

FTD-II-62-1301

299 679

CATALOGED BY ASTIA 299679
AS AD NO

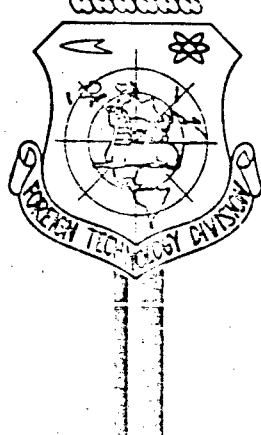
TRANSLATION

PROBLEMS OF MAGNETOHYDRODYNAMICS AND PLASMA DYNAMICS II

FOREIGN TECHNOLOGY DIVISION

AIR FORCE SYSTEMS COMMAND

WRIGHT-PATTERSON AIR FORCE BASE
OHIO



Reproduced From
Best Available Copy

19990923045

NOTICE: When government or other drawings, specifications or other data are used for any purpose other than in connection with a definitely related government procurement operation, the U. S. Government thereby incurs no responsibility, nor any obligation whatsoever; and the fact that the Government may have formulated, furnished, or in any way supplied the said drawings, specifications, or other data is not to be regarded by implication or otherwise as in any manner licensing the holder or any other person or corporation, or conveying any rights or permission to manufacture, use or sell any patented invention that may in any way be related thereto.

FTD-TT-62-1301/1+2

UNEDITED ROUGH DRAFT TRANSLATION

PROBLEMS OF MAGNETOHYDRODYNAMICS AND PLASMA DYNAMICS II

English Pages: 646

THIS TRANSLATION IS A RENDITION OF THE ORIGINAL FOREIGN TEXT WITHOUT ANY ANALYTICAL OR EDITORIAL COMMENT. STATEMENTS OR THEORIES ADVOCATED OR IMPLIED ARE THOSE OF THE SOURCE AND DO NOT NECESSARILY REFLECT THE POSITION OR OPINION OF THE FOREIGN TECHNOLOGY DIVISION.

PREPARED BY:

TRANSLATION SERVICES BRANCH
FOREIGN TECHNOLOGY DIVISION
AFB, OHIO.

FTD-TT-62-1301/1+2

Date 25 Feb. 19 63

S

Akademija Nauk Latvijskoy SSR
Institut Fiziki

VOPROSY MAGNITNOY GIDRODINAMIKI I DINAMIKI PLAZMY II

(Papers read to the 2nd Conference on Theoretical and Applied
Magnetohydrodynamics at Riga, 27 June to 2 July, 1960)

Izdatel'stvo Akademii Nauk Latvijskoy SSR
Riga 1962

Pages: 1-660

FID-RT-62-1301/1+2

TABLE OF CONTENTS

	PAGE
Poreword.....	
THEORETICAL PROBLEMS OF MAGNETOHYDRODYNAMICS.....	1
Fundamental Equations of Relativistic Magnetic Gas Dynamics, by K. P. Stanyukovich.....	1
Some Problems in Anisotropic Magnetic Gas Dynamics, by S. A. Kaplan, A. A. Logvinenko, V. V. Perfir'yev.....	25
Discussion Following the Paper, by R. V. Polovin.....	31
Contribution to the Theory of Stationary Flows in Magnetic Gas Dynamics, by M. F. Shirokov.....	33
Effect of Conductivity Anisotropy on the Structure of a Magnetohydrodynamic Shock Wave, by G. I. Lyubimov.....	44
Some Properties of Magnetohydrodynamic Flows in Shock Wave, by M. N. Kogan.....	49
Perturbations of the Magnetic Field in Wave and Jet Motions in a Conducting Medium, by L. I. Dorman.....	55
Laminar Flow of a Conducting Liquid in a Homopolar Engine, by V. S. Yargin.....	62
Concerning Turbulent Hydromagnetic Flow in a Homopolar Engine, by Ye. P. Vaulin, V. I. Babetskiy.....	73
Flow of Conducting Viscous Liquid in a Porous Annular Tube, by N. P. Dzhorbenadze, D. V. Sharikadze.....	81
Stability of Plane Couette Flow in the Presence of a Magnetic Field, by K. B. Pavlov.....	89

Flow of Viscous Conducting Liquid in Regions With Permeable Boundaries in the Presence of a Magnetic Field, by S. A. Regirer.....	97
Some Solutions of the System of Equations Describing One- Dimensional Flows in Magnetic Gasdynamics, by E. P. Zimin.....	105
Flow of Viscous Conducting Liquids in Pipes in the Presence of a Magnetic Field, by S. A. Regirer.....	116
Self-Similar Solutions of the Magnetohydrodynamic Equations, by N. I. Pol'skiy, I. T. Shvets.....	124
Quasi-Superimposable Fields of Finite Amplitude in Nonideal Magnetohydrodynamics, by V. S. Tkalich.....	130
Problem of Lubrication in Magnetohydrodynamics, by I. Ye. Tarapov.....	138
Experiments on the Generation of a Magnetic Field in Metals and the Question of the Origin of the Geomagnetic Field, by Yu. M. Volkov, L. I. Dorman, Yu. M. Mikhaylov.....	145
Magnetohydrodynamics of the Ocean, by V. V. Kontorovich.....	161
Hydromagnetic Turbulence in the Ionosphere, by Ye. A. Novikov.....	169
Character of Turbulence in Solar Wind, by L. I. Dorman.....	177
Flow Around Magnetic Inhomogeneities, by A. P. Kazantsev.....	181
Cylindrical Explosion and Straight Line Discharge in an Electri- cally Conducting Medium With Account of the Magnetic Field, by V. P. Korobeynikov.....	187
Deformation of a Conducting Liquid Sphere Under the Influence of a Magnetic Field, by V. V. Yankov.....	197

Magnetohydrodynamic Flow With Small Re_x , by M. D. Ladyzhenskiy.....	205
Approximate Method of Investigating Plane Vortical Flows in Magnetohydrodynamics, by I. I. Nochevkina.....	211
Investigation of Steady-State Ultrarelativistic Isentropic Flows in the Presence of Magnetic Field, by I. I. Nochevkina.....	216
Discussion Following the Paper, by V. S. Tkalich.....	219
Contribution to the Theory of the Magnetohydrodynamic Piston, by I. A. Akhiezar, G. Ya. Lyubarskiy, R. V. Polovin.....	221
On the "Law of Action Inversion" in Magnetic Gasdynamics, by L. A. Vulis, P. L. Gusika.....	222
Some Problems in the Theory of Simple Waves, by R. V. Polovin.....	223
Relativistic Shock Waves in Magnetohydrodynamics, by L. M. Kovrizhnykh.....	224
Structure of Low-Intensity Shock Waves in Magnetohydrodynamics, by Ye. P. Sirotina, S. I. Syrovatskiy.....	224
Special Case of Interaction Between A Magnetic Field and A Strong Shock Wave, by Yu. L. Zhilir.....	226
Absorption of Magnetohydrodynamic Waves In Waveguides, by Yu. F. Filippov.....	227
Meridional Flows of A Conducting Liquid, by G. L. Goodzovskiy, A. N. Dyukalov, V. V. Tokarev, A. N. Tolstykh.....	227
Turbulent Flow of a Conducting Liquid in a Homopolar Engine, by E. F. Fradkina, A. V. Kozyukov.....	228
Concerning the Steady Flow of a Conducting Liquid in a Rectangular Tube, by Ya. S. Uflyand.....	228
Plane Problem of Flow of Incompressible Liquid of Finite Conductivity Around a Solid Body in a Perpendicular Magnetic Field, by K. A. Lur'ye.....	229

Estimate of the Influence of the Earth's Magnetic Field on the Turbulence in the Lower Ionosphere, by G. S. Golitsyn.....	230
Effectiveness of Local Magnetic Field In Solar Corona, by E. E. Mogilevskiy.....	230
Effect of the Magnetic Field on Motion in Chromospheric Flares, by S. I. Gopasyuk.....	231
Generation of Cosmic Rays in a Solar Flare, by A. B. Severnyy, V. P. Shabanskiy.....	232
Formation of Active Regions in the Presence of a Magnetic Field, by S. B. Pikel'ner.....	234
THEORETICAL PROBLEMS IN PLASMA PHYSICS..... 235	
Some Problems in Relativistic Gasdynamics of Charged Particles, by V. N. Tsytovich.....	235
Plane and Cylindrical Waves in a Medium With Finite Conductivity, by L. B. Levitin, M. I. Kiselev, K. P. Stanyukovich.....	247
Concerning One Analogy Between Waves on the Surface of a Heavy Liquid and Nonlinear Plasma Oscillations, by R. Z. Sagdeev.....	264
Properties of a Magnetic Trap in a Plasma Ejected From the Sun, by L. I. Derman.....	269
Concerning the Stability of a Plasma Pinch, by V. D. Ladyzhenskiy..	277
Natural Oscillations of a Bounded Plasma, by D. A. Frank- Kamenetskiy.....	283
Magnetohydrodynamics Instability of a Plasma Stream Moving Through an Ionized Gas, by V. P. Dokuchayev.....	290
Interaction of Ion Beam With Magentoactive Plasma*, by N. L. Tsintsasize, D. G. Lominadze.....	298

Magnetohydrodynamic Equations For a Nonisothermal Collision-Free Plasma, by Yu. L. Klimontovich, V. P. Sulin.....	302
Instability of a System of Two Electron Beams in a Magnetic Field, by V. N. Rutkevich.....	311
Cherenkov Generation of Hydromagnetic and Magnetic Sound Waves in Low-Density Anisotropic Plasma, by N. L. Tsintsadze, A. D. Pataraya.....	325
Effect of Fluctuating Microfields on Multiple Collisions in a Gas of Charged (or Gravitating) Particles, by V. I. Kogan.....	330
Kinetic Analysis of the Structure of the Boundary of a Plasma in a Magnetic Field, by A. I. Morozov, L. S. Solov'yev.....	331
Structure of Transition Layer Between a Plasma and a Magnetic Field, by V. P. Shabanskiy.....	331
Effect of External Magnetic Field on the Boundary Layer in a Plasma, by E. I. Andriankin, Yu. S. Sayasov.....	333
Motion of Viscous Plasma in a Magnetic Field For Arbitrary WT, by A. I. Cubanov, Yu. P. Lun'kin.....	334
Magnetic "Wringing" of Free-Molecule Plasma Current, by V. N. Zhigulev.....	335
Stability of Plane Poiseuille Flow of a Plasma With Finite Conductivity in a Magnetic Field, by Yu. A. Tarasov.....	336
Investigation of the Stability of a Plasma With the Aid of the Generalized Energy Principle, by V. F. Aleksin, V. I. Yashin.....	337
Some Problems in the Magnetohydrodynamic Stability of a Thin Annular Pinch, by Yu. V. Vandal'kurov.....	337
Instability of Electromagnetic Waves in a System of Interpenetrating Plasmas, by A. A. Rukhadze.....	338

Propagation of Electromagnetic Waves in a Half Space Filled With Plasma, by Yu. N. Dnestrovskiy, D. P. Kostomarov.....	338
Some Singularities of Transverse Propagation of Electromagnetic Waves in a Plasma Situated in a Constant Magnetic Field, by B. N. Gershman.....	339
Tendency of Compression Waves to "Tumble" and Lose Their Isentropic Nature in the Absence of Collisions Between the Particles of the Plasma Medium, by V. A. Belokon'.....	341
Oscillations of an Inhomogeneous Plasma, by L. I. Rudakov.....	345
Plasma Oscillations Between Two Electrodes, by S. V. Iordanskiy...	345
Nonlinear Langmuir Oscillations of Ions in a Plasma, by M. V. Konyukov.....	346
Transition Radiation of a Charge on the Front of a Shock Wave, by L. S. Bogdankevich, B. M. Bolotovskiy, A. A. Rukhadze.....	347
Cyclotron Radiation of a Plasma, by V. I. Pakhomov, K. N. Stepanov.....	347
EXPERIMENTAL PROBLEMS OF PLASMA PHYSICS.....	348
Behavior of a Plasma in Strong Electric Fields, by L. V. Dubovoy, A. G. Ponomarenko, O. M. Shvets.....	348
On the Role of Space Charge in a Discharge With Oscillating Electrons in a Magnetic Field, by M. N. Vasil'yeva, E. M. Reykhruzel'.....	356
Experimental Determination of the Nature and Concentration of Easily Ionized Impurities by Means of Absorption of Radio Waves Behind a Shock Wave, by T. V. Bazhenova, Yu. S. Lebastov.....	367
Experimental Determination of the Concentration of Charged Particles in Argon and Krypton Behind a Shock Wave, by V. N. Alyamovskiy, A. P. Bronov, V. P. Kitayeva, A. G. Sviridov, N. N. Sobolev.....	376

Pyrometric Investigation of a Gas Behind a Shock Wave, by Ye. M. Kudryavtsev, N. N. Scholev, L. N. Tunitskiy, F. S. Fayzullov.....	387
Magnetic Compression of Plasma, by I. M. Zolototrubov, Yu. M. Novikov, N. M. Ryzhov, I. P. Skoblik, V. T. Tolok.....	399
New Data on the Influence of a Magnetic Field on the Departure of Ions From the Plasma of Inert Gases, by I. A. Vasil'yeva, V. L. Granovskiy.....	406
Investigation of the Motion of a Conducting Gas Accelerated by Crossed Electric and Magnetic Fields, by A. K. Musin, V. L. Granovskiy.....	414
Investigation of the Motion of a Conducting Gas Accelerated by Crossed Electric and Magnetic Fields, by L. S. Lomonosova, V. I. Serbin, G. G. Timofeyeva, V. L. Granovskiy.....	421
Observation of Hydromagnetic Oscillations in the Plasma of a Pulsed Electrodeless Discharge, by M. D. Gabovich, I. M. Mitropan.....	428
Schemes of Electrogasdynamic Machines, by Ye. I. Yantovskiy.....	429
Circle Diagram of an Induction Magnetogasdodynamic Generator, by L. M. Dronnik.....	452
Some Experiments With a Plasma Jet, by B. F. Bobylev, V. Ye. Stryzhak.....	457
Acceleration of a Conducting Gas by a Traveling Magnetic Field, by V. B. Baranov.....	460
Equations of Motion of Plasmoids in External Magnetic Field, by K. D. Sinel'nikov, N. A. Khizhnyak, B. G. Saforonov.....	468

Concerning the Interaction Between Plasma and a Magnetic Field, by I. M. Podgornyy, V. I. Sumarokov.....	468
Conductivity of a Plasma of a Straight-Line Pinch, by M. D. Borisov, T. A. Suprunenko, Ye. A. Sukhomlin, Ye. D. Volkov, N. I. Briniev.....	469
Investigation of the Propagation of Shock Waves in a Discharge Tube, by L. G. Chernikova, M. D. Ladyzhenskiy.....	469
Investigation of a Shock Wave in a Conical Discharge Tube, by D. V. Orlinskii.....	470
Instability of a Plasma With Anisotropic Distribution of Ion and Electron Velocities, by A. B. Kitsenko, K. N. Stepanov.....	470
Interaction of an Electron Beam With A Plasma in a Magnetic Field, by I. F. Kharchenko, Ya. B. Faynberg, R. M. Nikolayev, Ye. A. Kurnilov, Ye. I. Lutsenko, N. S. Pedenko.....	471
Investigation of the High-Frequency Oscillations of the Plasma Pinch of a Vacuum Arc, by B. G. Safronov, R. V. Mitin, A. A. Kalmykov, V. G. Konovalov.....	471
Study of Magnetic Properties of a Plasma Behind the Front of a Strong Shock Wave, by K. D. Sinelnikov, V. G. Safronov, G. G. Aseyev, Th. S. Azovskiy, V. S. Voytsenya.....	472
Experiments With Plasma Jets in a Magnetic Field, by A. M. Kostylev, A. A. Porotnikov.....	473
High-Frequency Discharge in Moving Gas, by A. M. Khazen.....	487
Contribution to the Theory of the Synchronous Magnetogasdynamic Machine, by L. Yu. Ustimenko, Ye. I. Yantovskiy.....	487
Electric Dipole Field in a Plasma in an External Magnetic Field, by B. P. Kononov, A. A. Rukhadze, G. V. Solodukhov.....	488

APPLIED MAGNETOHYDRODYNAMICS.....	489
Status and Problems Involved in the Development of the Theory of Electromagnetic Processes in Induction Pumps and in Machinery With Open Magnetic Circuits, by A. I. Vol'dek.....	489
Transverse Edge in Planar Induction Pumps Using a Liquid Metal Channel With Conducting Walls, by A. I. Vol'dek, Kh. I. Yanes....	490
Longitudinal Edge Effect in Secondary Circuit of Liquid Metal Induction Pumps With Open Magnetic Circuit, by A. I. Vol'dek, Kh. K. Ross.....	499
Equivalent Circuit of D. C. Pump Channel, by Yu. A. Birzvalk....	500
Determination of Certain Parameters of Electromagnetic Pumps With the Aid of an Electrolytic Trough, by L. V. Nitsetskiy, E. K. Yankop.....	501
Experimental Investigation of Planar Induction Pumps, by A. I. Vol'dek, Kh. I. Yanes.....	507
Design of D. C. Pump for Maximum Efficiency, by Yu. A. Birzvalk.....	514
Centrifugal Induction Pump, by A. K. Veze, I. M. Kirko, O. A. Lielausis.....	516
Magnetohydrodynamic Phenomena in a Channel of a Planar Induction Pump With Account of Attenuation of the Electromagnetic Field, by N. M. Okhremenko.....	520
Hydrodynamic Processes in the Channel of an Electromagnetic Induction Pump, by Ya. Ya. Lielpeter.....	532
Nonstationary Flow of a Liquid Metal in the Channel of a Planar Induction Pump, by N. M. Okhremenko.....	541

Development of Laminar Flow of a Viscous Electrically Conducting Liquid Between Parallel Planes Under the Influence of a Transverse Magnetic Field, by N. M. Okhremenko.....	547
Batching of Liquid Metal With the Aid of Electromagnetic Induction Pumps, by I. M. Kirko, Ya. Ya. Lielpeter.....	554
Concerning the Transverse Edge Effect in Induction Pumps, by L. Ya. Ulmanis.....	555
Measurement of Velocities of a Liquid in Magnetohydrodynamics by the Electromagnetic Method, by Yu. M. Mikhaylov.....	562
Use of Electromagnetic Flow Meters for the Measurement of the Flow of Liquid Media With Ionic Conductivity, by L. M. Korsunskiy.....	566
Some Results of an Experimental Investigation of Turbulent Flow of Liquid Metal in a Transverse Magnetic Field, by G. G. Branover, O. A. Lielausis.....	567
Effect of the Magnetic Field on the Resistance in the Flow of Mercury Around Some Bodies, by O. A. Lielausis, A. B. Tsinober.....	574
Effect of Transverse Magnetic Field on the Local Hydraulic Resistance in a Mercury Stream, by G. G. Branover, O. A. Lielausis.....	579
Effect of Magnetic Field on Turbulent Transport Processes in a Stream of Mercury, by G. G. Branover, O. A. Lielausis.....	583
Certain Problems in the Contact Properties of Metallic Surfaces, by R. K. Dukure, G. P. Upit.....	586
Concerning the Stability of Free Suspension of a Drop of Liquid Metal in an Alternating Magnetic Field, by I. M. Kirko, A. E. Mikel'son.....	587

Motion of Nonintermixing Layers of Liquid Metal and Nonelectrically Conducting Liquid in a Traveling Magnetic Field, by V. A. Briskman.....	595
Mixing of Metal Inside a Freely Suspended Drop, by A. E. Mikel'son.....	596
Basic Parameters and Constructions of Electromagnetic Stirring Devices for Electric Arc Furnaces, by Ya. P. Zvorono.....	603
Electromagnetic Stirring of Steel in the Ladle, by M. G. Rezin.....	611
Power Supplies For Installations for Electromagnetic Stirring of Liquid Steel in Ladles, by Ya. I. Drobinnin.....	619
Hydrogas Analogy in Magnetohydrodynamics, by L. A. Vulis, P. L. Gusika.....	625
Certain Properties of Suspended Layer of Ferromagnetic Particles in a Magnetic Field, by M. V. Filippov.....	626
Magnetic Separation of Particles in Suspended State, by M. V. Filippov.....	633
Experimental Study of the Influence of Electromagnetic Forces on the Flow of an Electrolyte Around Some Bodies, by R. K. Dukure, O. A. Lielausis.....	636
Heat Transfer to Liquid Metals, by V. M. Borishanskiy.....	640
Some Physical and Chemical Phenomena Observed in Flows of Liquid Metal Collants, by A. S. Andreyev.....	643

FOREWORD

In accordance with the plan of the Science Council on Magnetism at the Academy of Sciences USSR and the resolution of the presidium of the Academy of Sciences of the Latvian SSR, the Institute of Physics of the Latvian SSR Academy of Sciences has called together in Riga, in June 1960, the second conference on magnetohydrodynamics.

The work of the conference was done in four sections: theoretical magnetohydrodynamics, plasma theory, experimental plasma physics, and applied magnetohydrodynamics.

In attendance at the conference were approximately 500 persons from different cities of the Soviet Union. More than 140 papers and communications were heard.

The present collection contains the abbreviated texts or abstracts of most papers delivered at the conference. The texts of the papers were presented by the authors themselves, and the editorial staff made no changes in them. Consequently, there is no adherence to a rigorously unified notation for the physics quantities in the collection.

THEORETICAL PROBLEMS OF MAGNETOHYDRODYNAMICS

FUNDAMENTAL EQUATIONS OF RELATIVISTIC MAGNETIC GAS DYNAMICS

K. P. Stanyukovich
Moscow

In the present paper we present a rigorous derivation of the equations of relativistic magnetic gas dynamics in the case of finite conductivity, and a transition to the classical limit is given.

We do not give here the precise dependences of ϵ and μ on the character of the processes that occur in the medium, but these quantities are assumed to be variable.

In specific problems where there is a considerable electric field in the system's own frame of reference, and also in other cases, complete solution of these problems calls for knowledge of ϵ and μ as functions of the process or of the state of the system; this, however, is already in the realm of relativistic plasma kinetics, in the derivation of which we shall not engage in the present paper.

Many problems arising in the case of good conductivity of the medium can be solved by means of the relations indicated here, some of which are presented for the first time in the form proposed here.

Of greatest interest are motions possessing symmetry.

1. DERIVATION OF FUNDAMENTAL EQUATIONS

Let us derive the fundamental equations of magnetic gas dynamics in general form for the relativistic case.

The motion and energy equations can be obtained from the well-known expression [1]

$$\frac{\partial}{\partial x_k} (T_{ik}^* + T_{ik}) = 0. \quad (1)$$

where

$$T_{ik}^* = (\rho + \epsilon) u_i u_k + \delta_{ik} p + \tau_{ik} - \quad (2)$$

is the macroscopic symmetrical energy momentum tensor;

$$\begin{aligned} \tau_{ik} = & -\eta \left[\frac{\partial u_i}{\partial x_k} + \frac{\partial u_k}{\partial x_i} + u_i u_l \frac{\partial u_l}{\partial x_k} + u_k u_l \frac{\partial u_l}{\partial x_i} \right] - \\ & - \left(\zeta - \frac{2}{3} \eta \right) (\delta_{ik} + u_i u_k) \frac{\partial u_l}{\partial x_l} - \end{aligned}$$

is a tensor that takes into account the dissipative processes (viscosity); η and ζ are viscosity coefficients; $\epsilon = \rho c^2$ is the volume energy density, where ρ is the density (including the internal density); $u_a = a_a/c\epsilon$; $u_4 = 1/\epsilon$ are the four-velocity components; a_a are the components of ordinary velocity; $\epsilon = \sqrt{1 - (a^2/c^2)}$, where a is the total velocity. Besides, the quantities ρ and ϵ are reckoned in a reference frame in which each element of the medium is at rest (the K reference frame), and T_{ik} is the symmetrical electromagnetic field tensor.

The usual expression for the tensor T_{ik} with $\epsilon \neq 1$ and $\mu \neq 1$ has the form

$$T_{ik} = \frac{1}{4\pi} \left\{ F'_{il} H'_{lk} - \frac{\delta_{ik}}{4} \cdot F'_{im} H'_{lm} \right\}. \quad (3)$$

Here F'_{ik} and H'_{ik} are referred to the K' (observer) frame, relative to which the K frame moves with velocity \vec{a} (along the x axis). This tensor is not symmetrical. However, the tensor T_{ik} must also be symmetrical (the tensors F_{ik} and H_{ik} are antisymmetrical).

It was already shown by Abraham [2, 3] that a symmetrical tensor T_{ik} can be expressed in the form

$$T_{ik} = \frac{1}{8\pi} \left\{ F'_d H'_{ik} + H'_d F'_{ik} - \frac{\delta_{ik}}{2} \cdot F'_{im} H'_{lm} - (\epsilon_1 - 1)(\Omega'_i u_k + u_i \Omega'_k) \right\}. \quad (4)$$

where

$$\begin{aligned} \Omega'_i &= u_i F'_i (H'_{ik} u_k + H'_k u_i + H'_i u_k); \quad F'_i = F'_{ik} u_k, \\ \Omega'_k &= u_i H'_i (F'_{ik} u_k + F'_{ki} u_i + F'_{kk} u_i); \quad H'_i = H'_{ik} u_k, \end{aligned}$$

The expressions for T_{1k} can be written in the form

$$T_{1k} = \frac{1}{4\pi} \left\{ H'_4 F'_{14} - \frac{3}{4} F'_{14} H'_{14} - (\epsilon_4 - 1) u_4 \Omega'_4 \right\}. \quad (5)$$

However, it is most convenient to use an expression of the form

$$T_{1k} = \frac{1}{4\pi} \left\{ F'_{14} H'_{14} - \frac{3}{4} F'_{14} H'_{14} - (\epsilon_4 - 1) u_4 \Omega'_4 \right\} = \bar{T}_{1k} - \frac{\epsilon_4 - 1}{4\pi} u_4 \Omega'_4. \quad (6)$$

It is easy to verify that in the reference frame (K) in which each element of the medium is at rest, the expressions (4-6) for T_{1k} are equivalent and consequently they are equivalent in any inertial reference frame K'.

In the system K we have $u_k = u_\beta = 0$, $u_k = u_4 = 1$, and therefore the separate entry tensor is

$$\xi_{ik} = u_k \dot{\Omega}_i = \xi_{i4} = i \Omega_i, \quad \xi_{ij} = 0.$$

Further, $F_{14} = i F_{14}$, and therefore

$$\Omega_i = -F_{ii}(H_{ii}u_i + H_{44}u_4 + iH_{ii}).$$

The first term of this expression obviously is equal to zero. In fact, when $i = 1, 2, 3$, we have $u_i = 0$ and when $i = 4$ we have $F_{14} = F_{44} = 0$.

It is obvious also that when $i = 4$ we have $\Omega_4 = 0$, inasmuch as

$$F_{ii}(H_{ii}u_i + iH_{ii}) = iF_{ii}(H_{ii} + H_{ii}), \quad H_{ii} = -H_{ii}.$$

When $i = \alpha$ we have

$$\Omega_\alpha = -iF_{ii}H_{i\alpha} = [\vec{EH}]_\alpha. \quad (7)$$

Inasmuch as

$$\xi_{i\beta} = 0, \quad \xi_{i\alpha} = 0, \quad \xi_{i4} = i\Omega_\alpha = F_{ii}H_{i\alpha},$$

we get

$$\frac{\partial \xi_{i\alpha}}{\partial x_\beta} = \frac{\partial \xi_{i\beta}}{\partial x_\alpha} + \frac{\partial \xi_{i4}}{\partial x_\alpha} = \frac{\partial \xi_{i4}}{\partial x_\alpha}.$$

If $i = 4$ then $\partial \xi_{i4}/\partial x_\alpha = 0$. When $i = \alpha$ we have

$$\frac{\partial \xi_{i\alpha}}{\partial x_\alpha} = \frac{\partial \xi_{i4}}{\partial x_\alpha} = \frac{\partial (F_{ii}H_{i\alpha})}{\partial x_\alpha} = \frac{\partial [\vec{EH}]_\alpha}{\partial x_\alpha}. \quad (8)$$

In the K' frame, relative to which the K frame moves along the x axis with velocity a, we have

$$u_1 = \frac{a}{c\Theta}, \quad u_2 = u_3 = 0, \quad u_4 = \frac{t}{\Theta}.$$

$$\Omega'_1 = \frac{\Omega_x}{\Theta}, \quad \Omega'_{23} = \Omega_{y,z}, \quad \Omega'_4 = \frac{ta\Omega_x}{c\Theta}.$$

$$\xi'_k = u_k \Omega'_i = \begin{bmatrix} \frac{a}{c\Theta^2} \Omega_x & 0 & 0 & \frac{t}{\Theta} \Omega_x \\ \frac{a}{c\Theta} \Omega_y & 0 & 0 & \frac{t}{\Theta} \Omega_z \\ \frac{a}{c\Theta} \Omega_z & 0 & 0 & \frac{t}{\Theta} \Omega_x \\ \frac{ta^2}{c^2\Theta^2} \Omega_x & 0 & 0 & -\frac{a}{c\Theta^2} \Omega_z \end{bmatrix} \quad (9)$$

Inasmuch as

$$\frac{\partial \vec{v}_{ik}}{\partial x_k} = u_k \frac{\partial \Omega'_i}{\partial x_k} + \Omega'_i \frac{\partial u_k}{\partial x_k} = \frac{d \Omega'_i}{ds} + \Omega'_i \operatorname{Div} \vec{u}, \quad (10)$$

where $ds = \epsilon c dt$, we get

$$\begin{aligned} \operatorname{Div} \vec{u} &= \frac{\partial u_k}{\partial x_k} = \frac{1}{c} \left(\operatorname{div} \frac{\vec{a}}{\Theta} + \frac{\partial (\vec{a}/\Theta)}{\partial t} \right) = \\ &= \frac{1}{c\Theta} \left[\operatorname{div} \vec{a} + \frac{\vec{a}}{c^2\Theta^2} (\vec{a} \cdot \operatorname{grad}) \vec{a} + \frac{\vec{a}}{c^2\Theta^2} \cdot \frac{\partial \vec{a}}{\partial t} \right]. \end{aligned}$$

where

$$\Omega'_i = \left\{ \frac{1}{\Theta} [\vec{EH}]_x; [\vec{EH}]_y; [\vec{EH}]_z; \frac{ta}{c\Theta} [\vec{EH}]_x \right\}.$$

We can write

$$\begin{aligned} \frac{\partial \xi'_{1k}}{\partial x_k} &= \frac{1}{c\Theta^2} \cdot \frac{d[\vec{EH}]_x}{dt} + \frac{[\vec{EH}]_x}{c\Theta^2} \left\{ \operatorname{div} \vec{a} + \frac{\vec{a}}{c^2\Theta^2} \frac{\partial \vec{a}}{\partial t} \right\}, \\ \frac{\partial \xi'_{23k}}{\partial x_k} &= \frac{1}{c\Theta} \frac{d[\vec{EH}]_{y,z}}{dt} + \frac{[\vec{EH}]_{y,z}}{c\Theta} \left\{ \operatorname{div} \vec{a} + \frac{\vec{a}}{c^2\Theta^2} \frac{\partial \vec{a}}{\partial t} \right\}, \\ \frac{\partial \xi'_{4k}}{\partial x_k} &= \frac{ta}{c^2\Theta^2} \cdot \frac{d[\vec{EH}]_x}{dt} + \frac{ta}{c^2\Theta^2} [\vec{EH}]_x \left\{ \operatorname{div} \vec{a} + \frac{\vec{a}}{c^2\Theta^2} \frac{\partial \vec{a}}{\partial t} \right\}. \end{aligned} \quad (11)$$

The tensor T_{ik} refers to the K' frame, and therefore the tensor components T_{ik} , F_{ik} , H_{ik} , ξ'_{ik} should also be referred to the K' frame.

Thus,

$$T_{ik} = \frac{1}{4\pi} \left\{ F_{ik} H_{ii} - \frac{3}{4} F_{in} H'_{in} - (i_p - 1) \xi'_{ik} \right\}. \quad (12)$$

In the case of an arbitrary vector \vec{a} we must $\xi_{ik} = U_{ik} L_i$ to mean

the tensor obtained from the tensor $\xi_{ik} = U_k L_1$ by means of the ordinary Lorentz transformations. The same remark pertains also to the vector L_1 .

The field tensors are

$$F_{ik}' = \begin{bmatrix} 0 & B'_x - B'_y - iE'_z \\ -B'_x & 0 & B'_x - iE'_y \\ B'_y - B'_x & 0 & -iE'_z \\ iE'_z & iE'_y & iE'_x & 0 \end{bmatrix}; H'_{ik} = \begin{bmatrix} 0 & H'_x - H'_y - iD'_z \\ -H'_x & 0 & H'_x - iD'_y \\ H'_y - H'_x & 0 & -iD'_z \\ iD'_z & iD'_y & iD'_x & 0 \end{bmatrix}. \quad (13)$$

where \vec{H}' , \vec{B}' , \vec{E}' , \vec{D}' are the vectors of the magnetic and electric fields and inductions, referred to the laboratory frame (K') (stationary observer).

In order to change over to the K frame in which each element of the medium is at rest, it is necessary to carry out the Lorentz transformation.

In the particular case, assuming that the motion of the frame is along the x axis with velocity a , we arrive at the relations

$$\begin{aligned} E'_x &= E_x & E'_y &= \frac{1}{\Theta} \left(E_y + \frac{a}{c} B_z \right) & E'_z &= \frac{1}{\Theta} \left(E_z - \frac{a}{c} B_y \right) \\ D'_x &= D_x & D'_y &= \frac{1}{\Theta} \left(D_y + \frac{a}{c} H_z \right) & D'_z &= \frac{1}{\Theta} \left(D_z - \frac{a}{c} H_y \right) \\ H'_x &= H_x & H'_y &= \frac{1}{\Theta} \left(H_y - \frac{a}{c} D_z \right) & H'_z &= \frac{1}{\Theta} \left(H_z + \frac{a}{c} D_y \right) \\ B'_x &= B_x & B'_y &= \frac{1}{\Theta} \left(B_y - \frac{a}{c} E_z \right) & B'_z &= \frac{1}{\Theta} \left(B_z + \frac{a}{c} E_y \right). \end{aligned} \quad (14)$$

where \vec{H} , \vec{B} and \vec{E} , \vec{D} are referred to the frame in which each element of the medium is at rest, it being assumed further that $\vec{B} = \mu \vec{H}$ and $\vec{D} = \epsilon \vec{E}$.

In the general case it is necessary to take the projections of the velocity a along the coordinate axes a_x , a_y , a_z and carry out a general Lorentz transformation, or assume that the orientation of the x axis changes from one element of the medium to another. For motions having central symmetry it is necessary to identify the x axis with the radius r , and then the transformations will be valid for a special element of the medium (the observer is at the symmetry center).

Let us write T_{ik} in the form

$$T_{ik} = \bar{T}_{ik} - \frac{\epsilon_0 - 1}{4\pi} \xi'_{ik}, \quad (15)$$

where in the K' frame \bar{T}_{ik} is given by Expression (3):

$$\bar{T}_{ik} = \frac{1}{4\pi} \left\{ F'_{ik} H'_k - \frac{\delta_{ik}}{4} F'_{lm} H'_{lm} \right\}.$$

As is well known [4]

$$\begin{aligned} \frac{\partial \bar{T}_{ik}}{\partial x_k} &= -\frac{1}{c} F'_{ik} j'_k + \frac{1}{16\pi} \left\{ H'_{lm} \frac{\partial F'_{ik}}{\partial x_l} - F'_{lm} \frac{\partial H'_{ik}}{\partial x_l} \right\} = \\ &= -\frac{1}{c} F'_{ik} j'_k + \theta'_k. \end{aligned} \quad (16)$$

Here j'_k are the components of the total current vector (the sum of the conduction and charging currents).

$$j'_i = (j'_x, j'_y, j'_z, lc\delta); \quad (17)$$

$$j'_x = \frac{1}{\Theta} (J_x + a\delta), \quad j'_{y,z} = J_{y,z}, \quad j'_i = lc\delta' = \frac{lc}{\Theta} \left(\delta + \frac{a}{c^2} J_z \right) \quad (18)$$

(δ is the charge density), and $j_a = (j_x, j_y, j_z)$ are the components of the conduction current;

$$\frac{\partial T_{ik}}{\partial x_k} = i'_i = - \left[\frac{1}{c} F'_{ik} j'_k + \frac{\epsilon_0 - 1}{4\pi} \cdot \frac{\partial \xi'_{ik}}{\partial x_k} + \frac{\xi'_{ik}}{4\pi} \frac{\partial (\epsilon_0)}{\partial x_k} \right] + \theta'_k, \quad (19)$$

where f'_{ik} is the force exerted (in the K' frame) by the field on the conducting medium.

From (1) we have

$$\frac{\partial T_{ik}}{\partial x_k} = -\frac{\partial T_{ik}}{\partial x_k} = -i'_i = \frac{1}{c} F'_{ik} j'_k + \frac{\epsilon_0 - 1}{4\pi} \frac{\partial \xi'_{ik}}{\partial x_k} + \frac{\xi'_{ik}}{4\pi} \frac{\partial (\epsilon_0)}{\partial x_k} - \theta'_k. \quad (20)$$

Calculations yield

$$\frac{1}{c} F'_{ik} j'_k = \frac{1}{c} [\vec{j}' \vec{B}']_x + \delta' E'_x; \quad \frac{1}{c} F'_{ik} j'_i = \frac{l}{c} \vec{j}'_x \vec{E}'_x; \quad (21)$$

$$\theta'_i = \frac{1}{8\pi} \left\{ E^2 \frac{\partial \delta}{\partial x_i} + H^2 \frac{\partial \mu}{\partial x_i} \right\} - \frac{\epsilon_0 - 1}{4\pi c} \cdot \frac{[\vec{E} \vec{H}]_x}{\Theta^2} \frac{\partial \alpha}{\partial x}. \quad (22)$$

$$\frac{\xi'_{ik}}{4\pi} \frac{\partial (\epsilon_0)}{\partial x_k} = \frac{[\vec{E} \vec{H}]_x}{4\pi \Theta} \frac{d(\epsilon_0)}{ds}; \quad \frac{\xi'_{2ik}}{4\pi} \frac{\partial (\epsilon_0)}{\partial x_k} = \frac{[\vec{E} \vec{H}]_{y,x}}{4\pi} \frac{d(\epsilon_0)}{ds};$$

$$\frac{\xi'_{ik}}{4\pi} \frac{\partial (\epsilon_0)}{\partial x_k} = \frac{la [\vec{E} \vec{H}]_x}{4\pi \Theta} \frac{d(\epsilon_0)}{ds}. \quad (23)$$

(We see that inclusion of the supplementary tensor ξ'_{ik} gives in general a small correction to the main tensor, of order $1/c\tau$, where l and τ are the characteristic length and time for the investigated process.)

Thus

$$-\mathbf{f}_z = \frac{1}{c} [\vec{B}' \vec{B}']_z + \tilde{\epsilon} E_z - \frac{1}{8\pi} \left(E^2 \frac{\partial \epsilon}{\partial x_z} + H^2 \frac{\partial \mu}{\partial x_z} \right) + \\ + \frac{[\vec{E}\vec{H}]_z}{4\pi\theta^3} \frac{d(\epsilon\mu)}{ds} + \frac{\epsilon\mu-1}{4\pi} \left\{ \frac{[\vec{E}\vec{H}]_z}{c\theta^2} \frac{\partial a}{\partial x_z} + \frac{d(\vec{E}\vec{H})_z}{ds} + \frac{[\vec{E}\vec{H}]_z}{\theta^3} \operatorname{Div} u \right\}, \quad (24)$$

where $\beta = 1$ when $\alpha = 1$ and $\beta = 0$ when $\alpha = 2, 3$;

$$-\mathbf{f}_i = \frac{i}{c} \vec{j}' \vec{E} + \frac{i}{8\pi c} \left\{ E^2 \frac{\partial \epsilon}{\partial t} + H^2 \frac{\partial \mu}{\partial t} \right\} + \frac{ia}{4\pi c} \cdot \frac{[\vec{E}\vec{H}]_z}{\theta} \frac{d(\epsilon\mu)}{ds} + \\ + \frac{(\epsilon\mu-1)i}{4\pi c} \left\{ - \frac{[\vec{E}\vec{H}]_z}{c\theta^2} \frac{\partial a}{\partial t} + \frac{d\left(\frac{a}{\theta} [\vec{E}\vec{H}]_z\right)}{ds} + \frac{2}{\theta} [\vec{E}\vec{H}]_z \operatorname{Div} u \right\}; \quad (25)$$

$$\frac{\partial T_{ik}}{\partial x_k} = - \frac{\partial T_{ik}}{\partial x_k} = -\mathbf{f}_{ik}. \quad (26)$$

$$\frac{\partial T_{ii}}{\partial x_k} = - \frac{\partial T_{ii}}{\partial x_k} = -\mathbf{f}_{ii}. \quad (27)$$

In order for the system (26, 27) to be closed, we must use Maxwell's equations

$$\frac{\partial F'_{ik}}{\partial x_i} + \frac{\partial F'_{il}}{\partial x_l} + \frac{\partial F'_{il}}{\partial x_k} = 0; \quad \frac{\partial H'_{ik}}{\partial x_k} = \frac{4\pi}{c} j_i. \quad (28)$$

In vector form these equations are known to be

$$\operatorname{div} \vec{B}' = 0; \quad \operatorname{rot} \vec{H}' = \frac{4\pi}{c} \vec{j}' + \frac{1}{c} \frac{\partial \vec{D}'}{\partial t}; \\ \operatorname{div} \vec{D}' = 4\pi \vec{e}'; \quad \operatorname{rot} \vec{E}' = - \frac{1}{c} \frac{\partial \vec{B}'}{\partial t}. \quad (29)$$

We recall that the system (29) has only six independent equations, since the components $\operatorname{rot} \vec{H}'$ and $\operatorname{rot} \vec{E}'$ are connected by the relations $\operatorname{div} \operatorname{rot} \vec{H}' = 0$; $\operatorname{div} \operatorname{rot} \vec{E}' = 0$. In addition, it is necessary to use Ohm's law and the equations of state (the connections between \vec{D} and \vec{E} , \vec{B} and \vec{H}). For a moving medium Ohm's law has (in the K' frame) the following form [3]:

$$j_x + \sigma_a j_x = \lambda u F_{ax}, \quad (30)$$

where λ is the conductivity.

In vector form Ohm's law is

$\text{for } \vec{E} \parallel \vec{a}$ $j_x - a\dot{z} = j_{x_0} =$ $= \lambda \theta \left\{ E_x + \left[\frac{a}{c} \vec{B} \right]_x \right\} =$ $= \lambda \theta E_x = \lambda \theta E_x;$ $j_x = \frac{1}{\theta} (\lambda E_x + a\dot{z})$	$\text{for } \vec{E} \perp \vec{a}$ $j_{yx} = j_{y,x} = \frac{\lambda}{\theta} \left\{ E_{y,x} + \left[\frac{a}{c} \vec{B} \right]_{y,x} \right\} =$ $= \frac{\lambda}{\theta} \left(E_{y,x} + \frac{a}{c} B_{z,y} \right) = \lambda E_{y,x}$
--	---

(31)

When $a = 0$ (in the K frame) we have

$$j = j_0 = \lambda E, \quad (32)$$

where \vec{j}_0 is the conductivity vector.

The equations of state for moving media have the form [3]

$$H'_{ik} u_k = \epsilon F'_{ik} u_i, F'_{ik} u_i + F'_{ki} u_i + F'_{ii} u_k = \mu (H'_{ik} u_i + H'_{ki} u_i + H'_{ii} u_k). \quad (33)$$

In vector form these expressions can be written

$\text{for } \vec{E} \parallel \vec{a}$ $\vec{D}' = \epsilon \vec{E}' + \frac{\epsilon_p - 1}{1 - \epsilon_p} \left[\frac{a}{c} \vec{H}' \right] =$ $= \epsilon (\vec{E}' + \vec{E}^1);$	$\text{for } \vec{E} \perp \vec{a}$ $\vec{D}' = \epsilon \vec{E}' + \frac{\epsilon_p - 1}{1 - \epsilon_p} \left\{ \left[\frac{a}{c} \vec{H}' \right] + \frac{\epsilon \vec{E}' a^2}{c^2} \right\} = \epsilon (\vec{E}' + \vec{E}^2);$
$\text{for } \vec{H}' \parallel \vec{a}$ $\vec{B}' = \mu \vec{H}' + \frac{\epsilon_p - 1}{1 - \epsilon_p} \left[\frac{a}{c} \vec{E}' \right] =$ $= \mu (\vec{H}' + \vec{H}^1)$	$\text{for } \vec{H}' \perp \vec{a}$ $\vec{B}' = \mu \vec{H}' + \frac{\epsilon_p - 1}{1 - \epsilon_p} \left\{ \left[\frac{a}{c} \vec{E}' \right] + \frac{\mu \vec{H}' a^2}{c^2} \right\} = \mu (\vec{H}' + \vec{H}^2)$

(34)

Here \vec{E}^1 , \vec{E}^2 and \vec{H}^1 , \vec{H}^2 are small corrections to the quantities \vec{E}' and \vec{H}' . Let us now transform the fundamental equations

$$\frac{\partial T_{ik}}{\partial x_k} = \frac{\partial (\rho + \epsilon) u_i u_k}{\partial x_k} + \frac{\partial \rho}{\partial x_i} = - \left(\dot{l}_i - \frac{\partial \tau_{ik}}{\partial x_k} \right). \quad (35)$$

We introduce the heat content $W = (p + \epsilon)V$, where V is the specific volume; then, neglecting the viscosity, i.e., putting $\tau_{ik} = 0$, we can

rewrite (35) in the form

$$u_k \frac{\partial (Wu_i)}{\partial x_k} + VWu_i \frac{\partial \frac{u_k}{V}}{\partial x_k} + V \frac{\partial p}{\partial x_i} = -Vf'_i.$$

Inasmuch as $dW = Td\sigma + Vdp$, where T is the temperature and σ the entropy, we get

$$\frac{d(Wu_i)}{ds} + \frac{dW}{dx_i} + VWu_i \frac{\partial \frac{u_k}{V}}{\partial x_k} = T \frac{d\sigma}{ds} - Vf'_i. \quad (36)$$

Taking the scalar product of (36) and u_1 , we obtain

$$VW \frac{\partial \frac{u_k}{V}}{\partial x_k} = -T \frac{d\sigma}{ds} + Vf'_i u_1. \quad (37)$$

We now write relations for the material flux density

$$\frac{\partial (nu_k)}{\partial x_k} = -\frac{\partial V_k}{\partial x_k}, \quad (38)$$

where $n \sim 1/V$ is the number of particles, V_k the components of the vector that take the heat conduction into account

$$V_k = -\frac{\kappa}{c} \left(\frac{T}{W} \right)^2 \left[\frac{\partial \bar{\mu}}{\partial x_i} + u_i u_k \frac{\partial \bar{\mu}}{\partial x_k} \right].$$

κ is the heat conduction coefficient, and $\bar{\mu} = W - T\sigma$ the chemical potential of the medium.

Neglecting heat conduction, we obtain from (38)

$$\frac{\partial \frac{u_k}{V}}{\partial x_k} = 0, \quad (39)$$

and therefore

$$\frac{T}{V} \frac{d\sigma}{ds} = \frac{dQ}{V ds} = f'_i \mu_r \quad (40)$$

where dQ is the elementary amount of Joule heat.

Inasmuch as the ratio T/V (for any medium) is invariant (against the Lorentz transformations), and ds and $d\sigma$ are also invariant, the relation (40) will hold true also in the K' frame. When $u_\alpha = 0$, $u_4 = 1$ we have in the K frame

$$\frac{T}{V} \frac{ds}{ds} = \frac{T}{cV} \frac{dz}{dt} = iI_s = \frac{1}{c} jE + \frac{1}{8\pi c} \left(E^2 \frac{\partial z}{\partial t} + H^2 \frac{\partial p}{\partial t} \right). \quad (41)$$

Inasmuch as $E = j/\lambda$, we have

$$\frac{T}{V} \frac{ds}{ds} = \frac{T}{cV} \frac{dz}{dt} = \frac{Tdz}{cdt} = \frac{j^2}{c\lambda} + \frac{1}{8\pi c} \left(j^2 \frac{\partial z}{\partial t} + H^2 \frac{\partial p}{\partial t} \right) \quad (42)$$

or

$$\frac{dQ}{dt} = \frac{Vj^2}{\lambda} + \frac{V}{8\pi} \left(j^2 \frac{\partial z}{\partial t} + H^2 \frac{\partial p}{\partial t} \right),$$

where dQ/dt is the Joule heat produced in the medium per second as a result of its finite conductivity.

In any frame K' we have

$$\frac{dQ}{Vds} = \frac{Tds}{Vds} = \frac{j^2}{c\lambda} + \frac{j^2}{8\pi\lambda^2} \frac{dt}{ds} + \frac{H^2}{8\pi} \frac{dp}{ds}. \quad (43)$$

In the case of infinite conductivity

$$(\lambda \rightarrow \infty), \quad \frac{dQ}{dt} = \frac{VH^2}{8\pi} \frac{dp}{dt}. \quad (44)$$

If μ is constant we have

$$dQ/dt = 0, \quad (45)$$

Let us now rewrite (36) (neglecting viscosity) in the form

$$\frac{d(Wa_i)}{ds} + \frac{\partial p}{\partial x_i} = -f_i. \quad (46)$$

When $i = \alpha$ we have, using Maxwell's equations

$$\begin{aligned} \frac{d}{V\theta c^2 dt} \frac{W a_\alpha}{\Theta} + \frac{\partial p}{\partial x_\alpha} &= \frac{1}{4\pi} \left\{ [\text{rot } \vec{H}] \vec{B}_z - \frac{1}{c} \left[\frac{\partial \vec{D}}{\partial t} \vec{B} \right]_z + E'_z \text{div } \vec{D}' \right\} + \\ &+ \frac{[EH]_z}{4\pi\theta^{1+\beta}} \frac{d(\epsilon\mu)}{dt} + \frac{\epsilon\mu - 1}{4\pi} \left\{ \frac{[EH]_z}{c\theta^2} \frac{\partial a}{\partial x_z} + \frac{[EH]_z}{\theta^3} \left(\frac{\epsilon\alpha}{c\theta^2} \frac{da}{dt} + \text{Div } \vec{u} \right) \right\} + \\ &+ \frac{d[EH]_z}{c\theta^{1+\beta} dt} \left\} - \frac{1}{8\pi} \left\{ E^2 \frac{\partial z}{\partial x_\alpha} + H^2 \frac{\partial p}{\partial x_\alpha} \right\}; \end{aligned} \quad (47)$$

($\beta = 1$ for $\alpha = 1$, $\beta = 0$ for $\alpha = 2, 3$); for $i = 4$ we have

$$\begin{aligned} \frac{d}{V\theta dt} \frac{W}{\Theta} - \frac{\partial p}{\partial t} &= \frac{1}{4\pi} \left\{ c \vec{E} \text{rot } \vec{H} - \frac{\partial \vec{D}}{\partial t} \vec{E} \right\} + \frac{a[EH]_z}{4\pi\theta^2} \frac{d(\epsilon\mu)}{dt} + \\ &+ \frac{1}{8\pi} \left\{ E^2 \frac{\partial z}{\partial t} + H^2 \frac{\partial p}{\partial t} \right\} + \frac{\epsilon\mu - 1}{4\pi\theta} \left\{ [EH]_z \left(-\frac{1}{c\theta} \frac{da}{dt} + \frac{da}{c\theta^2 dt} \right) + \right. \end{aligned}$$

$$+ a \operatorname{Div} \vec{u} \Big) + \frac{a}{c\theta} \frac{d|\vec{E}\vec{H}|_x}{dt} \Big\} + \frac{1}{8\pi} \left\{ E^2 \frac{\partial \epsilon}{\partial t} + H^2 \frac{\partial \mu}{\partial t} \right\}. \quad (48)$$

Here

$$\frac{d}{dt} = \frac{\partial}{\partial t} + a_3 \frac{\partial}{\partial x_3}.$$

In these equations it is necessary to change over with the aid of the transformation (14) and the equation of state from the quantities \vec{D}' , \vec{B}' and \vec{E}' , \vec{H}' to the quantities \vec{E} and \vec{H} . Equation (48) is not independent and can be derived from the equations (47, 39, and 41).

The continuity equation (neglecting heat conduction) can be written in the form

$$\frac{\partial \frac{a_3}{V}}{\partial x_3} = 0; \quad \frac{d \ln V}{ds} = \operatorname{Div} \vec{u} = \frac{1}{c} \operatorname{div} \vec{a} + \frac{a}{c\theta^2} \frac{\partial a}{\partial t} \quad (49)$$

or in the form

$$\frac{d \ln V}{dt} = \frac{\partial \ln V}{\partial t} + a_3 \frac{\partial \ln V}{\partial x_3} = \operatorname{div} \vec{a} + \frac{a}{c\theta^2} \frac{\partial a}{\partial t}. \quad (50)$$

It is easy to verify that the system (47, 50, 29) together with the equations of state and Ohm's law is a closed system (in which the number of unknown functions equals the number of equations).

From Maxwell's equations we can obtain, by eliminating the electric field components (\vec{E}' and \vec{D}') a single equation relating the components of the magnetic field (\vec{H}' and \vec{B}') with the velocity. In fact, inasmuch as

$$j'_x = \frac{1}{\theta} (c E_x + i a) = \frac{1}{\theta} \left\{ i \left(E_x + \left[\frac{a}{c} \vec{B}' \right]_x \right) + i a \right\},$$

and

$$j'_{x,x} = \frac{1}{\theta} \left\{ E'_{x,x} + \left[\frac{a}{c} \vec{B}' \right]_{x,x} \right\},$$

we can write

$$\vec{j} = \frac{1}{\theta} \left\{ \vec{E} + \left[\frac{a}{c} \vec{B} \right] \right\} + i \frac{a_3}{\theta}. \quad (51)$$

Further, inasmuch as

$$\frac{4\pi}{c} \vec{J} - \text{rot} \vec{H} = \frac{1}{c} \frac{\partial \vec{D}}{\partial t}, \quad (52)$$

we have

$$-\vec{I} \frac{a\vec{s}}{\lambda} + \frac{c^2}{4\pi\lambda} \left(\text{rot} \vec{H} - \frac{1}{c} \frac{\partial \vec{D}}{\partial t} \right) = \vec{E} + \left[\frac{a}{c} \vec{B} \right]. \quad (53)$$

Taking the curl of both halves of the equation we get

$$\begin{aligned} \frac{\partial \vec{B}}{\partial t} - \text{rot} [\vec{a}\vec{s}] &= \vec{I} c \frac{\partial}{\partial z} \frac{a\vec{s}}{\lambda} - \vec{k} c \frac{\partial}{\partial y} \frac{a\vec{s}}{\lambda} + \\ &+ \frac{c^2}{4\pi} \text{rot} \left\{ \frac{\theta}{\lambda} \left(-\text{rot} \vec{H} + \frac{1}{c} \frac{\partial \vec{D}}{\partial t} \right) \right\}. \end{aligned}$$

Expressing λ in terms of the magnetic viscosity $v_m = c^2/4\pi\lambda$, we arrive at the equation

$$\begin{aligned} \frac{\partial \vec{B}}{\partial t} - \text{rot} [\vec{a}\vec{s}] &= \frac{4\pi}{c} \left\{ \vec{j} \frac{\partial}{\partial z} v_m a\vec{s} - \vec{k} \frac{\partial}{\partial y} v_m a\vec{s} \right\} + \\ &+ \text{rot} \left\{ v_m \theta \left(-\text{rot} \vec{H} + \frac{1}{c} \frac{\partial \vec{D}}{\partial t} \right) \right\}. \end{aligned} \quad (54)$$

In addition to (54), in solving the entire system of equations we must take into account the remaining three Maxwell's equations; we have already made use of one Maxwell equation (52).

If $\vec{a} = \vec{a}(r; t)$, i.e., the velocity in any noncurvilinear system of coordinates is directed along the radius vector, or if there are no charges, $\delta = 0$, then

$$\frac{\partial \vec{B}}{\partial t} - \text{rot} [\vec{a}\vec{s}] = \text{rot} \left\{ v_m \theta \left(-\text{rot} \vec{H} + \frac{1}{c} \frac{\partial \vec{D}}{\partial t} \right) \right\}. \quad (55)$$

If the conductivity is infinite $v_m = 0$, then

$$\frac{\partial \vec{B}}{\partial t} - \text{rot} [\vec{a}\vec{s}] = 0. \quad (56)$$

If the medium moves with a velocity approaching c ($\theta \rightarrow 0$), then the term $\text{rot} \left\{ v_m \theta \left(-\text{rot} \vec{H} + \frac{1}{c} \frac{\partial \vec{D}}{\partial t} \right) \right\} = 0$, the free charges also tend to zero ($\delta = 0$), and Eq. (56) holds true, for when $a = c$ only a pure field can exist.

It is convenient to introduce the vector potential $\vec{\phi}'$ of the magnetic field

$$\text{rot} \vec{\phi}' = \vec{B}', \quad (57)$$

then $\vec{E}' = -(1/c)(\partial \vec{\varphi}' / \partial t)$, where it is necessary to put $\operatorname{div} \vec{\varphi}' = 0$; Eq. (54) can then be rewritten as

$$\frac{\partial \vec{\varphi}'}{\partial t} - [\vec{a} \operatorname{rot} \vec{\varphi}'] = i \frac{4\pi}{c} v_m a \delta + v_m \Theta \left[-\operatorname{rot} \vec{H}' + \frac{1}{c} \frac{\partial \vec{D}'}{\partial t} \right]. \quad (58)$$

Carrying out the transformations we arrive at the equation

$$\begin{aligned} \frac{\partial \vec{\varphi}'}{\partial t} - [\vec{a} \operatorname{rot} \vec{\varphi}'] &= i \frac{4\pi}{c} v_m a \delta + v_m \Theta \left\{ \frac{1}{\mu} \Delta \vec{\varphi}' - \frac{\epsilon}{c^2} \frac{\partial^2 \vec{\varphi}'}{\partial t^2} + \right. \\ &\quad \left. + \operatorname{rot} \vec{H}' + \frac{1}{c} \frac{\partial (\epsilon \vec{E}')}{\partial t} + \frac{\vec{E}'}{c} \frac{\partial t}{\partial t} - \left[\nabla \frac{1}{\mu} \operatorname{rot} \vec{\varphi}' \right] \right\}; \end{aligned} \quad (59)$$

here $\vec{H}^0 = \vec{H}^1$ or $\vec{H}^0 = \vec{H}^2$; $\vec{E}^0 = \vec{E}^1$ or $\vec{E}^0 = \vec{E}^2$ (see (34)).

Inasmuch as we have on the right side the quantity $\frac{1}{\mu} \Delta \vec{\varphi}' - \frac{\epsilon}{c^2} \frac{\partial^2 \vec{\varphi}'}{\partial t^2}$, we can conclude that a disturbance propagates in a dispersive ("viscous") medium with a velocity $c^* = c/\sqrt{\epsilon \mu}$.

If $\epsilon = 1$, $\mu = 1$, then, inasmuch as $\vec{E}^0 = 0$, $\vec{H}^0 = 0$, we arrive at the equation

$$\frac{\partial \vec{\varphi}'}{\partial t} - [\vec{a} \operatorname{rot} \vec{\varphi}'] = i \frac{4\pi}{c} v_m a \delta + v_m \Theta \left\{ \Delta \vec{\varphi}' - \frac{1}{c^2} \frac{\partial^2 \vec{\varphi}'}{\partial t^2} \right\}. \quad (60)$$

If $\delta = 0$, then Eq. (60) for specified \vec{a} determines $\vec{\varphi}'$. When $\epsilon = 1$, $\mu = 1$ Eq. (54) can be reduced to the form

$$\begin{aligned} \frac{\partial \vec{H}'}{\partial t} - \operatorname{rot} [\vec{a} \vec{H}'] &= \frac{4\pi}{c} \left(j \frac{\partial}{\partial z} v_m a \delta - k \frac{\partial}{\partial y} v_m a \delta \right) + v_m \Theta \left(\Delta \vec{H}' - \frac{1}{c^2} \frac{\partial^2 \vec{H}'}{\partial t^2} \right) + \\ &\quad + \left[\nabla (v_m \Theta) \cdot \left(-\operatorname{rot} \vec{H}' + \frac{1}{c} \frac{\partial \vec{E}'}{\partial t} \right) \right]. \end{aligned} \quad (61)$$

In the classical approximation, (54) becomes

$$\begin{aligned} \frac{\partial \vec{B}}{\partial t} - \operatorname{rot} [\vec{a} \vec{B}] &= \frac{v_m}{\mu} \left\{ \Delta \vec{B} - \frac{\epsilon_m}{c^2} \frac{\partial^2 \vec{B}}{\partial t^2} - \mu \left[\nabla \frac{1}{\mu} \operatorname{rot} \vec{B} \right] - \frac{1}{c^2} \frac{\partial z}{\partial t} \frac{\partial \vec{B}}{\partial t} + \right. \\ &\quad \left. + \frac{1}{c} \frac{\partial}{\partial t} [\nabla \epsilon \vec{E}] \right\} + \left\{ \frac{\nabla v_m}{\mu} \left[\operatorname{rot} \vec{B} - \frac{\mu}{c} \frac{\partial [\epsilon \vec{E}]}{\partial t} \right] + \mu \left[\nabla \frac{1}{\mu} \vec{B} \right] \right\}. \end{aligned} \quad (62)$$

If $\epsilon = \text{const}$, $\mu = \text{const}$, then (62) assumes the form

$$\frac{\partial \vec{B}}{\partial t} - \operatorname{rot} [\vec{a} \vec{B}] = \frac{v_m}{\mu} \left(\Delta \vec{B} - \frac{\epsilon_m}{c^2} \frac{\partial^2 \vec{B}}{\partial t^2} \right) +$$

$$+ \left[\frac{\nabla \cdot \vec{E}}{\mu} \left(\text{rot} \vec{B} - \frac{\epsilon_0}{c} \frac{\partial \vec{E}}{\partial t} \right) \right]. \quad (63)$$

It is very frequently possible (and customary) to neglect the displacement currents (the quantity $\frac{1}{c} \frac{\partial \vec{D}}{\partial t}$); then (62) greatly simplifies

$$\begin{aligned} \frac{\partial \vec{B}}{\partial t} - \text{rot} [\vec{a} \vec{B}] &= \frac{\nu_m}{\mu} \left\{ \Delta \vec{B} - \mu \left[\nabla \frac{1}{\mu} \text{rot} \vec{B} \right] \right\} + \\ &+ \left\{ \frac{\nabla \cdot \vec{E}}{\mu} \left(\text{rot} \vec{B} + \mu \left[\nabla \frac{1}{\mu} \vec{B} \right] \right) \right\}; \end{aligned} \quad (64)$$

when $\mu = \text{const}$ we get

$$\frac{\partial \vec{B}}{\partial t} - \text{rot} [\vec{a} \vec{B}] = \frac{\nu_m}{\mu} \Delta \vec{B} + \frac{\nabla \cdot \vec{E}}{\mu} \text{rot} \vec{B}. \quad (65)$$

Equation (59) assumes in the classical case the form

$$\begin{aligned} \frac{\partial \vec{r}}{\partial t} - [\vec{a} \text{rot} \vec{r}] &= \nu_m \left\{ \frac{1}{\mu} \Delta \vec{r} - \frac{e}{c^2} \frac{\partial^2 \vec{r}}{\partial t^2} - \right. \\ &\left. - \left[\Delta \frac{1}{\mu} \text{rot} \vec{r} \right] + \frac{E}{c} \frac{\partial r}{\partial t} \right\}. \end{aligned} \quad (66)$$

If we neglect the displacement currents, we obtain

$$\frac{\partial \vec{r}}{\partial t} - [\vec{a} \text{rot} \vec{r}] = \nu_m \left\{ \frac{1}{\mu} \Delta \vec{r} - \left[\nabla \frac{1}{\mu} \text{rot} \vec{r} \right] \right\}; \quad (67)$$

when $\mu = \text{const}$ we get

$$\frac{\partial \vec{r}}{\partial t} - [\vec{a} \text{rot} \vec{r}] = \frac{\nu_m}{\mu} \Delta \vec{r}. \quad (68)$$

This equation is very convenient for the solution of specific problems.

2. PLANE AND CYLINDRICAL WAVES

Equations (35) in a cylindrical coordinate frame, in the case when the velocity is directed along \underline{r} and is a function of $(r; t)$, assume, inasmuch as

$$\frac{d}{dt} = \frac{\partial}{\partial t} + a \frac{\partial}{\partial r} \quad (a_1 = a; a_2 = a_3 = 0) \quad x_1 = r,$$

the form

$$\begin{aligned} \frac{W}{Vc^2 + a^2} \cdot \frac{1}{a^2} \left(\frac{\partial a}{\partial t} + a \frac{\partial a}{\partial r} \right) + \frac{a}{Vc^2 + a^2} \left(\frac{\partial W}{\partial t} + a \frac{\partial W}{\partial r} \right) + \\ + \frac{\partial p}{\partial r} = -P_i = -P_r. \end{aligned}$$

$$\frac{1}{Vt^2} \left(\frac{\partial W}{\partial t} + a \frac{\partial W}{\partial r} \right) - \frac{\partial p}{\partial t} + \frac{Wa}{Vc^2} \frac{1}{\Theta^2} \left(\frac{\partial a}{\partial t} + a \frac{\partial a}{\partial r} \right) = -\frac{1}{t} f'_r = l''_r. \quad (69)$$

Equation (50) can be written in the form

$$-\left(\frac{\partial \ln V}{\partial t} + a \frac{\partial \ln V}{\partial r} \right) + \frac{1}{\Theta^2} \left(\frac{\partial a}{\partial r} + a \frac{\partial a}{\partial t} \right) + \frac{Na}{r} = 0, \quad (70)$$

where $N = 0$ for plane waves and $N = 1$ for cylindrical waves. Since

$$\operatorname{Div} \vec{u} = \frac{1}{ct^2} \left[\frac{1}{\Theta^2} \left(\frac{\partial a}{\partial r} + a \frac{\partial a}{\partial t} \right) + \frac{Na}{r} \right],$$

we have

$$\begin{aligned} -l'_r &= \frac{1}{4\pi} \left\{ [\operatorname{rot} \vec{H} \vec{B}]_r - \frac{1}{c} \left[\frac{\partial \vec{D}'}{\partial t} \cdot \vec{B}' \right]_r + E_r \operatorname{div} \vec{D}' \right\}_r + \\ &\quad + \frac{[\vec{E} \vec{H}]_r}{4\pi c \Theta^2} \frac{d(\epsilon\mu)}{dt} - \frac{1}{8\pi} \left\{ E^2 \frac{\partial \epsilon}{\partial r} + H^2 \frac{\partial \mu}{\partial r} \right\}_r + \\ &\quad + \frac{\epsilon\mu - 1}{4\pi c \Theta^2} \left\{ [\vec{E} \vec{H}]_r \left[\frac{2}{\Theta^2} \left(\frac{\partial a}{\partial r} + a \frac{\partial a}{\partial t} \right) + \frac{Na}{r} \right] + \frac{d[\vec{E} \vec{H}]_r}{dt} \right\}; \end{aligned} \quad (71)$$

$$\begin{aligned} -l'_{2,3} &= \frac{1}{4\pi} \left\{ [\operatorname{rot} \vec{H} \vec{B}]_{2,3} - \frac{1}{c} \left[\frac{\partial \vec{D}'}{\partial t} \cdot \vec{B}' \right]_{2,3} + E_{2,3} \operatorname{div} \vec{D}' \right\}_{2,3} + \\ &\quad + \frac{[\vec{E} \vec{H}]_{2,3}}{4\pi c \Theta^2} \frac{d(\epsilon\mu)}{dt} - \frac{1}{8\pi} \left\{ E^2 \frac{\partial \epsilon}{\partial x_{2,3}} + H^2 \frac{\partial \mu}{\partial x_{2,3}} \right\}_{2,3} + \\ &\quad + \frac{\epsilon\mu - 1}{4\pi c \Theta^2} \left\{ [\vec{E} \vec{H}]_{2,3} \left[\left(1 + \frac{a^2}{c^2} \right) \frac{\partial a}{\partial r} + \frac{2a}{c^2} \frac{\partial a}{\partial t} + \frac{Na}{r} \right] + \frac{d[\vec{E} \vec{H}]_{2,3}}{dt} \right\}; \end{aligned} \quad (72)$$

$$\begin{aligned} -l'_i &= \frac{i}{4\pi c} \left\{ c \vec{E}' \cdot \operatorname{rot} \vec{H}' - \frac{\partial \vec{D}'}{\partial t} \cdot \vec{E}' \right\}_i + \frac{ia}{4\pi c \Theta^2} [\vec{E} \vec{H}]_r \frac{d(\epsilon\mu)}{cdt} + \\ &\quad + \frac{i}{8\pi c} \left\{ E^2 \frac{\partial \epsilon}{\partial t} + H^2 \frac{\partial \mu}{\partial t} \right\}_i + \frac{(\epsilon\mu - 1)ai}{4\pi c \Theta^2} \times \\ &\quad \times \left\{ [\vec{E} \vec{H}]_r \left[\frac{2}{\Theta^2} \left(\frac{\partial a}{\partial r} + a \frac{\partial a}{\partial t} \right) + \frac{Na}{r} \right] + \frac{d[\vec{E} \vec{H}]_r}{dt} \right\}. \end{aligned} \quad (73)$$

Maxwell's equations and (54) simplify somewhat in this case. The simplest and most interesting case of motion is when $f_2 = f_3 = 0$; then $p = p(r, t)$.

Here, obviously, $[\vec{E} \vec{H}]_{2,3} = 0$, from which it follows that there can be two cases of motion: either $E = E_2 = E_\varphi$; $H = H_3 = H_z$ or $E = E_3 = E_z$; $H = H_2 = H_\varphi$, in a cylindrical coordinate system in the K frame.

We then have identically in Eqs. (72) $f'_{2,2} = f'_{3,3} = 0$ and $\delta = 0$.

In the first case we have in the K' frame

$$H = \left\{ 0; 0; \frac{1}{\Theta} \left(H_z + \frac{a}{c} D_z \right) \right\}; \quad E = \left\{ 0; \frac{1}{\Theta} \left(E_z + \frac{a}{c} B_z \right); 0 \right\}.$$

In the second case

$$H' = \left\{ 0; \frac{1}{\Theta} \left(H_{z'} - \frac{a}{c} D_{z'} \right); 0 \right\}; \quad E' = \left\{ 0; 0; \frac{1}{\Theta} \left(E_{z'} - \frac{a}{c} B_{z'} \right) \right\}$$

(and corresponding expressions for B' and D').

In the case of plane waves (one-dimensional motion) the problem reduces to the first investigated case. Then

$$N = 0; \quad E_r = E_z; \quad r = x.$$

We consider now the case of infinite conductivity ($\lambda \rightarrow \infty$). Then

$$E = 0; \quad E_r = 0; \quad E_{z,z} = \pm \frac{a}{c\Theta} B_{z,\varphi}; \quad D_r = 0;$$

$$D'_{0,z} = \pm \frac{a}{c\Theta} H_{z,\varphi}; \quad H'_{z,\varphi} = \frac{H_{z,\varphi}}{\Theta}; \quad B'_{z,\varphi} = \frac{B_{z,\varphi}}{\Theta};$$

$$- I'_r = \frac{1}{4\pi} \left\{ [\text{rot} \vec{H}' \vec{B}']_r - \frac{1}{c} \left[\frac{\partial \vec{D}'}{\partial t} \vec{B}' \right] \right\} - \frac{H^2}{8\pi} \frac{\partial \mu}{\partial r}; \quad (74)$$

$$- I'_{2,3} = \frac{1}{4\pi} \left\{ [\text{rot} \vec{H}' \vec{B}']_{2,3} - \frac{1}{c} \left[\frac{\partial \vec{D}'}{\partial t} \vec{B}' \right]_{2,3} + E'_{z,z} \text{div} \vec{D}' \right\} - \frac{H^2}{8\pi} \frac{\partial \mu}{\partial x_{2,3}}, \quad (75)$$

$$dx_2 = r d\varphi,$$

$$dx_3 = dz$$

$$- I'_4 = \frac{1}{4\pi} \left\{ c \vec{E}' \text{rot} \vec{H}' - \frac{\partial \vec{D}'}{\partial t} \vec{E}' \right\} + \frac{H^2}{8\pi} \frac{\partial \mu}{\partial t}. \quad (76)$$

The equation $\partial \vec{B}' / \partial t - \text{rot} [\vec{a} \vec{B}'] = 0$ for the magnetic field (54) assumes in cylindrical coordinates the form

$$\frac{\partial \vec{B}_z}{\partial t} + \frac{\partial (a \vec{B}_\varphi)}{\partial r} = 0; \quad \frac{\partial (r \vec{B}_r)}{\partial t} + \frac{\partial (ar \vec{B}_\varphi)}{\partial r} = 0, \quad (77)$$

$$\vec{B}_r = \vec{B}_\varphi = \vec{B}(r),$$

but it follows from the condition $\text{div} \vec{B} = 0$ that $B_r = \text{const.}$

If $H = H_z$ or $H = H_\varphi$, then we have $f_{2,3} = 0$ identically in (75).

Let us examine in greater detail the two cases, when $H = H_z$ and

when $H = H_\varphi$. The first case was already considered by us previously for $N = 0$ [4].

In the first case we have in the K' frame

$$H'_r = \frac{H_r}{\Theta} = \frac{H}{\Theta}; \quad E'_r = \frac{aB_r}{c\Theta} = \frac{aB}{c\Theta}; \quad B'_r = \frac{B_r}{\Theta} = \frac{B}{\Theta};$$

$$D'_\varphi = \frac{aH_r}{c\Theta} = \frac{aH}{c\Theta};$$

$$I'_r = \frac{1}{4\pi} \left\{ B \left[\frac{\partial}{\partial r} \left(\frac{H}{\Theta} \right) + \frac{\partial}{c\partial t} \left(\frac{aH}{c\Theta} \right) \right] + \frac{H^2}{2} \frac{\partial \mu}{\partial r} \right\},$$

$$I'_t = \frac{i}{4\pi c} \left\{ \frac{aB}{\Theta} \left[\frac{\partial}{\partial r} \left(\frac{H}{\Theta} \right) + \frac{\partial}{c\partial t} \left(\frac{aH}{c\Theta} \right) \right] - \frac{H^2}{2} \frac{\partial \mu}{\partial t} \right\}, \quad (78)$$

$$\frac{\partial}{\partial t} \left(\frac{r^N B}{\Theta} \right) + \frac{\partial}{\partial r} \left(\frac{ar^N B}{\Theta} \right) = 0.$$

In the second case we have in the K' frame

$$H'_r = \frac{H_r}{\Theta} = \frac{H}{\Theta}; \quad -E'_r = \frac{aB_r}{c\Theta} = \frac{aB}{c\Theta}; \quad B'_r = \frac{B_r}{\Theta} = \frac{B}{\Theta};$$

$$-D'_\varphi = \frac{aH_r}{c\Theta} = \frac{aH}{c\Theta};$$

$$I'_r = \frac{1}{4\pi} \left\{ B \left(\frac{1}{r} \frac{\partial}{\partial r} \frac{rH}{\Theta} + \frac{\partial}{c\partial t} \frac{aH}{c\Theta} \right) + \frac{H^2}{2} \frac{\partial \mu}{\partial r} \right\},$$

$$I'_t = \frac{i}{4\pi c} \left\{ \frac{aB}{\Theta} \left(\frac{1}{r} \frac{\partial}{\partial r} \frac{rH}{\Theta} + \frac{\partial}{c\partial t} \frac{aH}{c\Theta} \right) - \frac{H^2}{2} \frac{\partial \mu}{\partial t} \right\}, \quad (79)$$

$$\frac{\partial}{\partial t} \frac{B}{\Theta} + \frac{\partial}{\partial r} \frac{aB}{\Theta} = 0.$$

Both cases can be combined. Inasmuch as

$$H' = \frac{H}{\Theta}; \quad B' = \frac{B}{\Theta}; \quad E' = \frac{aB}{c\Theta}; \quad D' = \frac{aH}{c\Theta}. \quad (80)$$

we have the following equations:

$$\frac{d}{c\Theta dt} \frac{W a}{\Theta} + \frac{\partial W}{\partial r} + \frac{1}{4\pi} \left\{ B \left(r - \frac{\partial}{\partial r} \frac{r^N H}{\Theta} + \frac{\partial}{c\partial t} \frac{aH}{\Theta} \right) + \frac{H^2}{2} \frac{\partial \mu}{\partial r} \right\} = T \frac{\partial \sigma}{\partial r}; \quad (81)$$

$$\frac{d}{\Theta dt} \frac{W}{\Theta} - \frac{\partial W}{\partial t} + \frac{V}{4\pi} \left\{ B \left(r - \frac{\partial}{\partial r} \frac{r^N H}{\Theta} + \frac{\partial}{c\partial t} \frac{aH}{\Theta} \right) - \frac{H^2}{2} \frac{\partial \mu}{\partial t} \right\} = -T \frac{\partial \sigma}{\partial t}; \quad (82)$$

$$\frac{\partial}{\partial t} \frac{r^{N(1-\alpha)} B}{\Theta} + \frac{\partial}{\partial r} \frac{r^{N(1-\alpha)} aB}{\Theta} = 0; \quad (83)$$

$$T \left(\frac{\partial \sigma}{\partial t} + a \frac{\partial \sigma}{\partial r} \right) = \frac{H^2 V}{8\pi} \left(\frac{\partial n}{\partial t} + a \frac{\partial n}{\partial r} \right). \quad (84)$$

Equation (82) is the consequence of Eqs. (81, 83, and 24). Here, $m = 0$ when $N = 0$. When $N = 1$ we have $m = 0$ if $H = H_z$ and $m = 1$ if $H = H_\phi$.

The continuity equation (70) can be written in the form

$$\frac{\partial \frac{r^N}{V\Theta}}{\partial t} + \frac{\partial \frac{ar^N}{V\Theta}}{\partial r} = 0. \quad (85)$$

Comparing (83 and 85) we find

$$BV = b(\sigma)r^{Nm} = b(\sigma)r^m, \quad (86)$$

where $b(\sigma)$ is the entropy function.

If $H = H_z$ (when $N = 0$ and $N = 1$), then

$$BV = b(\sigma). \quad (87)$$

If $H = H_\phi$, then

$$BV = b(\sigma)r. \quad (88)$$

We now introduce the total heat content

$$W^* = W + \frac{BHV}{4\pi} = W + \frac{b^2 r^{2m}}{4\pi \mu V}; \quad (89)$$

then Eqs. (81, 82) can be written in the form

$$\frac{d \frac{W^* a}{\Theta}}{c^2 \Theta dt} + \frac{\partial W^*}{\partial r} = T \frac{\partial \sigma}{\partial r} - \frac{H^2 V}{8\pi} \frac{\partial n}{\partial r} + \frac{BHV}{4\pi \Theta^2} \left(\frac{\partial \ln b}{\partial r} + \frac{a}{c^2} \frac{\partial \ln b}{\partial t} \right); \quad (90)$$

$$\frac{d \frac{W^*}{\Theta}}{\Theta dt} - \frac{\partial W^*}{\partial t} = - T \frac{\partial \sigma}{\partial t} + \frac{H^2 V}{8\pi} \frac{\partial n}{\partial t} + \frac{BHV a}{4\pi \Theta^2} \left(\frac{\partial \ln b}{\partial r} + \frac{a}{c^2} \frac{\partial \ln b}{\partial t} \right); \quad (91)$$

Inasmuch as

$$\frac{d \frac{W^*}{\Theta}}{\Theta dt} - \frac{\partial W^*}{\partial t} = a \left(\frac{d \frac{W^* a}{\Theta}}{c^2 \Theta dt} + \frac{\partial W^*}{\partial r} \right), \quad (92)$$

we can readily verify, by taking (84) into consideration, that the equations (90 and 91) are actually equivalent.

Thus, the solution of the problem reduces to the solution of the equations

$$\begin{aligned} \frac{d \frac{W^*}{\Theta}}{dt} - \frac{\partial W^*}{\partial t} &= -T \frac{\partial \sigma}{\partial t} + \frac{H^2 V}{S \pi} + \frac{B H V a}{4 \pi \Theta^2} \left(\frac{\partial \ln b}{\partial r} + \frac{a \partial \ln b}{c^2 \partial t} \right); \\ \frac{\partial \frac{r^N}{V \Theta}}{\partial t} + \frac{\partial \frac{a r^N}{V \Theta}}{\partial r} &= 0; \quad S V = b(\sigma) r^m; \\ \frac{T \frac{\partial \sigma}{\partial t}}{V \frac{\partial r}{\partial t}} &= \frac{H^2 \frac{\partial \ln b}{\partial t}}{8 \pi}. \end{aligned} \quad (93)$$

It is necessary to bear in mind here the equations of state of the medium $p = p(V; T)$ and the identity

$$\frac{\partial(p; V)}{\partial(T; s)} = 1. \quad (94)$$

If $\mu = \text{const}$ and $\sigma = \text{const}$, then the problem reduces to the solution of the equations

$$\frac{d \frac{W^*}{\Theta}}{dt} - \frac{\partial W^*}{\partial t} = 0; \quad \frac{\partial \frac{r^N}{V \Theta}}{\partial t} + \frac{\partial \frac{a r^N}{V \Theta}}{\partial r} = 0. \quad (95)$$

We must specify here the isentropic equation

$$W = W(V), \quad (96)$$

and then

$$W^* = W(V) + \frac{b \sigma^{2m}}{4 \pi \mu V}. \quad (97)$$

It is now convenient to rewrite the system (95) in the form

$$\frac{1}{\Theta^2} \left(\frac{\partial a}{\partial t} + a \frac{\partial a}{\partial r} \right) + c^2 \left(\frac{\partial \ln W^*}{\partial r} + \frac{a}{c^2} \frac{\partial \ln W^*}{\partial t} \right) = 0, \quad (98)$$

$$-\left(\frac{\partial \ln V}{\partial t} + a \frac{\partial \ln V}{\partial r} \right) + \frac{1}{\Theta} \left(\frac{\partial a}{\partial r} + \frac{a}{c^2} \frac{\partial a}{\partial t} \right) + \frac{N \sigma}{r} = 0. \quad (99)$$

It is convenient also to introduce the generalized velocity of sound in the medium [5]

$$\frac{v^*}{c^2} = -\frac{\frac{\partial \ln W^*}{\partial r}}{\frac{\partial \ln V}{\partial r}},$$

and then (98) assumes the form

$$\frac{1}{\Theta^2} \left(\frac{\partial a}{\partial t} + a \frac{\partial a}{\partial r} \right) - v^* \left(\frac{\partial \ln V}{\partial r} + \frac{a}{c^2} \frac{\partial \ln V}{\partial t} \right) = 0. \quad (100)$$

If

$$W = \frac{k}{k-1} A V^{k-2} + \frac{1}{2} V^2; \quad (p = A V^{-k})$$

with $\bar{\alpha} = 0$ for an ultrarelativistic gas and $\bar{\alpha} = 1$ for a relativistic gas, then

$$\begin{aligned}\frac{\omega^*}{c^2} &= \frac{kAV^{1-\bar{\alpha}} + \frac{b^2r^m}{4\pi\mu V} - \frac{2mb^2r^m}{4\pi\mu} \frac{d\ln r}{dV}}{k - \frac{1}{1-\bar{\alpha}} AV^{1-\bar{\alpha}} + \frac{b^2c^2}{4\pi\mu V}} = \\ &= \frac{kAV^{1-\bar{\alpha}} + \frac{BHV}{4\pi} \left(1 - 2m \frac{d\ln r}{d\ln V}\right)}{W^*}. \quad (101)\end{aligned}$$

Inasmuch as

$$dW^* = Vdp^* = Vdp + Vdp_M,$$

the supplementary magnetic pressure p_M can be determined from the relation

$$dp_M = \frac{1}{4\pi V} d(BHV).$$

Equations (99, 100) are very convenient for the solution of specific problems.

3. CLASSICAL TRANSITION

It is easy to obtain the classical approximation equation by starting from the relativistic equations.

The equations of motion and energy (disregarding viscosity and heat conduction) (see Eqs. (47 and 48)) assume the form

$$\begin{aligned}\frac{d(W\alpha_z)}{Vc dt} + \frac{\partial p}{\partial x_z} &= \frac{1}{4\pi} \left\{ [\text{rot } \vec{H} \vec{B}]_z - \frac{1}{c} \left[\frac{\partial \vec{D}}{\partial t} \cdot \vec{B} \right]_z + E_z \text{div } \vec{D} \right\} - \\ &- \frac{1}{8\pi} \left\{ E^2 \frac{\partial \epsilon}{\partial x_z} + H^2 \frac{\partial u}{\partial x_z} \right\}; \quad (102)\end{aligned}$$

$$\begin{aligned}\frac{dW}{Vdt} + \frac{W\alpha_z d\alpha}{Vc dt} - \frac{\partial p}{\partial t} &= \frac{c}{4\pi} \left\{ \vec{E} \text{rot } \vec{H} - \vec{E} \frac{\partial \vec{D}}{\partial t} \right\} + \\ &+ \frac{1}{8\pi} \left\{ E^2 \frac{\partial \epsilon}{\partial t} + H^2 \frac{\partial u}{\partial t} \right\}. \quad (103)\end{aligned}$$

Since $W = 1 + c^2$, where $\underline{1}$ is the classical heat content, these equations can be written, neglecting the displacement current, in the form (inasmuch as $V = 1/\rho$)

$$\frac{\partial \alpha_z}{\partial t} + \frac{\partial p}{\rho \partial x_z} = \frac{1}{4\pi} \left\{ [\text{rot } \vec{H} \vec{B}]_z + E_z \text{div } \vec{D} \right\} -$$

$$-\frac{1}{8\pi\rho} \left\{ E^2 \frac{\partial \epsilon}{\partial x_3} + H^2 \frac{\partial \mu}{\partial x_3} \right\}; \quad (104)$$

$$\frac{dt}{dt} + \frac{da}{dt} - \frac{1}{\rho} \frac{dp}{dt} = \frac{c \vec{E} \cdot \vec{\text{rot}} \vec{H}}{4\pi\rho} + \frac{1}{8\pi\rho} \left\{ E^2 \frac{\partial \epsilon}{\partial t} + H^2 \frac{\partial \mu}{\partial t} \right\}. \quad (105)$$

The continuity equation — see (49) — can be immediately written down in the form

$$\frac{d \ln \rho}{dt} + \text{div} \vec{a} = 0. \quad (106)$$

Introducing $\text{rot} \vec{\varphi} = \vec{B}$; $\frac{1}{c} \frac{d \vec{\varphi}}{dt} = -\vec{E}$, we can arrive at an equation that defines $\vec{\varphi}$ in the form (see Eq. (59))

$$\frac{\partial \vec{\varphi}}{\partial t} - [\vec{a} \cdot \text{rot} \vec{\varphi}] = v_m \left\{ \frac{1}{\mu} \Delta \vec{\varphi} - \frac{\epsilon}{c^2} \frac{\partial^2 \vec{\varphi}}{\partial t^2} + \frac{E}{c} \frac{\partial \vec{\varphi}}{\partial t} - \left[\nabla \frac{1}{\mu} \cdot \text{rot} \vec{\varphi} \right] \right\}. \quad (107)$$

Here, however, the last two terms are insignificant

$$\left(v_m = \frac{c^2}{4\pi\lambda} \right).$$

The equation for the Joule losses assumes the form (see Eq. (43))

$$\frac{dQ}{dt} = \frac{I^2}{\rho\lambda} \left(1 + \frac{1}{8\pi\rho} \frac{d\epsilon}{dt} \right) + \frac{H^2}{8\pi\rho} \frac{dp}{dt}. \quad (108)$$

The energy equation (105) is the consequence of the equations (104, 106, and 108).

In the case of infinite conductivity ($\lambda \rightarrow \infty$) we have

$$\frac{dQ}{dt} = \frac{H^2}{8\pi\rho} \frac{dp}{dt}. \quad (109)$$

Thus, Joule losses arise in the case of variable magnetic permeability.

4. ALLOWANCE FOR THE DEPENDENCE OF ϵ AND μ ON THE SPECIFIC VOLUME AND ON OTHER THERMODYNAMIC PARAMETERS

For several media (for example dielectrics and semiconductors), the parameters ϵ and μ depend in explicit form on the specific volume of the element of the medium under consideration and on other thermodynamic parameters [6].

Let us calculate this dependence in general relativistic form.

For this purpose we must add to the energy and momentum tensor T_{ik}

the corresponding symmetrical tensor M_{ik} , which should in the classical limit yield the ordinary expression

$$T'_{\alpha\beta} = T_{\alpha\beta} + M_{\alpha\beta} = \frac{1}{4\pi} \left\{ - (D_\alpha E_\beta + B_\alpha H_\beta) + \right. \\ \left. + \frac{\delta_{\alpha\beta}}{2} \left[\vec{DE} \left(1 + V_i \frac{\partial D}{\partial V_i} \right) + \vec{BH} \left(1 + V_i \frac{\partial B}{\partial V_i} \right) \right] \right\}$$

or

$$T'_{\alpha\beta} = \frac{1}{4\pi} \left\{ - (\epsilon E_\alpha E_\beta + \mu H_\alpha H_\beta) + \frac{\delta_{\alpha\beta}}{2} \left[E^i \left(\epsilon + V_i \frac{\partial \epsilon}{\partial V_i} \right) + \right. \right. \\ \left. \left. + H^i \left(\mu + V_i \frac{\partial \mu}{\partial V_i} \right) \right] \right\} \quad (110)$$

(where the derivatives are taken at constant E and H);

$$M_{\alpha\alpha} = 0; \quad T_{\alpha\alpha} = \frac{i}{c} [\vec{EH}]_{\alpha}; \quad T_{44} = - \frac{\vec{DE} + \vec{BH}}{8\pi} = \\ = - \frac{\epsilon E^4 + \mu H^4}{8\pi}. \quad (111)$$

Here V_τ are various independent thermodynamic parameters. In particular, when $\tau = 1$ we have $V_1 = V$, where V is a specific volume.

It is easy to verify that in the case when ϵ and μ depend explicitly on these parameters, the tensor M_{ik} should have in the K' frame the form

$$M'_{ik} = \frac{1}{4\pi} (\varepsilon_{ik} + u_i u_k) V_i \frac{\partial}{\partial V_i} \left\{ \frac{1}{4} F_{lm} H_{lm} + u_i u_l F_{lm} H_{lm} \right\}. \quad (112)$$

In the frame in which the given element is at rest we have $u_\alpha = 0$, $u_4 = 1$; therefore

$$\begin{aligned} u_i u_l F_{lm} H_{lm} &= - F_{ll} H_{ll} = \epsilon E^2, \\ \frac{1}{4} F_{lm} H_{lm} &= \frac{1}{2} (\mu H^2 - \epsilon E^2). \end{aligned} \quad (113)$$

Furthermore

$$\frac{1}{4} F_{lm} H_{lm} + u_i u_l F_{lm} H_{lm} = \frac{1}{2} (\mu H^2 + \epsilon E^2).$$

$$M_{23} = \frac{1}{8\pi} \tilde{\epsilon}_{23} \left(E^2 V_z \frac{\partial D}{\partial V_z} + H^2 V_z \frac{\partial B}{\partial V_z} \right); \\ M_{43} = 0. \quad (114)$$

It follows therefore that

$$M_{23} = \frac{1}{8\pi} (\tilde{\epsilon}_{23} + u_i u_k) \left(E^2 V_z \frac{\partial \epsilon}{\partial V_z} + H^2 V_z \frac{\partial p}{\partial V_z} \right); \quad (115) \\ \frac{\partial M_{23}}{\partial x_k} = \frac{\partial M_{23}}{\partial x_3} + \frac{\partial M_{23}}{\partial x_k} = \frac{\partial M_{23}}{\partial x_3}, \text{ since } M_{43} = 0.$$

Further

$$\frac{\partial M_{23}}{\partial x_3} = \frac{\partial M_{23}}{\partial x_3} + \frac{\partial M_{23}}{\partial x_4} = \frac{\partial M_{23}}{\partial x_3}. \quad (116)$$

since

$$M_{43} = 0.$$

Therefore

$$\frac{\partial M_{23}}{\partial x_k} = \frac{\partial M_{23}}{\partial x_3} = \frac{1}{8\pi} \frac{\partial}{\partial x_k} \left[E^2 V_z \frac{\partial \epsilon}{\partial V_z} + H^2 V_z \frac{\partial p}{\partial V_z} \right]. \quad (117)$$

In the K' frame we have analogously

$$\frac{\partial M'_{23}}{\partial x_k} = \frac{1}{4\pi} \frac{\partial}{\partial x_k} \left[\frac{1}{4} F'_{lm} H'_{lm} + u_n u_r F'_{ln} H'_{lr} \right] = \frac{\partial M'}{\partial x_k}, \quad (118)$$

where

$$M' = \frac{V'_z}{4\pi} \frac{\partial}{\partial V'_z} \left[\frac{1}{4} F'_{lm} H'_{lm} + u_n u_r F'_{ln} H'_{lr} \right].$$

Since the expression $F'_{lm} H'_{lm}/4 + u_n u_r F'_{ln} H'_{lr}$ is a scalar quantity, we have in any reference frame

$$\frac{1}{4} F'_{lm} H'_{lm} + u_n u_r F'_{ln} H'_{lr} = \frac{1}{2} (DE + BH) = \frac{1}{2} (eE + pH);$$

and therefore

$$M' = \frac{V'_z}{8\pi} \left\{ E^2 \frac{\partial \epsilon}{\partial V'_z} + H^2 \frac{\partial p}{\partial V'_z} \right\}. \quad (119)$$

Here V'_z are parameters in the K' frame, for example

$$V'_1 = V' = \theta V.$$

Thus, the quantity $\partial M'/\partial x_a$ is added to the force f'_a , so that the total force is

$$\begin{aligned}
-\vec{f}'_4 &= \frac{1}{c} [\vec{J}' \vec{B}']_z + \vec{v}' E'_z - \frac{1}{8\pi} \left\{ E^2 \frac{\partial \epsilon}{\partial x_3} + H^2 \frac{\partial \mu}{\partial x_3} \right\} + \\
&+ \frac{[\vec{E}\vec{H}]_z}{4\pi H^3} \frac{d(\epsilon\mu)}{ds} + \frac{\epsilon\mu - 1}{4\pi} \left\{ \frac{[\vec{E}\vec{H}]_z}{c t^2} \frac{\partial \alpha}{\partial x_3} + \frac{d[\vec{E}\vec{H}]_z}{ds} + \frac{[\vec{E}\vec{H}]_z}{H^3} \operatorname{Div} \vec{u} \right\} - \\
&- \frac{1}{8\pi} \frac{\partial}{\partial x_3} \left\{ E^2 V'_z \frac{\partial \epsilon}{\partial V'_z} + H^2 V'_z \frac{\partial \mu}{\partial V'_z} \right\} \quad (120)
\end{aligned}$$

The force \vec{f}'_4 remains unchanged.

In these expressions ϵ and μ are functions of the parameters V'_z , and therefore

$$d\epsilon = \frac{\partial \epsilon}{\partial V'_z} dV'_z; \quad d\mu = \frac{\partial \mu}{\partial V'_z} dV'_z.$$

The expression for the Joule heat remains the same as before.

REFERENCES

1. P. G. Bergman. Vvedeniye v teoriyu otnositel'nosti [Introduction to Relativity Theory] (Chapter VIII), Izd-vo inostr. lit. [Foreign Literature Press], 1947.
2. M. Abraham. Theorie der Elektrizitat [Theory of Electricity], (§§38, 39), third edition, Berlin, 1914.
3. V. Pauli. Teoriya otnositel'nosti [Relativity Theory], §35, Gostekhizdat [State United Publishing House for Technical and Theoretical Literature], 1947.
4. F. A. Baum, S. A. Kaplan and K. P. Stanyukovich. Vvedeniye v kosmicheskuyu gazodinamiku [Introduction to Cosmic Gas Dynamics] (Chapter II, Part III), Fizmatgiz [State Publishing House for Literature in Physics and Mathematics], 1958.
5. K. P. Stanyukovich, ZhETF [Journal of Experimental and Theoretical Physics], 36, 3, 1782, 1959.
6. L. D. Landau and Ye. M. Lifshits. Elektrodinamika sploshnykh sred [Electrodynamics of Continuous Media] (§10, 30). Gostekhizdat, 1957.

SOME PROBLEMS IN ANISOTROPIC MAGNETIC GAS DYNAMICS

S.A. Kaplan, A.A. Logvinenko, V.V. Porfir'yev
(L'vov)

In applying the methods of phenomenological magnetic gas dynamics to an investigation of a low-density plasma it is necessary, as was shown in [1], to take into account the anisotropy of the pressures. To be sure, ideas have been advanced recently that the time of equalization of the longitudinal and transverse pressures may be relatively short, owing to the internal instability of the plasma. In some problems, however, particularly in the investigation of rapid motions, the anisotropy of the pressures may lead to the appearance of singularities in the motions.

In magnetic gas dynamics with anisotropic pressure, one can also use the phenomenological equations of magnetic gas dynamics, in which the scalar gas pressure should be replaced by the tensor

$$P_{ik} = p_1 \delta_{ik} + \frac{p_1 - p_{\perp}}{H^2} H_i H_k. \quad (1)$$

Here p_1 and p_{\perp} are the longitudinal and transverse pressures, while H_i and H_k are the components of the magnetic field. In addition, it is necessary to include in place of the scalar heat function the "heat function tensor" W_{ik} , which is analogous to (1) and has as the corresponding components W_1 and W_{\perp} , which are the longitudinal and transverse heat functions, respectively. A similar tensor is used also to express the tensor of the square of the sound velocity

$$c_s^2 = c_1^2 \delta_{ik} + (c_1^2 - c_{\perp}^2) H_i H_j H^2.$$

To save space, we shall not write out the entire system of equations of anisotropic magnetic gas dynamics. By way of example we present only the expression for the energy flux (neglecting dissipative processes)

$$q = \gamma v \left(\frac{v^2}{2} + W_1 + \frac{H^2}{4\pi\rho} \right) - \frac{H(vH)}{4\pi} \left(1 - \frac{W_1 - W_1}{H^2/4\pi\rho} \right). \quad (2)$$

Here v is the velocity of the gas and ρ its density.

We consider here two examples of motion in anisotropic magnetic gas dynamics: discontinuities and flow around slender bodies.

In the investigation of discontinuities one sets up the usual conditions for the conservation of the flux on both sides of the discontinuity. In particular, the condition for the conservation of the energy flux q has the form

$$\{q\} = \left\{ \left(\frac{H}{\rho} \right)^2 \right\} + \frac{2H}{j^2} \{W_1\} = 0. \quad (3)$$

The braces stand here for the difference in the quantity on the two sides of the discontinuity, $j = \rho v_n = \text{const}$ is the mass flux, and $H_n = \text{const}$ is the magnetic field component normal to the discontinuity.

Equation (3) has been written out in a coordinate system in which the discontinuity is at rest, and the magnetic field is parallel to the velocity both ahead of the discontinuity front and behind it.

One might think that the width of the discontinuity (which is probably on the order of the Larmor radius) is shorter than the relaxation length of the longitudinal and transverse pressures. In such a case one can assume

$$\{W_1\} = \{j\} = 0.$$

It then follows from (3) that

$$\frac{H}{\rho} = \text{const} \quad (4)$$

in full agreement with the condition of Chew, Low, and Goldberger [1]

$$\frac{d}{dr} \left(\frac{p_1 H^2}{r^2} \right) = 0.$$

Using now the conditions for the conservation of momentum flux on going through the discontinuity, and introducing the notation

$$\frac{H_2}{H_1} = \frac{p_2}{p_1} = \frac{\cos \theta_1}{\cos \theta_2}, \quad (5)$$

where the subscript "1" denotes the values of the quantities prior to the passage of the wave front and "2" denotes the quantities behind the front, ϑ is the angle between the direction of the velocity (magnetic field) and the normal to the discontinuity front, we obtain after simple but cumbersome calculations an equation for the determination of the jump in the perpendicular pressures, the analog of the Hugoniot adiabat are

$$p_{\perp,2} - p_{\perp,1} = (p_{\perp,1} - p_{\perp,1}) \frac{\sin \theta_1}{\sin \theta_2} + \frac{H_1^2 \sin(\theta_2 - \theta_1) (\cos \theta_2 - \cos \theta_1)}{8\pi \sin \theta_2 \cos^2 \theta_2}. \quad (6)$$

In particular, if the pressure was isotropic ahead of the discontinuity, we get

$$p_{\perp,2} = p_{\perp,1} + \frac{H_1^2 \sin(\theta_2 - \theta_1) (\cos \theta_2 - \cos \theta_1)}{8\pi \sin \theta_2 \cos^2 \theta_2}. \quad (7)$$

It follows therefore that a decrease in the magnetic field and in the gas density in the discontinuity is accompanied by an increase in the transverse pressure, and vice versa. In this sense, anisotropic discontinuities are directly the opposite of shock waves in their properties. Anisotropic jumps are limited in magnitude. In particular, in jumps with an increase in the magnetic field one should have $H_2 \leq \sqrt{\delta n p_{\perp,1}}$, while in jumps with a decrease in the magnetic field one should have $H_2 < H_1 \cos \vartheta_1$. A similar investigation of the properties of anisotropic discontinuities was made by one of us (Logvinenko) in a different paper.

To investigate the flow around slender bodies in gas dynamics, an equation is set up for small deviations from the main flow. In anisotropic magnetic gas dynamics this equation has the form

$$(c_1^2 + u^2) \Delta \vec{v}' - \left[1 - \frac{c_a^2 - c_1^2}{u^2} \right] \vec{u} (\vec{u} \nabla) \operatorname{div} \vec{v}' + \\ + [(\vec{u} \nabla)^2 - (\vec{v} \nabla)^2] \vec{v}' - (\vec{u} \nabla) \operatorname{grad} (\vec{u} \vec{v}') = 0. \quad (8)$$

Here \vec{v}' is the perturbation in the velocity, \vec{v} is the velocity of the main stream (velocity of the body in the stream), and $\vec{u} = \vec{H} \sqrt{4\pi\rho}$, where \vec{H} is the intensity of the magnetic field. We note that the directions of \vec{H} and \vec{v} may not coincide. Equation (8) has been derived from the fundamental system of equations of anisotropic magnetic gas dynamics for the stationary state by excluding small quantities (perturbations in the main stream), except for the velocity, as is customarily done in gas dynamics, and ∇ is the nabla operator. Introducing the notation $c_a^2 = c_1^2 + u^2$ and transforming the last term in (8), we reduce this equation to the form

$$c_a^2 \Delta \vec{v}' - \frac{c_a^2 - c_1^2}{u^2} \vec{u} (\vec{u} \nabla) \operatorname{div} \vec{v}' - (\vec{v} \nabla) \vec{v}' - [\vec{u} \operatorname{rot} ((\vec{u} \nabla) \vec{v}')]. \quad (9)$$

A solution of this equation under the suitable boundary conditions for \vec{v}' does indeed determine the variation of this quantity in space.

The complicated equation (9) can be simplified by replacing it with a system of two equations. Taking the scalar product of (9) and \vec{u} , and taking the divergence of (9) (i.e., the scalar product of (9) and the ∇ operator), we obtain

$$[c_a^2 \Delta - (\vec{v} \nabla)^2] (\vec{u} \vec{v}') = (c_a^2 - c_1^2) \operatorname{div} ((\vec{u} \nabla) \vec{v}'), \\ \left(c_a^2 \Delta - (\vec{v} \nabla)^2 - \frac{c_a^2 - c_1^2}{u^2} (\vec{u} \nabla)^2 \right) \operatorname{div} \vec{v}' = \\ = \operatorname{div} [\vec{u} \operatorname{rot} ((\vec{u} \nabla) \vec{v}')]. \quad (10)$$

However, these equations in this form are too complicated to solve (they were solved by M. I. Kogan [2] under a set of simplifying assumptions).

tions in isotropic magnetic gas dynamics). In anisotropic magnetic gas dynamics they can be simplified either by assuming the flow to be potential, $\text{rot } \vec{v}' = 0$, or by introducing the somewhat artificial condition $c_a \approx c$, which is equivalent to assuming that the magnetic and longitudinal pressures are approximately equal. We have seen above that this condition does indeed hold true behind the front of the discontinuity.

For potential flow ($\text{rot } \vec{v}' = 0$) Eqs. (10) are rewritten in the form

$$\begin{aligned} (c_1^2 - (\vec{v} \cdot \nabla)^2) \vec{u} \cdot \vec{v}' &= 0, \\ (c_a^2 - (\vec{v} \cdot \nabla)^2 - (\vec{u} \cdot \nabla)^2) \text{div } \vec{v}' &= 0. \end{aligned} \quad (11)$$

Here $\vec{u}_e = \vec{u} / \sqrt{1 - \frac{c_1^2 - c_a^2}{u^2}}$. Thus, $\text{div } \vec{v}'$ and $(\vec{u}_e \cdot \vec{v}')$ can be determined separately. The solution of the first of these equations is obvious, while the second equation can also be reduced to the usual form of wave equation by changing over to an oblique system of coordinates. The complexity of the problem lies not in the equations, but in the need for specifying asymmetrical boundary conditions.

In the second case ($c_a^2 \approx c^2$), Eqs. (10) assume the form

$$\begin{aligned} (c_1^2 - (\vec{v} \cdot \nabla)^2) \vec{u} \cdot \vec{v}' &= 0, \\ (c_1^2 - (\vec{v} \cdot \nabla)^2 - (\vec{u} \cdot \nabla)^2) \text{div } \vec{v}' &= (\vec{u} \cdot \nabla) \cdot (\vec{u} \cdot \vec{v}'). \end{aligned} \quad (12)$$

We first solve independently the first equation, and then solve the inhomogeneous wave equation with known right half. In the present case the main difficulty also lies in formulating the boundary conditions.

Thus, an account of anisotropy in the investigation of flow around slender bodies in a gas magnetic stream does not lead to noticeable complications and to as complicated calculations. The qualitative results will apparently remain unchanged, but quantitative changes arising on the account of the anisotropy are quite possible.

REFERENCES

1. G. Chew, M. Goldberger, F. Low. Proc. Roy. soc., 236, 112, 1956.
2. M.I. Kogan. Prikl. matem. i mekh. [Appl. Math. and Mech.], 23, 70, 1959.

DISCUSSION FOLLOWING THE PAPER

R.V. Polovin

Khar'kov

The paper considers shock waves in an anisotropic plasma. The authors are not interested here in the structure of the shock wave and confine themselves to the consequences of the conservation laws. In the case of anisotropic pressure the number of conservation laws is one less than the number of magnetohydrodynamic variables. The question therefore arises of how to write out the lacking boundary condition. The authors propose to choose as this condition the continuity of the longitudinal pressure. We have also considered this question, jointly with N.L. Tsintsadze, and have arrived at different conclusions.

In the absence of collisions, it seems natural to assume as the lacking boundary condition the conservation of entropy. If the expression for the entropy per particle is written in the form $s = (k/2) \ln (p_{||} p_1^2 / \rho^5)$, then for stationary shock wave of low intensity we shall have the relation

$$v_{1x} = u_{1+} + \frac{v_{1x}^2 (5p_{||}^{(1)} + 3p_{\perp}^{(1)})}{2(p_{||}^{(1)} - p_{\perp}^{(1)})(v_{1x} + u_{1+})} \cdot \frac{\delta\rho}{\rho_1}. \quad (1)$$

where v_{1x} is the velocity of the shock wave relative to the medium located in front of it, u_{1+} is the velocity of the fast magnetohydrodynamic wave, $p_{||}^{(1)}$, $p_{\perp}^{(1)}$, and ρ_1 are the longitudinal pressure, transverse pressure, and the density of the medium ahead of the shock wave, $\delta\rho = \rho_2 - \rho_1$ is the density discontinuity on the shock waves; the longitudinal magnetic field H_n is set equal to zero. If $p_{||}^{(1)} < p_{\perp}^{(1)}$, then

the evolutionality condition $v_{1x} > u_{1+}$ contradicts Zemplen's theorem ($\delta\rho > 0$). Therefore, if stationary shock waves exist in the absence of collisions, the entropy in them increases.

If we assume that the magnetic moment per unit mass $p_1/\rho H$ is conserved in the shock wave, we obtain for a low intensity wave

$$v_{1x} = u_{1+} + \frac{3}{2} \cdot \frac{v_{1x}^2}{v_{1x} + u_{1+}} \cdot \frac{\delta\rho}{\rho_1}, \quad v_{2x} = u_{2+} - \frac{3}{2} \cdot \frac{v_{2x}^2}{v_{2x} + u_{2+}} \cdot \frac{\delta\rho}{\rho_2} \quad (2)$$

(the subscript "2" pertains to the region behind the discontinuity).

According to Eqs. (2), Zemplen's theorem leads to the evolutionality conditions $v_{1x} > u_{1+}$, $v_{2x} < u_{2+}$. Thus, no contradiction is obtained in this case. Another fact in evidence of the conservation of the magnetic moment is that the magnetic moment is an adiabatic invariant, and therefore it is conserved, with exponential degree of accuracy, in slowly varying fields.

CONTRIBUTION TO THE THEORY OF STATIONARY FLOWS
IN MAGNETIC GAS DYNAMICS

M.F. Shirokov

Moscow

In view of the absence of induced electric field in stationary flows [$\text{rot } \vec{E} = 0$] and the need for including in the initial system of equations the electrostatic equation, certain new solutions have been obtained for the magnetohydrodynamic equations for stationary plane parallel flows and plane shock waves.

GENERAL REMARKS

A feature of stationary flows in magnetic gas dynamics is the absence of an induced electric field, since in such flows $\text{rot } \vec{E} = 0$. For this reason, the field in such flows is determined by the distribution of the space charges δ outside and inside the gas, using some solution of the equation

$$\text{div } \vec{E} = 4\pi\delta \quad (1)$$

or electromotive forces that are applied from the outside. Yet in solving the magnetohydrodynamic problem this equation is usually discarded and the system of initial equations is reduced to relations that contain only the pressure p , the density ρ , and the velocity and magnetic field intensity vectors \vec{u} and \vec{H} . This leads, for example in the case of an incompressible conducting liquid, to the following system of equations [1]

$$\begin{aligned} \text{div } \vec{H} &= 0, \quad \text{div } \vec{u} = 0, \\ \frac{\partial \vec{H}}{\partial t} + (\vec{u} \nabla) \vec{H} &= (\vec{H} \nabla) \vec{u} + \frac{e^2}{4\pi\rho} \Delta \vec{H}, \end{aligned} \quad (2)$$

$$\frac{\partial \vec{u}}{\partial t} + (\vec{u} \nabla) \vec{u} = -\frac{1}{\rho} \nabla \left(p + \frac{H^2}{8\pi} \right) + \frac{1}{4\pi\eta} (\vec{H} \nabla) \vec{H} + \vec{u} \cdot \nabla \vec{u}$$

with corresponding boundary conditions for the vectors \vec{u} and \vec{H} . The solution of the problems formulated in this manner leads, generally speaking, to a random choice of one of the solutions of Eq. (1) and to neglect of its other solutions, which may be of appreciable interest.

We give here some of these neglected solutions, which pertain to plane parallel flows and shock waves.

1. PLANE PARALLEL FLOW

Let the conducting incompressible liquid move in stationary manner between two plane parallel walls perpendicular to the x_3 axis in an external magnetic field $H_0 = H_3^0$, $H_1^0 = H_2^0 = 0$ perpendicular to the walls, in the presence of a pressure gradient $P = dp/dx_1 = \text{const}$ throughout the flow region. The system (2) then assumes the form

$$H_0 \frac{du_1}{dx_3} + \frac{c^2}{4\pi\sigma} \frac{d^2H_1}{dx_3^2} = 0, \quad (3)$$

$$\eta \cdot \frac{d^2u_1}{dx_3^2} + \frac{H_0}{4\pi} \frac{dH_1}{dx_1} = P = \text{const.}$$

Its solution subject to the following boundary conditions on the walls

$$x_3 = \pm L \quad \begin{cases} H_1(+L) = -H_1(-L) = \text{const.} \\ u_1 = 0 \end{cases} \quad (4)$$

$$(5)$$

has the form

$$u_1 = A \left(1 - \frac{\operatorname{ch} \frac{Mx_3}{L}}{\operatorname{ch} M} \right), \quad (6)$$

$$H_1 = \frac{4\pi P}{H_0} x_3 + \frac{4\pi L H_0 \sigma}{c^2 M \operatorname{ch} M} A \operatorname{sh} \frac{Mx_3}{L}, \quad (7)$$

where

$$M = \frac{L H_0}{c} \sqrt{\frac{\sigma}{\eta}} \quad (8)$$

is the Hartmann number and A is an arbitrary constant determined by the boundary conditions (4) for the magnetic field H_1 at the channel

walls. From Ohm's law and from one of Maxwell's equations we have

$$\frac{dH_1}{dx_3} = \frac{4\pi j}{\epsilon} \left(E - \frac{u_1 H_0}{\epsilon} \right). \quad (9)$$

Substituting into this equation the values of u_1 and H_1 from (6) and (7) we get

$$A = \frac{\epsilon E}{H_0} - \frac{P t^2}{\epsilon H_0^2}. \quad (10)$$

From this relation we see that the choice of some particular set of boundary conditions for H_1 , conditions which determine A in (7), is equivalent to the choice of some value of the external electric field E , produced either by the surface charges on the channel walls, which are perpendicular to the x_2 axis, or by a potential difference φ applied to these walls from the outside. In either case, naturally, these walls must be assumed to be made of a conducting material, say metal. Walls of precisely this kind were used in the experiments of Hartmann and Lazarus [2] who used mercury filling in rectangular channels in an external magnetic field $H_0 = H_3^0$, $H_1^0 = H_2^0 = 0$, perpendicular to the velocity u_1 , and in some experiments by Lehnert [3]. The question arises, however, of the choice of E or, what is the same, of the boundary conditions (4) for H_1 . Usually, as was also done by Hartmann [2], one assumes in (4) const = 0, i.e., one assumes that

$$H_1(+L) = -H_1(-L) = 0, \quad (4a)$$

the vanishing of the field H_1 on the channel walls being motivated by the requirement that the tangential component of the magnetic field be continuous on the wall (see, for example, [4]), in spite of the fact that this condition is obviously satisfied for any choice of constant in the boundary condition (4). In fact, Condition (4a), as shown by integrating (9) with respect to x_3 within the limits $-L$ to $+L$, reduces to the requirement that the total current through the transverse cross section of the channel vanish. The same integration, with allowance

for (4a, 6, and 10) yields

$$E = \frac{Pc}{\sigma H_0} (\text{M} \operatorname{ctn} \text{M} - 1), \quad (11)$$

with the average velocity over the channel cross section being

$$\bar{u}_1 = u = \frac{cE}{H_0} = \frac{Pc^2}{\sigma H_0^2} (\text{M} \operatorname{ctn} \text{M} - 1). \quad (12)$$

This solution by Hartmann demonstrates well the random character of the choice of electric field E when the magnetohydrodynamic problems are reduced to the determination of only the hydrodynamic and magnetic fields. It is apparently indeed valid when the rectangular channel walls at $x_3 = \pm L$ are not conducting, while the walls perpendicular to the x_2 axis are metallic (in practice with conductivity $\sigma = \infty$). The channels used in the experiments of Hartmann and Lazarus [2] satisfy these requirements and therefore the use of Formula (12) was justified. The same cannot be said concerning its application to the experiments of Lehnert [3] and Murgatroyd [4] on the flow of mercury in a magnetic field, using channels made of glass and of steel insulated on the inside by a special coating.

Hartmann's solution (12) with Boundary Conditions (4a) for H_1 are cited in all books [1, 4] and articles without mentioning that it has a limited region of applicability. Yet there exist also other solutions, which describe flow conditions that in our opinion can be experimentally realized in a more clear-cut fashion. We wish to call attention to these.

If the conducting walls perpendicular to the x_2 axis used in the above-described rectangular channel are joined together by a wire of infinite conductivity, i.e., short-circuited, the electric field of the channel will become equal to zero. Then, putting $E = 0$ in (6) and (10), we obtain in place of (12) the relation

$$u = \frac{Pc^2}{\sigma H_0} \frac{M \operatorname{ch} M - 1}{M \operatorname{ch} M}. \quad (13)$$

In addition, in the parallel circuit joining the conducting walls we can introduce an electromotive force which produces any value of the field E in the liquid, and the external mechanical action can be removed, i.e., we can put $P = 0$. Then the conducting liquid will flow only under the influence of the ampere forces and in accord with (6) and (10) its average flow velocity in the channel will be

$$u = \frac{Ec}{H_0} \frac{M \operatorname{ch} M - 1}{M \operatorname{ch} M}. \quad (14)$$

The solutions (13) and (14) are interesting because they give a different dependence of the average velocity on the M number when $M \gg 1$. According to (12) this velocity is proportional to $1/M$ in this case, other conditions being equal, something that was confirmed although not quite clearly in the experiments of [2, 3, 5]. Yet in accordance with (13) it is proportional to $1/M^2$, and in accordance with (14), although it is again proportional to $1/M$, nevertheless when $M = 0$ we also have $u = 0$, this being due to the fact that in this case $H_0 = 0$ and the ampere force which sets the liquid in motion is also equal to zero. To the contrary, according to (12 and 13) we obtain when $M = 0$ the same connection between u and P , corresponding to a pure hydrodynamic laminar flow.

It seems to us that it would be interesting to check the conclusions drawn from the solutions (13 and 14) by means of specially set up experiments.

2. STATIONARY SHOCK WAVES IN A GAS OF HIGH CONDUCTIVITY ($\sigma = \infty$)

The general theory of shock waves, including nonstationary ones, in such a medium [1] is based on the use of the conservation laws on the front of the shock wave and of the hypothesis that there exists an electric field completely defined by the relation

$$\vec{E} = - \frac{[\vec{u} \vec{H}]}{c}. \quad (15)$$

In the case of stationary waves this equation, generally speaking, is not satisfied because there is no induced electric field ($\text{rot } \vec{E} = 0$). As we have already noted, in this case E is determined by the electrostatic equation (1) and the corresponding boundary conditions, and may have different values, including vanishing ones.

Owing to the nonfulfillment of (15) and owing to the electrostatic character of the field E , stationary waves may arise, not described by the ordinary theory, the very existence of which, as far as we know, has nowhere been mentioned.

We shall consider the simplest of these waves, which can be realized in plane parallel flow of a strongly conducting gas ($\sigma = \infty$) in a channel of rectangular cross section of the same type as used in the experiments of Hartmann and Lazarus, with an external magnetic field likewise parallel to the x_3 axis. Unlike the Hartmann problem we shall, however, assume that this field has a jump discontinuity in the plane $x_1 = 0$ given by

$$\begin{aligned} x_1 < 0; \quad H'_3 &= H_0 = \text{const}; \\ x_1 \geq 0; \quad H'_3 &= H_0 + \Delta H = \text{const}, \\ -\infty < x_1 &\leq +\infty \quad H_1^0 = H_2^0 = 0. \end{aligned} \quad (16)$$

The walls of the channel perpendicular to the x_2 axis are short-circuited by a wire or are connected in parallel to an external emf which produces a uniform electric field

$$-\infty < x_1 < +\infty \quad E_1^0 = \text{const} \quad (17)$$

When gas flows in the direction of the x_1 axis in the plane $x_1 = 0$, the jumplike change in the external magnetic field will bring about impact of the gas against the magnetic field with formation of a shock wave front in this plane. On going through the shock wave, all

the conservation laws will be satisfied in this case; these, if we denote by means of braces the difference $Q'' - Q'$ of the quantity Q ahead of and behind the front of the shock wave, assume the form

$$\{pu_1\} = 0, \quad g \left\{ I + \frac{u_1^2 + u_3^2}{2} \right\} + \frac{c}{4\pi} E_2^0 \{H_3\} = 0,$$

$$\left\{ pu_1^2 + p + \frac{H_3^2}{8\pi} \right\} = 0 \quad g \{u_3\} = \frac{H_1}{4\pi} \{H_3\},$$

where

$$g = \rho u_1 = \text{const.} \quad (18)$$

$$I = W + p v \quad (19)$$

is the heat content, W is the internal energy, and $v = p/\rho$. We shall assume that the channel walls $x_3 = \pm L$ are sufficiently far apart (in the limit $L = \infty$). Then we can put on the wave front portion $x_1 = 0$ that $H_1 = 0$, $u_3 = 0$, and consequently the conservation equations assume the form

$$\left. \begin{aligned} \{pu_1\} &= 0, \\ \left\{ pu_1^2 + p + \frac{H_3^2}{8\pi} \right\} &= 0, \\ g \left\{ I + \frac{u_1^2}{2} \right\} + \frac{c}{4\pi} E_2^0 \{H_3\} &= 0. \end{aligned} \right\} \quad (20)$$

We assume further that on both sides of the shock wave front gas flow is established in electric and magnetic fields (16 and 17) applied from the outside. Then E_2^0 and $\{H_3\} = \Delta H$ in Eq. (20) can be regarded as specified quantities, and in addition the function $I = I(p, \rho)$ can be assumed known, so that from the values of p , ρ , and u_1 ahead of the shock wave front we can determine with the aid of (20) their values behind the front. Thus, the problem of the impact of a conducting gas mass against an inhomogeneity of a magnetic field ΔH is completely solved.

Eliminating g and u_1 from the system of equations, we determine the equation for the "shock adiabat," confining ourselves for simplicity

to the case $E_2^0 = 0$

$$W'' - W' + \frac{(p'' + p')(v'' - v')}{2} + \frac{(v'' - v')(H_3'' - H_3'^2)}{16\pi} = 0. \quad (21)$$

The analogous equations in the theory of ordinary shock waves have the form

$$W'' - W' + \frac{(p'' + p')(v'' - v')}{2} + \frac{(v'' - v')(H_3'' - H_3'^2)}{16\pi} = 0. \quad (22)$$

Comparison of (21) with (22) shows that the new type of shock waves differ appreciably from the ordinary ones. This difference becomes even greater if the external electric field E_2^0 differs from zero.

We consider also another interesting case of shock waves, arising during the mechanical impact between a gas flowing along the x_1 axis with velocity u_1 against the body over which the gas flows, in an external homogeneous magnetic field $H_3^0 = H_0$, $H_1^0 = H_2^0 = 0$ in the absence of an external electric field $\vec{E} = 0$. The problem is completely analogous to the preceding one. The only difference lies in the fact that in place of the inhomogeneity of the magnetic field on the channel axis we introduce an obtuse body made of a well-conducting material with a cross section profile that is symmetrical with respect to the plane $x_3 = 0$ and is the same in the planes perpendicular to the x_2 axis, supported by the well-conducting channel walls perpendicular to the x_2 axis. Thus, these channel walls are short-circuited and the current j is determined by the relations

$$j_1 = -\frac{\sigma n_1 H_3}{c}, \quad j_2 = j_3 = 0. \quad (23)$$

since in this case the electric field is $E = 0$.

For such a shock wave, the same relations (20) will be satisfied, but in simpler form. One of the obvious simplifications is $E_2^0 = 0$. In addition, because of the homogeneity of the external magnetic field, there will be no discontinuity in its tangential component on the front

of the shock wave, something that follows directly from the integration of the Maxwell equation $dH_3/dx_1 = 4\pi j_2/c$ over the width of the shock front $x''_1 - x'_1 = d$, which we shall assume to be infinitesimally small.

Thus, in addition to $E_2^0 = 0$, we must put also in (20) $\{H_3\} = 0$, after which the equations assume the form

$$\{pu_1\} = 0; \quad \{u_1^2 + p\} = 0; \quad \left\{ I + \frac{u_1^2}{2} \right\} = 0. \quad (24)$$

Consequently, a magnetic field without sharp artificial inhomogeneities will not affect a shock wave of mechanical origin. We note that the mechanical use of the ordinary theory of shock waves would lead in this case to another conclusion, one not agreeing with reality. According to that theory there should arise an electric field E determined by Relation (15). In order for the tangential component to be continuous on the shock wave front while the normal component of the magnetic field H_1 is equal to zero, it would be necessary to have a jump in the tangential component H_3 given by the equation

$$\frac{p'}{p''} = \frac{H'_3}{H''_3}.$$

We do not wish to state here that ordinary shock wave theory is in general incorrect. We merely note the cases that are not included within the range of applicability of this theory. The fact that it does not apply in many cases to stationary shock waves is due essentially to the absence of an induced electric field \vec{E} , defined by (15), for these shock waves.

It is somewhat stated that such a field, which is not of induction origin, will nevertheless exist as the result of relativity theory also in stationary streams of a conducting medium, for if $\vec{E} = 0$ in the frame in which the medium is at rest, then in a different frame (say the laboratory frame), in which the medium moves with velocity \vec{u} , electric polarization arises with electric field E_1 , which cancels out the

induced field $[\bar{u}H]/c$ and is therefore determined by Relation (15). From this, in particular, it is sometimes concluded that such an electric field, given by Eq. (15), arises at the location of the stationary shock wave front.

However, if the occurrence of such a field \bar{E} is possible, it does not at all follow that it arises always in stationary flows and in shock waves. It is very easy to point out flows and shock waves in which the conditions (15) for its occurrence are not fulfilled. Such, for example, are plane parallel flows of a conducting medium in rectangular channels, which were theoretically and experimentally investigated by Hartmann and Lazarus [2], Lehnert [3], and Murgatroyd [5], and also stationary flows and waves described in the present paper. In general, in any stationary flow of a conducting liquid in an external magnetic field, in channels with conducting walls, it is known for certain that there will be no electric field described by (15). On the other hand, it is very difficult to point out the conditions under which such a field could exist. For example, one might think that in channels of rectangular and round cross sections with nonconducting walls, with which Lehnert [3] and Murgatroyd [5] experimented, the charges resulting from the polarization of the medium would concentrate in thin surface layers near the walls and would yield a field \bar{E} given by (15) in the entire stream as a whole. But then the current \bar{J} and the ampere force $[\bar{J}H]/c$ would vanish everywhere and there would be no interaction whatever between the stream and the magnetic field. If such interaction is observed in such a manner, that in one region of the flow, in spite of (15), we have $\bar{E} > -[\bar{u}H]/c$, and in the other we have $\bar{E} < -[\bar{u}H]/c$ and only in the symmetry plane do we get $\bar{E} = -[\bar{u}H]/c$.

The foregoing applies equally well to stationary shock waves. Thus, Marshall [6] developed a theory of such waves for uniform flow

of a conducting gas in a perpendicular magnetic field, starting from the assumption that on both sides of the shock wave front the electric field due to the polarization of the medium, $E = \text{const}$, satisfies Relation (15), which is equivalent to assuming the vanishing of the current and the lack of interaction between the medium and the magnetic field on both sides of the shock front. Marshall, however, does not concern himself with the real physical conditions under which such a flow with formation of a shock wave could be realized. Yet, in all probability, Marshall's one-dimensional stationary flow with a shock wave of this type would be completely unstable, since the smallest disturbance would violate Condition (15) and would give rise to ampere forces that would change this flow.

REFERENCES

1. L. Landau and Ye. Lifshits. Elektrodinamika sploshnykh sred [Electrodynamics of Continuous Media], GTTI [State Press for Theoretical and Technical Literature], 1957.
2. J. Hartman, F. Lasarus. Det Kgb. Dan. Vid. Selsk-Math.-fis. Meddel., XV, 6, 1937.
3. B. Lehnert. Ark. Fys., 5, 69, 1952.
4. T. Kauling. Magnitnaya gidrodinamika [Magnetohydrodynamics], Izd-vo inostr. lit. [Foreign Literature Press], 1959.
5. W. Murgartroyd. Phil. Mag., 44, 1348, 1955.
6. W. Marshall. Proc. Roy. Soc., ser. A, 233, 367, 1955.

EFFECT OF CONDUCTIVITY ANISOTROPY ON THE
STRUCTURE OF A MAGNETOHYDRODYNAMIC SHOCK WAVE

G. A. Lyubimov

Moscow

We consider the problem dealing with the structure of a shock wave in a gas which is sufficiently rarefied to permit the electrons to have a helical range ($\omega\tau \geq 1$).

Ohm's law is expressed in such a medium in the form

$$\sigma \left(\vec{E} + \frac{1}{c} [\vec{V} \times \vec{H}] + \frac{1}{ne} \text{grad } p_e \right) = \vec{j} + \frac{\omega e}{H} \vec{U} \times \vec{H} \quad (1)$$

The problem of the structure of the shock wave in an analogous formulation was considered in [1], where only part of the equations describing the problem were considered, so that the qualitative results obtained do not hold true for the complete system of equations and consequently for the entire problem as a whole.

We shall henceforth assume that the energy dissipation occurs in the wave only as the result of the dissipation of the electric current energy, i.e., we shall neglect viscosity and electric conductivity of the gas.

Since we cannot describe the research in detail, we shall indicate here only the research scheme and the formulation of the conclusions.

The problem of the structure of a shock wave reduces in the classical formulation in this case to a system of five algebraic equations, which represent the laws of conservation of mass, the three momentum projections, and the energy, as well as two differential equations

which represent the projections of (1) on coordinate axes that lie in a plane tangent to the wave.

The projection of (1) on the normal to the discontinuity surface serves to determine the transverse component of the electric field E_x , if the electron pressure is known.

It is thus necessary to solve the following system of equations

$$\begin{aligned} mu + p + \frac{H^2}{8\pi} &= I_1, \\ mv - \frac{H_x}{4\pi} H_y &= I_2, \\ mw - \frac{H_x}{4\pi} H_z &= I_3, \end{aligned} \quad (2)$$

$$\begin{aligned} m \left(\frac{u^2 + v^2 + w^2}{2} + \frac{\gamma - 1}{\gamma - 1} \frac{p}{\rho} \right) &= \epsilon, \\ \frac{dH_z}{dx} &= \beta [xH_x(uH_y - vH_z) - (wH_x - uH_z)] \\ \frac{dH_y}{dx} &= \beta [aH_x(wH_z - uH_y) + (uH_y - vH_z)] \\ \alpha = \frac{\omega}{H}, \quad \beta = \frac{4\pi}{c^2} \frac{\sigma}{1 + \alpha^2 H_x^2}, \quad H_x &= \text{const.} \end{aligned} \quad (3)$$

The constants m , I_1 , I_2 , I_3 , ϵ , and H_x are determined from the parameters of the flow ahead of the shock wave.

We introduce dimensionless quantities defined by the formulas

$$\begin{aligned} u &= u_0 u^*, \quad v = u_0 v^*, \quad w = u_0 w^*, \\ RT &= \theta u_0^2, \quad u^* p = \rho_0 u_0^2 \theta, \\ H_i &= \sqrt{8\pi \rho_0 u_0^2} h_i, \quad i = x, y, z. \end{aligned}$$

The subscript "0" pertains to the parameters ahead of the shock wave. Changing over in (3) to dimensionless coordinates, we obtain

$$\begin{aligned} \frac{1}{\rho^*} h'_z &= (u^* - 2h'_z)(x^* h_x h'_y + h'_z) - z^* h'_z f'_z, \\ \frac{1}{\rho^*} h'_y &= (u^* - 2h'_z)(h_y - a^* h_x h'_z) - h_x h'_z f'_z, \end{aligned} \quad (4)$$

where

$$\begin{aligned} x^* &= \frac{\alpha x}{c}, \quad f'_z = \frac{h_x}{h_x} (1 - 2h'_z), \\ f'_z &= 1 + \theta_0 + h'_z, \\ a^* &= \sqrt{8\pi \rho_0 u_0^2} z, \quad \beta^* = \beta \frac{c^2}{\sigma}. \end{aligned}$$

Changing over to dimensionless coordinates in (2) and eliminating from the latter v^* , w^* , and ϵ^* , we obtain a relation between u^* , h_y , and h_z :

$$\frac{1}{2}(\gamma+1)u^{*2} + \gamma u^*(h_y^2 + h_z^2) - 2(\gamma-1)h_x^2(h_y^2 + h_z^2) - \gamma h_x^2 - 2(\gamma-1)h_x^2 h_y - \frac{1}{2}(\gamma-1)h_x^2 + (\gamma-1)\epsilon^* = 0. \quad (5).$$

To complete the solution of the problem it is necessary to express u^* from (5) in terms of h_y and h_z , substitute it into (4), and integrate the system (4).

Let us investigate the system (4)-(5) qualitatively. In the u^* , h_y , h_z space Eq. (5) defines a certain surface, on which the integral curves of the equations in (4) should lie. Since the solution describing the structure of the shock wave goes over at $x = \pm\infty$ into translational flow, the points on the surface (5), corresponding to $x = \pm\infty$, lie on the intersection between the surfaces

$$(u^* - 2h_x^2)(\alpha^* h_x h_y + h_z) - \alpha^* h_x^2 h_z^2 = 0, \quad (6)$$

$$(u^* - 2h_x^2)(h_y - \alpha^* h_x h_z) - h_x^2 h_z^2 = 0.$$

Relations (6) have been obtained by equating to zero the right halves of (4). The points of intersection of (5)-(6) are the singular points of the system (4).

The character of the integral curve of the system (4), and consequently also the qualitative singularities of the flow within the zone representing the shock wave, depend on the character of these singular points.

The character of the singular points is determined by the sign of the discriminant of the characteristic equation, made of the coefficients of the linear terms in the right halves of the equation in (4)

$$D = \frac{h_x^4}{(1-\theta_0)^2} + \alpha^* h_x^2 (1-2h_x^2) h_{xy} \left[\frac{2h_x}{1-\theta_0} - \frac{1-2h_x^2}{h_x} \right].$$

Without dwelling on the details of the further research, let us

formulate the qualitative conclusions to which the research leads.

If the shock wave is fast and its intensity is such that the velocity behind the wave is larger than the gasdynamic velocity of sound, then the motion inside the zone of the wave is continuous. Furthermore, if $a^2 h_x^2$ is small, then all the parameters in the flow zone change monotonically, but if $a^2 h_x^2$ is large, i.e., the helical range of the electrons is large, then u^* and the components of the magnetic field near the initial points do not change monotonically (the initial point is in this case the focus for the system of integral curves). In the latter case the end point of the magnetic field intensity vector describes in space a regular curve, but it does not rotate in this case around the normal to the discontinuity surface.

If the intensity of the fast wave is large, so that the velocity behind it is subsonic, then a continuous flow cannot exist within the zone representing the shock wave.

The flow near the initial point is the same as for a wave of low intensity. The flow zone is terminated in this case by a gasdynamic isomagnetic discontinuity.

If the gas velocity ahead of a slow shock wave is subsonic, the flow is continuous. The flow is monotonic in the case of small $a^2 h_x^2$ and in the case of large $a^2 h_x^2$ near the end point the motion is similar to the motion near the initial point in a fast wave with large $a^2 h_x^2$.

If the gas velocity ahead of a slow wave is supersonic, then the flow begins with a gasdynamic isomagnetic discontinuity, followed by a region of continuous flow. The behavior of the flow near the end point is the same as in the preceding case.

Thus, the character of the flow within the zone representing the shock wave depends in essential fashion on the magnitude of the helical range of the electrons and on the character of the wave itself (fast

or slow). As $\alpha^* \rightarrow 0$ the flow goes over into one describing the structure of an ordinary magnetohydrodynamic shock wave.

An essential feature of the structure of the shock wave in a gas with anisotropic conductivity is the presence of a transverse electric field component, and consequently space charge, within the zone of the wave.

We note that in a medium with anisotropic conductivity the thickness of the shock wave is larger than in an ordinary magnetohydrodynamic shock wave.

If $\omega\tau \sim 1$, then

$$l \sim \frac{c^2}{4\pi\sigma u_0} (1 + \alpha^2 H_x^2);$$

if $\omega\tau \gg 1$, then

$$l \sim \frac{c^2}{4\pi\sigma u_0} \frac{(1 + \alpha^2 H_x^2)}{\alpha H_x} \sim \frac{c^2}{4\pi\sigma u_0} \omega\tau.$$

In this case for a medium with a large helical range of electrons the thickness of the shock wave is of the order of the Larmor radius

$$l \sim \frac{c^2}{4\pi\sigma u_0} \omega\tau = \frac{cH}{4\pi n e u_0} = \frac{cI^2 \mu u_0}{4\pi n e u_0^2 H m} = \frac{H^2}{4\pi\sigma u_0^2} R_L \sim R_L$$

For comparison we indicate that the thickness of an ordinary magnetohydrodynamic shock wave is of the order of

$$l \sim \frac{c^2}{4\pi\sigma u_0}.$$

REFERENCE

1. S.A. Kaplan. Vliyaniye anizotropii providimosti v magnitnom pole na strukturu udarnoy volny v magnitnoy gazodinamike [Influence of Conduction Anisotropy in a Magnetic Field on the Structure of Shock Waves in Magnetohydrodynamics], ZhETP [Journal of Experimental and Theoretical Physics], 1, 1960.

SOME PROPERTIES OF MAGNETOHYDRODYNAMIC FLOWS IN SHOCK WAVES

M. N. Kogan
Moscow

§1. STABILITY OF SHOCK WAVE

According to [1], shock waves are stable against small disturbances if

$$u_{1-} < v_{n1} < w_{n1}, \quad v_n < u_{2+} \quad (1.1)$$

or

$$u_{1+} < v_{n1}, \quad w_{n1} < v_n < u_{2+}, \quad (1.2)$$

where v_n is the component of the stream velocity normal to the wave, $w = H/\sqrt{4\pi\rho}$ is the Al'fven velocity, $w_n = H_n/\sqrt{4\pi\rho}$, $a = \sqrt{\kappa p/\rho}$ is the velocity of light, and

$$u_{\pm}^2 = \frac{1}{2} [w^2 + a^2 \pm \sqrt{(w^2 + a^2) - 4a^2 w_n^2}]$$

The subscripts "1" and "2" denote the states ahead of and behind the wave, respectively. The coordinate system is fixed to the wave.

In the investigation of plane stationary flows it is convenient to use the planes of the velocity hodograph and the magnetic field, since we have in these planes the characteristic manifold [2] and the polars of the shock wave [3]. Figures 1-4 show the shock polars plotted in Reference [3]. These polars were derived from the conditions for the conservation of the mass, momentum, and energy of the flow and the conditions that the entropy increase.

The results of the stability analysis on the basis of (1.1) and (1.2) are shown in Figs. 1-4. $M = v/a$, $N = w/a$, V_1 is the critical

velocity of sound, and σ is the angle of inclination of the wave to the coinciding velocity and magnetic field vectors ahead of the wave. In Figs. 1 and 2 the stable modes are designated by continuous lines and the unstable ones by dashed lines. A clearer picture is obtained

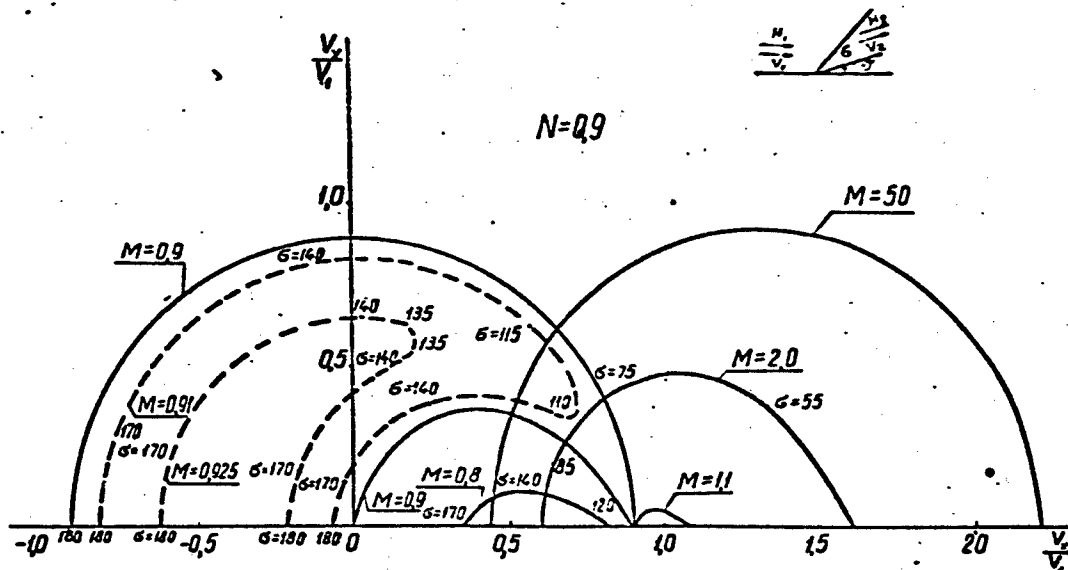
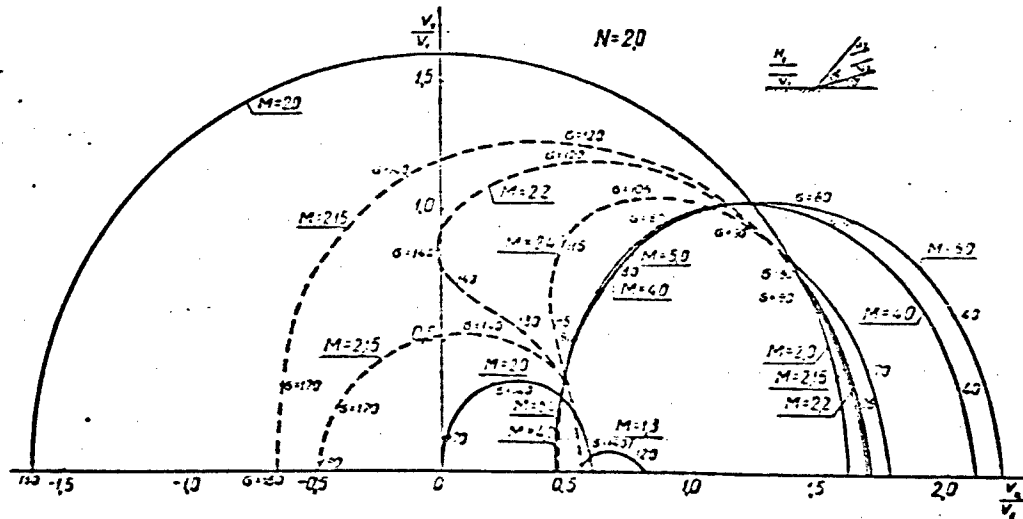


Fig. 1



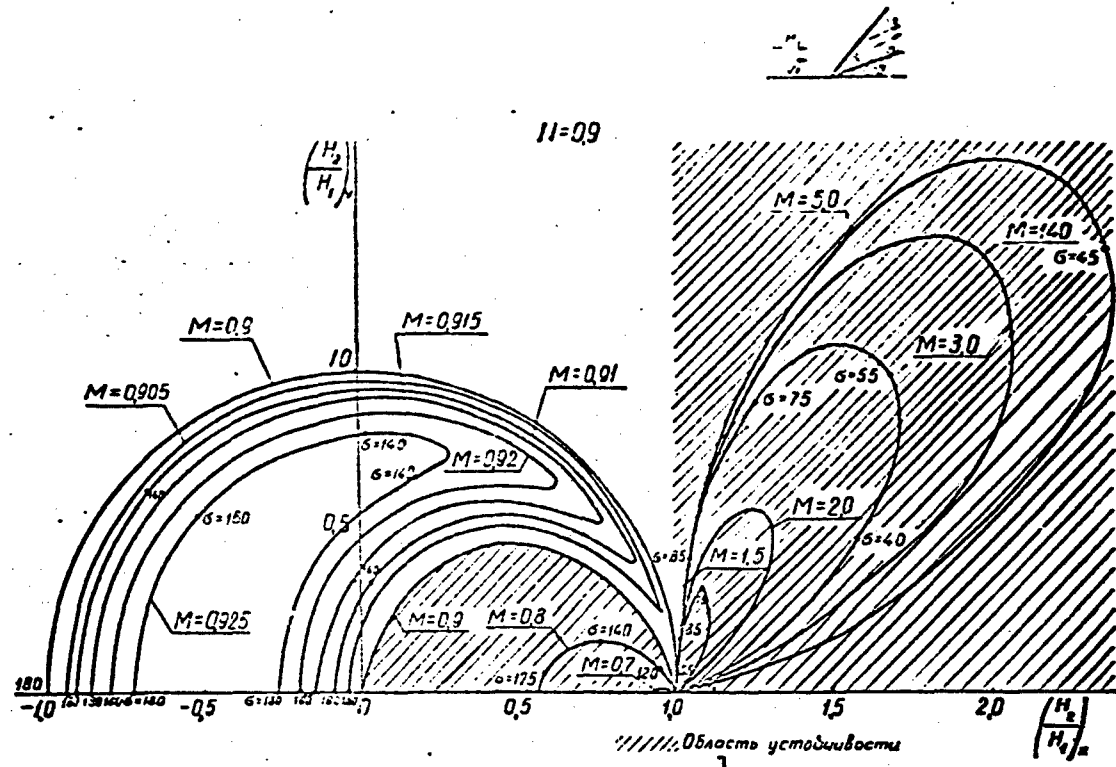


Fig. 3. 1) Stability region.

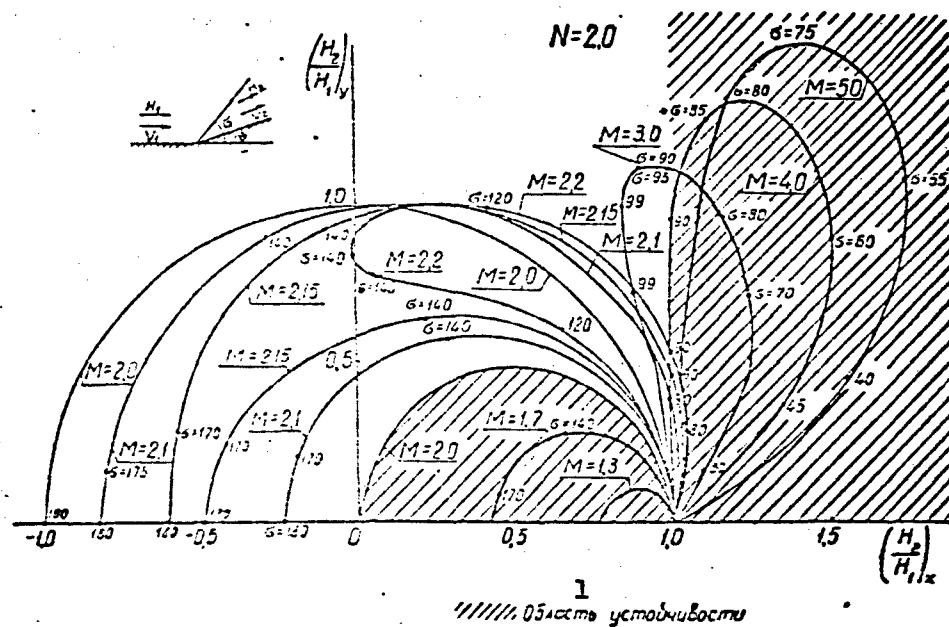


Fig. 4. 1) Stability region.

and (1.2) have a simple geometrical interpretation [1]: the stable

modes are those in which the tangential component of the magnetic field does not reverse sign on going through the wave. It is easy note that the stability regions, in accordance with this rule, will be those shown shaded in Figs. 3 and 4.

Let us note some properties of shock polars.

1. A stability occurs where multiple valuedness occurs, i.e., where the same conditions ahead of the wave correspond to several possible modes behind the wave.

When $N_1 > 1$ such a multiple valuedness region exists [3] in the range

$$N_1^2 < M_1^2 < \frac{\kappa+1}{\kappa-1} \left(N_1^2 - \frac{2}{\kappa+1} \right). \quad (1.3)$$

where κ is the ratio of the specific heat.

When $N < 1$ a multiple valuedness exists at $N_1 < M_1 < 1$. The polars corresponding to this mode are completely unstable.

2. The ordinary direct shock wave is unstable in the range (1.3).
3. In the range (1.3) there exist unstable fast shock waves ($v_{nl} > u_{l+}$).
4. Small shock waves of the first kind [3] are stable both when $M_1 > 1$ and when $M_1 < 1$.
5. Waves traveling against the stream are stable when

$$\sqrt{N_1^2 + N_1^2} < M_1 < \min(N_1, 1) \text{ for } N_1 < 1$$

and when

$$1 < M_1 < N_1 \text{ for } N_1 > 1.$$

6. All the polars are stable when they are qualitatively similar to the polars of normagnetic gasdynamics, occurring when $M_1^2 > \frac{\kappa+1}{\kappa-1} \times \left(N_1^2 - \frac{2}{\kappa+1} \right)$ for $N_1 > 1$ and when $M_1 > 1$ when $N_1 < 1$.

§2. WIDTHS OF DISCONTINUITIES

To estimate the thickness of the shock wave we can use the equation

$$\rho_1 u_1 T s' = \rho_1 u' + \eta_1 (\rho_1 u' + v' + w') + (\lambda T)' + \frac{c^2}{16\pi^2} H_y^2. \quad (2.1)$$

Here u, v, and w are the components of the velocity vectors along the axes x, y, and z, ρ is the density, T is the temperature, s is the entropy, H_y is the component of the magnetic field along the y axis, ξ and η are the viscosity coefficients, λ is the heat conduction coefficient, σ is the electric conductivity, and c is the velocity of light. The x axis is directed along the normal to the wave. The velocity vector \vec{v}_1 lies in the xy plane. The primes denote differentiation with respect to x.

Integrating (2.1) over the width of the discontinuity we obtain the following estimate for the thickness of the wave δ :

$$\delta = \delta_1 + \delta_2 + \delta_3,$$

where

$$\begin{aligned} \delta_1 &= \frac{(\zeta + 4/3 \eta_1)(\Delta u)^2}{\rho_1 u_1 T \Delta s}; & \delta_2 &= \frac{\eta_1 [(\Delta v)^2 + (\Delta w)^2]}{\rho_1 u_1 T \Delta s}; \\ \delta_3 &= \frac{c^2 (\Delta H_y)^2}{16\pi^2 \rho_1 u_1 T \Delta s}. \end{aligned}$$

Here $\Delta A = A_2 - A_1$ and the quantities that are variable in the front are replaced by certain mean values. The quantity Δw differs from zero in rotational discontinuities.

Denoting Δp by Δ , we obtain the following estimate for weak shock waves of the first kind [3]:

$$\varepsilon_1 \sim \varepsilon_2 \sim \frac{\sqrt{F\rho}}{\Delta}, \quad \varepsilon_3 \sim \frac{\sqrt{v_m \rho \rho}}{\Delta},$$

where v is the kinematic viscosity and $v_m = c^2/4\pi\sigma$ is the magnetic viscosity.

As shown in [3], when $M^2 = N^2 + \varepsilon^2$, where ε is a small quantity, weak waves of the second kind exist. In moving along such a polar, the entropy drop changes from $\Delta s \sim \Delta^3$ to $\Delta s \sim \Delta$. However, the corresponding change in Δv and ΔH leads to the estimate $\delta \sim \Delta^{-1}$. Weak shock waves of

the second kind go over into the limit to rotational discontinuities, in which $\Delta = 0$ and $\Delta s = 0$. Therefore the thickness of such a discontinuity is infinite, i.e., there are no stationary discontinuities of this kind. Inasmuch as in an incompressible liquid the only possible rotational discontinuities are shock waves, it is clear that the solutions with shock waves obtained for flows of an incompressible liquid cannot be realized. They are, however, of certain interest for by using similitude criteria it is possible to change over from them to the corresponding solutions of the elliptical-hyperbolic problems for a gas.

Along with waves whose thickness increases with decreasing intensity, there exist in magnetohydrodynamics waves whose thickness increases with increasing intensity. These are waves that are close to tangential discontinuities, the thickness of which, as can be readily seen from (2.1) tends to infinity as $\sigma \rightarrow \pi$.

REFERENCES

1. A.I. Akhiyezer, G.Ya. Lyubarskiy and R.V. Polovin. Ob ustoychivosti udarnykh voln v magnitnoy gazodinamike [On the Stability of Shock Waves in Magnetohydrodynamics], ZhETF [Journal of Experimental and Theroretical Physics], 25, 3, 9, 1958.
2. M.N. Kogan. Magnitudinamika ploskikh i osesimmetricheskikh techeniy gaza s beskonechnoy elektropravodnost'yu [Magnetodynamics of Plane and Axially Symmetrical Flows of a Gas with Infinite Conductivity], PMM [Applied Mathematics and Mechanics], XXIII, 1, 1959.
3. M.N. Kogan. Udarnyye volny v magnitnoy gidrodinamike [Shock Waves in Magnetohydrodynamics], PMM, XXIII, 3, 1959.

PERTURBATIONS OF THE MAGNETIC FIELD IN WAVE
AND JET MOTIONS IN A CONDUCTING MEDIUM

L. I. Dorman

Moscow

§1. PERTURBATION OF MAGNETIC FIELD IN WAVE MOTIONS OF A CONDUCTING MEDIUM

Let us find the perturbation of a magnetic field occurring in the propagation of gravitational waves over the surface of a liquid situated in a homogeneous magnetic field, in the case of small magnetic Reynolds numbers. We shall assume here that the amplitude a of the wave is much smaller than the wavelength λ . In this case we can neglect in the Navier-Stokes equation the term $(\vec{v}\vec{v})\vec{v}$ compared with the term $\frac{\partial \vec{v}}{\partial t}$, and the velocity distribution in the moving liquid will have in accordance with [1] the form

$$\begin{aligned} v_x &= -Ake^{kx} \sin(kz - \omega t); & v_y &= 0; \\ v_z &= Ake^{kx} \cos(kz - \omega t). \end{aligned} \quad (1.1)$$

where $k = 2\pi/\lambda$, $\omega = \sqrt{kg}$, and g is the acceleration due to gravity. The coefficient A is connected with the wave amplitude a and with the velocity of propagation $u = \frac{\partial \omega}{\partial k} = \frac{1}{2}\sqrt{g/k}$ by the relation $A = 2ua = a\sqrt{g/k}$. Here the z axis is directed vertically upward and the xy plane is chosen to be the equilibrium plane surface of the liquid. The perturbations of the magnetic field \vec{h} for small magnetic Reynolds numbers and small Hartmann numbers is given by the equation

$$\vec{\Delta h} = -\frac{4\pi\sigma}{c^2} \text{rot}[\vec{v}\vec{H}] \quad (1.2)$$

where σ is the conductivity of the medium and \vec{H} is the external field

(in our case, homogeneous). Substituting (1.1) in (1.2) we obtain

$$\left. \begin{aligned} \Delta h_x &= \frac{4\pi\sigma Ak^2}{c^2} e^{kz} [H_x \cos(kx - \omega t) + H_z \sin(kx - \omega t)] \\ \Delta h_y &= 0 \\ \Delta h_z &= \frac{4\pi\sigma Ak^2}{c^2} e^{kz} [H_x \sin(kx - \omega t) - H_z \cos(kx - \omega t)] \end{aligned} \right\} \text{for } z < 0. \quad (1.3)$$

$$\left. \begin{aligned} \Delta h_x &= 0 \\ \Delta h_y &= 0 \\ \Delta h_z &= 0 \end{aligned} \right\} \text{for } z > 0. \quad (1.4)$$

We seek a solution of (1.3) and (1.4) in the form

$$h_x = \varphi(z) \frac{4\pi\sigma}{c^2} Ak^2 [H_x \cos(kx - \omega t) + H_z \sin(kx - \omega t)]. \quad (1.5)$$

Substituting (1.5) in (1.3) and (1.4) we obtain for $\varphi(z)$ the equation

$$\varphi''(z) - k^2 \varphi(z) = \begin{cases} e^{kz} & \text{for } z < 0, \\ 0 & \text{for } z > 0, \end{cases} \quad (1.6)$$

the solution of which has the form

$$\varphi(z) = \begin{cases} \frac{e^{kz}}{2k} \left(z - \frac{1}{2k} \right) + c_1 e^{kz} + c_2 e^{-kz} & \text{for } z < 0, \\ c_3 e^{kz} + c_4 e^{-kz} & \text{for } z > 0. \end{cases} \quad (1.7)$$

From the fact that the solution must be bounded at infinity, it follows that $c_2 = c_3 = 0$. The constants c_1 and c_4 are determined from the condition that the solutions must be joined together on the boundary at $z = 0$, namely $c_1 = 0$; $c_4 = -1/4k^2$.

Substituting the obtained value of $\varphi(z)$ in (1.5) we obtain

$$\begin{aligned} h_x &= R_m [H_x \cos(kx - \omega t) + H_z \sin(kx - \omega t)] \times \\ &\times \begin{cases} e^{kz} (1 - 2kz), & \text{if } z \leq 0, \\ e^{-kz}, & \text{if } z > 0, \end{cases} \end{aligned} \quad (1.8)$$

where

$$R_m = \frac{\pi\sigma A}{c^2} = \frac{\pi\sigma \cdot 2\omega a}{c^2} = \frac{\sigma a \sqrt{g \lambda \pi}}{c^2 \sqrt{2}}. \quad (1.9)$$

Analogously we get

$$\begin{aligned} h_y &= 0, \\ h_z &= -R_m [H_x \sin(kx - \omega t) - H_z \cos(kx - \omega t)] \times \end{aligned} \quad (1.10)$$

$$\times \begin{cases} e^{kz} (1 - 2kz), & \text{if } z \leq 0, \\ e^{-kz}, & \text{if } z > 0, \end{cases} \quad (1.11)$$

Thus, the field perturbation is represented by a vector with amplitude

$$|\vec{h}| = R_m \sqrt{H_x^2 + H_y^2} \begin{cases} e^{ikz} (1 - 2kz), & \text{if } z < 0, \\ e^{-ikz}, & \text{if } z > 0, \end{cases} \quad (1.12)$$

which rotates in the x, z plane with frequency ω . From (1.12) it follows that the maximum of the perturbation $|\vec{h}|$ is located at a depth $z = -1/2k = -\lambda/4\pi$. The dependence of $|\vec{h}|$ on z is plotted in Fig. 1.

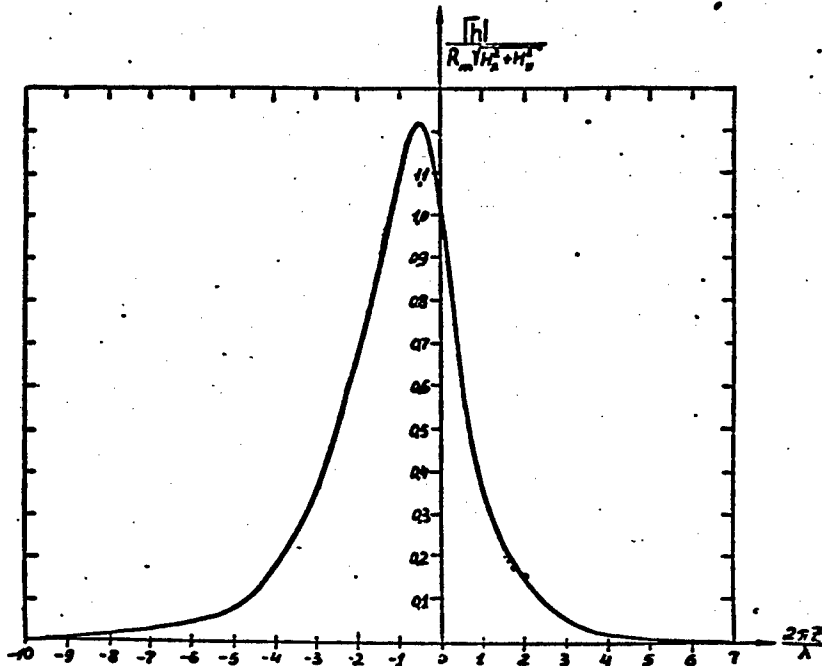


Fig. 1. Dependence of the amplitude of the perturbation of the field on z .

By way of an example let us estimate the field perturbation due to gravitational waves in liquid sodium and in sea water. Since in the former case $\sigma \sim 10^{17}$ we obtain, putting $a \sim 1$ cm and $\lambda \sim 10$ cm, $R_m \sim 10^{-2}$ and in the earth's field at $H \sim 0.5$ gauss we get $h \sim M_{oe}$ at $z = 0$. Such a perturbation can be readily measured. Putting in the second case $\sigma \sim 2 \cdot 10^{10}$, $a \sim 1$ meter and $\lambda \sim 10$ meters, we obtain according to (1.9) $R_m \sim 4 \cdot 10^{-6}$ and in the earth's field at $H \sim 0.5$ gauss the expected field perturbation is $h \sim 0.2\gamma$ on the interphase, approximately

0.24γ at a depth of 1 meter, and it should decrease rapidly with increasing distance from the interface in accordance with the curve of Fig. 1.

Concluding this section, we note that the result obtained can be readily generalized also to include ripple and gravitation-ripple waves. In this case, in accord with [1, page 290], the equations remain the same as before, but

$$\omega^2 = kg + \frac{\alpha}{\rho} k^2 \quad (1.13)$$

where α is the coefficient of surface tension and ρ is the density. We then obtain for R_m in place of (1.9)

$$R_m = \frac{\pi \alpha A}{c^2} = \frac{\pi \alpha \sqrt{g/k + \alpha/k}}{c^2}. \quad (1.14)$$

If $g/k \gg \alpha k / \rho$, then gravitational waves will occur, if $g/k \ll \alpha k / \rho$, the waves will be capillary (or ripple), while if $g/k \sim \alpha k / \rho$, the waves will be capillary-gravitational. The dependence on x , t , and z remains the same as before and is given by (1.8), (1.10), and (1.11), where R_m should in general be taken to be as defined by (1.14).

§2. PERTURBATION OF MAGNETIC FIELD IN THE CASE OF JET FLOW IN A CONDUCTING LIQUID

2.1. Straight Line Submerged Jet with Exponential Velocity Distribution

Assume that the distribution of the liquid velocity has the form

$$v_x = 0; \quad v_y = 0; \quad v_z = v_0 e^{-x/c_0} \quad (2.1)$$

and the unperturbed homogeneous magnetic field is $\vec{H} = \{H_x, H_y, H_z\}$.

Hence

$$[\vec{v} \cdot \vec{H}]_x = -v_z e^{-x/c_0} H_y; \quad [\vec{v} \cdot \vec{H}]_y = v_z e^{-x/c_0} H_x; \quad [\vec{v} \cdot \vec{H}]_z = 0. \quad (2.2)$$

Substituting (2.2) in (1.2) we obtain the initial equations for the field perturbation

$$\begin{aligned} \Delta h_x &= 0; \quad \Delta h_y = 0; \\ \Delta h_z &= \frac{4\pi \alpha \gamma}{c_0^2 \rho} e^{-x/c_0} \{ H_x \cos \varphi + H_y \sin \varphi \} \end{aligned} \quad (2.3)$$

We seek a solution in the form

$$h_z = f(\rho) [H_x \cos \varphi + H_y \sin \varphi]. \quad (2.4)$$

Substituting it in (2.3) we obtain an equation for $f(\rho)$

$$f'' + \frac{1}{\rho} f' - \frac{1}{\rho^2} f = \frac{4\pi\sigma}{c^2} \frac{v_0}{\rho_0} e^{-\rho/\rho_0}. \quad (2.5)$$

Its solution is given in the form

$$f(\rho) = \frac{4\pi\sigma v_0 \rho_0}{c^2} e^{-\rho/\rho_0} \left(\frac{\rho_0}{\rho} + 1 \right) - \frac{c_1}{2\rho} + c_2 \rho. \quad (2.6)$$

From the condition that the solution must be bounded as $\rho \rightarrow \infty$ and $\rho \rightarrow 0$ we obtain $c_2 = 0$; $c_1 = (2 \cdot 4\pi\sigma v_0 \rho_0^2)/c^2$, hence

$$h_z = -R_m \left[\frac{\rho_0}{\rho} (1 - e^{-\rho/\rho_0}) - e^{-\rho/\rho_0} \right] (H_x \cos \varphi + H_y \sin \varphi), \quad (2.7)$$

where

$$R_m = \frac{4\pi\sigma v_0 \rho_0}{c^2}. \quad (2.8)$$

For the remaining field components we obtain $h_x = 0$; $h_y = 0$.

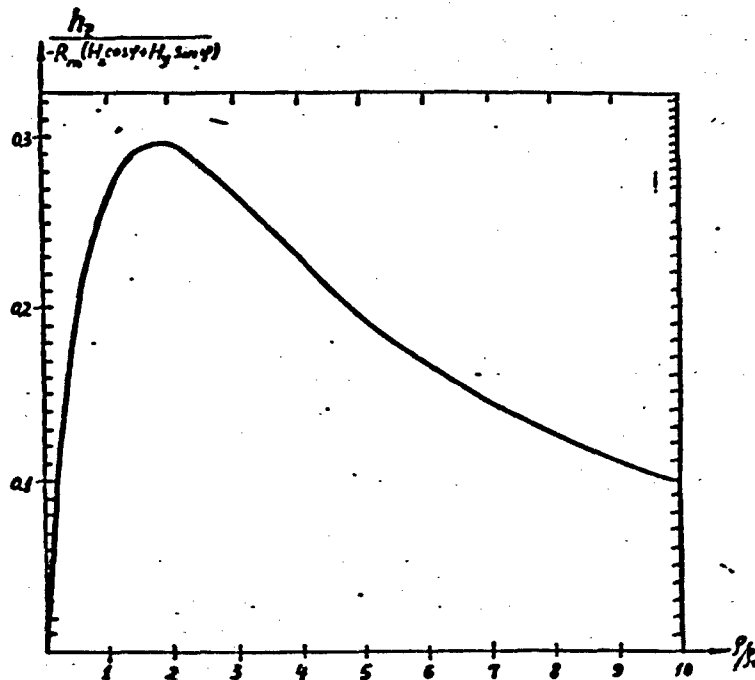


Fig. 2. Dependence of the amplitude of the field perturbation on ρ/ρ_0 .

Figure 2 shows the dependence of $h_z/R_m(H_x \cos \varphi + H_y \sin \varphi)$ on ρ/ρ_0 .

2.2. Field Perturbation in the Flow of a Viscous Conducting Liquid in a Submerged Pipe

Let ρ_0 be the radius of the pipe, v_0 the velocity on the pipe axis, the z axis chosen in the flow direction, the external homogeneous field $\vec{H} = (H_x, H_y, H_z)$, and

$$v_x = 0; v_y = 0; v_z = v_0 \left[1 - \left(\frac{\rho}{\rho_0} \right)^2 \right]. \quad (2.9)$$

Then, in accordance with (1.2), we obtain

$$\begin{aligned} \Delta h_x &= 0; \Delta h_y = 0; \\ \Delta h_z &= \begin{cases} \frac{8\pi\sigma v_0}{c^2\rho_0^2} \rho (H_x \cos \varphi + H_y \sin \varphi), & \text{if } \rho \leq \rho_0 \\ 0, & \text{if } \rho \geq \rho_0 \end{cases} \end{aligned} \quad (2.10)$$

We seek h_z in the form

$$h_z = f(\rho) (H_x \cos \varphi + H_y \sin \varphi). \quad (2.11)$$

For $f(\rho)$ we obtain the equation

$$f'' + \frac{1}{\rho} f' - \frac{1}{\rho^2} f = \begin{cases} \frac{8\pi\sigma v_0}{c^2\rho_0^2} \rho, & \text{if } \rho \leq \rho_0 \\ 0, & \text{if } \rho \geq \rho_0 \end{cases} \quad (2.12)$$

The solution of Eq. (2.12) has the form

$$f(\rho) = \begin{cases} \frac{\pi\sigma v_0}{c^2\rho_0^2} \rho^3 + \frac{c_1}{\rho} + c_2 \rho, & \text{if } \rho \leq \rho_0 \\ \frac{c_3}{\rho} + c_4 \rho, & \text{if } \rho \geq \rho_0 \end{cases} \quad (2.13)$$

From the requirement that the solution be bounded as $\rho \rightarrow 0$ and $\rho \rightarrow \infty$ we obtain $c_1 = c_4 = 0$. The conditions that the solutions must be joined at $\rho = \rho_0$ yield $c_2 = -2\pi\sigma v_0/c^2$; $c_3 = \pi\sigma v_0 \rho_0^2/c^2$. Substituting (2.13) in (2.12) we obtain

$$h_z = -R_m (H_x \cos \varphi + H_y \sin \varphi) \begin{cases} \frac{\rho}{\rho_0} \left(2 - \frac{\rho^2}{\rho_0^2} \right), & \text{if } \rho \leq \rho_0 \\ \frac{\rho_0}{\rho}, & \text{if } \rho \geq \rho_0 \end{cases} \quad (2.14)$$

where

$$R_m = \frac{\pi\sigma v_0 \rho_0}{c^2}. \quad (2.15)$$

For the remaining components we obtain $h_x = h_y = 0$.

The dependence of h_z on ρ is shown in Fig. 3. The jet in a pipe submerged in liquid sodium at $\sigma \sim 10^{17}$, $v_0 \sim 10$ cm/sec, $\rho_0 \sim 3$ cm, gives a field perturbation defined by $R_m \sim 10^{-2}$. In sea water at $\sigma \sim 3 \cdot 10^{10}$, flow with a cross section defined by $\rho_0 \sim 100$ meters with a velocity $v_0 \sim 3$ km/hr gives rise to a perturbation defined by $R_m \sim 10^{-4}$, and in the earth's field this yields $h \sim 5\gamma$.

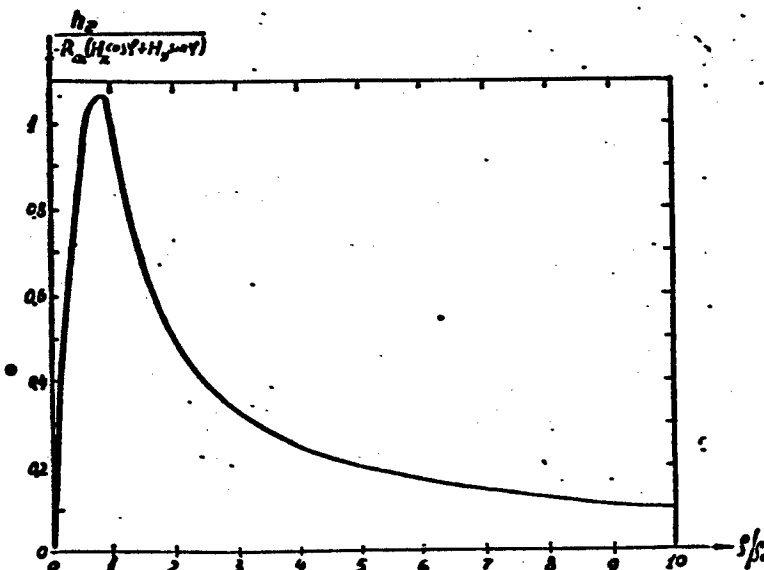


Fig. 3. Character of decrease in the field perturbation with increasing distance from the pipe axis.

REFERENCE

1. L. D. Landau and Ye. M. Lifshits. Mekhanika sploshnykh sred [Mechanics of Continuous Media], Gostekhizdat [State Publishing House for Theoretical and Technical Literature], Moscow, 1950.

LAMINAR FLOW OF A CONDUCTING LIQUID
IN A HOMOPOLAR ENGINE

V.S. Yargin
Moscow

* * *

In the present paper we solve the problem of isothermal flow of an incompressible conducting liquid in a homopolar engine of finite height. The case of small Hartmann numbers (M) is considered. Using an expansion in M^2 as a small parameter, expressions are derived for the flow velocity, the magnetic field, and the current field in first and second approximations. The coefficient of hydraulic resistance is introduced and its dependence on the geometrical dimensions of the setup is investigated.

* * *

The homopolar engine is an axially symmetrical setup consisting of two coaxial cylindrical electrodes, bounded on the ends with dielectric covers, and filled with a conducting liquid. In addition to the electric field between the electrodes, a homogeneous axial magnetic field H_0 is produced in the apparatus. Under the influence of the ampere force produced in the crossed fields, the liquid in the homopolar engine is set in motion.

The theory of this motion has been little studied. Only particular cases of isothermal flow of an incompressible liquid were investigated. Thus, S.I. Braginskii [4] has investigated the case of large numbers $M = (\mu H_0 L/c) \sqrt{\sigma/\eta}$ and $N = \mu^2 H^2 L c / c^2 \rho v$, when the magnetic forces are

much larger than the viscous and inertial forces. Chang and Lundgren [5] investigated the flow in a very thin homopolar engine, neglecting the influence of the side walls; they have considered only one of the possible solutions, in which the velocity and the azimuthal magnetic field are inversely proportional to the distance from the axis of the apparatus. The work of G.V. Gordeyev [6] concerning the flow of liquid in a homopolar engine of finite height contains erroneous assumptions, which will be discussed below.

In our paper we consider stationary isothermal flow of an incompressible liquid in a homopolar engine of finite height at small Hartmann numbers ($M < 1$).

The problem posed can be completely formulated by means of the following set of equations [1, 3]:

$$\begin{aligned} (\vec{U}\nabla)\vec{U} - \frac{1}{4\pi\rho}(\vec{H}\nabla)\vec{H} &= -\frac{1}{\rho}\nabla\psi + \nu\nabla^2\vec{U}, \\ (\vec{U}\nabla)\vec{H} - (\vec{H}\nabla)\vec{U} &= D_m\nabla^2\vec{H}, \\ \nabla\cdot\vec{U} &= 0, \end{aligned} \quad (1)$$

where $\nu = \eta/\sigma$ is the kinematic coefficient of viscosity, $D_m = c^2/4\pi\sigma$ is the coefficient of diffusion of the magnetic field, and

$$\psi = p + \frac{H^2}{8\pi}.$$

It is assumed here that the ordinary conditions under which the magnetohydrodynamic equations are valid [1-3] are satisfied.

Let us change over to dimensionless quantities, putting

$$\begin{aligned} r &= L_0 r, & z &= L_1 z; & \vec{U} &= V_0 \vec{V} \\ H_r &= H_0 h_r; & H_z &= H_0 h_z; & H_\theta &= H_0 h_\theta \\ \psi &= p_0 \psi = p_0 \left(p + \frac{1}{2} \frac{S}{E} h^2 \right). \end{aligned}$$

where L_0 and L_1 are the outside radius and half the height of the apparatus, p_0 is the pressure near the outside wall; H_0 is a constant,

for the time being undetermined, having the dimensionality of the magnetic field intensity; $V_0 = H_0 H_1 L_0 / 4\pi \eta$ is the characteristic velocity; $E = p_0 / \rho V_0$ is the Euler number, and $S = \mu H^2 / 4\pi \rho V_0^2$.

Then, taking into account the cylindrical symmetry of the problem, we obtain the following system of equations:

$$\begin{aligned} \nabla^2 V_r - \frac{V_r}{r^2} &= RE \frac{\partial V_r}{\partial r} - \frac{1}{a} \left(h_r \frac{\partial h_r}{\partial r} + h_z \frac{\partial h_z}{\partial r} - a^2 \frac{h_\varphi^2}{r} \right) + \\ &+ R \left(V_r \frac{\partial V_r}{\partial r} + V_z \delta \frac{\partial V_r}{\partial z} + \frac{V_\varphi^2}{r} \right); \end{aligned} \quad (2)$$

$$\begin{aligned} \nabla^2 V_\varphi - \frac{V_\varphi}{r^2} &= - \left(h_r \frac{\partial h_\varphi}{\partial r} + h_z \delta \frac{\partial h_\varphi}{\partial z} + \frac{h_r h_z}{r} \right) + \\ &+ R \left(V_r \frac{\partial V_\varphi}{\partial r} + V_z \delta \frac{\partial V_\varphi}{\partial z} + \frac{V_\varphi V_r}{r} \right); \end{aligned} \quad (3)$$

$$\begin{aligned} \nabla^2 V_z &= RE \frac{\partial V_z}{\partial z} - \frac{1}{a} \left(h_r \frac{\partial h_z}{\partial r} + h_z \delta \frac{\partial h_z}{\partial z} \right) + \\ &+ R \left(V_r \frac{\partial V_z}{\partial r} + V_z \delta \frac{\partial V_z}{\partial z} \right); \end{aligned} \quad (4)$$

$$\nabla^2 h_r - \frac{h_r}{r^2} = a M^2 \left(V_r \frac{\partial h_r}{\partial r} + V_z \delta \frac{\partial h_r}{\partial z} - h_r \frac{\partial V_r}{\partial r} - h_z \delta \frac{\partial V_z}{\partial z} \right); \quad (5)$$

$$\begin{aligned} \nabla^2 h_\varphi - \frac{h_\varphi}{r^2} &= - M^2 \left(h_r \frac{\partial V_\varphi}{\partial r} + h_z \delta \frac{\partial V_\varphi}{\partial z} - \frac{V_\varphi h_r}{r} \right) + \\ &+ a M^2 \left(V_r \frac{\partial h_\varphi}{\partial r} + V_z \delta \frac{\partial h_\varphi}{\partial z} - \frac{V_\varphi h_\varphi}{r} \right); \end{aligned} \quad (6)$$

$$\nabla^2 h_z = a! M^2 \left(V_r \frac{\partial h_z}{\partial r} + V_z \delta \frac{\partial h_z}{\partial z} - h_r \frac{\partial V_r}{\partial r} - h_z \delta \frac{\partial V_z}{\partial z} \right); \quad (7)$$

$$\frac{\partial V_r}{\partial r} + \frac{V_r}{r} + \frac{\partial V_z}{\partial z} = 0, \quad (8)$$

where $R = \rho L_0 V_0 / \eta$ is the Reynolds number; $\delta = L_0 / L_1$; $a = H_1 / H_0$; $\nabla^2 = (\partial^2 / \partial r^2) + (\partial / r \partial r) + (\delta^2 \partial^2 / \partial z^2)$. Under the conditions of our problem, $a \leq 1$.

In these equations the connection between the motion of the conducting medium and the magnetic field is characterized by the Hartmann number. If $M < 1$, the interaction between them is weak and the system

of equations (2-8) can be solved by expansion in M^2 as a small parameter.

Using this expansion and neglecting in first approximation the axial and radial velocities, we obtain the following first approximation system of equations:

$$\nabla^2 V_\varphi^{(1)} - \frac{V_\varphi^{(1)}}{r^2} + \delta \frac{\partial h_\varphi^{(1)}}{\partial z} = 0; \quad (9)$$

$$\frac{V_\varphi^{(1)2}}{r} = E \frac{\partial \psi^{(1)}}{\partial r} + S \frac{\partial h_\varphi^{(1)}}{\partial r} = E \frac{\partial p^{(1)}}{\partial r}; \quad (10)$$

$$\frac{\partial \psi^{(1)}}{\partial z} = 0; \quad (11)$$

$$\nabla^2 h_\varphi^{(1)} - \frac{h_\varphi^{(1)}}{r^2} = 0. \quad (12)$$

From among the second approximation equations, we give the equation for $h_\varphi^{(2)}$

$$(h_x^{(2)} = h_z^{(2)} = 0),$$

which is determined only by the first-approximation quantities

$$\nabla^2 h_\varphi^{(2)} - \frac{h_\varphi^{(2)}}{r^2} = -\delta \frac{\partial \tilde{V}_\varphi^{(1)}}{\partial z}. \quad (13)$$

The boundary conditions for the velocity will be assumed in the form

$$\begin{array}{ll} V_\varphi = 0 & V_\varphi = 0 \\ r = z; & \\ r = 1 & z = \pm 1. \end{array} \quad (14)$$

where $\epsilon = r = r_1/r_2$.

On the side walls, in view of their ideal conductivity, we have

$$E_\varphi = 0, \quad E_z = 0.$$

On the ends we have $E_\varphi = 0$ and $h_\varphi = -I_0 z/c L_0 H_1 r$ or $h_\varphi = -\delta z/r$, $z = \pm 1$, if we define the constant H_1 as $z = \pm 1$,

$$H_1 = \frac{2I_0}{c}, \quad J_1 = \frac{I_0}{2L_1}. \quad (15)$$

Going over to the magnetic field intensity and using the assump-

tions made above, we obtain the boundary conditions for $h_\phi^{(1)}$:

$$h_\phi^{(1)} = \mp \frac{1}{\delta} \frac{1}{r} \quad \frac{1}{r} \frac{\partial}{\partial r} r h_\phi^{(1)} = 0 \\ z = \pm 1, \quad r = e \\ r = 1, \quad (16)$$

$$h_\phi^{(1)} = 0 \quad \frac{1}{r} \frac{\partial}{\partial r} r h_\phi^{(1)} = 0 \\ z = \pm 1, \quad r = e \\ r = 1. \quad (17)$$

In the first approximation the magnetic field is independent of the liquid flow and is formed by the axial field $h_z^{(1)} = 1$ and by the azimuthal field $h_\phi^{(1)}$. The latter is described by Eq. (12) with Boundary Conditions (17) and represents the field of a current flowing in the inner electrode

$$h_\phi^{(1)} = -\frac{1}{\delta} \frac{z}{r}. \quad (18)$$

This magnetic field corresponds to a radial electric current $j_r = \text{const}/r$, which is independent of the coordinate z .

It is possible to neglect the velocities v_r and v_z if the following conditions are satisfied

$$\epsilon > 1; \quad \frac{H_1^2}{8\pi} \ll \rho_0 + \frac{H_0}{8\pi}$$

which follow from Eqs. (10 and 11). In this case $p = 1$.

Thus, in the first approximation the pressure is constant over the entire volume of the apparatus, the electric current has only a radial component which is independent of the coordinate z , and the velocity of flow is described by the equation

$$\frac{\partial^2 V_r^{(1)}}{\partial r^2} + \frac{1}{r} \frac{\partial V_r^{(1)}}{\partial r} + \delta^2 \frac{\partial^2 V_r^{(1)}}{\partial z^2} - \frac{V_r^{(1)}}{r^2} = \frac{1}{r}. \quad (19)$$

The applicability of the proposed method of solution for liquid metals is determined by the possibility of expansion in δ^2 and is therefore limited to the region of weak magnetic fields. For electrolytes, a more important factor is the possibility of neglecting v_r and

v_z , i.e., the condition $E > 1$, which limits the flow velocity ($v_0 \leq 10^3$ cm/sec) and the magnitude of the ampere force ($J_1 H_0$). This is particularly noticeable when $J_1 \geq 1$ a/cm, when the condition $M < 1$ is automatically satisfied.

A comparison of the system of equations and boundary conditions (9, 12, 14, 15) and of Reference [5] with that proposed by G.V. Gordyev [6] shows that the latter was inconsistent and consequently Eq. (2) of his paper contains a term $\sigma H_0 \partial^2 V_\phi / \partial z^2$. Under his assumption that only a radial current exists and with his formulation of the boundary condition for the current on the side walls, which hold true only when $M \ll 1$, the term mentioned above should be discarded. Its retention leads to the violation of the current continuities law. In addition, the author shows the problem for a boundary condition that is known to be incorrect, assuming the current in the liquid at the end covers to be equal to zero, which is clearly a misunderstanding.

As a result of these circumstances, the solution given in [6] is in error and it is necessary to give a new one, something that is done below for the first approximation equation.

The solution of Eq. (19) will be sought in the form

$$V_r(r, z) = R(r) Z(z) + V_\infty(r) \quad (20)$$

(the symbol (1) has been left out for convenience in notation).

Substituting (20) in (19) and separating the variables, we obtain equations for the determination of the functions $R(r)$, $Z(z)$, and $V_\infty(r)$

$$\left. \begin{aligned} R'' + \frac{1}{r} R' + \left(\lambda_n^2 - \frac{1}{r^2} \right) R &= 0 \\ Z'' - \left(\frac{\lambda_n}{r} \right)^2 Z &= 0 \\ V_\infty'' + \frac{1}{r} V_\infty' - \frac{1}{r^2} V_\infty - \frac{1}{r} &= 0 \end{aligned} \right\}. \quad (21)$$

where λ_n is the variable separation constant.

The boundary conditions for these equations follow from (14):

$$R_{(1)} = R(\varepsilon) = 0; \quad V_\infty(l) = V_\infty(\varepsilon) = 0; \\ R(r)Z(\pm l) + V_\infty(r) = 0. \quad (22)$$

After finding the solutions of Eqs. (21) and substituting them in (20), we obtain the following expressions for the flow velocity

$$V_r(r, z) = \frac{1}{2} \left[A \left(r - \frac{1}{r} \right) + r \ln r + \sum_{n=1}^{\infty} A_n B_n(\lambda_n r) \operatorname{ch}(\nu_n z) \right], \quad (23)$$

where $B_n(\lambda_n r)$ are cylindrical functions of order 1.

$$B_n(\lambda_n r) = J_n(\lambda_n r) - \frac{J_1(\lambda_n r)}{N_1(\lambda_n)} N_n(\lambda_n r),$$

λ_n is the root of the equation $J_1(\varepsilon \lambda_n) N_1(\lambda_n) - J_1(\lambda_n) N_1(\varepsilon \lambda_n) = 0$,

$$A_1 = \frac{\varepsilon^2 \ln \varepsilon}{1 - \varepsilon^2}; \quad A_n = -\frac{4}{\lambda_n \delta \nu_n} b_n; \quad v_n = \frac{\lambda_n}{\delta};$$

$$b_n = \frac{1}{\lambda_n^2} \frac{B_0(\lambda_n) - B_0(\varepsilon \lambda_n)}{[B_0(\lambda_n)]^2 - [\varepsilon B_0(\varepsilon \lambda_n)]^2}.$$

The influence of the end covers on the velocity is described by the term $\sum_{n=1}^{\infty} A_n B_n(\lambda_n r) \operatorname{ch}(\nu_n z)$. For the central cross section ($z \ll 1$) the value of this term decreases with increasing length of the apparatus.

When $\delta \rightarrow 0$ we get

$$V_r(r, z) \rightarrow V_\infty(r) = \frac{1}{2} \left[A \left(r - \frac{1}{r} \right) + r \ln r \right],$$

which coincides with the solution obtained for infinitely long cylinders by G.V. Gordeyev and A.I. Gubanov [3].

The profile of the velocity field depends on the ratio of the radii. The maximum of the velocity is always shifted toward the internal electrode. When $\varepsilon = 0$ (the internal electrode is a filament), the velocity has a maximum at $r = 0.368$ and reaches $0.18 V_0$. With increasing ε , the maximum of the velocity increases, approaching the center of the distance between electrodes. The influence of the end covers smooths out the velocity profile without changing noticeably the position of the maximum. This influence is particularly noticeable for shortened cylinders.

The average flow velocity is

$$V_r(z, \delta) = -\frac{1}{9} \frac{1}{1-\epsilon^2} \left\{ 1 - \epsilon^2 + 6 \frac{\epsilon^2 \ln \epsilon}{1+\epsilon} - \right. \\ \left. - 36 z \sum_{n=1}^{\infty} \frac{\operatorname{th} v_n}{\lambda_n} b_n [S_{1,1}(\lambda_n) B_n(\lambda_n) - z S_{1,1}(\epsilon \lambda_n) B_n(\epsilon \lambda_n)] \right\}, \quad (24)$$

where $S_{1,1}(r)$ is the Lommel function [7].

The average velocity increases with decreasing δ and ϵ . As $\delta \rightarrow 0$ and $\epsilon \rightarrow 0$ we have $V_r \rightarrow V_0/9$ and amounts to approximately 0.6 of the maximum value.

Substituting (23) in (13) we obtain an equation for the determination of $h_\varphi^{(2)}$:

$$\frac{\partial^2 h_\varphi^{(2)}}{\partial r^2} + \frac{1}{r} \frac{\partial h_\varphi^{(2)}}{\partial r} + \delta^2 \frac{\partial h_\varphi^{(2)}}{\partial z^2} - \frac{h_\varphi^{(2)}}{r^2} = \\ = \frac{1}{2} \sum_{n=1}^{\infty} \lambda_n A_n B_1(\lambda_n r) \operatorname{sh}(v_n z). \quad (25)$$

Its solution has the form

$$h_\varphi^{(2)} = \sum_{n=1}^{\infty} \left[R_1(k_n r) \sin \pi n z + \frac{1}{6} \frac{b_n}{\lambda_n} B_1(\lambda_n r) S_1(v_n z) \right], \quad (26)$$

where

$$R_i(k_n r) = C_n I_i(k_n r) - (-1)^i D_n K_i(k_n r), \\ k_n = \pi n \delta, \\ S_1(v_n z) = \frac{\operatorname{sh}(v_n z)}{\operatorname{sh}(v_n)} - z \frac{\operatorname{ch}(v_n z)}{\operatorname{ch}(v_n)}, \\ C_n = (-1)^n 2 \frac{\sum_{m=1}^{\infty} b_m \frac{1+2v_m}{k_n^2 + \lambda_m^2} \operatorname{th} v_m [B_0(\lambda_m) K_0(\epsilon k_n) - B_0(\epsilon \lambda_m) K_0(k_n)]}{I_0(k_n) K_0(\epsilon k_n) - I_0(\epsilon k_n) K_0(k_n)}, \\ D_n = (-1)^n 2 \frac{\sum_{m=1}^{\infty} b_m \frac{1+2v_m}{k_n^2 + \lambda_m^2} \operatorname{th} v_m [B_0(\lambda_m) I_0(\epsilon k_n) - B_0(\epsilon \lambda_m) I_0(k_n)]}{I_0(k_n) K_0(\epsilon k_n) - I_0(\epsilon k_n) K_0(k_n)}.$$

To change over to the current field, we use the equations

$$I_r = -\delta \frac{\partial h_\varphi}{\partial z}; \quad I_z = \frac{\partial h_\varphi}{\partial r} + \frac{h_\varphi}{r}.$$

where $\bar{J} = \vec{J}/j_0$ is the dimensionless current density; $j_0 = c H_1 / 4\pi L_0 = j_r^{(1)}$.

On the basis of these equations we obtain

$$I_r^2 = - \sum_{n=1}^{\infty} \left[k_n R_1(k_n r) \cos n\pi z + \frac{b_n}{\delta} B_1(k_n r) S_1(v_n z) \right],$$

$$I_r^3 = \sum_{n=1}^{\infty} \left[k_n R_1(k_n r) \sin n\pi z + \frac{b_n}{\delta} B_1(k_n r) S_1(v_n z) \right].$$

where

$$S_1(v_n z) = S_1'(v_n z) = v_n \left[\frac{\operatorname{ch} v_n z}{\operatorname{sh} v_n} - z \frac{\operatorname{sh} v_n z}{\operatorname{ch} v_n} \right] - \frac{\operatorname{ch} v_n z}{\operatorname{ch} v_n}.$$

We see from (27) that in the central cross section and near the ends, the second approximation radial current is maximal, while the axial is equal to zero. Thus, the second approximation current is an eddy current in the meridional planes, while near the ends it coincides in direction with the first approximation current, and in the central section it is directed opposite to it.

The volume force $J_r H_0 / r$ assumes for the flow of conducting liquid in the homopolar engine the role of a pressure gradient, and it is therefore convenient to introduce a hydraulic resistance coefficient ξ , defined by the relation

$$\frac{J_r H_0}{r} = \xi \frac{\rho V^2}{2d}. \quad (28)$$

where $d = r_2(1 - \epsilon)$ is the distance between electrodes; $R = \rho V d / \eta$ is the Reynolds number.

For laminar flow it is usually assumed that ξ has the following dependence on the properties of the liquid and the dimensions of the apparatus [2]:

$$\xi = \frac{1}{R} \Phi(\epsilon, \delta), \quad (29)$$

where $\Phi(\epsilon, \delta)$ is a form factor that depends only on the geometrical dimensions of the homopolar engine.

Using (24, 28, and 29) we obtain

$$\frac{\Phi(\epsilon, \delta)}{\Phi(\epsilon, 0)} = \left\{ 1 - \frac{36(1+\epsilon)\delta}{(1-\epsilon)^2(1+\epsilon) + 6\epsilon^2 \ln \epsilon} \right\} X$$

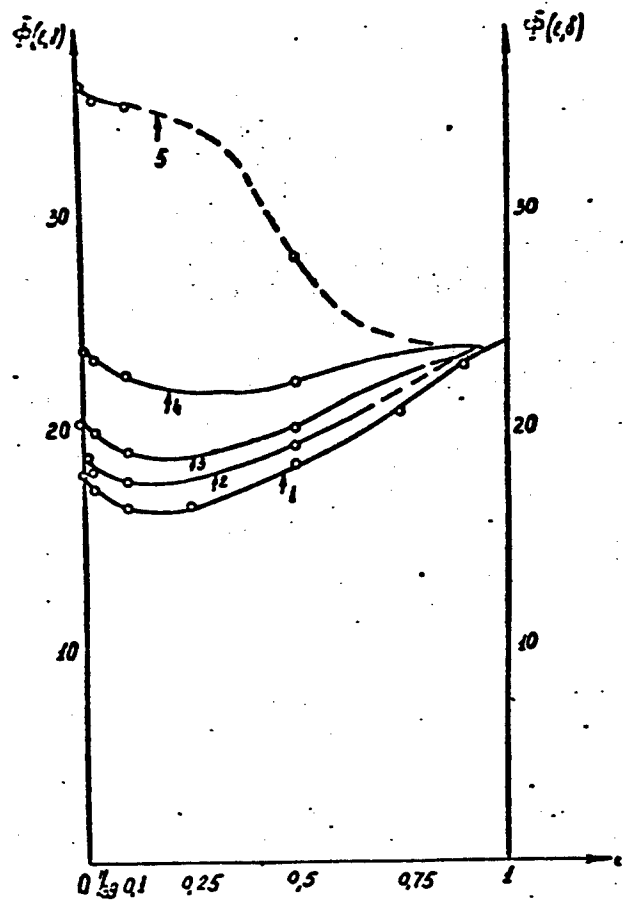


Fig. 1. Dependence of the value of the form factor $\Phi(\epsilon, \delta)$ on $\epsilon = r_1/r_2$ for different $\delta = L_0/L_1$. 1) $\Phi(\epsilon, \delta)$ for $\delta = 0$; 2) $\Phi(\epsilon, \delta)$ for $\delta = 0.25$; 3) $\Phi(\epsilon, \delta)$ for $\delta = 0.5$; 4) $\Phi(\epsilon, \delta)$ for $\delta = 1$; 5) $\Phi(\epsilon, \delta)$ for $\delta = 2$.

$$\times \left\{ \sum_{n=1}^{\infty} \frac{1}{\lambda_n^3} b_n [S_{1,1}(\lambda_n) B_0(\lambda_n) - S_{1,1}(\epsilon \lambda_n) B_0(\epsilon \lambda_n)] \right\}^{-1},$$

where

$$\Phi(\epsilon, 0) = \frac{18(1+\epsilon)^2(1-\epsilon)^3}{(1-\epsilon)^3(1+\epsilon) + 6\epsilon^2 \ln \epsilon} -$$

is the form factor for infinitely long apparatus.

The dependence of $\Phi(\epsilon, \delta)$ on ϵ and δ is plotted in Fig. 1.

For elongated cylinders ($\delta < 1$) the value of $\Phi(\epsilon, \delta)$ increases

slowly with increasing δ . When $\delta = 1/2$, the relative value of the form factor [$\phi(\epsilon, \delta)/\phi(\epsilon, 0)$] is equal to 1.1. When $\delta = 1$, this ratio reaches 1.2-1.36, depending on ϵ . For foreshortened installations ($\delta > 1$), the value of $\phi(\epsilon, \delta)$ increases more rapidly with increasing δ and the role of the end covers rapidly increases and soon becomes decisive. When $\delta = 2$ the relative magnitude of the form factor is 1.5-2, and when $\delta = 4$ it is already 3-5.

In conclusion, I consider it a pleasant duty to express deep gratitude to Professor M.F. Shirokov for interest in the work and for useful consultations.

REFERENCES

1. L.D. Landau and Ye.M. Lifshits. Elektrodinamika sploshnykh sred [Electrodynamics of Continuous Media], Fizmatgiz [State Publishing House for Literature on Physics and Mathematics], 1959.
2. M.F. Shirokov. Fizicheskiye osnovy gazodinamiki [Physical Foundations of Gas Dynamics], Fizmatgiz, 1958.
3. G.V. Gordeyev and A.I. Gubanov, ZhTF [Journal of Technical Physics], XXVIII, 9, 1958.
4. S.I. Braginskiy, ZhETF [Journal of Experimental and Theoretical Physics], XXXVII, 5, 1959.
5. C.C. Chang, T.S. Lundgren. The Physics of Fluids, 2, 5, 1959.
6. G.V. Gordeyev, ZhTF, XXIX, 6, 1959.
7. G.N. Watson [Watson]. Teoriya besselevykh funktsiy [Theory of Bessel Functions], Izd-vo inostr. lit. [Foreign Literature Press], 1949.

CONCERNING TURBULENT HYDROMAGNETIC FLOW
IN A HOMOPOLAR ENGINE

Ye. P. Vaulin, V. I. Babetskiy
Moscow

Turbulent flow of a conducting liquid between coaxial cylinders in a homogeneous magnetic field directed along the axis of the cylinders is considered. Formulas are derived for the calculation of the profile of the average velocity and for the resistance coefficient.

1. TURBULENT FLOW BETWEEN COAXIAL CYLINDERS WITHOUT A MAGNETIC FIELD

Before we proceed to consider hydromagnetic flow, let us analyze briefly ordinary hydrodynamic pressure flow between coaxial cylinders.

It is known [1] that in the core of a completely turbulent stream in a curvilinear channel the product of the velocity and the radius vary little with the radius, i.e., $ur \approx M_0 = \text{const}$. This enables us to represent the distribution of the angular momentum in the core of the flow in the form

$$ur = M_0 - m_0 f(\xi), \quad (1)$$

where M_0 is the maximum value of the angular momentum, m_0 is the scale of the angular momentum of the pulsating motion, ξ is the dimensionless coordinate, to be defined below.

The quantity ur reaches the value M_0 at a certain point r_p . A circle of radius r_p divides the channel into two parts of width $b_1 = r_p - r_1$ and $b_2 = r_2 - r_p$, where r_1 and r_2 are the radii of the internal and external cylinders, respectively. The radius r_p characterizes the influence of the channel curvature on the flow. In each of

the parts of the channel we shall use as a dimensionless coordinate the quantity $\xi = y/b$, where y is the distance from the wall and $b = b_1$ or b_2 .

The flow in the channel is determined by the following independent quantities: the pressure gradient $dp/d\varphi$, the density ρ , the kinematic viscosity ν , the channel width $d = b_1 + b_2 = r_2 - r_1$ and the radius r_p as the curvature parameter. From these we can make up a quantity which has the dimension of velocity and is the velocity scale [1]:

$$u^* = \sqrt{\frac{1}{\rho} \frac{1}{r_p} \frac{dp}{d\varphi}} b. \quad (2)$$

As the angular momentum scale reaches the quantity

$$m_0 = u^* r_p. \quad (3)$$

We introduce the Reynolds number

$$R^* = \frac{u^* b}{\nu}.$$

Thus, the flow in the channel is determined by the two dimensionless quantities R^* and ξ .

We have

$$\frac{ur}{m_0} = f_1(R^*, \xi). \quad (4)$$

In the core of the flow, Relation (1) holds true and can be written in the form

$$\frac{M_0 - ur}{m_0} = f_2(\xi). \quad (5)$$

The flow near the wall is independent of the channel width, so that we assume, as is customary, for the region next to the wall

$$\frac{ur}{m_0} = f_3(R^* \xi). \quad (6)$$

In some region Eqs. (5) and (6) should be satisfied simultaneously.

From Eq. (4) we have

$$\frac{M_0}{m_0} - f_1(R^*, 1) = \varphi(R^*). \quad (7)$$

Equation (5), with account of Eq. (7), can be written in the form

$$\frac{ur}{m_0} = \varphi(R^*) - f_2(\xi). \quad (8)$$

Comparing (6) with (8), and also recognizing that $f_2(1) = 0$, we get

$$\frac{ur}{m_0} = f_2(R^*\xi) = A \ln(R^*\xi) + C, \quad (9)$$

$$\frac{M_0}{m_0} = \varphi(R^*) = A \ln R^* + C, \quad (10)$$

$$\frac{M_0 - ur}{m_0} = f_2(\xi) = -A \ln \xi, \quad (11)$$

or, going over to the velocity distribution

$$\frac{u}{u^*} = \frac{r_p}{r} [A \ln(R^*\xi) + C], \quad (12)$$

$$\frac{u_p}{u^*} = \frac{r_p}{r} [A \ln(R^*) + C]. \quad (13)$$

$$\frac{u_p - u}{u^*} = -\frac{r_p}{r^*} A \ln \xi, \quad (14)$$

where $u_p = M_0/r$.

Wattendorf has found [1] that in the core of a turbulent stream the "velocity defect" $(u_p - u)/u^*$ is a universal function of ξ , which is the same for both walls of the channel, something that does not contradict (14), since in his experiment the quantity r_p/r was of the order of unity. The correctness of the "velocity defect" law (14) needs experimental verification in channels with appreciable curvature, i.e., those for which $(r_2 - r_1)/r_1$ is not very small. It is easy to see that Eqs. (12, 13, and 14) go over into the ordinary velocity laws for flows in straight channels when $(r_2 - r_1)/r_1 \rightarrow 0$.

Resistance Coefficient

We define the resistance coefficient of the channel under consideration in the following manner

$$f = \frac{1}{r_p} \frac{dp}{dr} \frac{2D}{\frac{ur^2}{r_p^2}}, \quad (15)$$

where D is the so-called "hydraulic diameter."

We introduce the average values of the angular momenta for the two halves of the channel, $\bar{u}_1 r$ and $\bar{u}_2 r$, and form the quantities f_1 and f_2 by means of the formulas

$$\frac{\bar{u}_1 r}{m_{01}} = \sqrt{\frac{2}{f_1}}, \quad \frac{\bar{u}_2 r}{m_{02}} = \sqrt{\frac{2}{f_2}}. \quad (16)$$

The average value of the momentum over the section of the channel is

$$\bar{u}r = \frac{\bar{u}_1 r b_1 + \bar{u}_2 r b_2}{d}, \quad (17)$$

where d is the width of the channel.

Combining (2, 15, 16, and 17) we obtain

$$f = \frac{D}{(\sqrt{b_1/f_1} + \sqrt{b_2/f_2})^2}. \quad (18)$$

On going to the limit of a straight channel, the quantities f , f_1 , and f_2 go over into the resistance coefficient of a straight channel, defined in the original manner.

We can derive for the quantities f_1 and f_2 a law which is similar to the law of resistance of straight channels.

Indeed, from (11) we obtain, for example, for the internal wall

$$\frac{M_0 - \bar{u}_1 r}{m_{01}} = \int_0^1 f_1(\xi_1) d\xi_1, \quad (19)$$

which together with (10, 11, 15, and 16) yields

$$\sqrt{\frac{2}{f_1}} = A \ln R_i + C - A. \quad (20)$$

2. MAGNETOHYDRODYNAMIC FLOW BETWEEN COAXIAL CYLINDERS

We now consider the flow of a conducting liquid in the presence of a magnetic field, directed along the axis of the cylinder. An example of such a flow may be the flow in a homopolar engine, where the role of the pressure gradient $dp/d\varphi$ is assumed by the ampere force JH ,

where J is the total current. It becomes possible here to carry out a dimensionless analysis, similar to what was done by Harris for straight channels [2].

In addition to the dimensionless parameters R^* and ξ introduced above, it is also necessary to include one magnetohydrodynamic parameter, namely the Hartmann number, defined by the formula $M^2 = \sigma H_0^2 b^2 / \eta$. Here b is the same as before, η is the viscosity, and H_0 is the field along the cylinder axis.

We thus have

$$\frac{ur}{m_0} = f_1(R^*, M, \xi). \quad (21)$$

Near the wall the flow is independent of the channel dimensions, so that we should have for the region near the wall

$$\frac{ur}{m_0} = f_2(R^* \xi, M \xi). \quad (22)$$

Within the core of the turbulent flow, the influence of the viscosity does not come into effect, and therefore we have away from the walls

$$\frac{M_0 - ur}{m_0} = f_3\left(\frac{M^2}{R^*}, \xi\right). \quad (23)$$

In some region Eqs. (22) and (23) are valid simultaneously, so for that region we have

$$\frac{ur}{m_0} = f_2(R^* \xi, M \xi) = \varphi(R^*, M) - f_3\left(\frac{M^2}{R^*}, \xi\right), \quad (24)$$

where $\varphi(R^*, M) = M_0/m_0$.

Differentiating (24) with respect to ξ , R^* , and M we obtain

$$\frac{\partial(u_r/m_0)}{\partial \xi} = R^* \frac{\partial f_2}{\partial(R^* \xi)} + M \frac{\partial f_2}{\partial(M \xi)} = - \frac{\partial f_3}{\partial \xi}. \quad (25)$$

$$\frac{\partial(u_r/m_0)}{\partial R^*} = \xi \frac{\partial f_2}{\partial(R^* \xi)} = \frac{\partial \varphi}{\partial R^*} + \left(\frac{M}{R^*}\right)^2 \frac{\partial f_3}{\partial(M^2/R^*)}. \quad (26)$$

$$\frac{\partial(u_r/m_0)}{\partial M} = \xi \frac{\partial f_2}{\partial(M \xi)} = \frac{\partial \varphi}{\partial M} - 2 \frac{M}{R^*} \frac{\partial f_3}{\partial(M^2/R^*)}. \quad (27)$$

Substituting (26) and (27) in (25) we get

$$R^* \frac{\partial \varphi}{\partial R^*} + M \frac{\partial \varphi}{\partial M} = -\xi \frac{\partial f_3}{\partial \xi} + \frac{M^2}{R^*} \frac{\partial f_1}{\partial (M^2/R^*)}. \quad (28)$$

Inasmuch as the left half depends only on R^* and M , and the right one only on ξ and M^2/R^* , both halves can be functions of M^2/R^* only, i.e.,

$$R^* \frac{\partial \varphi}{\partial R^*} + M \frac{\partial \varphi}{\partial M} = g_1 \left(\frac{M^2}{R^*} \right) \quad (29)$$

and

$$-\xi \frac{\partial f_3}{\partial \xi} + \frac{M^2}{R^*} \frac{\partial f_1}{\partial (M^2/R^*)} = g_1 \left(\frac{M^2}{R^*} \right). \quad (30)$$

Analogously, eliminating f_3 from (26 and 28), we get

$$2R^* \xi \frac{\partial f_2}{\partial (R^* \xi)} + M \xi \frac{\partial f_2}{\partial (M \xi)} = g_2 \left(\frac{M}{R^*} \right), \quad (31)$$

$$2R \frac{\partial \varphi}{\partial R^*} + M \frac{\partial \varphi}{\partial M} = g_2 \left(\frac{M}{R^*} \right). \quad (32)$$

From (29 and 32) we determine the function φ in terms of the functions g_1 and g_2

$$\varphi(R^*, M) = G_1 \left(\frac{M^2}{R^*} \right) + G_2 \left(\frac{M}{R^*} \right). \quad (33)$$

Here

$$G_1(x) = \int \frac{g_1(x)}{x} dx, \quad G_2(x) = \int \frac{g_2(x)}{x} dx. \quad (34)$$

In exactly the same way we have from (30, 31)

$$f_3 \left(\frac{M^2}{R^*}, \xi \right) = G_3 \left(\frac{M^2 \xi}{R^*} \right) + G_1 \left(\frac{M^2}{R^*} \right), \quad (35)$$

$$f_2(R^* \xi, M \xi) = G_2 \left(\frac{M^2 \xi}{R^*} \right) + G_1 \left(\frac{M}{R^*} \right). \quad (36)$$

Inasmuch as $f_3(M^2/R^*, 1) = 0$, we should have $G_3(x) = -G_1(x)$, and in order to satisfy (24) we should have

$$G_4(x) = G_1(x).$$

Thus, all three functions, φ , f_2 , and f_3 , are expressed in terms of G_1 and G_2 :

$$\xi(R^*, M) = G_1\left(\frac{M^2}{R^*}\right) + G_2\left(\frac{M}{R^*}\right), \quad (37)$$

$$f_1\left(\frac{M^2}{R^*}, \xi\right) = -G_1\left(\frac{M^2\xi}{R^*}\right) + G_2\left(\frac{M^2}{R^*}\right). \quad (38)$$

$$f_2(R^*\xi, M\xi) = G_1\left(\frac{M^2\xi}{R^*}\right) + G_2\left(\frac{M}{R^*}\right). \quad (39)$$

In order to determine the connection between the solutions obtained here and the solutions for flow without a magnetic field, we introduce in place of G_1 and G_2 other functions, namely:

$$G_1(x) = A \ln x + F_1(x), \quad (40)$$

$$G_2(x) = -2A \ln x + C + F_2(x). \quad (41)$$

Then the sought functions will have the form

$$\frac{M_0}{m_0} = A \ln R^* + C + F_1\left(\frac{M^2}{R^*}\right) + F_2\left(\frac{M}{R^*}\right). \quad (42)$$

$$\frac{M_0 - ur}{m_0} = -A \ln \xi - F_1\left(\frac{M^2\xi}{R^*}\right) + F_2\left(\frac{M^2}{R^*}\right). \quad (43)$$

$$\frac{ur}{m_0} = A \ln(R^*\xi) + F_1\left(\frac{M^2\xi}{R^*}\right) + F_2\left(\frac{M}{R^*}\right). \quad (44)$$

When $M = 0$ we have $F_1 = F_2 = 0$ and Relations (42-44) go over into the corresponding expressions (9-11).

The resistance coefficient is determined as before by means of Formulas (15, 16, 18).

From the velocity defect law (43) we have, for example for the internal wall,

$$\frac{M_0 - \bar{u}_i r}{m_{u_i}} = A + F_2\left(\frac{M_i^2}{R_i}\right) - \int_{0}^{1} F_1\left(\frac{M_i^2 \xi_i}{R_i}\right) d\xi_i, \quad (45)$$

which with allowance for (42) yields the following resistance law:

$$\sqrt{\bar{f}_i} = A \ln R_i + C - A + \int_{0}^{1} F_1\left(\frac{M_i^2 \xi_i}{R_i}\right) d\xi_i - F_2\left(\frac{M_i^2}{R_i}\right). \quad (46)$$

In conclusion we note that it follows from the mean of the derivation of the relations (9-11) and (42-44) and from the necessity that

they go over into the corresponding relations for plane channels, that the constants A and C as well as the form of the functions F_1 and F_2 apparently be the same as in straight channels, which, incidentally, calls for an experimental verification.

REFERENCES

1. F. Wattendorf. Proc. Roy. Soc., A, 148, 565, 1935.
2. L.P. Harris. Hydromagnetic Channel Flows, N.Y.-L., 1960.

FLOW OF CONDUCTING VISCOUS LIQUID
IN A POROUS ANNULAR TUBE

N.P. Dzhorbenadze, D.V. Sharikadze
Tbilisi

The flow of viscous incompressible liquid in areas with bounded porous surfaces has recently been studied in [1-3] and in several other papers, while the known papers by Hartmann [4] and [5-7] are devoted to the flow of a viscous electrically conducting liquid in regions with solid boundaries situated in a magnetic field.

In the present work we consider two-dimensional stationary and nonstationary flow of a conducting viscous incompressible liquid in a porous annular tube of infinite length, when an external homogeneous magnetic field is applied perpendicular to the cylinder axes.*

Assume that the main flow of liquid is parallel to the cylinder axes and that liquid enters through the pores of one cylinder into the region of main flow and leaves through the pores of the second cylinder behind the region of motion, i.e., that the motion is cruciform. We choose a cylindrical coordinate system r , θ , z and align the oz axis with the cylinder axis. We denote the cylinder radii by a and b , with $a > b$.

We assume that the amount of liquid leaking in is equal to the amount of liquid leaking out. This will occur if the following condition is satisfied

$$av_a(t) = bv_b(t), \quad (1)$$

where $v_a(t)$ and $v_b(t)$ are the specified values of the corresponding

velocity component on the surfaces of the cylinders.

Let the specified external transverse magnetic field H_0 satisfy the condition

$$H_0 = \delta H_0^* \quad (2)$$

where H_0^* is the value of the external magnetic field on the inner cylinder, and $\delta = b/a$.

The fundamental equations of magnetohydrodynamics in cylindrical coordinates, when the liquid flow is symmetrical relative to the oz axis and the velocity and magnetic field intensity components depend only on r and t will have the following form:

$$\frac{\partial v_r}{\partial t} + v_r \frac{\partial v_r}{\partial r} = \frac{1}{4\pi\rho} H_r \frac{\partial H_r}{\partial r} + v \left[\frac{1}{r} \frac{\partial}{\partial r} (rv_z) \right] - \frac{1}{\rho} \frac{\partial}{\partial r} \left(p + \frac{H^2}{8\pi} \right). \quad (3)$$

$$\frac{\partial v_z}{\partial t} + v_r \frac{\partial v_z}{\partial r} = \frac{1}{4\pi\rho} H_z \frac{\partial H_z}{\partial r} + v \left(\frac{\partial^2 v_z}{\partial r^2} + \frac{1}{r} \frac{\partial v_z}{\partial r} \right) - \frac{1}{\rho} \frac{\partial}{\partial z} \left(p + \frac{H^2}{8\pi} \right). \quad (4)$$

$$\frac{\partial H_r}{\partial t} + v_r \frac{\partial H_r}{\partial r} = H_r \frac{\partial v_r}{\partial r} + v_m \left(\frac{\partial^2 H_r}{\partial r^2} + \frac{1}{r} \frac{\partial H_r}{\partial r} - \frac{H_z}{r^2} \right). \quad (5)$$

$$\frac{\partial H_z}{\partial t} + v_r \frac{\partial H_z}{\partial r} = H_z \frac{\partial v_z}{\partial r} + v_m \left(\frac{\partial^2 H_z}{\partial r^2} + \frac{1}{r} \frac{\partial H_z}{\partial r} \right), \quad (6)$$

$$\frac{1}{r} \frac{\partial}{\partial r} (rv_z) = 0, \quad (7)$$

$$\frac{1}{r} \frac{\partial}{\partial r} (rv_r) = 0, \quad (8)$$

where v_r and v_z are the components of the velocity, H_r and H_z are the components of the magnetic field intensity along the cylindrical coordinate axes r and z , ρ is the density of the liquid, p is the hydrodynamic pressure, $v = \mu/\rho$ is the kinematic coefficient of viscosity, and $v_m = c^2/4\pi\sigma$, where σ is the coefficient of electric conductivity.

The solution of the system (3-8) must be sought under the following boundary conditions

$$\left. \begin{aligned} v_r(r, 0) &= v_r^0(r) \\ v_z(r, 0) &= v_z^0(r) \\ v_r(a, t) &= v_z(b, t) = 0 \\ v_r(a, t) &= v_z(t) \\ v_r(b, t) &= v_z(t) \end{aligned} \right\} \quad (9)$$

$$\left. \begin{aligned} H_r(r, 0) &= H_r^0(r) \\ H_z(r, 0) &= H_z^0(r) \\ H_r(a, t) &= H_z(b, t) = 0 \\ H_r(z, t) &= H_z \\ H_r(b, t) &= H_z^0 \end{aligned} \right\} \quad (10)$$

where $v_z^0(r)$, $v_r^0(r)$, $H_z^0(r)$, $H_r^0(r)$ are the values of the velocity and magnetic field intensity components at the initial instant of time, and the boundary condition for H_z is obtained from the condition that the tangential component of the vector \mathbf{H} be continuous. At the initial instant of time $v_a(t)$ and $v_b(t)$ are equal, respectively, to v_a and v_b , which are given.

In the nonstationary case we obtain directly from (1, 2, 7, and 8) for the radial velocity and magnetic field intensity components v_r and H_r :

$$v_r = \frac{av_a(t)}{r} = \frac{bv_b(t)}{r}, \quad (11)$$

$$H_r = \frac{aH_0}{r} = \frac{bH_0}{r}. \quad (12)$$

Substitution of (11 and 12) into the main system of equations (3-6) shows that Eq. (5) is satisfied automatically and from (3) we obtain

$$\frac{\partial}{\partial r} \left(p + \frac{H^2}{8\pi} \right) = f(r, t).$$

From this and from (4) it follows that $\partial p / \partial z$ is a function of t only, and to determine the longitudinal components of the velocity v_z and of the magnetic field intensity H_z we obtain the following system of equations:

$$v \frac{\partial^2 v_z}{\partial r^2} - \frac{\partial v_z}{\partial t} = \frac{A(t)}{r} \frac{\partial v_z}{\partial r} + \frac{B}{4\pi\rho r} \frac{\partial H_z}{\partial r} - f(t), \quad (13)$$

$$v \frac{\partial^2 H_z}{\partial r^2} - \frac{\partial H_z}{\partial t} = \frac{A_1(t)}{r} \frac{\partial H_z}{\partial r} + \frac{B}{r} \frac{\partial v_z}{\partial r}, \quad (14)$$

where

$$\begin{aligned} A(t) &= v - av_a(t) = v - bv_b(t), \\ A_1(t) &= v_a - av_a(t) = v_a - bv_b(t), \\ B &= H_0 = \delta H_0, \\ f(t) &= \frac{1}{p} \frac{\partial p}{\partial z}. \end{aligned} \quad (15)$$

We assume that the voltage drop along the tube axis changes from

the instant $t = 0$ in accordance with a specified law, i.e., we assume the function $f(t)$ to be known.

The solution of the system (13, 14) subject to the conditions (9, 10) can be reduced to the following integral-differential equations [2, 3, 9]:

$$v_z = F_1(r, t) + \int_0^t \int_0^r \left[\frac{A(\tau)}{\eta} \frac{\partial v_z}{\partial \eta} + \frac{B}{4\pi r \eta} \frac{\partial H_z}{\partial \eta} \right] G(r, \eta, t - \tau) d\eta d\tau, \quad (16)$$

$$H_z = F_2(r, t) + \int_0^t \int_0^r \left[\frac{A_1(\tau)}{\eta} \frac{\partial H_z}{\partial \eta} + \frac{B}{\eta} \frac{\partial v_z}{\partial \eta} \right] G(r, \eta, t - \tau) d\eta d\tau,$$

where $F_1(r, t)$ and $F_2(r, t)$ are the solutions of the heat conduction equation

$$\frac{\partial F_1}{\partial t} - v \frac{\partial^2 F_1}{\partial r^2} = f(t),$$

$$\frac{\partial F_2}{\partial t} - v \frac{\partial^2 F_2}{\partial r^2} = 0,$$

which satisfy the conditions (9, 10), and G is the Green's function of the heat conduction equation. The determination of F_1 and F_2 reduces to a system of Volterra integral equations of the second kind with regular kernel.

We seek the solution of (16) by the method of successive approximations. For this purpose, after differentiating the system (16) once with respect to r and considering in place of this system one with parameter a , we obtain for the determination of $\partial v_z / \partial r$ and $\partial H_z / \partial r$ the following system of integral equations

$$\frac{\partial v_z}{\partial r} = \frac{\partial F_1}{\partial r} + z \int_0^t \int_0^r \left[\frac{A(\tau)}{\eta} \frac{\partial v_z}{\partial \eta} + \frac{B}{4\pi r \eta} \frac{\partial H_z}{\partial \eta} \right] \frac{\partial G}{\partial r} d\eta d\tau, \quad (17)$$

$$\frac{\partial H_z}{\partial r} = \frac{\partial F_2}{\partial r} + z \int_0^t \int_0^r \left[\frac{A_1(\tau)}{\eta} \frac{\partial H_z}{\partial \eta} + \frac{B}{\eta} \frac{\partial v_z}{\partial \eta} \right] \frac{\partial G}{\partial r} d\eta d\tau.$$

We seek the solution of (17) in series form

$$\frac{\partial \sigma_1}{\partial r} = \sum_{n=1}^{\infty} a^n \Phi_n, \\ \frac{\partial H_1}{\partial r} = \sum_{n=1}^{\infty} a^n \Psi_n. \quad (18)$$

For the coefficients of the series (18) we obtain the following recurrence formulas:

$$\Phi_0 = \frac{\partial F_1}{\partial r}, \quad \Psi_0 = \frac{\partial F_1}{\partial r}, \\ \Phi_n(r, t) = \int \int \left[\frac{A(\tau)}{\tau} \Phi_{n-1}(\tau, \tau) + \frac{B}{4\pi\rho\eta} \Psi_{n-1}(\tau, t) \right] \frac{\partial G}{\partial r} d\eta d\tau, \quad (19) \\ \Psi_n(r, t) = \int \int \left[\frac{A_1(\tau)}{\tau} \Psi_{n-1}(\tau, \tau) + \frac{B}{\eta} \Phi_{n-1}(\eta, \tau) \right] \frac{\partial G}{\partial r} d\eta d\tau.$$

To prove the convergence of the series in (18) we note that the following inequality holds true

$$\int \sqrt{t-\tau} \left| \frac{\partial G(r, \eta, t-\tau)}{\partial r} \right| d\eta < N. \quad (19a)$$

Let K and L be constants such that the following inequalities are obtained:

$$\left| \frac{\partial F_1}{\partial r} \right|, \left| \frac{\partial F_2}{\partial r} \right| < K, \left| \frac{A(\tau)}{\tau} \right|, \left| \frac{A_1(\tau)}{\tau} \right|, \left| \frac{B}{4\pi\rho\eta} \right|, \left| \frac{B}{\eta} \right| < L; \quad (19b)$$

by virtue of (19, 19b) we have the following estimates

$$|\Phi_0|, |\Psi_0| < K.$$

$$|\Phi_1|, |\Psi_1| < 2KLN \int_0^t \frac{d\tau}{\sqrt{t-\tau}} = 2KLN\sqrt{t} \frac{\Gamma(1/2)}{\Gamma(3/2)}.$$

where Γ is the Euler gamma function.

Continuing this process, we obtain the general estimates

$$|\Phi_n|, |\Psi_n| < K(2LN)^n t^{\frac{n}{2}} \frac{\Gamma(1/2)}{\Gamma(n/2 + 1)}.$$

From this we find directly that the series (18) converge absolutely and uniformly when $b \leq r \leq a$ and $t < \infty$, the sums of the series

(18) yielding the solutions of our problem when $\alpha = 1$.

In the case of stationary flow of a conducting liquid situated in a magnetic field in an annular porous tube, the introduction of the dimensionless quantity

$$\xi = \frac{r}{a}, \quad 0 \leq \xi \leq 1$$

for the radial component of the velocity and of the magnetic field intensity yields directly from (7,8)

$$v_\xi = \frac{v_r}{\xi}, \quad H_\xi = \frac{H_r}{\xi}.$$

and for the longitudinal components of the velocity and magnetic field intensity we obtain from (13 and 14)

$$\frac{d^2 v_z}{d\xi^2} + \frac{M^2}{N} \frac{1}{\xi} \frac{dH_z}{d\xi} - \frac{R-1}{\xi} \frac{dv_z}{d\xi} = P_1; \quad (20)$$

$$\frac{d^2 H_z}{d\xi^2} + \frac{N}{\xi} \frac{dv_z}{d\xi} - \frac{R_m-1}{\xi} \frac{dH_z}{d\xi} = 0, \quad (21)$$

where $M = (aH_0/c)\sqrt{\sigma/\mu}$ is the Hartmann number, $R = av_a/v$, $R_m = av_a/v_m$ are the ordinary and magnetic Reynolds numbers corresponding to the transverse flow, $N = aH_0/v_m = 4\pi M \sqrt{\sigma\mu/c}$, $P_1 = -a^2 \partial P/\mu \partial z = \text{const}$, and the boundary conditions (9 and 10) yield

$$v_z|_{\xi=0} = v_z|_{\xi=1} = 0, \quad H_z|_{\xi=0} = H_z|_{\xi=1} = 0. \quad (22)$$

From (20 and 21) subject to Conditions (22) we obtain for v_z the following expression

$$v_z = D \left\{ \left(\xi^2 - \frac{1+\xi^2}{2} \right) + \frac{(1-\xi^2)}{(k_2-k_1)(R_m-2)} \left[J_1 \left(\xi^{k_1} - \frac{1+\xi^{k_1}}{2} \right) - J_2 \left(\xi^{k_2} - \frac{1+\xi^{k_2}}{2} \right) \right] \right\}, \quad (23)$$

where

$$J_1 = \frac{2RR_m - 4R + 2 - M^2 - k_1(R_m-2)}{1-\xi^{k_1}},$$

$$J_2 = \frac{2RR_m - 4R + 2 - M^2 - k_2(R_m-2)}{1-\xi^{k_2}},$$

$$D = \frac{(R_m-2)P_1}{2(2R+2R_m-RR_m+M^2-4)}.$$

$$k_{12} = \frac{R - R_m \pm \sqrt{(R - R_m)^2 + 4M^2}}{2}$$

An expression for H_z is obtained analogously.

We investigate the influence of the magnetic field and of the porosity on the motion of a conducting liquid in an annular tube, let us find the ratio of the longitudinal velocity component to its mean value v_z/\bar{v}_z , where

$$\bar{v}_z = \frac{2}{1-\beta} \int_0^1 \xi v_z d\xi;$$

this ratio is given by the expression

$$\frac{v_z}{\bar{v}_z} = \frac{\left(\frac{\pi}{2} - \frac{1+\delta^2}{2}\right) + \frac{(1-\delta^2)}{(k_2-k_1)(R_m-2)} \left[J_1 \left(\xi^2 - \frac{1+\delta^2}{2} \right) - \frac{2}{(k_2-k_1)(R_m-2)} \left\{ J_1 \left(\frac{1-\delta^{2+2}}{k_1+2} - \frac{(1-\delta^2)(1+\delta^2)}{4} \right) - J_1 \left(\xi^2 - \frac{1+\delta^2}{2} \right) \right\} \right]}{-J_1 \left(\frac{1-\delta^{2+2}}{k_2+2} - \frac{(1-\delta^2)(1+\delta^2)}{4} \right)}$$

This formula makes it possible to obtain different profiles for the longitudinal component of the velocity of a conducting liquid with different values of the Hartmann number and with different R and R_m .

REFERENCES

1. A.S. Berman. Laminar Flow in Channels with Porous Walls. *J. Appl. Phys.*, 24, 9, 1953.
2. D.Ye. Dolidze. O nestatsionarnom techenii vyazkoy zhidkosti medzhdu parallel'nymi poristymi stankami [On Nonsteady Flow of a Viscous Fluid Between Parallel Porous Walls], DAN SSSR [Proceedings of the Academy of Sciences USSR], 17, 3, 1957.
3. N.P. Dzhorbenadze. O nestatsionarnom techenii vyazkoy zhidkosti v poristoy krugloy kol'tsevoy trube [On Nonsteady Flow of a Viscous Fluid in a Porous Toroidal Tube], Soobshcheniya AN GSSR [Communications of the Academy of Sciences Georgian SSR],

XIV, 5, 1960.

4. J. Hartmann. Hg-Dynamics. J. Kgl. Danske Vidensk. Selskab. Math.-fys. Medd., 15, 6, 1937.
5. J.A. Shercliff. Steady Motion of Conducting Fluids in Pipes Under Transverse Magnetic Fields. Proc. Cambr. phil. soc. 49, 1, 136-144, 1953.
6. S.A. Regirer. Neustanovivshyesya techeniye elektroprovodnoy zhidkosti v prisutstvii magnitnogo polya [Nonsteady Flow of a Conducting Fluid in the Presence of a Magnetic Field], Inzh.-fiz. zhurnal [Engineering-Physics Journal], II, 8, 43, 1959.
7. I.B. Chekmarev. O statsionarnom technii provodyashchiy zhidkosti mezhdu koaksial'nymi neprovodyashchimi tsilindrami pri nalichii radial'nogo magnitnogo polya [On Steady-State Flow of a Conducting Fluid between Nonconducting Coaxial Cylinders in the Presence of a Radial Magnetic Field], Nauch.-tekhn. inform. byull. [Scientific-Technical Information Bulletin], 8, Leningrad Polytechnic Institute, Division of Physical-Mathematical Sciences, 1959.
8. I.B. Chekmarev. Nekotoryye voprosy statsionarnogo techeniya provodyashchey zhidkosti v beskonechno dlinnoy kol'tsevoy trube pri nalichii radial'nogo magnitnogo polya [Certain Problems of Steady-State Flow of a Conducting Liquid in an Infinitely Long Toroidal Tube in the Presence of a Radial Magnetic Field], ZhTF [Journal of Technical Physics], 30, 6, 1960.
9. N.P. Dzhorbenadze and D.V. Sharikadze. O techenii provodyashchey vyazkoy zhidkosti mezhdu dvumya poristymi ploskostyami [On Flow of a Conducting Viscous Fluid Between Porous Planes], DAN SSSR [Proceedings of the Academy of Sciences USSR], 133, 2, 1960.

Manu-
script
Page
No.

[Footnote]

81

It was learned later that the stationary problem was con-
sidered by I.B. Chekmarev [8].

STABILITY OF PLANE COUETTE FLOW IN
THE PRESENCE OF A MAGNETIC FIELD

K.B. Pavlov

Moscow

The motion of a viscous conducting liquid resulting from the relative displacement of two infinite parallel plates is called plane Couette flow. If a homogeneous external magnetic field $\vec{H}_0(0, H_0, 0)$ is applied perpendicular to the plates, then taking the x axis along the direction of the velocity $\vec{U}_0(U_0, 0, 0)$ of the lower plate relative to the stationary upper plate (we choose the origin in the plane of the lower plate), it is easy to obtain from the system of magnetohydrodynamic equations [1] the following distributions of the dimensionless velocity $\vec{w}(w, 0, 0)$ and magnetic field $\vec{h}(h_x, h_y, 0)$ in the space between the plates (Fig. 1):

$$w = 0.5 \left[1 - \frac{\operatorname{sh} M(y-0.5)}{\operatorname{sh} 0.5M} \right], \quad (1)$$

$$h_x = \frac{0.5 R_g}{M} \cdot \frac{\operatorname{ch} M(y-0.5) \operatorname{ch} 0.5M}{\operatorname{sh} 0.5M}, \quad h_y = 1, \quad (2)$$

where $M = A(R_g R_m)^{1/2}$ is the Hartmann number, $A = H_0/(4\pi\rho)^{1/2} U_0$ is the Alfvén number, ρ is the density, R_g and R_m are, respectively, the ordinary and magnetic Reynolds numbers; the characteristic values of the magnetic field, the velocity, and the length are chosen to be, respectively, H_0 , U_0 , and the distance between the plates.

We know that when $M = 0$ a flow having a velocity profile (1) is stable against infinitesimally small disturbances [2]. When $M \neq 0$ the profile (1) has a point of inflection $y = y_s = 0.5$; this, however, does

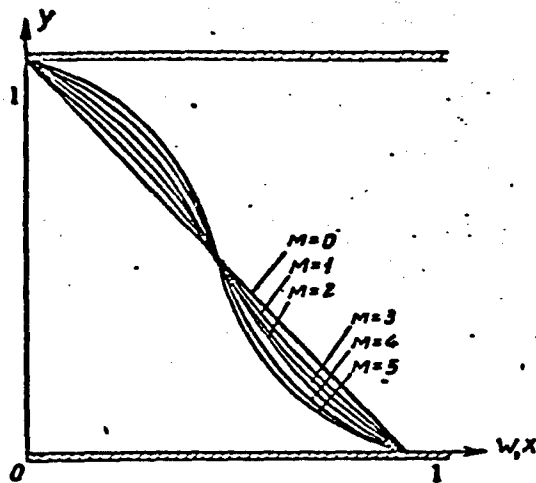


Fig. 1

not mean that instability is possible even in the limiting case when there is no viscosity. The point is that the Rayleigh-Tollmien theory, according to which the presence of the point of inflection is a necessary and sufficient condition for the existence in the nonviscous limit of neutral and growing disturbances, holds true only for symmetrical distributions of the velocity $w(y)$ and of distributions of the boundary layer type. For antisymmetrical distributions, such as for example (1), the presence of the point of inflection is not a sufficient condition for the existence of such disturbances [3]. One can therefore draw no conclusions whatever regarding the stability of plane Couette flow in a perpendicular magnetic field by considering the nonviscous approximation. It is necessary to examine the complete problem with inclusion of viscosity, when the stability is controlled to a considerable degree by the action of the viscosity, the effect of which may vary.

If we consider in the complete system of magnetohydrodynamic equations, written in dimensionless forms, all quantities to consist of a large stationary term and of a small perturbation that depends on the time, then, by assuming the perturbations of the y component of the

velocity and of the magnetic field to be, respectively,

$$\begin{aligned}\Psi(y) \exp\{i[\alpha_1(x - ct) + \alpha_2 z]\} \\ \Phi(y) \exp\{i[\alpha_1(x - ct) + \alpha_2 z]\}\end{aligned}\quad (3)$$

(α_1 and α_2 are the dimensionless wave numbers along the x and z axes and c is the dimensionless complex frequency), we can obtain in the usual fashion [4] for the case of arbitrary stationary flow in a perpendicular magnetic field the following system for the amplitudes Ψ and Φ of the perturbations

$$\begin{aligned}h_x \Psi - \frac{i}{\alpha_1} \Psi'' = (\omega - c)\Phi + \frac{i}{\alpha_1 R_g} (\Phi'' - \alpha^2 \Phi), \\ (\omega - c)(\Psi'' - \alpha^2 \Psi) - \omega'' \Psi + \frac{i}{\alpha_1 R_g} (\Psi''' - 2\alpha^2 \Psi'' + \alpha^4 \Psi) = \\ = \frac{M^2}{R_g R_m} \left[h_x (\Phi'' - \alpha^2 \Phi) - \frac{i}{\alpha_1} (\Phi''' - \alpha^2 \Phi') - h_x' \Phi \right].\end{aligned}\quad (4)$$

where $\alpha^2 = \alpha_1^2 + \alpha_2^2$, and the prime denotes differentiation with respect to the dimensionless coordinate y. In cases of plane Couette flow, the solutions Ψ and Φ should satisfy the boundary conditions

$$\Psi(y) = \Psi'(y) = \Phi(y) = 0 \text{ for } y = 0.1. \quad (5)$$

If $R_m \ll 1$ (this condition is satisfied, for example, for mercury), then the system (4) reduces with sufficient accuracy to a single equation for Ψ :

$$\begin{aligned}(\omega - c)(\Psi'' - \alpha^2 \Psi) - \omega'' \Psi + \frac{i}{\alpha_1 R_g} (\Psi''' - 2\alpha^2 \Psi'' + \alpha^4 \Psi) = \\ = \frac{i M^2}{\alpha_1 R_g} \Psi''.\end{aligned}\quad (6)$$

If we assume M to be invariant, we can put in Eq. (6) $\alpha_1 R_g = \alpha \bar{R}_g$. In this case $\bar{R}_g \leq R_g$, since $\alpha \geq \alpha_1$, and the two-dimensional disturbances turn out to be more dangerous than the three-dimensional ones (Squire's theorem [3]). It is therefore sufficient to investigate the equation

$$\begin{aligned}(\omega - c)(\Psi'' - \alpha^2 \Psi) - \omega'' \Psi + \frac{i}{\alpha R_g} (\Psi''' - 2\alpha^2 \Psi'' + \alpha^4 \Psi) = \\ = \frac{i M^2}{\alpha R_g} \Psi''.\end{aligned}\quad (7)$$

with boundary conditions

$$\Psi(y) = \Psi'(y) = 0 \quad \text{for } y = 0.1. \quad (8)$$

The first pair of independent particular solutions of Eq. (7) is found from the so-called "nonviscous" equation

$$(w - c)(\Psi''' - z\Psi) - z''\Psi = 0, \quad (9)$$

which gives the zeroth approximation of the solution Ψ , if the latter is represented in the form of the asymptotic series

$$\Psi = \Psi^0 + \frac{1}{aR_\epsilon} \Psi^1 + \dots \quad (10)$$

The solutions of Eq. (9) can be found in the form of power series in $y - y_c$, where y_c is a point at which $w = c$. As a result we have

$$\begin{aligned} \Psi_1 &= (y - y_c) + a_1(y - y_c)^2 + a_2(y - y_c)^3 + \dots \\ \Psi_2 &= \Psi_1 \cdot B \cdot \ln(y - y_c) + 1 + b_1(y - y_c) + b_2(y - y_c)^2 + \dots, \end{aligned} \quad (11)$$

where

$$\begin{aligned} B &= \frac{w''(y_c)}{w'(y_c)}; \quad a_1 = b_1 = 0.5B; \quad a_2 = 0.1666(z^2 + M^2); \\ a_3 &= 0.0555z^2B + 0.0416M^2B; \quad a_4 = 0.0083(z^4 + M^4) + \\ &\quad + z^2(0.0166M^2 - 0.00135); \quad a_5 = 0.0021a^4B + \\ &\quad + z^2(0.0004B^2 + 0.0029M^2B) + 0.0013M^4B; \\ a_6 &= 0.0002(z^6 + M^6) + z^4(0.0005M^2 + 0.0001B^2) + \\ &\quad + z^2(0.0005M^4 + 0.0001M^2B^2 - 0.0001B^4); \quad b_2 = 0.5M^2 - 0.75B^2; \\ b_3 &= -0.125B^2; \quad b_4 = 0.0416M^4 - 0.1041M^2B^2 + 0.0208B^4; \\ b_5 &= -(0.0048M^4B + 0.0052B^5); \\ b_6 &= 0.0013M^6 - 0.0031M^4B^2 - 0.0013M^2B^4 + 0.0015B^6. \end{aligned}$$

The other pair of independent particular solutions of Eq. (7) is found in the form

$$\Psi = \exp(\int g dy); \quad z = \sqrt{zR_\epsilon} \cdot z_1 + g_1 + \frac{1}{\sqrt{zR_\epsilon}} z_2 + \dots \quad (12)$$

Substituting (12) in (7) and equating the coefficients of like powers of aR_ϵ , we get

$$\begin{aligned} \Psi_3 &= (w - c)^{-\frac{s}{4}} e^{\int \sqrt{zR_\epsilon} \frac{dy}{z - c}} \equiv D(y) e^{\int \frac{dy}{z - c}}, \\ \Psi_4 &= (w - c)^{-\frac{s}{4}} e^{\int \sqrt{zR_\epsilon} \frac{dy}{z - c}} \equiv D(y) e^{\int \frac{dy}{z - c}}. \end{aligned} \quad (13)$$

The solutions γ_3 , γ_4 , and γ_2 have at the point $y = y_c$ an algebraic and a logarithmic branch point, respectively. The correct branch is determined from the inequalities

$$-\frac{\pi}{6} < \arg(y - y_c) < \frac{7\pi}{6}. \quad (14)$$

which are found from a comparison of the solutions $\Psi = \Psi_{1,2,3,4}$ with the solutions near y_c , after which a use is made of the asymptotic expansion of the Hankel functions. From (1) and (14) it follows that

$$\begin{aligned} \omega - c &= |\omega - c| && \text{for } y < y_c \\ \omega - c &= |\omega - c| e^{-i\pi} && \text{for } y > y_c \end{aligned} \quad (15)$$

The general solution of (7) can be represented in the form

$$\Psi = c_1 \Psi_1 + c_2 \Psi_2 + c_3 \Psi_3 + c_4 \Psi_4. \quad (16)$$

In the problem dealing with the determination of the eigenvalues of a , c , and R_g from (16) and the boundary conditions (8) it is necessary to write for the secular determinant

$$\begin{vmatrix} \Psi_{11} & \Psi_{21} & \Psi_{31} & \Psi_{41} \\ \Psi'_{11} & \Psi'_{21} & \Psi'_{31} & \Psi'_{41} \\ \Psi_{12} & \Psi_{22} & \Psi'_{32} & \Psi'_{42} \\ \Psi'_{12} & \Psi'_{22} & \Psi'_{32} & \Psi'_{42} \end{vmatrix} = 0, \quad (17)$$

where the second subscript 1 or 2 designating the particular solutions Ψ_i denote their values at the boundary points 0 or 1, respectively. Expanding the secular determinant in terms of the elements of the fourth column and then expanding each of the third order determinants in elements of the third column, we get

$$\begin{aligned} &(\Gamma_{11}\Psi'_{31} - \Psi'_{41}\Gamma_{11})\gamma_1 + (\Gamma_{12}\Gamma_{31} - \Psi_{41}\Psi_{31})\gamma_2 + \\ &+ (\Gamma_{11}\Gamma_{32} - \Psi'_{41}\Gamma_{32})\gamma_3 + (\Psi'_{41}\Gamma_{32} - \Psi_{42}\Psi'_{31})\gamma_4 + \\ &+ (\Gamma'_{11}\Psi'_{31} - \Psi'_{41}\Psi'_{31})\gamma_5 + (\Gamma_{12}\Gamma'_{32} - \Psi'_{42}\Psi_{32})\gamma_6 = 0, \end{aligned} \quad (18)$$

where γ_i are second order determinants, for example

$$\begin{aligned} \gamma_3 &= \Psi'_{11}\Gamma_{32} - \Psi'_{21}\Gamma_{32}, & \gamma_4 &= \Psi_{11}\Psi'_{32} - \Psi_{21}\Psi'_{32}, \\ \gamma_5 &= \Psi_{11}\Gamma_{32} - \Psi_{21}\Gamma_{32} \end{aligned} \quad (19)$$

Assuming that the differentiation of the "nonviscous" solutions (11)

does not bring about an essential increase in their order of magnitude and neglecting in (18) terms of order $\frac{1}{\epsilon^6}$ and $\frac{1}{\epsilon^8}$, and then $1/\alpha R_g$, compared with unity, we get

$$\begin{aligned} & -D(0)D(1)\sqrt{izR_g(-c)}\gamma_3 + D(0)D(1)\sqrt{izR_g(1-c)}\gamma_4 + \\ & + D'(0)D(1)\sqrt{izR_g(-c)}\gamma_5 - D(0)D'(1)\sqrt{izR_g(1-c)}\gamma_6 - \\ & - D(0)D(1)\sqrt{izR_g(-c)}\cdot 1/\sqrt{izR_g(1-c)}\gamma_7 = 0. \end{aligned} \quad (20)$$

Taking (15) into account and leaving out the intermediate transformations, we arrive at a final relation

$$\begin{aligned} R_g = & \frac{i}{\alpha} \{ c^{-1/2} [\gamma_4\gamma_5 - 1.25 w'_r c^{-1}] + \\ & + i(1-c)^{-1/2} [\gamma_3\gamma_6 + 1.25 w'_r (1-c)^{-1}] \}, \end{aligned} \quad (21)$$

where $w'_r = w'(0) \equiv w'(1)$.

For neutral disturbances, the values of c are real. If c and α in (21) have arbitrary real values, then the values of R_g are, generally speaking, complex; on the other hand, if there exist such real c and α for which R_g are also real, these are the sought eigenvalues involved in the determination of the neutral disturbances.

Direct calculations carried out for the values $M = 2-6$ show that the only possible eigenvalues of c are $c = w_s = 0.5$; in this case the values of α and R_g are subject to definite relationships, which form in the (α, R_g) plane curves for the neutral stability (Fig. 2). One can verify that the points to the right of any of these curves correspond to the instability region; for these we have $c = c_r + ic_1$, $c_1 > 0$; lying to the left is the stability region, $c_1 < 0$.

Disturbances with large values of α are physically unreal [2, 3]. In this connection there is no point in continuing the obtained curves into the region of values $\alpha > 2$. Nonetheless, the results obtained enable us to make the following two conclusions.

1. In the presence of a perpendicular magnetic field, plane Couette flow becomes unstable against infinitesimally small disturbances, and

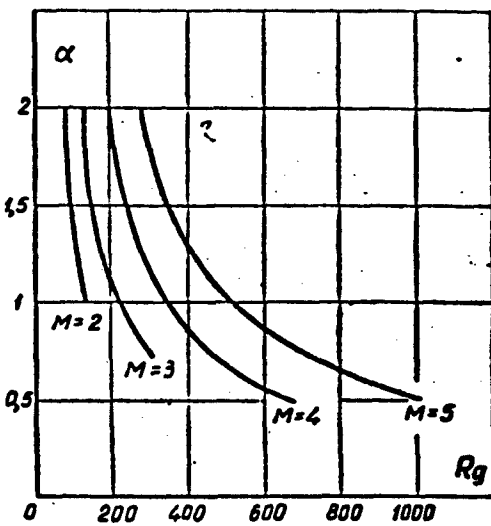


Fig. 2

the instability arises when $R_g \text{ crit} \sim 10^2$ for $M = 2-6$.

2. The instability arising in the presence of a perpendicular magnetic field is the consequence of the deformation of the velocity profile and the accompanying occurrence of a point of inflection. Compared with this effect, as in the case of Hartmann flow [4, 5], the stabilizing action exerted by the magnetic field on the disturbances is insignificant, and the apparent slight increase in stability with increasing field is also the consequence of a change in the profile.

The use of the asymptotic methods developed above for the solution of Eq. (7) is impossible when $M < 2$, so that the transition to the limit of a flow with $M = 0$ cannot be traced.

In conclusion, the author expresses his deep gratitude to Professor K.P. Stanyukovich for a discussion of the results.

REFERENCES

1. L.D. Landau and Ye.M. Lifshits. Elektrodinamika sploshnykh sred [Electrodynamics of Continuous Media], Gostekhizdat [State Publishing House for Theoretical Literature], Moscow, 1957.
2. W. Wasow. J. res. nat. bur. stand., 51, 195, 1953.

3. Lin' Tszyz-Tszyao. Teoriya gidrodinamicheskoy ustoychivosti [Theory of Hydrodynamic Stability], Izd-vo inostr. lit. [Foreign Literature Press], Moscow, 1958.
4. R.C. Lock. Proc. roy soc., A. 233, 105, 1955.
5. K.B. Pavlov and Yu. A. Tarasov, PMM [Applied Mathematics and Mechanics], 24, 723, 1960.

FLOW OF VISCOUS CONDUCTING LIQUID IN REGIONS WITH
PERMEABLE BOUNDARIES IN THE PRESENCE OF A MAGNETIC FIELD

S.A. Regirer
Vorkuta

§1

Methods for the control of the boundary layer by drawing away or blowing in liquid through the surface exposed to the flow have been developed in recent years. In the case of the flow of a conducting liquid, the possibilities were investigated of exercising such control by means of electric and magnetic fields. It is of interest to investigate the effects arising upon simultaneous utilization of both methods. In the present paper we present a brief survey of the results obtained in this field.

We assume first that an infinitely long cylindrical surface Σ is placed inside the main stream, which flows in the direction of a generatrix parallel to the OZ axis, with all the flow parameters being functions of the coordinates x and y only. An external magnetic field, which is likewise invariant along the OZ axis, is applied to the flow. The surface is assumed permeable, that is, the normal component of velocity on Σ differs from zero. Let us write down the general equations of magnetohydrodynamics for the stationary case [1]

$$\rho(\vec{V}\nabla)\vec{V} = -\nabla p^* + \kappa(\vec{H}\nabla)\vec{H} + \tau_s \vec{V}, \quad (1.1)$$

$$(\vec{V}\nabla)\vec{H} = (\vec{H}\nabla)\vec{V} + \nu_m \vec{V}\vec{H}, \quad (1.2)$$

$$\operatorname{div} \vec{V} = 0, \quad \operatorname{div} \vec{H} = 0, \quad (1.3)$$

where $p^* = p + \mu H^2/3\pi$, $\kappa = \mu/4\pi$ and the remaining symbols are standard;

all the physical properties of the liquid are assumed constant. These equations can be analyzed in order to determine the linearizability conditions in the same manner as in [2], representing \vec{V} and \vec{H} in the form of sums of plane and axial vectors: $\vec{V} = \vec{V}_n + \vec{i}_n v$, $\vec{H} = \vec{H}_n + \vec{i}_n h$. In particular, if we put $\vec{H}_n = a\vec{V}_n$, $a = \text{const}$, when the "controlling" flow is directed along the force lines of the transverse field, then the system (1.1-1.3) is transformed into

$$(z - z_0^2)(\vec{V}_n \nabla) \vec{V}_n = -\tilde{\nabla} p^* \quad (\tilde{\nabla} = \vec{i}_x \frac{\partial}{\partial x} + \vec{i}_y \frac{\partial}{\partial y}). \quad (1.4)$$

$$\vec{V}_n \nabla (\varphi v - z_0 h) = -\frac{\partial p^*}{\partial z} + i_z v, \quad (1.5)$$

$$\vec{V}_n \nabla (h - z_0 v) = v_n \Delta h, \quad (1.6)$$

$$\text{div } \vec{V}_n = 0, \quad \frac{\partial h}{\partial z} = 0, \quad (1.7)$$

$$\text{rot } \vec{V}_n = -i_z \vartheta_n \quad (1.8)$$

where ϑ_v and ϑ_h are constants. The structure of these equations, as can be readily seen, depends essentially on the Alfvén number $\varepsilon = a\sqrt{(\kappa/\rho)}$.

The formulation of the boundary conditions and problems involving external flow was considered in detail in an article by M.D. Ladyzhenskiy [3]. In the case of a permeable flow, no new circumstances arise in principle, if the permeable wall is replaced by a wall with uniformly distributed sources. On the other hand, if it is assumed that a finite layer in which the liquid moves and a magnetic field exist inside the body placed in the stream, then additional equations must be considered for this region.

By way of the main example, we present the solution of the problem involving flow around an infinite permeable plate.* Let the liquid fill the half space $y > 0$ and let its velocity in the OZ direction have a finite value as $y \rightarrow \infty$. Regarding this as a plane problem, we

readily see that the velocity vector has the form $\vec{V} = v_0 \vec{i}_y + v(y) \vec{i}_z$. We assume that the vector potential of the field $A(y, z)$ depends linearly on z . It is possible to show that flow of this type is realizable in the presence of transverse fields of two types: $H_y = H_0 = \text{const}$ and $H_y = H_1 e^{v_0 y / v_m}$.

If the transverse field is homogeneous, then the quantities v and $h = H_z$ can be derived from a fourth order system, the general integral of which is

$$h = C_1 + C_2 e^{\nu y} + C_3 e^{-\nu y}, \quad (1.9)$$

$$v = C_4 + \frac{v_0}{H_0} [C_2(1 - R_1)e^{\nu y} + C_3(1 - R_2)e^{-\nu y}]. \quad (1.10)$$

Here $r_{1,2} = v_0 R_{1,2} / v_m$, $R_{1,2} = N + 1 \mp \sqrt{(N + 1)^2 - 4N(1 - \epsilon^2)}$, $N = v_m/v$, $\epsilon^2 = \kappa H_0^2 / \rho v_0^2$. Depending on the signs of the numbers r_1 and r_2 , three particular cases can arise for the determination of the constants C_i ($i = 1, \dots, 4$).

In the case of a blown-in current ($v_0 > 0$), if $\epsilon^2 \leq 1$ then $r_1 \geq 0$, $r_2 > 0$ and there exists only one trivial solution $v = \text{const}$, $h = \text{const}$. If $\epsilon^2 \geq 1$, $v_0 < 0$ or $\epsilon^2 > 1$, $v_0 > 0$, then one of the r_i is nonnegative, and therefore only three unknown constants remain in (1.9, 1.10) (one should vanish because v and h are bounded), and it is possible to impose three boundary conditions, for example to specify any three of the four values of v and h when $y = 0$ and $y \rightarrow \infty$: $v^x, v_\infty, h^x, h_\infty$. Finally, in the case of drawn-out current ($v_0 < 0$) and $\epsilon^2 < 1$, all four constants are independent and are determined from these four boundary values.

Thus, in the case of sub-Alfven velocity of permeation ($\epsilon^2 > 1$) the flow pattern does not differ essentially from ordinary hydrodynamics (with the exception of possible flow with in-blast). However, in the case of drawn-out flow with super-Alfven velocity, flows of a new

type are possible.* This circumstance was not taken into consideration by Gupta [4/5], who confined himself to an examination of the case $\epsilon^2 > 1$ only.

For the new type of flow ($v_0 < 0$, $\epsilon^2 < 1$), the stress due to friction against the plate is given by the formula

$$:= v_\infty (v^\infty - v_\infty) (1 - \Pi), \quad (1.11)$$

where $\Pi = (h^\infty - h_\infty) H_0 \epsilon / (v^\infty - v_\infty) v_0 \rho$ is a dimensionless parameter of the same type as the Alfvén number. When $\Pi = 1$ we have $\tau = 0$, i.e., the viscous resistance on the plate vanishes. The velocity profile has in this case a point of inflection, and the flow is close to potential near the surface, and there is no boundary layer in the usual sense. Naturally, one cannot speak here of the disappearance of resistance in general, for we also have magnetic forces applied to the field sources that are fixed to the plate. The effect obtained is interesting essentially because it makes it possible to reduce the viscous heat release near the plate (a more detailed calculation shows that the over-all heat release may also be reduced). It is also useful to note that usually the drawing out of the laminar boundary layer leads to a certain increase in viscous resistance, but here the opposite effect is obtained. It is easy to show furthermore that in the flow considered here (of course, with $\Pi \neq 1$) a velocity profile can be obtained having a maximum point, i.e., runaway of the conducting medium may be produced. All these results are interesting also because the solution (1.9, 1.10) satisfies simultaneously the equations of a magnetic boundary layer of the first kind [6] if $v_\infty H_0 = v_0 h_\infty$ (when $E_z = 0$). In other words, this solution and solutions similar to it characterize when $E_z = 0$ processes in an asymptotic boundary layer.

For the case of an inhomogeneous transverse field that varies exponentially, the solution of the equations is represented with the aid

of cylindrical functions. We shall not develop it here and confine ourselves only to an indication that this solution also leads to the vanishing of viscous friction on the plate under certain conditions.

In order to estimate the influence of the curvature of the surface, we analyze the problem of longitudinal flow over an infinite round cylinder (this problem was considered independently in a paper by Yasuhara [8]). It turned out that all the flow properties observed above will occur also in this case, and the vanishing of the viscous friction on the surface is also determined by the condition (1.11). We note that Yasuhara, unlike Gupta, considered precisely the case with four arbitrary constants, when $v_0 < 0$, $\epsilon^2 < 1$, but the boundary conditions which he set up ($v^x = 0$, $v_\infty \neq 0$, $h_\infty = 0$, $E_\phi = -\mu v_\infty H_0/C$) cannot yield the results described here.

We investigated still another exact solution of similar type for the problem involving the rotation of a permeable cylinder in a unbounded medium, when $v_r = v_0 r_0/r$, $H_r = H_0 r_0/r$ (the same as in the preceding problem) and $E_z = 0$. Unlike the problems considered above (as in ordinary hydrodynamics), it becomes necessary to introduce here more stringent damping conditions at infinity (for example, $\int v dr < \infty$ in place of $v \rightarrow \text{const}$). In all other respects the analysis of the general solution, which has the form

$$h = \frac{C_1}{r} + C_2 r^{m-1} + C_3 r^{m+1}, \quad (1.12)$$

$$v = \frac{v_0}{H_0} \left[\frac{C_1}{r} + C_2 \left(1 - \frac{m_1}{R_m}\right) r^{m-1} + C_3 \left(1 - \frac{m_2}{R_m}\right) r^{m+1} \right], \quad (1.13)$$

$$m_{1,2} = \frac{R_m}{2} \left[N + 1 \pm \sqrt{(N+1)^2 - 4N(1-\epsilon^2) - \frac{8}{R_m}} \right], \quad R_m = \frac{v_0 r_0}{v_\infty}, \quad (1.14)$$

leads to the conclusions which we already know.

§2

In all the problems considered above the flow of liquid in the direction of the main stream is constant, and the flow region is not

bounded. One can raise many other problems having the same property, but in this case not with one but with two solid boundaries.

In particular, if the flow is between two cylindrical surfaces with parallel generatrices, and the liquid blown in through one surface is completely drawn out through the other surface, then the general arguments of §1 remain in force.

Solutions of problems of this type are known for flows between parallel walls [9] or in an annular tube [10, 11]. It is easy to generalize the solutions of [11] to include the case of circular or helical flow between rotating permeable cylinders. Still another solution is obtained if the main flow is assumed to be radial. Putting

$$v_r = \frac{1}{r} v(\tilde{r}), H_r = \frac{1}{r} h(\tilde{r}), v_{\tilde{r}} = \frac{v_0}{r}, h_{\tilde{r}} = \frac{h_0}{r} \quad (2.1)$$

in Eqs. (1.1-1.3) we obtain for v and h the nonlinear systems

$$\tilde{r}(v_0 v' - v^2 - v_0^2) = -4\gamma v + C + \chi(h_0 h' - h^2 - h_0^2) + \gamma v^3, \quad (2.2)$$

$$h v_0 - v h_0 = v_0 h', \quad (2.3)$$

which does not reduce to quadratures in general form. One of the particular cases of solution (for infinite conductivity) was considered by Vatazhin [12].

Ordinary equations which cannot be integrated in quadratures are obtained also in problems concerning the flow near the critical point for a plane or axially symmetrical stream striking a permeable wall. In these problems allowance for the permeance is connected only with a suitable change in the boundary condition. For plane flow, for example, the equations obtained in [13] remain in force.

Still another group of problems is connected with flow in pipes and channels with permeable walls, when the quantity of liquid flowing varies along the axis of the tube. A simpler example is flow between parallel walls with liquid drawn away on both sides (the Berman prob-

lem). In this problem, and in the axially symmetrical problems analogous to it, the magnetohydrodynamic equations reduce to ordinary differential equations. The general case of flow in a pipe of arbitrary profile it becomes possible to reduce the number of independent variables to two. All these problems are nonlinear and cannot be solved in quadratures. It is interesting that the ordinary equations obtained for them are similar to the equations of flow near the critical point. For an approximate solution of the problem of flow in permeable tubes one can use the method proposed by the author in the ordinary hydrodynamic formulations [14].

REFERENCES

1. L.D. Landau and Ye. M. Lifshits, Elektrodinamika sploshnykh sred [Electrodynamics of Continuous Media], Gostekhizdat [State Publishing House for Technical and Theoretical Literature], Moscow, 1957.
2. S.A. Regirer, present collection page 125.
3. M.D. Ladyzhenskiy, PMM [Applied Mathematics and Mechanics], 23, 2, 292, 1959.
- 4/5. A.S. Gupta. Z. angew. Math. u. Phys., [Journal of Applied Mathematics and Physics], 11, 1, 43, 1960.
6. H.P. Greenspan, G.F. Carrier. J. Fluid Mech., 6, 1, 77, 1959.
7. V.N. Zhigulev, DAN SSSR [Proceedings of the Academy of Sciences USSR], 124, 5, 1001, 1959.
8. M. Yasuhara. J. phys. soc. Japan, 15, 2, 321, 1960.
9. N.P. Dzhorbenadze and D.V. Sharikadze, DAN SSSR, 133, 2, 299, 1960.
10. N.P. Dzhorbenadze and D.V. Sharikadze, present collection, page 91.
11. I.B. Chekmarev, ZhTF [Journal of Technical Physics], 30, 6, 601,

1960.

12. A.B. Vatazhin, PMM [Applied Mathematics and Mechanics], 24, 3, 524, 1960.
13. I. Neyringer and U. Mak-IIroy[MacElroy], collected translations, Mekhanika [Mechanics], 1, 39, 1959.
14. S.A. Regirer, ZhETF [Journal of Technical Physics], 30, 6, 639, 1960.

Manu-
script
Page
No.

[Footnotes]

- 98 We omit the intermediate derivations throughout, since a detailed exposition is the subject of a separate publication. In addition, some of them can be found in the papers of Gupta [4/5].
- 100 It must be noted that in other two-dimensional problems an analogous connection was observed between the value of the parameter ϵ^2 and the possibility of imposing boundary conditions [6].

SOME SOLUTIONS OF THE SYSTEM OF EQUATIONS DESCRIBING
ONE-DIMENSIONAL FLOWS IN MAGNETIC GASDYNAMICS

E.P. Zimin

Khar'kov

In the present paper we obtain solutions that describe one-dimensional stationary flow of a compressible electrically conducting gas in magnetic and electric fields.

1. The system of equations of magnetic gasdynamics for the case of one-dimensional stationary flow of a nonviscous and nonheat-conducting gas has the following form [1]

$$\frac{d}{dx}(\rho W) = 0, \quad (1.1)$$

$$\rho W \frac{dp}{dx} + \frac{dp}{dx} = -\mu_e H \frac{dH}{dx}, \quad (1.2)$$

$$\frac{1}{k-1} W \frac{dp}{dx} + \frac{k}{k-1} p \frac{dW}{dx} = \frac{1}{\sigma} \left(\frac{dH}{dx} \right)^2, \quad (1.3)$$

$$\mu_e \sigma \frac{d}{dx}(WH) = \frac{d^2H}{dx^2}. \quad (1.4)$$

$$p = \rho RT - \text{where the gas is assumed to be ideal. (1.5)}$$

Here H is the intensity of the magnetic field, μ_e is the magnetic permeability, and σ is the electric conductivity of the gas; all other symbols are standard. All quantities, with the exception of W , H , p , ρ , and T are assumed constant.

Since the current density in the one-dimensional case is

$$j = \sigma H / dx \quad (1.6)$$

(if H is directed along the y axis then j is directed along the z axis), the right half of (1.2) determines the ponderomotive force and the

right half of (1.3) the Joule heat j^2/σ . Equation (1.4) is the so-called induction equation [2].

Equations (1.1) and (1.2) can be integrated directly

$$\rho W = m,$$

$$mW + p + \mu_e \frac{H^2}{2} = J.$$

In the general case we can also obtain the first integral of (1.4):

$$\mu_e WH = \frac{dH}{dx} + \text{const.} \quad (1.7)$$

Further solution of the system (1.1-1.4) is possible only by numerical means. However, we can obtain an exact solution of this system for two particular cases which are of practical interest.

2. If there is no external electric field E , then from (1.6) and from Ohm's law

$$j = \mu_e \sigma WH,$$

where $\mu_e WH$ is the emf induced in the moving gas, we can see that in this case the constant in (1.7) is equal to zero.

Then, combining (1.2) and (1.3), which are rewritten in the forms

$$m \frac{dW}{dx} + \frac{dp}{dx} = -\mu_e^2 \sigma W H^2$$

and

$$\frac{1}{k-1} W \frac{dp}{dx} + \frac{k}{k-1} p \frac{dW}{dx} = \mu_e^2 \sigma W^2 H^2,$$

we obtain after integration

$$\frac{W^2}{2} + \frac{k}{k-1} \frac{p}{\rho} = L$$

or

$$\frac{W^2}{2} + c_p T = c_p T_0 = \text{const.}$$

where c_p is the isobaric specific heat and T_0 is the stagnation temperature.

Consequently, the system of equations can be rewritten for $E = 0$

in the form

$$\rho W = m, \quad (2.1)$$

$$mW + p + \mu_e \frac{H^2}{2} = J, \quad (2.2)$$

$$c_p T + \frac{W^2}{2} = c_p T_0. \quad (2.3)$$

$$\mu_e \sigma W H = \frac{dH}{dx}. \quad (2.4)$$

3. In this formulation ($E = 0$) the problem can be solved with account of friction. If we consider flow between plane parallel infinite plates in the quasi-one-dimensional approximation, then by introducing the friction force in terms of the resistance coefficient ξ [3] and recognizing that the critical sound velocity $a_* = \sqrt{2kRT_0/(k+1)}$ is constant over the entire region of flow, the equation of motion can be written in the form

$$\frac{k+1}{k} \left(\frac{1}{\lambda^2} - 1 \right) \frac{d\lambda}{d\bar{x}} = \left(\xi + \frac{2\mu_e^2 b}{m} H^2 \right) \lambda, \quad (3.1)$$

where $\lambda = W/a_*$ is the velocity coefficient, $\bar{x} = x/b$, and b is the width of the channel.

If the magnetic Reynolds number $R_m = 2\mu_e \sigma W b \ll 1$, then we can assume that $H \approx H_0$ everywhere, where H_0 is the external homogeneous magnetic field. Then the solution of (3.1) has the form [4]

$$\left(\frac{2\mu_e^2 H_0^2 b}{m} + \xi \right) \bar{x} = x(\lambda_1) - x(\lambda), \quad (3.2)$$

where $\kappa(\lambda) = (k+1)/2k(2 \ln \lambda + 1/\lambda^2)$. For laminar flows, the order of the ratio of the first term in the brackets to the second is characterized by the square of the Hartmann number

$$N^2 = \frac{2\mu_e^2 H_0^2 b}{m\xi} \sim \frac{\mu_e^2 H_0^2 b^2}{p}.$$

If we take it into consideration that

$$m = \rho W = \rho_* a_* \cdot q(\lambda) = \rho_* a_* \cdot \left(\frac{k+1}{2} \right)^{\frac{1}{k-1}} \lambda \cdot \left(1 - \frac{k-1}{k+1} \lambda^2 \right)^{\frac{1}{k-1}},$$

then we can transform (3.2) to

$$\frac{R^*}{M_m^*} \left(1 + \frac{1}{N^2}\right) \cdot \bar{x} = g(\lambda_1) \cdot [x(\lambda_1) - x(\lambda)].$$

Here $R^* m = 2\mu_e \sigma a_* b$ and $M^* m = (a_* / H_0) \sqrt{\rho_* / \mu_e}$.

Figure 1 shows a plot of the critical length

$$\frac{R^*}{M_m^*} \bar{l}_c = \frac{1}{1 + \frac{1}{N^2}} g(\lambda_1) [x(\lambda_1) - x(\lambda)]$$

as a function of the velocity coefficient at the input to the channel, λ_1 , for different values of N . We see that at sufficiently large N the gasdynamic friction can be neglected compared with the "magnetic" friction.

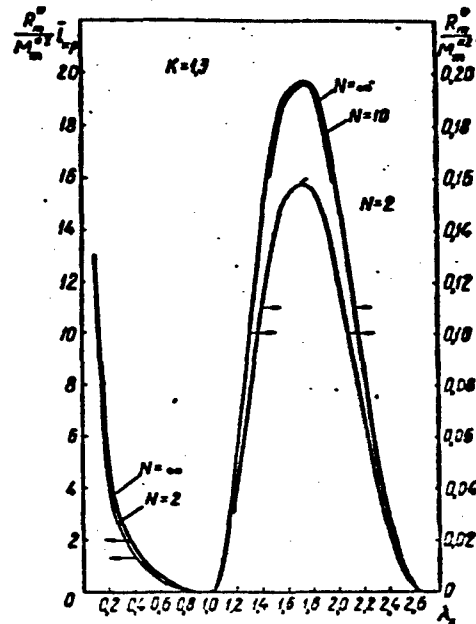


Fig. 1

If we take into account the induced magnetic field, then to obtain the solution it is sufficient to determine H from (3.1) and substitute it in the induction equation

$$\frac{1}{2} R^* \lambda \bar{H} = \frac{d\bar{H}}{dx}. \quad (3.3)$$

where $\bar{H} = H/H_1$, H_1 is the value of H at $\bar{x} = 0$.

The problem then reduces to solving the equation

$$R_m \lambda \left[\frac{k+1}{k} \left(\frac{1}{\lambda^3} - \frac{1}{\lambda} \right) \frac{d\lambda}{dx} - \frac{1}{\lambda} \right] = \frac{k+1}{k} \frac{d}{dx} \left[\left(\frac{1}{\lambda^3} - \frac{1}{\lambda} \right) \frac{d\lambda}{dx} \right]. \quad (3.4)$$

This equation reduces to the quadrature

$$\bar{x} = \int_{\lambda_1}^{\lambda} \frac{1-\lambda^2}{\lambda^3} \cdot \frac{d\lambda}{\theta(\lambda)}.$$

Here $\theta(\lambda)$ is the solution of the transcendental equation

$$\theta + \frac{k\xi}{k+1} \ln \left(\theta - \frac{k\xi}{k+1} \right) = - R_m \frac{1+\lambda^2}{\lambda} + C$$

and C is the integration constant.

By making several assumptions, we can obtain a solution in explicit form. Thus, if $0 < \theta - k\xi/(k+1) \leq 2$, then by expanding $\ln(\theta - k\xi/(k+1))$ in a series and retaining the first term of the expansion, we obtain a solution in the following form:

$$R_m \bar{x} = \frac{C_1}{2} \ln \frac{\lambda_1^2 (\lambda^2 - C_1 \lambda + 1)}{\lambda^2 (\lambda_1^2 - C_1 \lambda_1 + 1)} + \left(\frac{1}{\lambda} - \frac{1}{\lambda_1} \right) + \\ + \begin{cases} \sqrt{4 - C_1} \left(\arctg \frac{2\lambda - C_1}{\sqrt{4 - C_1}} - \arctg \frac{2\lambda_1 - C_1}{\sqrt{4 - C_1}} \right); & C_1 < 2 \\ \frac{4 - C_1^2}{2\sqrt{C_1 - 4}} \ln \frac{(2\lambda - C_1 - \sqrt{C_1 - 4})(2\lambda_1 - C_1 + \sqrt{C_1 - 4})}{(2\lambda - C_1 + \sqrt{C_1 - 4})(2\lambda_1 - C_1 - \sqrt{C_1 - 4})}; & C_1 > 2 \end{cases}. \quad (3.5)$$

$$\text{Here } R_m = \frac{R_m^*}{\frac{k\xi}{k+1} + 1} \text{ and } C_1 = \frac{C + \frac{k\xi}{k+1} \left(\frac{k\xi}{k+1} + 1 \right)}{R_m^*}.$$

4. If we neglect friction ($\xi \equiv 0$), then for any value of the magnetic Reynolds number R_m the equations (3.1) and (3.3) reduce to the quadrature

$$R_m^* \bar{x} = \int_{\lambda_1}^{\lambda} \frac{(\lambda^2 - 1) d\lambda}{\lambda^2 (\lambda^2 - B\lambda + 1)}, \quad (4.1)$$

which has two solutions of the form (3.8), for $B > 2$ and for $B < 2$.

Here $i = [2k/(k+1)] \cdot (J/m_a)$, where J is the constant of the magnetic analog of the Bernoulli equation (2.2). Consequently, the struc-

ture of the solution is determined by specifying the boundary conditions.

Let us analyze the boundary conditions. Equation (2.2) can be reduced to the form

$$\lambda + \frac{1}{\lambda} + \frac{k}{k+1} \cdot \frac{B^2}{M_m^2} = B, \quad (4.2)$$

where $M_m^* = (1/H_1) \sqrt{m a_* / \mu_e}$. Since when $\bar{x} = 0$ we have $\lambda = \lambda_1$ and $H = 1$, we get

$$B = \lambda_1 + \frac{1}{\lambda_1} + \frac{k}{k+1} \cdot \frac{1}{M_m^2}. \quad (4.3)$$

From (4.3) we can readily find the values of λ_1 , which determine, for fixed B , the interval of value λ_1 for which flow is possible. For this it is sufficient to put $M_m^* = \infty$ and find the roots (λ'_1 and λ''_1) of the equation

$$\lambda_1^2 - B\lambda_1 + 1 = 0. \quad (4.4)$$

Thus, the boundary conditions in the presence of a magnetic field cannot be specified arbitrarily, but must satisfy the following conditions

$$\left. \begin{aligned} & \frac{B}{2} + \sqrt{\frac{B^2}{4} - 1} > \lambda_1 > \frac{B}{2} - \sqrt{\frac{B^2}{4} - 1} \\ & B = \lambda_1 + \frac{1}{\lambda_1} + \frac{k}{k+1} \cdot \frac{1}{M_m^2} \end{aligned} \right\} \quad (4.5)$$

The region where flow can be realized is shown in Fig. 2; by way of an example, the same figure shows the region of flow for $M_m^* = 0.5$ between the branches of the dashed curve.

Since Eq. (4.4) has no roots when $B < 2$ (the roots are imaginary), the solution of Eq. (4.1) assumes the form

$$\begin{aligned} R \bar{x} = & \frac{B}{2} \ln \frac{\lambda_1^2 (\lambda_1^2 - B\lambda_1 + 1)}{\lambda^2 (\lambda_1^2 - B\lambda_1 + 1)} + \left(\frac{1}{\lambda} - \frac{1}{\lambda_1} \right) + \\ & + \frac{4 - B^2}{2\sqrt{B^2 - 4}} \ln \frac{(2\lambda_1 - B - \sqrt{B^2 - 4})(2\lambda_1 - B + \sqrt{B^2 - 4})}{(2\lambda_1 - B + \sqrt{B^2 - 4})(2\lambda_1 - B - \sqrt{B^2 - 4})}. \end{aligned} \quad (4.6)$$

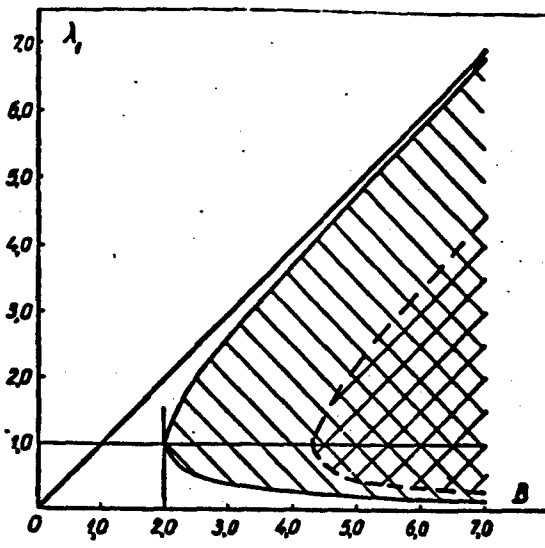


Fig. 2

For the magnetic field we obtain, accordingly,

$$\bar{H}^2 = \frac{\lambda_1 \cdot \lambda^2 - B\lambda + 1}{\lambda \cdot \lambda_1^2 - B\lambda_1 + 1}. \quad (4.7)$$

Figure 3 is a plot of the function

$$\bar{H}_{sp} = \sqrt{\frac{\lambda_1(2-B)}{\lambda_1^2 - B\lambda_1 + 1}}.$$

Here \bar{H}_{kr} is the value of the magnetic field intensity at the critical cross section. We see that a considerable intensification of the field occurs toward the critical cross section at values of λ_1 close to characteristic.

To determine the solution for the magnetic field in the form $H = \bar{H}(\bar{x})$, let us determine λ from (3.3) and substitute in (4.2):

$$\frac{d\bar{H}}{d\bar{x}} = \frac{\frac{R_m^2}{4} \bar{H}^2}{\frac{R_m}{2} \left(B - \frac{k}{k+1} \cdot \frac{\bar{H}^2}{M_{sp}^2} \right) \bar{H} - \frac{d\bar{H}}{dx}}. \quad (4.8)$$

This equation is a particular case of the equation to which the system (1.1-1.4) reduces in the general case [1].

Solving Eq. (4.8) with respect to $d\bar{H}/d\bar{x}$, we obtain an equation that reduces to a quadrature of the form

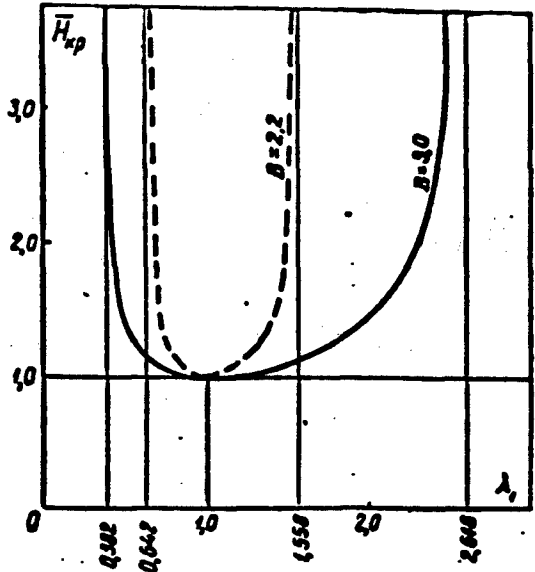


Fig. 3

$$\frac{R_m}{2} \bar{x} = \int_1^{\bar{H}} \frac{\frac{d\bar{H}}{\bar{H}}}{\left(B - \frac{k}{k+1} \cdot \frac{\bar{H}^2}{M_m^2}\right) - \sqrt{\left(B - \frac{k}{k+1} \cdot \frac{\bar{H}^2}{M_m^2}\right)^2 - 1}}.$$

Using the substitution

$$\sqrt{\left(B - \frac{k}{k+1} \cdot \frac{\bar{H}^2}{M_m^2}\right)^2 - 1} = t - \left(B - \frac{k}{k+1} \cdot \frac{\bar{H}^2}{M_m^2}\right),$$

we obtain a solution in the following form ($B > 2$):

$$R_m \bar{x} = B \cdot \ln \frac{t}{t^2 - 2Bt + 1} - \frac{1}{t} + \frac{B^2}{\sqrt{B^2 - 1}} \cdot \ln \frac{t - B - \sqrt{B^2 - 1}}{t - B + \sqrt{B^2 - 1}} + A,$$

where A is the integration constant, which is obtained from the boundary conditions ($\bar{x} = 0$, $\bar{H} = 1$).

In similar formulation ($E = 0$) but using a different method, the problem (4) was solved by I.B. Chekmarev [5].

5. Let us consider the quasi-one-dimensional flow of a compressible electrically conducting gas in magnetic and electric fields that cross at a right angle. The direction of gas flow coincides with the direction of the normal to the E-H plane.

Since we introduce in this case an additional parameter, the electric field intensity (E), then we can introduce in accordance with the π theorem of similitude theory [6] a supplementary similitude criterion.

The equation of motion in dimensionless form is [7]

$$\begin{aligned} \frac{I_0}{W_0 J_0} \cdot \frac{\partial \vec{W}_*}{\partial r_*} + (\vec{W}_* \cdot \nabla_*) \vec{W}_* &= -\nabla_* p_* + \\ + \frac{\mu_0}{\rho_0 W_0 J_0} \cdot \frac{\mu_0}{\rho_*} \left(\lambda_* \vec{W}_* + \frac{1}{3} \nabla_* \nabla_* \cdot \vec{W}_* \right) + \frac{\mu_0 E_* H_* I_0}{\rho_0 W_0^2} \cdot \frac{1}{\rho_*} [\vec{E}_* \vec{H}_*] + \\ + \frac{H_0^2 \sigma \mu_0^2}{\rho_0 W_0} \cdot \frac{1}{\rho_*} [[\vec{W}_* \vec{H}_*] \vec{H}_*]. \end{aligned} \quad (5.1)$$

Here the 0 subscript denotes scaled parameters and the * subscript denotes dimensionless parameters.

If the magnetic Reynolds number is $R_m = \mu_e \sigma W_0 l_0$ and the magnetic analog of the Mach number is $M_m = (W_0 / H_0) \sqrt{\rho_0 / \mu_e}$, then the dimensionless coefficient of the third term of the right half of (5.1) can be represented in the form

$$\frac{\mu_0 \sigma E_* H_* I_0}{\rho_0 W_0^2} = \frac{R_m}{M_m^2} \cdot \frac{E_0}{\mu_e H_0 W_*}.$$

The quantity $V = E_0 / \mu_e H_0$ has the dimension of velocity. Let us introduce the symbol

$$F = \frac{W}{V} = \frac{\mu_e H}{E}.$$

The physical meaning of the velocity V can be readily determined from the formula for the action law in the case of flow in magnetic and electric fields [8]:

$$(M^2 - 1) \frac{1}{W} \frac{dW}{dx} = - \frac{k \mu_e \sigma E H}{m a^2} (F - 1) \left(F - \frac{k-1}{k} \right).$$

In the critical cross section $F = 1$, i.e., $E = \mu_e W H$, the induced electric field is attenuated toward the outside. At velocities different from $V = E / \mu_e H$, acceleration or deceleration of the stream takes place, depending on the values of F and M . The flow conditions in such a formulation of the problem were considered in detail in a paper by Resler

and Sears [8].

Assuming $E = E_0 = \text{const}$ and $R_m \ll 1$ ($H = H_0 = \text{const}$), the problem has an analytic solution which is also the particular case of the general solution of the system (1.1-1.4).

Under the assumptions indicated above, the equation of motion and the energy equation can be written in the form

$$m \frac{dW}{dx} + \frac{dp}{dx} = \mu_r z (E_0 - \mu_r W H_0) H_0.$$

$$m \frac{d}{dx} \left(c_p T + \frac{W^2}{2} \right) = z E_0 (E_0 - \mu_r W H_0).$$

Combining these two equations and integrating, we obtain

$$\frac{1}{V} \left(c_p T + \frac{W^2}{2} \right) = W + \frac{p}{m} + A_1. \quad (5.2)$$

Using (5.2), we can transform the equation of motion into

$$\left[\frac{F-1}{1 - \frac{k}{k-1} F} + \frac{\frac{k}{k-1} \left(\frac{F^2}{2} - F + A_1 \right)}{\left(1 - \frac{k}{k-1} F \right)^2} + 1 \right] \frac{dF}{dx} = \frac{\mu_r^2 H_0^2 b}{m} (1 - F).$$

After integration, subject to boundary conditions $\bar{x} = 0$ $F = F_1$, we obtain

$$\begin{aligned} \frac{R_m}{M_m^2} \bar{x} &= z \ln \frac{1-F}{1-F_1} + \beta \ln \frac{\frac{k}{k-1} F - 1}{\frac{k}{k-1} F_1 - 1} + \\ &\quad + \gamma \left(\frac{1}{1 - \frac{k}{k-1} F} - \frac{1}{1 - \frac{k}{k-1} F_1} \right). \end{aligned}$$

where

$$z = \frac{1}{2} k(k-1)(2A_2 - 1) - 1,$$

$$\beta = [k^2(2A_2 - 1) + 1],$$

$$\gamma = \frac{1}{2} \left[2A_2 k - \frac{k^2 - 1}{k} \right] \times A_2 = -\frac{A_2}{V}.$$

REFERENCES

1. G.S. Golitsyn and K.P. Stanyukovich, ZhETF [Journal of Experimental and Theoretical Physics], 33, 6, 1957.
2. L.D. Landau and Ye.M. Lifshits, Elektrodinamika sploshnykh sred [Electrodynamics of Continuous Media], Fizmatgiz [State Publishing House For Literature on Physics and Mathematics], 1959.
3. S.A. Khristianovich (ed.), Prikladnaya gazovaya dinamika [Applied Gas Dynamics], 1948.
4. E.P. Zimin and Ye.I. Yantovskiy, Izvestiya AN SSSR, OTN, Mekhanika i mashinostroyeniye [Bulletin of the Academy of Sciences USSR, Division of Technical Sciences, Mechanics and Machine Building], 4, 1961.
5. I.B. Chekmarev, PMM [Applied Mathematics and Mechanics], 2, 1960.
6. L.I. Sedov, Metody podobiya i razmernosti v mekhanike [Methods of Similitude and Dimensional Analysis in Mechanics], 1958.
7. I.M. Kirko, Elektrichestvo [Electricity], 4, 1959.
8. Resler, Sears. JAS, 25, 4, 1958; collection of translations, Mekhanika [Mechanics], 6, 1958.

Manu-
script
Page
No.

[List of Transliterated Symbols]

108 $k_p = kr = kriticheskiy = critical$

FLOW OF VISCOUS CONDUCTING LIQUIDS IN PIPES
IN THE PRESENCE OF A MAGNETIC FIELD

S. A. Regirer
Vorkuta

§1

The present work is devoted to a study of laminar flow of a viscous incompressible liquid with finite conductivity in pipes, in the presence of a magnetic field.

Assume that a cylindrical pipe with generatrices parallel to the Oz axis has a cross section in the form of a connected region B, bounded by piecewise-smooth contours Σ_1 . Some of the boundaries can move uniformly along the Oz axis with a specified velocity. The liquid stream lines are assumed parallel to the same axis, and consequently $\vec{V} = \vec{i}_z v$, which corresponds to flow over a sufficient distance from the inlet portion. The pipe is placed in an external magnetic field, i.e., one independent of the flow, but which, however, can be distorted by the influence of the induced fields.

Let us write down the magnetohydrodynamic equations under the assumption that the physical properties of the liquid are constant and the processes stationary* [1]:

$$\rho(\vec{V}\nabla)\vec{V} = -\nabla p^* + \times(\vec{H}\nabla)\vec{H} + \tau A \vec{V} + \vec{F}_A \quad (1.1)$$

$$(\vec{V}\nabla)\vec{H} = (\vec{H}\nabla)\vec{V} + v_A A \vec{H}, \quad (1.2)$$

$$\operatorname{div} \vec{V} = 0, \quad \operatorname{div} \vec{H} = 0. \quad (1.3)$$

Here $p^* = p + \mu H^2/8\pi$, $\kappa = \mu/4\pi$, $\vec{F}_A = -\rho \beta T \vec{g}$ is the Archimedean force, and the remaining symbols are standard. If there is no free convection,

then $\vec{F}_A = 0$.

For nonisothermal flow one adds to the system (1.1-1.3) the energy equation

$$\rho(\vec{V}\nabla T) = kT + \Phi, \quad (1.4)$$

which contains the dissipation function

$$\Phi = \nu [|\operatorname{rot} \vec{V}|^2 + 2\operatorname{div}(\vec{V}\nabla)\vec{V}] + \nu_m |\operatorname{rot} \vec{H}|^2. \quad (1.5)$$

Let us agree further on some notation. First, we shall write $\vec{H} = \vec{H}_n + h\vec{i}_z$, where $\vec{H}_n = H_x\vec{i}_x + H_y\vec{i}_y$, thereby resolving the magnetic field into a planar (transverse) and axial (longitudinal) component. Further, we shall designate by the symbol \sim the planar component of a vector, for example, $\tilde{\nabla}p^* = \vec{i}_x \frac{\partial p^*}{\partial x} + \vec{i}_y \frac{\partial p^*}{\partial y}$.

Projecting Eqs. (1.1, 1.2) on the plane XOY and on the axis OZ we obtain, taking into account the new notation and the equality $\vec{V} = \vec{i}_z v$:

$$\tilde{\nabla}p^* = \nu \left[(\vec{H}_n \nabla) \vec{H}_n + h \frac{\partial \vec{H}_n}{\partial z} \right] + \tilde{\vec{F}}_A. \quad (1.6)$$

$$\nu \frac{\partial \vec{H}_n}{\partial z} = v_n \Delta \vec{H}_n. \quad (1.7)$$

$$\frac{\partial p^*}{\partial z} = \nu \left[\vec{H}_n \nabla h + h \frac{\partial h}{\partial z} \right] + \nu \Delta v + F_{Az}, \quad (1.8)$$

$$\nu \frac{\partial h}{\partial z} = \vec{H}_n \nabla v + v_n \Delta h, \quad (1.9)$$

and furthermore $v = v(x, y)$, which follows from the condition $\operatorname{div} \vec{V} = 0$.

Together with the continuity equation for the field

$$\operatorname{div} \vec{H}_n + \frac{\partial h}{\partial z} = 0 \quad (1.10)$$

and the energy equation

$$\rho v \frac{\partial T}{\partial z} = kT + \Phi \quad (1.11)$$

the equations (1.6-1.9) form a closed system.

The boundary conditions for this system are formulated in the usual manner, i.e., on the interface between the boundaries we have $v = U_1$, $\mu \vec{H}_{nr} = \mu \vec{H}_{nri}$, $\vec{H}_{n\tau} = \vec{H}_{n\tau i}$, $h = h_1$, $\vec{J}_n = \vec{J}_{ni}$, $\vec{E}_\tau = \vec{E}_{\tau i}$, $\alpha_1(T -$

$-T_1) + \rho_1(\partial T/\partial n - \partial T_1/\partial n) = \gamma_1$, where the subscript 1 designates quantities pertaining to the external regions B_1 and obeying, generally speaking, certain equations formulated separately for each specific problem. Usually the vectors \mathbf{j}_1 , \vec{H}_1 , \vec{E}_1 satisfy Maxwell's equations and the corresponding boundary conditions. As a rule, the value of the liquid flow $Q = \int \mathbf{v} dB$ is also specified.

In problems where free convection is disregarded ($\vec{F}_A = 0$), Eqs. (1.6-1.10) can be solved independently of the energy equation. If it is possible to obtain in some manner the transverse field vector \vec{H}_n , then Eqs. (1.8, 1.9) are linear in \mathbf{v} and h . For flows occurring under free convection conditions, it is necessary to know in addition to \vec{H}_n also the temperature gradient $\partial T/\partial z$ in the direction of motion and to neglect the energy dissipation due to the induced currents and viscosity. We then have likewise a linear system for the determination of \mathbf{v} , h , and T .

The determination of \vec{H}_n is in general very difficult, but an attempt can be made to find such particular cases, in which \vec{H}_n satisfies certain linear equations and the problem reduces to a successive solution of linear systems.

§2

Let us assume that the flow is isothermal ($\vec{F}_A = 0$) and that the transverse field vector \vec{H}_n does not vary in the flow direction, i.e., $\partial \vec{H}_n / \partial z = 0$. In this case it follows from (1.10) that $\partial^2 h / \partial z^2 = 0$, i.e., $h = h_0(x, y) + z\psi(x, y)$ and $\operatorname{div} \vec{H}_n = -\theta$. Substituting this result into (1.9) we obtain after separating the terms containing z ,

$$z\theta = \vec{H}_n \cdot \nabla \psi + v_n \Delta h_0 - \lambda \theta = 0. \quad (2.1)$$

It is also easy to see that $\nabla h = \nabla h_0 + z\nabla \psi + \vec{I}_z \psi$ so that we obtain from (1.8)

$$\frac{\partial \psi}{\partial z} = -(\vec{H}_n \cdot \nabla h_0 + h_0 \theta) + \tau \Delta \psi + C_1 z, \quad (2.2)$$

$$\vec{H}_a \nabla \theta + \Theta^2 = C_1, \quad (2.3)$$

where $C_1 = \text{const}$. The latter follows from an examination of the derivatives $\partial p^*/\partial z$, $\partial^2 p^*/\partial z^2$, which are calculated in accordance with (1.6) and (1.8), respectively. Let us further apply to Eq. (1.10) the operation of scalar multiplication by $\vec{\nabla}$, which yields, with allowance for the assumptions made and for Eq. (1.7),

$$\text{rot} \text{rot} \vec{H}_a + \nabla \theta = 0. \quad (2.4)$$

Putting $\text{rot} \vec{H}_a = -\vec{i}_z \vartheta(x, y)$ and taking into account the fact that ϵ is harmonic, we can readily show that ϑ is a harmonic function, which is conjugate to ϵ : $\partial \epsilon / \partial x = \partial \vartheta / \partial y$, $\partial \epsilon / \partial y = -\partial \vartheta / \partial x$. In this case ϑ determines, apart for a factor, the z component of the current density vector, since

$$\vec{j} = \frac{\epsilon}{4\pi} \text{rot} \vec{H} = \frac{\epsilon}{4\pi} \left(\vec{i}_x \frac{\partial h}{\partial y} - \vec{i}_y \frac{\partial h}{\partial x} - \vec{i}_z s \right).$$

It turns out that for the given field structure the axial component of \vec{j} depends only on the planar component of \vec{H} and the planar component of \vec{j} only on the axial component of \vec{H} .

Let us apply, finally, the curl operation to Eq. (1.6), after which we obtain

$$\text{rot}(\vec{H}_a \vec{\nabla}) \vec{H}_a = -\vec{i}_z (\vec{H}_a \nabla \vartheta - \vartheta \theta) = 0. \quad (2.5)$$

Thus, the quantities H_x , H_y , ϵ , and ϑ are connected by the following four relations:

$$\begin{aligned} \text{div} \vec{H}_a &= -\theta, \quad \text{rot} \vec{H}_a = -\vec{i}_z \vartheta, \quad \vec{H}_a \nabla \theta + \theta^2 = C_1, \\ \vec{H}_a \nabla \vartheta - \vartheta \theta &= 0, \end{aligned} \quad (2.6)$$

where ϵ and ϑ are conjugate harmonic functions. This system has the simple solution $\epsilon = \text{const}$, $\vartheta = \text{const}$ with one constant having zero value and the other specified. We shall prove here that there exist no other solutions with respect to θ and ϑ .

Let us assume that ϵ and ϑ are not constant. Combining the first

and last equations in (2.6) we can write $\vec{H}_n = (1/\vartheta) \operatorname{rot} \vec{i}_z L(x, y)$. Introducing this expression into the last two equations of (2.6) and solving them with respect to $\operatorname{rot} \vec{i}_z L$ we obtain

$$\operatorname{rot} \vec{i}_z L = \frac{\vartheta^2 \nabla \vartheta + (C_1 - \theta^2) \vartheta \nabla \theta}{W} = -\frac{\vec{i}_z \times \nabla q}{2W}, \quad (2.7)$$

where $q = \vartheta^2(C_1 - \theta^2)$, $W = |\nabla \vartheta|^2$. It follows therefore that

$$\operatorname{div} \frac{\vec{i}_z \times \nabla q}{2W} = -\vec{i}_z \cdot \operatorname{rot} \frac{\nabla q}{2W} = 0.$$

Inasmuch as the second factor is collinear with \vec{i}_z , we have $\operatorname{rot}(\nabla q/2W) = 0$ and we arrive after some calculations to the necessity of the equality $W = F(q)$, where F is an arbitrary function. By using the representation of \vec{H}_n introduced above, we can further transform the second equation in (2.6) into

$$-\frac{\nabla \vartheta}{\vartheta^2} \times \operatorname{rot} \vec{i}_z L + \frac{1}{\vartheta} \operatorname{rot} \operatorname{rot} \vec{i}_z L = -\vec{i}_z \vartheta. \quad (2.8)$$

Substituting into the first and second terms, respectively, the first and second expressions for $\operatorname{rot} \vec{i}_z L$ from (2.7) we get after simplification

$$\frac{\Delta q}{2W} - \frac{\nabla q \cdot \nabla W}{W^2} = C_1 - \theta^2 + \vartheta^2. \quad (2.9)$$

Elementary calculation shows that $\Delta q = 2W(C_1 - \theta^2 - \vartheta^2)$, $\nabla W = F'(q)\nabla q$, $|\nabla q|^2 = 4W[(C_1 - \theta^2)^2 \vartheta^2 + \vartheta^4 \theta^2]$. We can therefore write ultimately in place of (2.9)

$$\frac{2F(q)}{F'(q)} = -\frac{1}{(C_1 - \theta^2)^2 - \vartheta^2 \theta^2}. \quad (2.10)$$

The right half should be a function of q only, and this is impossible unless θ and ϑ are constants. This completes the proof. Thus, if the transverse field vector \vec{H}_n is invariant in the flow direction, then it is either solenoidal with constant curl or potential with constant divergence. In either case, the first two equations of (2.6), which are linear, are used to determine \vec{H}_n , while v and h are determined from

(2.1) and (2.2). This attains the purpose designated in §1.

Further analysis of the equations, for a solenoidal transverse field, is given in the author's note [2]. There are several known investigations dealing with flows of this type. Particular solutions of problems involving the flow between parallel plates with $\bar{H}_n = \text{const}$ were obtained by Hartmann [3], Lehnert [4], and were subsequently cited in many papers [1, 5, 6]. Shercliff [7] considered flow in a rectangular tube for a homogeneous transverse field. I.B. Chekmarev [8] and Globe [9] solved the problem for an annular tube with $H_\varphi = 0$, $H_r \sim 1/r$. In all the mentioned problems it was assumed that $\theta = v = 0$, i.e., there was no current in the direction of the flow. By way of a further example we can point out the possibility of investigating the generalized Couette flow between cofocal elliptical cylinders by introducing curvilinear coordinates.

For a potential transverse field, solutions of some specific problems are also known. Thus, for a round pipe when $H_\varphi = 0$, $H_r \sim r$, a solution was obtained by Pai [10]. The problem for a half space and a flat pipe with inhomogeneous transverse field, linearly dependent on the transverse coordinate, was considered by the author [11]. No other simple solutions were found.

To conclude the section we must point out that the possibility of reducing the problem to linear equations is not limited to the case when $\partial \bar{H}_n / \partial z = 0$. However, solutions with any degree of simplicity are apparently obtained only under this assumption.

§3

The analysis carried out in the present paper admits of several useful generalizations for nonisothermal flows. The case of forced convection is in principle the simplest, since the energy equation is linear in the temperature. R. Zigel' [12] and the author [13] gave ex-

amples of solutions of problems of this type. Great interest is attached to the solution of the problem of the Graetz-Nusselt type, which for a flat pipe reduces to the Mathieu equation. As indicated above, free convection phenomena are somewhat more complicated to analyze. It is possible, however, to prove in general form that in the case of negligibly small energy dissipation, as in ordinary hydrodynamics [14], straight line motion in a vertical pipe is possible only for a vertical constant temperature gradient, while for an inclined pipe with closed cross section this motion should be equal to zero. Problems concerning free convection in pipes were considered, for example, in [15-17]. It is possible also to obtain some exact solutions for axially symmetrical problems. It is possible to obtain simultaneously the conditions for the stable equilibrium of an unevenly heated liquid in a vertical channel.

REFERENCES

1. L.D. Landau and Ye.M. Lifshits, Elektrodinamika sploshnykh sred [Electrodynamics of Continuous Media], Gostekhizdat [State Publishing House for Theoretical and Technical Literature], Moscow, 1957.
2. S.A. Regirer, PMM [Applied Mathematics and Mechanics], 24, 3, 541, 1960.
3. J. Hartmann. Mat. fys. Medd. 15, 6, 1937.
4. B. Lehnert. Arkiv fys., 5, 1 - 2, 69, 1952.
5. T. Kauling, Magnitnaya gidrodinamika [Magnetohydrodynamics], Izd-vo inostr. lit. [Foreign Literature Press], Moscow, 1959.
6. R. Lock. Proc. Roy. soc., 233A, 105, 1955.
7. J.A. Shercliff. Proc. Cambr. phil. soc., 49, 1, 136, 1953.
8. I.B. Chekmarev, Nauchno-tekhn. inform. byull. LPI [Scientific-Technical Information Bulletin of Leningrad Polytechnic Institute],

- 8, 1959 - Physical-Mathematical Sciences Division 43.
9. S. Globe. Phys. of Fluids, 2, 4, 404, 1959.
 10. S.I. Pai. J. appl. phys., 25, 9, 1205, 1954.
 11. S.A. Regirer, PMM, 24, 2, 383, 1960.
 12. R. Zigel', collected translations, Mekhanika [Mechanics], 3 (55), 65, 1959.
 13. S.A. Regirer, PMM, 23, 5, 948, 1959.
 14. G.A. Bugayenko, PMM, 17, 4, 496, 1953; 18, 2, 212, 1954.
 15. G.Z. Gershuni and Ye.M. Zhukovitskiy, ZhETF [Journal of Experimental and Theoretical Physics], 34, 3, 670, 1958.
 16. Ye.M. Zhukovitskiy, Fizika met. i metalloved. [Physics of Metals and Metallography], 6, 3, 385, 1958.
 17. S.A. Regirer, ZhETF, 37, 1, 212, 1959.

Manu-
script
Page
No.

[Footnote]

116 It is not essential for what follows to assume that the flow is stationary. All the arguments can be readily carried over to the nonstationary case.

SELF-SIMILAR SOLUTIONS OF THE MAGNETOHYDRODYNAMIC EQUATIONS

N. I. Pol'skiy, I. T. Shvets
Kiev

In many magnetohydrodynamic problems the magnetic field induced by the electric current in the liquid is negligibly small compared with the applied magnetic field. As shown in [1], such a situation obtains, for example, in the problem involving the investigation of flow in the vicinity of the critical point of a blunt-nose body in a supersonic stream. The reason why the applied magnetic field is practically undistorted by the electric currents in the liquid lies in the small values of the magnetic Reynolds numbers.

Neglecting the distortion of the applied magnetic field, we can greatly simplify the system of magnetohydrodynamic equations and reduce the problem to an investigation of boundary layer equations, in which the ponderomotive force due to the action of the magnetic field is suitably taken into account. In investigations of heat exchange it is necessary, generally speaking, to include the Joule dissipation in the energy equation.

We consider below precisely such a system of differential equations for a laminar boundary layer in the presence of heat exchange.

In addition to Reference [1] cited above, such a system of equations was used also in [2, 3] under certain assumptions.

In all these investigations, self-similar solutions were sought. In [2], in particular, it was shown that for a compressible gas self-similar solutions can be obtained in the case when the velocity out-

side the boundary layer and the magnetic field intensity vary along the body in the stream in accordance with interrelated expressions in powers of suitably chosen variables (and not in the initial physical plane). It was further assumed every time that the magnetic field intensity does not vary transversely to the boundary layer.

A method can be indicated for determining all the possible self-similar solutions and to obtain some new solutions. The general pattern for finding such solutions was indicated by us in [4], where cases of compressible and incompressible liquids were considered. We shall make here a few additional remarks pertaining to [4]. For the sake of simplicity we confine ourselves to the case of an incompressible liquid. The extension of the methods employed to the case of a compressible liquid is given in [4].

We write down the initial system of differential equations for a laminar boundary layer in an incompressible liquid in the form

$$\begin{aligned} u \frac{\partial u}{\partial x} + v \frac{\partial u}{\partial y} &= -\frac{1}{\rho} \frac{dp}{dx} + v \frac{\partial^2 u}{\partial y^2} - \frac{\sigma}{\rho} B^2 u; \quad \frac{\partial u}{\partial x} + \frac{\partial v}{\partial y} = 0; \\ u \frac{\partial \theta}{\partial x} + v \frac{\partial \theta}{\partial y} &= \frac{\nu}{Pr} \frac{\partial^2 \theta}{\partial y^2} + v \left(\frac{\partial u}{\partial y} \right)^2 + \frac{\sigma}{\rho} B^2 u^2. \end{aligned} \quad (1)$$

Here $\Theta(x, y)$ is the difference between the enthalpy per unit mass at the point x, y of the boundary layer and in the external stream; the other symbols are standard. The last term in the equation of motion characterizes the magnetic ponderomotive force, and the last two terms in the energy equation characterize the viscous and Joule dissipation, respectively.

The boundary conditions are

$$\begin{aligned} u(x, 0) &= v(x, 0) = 0; \quad u(x, \infty) = U_e(x); \quad \Theta(x, 0) = \tau(x); \\ \Theta(x, \infty) &= 0. \end{aligned}$$

We note immediately that by virtue of the presence of ponderomotive magnetic forces in the external stream, the distribution of the

velocities $U_e(x)$ outside the layer is not connected with the pressure by means of the Bernouli equation. In other words $-U_e'(x)U'_e(x) \neq -dp/\rho dx$.

Let \underline{x} and x^* be two arbitrary points on the stream-over profile in the \underline{x}, y plane. In this case $u(x, y)$, $\Theta(x, y)$ and $u(x^*, y)$, $\Theta(x^*, y)$ are the corresponding profiles of the quantities u and Θ in the indicated points. The question arises whether it is possible to carry out along the axes y , u , and Θ similarity transformations (with generally speaking different coefficients of extension or contraction), such that the profiles $u(x, y)$ and $\Theta(x, y)$ become exactly congruent with the profiles $u(x^*, y)$ and $\Theta(x^*, y)$. The similarity coefficients for fixed x^* are, of course, functions of \underline{x} . If the indicated transformation is possible for any \underline{x} , then it is stated that the problem has a similar or self-similar solution.

In accordance with the results of [5, 6], the determination of all the self-similar solutions is equivalent to finding all those sets of functions $U(x)$, $\tau(x)$, $K(x)$ for which

$$u(x, y) = U(x)\varphi(\xi); \quad \Theta(x, y) = \tau(x)g(\xi); \quad \xi = yK(x) \quad (2)$$

and the initial differential equations (1) become ordinary differential equations for the functions $\varphi(\xi)$ and $g(\xi)$ in the variable ξ . In the given case we must add that we are seeking in addition to the sets of functions $U(x)$, $\tau(x)$, $K(x)$ also all possible functions $B(x)$.

The boundary conditions for the functions $\varphi(\xi)$ and $g(\xi)$ assume in this case the form

$$\varphi(0) = \varphi'(0) = 0; \quad \varphi'(\infty) = C; \quad g(0) = 1; \quad g(\infty) = 0, \quad (3)$$

where the constant $C > 0$ has not yet been determined. From the first equation in (2) it merely follows that

$$U_e(x) = CU(x) \quad (4)$$

It is easy to see that the continuity equation is satisfied if we

put along with (2)

$$\nu(x, y) = \left\{ \frac{U K'}{K^2} - \frac{U}{K} \right\} \tau(\xi) - \frac{U K'}{K^2} \xi \tau'(\xi). \quad (5)$$

Substituting (2) and (5) in (1), we obtain after simple transformations

$$\tau'' - \left\{ 1 - \frac{U K'}{U' K} \right\} \tau''' = \frac{1}{U U'} \left\{ - \frac{1}{\rho} \frac{dp}{dx} \right\} + \frac{K^2}{U'} \tau'''' + \frac{\alpha B^2}{\rho U'} \tau'; \quad (6)$$

$$\frac{U \tau'}{U' \tau} g \tau' - \left\{ 1 - \frac{U K'}{U' K} \right\} g' \tau = \frac{\alpha K^2}{\rho U' \tau} g'' + \frac{\alpha B^2 U^2}{\rho U' \tau} \tau'' + \frac{U^2 K^2}{\tau U'} \tau'''.$$

It is easy to verify that Eqs. (6) will be ordinary differential equations if and only if

$$\frac{1}{U U'} \left\{ - \frac{1}{\rho} \frac{dp}{dx} \right\} = \text{const} \quad (7)$$

and, under suitable normalization of the function $K(x)$

$$1 - \frac{U K'}{U' K} = \frac{1}{\beta}; \quad \frac{K^2}{U'} = \frac{1}{\beta}; \quad \frac{U^2}{\tau} = \alpha; \quad \frac{U \tau}{U' \tau} = \gamma, \quad (8)$$

where α , β , and γ are constants. In addition, the quantity $\alpha B^2 / \rho U'$ should be a function of ξ only.

Inasmuch as the function $U(x)$ is connected with the still undetermined constant C by means of Eq. (4), and $U(x)$ is determined below with accuracy to within a constant factor, we can assume without loss of generality that the constant in the right half of (7) is equal to unity. In other words, this means that the function $U(x)$, unlike the function $U_e(x)$, is connected with the pressure $p(x)$ by the Bernoulli equation.

If we retain at least one of the last two terms characterizing the dissipation in the energy equation, then $\alpha \neq 0$ and it follows from the last equations in (8) that $\gamma = 2$. On the other hand, if there are no dissipative terms, then there is no combination $U^2/\tau = \alpha$ in (6), i.e., we can assume that in the system (6) $\alpha = 0$ and γ is arbitrary.

As in [6, 7], we can determine from (8) those functions $U(x)$, $\tau(x)$,

$K(x)$, for which self-similar solutions are possible. Namely

$$U \sim x^\beta, \quad \left(\beta = \frac{2n}{n+1} \right) \quad \text{or} \quad U \sim e^{\alpha x}, \quad (\beta = 2); \quad z \sim U^\beta. \quad (9)$$

In addition, $K \sim \sqrt{U'}$ and $\gamma = 2$ in the presence of dissipative terms.

On the basis of (6) we can readily understand that self-similar solutions are possible only when the magnetic parameter

$$\zeta = \frac{\sigma}{\rho} \frac{B^2}{U^\beta}$$

is constant. From this it follows in accordance with (9) that

$$B(x) \sim x^{\frac{n}{\beta}} \quad \text{or} \quad B(x) \sim e^{\frac{\alpha x}{\beta}}. \quad (10)$$

If Conditions (9) and (10) are satisfied, the equations in (6) turn into ordinary differential equations

$$\begin{aligned} \varphi''' + \gamma \varphi'' &= \beta(\varphi'' - 1) + \zeta \varphi'; \\ \frac{1}{P_f} g'' + g' \varphi - \beta \gamma g \varphi' + \alpha \varphi''' + \alpha \zeta \varphi'' &= 0, \end{aligned} \quad (11)$$

which describe self-similar solutions. The boundary conditions are given in (3). In addition, on the basis of the foregoing, $\gamma = 2$ if $\alpha \neq 0$.

If we go to the limit of $\xi \rightarrow \infty$ in Eq. (11), we obtain

$$\beta(C - 1) + \zeta C = 0.$$

In the absence of interaction between the magnetic field and the current, $\zeta = 0$. Then $C = 1$ and on the basis of (4) $U_e = U$.

We note that we have listed above all the possible self-similar solutions of (1) with the exception of two cases. The point is that in the derivation of the equations in (6) we divided by U' , i.e., we assumed that $U \neq \text{const}$, and in the conditions (8) we excluded the case $1 - UK'/U'K = 0$, i.e., $\beta = \infty$. In both these cases it is also possible to obtain self-similar solutions. We note that in the first case we obtain the solution of the problem concerning longitudinal flow over a plate. These cases were considered in [4].

This covers completely the question of finding the self-similar solutions of the system of equations (1).

As indicated above, an analogous problem which includes also the case of a compressible liquid is considered in [4].

REFERENCES

1. R.C. Mayer. J. Aero-Space Sci., 25, 9, 1958.
2. P.S. Lykoudis. Preprints of the heat transfer and fluid. Mech. inst. Stanford 1958.
3. P.S. Lykoudis. J. Aero-Space Sci., 26, 5, 1959.
4. N.I. Pol'skiy and I.T. Shvets, DAN SSSR [Proceedings of the Academy of Sciences USSR], 136, 5, 1961.
5. N.I. Pol'skiy, Sb. trudov Instituta teploenergetiki AN USSR [Collected Transactions of the Thermal-Power-Engineering Institute of the Academy of Sciences Ukrainian SSR], 14, 1958.
6. N.I. Pol'skiy, Izvestiya vyssh. ucheb. zaved., Seriya "Aviatsionnaya tekhnika" [Bulletin of the Higher Educational Institutions, Series entitled Aviation Engineering], 3, 1959.

QUASI-SUPERIMPOSABLE FIELDS OF FINITE AMPLITUDE
IN NONIDEAL MAGNETOHYDRODYNAMICS

V.S. Tkalich

Sukhumi

1. The system of magnetohydrodynamic equations for an incompressible nonideal liquid has in nondimensional variables the form [1, 2]

$$\left. \begin{aligned} \frac{\partial \vec{h}}{\partial t} + (\vec{v} \nabla) \vec{h} &= (\vec{h} \nabla) \vec{v} + \mu_0 \vec{M}, \quad \operatorname{div} \vec{h} = 0, \\ \frac{\partial \vec{v}}{\partial t} + (\vec{v} \nabla) \vec{v} + \nabla p &= (\vec{h} \nabla) \vec{h} + \mu \vec{M}, \quad \operatorname{div} \vec{v} = 0. \end{aligned} \right\} \quad (1.1)$$

The physical quantities in the absolute Gaussian system of units are related with the introduced dimensionless units (μ_0 , μ , x_1 , t , \vec{v} , \vec{h} , p) in the following fashion: the coordinates are ($x_1 L$); the time is ($t T$); the velocity is ($\vec{v} L/T$); the magnetic field is ($\vec{h} \sqrt{4\pi \rho L/T}$); the total pressure is $p \rho (L/T)^2 \equiv \Pi + F + (\vec{h} \sqrt{4\pi \rho L/T})^2 / 8\pi$, where Π is the ordinary hydrodynamic pressure, F the potential of the external forces and ρ the density; L and T are certain characteristic constants with dimensions of length and time. The quantities μ and μ_0 are the reciprocals of the analog of the ordinary and magnetic Reynolds numbers [2]

$$\mu \equiv \gamma T / L^2, \quad \mu_0 \equiv c^2 T / 4\pi \rho L^2,$$

where γ is the kinematic viscosity coefficient, c the velocity of light, and σ the conductivity.

2. Quasi-superimposable fields. We denote by \underline{a} the complete set of sought functions of the system (1.1)

$$\underline{a} \equiv (\vec{h}, \vec{v}, p). \quad (2.1)$$

Let $\underline{a} = A_0$, where

$$A_0 \equiv (\vec{H}_0, \vec{V}_0, P_0) - \quad (2.2)$$

is a certain known solution of the system (1.1). It is then advantageous to seek a certain class of solutions of the system (1.1) in the form

$$a = A_0 + A, \quad (2.3)$$

where A is a new set of the sought physical quantities

$$A \equiv (\vec{H}, \vec{V}, P), \quad (2.4)$$

connected with the initial set as follows:

$$\vec{h} = \vec{H}_0 + \vec{H}, \quad \vec{v} = \vec{V}_0 + \vec{V}, \quad p = P_0 + P. \quad (2.5)$$

If the following conditions hold true

$$(\vec{V}\nabla)\vec{V} = (\vec{V}\nabla)\vec{H} = (\vec{H}\nabla)\vec{V} = (\vec{H}\nabla)\vec{H} = 0, \quad (2.6)$$

then, using (1.1) and (2.2-2.5) we obtain a system of equations that are linear in A

$$\left. \begin{aligned} D_0\vec{H} - (\vec{H}\nabla)\vec{V}_0 &= (\vec{H}_0\nabla)\vec{V} - (\vec{V}\nabla)\vec{H}_0, & \text{div } H = 0, \\ D\vec{V} + (\vec{V}\nabla)\vec{V}_0 + \nabla P &= (\vec{H}_0\nabla)\vec{H} + (\vec{H}\nabla)\vec{H}_0, & \text{div } V = 0, \end{aligned} \right\} \quad (2.7)$$

with generally speaking variable coefficients. D and D_0 are the linear differential operators

$$D \equiv \partial/\partial t + (\vec{V}_0\nabla) - \mu_1 \Delta, \quad D_0 \equiv \partial/\partial t + (\vec{V}_0\nabla) - \mu_0 \Delta. \quad (2.8)$$

If the conditions (2.6) are valid for any solution A from a certain class of solutions $\{A\}$ of the system (2.7) then by virtue of the linearity, the superposition principle holds for A .

The field $a \equiv A_0 - A$, which consists of the "main" field A_0 and the superimposed field A , will be called "quasi-superimposable." Fields of this type were investigated in magnetohydrodynamics and in multi-component magnetohydrodynamics [3/4]. Superimposable fields (and fields close to them) were considered previously [1, 5-10] from different points of view.

3. One-dimensional fields. If the vector fields \vec{H} and \vec{V} are one dimensional and are independent of x_1 (the analysis is carried out in a rectangular coordinate system)

$$\vec{H} = \vec{e}_1 H(x_2, x_3, t), \quad \vec{V} = \vec{e}_1 V(x_2, x_3, t). \quad (3.1)$$

then the linearity conditions (2.6), and also the solenoidal conditions (2.7), are satisfied identically.

Let us stipulate that each term in the system (2.7) be independent of x_1 . We consider one characteristic term from each group

$$(\vec{V}_0 \nabla) \vec{V} = \vec{e}_1 (V_{0\alpha} \partial / \partial x_\alpha) V, \quad (\vec{V} \nabla) \vec{V}_0 = V \partial \vec{V}_0 / \partial x_1, \quad (3.2)$$

where summation from 2 to 3 over repeated Greek letter indices is implied. It follows from the first relation in (3.2) that only V_{01} can depend on x_1 , and from the second relation it follows that the dependence can be only linear. Analogous conclusions hold true also for the vector \vec{H}_0 . Consequently, we can put

$$\vec{H}_0 = (B_0 + x_1 B_1) \vec{e}_1 + \vec{H}_0^*, \quad \vec{V}_0 = (U_0 + x_1 U_1) \vec{e}_1 + \vec{V}_0^* \quad (3.3)$$

The asterisk on the vector symbol denotes that the vector is parallel to the plane (x_2, x_3) . The quantities $B_0, B_1, \vec{H}_0^*, U_0, U_1, \vec{V}_0^*$ are independent of x_1 . Substituting (3.3) in (3.2) we obtain

$$(\vec{V}_0 \nabla) \vec{V} = \vec{e}_1 (\vec{V}_0 \nabla) V, \quad (\vec{V} \nabla) \vec{V}_0 = \vec{e}_1 U_1 V,$$

consequently all the vector terms in the system (2.7) are directed along the first axis. Therefore the pressure P has the form

$$P = Q(t) + x_1 Q_1(t), \quad (3.4)$$

where Q and Q_1 are arbitrary functions of the time.

Substituting (3.1, 3.3) and (3.4) in (2.7) we obtain the following closed system of equations, which are linear in A :

$$(D_0^* - U_1) H = [(\vec{H}_0^* \nabla) - B_1] V, \\ (D^* + U_1) V + Q_1(t) = [(\vec{V}_0^* \nabla) + B_1] H. \quad (3.5)$$

The operators D^* and D_0^* are obtained by making the substitution $(\vec{V}_0 \nabla) \rightarrow (\vec{V}_0^* \nabla)$ in Expressions (2.8) for D and D_0 .

Choosing the pressure P_0 in the form

$$P_0 = Q_0(x_2, x_3, t) + x_1 Q_{01}(t) + \frac{x_1^2}{2} Q_{02}(t) \quad (3.6)$$

and substituting the expressions (3.3, 3.6) for the main field A_0 in the system (1.1), resolving into components, and equating to zero the coefficients of x_1 , we obtain

$$\left. \begin{aligned} D_v^* \vec{H}_0 &= (\vec{H}_0 \nabla) \vec{V}_0, \quad D^* \vec{V}_0 + \nabla^* Q_0 = (\vec{H}_0 \nabla) \vec{H}_0 \\ D_v^* B_1 &= (\vec{H}_0 \nabla) U_1, \quad D^* U_1 + U_1^2 + Q_{01}(t) = (\vec{H}_0 \nabla) B_1 + B_1^2, \\ (D_v^* - U_1) B_0 &= [(\vec{H}_0 \nabla) - B_1] U_0, \end{aligned} \right\} \quad (3.7)$$

$$\left. \begin{aligned} (D^* + U_1) U_0 + Q_{01}(t) &= [(\vec{H}_0 \nabla) + B_1] B_0 \\ U_1 &= -\partial V_{0a}/\partial x_a, \quad B_1 = -\partial H_{0a}/\partial x_a. \end{aligned} \right\} \quad (3.8)$$

Let us transform the system (3.7). Using (3.8), we eliminate from it B_1 and U_1 . Taking the divergence of the first equation, we obtain the third. Taking the divergence of the second equation, we reduce the fourth to a simpler form. We obtain a system of five equations

$$\left. \begin{aligned} D_v^* \vec{H}_0 &= (\vec{H}_0 \nabla) \vec{V}_0, \quad D^* \vec{V}_0 + \nabla^* Q_0 = (\vec{H}_0 \nabla) \vec{H}_0 \\ \Delta Q_0 + Q_{02}(t) + \left(\frac{\partial V_{0a}}{\partial x_a} \right)^2 + \frac{\partial V_{0a}}{\partial x_3} \frac{\partial V_{03}}{\partial x_a} &= \left(\frac{\partial H_{0a}}{\partial x_a} \right)^2 + \\ &+ \frac{\partial H_{03}}{\partial x_a} \frac{\partial H_{0a}}{\partial x_3}, \end{aligned} \right\} \quad (3.9)$$

which contains five unknown functions (H_{0a} , V_{0a} , Q_0) of the coordinates and of the time, which can be solved independently of the remaining equations. Solving this system, we determine B_1 and U_1 from (3.8); to determine B_0 and U_0 we obtain a system of two linear equations

$$\left. \begin{aligned} \left(D_v^* + \frac{\partial V_{0a}}{\partial x_a} \right) B_0 &= [(\vec{H}_0 \nabla) + \partial H_{0a}/\partial x_a] U_0 \\ (D^* - \partial V_{0a}/\partial x_a) U_0 + Q_{01}(t) &= [(\vec{H}_0 \nabla) - \partial H_{0a}/\partial x_a], \end{aligned} \right\} \quad (3.10)$$

which coincides with (3.5), apart from the symbols; consequently, the part ($B_0 \vec{e}_1$, $U_0 \vec{e}_1$, $Q_{01} x_1$) of the main field A_0 "belongs" simultaneously to the superimposable class $\{A\}$. We shall henceforth regard this part as belonging to $\{A\}$; without loss of generality we can put $B_0 = U_0 = Q_{01} = 0$.

If the main field A_0 is chosen in the form

$$\vec{H}_0 = \vec{H}_0^* = \text{const.}, \quad \vec{V}_0 = \vec{V}_0(t), \quad P_0 = Q_{00}(t) - \vec{r} d\vec{V}_0/dt, \quad (3.11)$$

where \vec{H}_0^* is an arbitrary constant while $\vec{V}_0^*(t)$ and $Q_{00}(t)$ are arbitrary functions of the time, then the system (3.8-3.10) is identically satisfied. For the superimposable field A we obtain from (3.5) the system

$$D^*H = (\vec{H}_0^*\nabla)\vec{V}, \quad D^*V + Q_1(t) = (\vec{H}_0^*\nabla)H, \quad (3.12)$$

which coincides when $\vec{V}_0^* \equiv 0$ with that given by Shercliff [5]. If $\vec{H}_0^* = 0$, then the system (3.12) splits up into two independent equations

$$D^*H = 0, \quad D^*V + Q_1(t) = 0. \quad (3.13)$$

4. Two-dimensional fields. If the vector fields \vec{H} and \vec{V} are two dimensional and are independent of (x_2, x_3)

$$\vec{H} = \vec{H} = \vec{H}(x_1, t), \quad \vec{V} = \vec{V} = \vec{V}(x_1, t), \quad (4.1)$$

then both the linearity conditions (2.6) and the solenoidal conditions (2.7) are satisfied identically.

Let us stipulate that all the terms in (2.7) be independent of x_2 and x_3 . Considering typical terms

$$(\vec{V}\nabla)\vec{V} = V_{01}\partial\vec{V}/\partial x_1, \quad (\vec{V}\nabla)\vec{V}_0 = V_{01}\partial\vec{V}_0/\partial x_1, \quad (4.2)$$

we obtain from the first relation in (4.2) that only \vec{V}_0 can depend on (x_2, x_3) . From the second equation it follows that the dependence on (x_2, x_3) can only be linear. Similar conclusions hold true also for the vector \vec{H}_0 . Consequently the fields \vec{H}_0 and \vec{V}_0 have the form

$$\vec{H}_0 = H_{01}\vec{e}_1 + \vec{B}_0 + x_2\vec{B}_a, \quad \vec{V}_0 = V_{01}\vec{e}_1 + \vec{U}_0 + x_2\vec{U}_a, \quad (4.3)$$

where H_{01} , V_{01} , \vec{B}_0 , \vec{U}_0 , \vec{B}_a , \vec{U}_a are independent of (x_2, x_3) with the vectors \vec{B}_0 , \vec{U}_0 , \vec{B}_a , \vec{U}_a parallel to the plane (x_2, x_3) .

Since all the terms in (2.7) do not have a first component and are independent of (x_2, x_3) , the pressure P has the form

$$P = Q(t) + x_2Q_a(t), \quad (4.4)$$

where Q and Q_a are functions of the time.

Substituting (4.1, 4.3) and (4.4) in (2.7), we obtain a closed

system consisting of two vector linear equations

$$\left. \begin{aligned} D_0^1 \vec{H}_0 - \vec{U}_0 H_0 &= H_{01} \partial \vec{V}_0 / \partial x_1 - \vec{B}_0 V_0, \\ D^1 \vec{V}_0 + \vec{U}_0 V_0 + \vec{Q}(t) &= H_{01} \partial \vec{H}_0 / \partial x_1 + \vec{B}_0 H_0. \end{aligned} \right\} \quad (4.5)$$

The operators D^1 and D_0^1 are obtained by making the substitution $(\vec{V}_0, V_0) \rightarrow V_{01} \partial / \partial x_1$ in Expressions (2.8) for D and D_0 .

- If the pressure P_0 has the form

$$P_0 = Q_0(x_1, t) + x_a Q_{0a}(t) + \frac{x_a x_b}{2} Q_{ab}(t), \quad (4.6)$$

then the main field A_0 determined by Relations (4.3) and (4.6) is identical to that considered by Lin [6]. Substituting the expressions (4.3) and (4.6) in (1.1), resolving them into components, and equating to zero the coefficients of x_a , we separate the system

$$D_0^1 H_{01} = H_{01} \partial V_{01} / \partial x_1, \quad D^1 V_{01} + \partial Q_0 / \partial x_1 = H_{01} \partial H_{01} / \partial x_1, \quad (4.7)$$

$$\partial H_{01} / \partial x_1 + B_{12} = 0, \quad \partial V_{01} / \partial x_1 + U_{aa} = 0,$$

$$\left. \begin{aligned} D_0^1 \vec{B}_0 + \vec{U}_{02} \vec{B}_3 &= H_{01} \partial \vec{U}_0 / \partial x_1 + \vec{B}_{02} \vec{U}_3, \\ D^1 \vec{U}_0 + \vec{U}_{02} \vec{U}_3 + \vec{Q}_0(t) &= H_{01} \partial \vec{B}_0 / \partial x_1 + \vec{B}_{02} \vec{B}_3. \end{aligned} \right\} \quad (4.8)$$

Solving this system, we obtain for \vec{B}_0 and \vec{U}_0 a system of two linear equations

$$\left. \begin{aligned} D_0^1 \vec{B}_0 - \vec{U}_{02} B_{03} &= H_{01} \partial \vec{U}_0 / \partial x_1 - \vec{B}_{02} U_{03}, \\ D^1 \vec{U}_0 + \vec{U}_{02} U_{03} + \vec{Q}_0(t) &= H_{01} \partial \vec{B}_0 / \partial x_1 + \vec{B}_{02} B_{03}, \end{aligned} \right\} \quad (4.9)$$

which coincides with (4.5), apart from the notation. Consequently, the part $(\vec{B}_0, \vec{U}_0, Q_{0a} x_a)$ of the main field A_0 has the structure of the superimposable one $\{A\}$. We shall henceforth regard this part as belonging to $\{A\}$; without loss of generality, we put formally $\vec{B}_0 = \vec{U}_0 = \vec{Q}_0 = 0$.

Assume that the main field A_0 has the form

$$\vec{H}_0 = H_{01} \vec{e}_1, \quad \vec{V}_0 = V_{01}(t) \vec{e}_1, \quad P_0 = Q_{00}(t) - x_1 dV_{01} / dt, \quad (4.10)$$

where H_{01} is an arbitrary constant and V_{01} and Q_{00} are arbitrary functions of the time. The system (4.7, 4.8) is identically satisfied; for the superimposable field A we obtain from (4.5)

$$D^i \vec{H} = H_0 \partial \vec{V} / \partial x_i, \quad D^i \vec{V} + \vec{Q}(t) = H_0 \partial \vec{H} / \partial x_i. \quad (4.11)$$

If $H_{01} = 0$, then the system (4.11) splits into two independent equations

$$D^i \vec{H} = 0, \quad D^i \vec{V} + \vec{Q}(t) = 0. \quad (4.12)$$

5. Stationary motions. Let the vector fields depend only on a single coordinate ($x_1 \equiv x$). We then obtain from the solenoidal condition (1.1)

$$h_1 \equiv H_0 = \text{const}, \quad v_1 \equiv V_0 = \text{const}.$$

Let us separate the first components from the vectors and consider henceforth only the two-dimensional vectors $\vec{H} \equiv (h_2, h_3)$, $\vec{V} \equiv (v_2, v_3)$.

It then follows from (1.1) that the pressure p has the form

$$p = Q_0(t) + x_1 Q_v, \quad Q_v = \text{const}. \quad (5.1)$$

Integrating (1.1) we obtain a system that is linear in \vec{H} and \vec{V}

$$\begin{aligned} (V_0 - \mu_0 d/dx) \vec{H} &= H_0 \vec{V} + \vec{C}_H, \\ (V_0 - \mu_0 d/dx) \vec{V} &= H_0 \vec{H} + \vec{C}_V - x \vec{Q}, \end{aligned} \quad (5.2)$$

where \vec{C}_H and \vec{C}_V are arbitrary constants. If the liquid is ideal, $\mu = \mu_0 = 0$, and there are no longitudinal field components, $H_0 = V_0 = 0$, then the vector fields are arbitrary functions of the coordinate, $\vec{H} = \vec{H}(x)$, $\vec{V} = \vec{V}(x)$, and the pressure is an arbitrary function of the time $p = p(t)$.

If $H_0 = 0$, then in the case $\mu_0 V_0 \neq 0$ the general solution of (5.2) is

$$\vec{H} = \frac{\vec{C}_H}{V_0} + \vec{B}_H e^{\frac{V_0 x}{\mu_0}}, \quad \vec{V} = \frac{\vec{C}_V}{V_0} - \frac{(V_0 x + p)}{V_0^2} \vec{Q} + \vec{B}_V e^{\frac{V_0 x}{\mu_0}}, \quad (5.3)$$

where \vec{B}_H and \vec{B}_V are integration constants. For ordinary hydrodynamics the general solution is given by the second formula of (5.3).

If $\mu_0 V_0 H_0 \neq 0$, we obtain from (5.2) for the magnetic field \vec{H} a linear differential second-order equation

$$[\mu_0 \mu_1 d^2/dx^2 - (\mu_1 + \mu_0) d/dx + (V_0^2 - H_0^2)] \vec{H} = V_0 \vec{C}_H + H_0 (\vec{C}_V - x \vec{Q}).$$

The velocity is expressed in terms of the magnetic field by

$$\vec{V} = (1/H_0) [(V_0 - \mu_0 d/dx) \vec{H} - \vec{C}_H]$$

We note that results similar to the foregoing were obtained by S.A. Regirer [11] for a straight-line stationary flow.

REFERENCES

1. Kh. Al'fven, Kosmicheskaya elektrodinamika [Cosmic Electrodynamics], Izd-vo inostr. lit. [Foreign Literature Press], Moscow, 1852.
2. I. M. Kirko, Issledovaniye elektromagnitnykh yavleniy v metallakh metodom razmernosti i podobiya [Investigation of Electromagnetic Phenomena in Metals by the Methods of Dimensional Analysis and Similitude], Riga, 1959.
- 3/4. V. S. Tkach, ZhETF [Journal of Experimental and Theoretical Physics], 39, 1 (7), 1960.
5. J. A. Shercliff. J. fluid mech., 1, 6, 1956.
6. C. C. Lin. Arch. rat. mech. and analysis, 1, 5, 1958.
7. V. S. Tkach, collection entitled Voprosy magnitnoy gidrodinamiki i dinamiki plasmy [Problems of Magnetohydrodynamics and Plasma Dynamics], Riga, 1959, page 191; Izv. AN SSSR, OTN, MM [Bulletin of the Academy of Sciences USSR, Division of Technical Sciences, Mechanics and Machine Building], 1, 1960.
8. J. N. Kapur. Bull. Calcutta math. soc., 51, 1, 1959; Appl. sci. res., A8, 2 - 3, 1959; A9, 2 - 3, 1960.
9. P. Ramamorthy. Appl. sci. res., A9, 2 - 3, 1960.
10. S. A. Regirer, PMM, 24, 2, 1960.
11. S. A. Regirer, present collection, page 107.

PROBLEM OF LUBRICATION IN MAGNETOHYDRODYNAMICS

I.Ye. Tarapov

Khar'kov

We consider the planar motion of a viscous incompressible electrically conducting liquid between two planes, the upper one of which ($y = h(x)$) is stationary in the chosen coordinate system, and the lower one ($y = 0$) has a velocity $-V_0$ along the x axis (Fig. 1).

The fundamental magnetohydrodynamic equations [2] are written in

the form

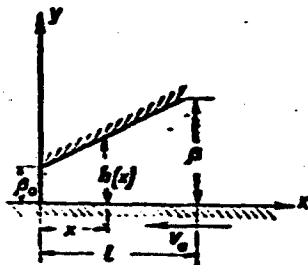


Fig. 1

$$\operatorname{div} \vec{H} = 0, \quad (1)$$

$$\operatorname{div} \vec{v} = 0, \quad (2)$$

$$\operatorname{rot} [\vec{v}, \vec{H}] + \frac{c^2}{4\pi\rho} \Delta \vec{H} = 0, \quad (3)$$

$$(\vec{V} \cdot \vec{\nabla}) \vec{V} = -\frac{1}{\rho} \vec{\nabla} \left(\rho + \frac{H^2}{8\pi} \right) +$$

$$+ \frac{1}{4\pi\rho} (\vec{H} \cdot \vec{\nabla}) \vec{H} + \Delta \vec{V}. \quad (4)$$

We assume, as is done in the theory of lubrication with a neutral liquid, that the gap between the planes is everywhere small, i.e., $\delta_0/l < \delta/l \ll 1$ (see Fig. 1), so that the motion is essentially along the x axis, i.e., $V_x \gg V_y$. We assume also that the dimensionless parameters (the ordinary and "magnetic" Reynolds numbers) $V_0 \delta^2/v_l$ and $V_0 \delta^2 \sigma/l c^2$ are small. This enables us to discard in Eq. (4) the inertial terms $(\vec{V} \cdot \vec{\nabla}) \vec{V}$, and to obtain from the projection of Eq. (3) on the y axis

$$\frac{\partial H_x}{\partial y} = 0. \quad (5)$$

We consider the flow of a liquid in a magnetic field whose transverse component H_y assumes on the planes $y = 0$ and $y = h(x)$ a constant value H_0 , and whose longitudinal component H_x vanishes on these planes. We then obtain from (5) in our approximation

$$H_y = H_0.$$

Thus, in the approximation considered we have from the projection of (3) on the x axis and from the two projections of Eq. (4) an approximate system for the determination of p , H_x , and V_x in the following form:

$$\left. \begin{aligned} H_0 \frac{\partial V_x}{\partial y} + \frac{c^2}{4\pi\sigma} \frac{\partial^2 H_x}{\partial y^2} &= 0, \\ \frac{\partial P}{\partial y} &= 0, \\ \frac{\partial P}{\partial x} &= \frac{H_0}{4\pi} \frac{\partial H_x}{\partial y} + \mu \frac{\partial^2 V_x}{\partial y^2}. \end{aligned} \right\} \quad (6)$$

where

$$P = p + \frac{H^2}{8\pi}.$$

In this case we have from Eq. (2) the constant flow condition

$$\int_{0}^{h(x)} V_x dy = -Q = \text{const.} \quad (7)$$

which will be used later on to satisfy the boundary conditions of the problem.

The boundary conditions have the form

$$\left. \begin{aligned} V_x(x, 0) &= -V_0, \\ V_x(x, h) &= V_x(x, 0) = V_y(x, h) = 0, \\ H_x(x, 0) &= H_x(x, h) = 0, \\ P(0, y) &= P(l, y) = p_0 = \text{const} \end{aligned} \right\} \quad (8)$$

By determining the functions V_x and H_x from the system (6), we obtain subject to the conditions (8)

$$V_x = -\frac{V_0}{2} \left(1 - \frac{\operatorname{sh} k \left(y - \frac{h}{2} \right)}{\operatorname{sh} \frac{kh}{2}} \right) - \frac{k}{2kp} \frac{dP}{dx} \left(\operatorname{ch} \frac{kh}{2} - \frac{\operatorname{ch} k \left(y - \frac{h}{2} \right)}{\operatorname{sh} \frac{kh}{2}} \right); \quad (9)$$

$$H_x = \frac{4\pi}{H_0} \frac{dP}{dx} \left(y - h \frac{\operatorname{sh} \frac{ky}{2}}{\operatorname{sh} \frac{kh}{2}} \operatorname{ch} \frac{k(y-h)}{2} \right) - \frac{4\pi H_0 V_0}{\kappa c^2} \frac{\operatorname{sh} \frac{ky}{2}}{\operatorname{sh} \frac{kh}{2}} \operatorname{sh} \frac{k(y-h)}{2}. \quad (10)$$

Here

$$h \equiv h(x) = \beta \left[(1 - \Delta) \frac{x}{l} + \Delta \right]; \quad \Delta = \frac{x_0}{\beta} < 1; \quad k = \frac{H_0}{c} \sqrt{\frac{\sigma}{\mu}}$$

Using Condition (7), we determine the function $P(x)$. We obtain after substituting the obtained value of V_x in (7)

$$\frac{\beta^2 (1 - \Delta)}{2\mu V_0^2} \frac{dP}{du} = m^2 \frac{(q - u) \operatorname{th} mu}{u(mu - \operatorname{th} mu)}, \quad (11)$$

where we introduced the notation

$$u = \frac{k}{\beta} = (1 - \Delta) \frac{x}{l} + \Delta; \quad q = \frac{2Q}{V_0 \beta}; \quad m = \frac{\beta H_0}{2c} \sqrt{\frac{\sigma}{\mu}}$$

Taking into account the boundary conditions for p and integrating (10) from Δ to 1 ($\Delta \leq u \leq 1$), we obtain the value of the constant q , which is the dimensionless flow of lubricant in the bearing

$$q = \frac{I_0}{I_{-1}},$$

where

$$I_k = m^2 \int_1^0 u^k \frac{\operatorname{th} mu}{mu - \operatorname{th} mu} du.$$

We note that from the integrals I_k we can calculate I_1 in final form:

$$I_1 = \ln \frac{m \operatorname{ch} m - \operatorname{sh} m}{m \Delta \operatorname{ch} m \Delta - \operatorname{sh} m \Delta}.$$

Now, integrating (9) from Δ to u , we obtain the pressure distribution function over the bearing

$$\frac{\beta^2(1-\Delta)}{2\mu l V_0} (p(u,0) - p_0) = qmr^3 \int_{\Delta}^u \frac{\tanh mx}{x(mu - \tanh mx)} dx - \\ - m^2 \int_{\Delta}^u \frac{\tanh mx}{mu - \tanh mx} dx. \quad (12)$$

Integrating this expression over the entire length of the bearing, we obtain an expression for the lifting force P

$$P = \frac{\mu V_0 l^2}{\beta^2} \cdot \frac{2I_1}{(1-\Delta)^2} \left(1 - \frac{f_0^2}{I_1 I_{-1}} \right). \quad (13)$$

Using the expression (9) for the velocity, we calculate the force of friction on the lower plane

$$F = \mu \int \left(\frac{\partial V_x}{\partial y} \right)_{y=0} dx = \frac{\mu V_0 l}{\beta(1-\Delta)} \left[I_1 \left(1 - \frac{f_0^2}{I_1 I_{-1}} \right) + \ln \frac{\sinh m\Delta}{\sinh m\Delta} \right]. \quad (14)$$

Using the electronic computer "Ural-1" we calculated the dependences of $\beta^2 P / \mu V_0 l^2$, $F\beta / \mu V_0 l$, g and $f \equiv Fl / P\beta$ on m and Δ .

The results of the calculations are listed in Table 1 and are plotted in Fig. 2.

From the table and from the plots we see that the lifting force and the friction force increase with increasing m , and when $m > 25$ the increase is almost linear; thus, the value of f tends for each Δ to a limiting value f_0 , with

$$f_0 = (1-\Delta) \times \left[1 + \left(1 - \frac{\Delta \ln^2 \Delta}{(1-\Delta)^2} \right)^{-1} \right].$$

As regards the value of g , it varies little with m (Fig. 3).

Let us consider several limiting cases.

In the case of parallel plates ($\Delta = 1$, $dP/dx = 0$) we obtain

$$V_x = -\frac{V_0}{2} \left(1 - \frac{\sinh \left(y - \frac{\Delta}{2} \right)}{\sinh \frac{\Delta}{2}} \right).$$

TABLE 1

λ	$m = 0$			$m = 0.5$			$m = 1.0$			$m = 1.5$		
	P	\bar{P}	q	P	\bar{P}	q	P	\bar{P}	q	P	\bar{P}	q
0.00	∞	∞	0.000	∞	∞	0.000	∞	∞	0.000	∞	∞	0.000
0.05	7.616	6.899	0.095	7.231	6.964	0.095	8.046	7.154	0.095	10.415	11.133	0.099
0.10	4.935	4.779	0.182	4.946	4.830	0.182	5.064	5.015	0.182	7.153	8.724	0.193
0.20	2.589	3.048	0.334	2.608	3.145	0.334	2.673	3.274	0.334	3.961	6.766	0.356
0.30	1.545	2.265	0.462	1.559	2.321	0.462	1.610	2.493	0.463	2.473	5.939	0.486
0.40	0.986	1.823	0.572	0.99	1.845	0.572	1.023	2.059	0.573	1.624	5.518	0.593
0.50	0.637	1.516	0.667	0.644	1.609	0.667	0.662	1.792	0.668	1.091	5.286	0.582
0.60	0.405	1.358	0.750	0.412	1.425	0.750	0.424	1.617	0.751	0.724	5.151	0.760
0.70	0.251	1.226	0.824	0.253	1.297	0.824	0.261	1.498	0.824	0.462	5.072	0.829
0.80	0.139	1.131	0.889	0.140	1.204	0.889	0.146	1.415	0.889	0.267	5.024	0.891
0.90	0.059	1.018	0.947	0.059	1.135	0.947	0.062	1.356	0.947	0.117	5.008	0.948
1.00	0.000	1.000	1.000	0.000	1.082	1.000	0.000	1.313	1.000	0.000	5.000	1.000

λ	$m = 10$			$m = 25$			$m = 50$			$m = 100$			$m = \infty$		
	P	\bar{P}	q	P	\bar{P}	q	P	\bar{P}	q	P	\bar{P}	q	$P_{\frac{1}{m}}$	$\bar{P}_{\frac{1}{m}}$	q
0.00	∞	∞	0.000	∞	∞	0.000	∞	∞	0.000	∞	∞	0.000	2.000	2.000	0.000
0.05	15.962	14.846	0.107	32.746	30.554	0.121	58.102	77.598	0.142	110.64	152.55	0.150	1.038	1.543	0.158
0.10	10.405	15.024	0.210	22.026	31.912	0.236	40.931	68.418	0.247	79.273	135.67	0.251	0.768	1.345	0.256
0.20	6.135	12.477	0.376	13.079	31.232	0.393	24.927	59.970	0.398	49.725	119.49	0.400	0.476	1.190	0.402
0.30	3.046	11.343	0.501	8.677	24.037	0.511	16.697	53.844	0.513	32.749	111.16	0.514	0.321	1.112	0.516
0.40	2.569	10.801	0.602	5.975	26.792	0.608	11.540	53.448	0.609	22.751	106.83	0.610	0.223	1.067	0.611
0.50	1.827	10.457	0.688	4.146	26.037	0.691	8.301	52.013	0.692	15.871	103.97	0.693	0.158	1.039	0.693
0.60	1.237	10.247	0.763	2.431	25.566	0.765	5.521	51.104	0.766	10.879	102.17	0.766	0.108	1.022	0.766
0.70	0.799	10.119	0.831	1.845	25.277	0.832	3.605	50.541	0.832	7.111	101.07	0.832	0.069	1.014	0.832
0.80	0.467	10.047	0.892	1.084	25.108	0.892	2.121	50.212	0.892	4.148	100.42	0.893	0.036	1.004	0.893
0.90	0.207	10.001	0.948	0.482	25.024	0.948	0.944	50.047	0.948	1.870	100.09	0.948	0.004	1.000	0.949
1.00	0.000	10.000	1.000	0.030	25.000	1.000	0.000	50.000	1.000	0.000	100.00	1.000	0.000	1.000	1.000

$$H_s = -\frac{4\pi j H_0 V_0}{kc^2} \cdot \frac{\sinh \frac{ky}{2}}{\sinh \frac{k\delta}{2}} \cdot \frac{\sinh k(y-\delta)}{2},$$

$$P=0; q=1,$$

$$F = \frac{\mu V_0}{\beta} m \cosh m.$$

For small values of m ($m \ll 1$) we can use the approximate formulas

$$\begin{aligned} q &= \frac{2\lambda}{1+\lambda} \left[1 + \frac{3m^2}{15} \left(1 + \frac{23 \ln \lambda}{1-\lambda^2} \right) \right], \\ \frac{\mu P}{\mu V_0 \beta} &= \frac{6}{(1-\lambda)^2} \left[\ln \frac{1}{\lambda} - 2 \frac{1-\lambda}{1+\lambda} \right] + \\ &+ \frac{8m^2}{5(1-\lambda)} \left[\frac{1+\lambda}{8} - \frac{1}{1+\lambda} \left(1 + \frac{3 \ln \lambda}{1-\lambda^2} \right) \right], \\ \frac{\mu F}{\mu V_0 \beta} &= \frac{4}{1-\lambda} \left[\ln \frac{1}{\lambda} - \frac{3}{2} \cdot \frac{1-\lambda}{1+\lambda} \right] + \\ &+ \frac{4}{5} m^2 \left[\frac{1+\lambda}{3} - \frac{1}{1+\lambda} \left(1 + \frac{3 \ln \lambda}{1-\lambda^2} \right) \right]. \end{aligned} \quad (15)$$

In the second limiting case of large values of m ($m \gg 1$) we obtain from the general formulas

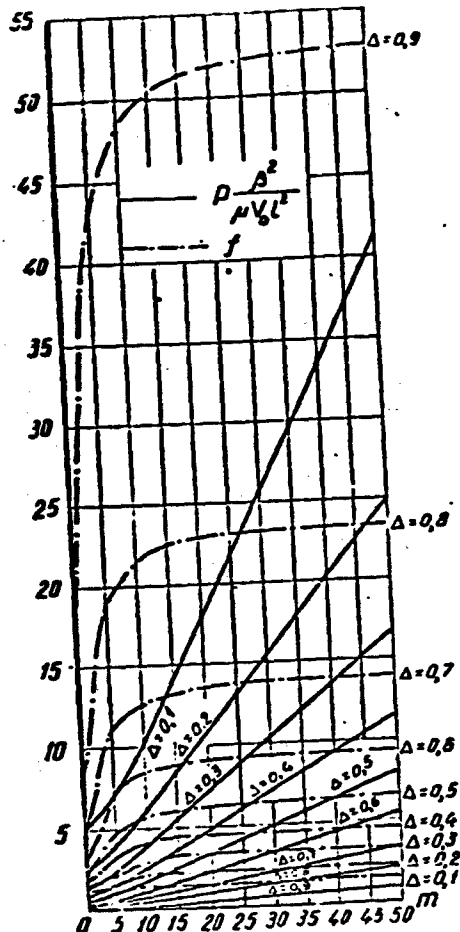


Fig. 2

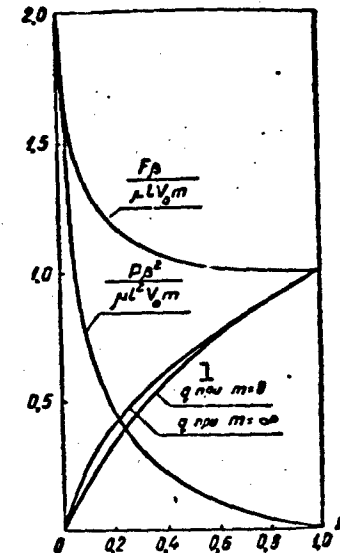


Fig. 3. 1) For.

$$q = \frac{\Delta}{1-\Delta} \ln \frac{1}{\Delta} - \frac{1+\Delta}{2m(1-\Delta)} \left(\ln \frac{1}{\Delta} - 2 \frac{1-\Delta}{1+\Delta} \right) + O\left(\frac{1}{m^2}\right).$$

$$\frac{F_p}{\mu^2 V_0} = \frac{2m}{1-\Delta} \left[1 - \frac{\Delta \ln^2 \Delta}{(1-\Delta)^2} \right] + \frac{1+\Delta}{(1-\Delta)^3} \ln \frac{1}{\Delta} \left(\ln \frac{1}{\Delta} - 2 \frac{1-\Delta}{1+\Delta} \right) + O\left(\frac{1}{m}\right).$$

$$\frac{F_f}{\mu^2 V_0} = m \left(2 - \frac{\Delta \ln^2 \Delta}{(1-\Delta)^2} \right) + \frac{1+\Delta}{2(1-\Delta)^2} \ln \frac{1}{\Delta} \left(\ln \frac{1}{\Delta} - 2 \frac{1-\Delta}{1+\Delta} \right) + O\left(\frac{1}{m}\right).$$

When $m = 0$ the expressions (15) obtained go over into the known expressions for a flat bearing with neutral lubricant [1].

Figure 3 shows plots of the principal terms of the dimensionless lifting force and friction force as functions of Δ for large values of m .

REFERENCES

1. Gidrodinamicheskaya teoriya smazki [Hydrodynamic Theory of Lubrication], GTTI [State Technical and Theoretical Editions], Moscow - Leningrad, 1934.
2. L.D. Landau and Ye.M. Lifshits. Elektrodinamika sploshnykh sred [Electrodynamics of Continuous Media], Moscow, 1959.

EXPERIMENTS ON THE GENERATION OF A MAGNETIC FIELD IN METALS
AND THE QUESTION OF THE ORIGIN OF THE GEOMAGNETIC FIELD

Yu.M. Volkov, L.I. Dorman, Yu.M. Mikhaylov
Moscow

§1. STATUS OF THE QUESTION OF GENERATION OF THE MAGNETIC FIELD IN METALS

The question of the generation of magnetic fields is one of the main branches of magnetohydrodynamics. This branch, which arose relatively long ago in connection with the problem of the magnetic field of the earth and of other celestial bodies, has been successfully progressing recently not only theoretically but also experimentally. The generation of the field can be explained by means of the following simple example.

We consider the motion of a conducting medium in a magnetic field. If a moving rectangular layer is in contact with a surrounding conducting medium (Fig. 1-a), then in accord with the law of induction a closed electric current is produced, which creates a secondary magnetic field parallel along the velocity and with magnitude $R_m H_0$, where R_m is the magnetic Reynolds number. In the case of rotating conductors, for example when cylinder A (Fig. 1-b) rotates relative to stationary cylinder B in an axial magnetic field, a toroidal magnetic field h_φ is produced. This phenomenon is the basis of the dynamo theory of the geomagnetic field. In connection with the possibility of obtaining under laboratory conditions magnetic Reynold numbers from 10 to 100, the suggestion has been made that a model of the dynamo can be created in the laboratory [2-4].

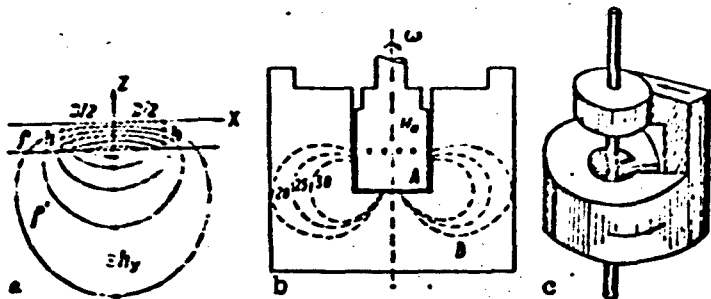


Fig. 1. Model for the generation of a magnetic field: a) generation of a magnetic field by rectangular motion of a conducting medium (the external magnetic field is vertical, the velocity of the medium and the induced field are directed perpendicular to the plane of the figure); b) generation by rotating cylinder A relative to stationary cylinder B. The magnetic field is directed along the axis of rotation. The induced magnetic field has only a ϕ component; c) Gellman and Bullard model of self-exciting dynamo.

Figure 1-c shows the model of self-exciting dynamo, proposed by Bullard and Gellman [3]. The system comprises a copper disk connected to a helical current lead. The construction of the current lead is such that the produced field reinforces the initial field. The rate of rotation of the system should be so large as to make the induced magnetic field larger than or equal to the initial field. Under this condition self-excitation of the system is possible. Estimates show that the system shown in Fig. 1-c, if made of copper, should be excited at $n \sim 10$ revolutions per second. Such a velocity is feasible under laboratory conditions.

It must be noted that the estimates given do not take account of many factors which greatly influence the experiment. These include the contact resistance, the redistribution of the current in the rotor upon interaction with the asymmetrical stator, and others. Apparently these factors exert an appreciable influence on the magnitude of the generated field, since no dynamo phenomena were observed in the experi-

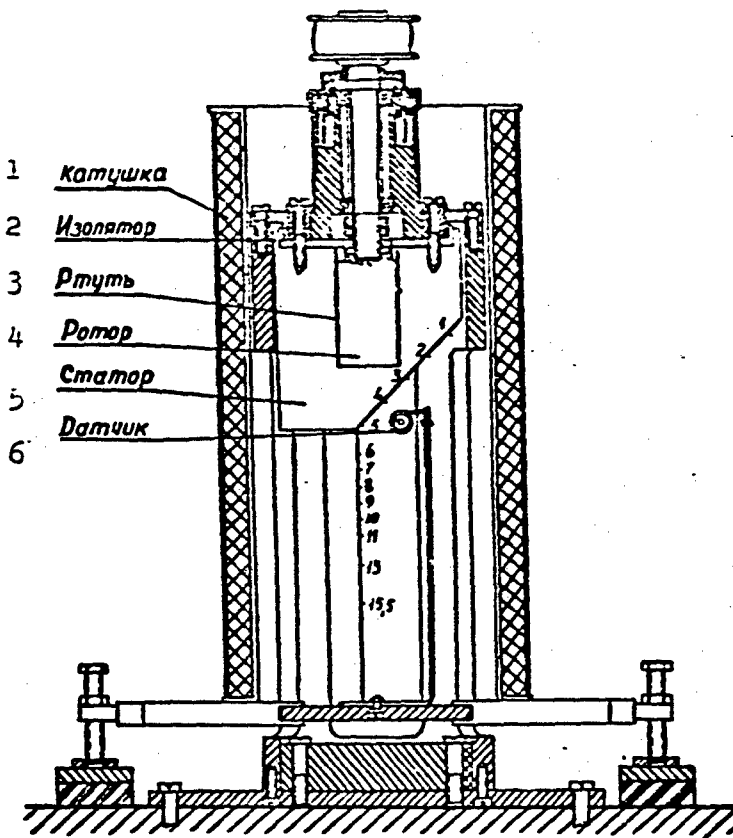


Fig. 2. Diagram of apparatus for the investigation of field generation in solid conductors.
 1) Coil; 2) insulator; 3) mercury; 4) rotor;
 5) stator; 6) transmitter.

mental works [1, 4] under conditions close to theoretical, and the measured value of the induced magnetic field turned out to be one or two orders of magnitude smaller than predicted by theory.

Herzenberg and Lowes [1] investigated the induced magnetic field in solid conductors. The apparatus they employed is shown in Fig. 2. The maximum field obtained at a distance 12 cm from the rotor was 10^{-4} of the initial field.

Lehnert [4] investigated magnetic fields in liquid sodium. A sodium installation with volume of 60 liters was used to investigate the fields. The magnetic Reynolds numbers reached 10, but the magni-

tude of the induced field remained not more than 1/4 of the initial value.

The magnitude of the measured field is essentially connected with the question of the leakage of the field outside the confines of the system. In 1949 Bullard [5] showed that in the case of axial symmetry the field outside the limits of the external conductor is equal to zero. Let us consider the system of cylinders shown in Fig. 1-b. From symmetry considerations $\frac{dh_\varphi}{d\varphi} = 0$. At the same time, $\oint h_\varphi d\varphi$ over any closed φ -contour beyond the limits of the external conductor is equal to zero, since the total current through the surface bearing against the given contact is equal to zero. Thus, the field beyond the limits of the external cylinder is $h_\varphi = 0$. The measurement of the field is possible only in the presence of asymmetry. Besides, the geometry of the asymmetry greatly influences the magnitude of the measured field. An analogous phenomenon occurs also in the case of straight-line motion of a liquid.

In the paper presented here we carry out further investigation of the generation of a field in liquid and solid conductors. In particular, we investigate the following questions, which, as far as we know, were not discussed in the literature before:

- 1) the dependence of the intensity of the generated field on the conductivity of the rotor, stator, and the conducting layer;
- 2) distribution of the generated field in space;
- 3) excitation of variable fields in an inhomogeneous structure.

In connection with the results obtained, we discuss also the question of the origin of the magnetic field of the earth and other celestial bodies, and also the origin of secular variations of the geomagnetic field.

§2. GENERATION OF MAGNETIC FIELD UPON ROTATION OF A SPHERE IN A SOLID OR LIQUID MEDIUM WITH ACCOUNT OF THE DIFFERENCE IN CONDUCTIVITY BETWEEN THE SPHERE AND THE MEDIUM

To obtain theoretical estimates of the magnitude and distribution of the generated field and to clarify the character of its dependence on the main parameters, let us consider the generation of a field by a solid sphere of radius a and with conductivity σ_1 , rotating in an external homogeneous magnetic field, directed along the axis of rotation. The sphere is in contact with a surrounding solid infinite medium with conductivity σ_3 , through a layer having a conductivity σ_2 and a thickness $\Delta = b - a$, where b is the outer radius of the layer. The conditions of the problem are specified by means of the equations

$$\text{rot } \vec{H} = \frac{4\pi}{c} \vec{j}; \quad (2.1)$$

$$\text{rot } \vec{E} = 0; \quad (2.2)$$

$$\vec{j} = \sigma \left(\vec{E} + \frac{1}{c} [\vec{v}, \vec{H}] \right); \quad (2.3)$$

$$\text{div } \vec{H} = 0. \quad (2.4)$$

Here, as usually, \vec{H} and \vec{E} are the intensity of the magnetic and electric fields, respectively, \vec{j} is the current density, \vec{v} is the velocity of motion and σ is the conductivity. We shall seek a solution in the form

$$\vec{H} = \vec{H}_0 + \vec{h}, \quad (2.5)$$

where \vec{H}_0 is the external field and \vec{h} is the induced field. From Eq. (2.2) it follows that it is possible to introduce an electric field potential φ :

$$\vec{E} = -\text{grad} \varphi. \quad (2.6)$$

The boundary conditions are determined by the expressions

$$\begin{cases} \varphi_1 = \varphi_2 \\ j_n = j_n \end{cases} \text{ for } r = a, \quad r = b; \quad \begin{cases} (2.7) \\ (2.8) \end{cases}$$

the velocity \vec{v} is specified in accordance with the conditions of the

problem in the form:

$$v_r = v_\theta = 0 \text{ in all of space, and}$$

$$v_\varphi = \begin{cases} \omega \sin \theta, & \text{if } r \leq a, \\ 0, & \text{if } r > a. \end{cases} \quad (2.9)$$

Substituting (2.9) in (2.3) and taking the divergence of both halves of the equation, we obtain

$$\Delta \varphi = \begin{cases} \frac{2\omega H_0}{c} & \text{for } r \leq a, \\ 0 & \text{for } r > a. \end{cases} \quad (2.10)$$

We seek the solution for the potential φ in the form

$$\frac{\varphi}{\omega H_0} = \begin{cases} (r^2 - a^2) \frac{1}{3} + A_1 r^2 P_2(\cos \theta), & \text{if } r \leq a, \\ P_2(\cos \theta) \left[4r^2 + A_3 \frac{a^5}{r^3} \right], & \text{if } a < r \leq b, \\ A_4 \frac{b^5}{r^3} P_2(\cos \theta), & \text{if } r > b, \end{cases} \quad (2.11)$$

where $P_2(\cos \theta)$ is the Legendre polynomial and A_1, A_2, A_3, A_4 are dimensionless constants which are determined from the boundary conditions (2.7) and (2.8). We then determine j from (2.3) and after substituting the resultant expression in (2.1) we obtain for \vec{h} a linear differential equation, the solution of which in the region $r > b$ is given in the form

$$n_r = 0,$$

$$h_\theta = 0,$$

$$h_\varphi = \frac{4\pi}{c^2} \omega H_0 a^5 \frac{\sin \theta \cos \theta}{r^3} \times$$

$$\times \frac{\sigma_1 \sigma_3}{(2\sigma_1 + 3\sigma_2) \left[3.5(1 - \sigma_1 \sigma_2) - (1 - \sigma_2/\sigma_1) \frac{\sigma_1 - \sigma_2}{2\sigma_1 + 3\sigma_2} \frac{6(a/b)^5}{5} - 1 \right]} \quad (2.12)$$

We can solve analogously the problem of the induction of the magnetic field \vec{h} resulting from the rotation of a solid sphere with conductivity σ_1 in a viscous conducting liquid with conductivity σ_2 in an external homogeneous field H_0 directed along the axis of rotation. The velocity distribution is specified in the following manner:

$$v_r = v_\theta = 0 \text{ in all of space}$$

$$v_\varphi = \begin{cases} \omega r \sin \theta, & \text{if } r \leq a, \\ \frac{\omega a^3 \sin \theta}{r^2}, & \text{if } r > a. \end{cases} \quad (2.13)$$

The solution of Eqs. (2.1-2.4) with Boundary Conditions (2.7) and (2.8) at $r = a$ for \vec{J} and φ defined by (2.6) is sought in the form $\vec{H} = \vec{H}_0 + \vec{h}$, where \vec{h} is the induced field. In this case we obtain in place of (2.10) the following equation for φ :

$$\Delta\varphi = \begin{cases} \frac{2\omega H_0}{c}, & \text{if } r \leq a, \\ \frac{2\omega a^3 H_0}{cr} P_1(\cos \theta), & \text{if } r > a. \end{cases} \quad (2.14)$$

Leaving out the intermediate steps, which are similar to those used in the preceding case, we obtain the solution in the region $r > a$ (which we propose to check experimentally) in the form

$$h_r = h_\theta = 0,$$

$$h_\varphi = \frac{2\pi\omega a^3 H_0 \sigma_2 \sin \theta \cos \theta}{cr} \left[1 - \frac{3\sigma_2}{2\sigma_1 + 3\sigma_2} \left(\frac{a}{r} \right)^2 \right]. \quad (2.15)$$

Comparison of (2.19) with (2.16) shows that the field in a viscous conducting liquid decreases much more slowly with distance away from the center of the sphere than the field in a solid medium (as $1/r$ and $1/r^3$, respectively).

§3. DESCRIPTION OF EXPERIMENTAL SETUPS

To check the results obtained in §2, we used two setups which enabled us to study the generation of the field upon rotation of a conducting rotor in both a solid and liquid medium, in a homogeneous magnetic field parallel to the axis of rotation. Because of the appreciable difficulties in the manufacture of a coaxial spherical structure, we used a copper cylinder as a rotor.

It was shown in [1] that the field distribution at a distance larger than the radius of the cylinder is in first approximation the same for a case of the spherical and for a cylindrical rotor of limited

height. In addition, the described setups enabled us to investigate the generation of fields in many cases that were "intermediate" between rotation in a liquid and in a solid medium. Thus, conducting and non-conducting blades could be used for the rotor. The solid stator could be made up of layers having different conductivities.

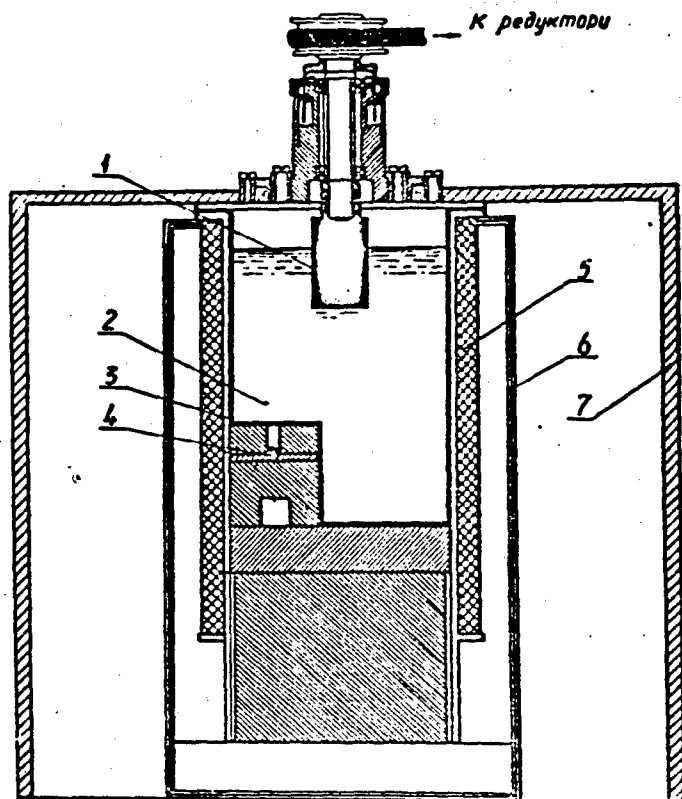


Fig. 3. Setup for the investigation of the generation of a field in mercury. 1) Rotor; 2) mercury; 3) rubber bag; 4) magnetic field transmitter; 5) solenoid; 6) stainless steel vessel; 7) wooden clamping frame. a) To reduction gear.

The setup with solid stator (see Fig. 2) is analogous to that described by Herzenberg and Lowes [1]. The rotor is a copper cylinder 40 mm in diameter and 70 mm high. The stator is a copper cylinder 120 mm in diameter and 120 mm high, with a slot cut on the side at an angle of 45° to produce asymmetry. The electric contact between the rotor

and the stator was with the aid of a mercury layer.

The setup for investigation of generation of a field in a liquid medium (Fig. 3) has a rotor part similar to that in the preceding setup. The rotor is a copper or nonconducting blade rotating in mercury, which is poured in a rubber bag. On the bottom of the bag is a ledge, also intended to produce asymmetry. The external field was produced by a solenoid 160 mm in diameter. The horizontal component of the earth's field was neutralized with the aid of Helmholtz coils.

The induced field was registered with the aid of a specially constructed magnetometer with maximum sensitivity 2.4γ per division. The magnetic field transmitter (cylinder 10 mm in diameter and 60 mm long) was a saturated ferromagnetic probe. The magnetometer is sensitive to the second harmonic of the auxiliary field exciting the transmitter.

The magnetometer readings were recorded by means of an EPPV-51 electronic potentiometer. The speed of the rotor was measured with a high-frequency NF-2 phase meter with selsyn transmitter. The vibrations of the transmitter in the earth's magnetic field and in the solenoid field were the main source of measurement error. To eliminate the influence of the vibrations, the transmitter was rigidly secured to the solenoid of the external field. This made it possible to reduce greatly the scatter in the magnetometer readings. An estimate of this and other factors influencing on the measurement accuracy shows that the relative error in the measurement with a solid stator does not exceed 10%, while in measurement with mercury it does not exceed 15 or 20%.

§4. EXPERIMENTAL RESULTS

4.1. Generation of Field in Solid Conductors

Owing to the asymmetry of the stator, the generated field emerges in part outside the stator. The degree of emergence of the field for a given configuration is not known exactly. We therefore determined in

our investigation only the character of the dependence of h_ϕ on several of the parameters contained in (2.12).

Dependence of h_ϕ on the external field H_0

The experiment confirms the linear dependence of h_ϕ on H_0 (Fig. 4) in accordance with Expression (2.12). The sign of h_ϕ changes with changing sign of H_0 and with changing direction of rotor rotation.

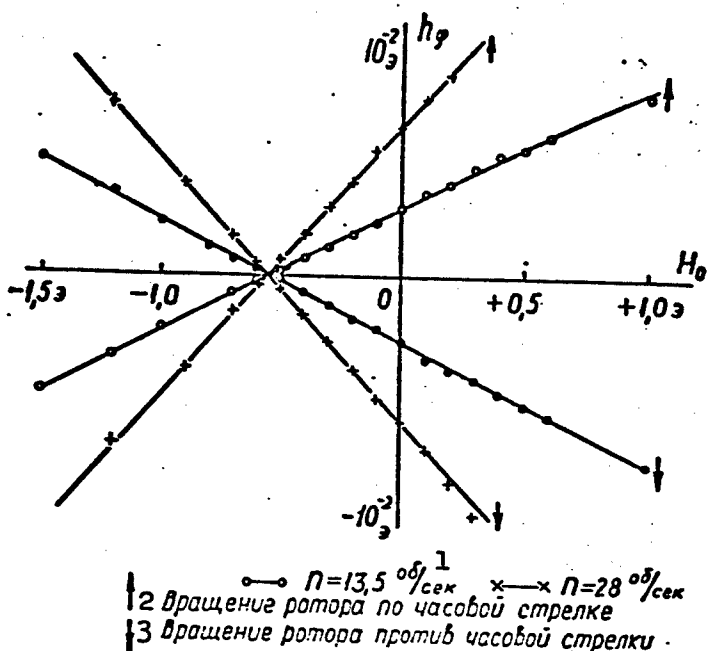


Fig. 4. Dependence of the generated field h_ϕ on the intensity of the homogeneous vertical magnetic field H_0 at two speeds of rotation

(the shifts of the lines on the abscissa axis is due to the fact that the vertical component of the earth's magnetic field was not neutralized). 1) Revolution per second; 2) rotor moving clockwise; 3) rotor moving counterclockwise.

Dependence of h_ϕ on the angular velocity ω

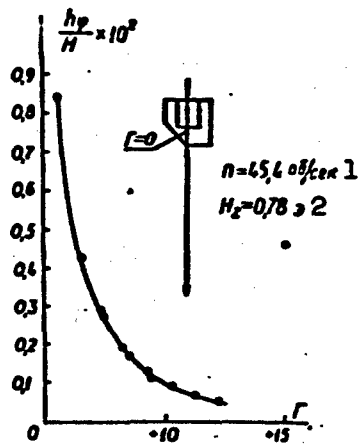
No special measurements of the dependence of h_ϕ on ω were made, since it was already established in [1] that this dependence is linear.

Our measurements at four speeds of rotation, namely 9, 13.5, 28, and

45.4 revolutions per second, confirmed the results of [1].

Spatial Distribution of h_φ

Figure 5 shows the dependence of h_φ on the distance to the bottom of the rotor, measured along the axis of rotation. Similar curves were



obtained in measurements of h_φ along other lines parallel to the axis of rotation and located different distances away from it. The maximum value of the field was obtained at the bottom of the stator at the center of the bevel cut. In the case when the rotor was a copper cylinder and the stator was also a copper cylinder (with a cut), the result was

$$h_\varphi = (3.97 \pm 0.4) \times 10^{-4} n \cdot H_0 \quad (4.1)$$

where n is the number of rotor revolutions (per second) and H_0 is the external field

(in oersted). The dependence shown in Fig. 5 is well approximated by the expression

(4.2)

in accordance with (2.12).

$$h_\varphi = \frac{\text{const}}{r^2}$$

Dependence of h_φ on the conductivities of the rotor, the stator, and the layer.

It is seen from Formula (2.12) that h_φ is also a function of the conductivities and dimensions of the individual parts of the setup. In order to determine this dependence, experiments were made with a stator made of copper with lead insert (the rotor was a copper cylinder), and also with a rotor made in the form of a blade of nonconducting material with a copper stator. The results of these measurements (as well as of measurements in a liquid medium) are listed in Table 1.

Let β be the ratio of the field h_φ , obtained for different combinations of rotor and stator conductivities to the value of h_φ for the setup where the rotor is made of copper, the layer of mercury, and the stator of copper. Table 1 shows good agreement between β_{eksp} and β_{teor} , calculated from (2.12) for the case of a solid stator and from (2.15) (with $r = a$) for a liquid stator.

TABLE 1

1) Ротор	2) Пряжка	3) Статор	$\beta_{\text{теор}}$	$\beta_{\text{эксп}}$	4) Примечание
5) Медь	Ртуть $\Delta = 1 \text{ мм}$	Медь 7	1,0	1,0	
	Медь $\Delta = 1 \text{ мм}$	Свинец	0,475	$0,45 \pm 0,04$	Свинцовый слой $\Delta = 6 \text{ мм}$ в медном статоре 9
6) Ртуть	Ртуть	Медь	0,111	$0,12 \pm 0,01$	Ротор — непроводящая лопатка 10
	Ртуть	Ртуть	0,067	$0,078 \pm 0,016$	Медная лопатка в ртути 11
Медь	Ртуть $\Delta = 0,5 \text{ мм}$	Латунь 8	0,454	$0,50 \pm 0,07$	Из работы [1] 12

- 1) Rotor; 2) layer; 3) stator; 4) remarks;
 5) copper; 6) mercury; 7) lead; 8) brass;
 9) lead layer $\Delta = 6 \text{ mm}$ in copper stator;
 10) rotor — nonconducting blade; 11) copper
 blade in mercury; 12) from Reference [1].

4.2. Generation of a Field in a Liquid Medium

When a field is generated in a liquid conducting medium, hydrodynamic phenomena begin to play an important role. The experiments were

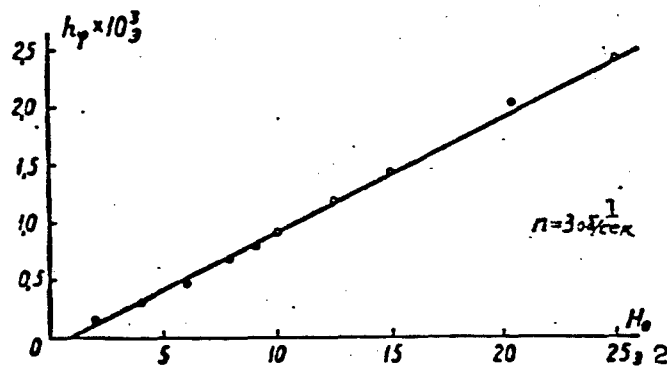


Fig. 6. Dependence of the generated field on H_0 for rotation of a copper blade in mercury. 1) Revolutions per second; 2) oersted.

carried out in such a way that there were no conditions under which the mercury becomes turbulent. Special measures were adopted to reduce the influence of vibration, since the interference due to vibration was particularly strong in this experiment.

Dependence of h_ϕ on the external field H_0

Figure 6 shows the results of the measurements of h_ϕ as a function of H_0 . Within the accuracy limits, a linear dependence is observed over a wide range of fields. Reversal of the sign of the external field is accompanied by the reversal of the sign of h_ϕ .

Dependence of h_ϕ on the speed of rotation

As in the case of the solid rotor, a linear relation exists between h_ϕ and the number of revolutions n per unit time (Fig. 7). The

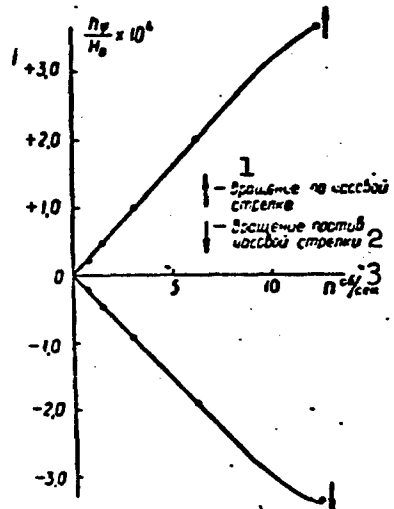


Fig. 7. Dependence of h_ϕ on the number of revolutions of a copper blade in mercury at $H_0 = 13.5$ oersted. 1) Clockwise rotation; 2) counterclockwise rotation; 3) revolutions per second.

sign of h_ϕ depends on the direction of rotation. At rotation speeds exceeding 8 revolutions per second, the proportionality breaks down, possibly owing to breakdown in the laminar nature of the flow of mercury.

Dependence of h_ϕ on the depth of immersion of the rotor

It was proposed to study the distribution of the field h_ϕ by immersing the rotor in mercury and bringing it closer to the transmitter. However, this disclosed no change in the readings of the transmitter, which stayed in all the measurements at a level of 270γ at $n = 3$ revolutions per second. This can be attributed to the fact that the maximum

generated field was produced somewhere near the inhomogeneity produced by the ledge in the bag, and that the immersion of the rotor did not influence the degree of this inhomogeneity in the hydrodynamic motion of the mercury.

Unfortunately, the strong influence of vibration, which made it necessary to secure the transmitter rigidly to the solenoid, as well as the construction of the setup, did not make it possible to shift the transmitter relative to the setup, i.e., to measure the spatial distribution of the field. In the case of the liquid rotor, the absolute value of the field was 13 times smaller than in the case with the solid copper rotor.

4.3. Generation of Alternating Field

In the case when the rotor is asymmetrical (for example, made in the form of a blade), one observes along with the constant field h_ϕ also the generation of an alternating field \tilde{h}_ϕ with fundamental frequency $f = nk$, where k is the number of blades, and n is the number of revolutions per second. The spectrum of the variable field \tilde{h}_ϕ has also higher harmonics with amplitudes that are smaller than the fundamental. The alternating field was registered with a ferrite transmitter of the inductive type. The voltage of frequency f was separated by a low pass filter, amplified by a factor 10^6 , and measured with a vacuum tube voltmeter. The transmitter was calibrated with the Helmholtz coils. Measurements have shown that in the case of a nonconducting blade

$$\tilde{h}_\phi = 0.8 \cdot 10^{-5} \cdot n H_0 \quad (4.3)$$

In the case of a conducting blade this field is 3-5 times larger.

§5. DISCUSSION OF THE RESULTS AND THE QUESTION OF THE ORIGIN OF THE GEOMAGNETIC FIELDS AND OF THE SECULAR VARIATIONS

We have thus determined the theoretical and experimental dependence of the generated field for different systems comprising conducting

liquid and solid media moving relative to each other in an external magnetic field as functions of various parameters: the configuration, speed of motion, intensity of external field, and ratio of conductivities, and we also estimated the distribution of the field in space. In particular, we have shown that the essential dependence of the magnitude of the generated field on the ratio of the conductivities of the different contacting media can be well explained by the theory. In equally good agreement with the theory are the obtained field distribution in space and the dependence of the generated field on the speed of motion and on the intensity of the external field. The magnitude of the generated field reached in this case $1/30$ the value of the external one.

In this connection we note that Bullard's theory [3, 5] presupposes generation of a dipole field with intensity approximately 0.01 of the specified azimuthal field. The generation of the field is brought about here by regular convection with speed of several hundredths of a centimeter per second, which corresponds, judging from the value of the magnetic Reynolds numbers, to the conditions prevailing in the described experiments. Apparently there are no principal difficulties involved in so modifying the experiment as to make the external field azimuthal, making the motion of the liquid correspond in its character to regular convection so that the generated field has in this case a dipole character. The results obtained are not only evident in favor of the hypothesis of the magnetohydrodynamic origin of the geomagnetic field, but indicate also the possibility of simulating, under laboratory conditions, the main processes occurring inside the earth and leading to the generation of both the dipole field and the secular variations (from this point of view, interest may attach to the data (4.3) on the generation of an alternating field in the pres-

ence of a certain asymmetry in the motion of the conducting liquid). We hope that the proposed modification of the experiment will enable us to check both the aspects of Bullard's theory and also certain aspects of Parker's theory [6] and a few magnetohydrodynamic theories.

REFERENCES

1. A. Herzenberg, F.J. Lowes. Phil. Trans. Roy. Soc., 243A, 509, 1957.
2. S.I. Braginskij. ZhETF [J. Expt. Theor. Phys.], 37, 1417, 1959.
3. E.C. Bullard, H. Gellman. Phil. Trans. Roy. Soc., 247A, 213, 1954.
4. B. Lehnert. Ark. för Fys. [Archives for Physics], 13, 109, 1958.
5. E.C. Bullard. Proc. Roy. Soc., 199A, 413, 1949.
6. E.N. Parker. Astrophys. J., 122, 293, 1955.

MAGNETOHYDRODYNAMICS OF THE OCEAN

V.M. Kontorovich

Khar'kov

1. ABSTRACT

The earth's seas and oceans can, in a certain sense, be included among the magnetohydrodynamic media.* To be sure, owing to the relatively low conductivity of sea water ($\sigma \sim 10^{10} \text{ sec}^{-1}$) and the weak hydromagnetic coupling in the earth's magnetic field, $B \sim 0.5$ oersted, the magnetohydrodynamic effects in sea water are quite weak and manifest themselves only in motions of sufficiently large scale. The possibility of such motion in the sea or in the ocean does indeed enable us to consider the latter as being magnetohydrodynamic media.

The influence of the earth's magnetism on the hydrodynamic motions is as a rule negligibly small, provided these motions exist in the absence of a magnetic field. Magnetohydrodynamic effects manifest themselves in the generation of current and an electromagnetic field by the hydrodynamic fields. Thus, the propagation of infrasound in the ocean is accompanied by the propagation of an undamped electromagnetic field coupled to it, the waves on the surface of the sea give rise to electromagnetic noise along with acoustic noise, and sea currents lead to local changes of the earth's magnetic field.

2. WIND CURRENTS

In the simplest case of Ekman wind currents [1], the magnetohydrodynamic equations can be solved exactly. One considers the stationary and homogeneous motion of a viscous conducting incompressible liquid

in the half space $z > 0$ ($\partial/\partial t = \partial/\partial x = \partial/\partial y = 0$) under the influence of the tangential friction force T (at $z = 0$) of a wind blowing along the y axis. It follows from $\operatorname{div} \vec{v} = 0$ and $\operatorname{div} \vec{B} = 0$ that $B_z = \text{const}$, $v_z = 0$. Using the boundary condition $\vec{v} = 0$, $d\vec{B}/dz = 0$ for $z = +\infty$, we obtain the magnetohydrodynamic equations (with account of the Coriolis force) for the complex velocity $w = v_x + iv_y$ and for a complex magnetic field $B = B_x + iB_y$ in the form

$$\frac{d^2w}{dz^2} - (b^2 \mp i2a^2) w = 0, \quad (1)$$

$$\frac{dB}{dz} = -\frac{4\pi\sigma}{c^2} B_z w, \quad (2)$$

where

$$a^2 = \frac{\Omega |\sin \varphi|}{v}, \quad b^2 = \frac{\sigma}{\eta c^2} B_z^2. \quad (3)$$

$\underline{l} = 1/a\sqrt{2}$ is the characteristic (vertical) scale of flow in the absence of a magnetic field, l/b is the characteristic scale connected with the action of the electrodynamic and viscous forces, $M = b/a\sqrt{2} = (B_z l/c)\sqrt{\sigma/\eta}$ is the Hartmann number, Ω is the angular velocity of the diurnal rotation of the earth, φ is the geographic latitude, η is the dynamic turbulent viscosity, and $v = \eta/\rho$. The upper sign pertains to the northern hemisphere and the lower one to the southern. The Hartmann number, which characterizes the influence of the magnetic field on the motion, has a particularly simple physical meaning in the case of a gas. Using the formulas of kinetic theory $\eta \sim nm\bar{v}^2\tau$, $\sigma \sim ne^2\tau/m$, we obtain $M \sim \underline{l}/r$, where $r = mc\bar{v}/eH$ is the torsion radius in the magnetic field.

Equation (1) with boundary conditions

$$\left. \frac{dw}{dz} \right|_{z=0} = \frac{iT}{\eta}, \quad w|_{z=+\infty} = 0 \quad (4)$$

has a solution

$$w = iUe^{-iz^2} e^{\pm i(z + w\eta)}, \quad (5)$$

$$U = \frac{T}{\eta |z|}, \quad 2a = \arccos M^2,$$

$$\epsilon' + i\epsilon'' = |\epsilon| e^{iz} = \sqrt{B^2 + i2a^2}, \quad \epsilon' > 0, \quad \epsilon'' > 0. \quad (6)$$

With exception of the direct vicinity of the equator (i.e., when $\varphi \leq \varphi_0 = \sigma B_z^2 / 2\Omega c^2 \rho \sim 10^{-8}$ for $\sigma = 4 \cdot 10^{10}$ and $B_z = 0.1$ oersted on the equator), we have $M \ll 1$ and the influence of the magnetic field on the velocity is negligibly small. In this case (5) goes over into the Ekman solution [1]:

$$w = iU_0 e^{-az} e^{(z+i)} \cdot \quad U_0 = \frac{T}{\eta a \sqrt{2}}. \quad (7)$$

The velocity vector on the surface is turned 45° to the right (in the southern hemisphere – to the left) relative to the wind and at increasing depths it turns to the right (in the southern hemisphere – to the left), exponentially decreasing in magnitude. The influence of the magnetic field on the flow can exist formally on the equator in those regions where $B_z \neq 0$. According to (6), $a \rightarrow 0$ when $\varphi \rightarrow 0$, $B_z \neq 0$, i.e., in the presence of a vertical magnetic field component on the equator, the velocity of flow on the surface is directed along the wind even in the deep sea.* As is well known, in ordinary hydrodynamics one arrives at this qualitative result by taking into account the finite depth of the sea.

Drift flow leads to the occurrence of an additional horizontal magnetic field (2), and also of a current

$$j = -i \frac{\sigma}{c} B_z w, \quad j_z = 0, \quad j \equiv j_x + j_y, \quad (8)$$

and a vertical electric field

$$E_z = -[\vec{v}, \vec{B}]_z/c, \quad E_x = E_y = 0.$$

Knowing the velocity w , we obtain the magnetic field from Eq. (2)

$$B - B_\infty = iH/c e^{-az} e^{iz(z+i)}, \quad H = \frac{4\pi z}{c^2} \frac{TB_z}{\eta |z|^2}. \quad (9)$$

where B_∞ is the limiting value of the field at $z \rightarrow +\infty$, which we iden-

tify with the unperturbed value of the horizontal component of the earth's magnetic field at $z = 0$.

For the magnetic field generated by the current (7), we obtain

$$B - B_\infty = II_0 e^{-\omega t} e^{\pm i(\frac{\pi}{2} + \alpha)} \quad (10)$$

where

$$H_0 = \frac{4\pi\gamma}{c^2} \cdot U_0 \cdot I \cdot B_\infty \quad (11)$$

This solution is the first term in the expansion of the exact solution (9) in powers of the small Hartmann number.

Thus, in wind currents there arises an additional horizontal magnetic field (10) on top of the earth's constant magnetic field. The field vector on the surface of the sea is turned 90° to the right (in the southern hemisphere – to the left) relative to the wind direction and 45° relative to the velocity direction when $B_z > 0$. With increasing depth, the field vector rotates together with the velocity vector, decreasing exponentially in magnitude with the same period of the damping constant.

Depending on the wind force, H_0 has an order of $0.1-10\gamma$, which is comparable with the amplitude of the diurnal variations of the earth's magnetic field (thus, we have $U_0 \sim 20$ cm/sec even at a wind velocity 6 m/sec); in medium latitude $H_0 \sim 0.1\gamma$ ($\gamma = 10^{-5}$ oersted).

The estimate $H \sim 4\pi\gamma v_0 l_0 B_\infty / c^2$, which is similar to (11), holds true in all problems where the variation of \vec{v} and \vec{H} in only one direction is significant, and where v_0 and l_0 are the characteristic velocity and scale of motion; this estimate is applicable, of course, not only to drift currents. For fast large scale currents, the additional magnetic field may reach tens or even hundreds of gammas.

3. LOW-FREQUENCY OSCILLATIONS

Magnetohydrodynamic effects manifest themselves also in large

scale low-frequency oscillations. Inasmuch as the detailed paper by Baños [2] does not include the limiting case of interest to us, that of the frequencies $\omega \sim \omega_s = 4\pi\sigma s^2/c^2$, we shall briefly dwell on a derivation of the dispersion relations. For plane waves ($\sim \exp i(\vec{k}\vec{r} - \omega t)$), neglecting the displacement current, all the quantities are conveniently expressed in terms of the current \vec{j} by means of the chain of formulas

$$\begin{aligned}\vec{j} &= \frac{B}{c} [\vec{j}, \vec{h}], \quad \vec{h} = \vec{B}/B, \\ \vec{v} &= \frac{i}{\rho\omega} \{L(\vec{x})\vec{x} + \vec{j}\}, \quad \vec{x} = \frac{\vec{k}}{k}, \quad L = \frac{s^2 k^2}{\omega^2 - s^2 k^2}, \\ p' &= \rho s^2 \frac{k}{\omega} (\vec{x} \vec{v}), \quad \rho' = \rho \frac{k}{\omega} (\vec{x} \vec{v}), \\ \vec{E} &= \frac{\vec{j}}{a} - \frac{B}{c} [\vec{v}, \vec{h}], \quad \vec{H} = \frac{ck}{\omega} [\vec{x}, \vec{E}].\end{aligned}\quad (12)$$

Here s is the velocity of sound in the sea, \vec{B} is the earth's magnetic field, \vec{v} , p' , ρ' , \vec{E} , \vec{H} are the amplitudes of the velocity, pressure, density, and electromagnetic field in the wave. The equations for the current, expressed in a coordinate system fixed in the wave,

$$\vec{\xi} = \vec{x}, \quad \eta = \frac{[\vec{x}, \vec{h}]}{\sin \theta}, \quad \dot{\xi} = \frac{[\vec{x} \vec{x}, \vec{h}]}{\sin \theta}, \quad \cos \theta = (\vec{x} \vec{h}), \quad (13)$$

have the following form ($j_\xi = 0$, $g = u^2 k^2 / \omega^2$, $a = c^2 k^2 / 4\pi\sigma\omega$, $u = B/\sqrt{4\pi\rho}$ is the Alfvén velocity):

$$j_\eta \cdot (1 + ia - g \cos^2 \theta) = 0. \quad (14)$$

$$j_\xi \cdot (1 + ia - g - gL \sin^2 \theta) = 0. \quad (15)$$

from which follow the dispersion equations which we give for $\omega \gg \omega_u = 4\pi\sigma u^2/c^2$ ($\omega_u \sim 10^{-12}$ cycles per second for the sea).

The oscillations which correspond at $\sigma = \infty$ to Alfvén waves ($j_\zeta \neq 0$) and to a slow magnetic sound wave ($j_\eta \neq 0$), do not propagate in the ocean and attenuate within the ordinary skin depth, following a dispersion law $k^2/\omega^2 = ic^2\omega/4\pi\sigma$. Modified sound (fast magnetic sound

wave at $\sigma = \infty$) corresponds to a dispersion law

$$\frac{k^2}{\omega^2} = \frac{1}{s^2} \left(1 - \frac{u^2}{s^2} \cdot \frac{\sin^2 \theta}{1 + i \frac{\omega}{\omega_s}} \right), \quad \omega_s = 4\pi\sigma \frac{s^2}{c^2}. \quad (16)$$

We shall call this wave from now on a sound wave. For the sea $u^2/s^2 \sim 10^{-12}$.

4. INFRASONIC WAVES

It is seen from (16) and (17) that the most interesting frequency region is $\omega \leq \omega_s$, where ω_s is the frequency at which the wavelength of the sound becomes equal to the length of the electromagnetic wave in sea water.*

When $\sigma = 4 \cdot 10^{10}$ we have $\omega_s/2\pi = 2$ cps. The magnitudes of the fields in the infrasonic wave are

$$\begin{aligned} \vec{H} &= \frac{B}{ps^3} \frac{[\vec{x}, \vec{h}] \vec{x}}{1 + i \frac{\omega}{\omega_s}} p', \quad \vec{E} = -\frac{B}{psc} \frac{[\vec{x}, \vec{h}]}{1 + i \frac{\omega}{\omega_s}} p', \\ \vec{j} &= i \frac{\omega c}{Bs} \frac{u^2}{s^2} \frac{[\vec{x}, \vec{h}]}{1 + i \frac{\omega}{\omega_s}} p'. \end{aligned} \quad (17)$$

When $\omega \approx \omega_s$ we have $E \sim 10^{-15} p'$, $H \sim 10^{-10} p'$ (in CGS units). The flux of electromagnetic energy \vec{s} is connected with the flux \vec{T} of acoustic energy in the wave by the relation

$$\vec{s} = \frac{u^2}{s^2} \frac{\sin^2 \theta}{1 + \left(\frac{\omega}{\omega_s}\right)^2} \vec{T}. \quad (18)$$

From (16) we obtain for the coefficient of absorption of infra-sound due to conductivity in the magnetic field (induction absorption):

$$Imk = \frac{\omega^2}{2s^3} \frac{u^2}{s^2} \frac{c^2}{4\pi\sigma} \cdot \frac{\sin^2 \theta}{1 + \left(\frac{\omega}{\omega_s}\right)^2}. \quad (19)$$

When $\omega \leq \omega_s$ this damping is of the same order of magnitude as the damping due to molecular viscosity. The damping coefficient is anisotropic.

Unique phenomena should occur on the interface (the surface of

the sea). When infrasound is incident on the surface of the sea, there is produced not only reflected and refracted sound, but also a damped Alfvén wave, a slow magnetic sound wave in the ocean, and an electromagnetic wave above the ocean. All these waves occur also when electromagnetic waves are incident on the interface (a total of six outgoing waves).*

It follows from Snell's law that when the sound wave from the sea has an angle of incidence $\alpha > s/c \sim 10^{-5}$, the electromagnetic waves arising above the sea have a surface character with a damping depth

$$\frac{1}{Imk_L} = \frac{\lambda}{2\pi \sin \alpha'}$$

where λ is the length of the sound wave in sea water. The electromagnetic wave propagates along the surface with a velocity equal to the horizontal component of the velocity of sound in water.

REFERENCES

1. V.V. Shuleykin. *Fizika morya* [Physics of the Sea], Izd-vo AN SSSR [Acad. Sci. USSR Press], 1953.
2. A. Baños. Proc. Roy. Soc., 233A, 350, 1955; "Problemy sovremennoj fiziki" [Problems of Contemporary Physics], 7, 62, 1957.

Manu- script Page No.	[Footnotes]
161	The contents of the paper were published in DAN SSSR, 137, 3, 576, 1961.
163	It is obvious, however, that with decrease in the horizontal component of the Coriolis force, other nonelectromagnetic forces come into play, as well as the inhomogeneity in the horizontal plane, so that the analysis given here is not suitable.
166	Accordingly, when $\omega = \omega_u$ the Alfvén wavelength and the length of the electromagnetic wave in the sea are equal.

Manu-
script
Page
No.

[Footnotes (Continued)]

- 167 For a discussion of this problem see the article by A. Gluts-yuk and the author in ZhETF, 41, 4, 1195, 1961.

HYDROMAGNETIC TURBULENCE IN THE IONOSPHERE

Ye.A. Novikov

Moscow

Turbulent motions of the conducting gas of the ionosphere induce in the earth's magnetic field electromagnetic fields, currents, and polarization charges. Because of the relatively large intensity of the magnetic field, ~0.5 gauss, the ponderomotive force acting on the induced currents may noticeably influence the motion of the gas (particularly in the upper layers of the ionosphere).

The conductivity of the ionosphere is sufficiently large to be able to neglect, in the case of hydrodynamic frequencies, the displacement current and the free charges. The corresponding condition has the form

$$4\pi\sigma_1 \gg \epsilon^{1/2} v^{-1}, \quad (1)$$

where σ_1 is the conductivity transversely to the earth's magnetic field, ϵ is the dissipation of kinetic energy per unit mass, and v is the kinematic viscosity. On the left side of (1) is the characteristic reciprocal relaxation time of the electric field and of the free charges, while on the right side is the highest frequency of the hydrodynamic motions, corresponding to the internal turbulence scale [1]. At the same time, the magnetohydrodynamics of the ionosphere can be considered also in the poor-conductivity approximation:

$$D_{ef} = 4\pi\sigma_{ef} c^{-1} V l \ll 1, \quad (2)$$

where D_{ef} is the effective magnetic Reynolds number, σ_{ef} is the effective conductivity (17), V and l are the velocity and scale of motion,

and c is the velocity of light. Under Condition (2), we can neglect the vertical part of the electric field compared with the potential field produced by the polarization charges, and the fluctuations of the magnetic field H' compared with the main field H_0 [see Formula (22)]. Condition (2) becomes most stringent for large scale motions in the upper layers of the ionosphere. An analysis of ionospheric data shows that (2) is satisfied in the "D" and "E" layers. In the "F" layer (starting at 200 km and above) this condition may, generally speaking, be violated for eddies with horizontal scales having hundreds of kilometers.*

Subject to Assumptions (1-2), the system of equations relating the various electromagnetic quantities with the velocity field has the form

$$\vec{J} = \sigma_L (\vec{n} \vec{E}) \vec{n} + \sigma_L [[\vec{n}, \vec{E}'], \vec{n}] + \sigma_H [\vec{n}, \vec{E}'], \vec{E}' = \vec{E} + H_0 c^{-1} [\vec{v}, \vec{n}], \quad (3)$$

$$\vec{E}' = -\nabla \varphi, \quad (4)$$

$$4\pi\rho_e = -\Delta \varphi, \quad (5)$$

$$\vec{F} = H_0 c^{-1} [\vec{j}, \vec{n}], \quad (6)$$

$$\rho e_m = \sigma_L (\vec{E}')^2 + (\sigma_L - \sigma_H) (\vec{n} \nabla \varphi)^2, \quad (7)$$

$$\text{rot } \vec{H}' = 4\pi c^{-1} \vec{j}, \quad (8)$$

$$\text{div } \vec{H}' = 0, \quad (9)$$

$$\sigma_L \vec{\varphi} + (\sigma_L - \sigma_H) (\vec{n} \nabla) \vec{\varphi} = \sigma_H H_0 c^{-1} (\text{div } \vec{v} - (\vec{n} \nabla) (\vec{n} \vec{v})) + \\ + \sigma_L H_0 c^{-1} (\vec{n} \text{rot } \vec{v}). \quad (10)$$

Here \vec{J} and ρ_e are the current and charge densities, \vec{n} is a unit vector in the direction of the main magnetic field, \vec{E} and φ are the intensity and potential of the electric field, \vec{F} and e_m are the electromagnetic force and the energy dissipation (the latter per unit mass of the gas), \vec{v} and ρ are the velocity and density of the gas, while σ_L and σ_H are the longitudinal and Hall conductivities.** Equation (10) is obtained by substituting (3) into the equation $\text{div } \vec{J} = 0$, which follows from

(8) (for the sake of simplicity, the conductivity coefficients are assumed constant).

So long as the influence of the magnetic field on the motion is insignificant (Criterion (25)), we can assume the turbulent velocity field to be locally isotropic. Assuming in addition incompressibility, we can obtain from (3-10) the relations between the one-dimensional spectral densities:*

$$I_E(p) = \left(\frac{H_0}{c}\right)^2 I_\sigma(p) \cdot \left\{ \frac{1}{8} \left(\frac{\sigma_\perp}{\sigma_\parallel} \right)^{1/2} \right\}^{1/2}, \quad (11)$$

$$I_H(p) = \left(\frac{H_0}{c}\right)^2 I_\sigma(p) \cdot \left\{ \frac{1}{3} \sigma^2 + \frac{\pi}{8} \sigma_\perp \sqrt{\sigma_\parallel \sigma_\perp} \right\}, \quad (12)$$

$$I_F(p) = \frac{2}{3} \left(\frac{H_0}{c}\right)^2 I_\sigma(p) \cdot \left\{ \frac{0.4 \sigma^2}{\sigma_\perp^2 + \sigma_\parallel^2} \right\}, \quad (13)$$

$$I_{t_m}(p) = \frac{1}{3p} \left(\frac{H_0}{c}\right)^2 I_\sigma(p) \cdot \left\{ \frac{0.7 \sigma}{\sigma_\perp} \right\}, \quad (14)$$

$$I_{H'}(p) = \left(\frac{4\pi}{cp}\right)^2 I_H(p), \quad (15)$$

$$I_{\rho_e}(p) = \left(\frac{p}{4\pi}\right)^2 I_E(p) \quad (16)$$

(p is the wave number). The upper lines in (11-14) correspond to isotropic conductivity ($\sigma_\parallel \approx \sigma_\perp \equiv \sigma \gg \sigma_H$), and the lower ones correspond to strong anisotropy ($\sigma_\parallel \gg \sigma_\perp, \sigma_H$).** The latter case takes place in the ionosphere, starting with 85 km and above, where the electron collision frequency [3] becomes much smaller than the Larmor rotation frequency in the magnetic field. In the transition layer 55-85 km (from isotropy to anisotropy of the conductivity), the coefficients in the formulas become more complicated. We can draw the following qualitative conclusions from (11-16): 1) the electric field, the currents, and the electromagnetic force are enclosed within the same scales as the velocity, 2) the magnetic field has a larger scale, 3) the polarization charge has a smaller scale (more accurately, it is enclosed in the

same scales as the velocity vortex), 4) the electromagnetic dissipation of energy, unlike the viscous dissipation, occurs within the scales of the main motion. From (11) and (12) we determine the effective conductivity coefficient

$$\sigma_{\text{ef}} = \sqrt{J/J_z} = \sqrt{\sigma_1 \sigma_1} \left(1 + \frac{8}{\pi} \frac{\sigma_H^2}{\sigma_1 \sqrt{\sigma_1 \sigma_1}} \right)^{1/2}, \quad (17)$$

which characterizes the ratio of current density to the electric field intensity in the turbulent stream of an anisotropically conducting gas (the second term in the round brackets is small above the "E" layer, and the sides $\sigma_{\text{ef}} = \sqrt{\sigma_{||} \sigma_{\perp}}$). From (11-15) we determine the characteristic values of the different quantities

$$E \approx \frac{H_0}{c} \left(\frac{\sigma_1}{\sigma_{||}} \right)^{1/4} V, \quad (18)$$

$$J \approx \frac{H_0}{c} \left(\frac{\sigma_1}{\sigma_{||}} \right)^{1/4} \sigma_{\text{ef}} V, \quad (19)$$

$$F \approx \left(\frac{H_0}{c} \right)^2 \sigma_F V, \quad \sigma_F = \sqrt{\sigma_1^2 + \sigma_H^2} \quad (20)$$

$$\epsilon_m \approx \sigma_{\perp} V^2, \quad \omega_{\perp} = \frac{H_0^2 \sigma_1}{\rho c^2}, \quad (21)$$

$$H' \approx H_0 \left(\frac{\sigma_1}{\sigma_{||}} \right)^{1/4} D_{\text{ef}} \quad (22)$$

The density of the polarization charge, which like the velocity vortex is enclosed within scales on the order of the internal turbulence scale $l_0 = v^{3/4} \epsilon^{-1/4}$ [1], can be related with ϵ . We have:

$$\begin{aligned} \bar{p}_e^2 &= 4\pi \int p^2 I_{p_e}(p) dp = \left(\frac{H_0}{4\pi c} \right)^2 4\pi \int p^4 I_{p_e}(p) dp \cdot \left\{ \frac{1}{3} \right. \\ &\quad \left. \frac{\pi}{8} \left(\frac{\sigma_1}{\sigma_{||}} \right)^{1/2} \right\} = \\ &= \left(\frac{H_0}{4\pi c} \right)^2 \frac{1}{v} \left\{ \frac{1}{3} \right. \\ &\quad \left. \frac{\pi}{8} \left(\frac{\sigma_1}{\sigma_{||}} \right)^{1/2} \right\}. \end{aligned} \quad (23)$$

In experiments on the scattering of radio waves by meteor trails [4] at altitudes 80-100 km, the mean square value of the turbulent velocity

was found to be ~ 25 meters per second. Substituting this value in (18-21) and putting $H_0 = 0.5$ gauss, $\sigma_{\parallel} = 9 \cdot 10^7 \text{ sec}^{-1}$, $\sigma_{\perp} = 1.3 \cdot 10^5 \text{ sec}^{-1}$, and $\sigma_H = 2.9 \cdot 10^6 \text{ sec}^{-1}$ [5], we obtain

$$E \approx 2.4 \cdot 10^{-6} \text{ v/cm}, \quad j \approx 7 \cdot 10^{-11} \text{ amp/cm}^2, \quad F \approx 2 \cdot 10^{-13} \text{ dyn/cm}^3,$$

$$\epsilon_m \approx 0.3 \text{ erg/g-sec.}$$

If we choose for the scale l the external horizontal turbulence scale ~ 150 km [4], then we get from (22) $H' \approx 1.3 \cdot 10^{-3}$ gauss.** In the same paper a value $\epsilon \sim 10^3$ erg/g-sec was obtained, and from this, putting $v = 2.4 \cdot 10^5 \text{ cm}^2/\text{sec}$ [2] we obtain from (23) $(\rho_e^{-2})^{1/2} \approx 2 \cdot 10^{-14} \text{ CGS esu/cm}^3$, while for the characteristic space charge we obtain $Q \approx (\rho_e^{-2})^{1/2} l_0^3 \approx 1.5 \cdot 10^{-4} \text{ CGS esu}$. The value obtained for j is comparable with the density of the current due to the tidal motions and producing the diurnal variations of the magnetic field at the earth's surface. However, the turbulent currents, unlike the tidal current, are random and when superimposed on one another do not produce so noticeable fluctuations of the magnetic field at the earth's surface. As regards the fluctuations of H' in the ionosphere, they turn out to be sufficiently large to be able to use them as an indicator of the turbulent motions at high altitudes. The polarization charges are relatively small and do not lead to any noticeable fluctuations of the electron density. However, the presence of polarization charges plays an important role in the formation of the turbulent currents. It can be shown that the contribution of the field $-\nabla \phi$ to the mean square value of the current is of the same order of magnitude as the contribution of the "dynamo field" $H_0 c^{-1} [\mathbf{v}, \mathbf{n}]$.

In the inertial interval of wave numbers, the spectral density of the kinetic energy is described by the following formula [6]:

$$\frac{1}{2} I_r(p) = \alpha' p^{-\alpha}, \quad (24)$$

where a is a constant on the order of unity. Substituting (24) in (11-16), we can obtain the spectral density of all the quantities of interest to us (the corresponding formula for $I_{H_1}(p)$ in the case of isotropic conductivity was derived earlier [7]).

- In order to estimate the influence of the earth's magnetic field on the turbulent motion, let us determine the order of magnitude of the ratio of the electromagnetic force (20) to the inertial force $\rho(\vec{v}\vec{v})\vec{v}$ in the equation of motion

$$N_F = \frac{\omega_F}{\omega}, \quad \omega_F = \frac{H_0 \sigma_F}{\rho c^2}, \quad \omega = \frac{V}{l}. \quad (25)$$

The ratio of the electromagnetic force to the viscous force $\eta \vec{v} \vec{v}$ determines the dimensionless parameter

$$M_F^2 = \left(\frac{l}{l_s} \right)^2, \quad l_s = \frac{c}{H_0} \sqrt{\frac{\eta}{\sigma_F}}. \quad (26)$$

which is a generalization of the Hartmann number to include the case of anisotropic conductivity. The ratio of the electromagnetic energy dissipation (21) to the viscous dissipation, which we denote M_1^2 , differs from (26) in that σ_F is replaced by σ_1 . From (25) we see that the magnetic field exerts an influence primarily on the low-frequency motions, and consequently on the large scale motions. An analysis of the ionospheric data shows that in the "D" and "E" layers the influence of the magnetic field on the turbulent motion can certainly be neglected. At an altitude of ~ 150 km, the magnetic field may exert an influence on the large scale eddies with horizontal scales amounting to hundreds of kilometers. We note that if we assume at this altitude $\epsilon \approx 10^3$ ergs/g-sec (the same as at altitudes 80-100 km [4]), then the internal turbulence scale is found to be ~ 3 km, which is merely one order of magnitude smaller than the "height of the homogeneous atmosphere," which is ~ 38 km [2]. Consequently, the turbulence cannot be highly developed. At an altitude ~ 250 km, the scale in which the electromagnetic

forces become equal to the inertial forces is of the same order of magnitude as the internal turbulence scale. This means that the inertial forces cease to play any role whatever. Consequently, at these altitudes no turbulence in the ordinary sense can arise, since the dynamics equations become linear with respect to the velocity. Random motions in the upper layer of the ionospheres are apparently in the nature of oscillations.

A more detailed paper will be published.

In conclusion I express my sincere gratitude to A.S. Monin for valuable remarks made by him during the course of an evaluation of the present research.

REFERENCES

1. A.N. Kolmogorov. DAN [Proceedings of the Academy of Sciences], 30, 4, 1941.
2. M. Nicolet. J. Geoph. Res., 64, 12, 1959.
3. M. Nicolet. Phys. of Fluid, 2, 2, 1959.
4. J.S. Greenhow and E.L. Neufeld. J. Geoph. Res., 64, 12, 1959.
5. W.G. Baker, D.F. Martin. Phil. Trans. Roy. Soc., 246, 913, 1953.
6. A.M. Obukhov. Izv. AN, ser. geogr. i geof. [Bulletin of the Academy of Sciences, Geography and Geophysics Series], 5, 1941.
7. G.S. Golitsyn. DAN, 132, 2, 1960.

Manu-
script
Page
No.

[Footnotes]

- 170 The vertical scales of the eddies are limited to the "height of the homogeneous atmosphere" $RT/\mu g$, which is of the order of 50 km in the "F" layer [2].
- 170 The coefficients of conductivity are proportional to the electron density and depend on the frequencies of collision between the electrons or ions with the molecules or with each other.

[Footnotes (Continued)]

- 171 The three-dimensional spectral functions of the electromagnetic quantities display an essential anisotropy, connected with the preferred direction \vec{n} and with the anisotropy of the conductivity.
- 171 Factors of the order of unity have been left out in the lower lines of (11) and (14).
- 173 The assumed values of σ_{\parallel} , σ_{\perp} , σ_H , and v (see below) correspond to a height of 100 km (lower limit of the "E" layer).
- 173 We note that the large scale turbulent motion is anisotropic (see the remark on page 170), so that our estimates, which are based on the assumption of local isotropy, are tentative in character.

CHARACTER OF TURBULENCE IN SOLAR WIND

L. I. Dorman

Moscow

1. It is known that with increasing solar activity the intensity of the cosmic rays on earth decrease, and the so-called "knee" of the latitude effect shifts toward the lower latitudes. As the minimum of solar activity is approached, the intensity of the cosmic rays reaches a maximum value, and the "knee" approaches the geomagnetic poles. The amplitude of the 11-year variations (with period of about 11 years, equal to the period of variation of the solar activity) reaches large values: about 6% in the muon component and about 25% in the neutron component at sea level. In the case of measurements in the stratosphere, these variations are even larger: at a height of 30 km, the intensity of the powerful ionizing component changes by a factor of two, and the number of particles at this altitude changes by almost four times. Using the data obtained by the International Network of Cosmic Ray Stations, by the method of coupling coefficients [1, Chapter IV], it is possible to find the energy spectrum of the primary 11-year variations. This spectrum has the following form [2]: the particles with low energies (less than several Bev) are practically completely lacking in the maximum of solar activity, compared with the flux in the minimum of the activity; the degree of absence of high energy particles decreases rapidly with increasing particle energy; the flux of the particles with energy > 100 Bev remains practically constant.

An investigation of the 11-year variations is of exceptional in-

terest, since they are connected with the electromagnetic properties of interplanetary medium.

2. Many of the hypotheses discussed in the literature concerning the origin of the 11-year variations meet with serious difficulties. The most promising is the hypothesis of Parker [3] concerning the so-called solar wind. Streams of magnetized plasma, ejected from the sun, are slowed down by the interplanetary medium and drag the latter as they move. A radial "wind" made up of magnetic field inhomogeneities is produced. The cosmic rays come to the earth from the galaxy as the result of diffusion by scattering on the inhomogeneities of the magnetic field. This is hindered by the convection transport due to the particle drift resulting from the motion of the scattering inhomogeneities, which is directed away from the sun. The stationary state is established as a result of the equality of both fluxes. Thus, for a definite "wind" geometry and for definite values of its radial velocity and diffusion coefficient $\kappa = v\lambda/3$ (where v is the particle velocity and λ is the mean free path for scattering on the inhomogeneities) it is easy to determine the difference between the cosmic ray intensity on Earth as compared with the intensity in the galaxy in the vicinity of the solar system (see [3, 4]). Inasmuch as v and λ depend on the particle energy, the expected variation $\delta(D\varepsilon)/D(\varepsilon)$ will also have a definite energy spectrum. Parker [3] suggested that the scattering is by field inhomogeneities measuring $\sim 2 \cdot 10^{11}$ cm, in which magnetic field of intensity $H \sim 2 \cdot 10^{-5}$ Oe are frozen in. Such an assumption leads to a spectrum that agrees with the experimental data only in the region of rather small energies ($< 2\text{-}3$ Bev). In the region of energies on the order of ten or several times ten Bev, the spectrum obtained in [3] differs appreciably, by a factor of several times ten, from that obtained in [2] from the experimental data. It was shown in [4] that no

change in the parameters employed by Parker (field intensity, velocity and geometry of the wind, dimension of the inhomogeneities) will lead to agreement with experiment simultaneously over the entire energy interval (for example, it is possible to choose the parameters such as to agree with experiment in the region of large energies, but then an appreciable discrepancy with experiment occurs in the region of moderate and low energies, etc.).

3. The only way out of this situation (if we retain the notion of the solar wind of magnetic inhomogeneities) is to assume that there exists not one characteristic dimension of the magnetic field inhomogeneities, but a whole spectrum with dimensions ranging from a certain minimum value \underline{l}_{\min} to a maximum one \underline{l}_{\max} . Then for particles with charge ze and momentum p , for which the radius of curvature is $\rho = cp/zeH$ (in the interplanetary magnetic field H) contained in the range from \underline{l}_{\min} to \underline{l}_{\max} , the mean free path for scattering λ will be proportional to ρ , i.e., proportional to cp . Indeed, scattering by small inhomogeneities with dimensions $\underline{l} \ll \rho$ yields a mean free path $\lambda \sim \rho^2/\underline{l} \gg \rho$, while scattering by very large inhomogeneities with $\underline{l} \gg \rho$ gives a mean free path $\lambda \sim \underline{l}$, also much larger than ρ , i.e., scattering on such inhomogeneities will be much less effective than scattering on inhomogeneities with $\underline{l} \sim \rho$, when $\lambda \sim \rho$. Thus, in the presence of such a spectrum for the inhomogeneities of the magnetic field, the diffusion coefficient will be proportional to the energy, up to energies of the particles with $\rho \sim \underline{l}_{\max}$, while for particles with $\rho > \underline{l}_{\max}$ the diffusion coefficient will be proportional to $\rho^2/\underline{l}_{\max}$, i.e., to the square of the energy. This deduction is in good agreement with the experimental data concerning the spectrum of the 11-year variations. In this case, to obtain agreement over the entire region of the spectrum, it is necessary to assume that the minimum dimension of

the inhomogeneities is $l_{\min} \sim 10^{11}$ cm, while the maximum is $l_{\max} \sim 10^{13}$ cm.

The presence of magnetic field inhomogeneities of this type is confirmed also by an analysis of the variation of the solar-diurnal variations with the solar activity, as obtained by data gathered with crossed cosmic ray telescopes.

REFERENCES

1. L. I. Dorman, Variatsii kosmicheskikh luchey [Variations of the Cosmic Rays], Gostekhizdat [State Publishing House for Technical and Theoretical Literature], Moscow, 1957.
2. L. I. Dorman, Rezul'taty MGG [Results of the IGY], Izd-vo AN SSSR, ser. kosmicheskikh luchey [Acad. Sci. USSR Press, Cosmic Radiation Series], 3, 205, 1961.
3. E. N. Parker. Phys. Rev., 110, 6, 1958.
4. L. I. Dorman, Trudy Mezhdunarodnoy konferentsii po kosmicheskim lucham [Trans. of the International Conference on Cosmic Rays], IV, 328, Izd-vo AN SSSR, 1960.

FLOW AROUND MAGNETIC INHOMOGENEITIES

A.P. Kazantsev
Novosibirsk

In the present communication we consider certain problems connected with the flow of an ideally conducting incompressible liquid around magnetic sources. In this case [1-3] the space is broken up into several regions, occupied either by the liquid or by the magnetic field. The regions located near the singularities of the magnetic field and free of liquid will be called, as is customary in hydrodynamics, cavities. It is obvious that on the boundary of the cavity the magnetic pressure $H^2/8\pi$ should be balanced by the pressure of the liquid. Assuming the flow of the liquid to be potential, the condition for the equilibrium in the case of stationary flow can be written with the aid of the Bernoulli integral in the following fashion

$$\frac{1}{2}\rho v^2 + \frac{H^2}{8\pi} = p_\infty + \frac{1}{2}\rho v_\infty^2 = p'_\infty. \quad (1)$$

The problem consists of determining the boundary of the cavity, assuming that the sources of the magnetic field are known.

1. An exact solution of the problem is possible only in a few very simple cases. For example, one can point out cases when the boundary of the cavity is made up of second order curves (only plane problems are considered). Thus, in the case of flow around a semi-infinite current carrying plate located along the incoming stream (Fig. 1, the magnetic force lines are shown dashed), the boundary of the cavity will be a parabola if $p_\infty = 0$. The end of the plate is in this case lo-

cated at the focus of the parabola

$$(y/2a)^2 = x/a + 1, \quad a = \frac{a^2}{4\pi\mu v_\infty^2}.$$

Here a characterizes the singularity of the magnetic field near the end of the plate ($H_x - iH_y = a/\sqrt{z}$). It can also be shown that in the case of flow around a current carrying plate of finite width, the boundary of the cavity is an ellipse, provided a certain connection exists between the current and the width of the plane, resulting from the requirement that the plate lie on the section line of the ellipse.

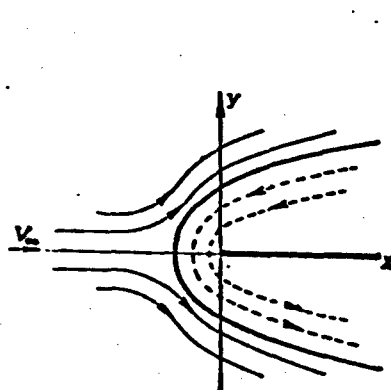


Fig. 1

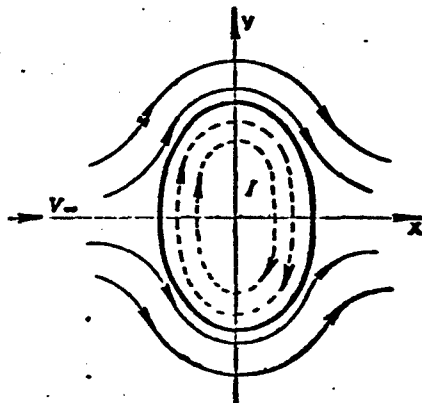


Fig. 2

2. In principle one can always write out, using the generalized Kirchhoff method [4], an exact system of equations for the cavity boundary. However, an exact solution of the system is possible only in those cases when the cavity boundary does not deviate greatly from a known one. This occurs when either the hydrodynamic pressure $\rho v^2/2$ or the magnetic pressure can be regarded as a perturbation. Let us consider two examples using Kirchhoff's method, namely the flow around a linear current and the scattering of a jet by a linear current. In the former case the streamline pattern is naturally assumed to be symmetrical about the x and y axes (Fig. 2). What would be in this case the exact system of equations describing the flow of liquid, the magnetic

field, and the cavity boundary? We introduce, as is customary, the complex potentials for the liquid, $w_1 = w_1(z_1)$, and for the magnetic field $w_2 = w_2(z_2)$, so that $v_x - iv_y = dw_1/dz_1$ and $H_x - iH_y = dw_2/dz_2$.

As is well known from hydrodynamics [4], it is more convenient to assume in problems of this type that the velocity $v(z_1)$ and the magnetic field $H(z_2)$ are functions of their complex potentials. We first map conformally the space outside the cavity on the outside area of the unit circle $|\zeta_1| > 1$, and the inside of the cavity on the inside of the circle $|\zeta_2| < 1$, so that the origin goes over into the center of the circle.

We then can write for the potentials the following expressions

$$w_1 = \lambda \left(\zeta_1 + \frac{1}{\zeta_1} \right) \text{ and } w_2 = 2i/\ln \zeta_2. \quad (2)$$

Here λ is a certain constant to be determined, and I is the strength of the current flowing through the conductor.

We shall seek $v(\zeta_1)$ and $H(\zeta_2)$ in the following form

$$v = v_\infty \left(1 - \frac{1}{\zeta_1} \right) e^{i\omega_1(\zeta_1)}, \quad H(\zeta_2) = \frac{i}{\zeta_2} \sqrt{\frac{p'_\infty}{8\pi}} e^{i\omega_2(\zeta_2)}. \quad (3)$$

We put also $\omega_k = \nu_k + i\mu_k$ and $\zeta_k = |\zeta_k| e^{i\tau_k}$. Then the condition (1) for mechanical equilibrium is written in the form

$$2\nu_\infty^2 \sin^2 \tau_1 e^{-2\mu_1(\tau_1)} + p'_\infty e^{-2\mu_2(\tau_2)} = p'_\infty. \quad (4)$$

Recognizing that the direction of the velocity on the boundary either coincides with the direction of the magnetic field or opposes it, we can write with the aid of (3)

$$\nu_1(\tau_1) - \tau_1 = \nu_2(\tau_2) - \tau_2. \quad (5)$$

Finally, it must be taken into consideration that the "events" occur at one point of the boundary ($dz_1 = dw_1/v = dz_2 = dw_2/H$):

$$\frac{1}{v_\infty} e^{\mu_1(\tau_1)} d\tau_1 = 2i \sqrt{\frac{8\pi}{p'_\infty}} e^{\mu_2(\tau_2)} d\tau_2 \quad (6)$$

Thus, we obtain a system of equations (4-6) for the three func-

tions ω_1 , ω_2 , and τ_1 , which depend on τ_2 . This system is readily solved only if ρv^2 can be regarded as small ($\rho v_\infty^2 \ll 2p_\infty$). Then ω_1 and ω_2 are small quantities and the equations can be linearized. In the first approximation in ρv_∞^2 the cavity has the form of an ellipse which is elongated in the transverse direction, something that is physically obvious.

In the case of linear flow, in view of the symmetry, there are no forces acting on the linear current.

If the flow is nonstationary (for example, if the current strength varies with the time), then the equilibrium condition on the cavity boundary has the form

$$\frac{\partial \varphi}{\partial t} + \frac{1}{2} v^2 + \frac{H^2}{8\pi\rho} = \text{const.}$$

In the case of flow around a linear current, the symmetry with respect to the x axis is disturbed and a force F (per unit length) arises, for which, in the case of sufficiently slow variation of the current strength ($|dI/dt| \rho v_\infty \ll 2\sqrt{\pi p_\infty^{3/2}}$) we can obtain the following expression:

$$F = \frac{\rho v_\infty}{2p_\infty} \frac{dp}{dt}.$$

We assume as before that $\rho v_\infty^2 \ll 2p_\infty$.

From the expression for F we see that as the current strength increases a braking force is produced, and when the current decreases a moving force is produced. The reason for it is that in the case when the current increases the rate at which the stream arrives on the left edge of the cavity (see Fig. 2) becomes less than the rate on the right side, the pressure on the left edge becomes larger, and the left edge of the cavity is located closer to the conductor than the right edge. When the current strength decreases, the opposite picture obtains.

3. In the scattering of a flat jet on a linear current, the streamline pattern can be assumed to be symmetrical with respect to the y axis (Fig. 3). In this case we can also write the exact system of the Kirchhoff equations; the canonical regions in this case will be a strip for the liquid and a half plane for the magnetic field. We confine ourselves, however, to the scattering of a jet in small angles, i.e., we regard the magnetic field as a perturbation

$$\frac{p}{\pi S^2} \ll v_\infty^2$$

(here S is the impact parameter).

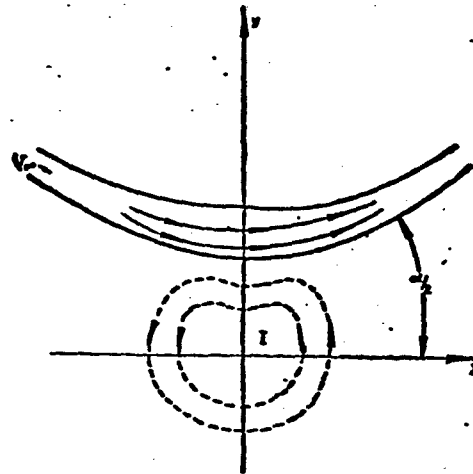


Fig. 3

In the plane $\zeta = w_1/L_\infty v_\infty$ the jet is mapped on the plane $0 \leq \operatorname{Im}\zeta \leq 1$; L_∞ is the width of the jet at infinity. We seek $v(\zeta)$, as before, in the form $v = v_\infty e^{i\omega(\zeta)} \approx v_\infty (1 + i\omega(\zeta))$. Then we have $\mu = 0$ when $\operatorname{Im}\zeta = 1$ and when $\operatorname{Im}\zeta = 0$ μ is determined from the condition (1) (in this case we must put $p_\infty = 0$)

$$\mu(t) = \frac{2tS^2}{\pi^2 v_\infty^2 (t^2 L_\infty^2 + S^2)}, \quad t = Re\zeta \quad (7)$$

In the first approximation in t^2 , the magnetic field coincides with the field of a linear current near a flat wall. Further, taking

into account the fact that the angle through which the jet is scattered, α , is connected with v ($v = R\omega$) by the simple relation

$$\alpha = v(+\infty) - v(-\infty).$$

we obtain with the aid of the Schwartz integral for a strip [5]

$$\alpha = \int_{-\infty}^{+\infty} \mu(t) dt = \frac{P}{SL_a \rho v_\infty^2}.$$

REFERENCES

1. Zh. Burgers. Collection entitled "Magnitnaya gidrodinamika" [Magnetohydrodynamics], Atomizdat [State Press for Literature on Atomic Energy], 1958.
2. V. N. Zhigulev, DAN SSSR [Proc. Acad. Sci. USSR], 126, 3, 1959.
3. A. P. Kazantsev, DAN SSSR, 133, 2, 1960.
4. N. Ye. Kochin, Tochnoye opredeleniye ustanovivshikhsya voln [Exact Determination of Stationary-State Waves], Collected Works, II, Izd-vo AN SSSR [Acad. Sci. USSR Press], 1949.
5. M. A. Lavrent'yev and B. V. Shabat, Metody teorii funktsiy kompleksnogo peremennogo [Methods of the Theory of Functions of Complex Variables], 1958.

CYLINDRICAL EXPLOSION AND STRAIGHT LINE DISCHARGE
IN AN ELECTRICALLY CONDUCTING MEDIUM WITH
ACCOUNT OF THE MAGNETIC FIELD

V.P. Korobeynikov
Moscow

The problem of a strong pointlike explosion along a straight line in an infinitely conducting gas will be considered under the assumption that the initial magnetic field has the following components in the cylindrical coordinate system r , φ , z :

$$H_r = kr^{-1}, \quad H_\varphi = 0$$

for arbitrary values of the adiabatic exponent γ :

$$H_r = kr^{-1}, \quad H_z = \text{const for } \gamma = 2$$

The component H_r will be assumed to be equal to zero throughout.

The formulation of the problem of a strong cylindrical explosion differs from the formulation of the analogous gasdynamic problem [1] only in the presence of the magnetic field in the conditions and in the equations of the problem.

The gas motion arising in the explosion will be one dimensional with cylindrical symmetry. The equations necessary for the mathematical description of such motions are given in [2]. In the case of a pure annular magnetic field with initial distribution $H_{\varphi_1} = kr^{-1}$ the explosion problem is self-similar and reduces to the integration of a system of four ordinary differential first-order equations. The necessary boundary conditions of the problem follow from the need of satisfying the conservation laws on the front of the shock wave and the symmetry condition on the explosion axis. The system of differential equations

has three first algebraic integrals [3]: the adiabaticity integral, the energy integral, and the freezing-in integral. The arbitrary constants contained in the analytic expression for the integrals are obtained from the boundary conditions on the front of the shock wave. With the aid of the integrals the problem reduces to an investigation of one ordinary differential equation, which can be written in the following form

$$\frac{d \ln y}{dV} = \frac{2(\gamma V - 1) \left[\Psi_1(y, V) + \frac{\gamma - 2}{\gamma} y(V - 0.5)^2 + (\gamma - 1) \Psi_2 \right]}{(V - 0.5) \Psi_2}, \quad (1)$$

where

$$\Psi_1 = (V - 0.5) V^{-2} \left[1/\gamma \left(2V - \frac{1}{\gamma - 1} \right) - 0.5yV^2 \right],$$

$$\Psi_2 = V(V - 1)(V - 0.5)y + 1/\gamma - 2V,$$

$$y = \frac{r^2}{\gamma^2 R} T^{-1}, \quad V = \frac{v}{r} t,$$

r is the radius, t the time, T the temperature, v the velocity, and R the gas constant.

We shall henceforth designate by the subscript 1 quantities characterizing the unperturbed state of the gas, and by the subscript 2 quantities directly behind the front of the shock wave. Using the conditions on the shock wave, we obtain the dependence of y_2 on V_2 and γ :

$$y_2^{-1} = \gamma(\gamma - 1) \left[0.5V_2^2 + \left(1 + \frac{0.5}{V_2 - 0.5} + 2V_2 \right) H_1 \right], \quad (2)$$

$$H_1 = \frac{0.5V_2 \left[(0.5 - V_2) \frac{1}{\gamma - 1} - 0.5V_2 \right]}{\frac{1}{\gamma - 1}(V_2 - 0.5) + \frac{(\gamma - 2)}{4(\gamma - 1)} \cdot \frac{1}{V_2 - 0.5} + V_2 + 0.5}.$$

From the condition $D^2 \geq H_{\varphi 1}^2 / 4\pi\rho_1$ (D is the velocity of the shock wave) and from Eqs. (2) it follows that

$$\frac{(\gamma + 1)^2}{0.5\gamma(\gamma - 1)} < y_2 < \infty, \quad \frac{1}{\gamma + 1} > V_2 > 0, \quad (H_1 < \frac{1}{4}).$$

We note that in the gasdynamic problem involving a pointlike explosion

the connection between y_2 and V_2 for a fixed value of γ was represented on the V_2 , y_2 plane by a point, whereas in the problem considered here the presence of the magnetic field leads to a $y_2(V_2)$ dependence given by Relations (2). An analysis of Eq. (1) shows that corresponding to the solution of the strong explosion problem in the V , y plane are integral curves starting with the points of the curve $y_2(V_2)$ and entering into the singular point $(0, 0)$ tangent to the abscissa axis. The integral curves obtained numerically for the cases

$$\begin{aligned} V_2 &= 0.3 & y_2 &= 14.8, \quad (\gamma = 2) \\ V_2 &= 0.3 & y_2 &= 33.3 \quad (\gamma = 5/3), \end{aligned}$$

are shown in Fig. 1.

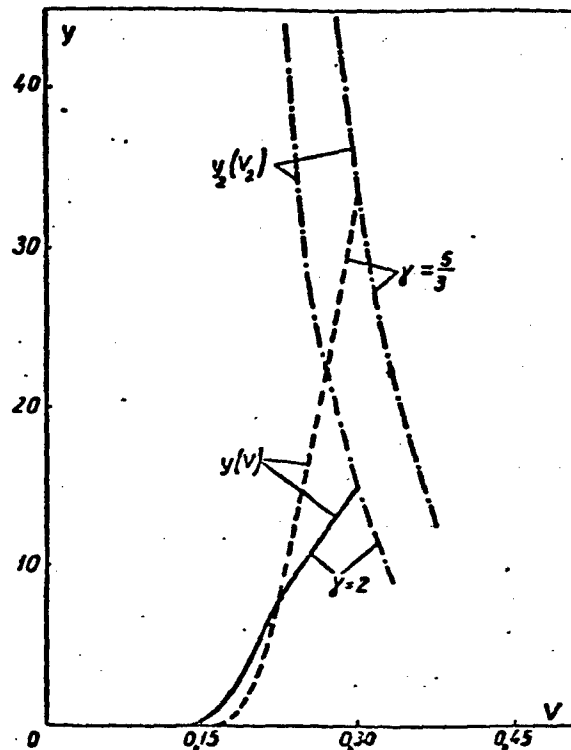


Fig. 1

Let r_2 be the radius of the shock wave. The dependence of $r/r_2 = \lambda$ on V is determined either by quadrature or with the aid of first in-

tegrals. Then, using the integrals and the very simple transformations, we obtain the dependences

$$T/T_2, \quad v/v_2, \quad p/p_2, \quad \varrho/\varrho_2, \quad H_\varphi^2/H_{\varphi 2}^2$$

on λ .

For the dependences $r_2(t)$ and $D(t)$ we have

$$r_2 = \left(\frac{r_0}{\alpha r_1} \right)^{1/2} t^{1/2}, \quad D = \frac{1}{2} \left(\frac{r_0}{\alpha r_1} \right)^{1/2} t^{-1/2},$$

where α is a constant determined during the course of solving the problem from the integral law of conservation of the total energy.

Plots of the variation of T/T_2 , v/v_2 , p/p_2 , and $H_\varphi^2/H_{\varphi 2}^2$ with increasing λ are shown in Fig. 2. We can note the following difference between the solution obtained here and the solution of the gasdynamic problem:

- a) the intensity of the shock wave is smaller than in the gasdynamic case,
- b) $H_\varphi \neq 0$, and near the center $H_\varphi \sim 1/r$,
- c) for the same values of λ , the speed of the gas is smaller than in the gasdynamic case,
- d) the temperature T in the flow region decreases when account is taken of the influence of the magnetic field.

For $\gamma = 2$ the problem can be readily generalized to include the case of a helical field with $H_{z1} = \text{const}$.

For this purpose it is sufficient to take

$$\begin{aligned} v &= v_\varphi, & p &= p_\varphi - H_z^2/8\pi, & \varrho &= \varrho_\varphi, \\ H_r &= H_\varphi, & H_z &= H_\varphi \frac{p}{p_1}, \end{aligned}$$

where the quantities marked by the subscript φ correspond to the problem considered above, with $H_z = 0$ and $\gamma = 2$.

This follows from the boundary conditions and the differential equations under the assumption that $p_2 + H_{z2}^2/8\pi \gg p_1 + H_{z1}^2/8\pi$.

For a weak axial magnetic field, the problem can be extended to include the case of finite conductivity of the medium. In this case we can neglect in first approximation the influence of the magnetic field on the motion of the gas and take into account the influence of the motion on the initial field.

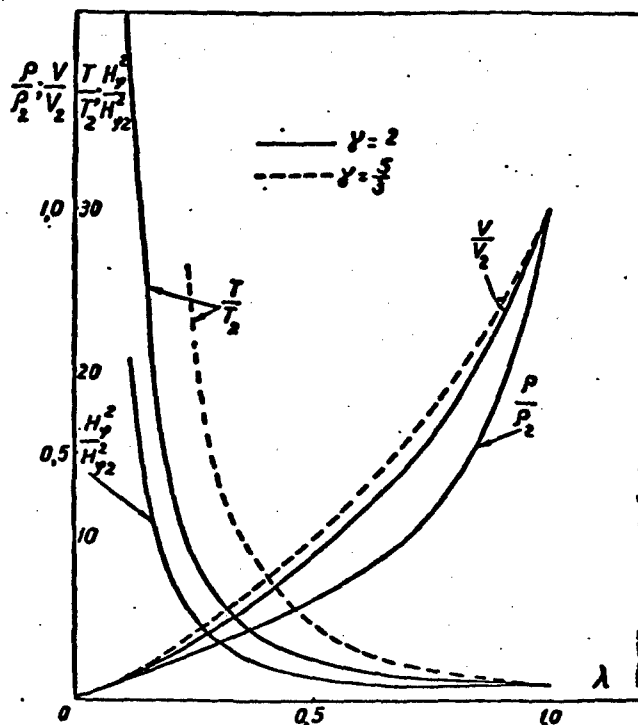


Fig. 2

We denote the initial magnetic field by H_{z0} , and assume the conductivity of the gas behind the front of the shock wave to be constant. For the value of the field ahead of the shock wave we obtain

$$h_1 = C_1 \int \lambda^{-1} e^{-\frac{1}{C_1} \lambda} d\lambda + 1,$$

where

$$C_1 = \text{const},$$

$$x = \left(\frac{x_2}{x_1}\right)^{\frac{1}{\gamma-1}} v_m, \quad h = \frac{H_z}{H_{z0}}.$$

To find H_z in the flow region, we must solve the linear equation

$$2V(V - 0.5) = - h(2V + \lambda V') + \kappa_2 \lambda^{-1} (h') \quad (3)$$

with allowance for the boundary conditions on the shock wave

$$V_1 h_1 - \kappa_2 h'_1 = - \kappa_1 h'_1, \quad h_1 = h_0. \quad (4)$$

where $h' = dh/d\lambda$.

From (4) it is seen that we assume $\kappa_2 \neq \kappa_1$ and presuppose the continuity of the magnetic field. The function $V(\lambda)$ contained in (3) is assumed known from the solution of the gasdynamic problem [1]. The dependence $h(\lambda)$ can be determined numerically. In this case it is necessary to take into account the form of $h_1(\lambda)$ and the representation of $h(\lambda)$ near $\lambda = 0$

$$h = C_2 \left(1 + 0.5V(0) \frac{\lambda^2}{\kappa_2} + \dots \right), \quad C_2 = \text{const.}$$

In the strong explosion problems considered here it is assumed that in the initial instant of time the energy is released instantaneously along the explosion axis. When applied to an electric straight-line discharge this means that the discharge occurs instantaneously and is characterized only by the release of energy. However, when current flows through a thin straight-line conductor the discharge may occur not instantaneously, but over a certain time. The flow of current through the conductor will give rise to an annular magnetic field. In the case of infinite conductivity of the medium, a gas flow will be produced by the expanding magnetic piston.

For simplicity we shall assume that the initial magnetic field in the plasma is zero. Assume that the current flowing in the conductor is I and varies as $I = \sigma_1 t^m$.

By virtue of the infinite conductivity, the magnetic field of the current

$$h_{r_0} = \frac{P}{2\sigma_1 r_0^m}$$

(where r_0 is the distance to the plasma boundary) will expel the gas

from the region adjacent to the axis, and will assume the role of a piston that expands as $r = r_0(t)$.

On the piston we have the boundary conditions

$$p(r_0, t) = p_0 := h_{70}, \quad v(r_0, t) = \frac{dr_0}{dt}.$$

An analysis of this problem with $p_1 = \text{const}$, $p_1 = 0$ (for $m \neq 1$) shows that since this problem is self-similar we have

$$r_0 = \frac{2\sigma_2}{m+1} t^{\frac{m+1}{2}},$$

where σ_2 is the unknown constant. The problem for a linear current corresponds to the expansion of a piston with constant velocity. In this case one can find by numerical integration the dependence of the parameters of the shock wave front on σ_1 .

The problem of a straight-line discharge for a current that increases in accordance with a power law (the inverse pinch effect) can also be investigated for the case

$$0 < m < 1.$$

We note that the analogous gasdynamic problem was investigated in sufficient detail [4]. Without dwelling on the details of the research, we shall point out only the asymptotic formulas which hold true for values of λ close to $\lambda_0 = r_0/r_2$,

$$\begin{aligned} T/T_2 &= A_1 \lambda^2 (1 - \lambda^2 \lambda^{-2})^{-\beta}, \\ p/p_2 &= A_2 (1 - \lambda^2 \lambda^{-2})^\beta, \end{aligned}$$

where $\beta = \frac{1-m}{m-1+\gamma(1+m)}$, $A_1, A_2 = \text{const}$.

The results of the calculation for the case $\gamma = 5/3$, $m = 0.9$ are shown in Fig. 3.

It follows from the plots that the temperature increases sharply on approaching the plasma boundary and that the gas density decreases sharply to zero in a narrow zone near the piston boundary. It was also found that

$$r_2 = 1.217 \sigma_1 t^{0.8}, \quad \sigma_1 = \sigma_1^{\text{in}} (2\pi c^2 \cdot 0.94 \rho_1)^{-1}, \\ \lambda_0 = 0.865.$$

An investigation of the problem of discharge along a straight line at values of m close to unity shows that the density behind the shock wave can be approximately regarded as constant. This pertains, in particular, to problems for which the current built up at sufficiently small t is nearly sinusoidal. In this case there is no need for regarding the radius of the conductor as infinitesimally small, and the solution of the problem greatly simplifies, since the equations of motion of the gas can be completely integrated. For a strong shock wave the general solution has the form

$$p = -\rho_1 \left(\frac{df}{dt} \ln r + 0.5 v^2 \right) + \psi(t), \\ v = f(t) r^1, \quad p = p_2 = \frac{\gamma+1}{\gamma-1} \rho_1,$$

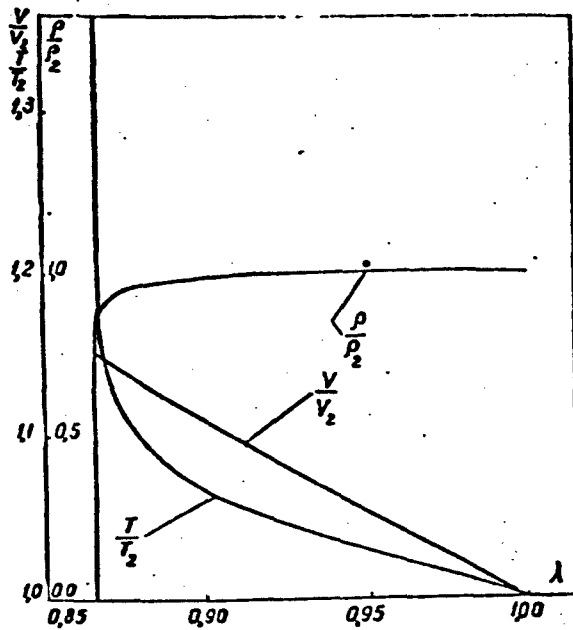


Fig. 3

where $f(t)$ and $\psi(t)$ are arbitrary functions determined from the boundary conditions on the boundary of the magnetic piston and on the front

of the shock wave.

If the conductivity of the gas is assumed to be finite, then the magnetic field of the current will penetrate into the plasma, in which current will start flowing. The effect of the magnetic field on the gas will be transmitted not through a narrow layer, as in the case of very large electric conductivity, but through a gas layer of finite width. The solution of the discharge problems becomes more complicated. This is formally related with the increase in the order of the system of differential equations of magnetohydrodynamics and the more complicated boundary conditions. The solution becomes simpler if the problem is self-similar. If a power law governs the buildup of the current and the dependence of the magnetic viscosity ν_m on ρ and T has the form

$$\nu_m \sim \rho^{\alpha_1} T^{\alpha_2}$$

then the self-similar conditions will be satisfied subject to the supplementary condition

$$-3\alpha_2 + 2 + 3\alpha_1 + \frac{z_1 m + 5z_2 - 2}{m+1} = 0$$

The problems considered above can be used to calculate a complicated discharge consisting of a combination of a direct and inverse pinch effect.

If a discharge is produced in the center of a gas through conductors and current is made to flow simultaneously or with some delay in the cylindrical gas columns surrounding this conductor, or else if a magnetic piston with converging wave is produced, then the interaction of the shock waves causes an appreciable increase in the temperature and pressure during the instant when the shock waves collide. Calculation of the gas parameters for the instant of time close to the instant when the waves collide can be carried out by means of the well-known gasdynamic procedures, using the results of the calculation for

a converging shock wave [5, 6] and the result obtained above for a diverging wave.

REFERENCES

1. L.I. Sedov, Metody podobiya i razmernosti v mekhanike [Methods of Similitude and Dimensional Analysis in Mechanics], 4th edition, Gostekhizdat [State Publishing House for Technical and Theoretical Literature], Moscow, 1957.
2. V.P. Korobeynikov and Ye.V. Ryazanov, Nekotorye resheniya uravneniy odnomernoy magnitnoy gidrodinamiki i ikh prilozheniya [Certain Solutions to the Equations of One-Dimensional Magnetohydrodynamics and Their Applications], PMM [Applied Mathematics and Mechanics], XXIV, 1, 111-120, 1960.
3. V.P. Korobeynikov, Odnomernye avtomodel'nye dvizheniya povedyashchego gaza v magnitnom pole [One-Dimensional Self-Simulating Motion of a Conducting Gas in a Magnetic Field], DAN SSSR [Proceedings of the Academy of Sciences USSR], 121, 4, 613-615, 1958.
4. N.N. Kochina and N.S. Mel'nikova, O neustanovivshemsya dvizhenii gaza, vtyesnyaemogo porshnem [Nonsteady Motion of a Gas being Displaced by a Piston], PMM, XXII, 1, 446-451, 1958.

DEFORMATION OF A CONDUCTING LIQUID SPHERE
UNDER THE INFLUENCE OF A MAGNETIC FIELD

V.V. Yankov
Moscow

ABSTRACT

I. We have continued the investigation of the deformation of an incompressible liquid sphere of infinite electric conductivity, brought about by the action of an inhomogeneous magnetic field. The magnetic energy of the sphere is calculated in the next, second approximation relative to the small perturbation parameters. A new type of deformation, wherein the magnetic energy is decreased, is observed.

II. We also discuss the effect exerted on the stability of a sphere by a homogeneous magnetic field passing through it.

1. Chandrasekhar and Fermi considered [1] in connection with the astrophysical problem of the stability of magnetic stars, the equilibrium of an infinite-conductivity incompressible liquid sphere of radius R with homogeneous internal magnetic field

$$H_r^{(0)} = H \cdot \cos \theta, \quad H_\theta^{(0)} = -H \cdot \sin \theta$$

and a dipole external magnetic field

$$H_r^{(0)} = H(R/r)^3 \cdot \cos \theta, \quad H_\theta^{(0)} = (H/2)(R/r)^3 \cdot \sin \theta \quad (1)$$

relative to the so-called P_1 deformations, which convert the sphere into a figure of revolution, the surface equation of which in spherical coordinates (r, ϑ, ϕ) has the form $r(\vartheta) = R + \epsilon \cdot P_1(\cos \vartheta)$, where $P_1(\cos \vartheta)$ is the Legendre polynomial of degree 1 .

The same authors have established that in first approximation rela-

tive to the small deformation parameter $\epsilon \ll R$ the sphere attempts to assume the form of an oblate spheroid ($l = 2$) and is insensitive to more complicated zonal perturbations ($l > 2$), for which the spherical configuration is an equilibrium one.

We investigated below the magnetohydrodynamic stability of a sphere in the presence of a field (1), relative to an arbitrary weak deformation. The latter can be expanded in spherical harmonics $T_1^m(\vartheta, \phi)$. We shall consider, as is customary, the " T_1^m "-deformation, described by a surface equation

$$r(\vartheta, \phi) = R + \epsilon \cdot T_1^m(\vartheta, \phi). \quad (2)$$

The displacement vector $\vec{\xi}$ of each point of the incompressible liquid in the case of deformation is determined, as in [1], from the system of equations $\vec{\xi} = \nabla \psi$, $\Delta \psi = 0$, the solution of which, satisfying the boundary condition that follows from (2), is

$$\vec{\xi} = \{\xi_r, \xi_\theta, \xi_\phi\} = \frac{\epsilon}{l} \left(\frac{r}{R} \right)^{l-1} \cdot \left\{ l Y_l^m, \frac{\partial Y_l^m}{\partial \theta}, \sin^{-1} \theta \frac{\partial Y_l^m}{\partial \phi} \right\}. \quad (3)$$

The local change in the internal effective magnetic field due to the dragging of the magnetic force lines by the medium is, as is well known, $\delta \vec{H}^{(1)} = \text{rot} [\vec{\xi} \vec{H}]$, which together with (1 and 3) yields

$$\vec{\xi} \vec{H}^{(1)} = \frac{\epsilon H l + m}{R} \left(\frac{r}{R} \right)^{l-2} \cdot \left\{ (l-1) Y_{l-1}^m, \frac{\partial Y_{l-1}^m}{\partial \theta}, \sin^{-1} \theta \frac{\partial Y_{l-1}^m}{\partial \phi} \right\}. \quad (4)$$

The perturbation of the external field, which is expressed as usual in terms of the magnetostatic potential ($\vec{\delta H}^{(e)} = \nabla \Phi$, $\Delta \Phi = 0$), is determined from the requirement that the normal component of the field be continuous on the deformed boundary surface, and is given by the formulas

$$\begin{aligned} \vec{\xi} \vec{H}_r^{(e)} &= \frac{\epsilon H}{R} \left[\frac{(l+m)(l-1)(l+2)}{2l(2l+1)} \left(\frac{R}{r} \right)^{l+1} Y_{l-1}^m + \right. \\ &\quad \left. + \frac{3(l-m+1)(l+2)}{2(2l+1)} \left(\frac{R}{r} \right)^{l+3} \cdot Y_{l+1}^m \right], \\ \vec{\xi} \vec{H}_\theta^{(e)} &= - \frac{\epsilon H}{R} \left[\frac{(l+m)(l-1)(l+2)}{2l^2(2l+1)} \left(\frac{R}{r} \right)^{l+1} \frac{\partial Y_{l-1}^m}{\partial \theta} + \right. \end{aligned}$$

$$+ \frac{3(l-m+1)}{2(2l+1)} \left(\frac{R}{r} \right)^{l+3} \cdot \frac{\partial Y_{l+1}}{\partial \varphi}, \quad (5)$$

$$\begin{aligned} \varepsilon H_i^{(e)} = - \frac{\varepsilon H}{R} & \left[\frac{(l+m)(l-1)(l+2)}{2^l(2l+1)} \left(\frac{R}{r} \right)^{l+1} \cdot \frac{\partial Y_{l-1}}{\partial \varphi} + \right. \\ & \left. + \frac{3(l-m+1)}{2(2l+1)} \left(\frac{R}{r} \right)^{l+3} \cdot \frac{\partial Y_{l+1}}{\partial \varphi} \right] \cdot \sin^2 \theta. \end{aligned}$$

To determine the change in the total magnetic energy of the sphere in the case of T_1^m deformation, we make use of the fact that the energy is equal to the work performed by the ponderomotive forces, taken with the opposite sign. Such an approach greatly simplifies the calculation compared with direct calculations [1]. There are no electrodynamic forces within the sphere, in view of the potential character of the magnetic field vector $\vec{H}^{(1)} + \delta\vec{H}^{(1)}$. The ponderomotive force applied to a unit surface separating the liquid and the vacuum is derived from the Maxwell stress tensor and in this case ($\mu = 1$) is equal to

$$\vec{f} = \frac{1}{4\pi} \vec{H}_1 (\vec{H}_2 - \vec{H}_1) - \frac{1}{8\pi} (\vec{H}_1^2 - \vec{H}_2^2) \cdot \vec{n}, \quad (6)$$

where \vec{n} is the outward normal to the surface, while \vec{H}_1 and \vec{H}_2 denote the magnetic fields inside and outside the deformed sphere, including the small corrections: $\vec{H}_1 = \vec{H}^{(1)} + \delta\vec{H}^{(1)}$, etc. Substituting (1, 4, 5) in (6) and then neglecting terms of higher order of smallness in ε , we obtain an approximate expression for the force components

$$\begin{aligned} f_r &= \frac{3H^2}{32\pi} \sin^2 \theta + \frac{\varepsilon H^2}{8\pi R} \cdot \left\{ \frac{3}{2} \sin^2 \theta \cdot Y_l^m - \right. \\ &\quad \left. - \frac{\sin \theta}{2} \left[\frac{(l+m)(7l^2+3l+2)}{l^2(2l+1)} \frac{\partial Y_{l-1}}{\partial \varphi} - \frac{3(l-m+1)}{2l+1} \frac{\partial Y_{l+1}}{\partial \varphi} \right] \right\}, \\ f_\theta &= \frac{3H^2}{8\pi} \sin \theta \cos \theta + \frac{\varepsilon H^2}{8\pi R} \cdot \left\{ -\frac{3}{2} \sin 2\theta \cdot Y_l^m - \right. \\ &\quad \left. - \cos \theta \left[\frac{(l+m)(5l^2+3l-2)}{l^2(2l+1)} \frac{\partial Y_{l-1}}{\partial \varphi} + \frac{3(l-m+1)}{2l+1} \frac{\partial Y_{l+1}}{\partial \varphi} \right] + \right. \\ &\quad \left. + \frac{3}{4} \sin \theta \left[\frac{(l+m)(5l^2-7l-4)}{l(2l+1)} Y_{l-1}^m + \frac{3l(l-m+1)}{2l+1} Y_{l+1}^m \right] \right\}, \\ f_\varphi &= - \frac{\varepsilon H^2}{8\pi R} \cdot \left\{ \frac{3}{4} \sin \theta \frac{\partial Y_l^m}{\partial \varphi} + \right. \end{aligned}$$

$$+ \frac{\cos^2}{\sin^2} \left[\frac{(l+m)(5l^2+3l-2)}{l(l+1)} \frac{\partial \Gamma_l^m}{\partial r} + \frac{3(l-m+1)}{2l+1} \frac{\partial \Gamma_{l+1}^m}{\partial r} \right]. \quad (7)$$

To find the work done by this force, accurate to ϵ^2 inclusive, we employ a method developed in [1] in the calculation of the change in gravitational potential energy. Assume that for a specified small quantity ϵ the amplitude of the deformation experiences an infinitesimally small increment $\delta\epsilon$. The corresponding displacement $\delta\vec{r}$ is obtained by simply substituting $\delta\epsilon$ for ϵ in (3), namely

$$\delta\vec{r} = \frac{\delta\epsilon}{l} \left(\frac{r}{R} \right)^{l-1} \cdot \left\{ \Omega_l^m, \frac{\partial \Gamma_l^m}{\partial \vartheta}, \sin^{-1} \vartheta \cdot \frac{\partial \Gamma_l^m}{\partial \varphi} \right\}. \quad (8)$$

The change in the magnetic energy of the sphere connected with the infinitesimally small deformation is expressed by the integral of the work consumed in displacement of the surface element $d\sigma$ by a distance $\delta\vec{r}$ in the field of the forces (7), taken over the entire surface, i.e.,

$$\begin{aligned} \delta M &= - \oint (\delta\vec{r} \cdot \vec{f}) d\sigma = \\ &= - \int_0^{2\pi} \int_0^\pi (\delta\vec{r} \cdot \vec{f}) \left[1 + \frac{1}{r^2} \left(\frac{\partial r}{\partial \vartheta} \right)^2 + \frac{1}{r^2 \sin^2 \vartheta} \left(\frac{\partial r}{\partial \varphi} \right)^2 \right]^{\frac{1}{2}} r^2 \sin \vartheta d\vartheta d\varphi. \end{aligned} \quad (9)$$

The integration (9) is carried out with the aid of Relations (2, 7, 8), and in the final result one retains only the terms containing ϵ in the zeroth and first degree. Leaving out intermediate steps, we write out the final result

$$\delta M = \delta\epsilon \cdot \frac{H^2 R^2}{8\pi} \left(\frac{7}{2} \delta_{ll} \cdot \delta_{mm} - \frac{\epsilon}{R} \cdot \Omega_{lm} \right) \int_0^{\frac{\pi}{2}} \int_0^{\frac{\pi}{2}} (\Gamma_l^m)^2 \sin \vartheta d\vartheta d\varphi, \quad (10)$$

where $\delta_{\alpha\beta}$ is the Kronecker-Weierstrass symbol, and

$$\Omega_{lm} = \frac{l-1}{2l+3} \left[\frac{9}{2} - \frac{(26l^2+97l^2+70l^2+11l-6)(l^2-m^2)}{l(l+1)(2l-1)} \right].$$

Integrating (10) with respect to ϵ from 0 to ϵ , we arrive at a final formula for the change in the total magnetic energy of the sphere in T_l^m deformation in the second approximation*

$$M = \frac{7}{20} \epsilon H^2 R^2 \delta_{ll} \cdot \delta_{mm} - \frac{1}{16\pi} \epsilon^2 H^2 R \cdot \Omega_{lm} \int_0^{2\pi} \int_0^\pi (\Gamma_l^m)^2 \sin \vartheta d\vartheta d\varphi. \quad (11)$$

Since the quantity Ω_{lm} is positive when $m = \underline{l}$ and negative in all other cases, only the deformation with $m = \underline{l}$ from among all the non-spheroidal $T_{\underline{l}}^m$ deformations ($\underline{l} > 2; \underline{l} = 2, m \neq 0$) decrease the magnetic energy.

Deformations of this type ($m = \underline{l}$) also decrease the magnetic potential energy of an ideally conducting sphere placed in an external quasi-homogeneous magnetic field [2].

The effects noted in [1] and here are due to the action of both the magnetic pressure normal to the surface and (unlike the case analyzed in [2]) to the tangential component of the ponderomotive force due to the bend of the force lines on the surface. For example, it is easy to show that the contribution made to the main T_2^0 deformation by the tangential component is six times larger than that of the normal component.

It is easy to show that deformations that differ in their azimuthal number m are independent of one another.

The nonequilibrium of the sphere relative to axially symmetrical disturbances ($m = 0$) was investigated in [1].

Although a T_m^m deformation ($m \neq 0$) when taken separately may turn out to be dynamically unrealizable because of the limitations imposed by the equations of motion [3], nonetheless the negative sign of M in this case is indisputable proof of the presence of perturbations which perhaps enter in the more extensive class of deformations of the form

$$r_m(0, \varphi) = R + \sum_{l=1}^{\infty} r_{lm} T_l^m(0, \varphi) (m \neq 0),$$

with respect to which the sphere is known to be unstable.

Consequently, in spite of the fact that the magnetic field (1) flattens the sphere into a spheroid, it also contributes to an increase in the axially asymmetrical perturbations and may serve as a cause of

instabilities of the type indicated above.

2. Let us examine the effect exerted on the character of the stability of an ideally conducting incompressible liquid sphere by a homogeneous magnetic field passing through it [4]

$$H_r^{(0)} = H_r^{(0)} = H \cdot \cos \theta, \quad H_\theta^{(0)} = H_\theta^{(0)} = -H \cdot \sin \theta. \quad (12)$$

Such a "frozen-in" magnetic field is remarkable in that, without effecting the equilibrium of the original sphere, it starts to interact with the sphere only when the latter becomes deformed. The increment in the magnetic energy due to a deformation of the type (2) is equal in this case to

$$M_{lm} = \frac{1}{8\pi} \epsilon_{lm}^2 H^2 R \cdot \frac{(l-1)(2l+1)(l-m^2)}{l} \int_0^{2\pi} \int_0^\pi (l_l^m)^2 \sin \theta d\theta d\phi. \quad (13)$$

After calculations that follow the scheme indicated above [5] it is easy to show that the individual different \underline{T}_1^m deformations are independent of one another. Therefore a generalization of Formula (13) to include the case of a perturbation of arbitrary form

$$r(\theta, \varphi) = R + \sum_{l=2}^{\infty} \sum_{m=-l}^l \epsilon_{lm} l_l^m(\theta, \varphi)$$

reduces simply to the summation

$$M = \sum_{l=2}^{\infty} \sum_{m=-l}^l M_{lm}.$$

We see that all the harmonics with $m \neq \underline{l}$ are stable. Nonetheless, the vanishing of M_{lm} when $m = \underline{l}$ undoubtedly indicates that there exists an unlimited number of deformations of the type $m = \underline{l}$, with respect to which the sphere stays in the state of indifferent equilibrium and which, consequently, are not stabilized by the homogeneous magnetic field (12) that penetrates inside the sphere.

In addition to the astrophysical applications already mentioned [1], the result obtained above can be of interest also in the solution

of the "electromagnetic crucible" problem, and also in the study of the conditions for the stabilization of a sphere-like high conductivity plasma formation (simulated by liquid metal) by external alternating electromagnetic fields in conjunction with a "frozen-in" constant magnetic field [4, 6].

The author is most grateful to M.L. Levin and M.S. Rabinovich for useful remarks and for a discussion of the present article.

REFERENCES

1. S. Chandrasekhar and E. Fermi. *Astrophys. J.*, 118, 116, 1953.
(translation: *Probl. sovr. fiziki* [Problems of Temporary Physics], 2, 108, 1954).
2. V.V. Yanov, *ZETF* [Journal of Experimental and Theoretical Physics], 37, 224, 959.
3. J. Berkowitz et al. Problems in magnetohydrodynamik stability. *Trudy vtoroy Mezhdunarodnoy konferentsii po mirnomu ispol'zovaniyu atomnoy energii* [Transactions of the Second International Conference on the Peaceful Uses of Atomic Energy], (Report No. 376, USA), Geneva, 1958.
4. J.W. Butler. Stability of electromagnetic plasma confinement in spherical geometry. Technical memorandum No. 21 of reactor engineering division of Argonne national laboratory, 1959.
5. V.V. Yankov, *ZTF* [Journal of Technical Physics], 31, 1077, 1961.
6. M.L. Levin, M.S. Rabinovich and G.A. Askaryan. On the stability and focusing of plasma bunches accelerated by radiation. Proc. Intern. conf. on high-energy accelerators and instrumentation, Bern 1959.

Manu-
script
Page
No.

[Footnote]

- 200 Some disparity between the numerical coefficients of the first approximation given here and in [1] ($7/20$ in place of $9/20$) is due to the error that crept in the latter in the calculation of the external magnetic deformation energy [Formulas (147-150)].

MAGNETOHYDRODYNAMIC FLOW WITH SMALL Re_m

M.D. Ladyzhenskiy
Moscow

1. In Cartesian (cylindrical) coordinates \underline{x} , \underline{y} the equations of steady-state plane ($v = 0$) or axially symmetrical ($v = 1$) flow of a gas with finite electric conductivity have in the presence of a magnetic field the form

$$\begin{aligned} u \frac{\partial u}{\partial x} + v \frac{\partial u}{\partial y} + \frac{1}{\rho} \frac{\partial p}{\partial x} &= h_y \frac{q}{\rho} (vh_x - uh_y), \quad q = \frac{\sigma L H^2}{c^2 R V}, \\ u \frac{\partial v}{\partial x} + v \frac{\partial v}{\partial y} + \frac{1}{\rho} \frac{\partial p}{\partial y} &= h_x \frac{q}{\rho} (uh_y - vh_x), \\ \frac{\partial u}{\partial x} + \frac{\partial v}{\partial y} + \frac{v}{y} &= 0, \quad \frac{u^2 + v^2}{2} + \frac{x}{x-1} \frac{p}{\rho} = \frac{1}{2}, \\ \frac{\partial h_x}{\partial x} + \frac{\partial h_y}{\partial y} &= 0, \quad \frac{\partial h_y}{\partial x} - \frac{\partial h_x}{\partial y} = R_m (uh_y - vh_x), \\ R_m &= \frac{4\pi\sigma VL}{c^2}. \end{aligned} \tag{1}$$

Here u and v are the components of the velocity vector along the axes \underline{x} and \underline{y} , h_x and h_y are the components of the magnetic field vector, ρ , p , κ , c , σ are, respectively, the density, pressure, ratio of specific heat, velocity of light, and specific electric conductivity. All the quantities are reduced to a dimensionless form, and the characteristic quantities chosen for the velocity, magnetic field intensity, density, pressure, and length, respectively, are V , H , R , RV^2 , L .

Let us represent the magnetic intensity vector in the form $\vec{h} = \vec{h}_* + \vec{h}'$, where \vec{h}_* is the given field and \vec{h}' is the induced field. We assume that the magnetic Reynolds number is small compared with unity; this, as is well known, makes it possible to neglect in the equations

of motion the induced field compared with the given field. Let the given field \vec{h}_* have at the origin a singularity of the form

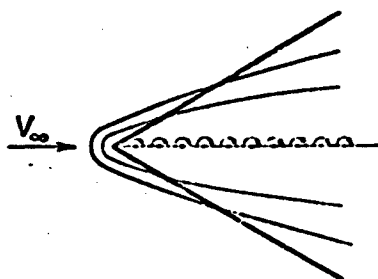


Fig. 1

$$\vec{h}_* = \frac{1}{\sqrt{x}} \hat{\Phi} \left(\frac{y}{x} \right), \quad (2)$$

where $\hat{\Phi}$ is a vector function determined by the given configuration of the field sources. In this case, as can be readily seen, the equations of motion of the gas admit of a class of self-similar solutions, in which the velocity vector, the pressure,

and the density depend on $\eta = y/x$.

2. Let us consider the following problem: a plane semi-infinite plate is located in a plane supersonic steady-state stream of a compressible nonviscous gas flowing in a direction perpendicular to the forward edge of the plate (Fig. 1). Surface currents isolated from the external flux flow in the plate in a direction perpendicular to the plane of the stream; the density of the surface currents j is given by the relation

$$j = -\frac{A}{\sqrt{x}}. \quad (3)$$

The magnetic field (we denote dimensional quantities by upper-case letters) corresponding to this distribution j is given by the equations

$$H_x = \frac{\sqrt{2}\pi A}{c\sqrt{x}} \frac{\eta}{\sqrt{(1+\eta^2)^2 - (1+\eta^2)}} = \frac{\sqrt{2}\pi A}{c\sqrt{x}} f(\eta), \quad (4)$$

$$H_y = \frac{\sqrt{2}\pi A}{c\sqrt{x}} [\eta f(\eta) - 1/(1+\eta^2)^{1/2} - 1] = \frac{\sqrt{2}\pi A}{c\sqrt{x}} \varphi(\eta). \quad (5)$$

It is assumed that the magnetic field under consideration produces in the gas an "ordinary" shock wave, emerging from the forward edge of the plate, and that behind the shock wave the conductivity is finite and the induced field is negligibly small. Ahead of the shock wave the conductivity is assumed equal to zero. In this case the problem does

not have a characteristic linear dimension, the magnetic field satisfies Relation (2), and the flow belongs to the aforementioned class of self-similar solutions, depending on the dimensionless parameters $\eta = y/x$ and $q = 2\sigma A^2 \pi^2 / c^4 RV$.

We note that in the axially symmetrical case there exists an analogous self-similar solution provided one distributes along the x axis dipoles whose axes are directed along the x axis and whose density increases in proportion to $x^{3/2}$. In this case the given field is expressed as before in Form (2). We shall henceforth confine ourselves to an analysis of plane flow.

We consider the case $\sigma = \text{const}$, but generalization is possible to the case of a σ that depends on the temperature and on the pressure. By way of the characteristic quantities we choose the density and the velocity of the unperturbed stream. The usual gasdynamic relations are satisfied on the shock wave, which is represented by an inclined straight line. The equations of motion (1) can be reduced to three ordinary differential equations in u, v, and ρ ; these equations have the form

$$u' \beta [\beta^2 - a^2(1 + \eta^2)] = q\gamma [a(a^2 - v\beta) + z\eta\beta\gamma]. \quad (6)$$

$$v' \beta [\beta^2 - a^2(1 + \eta^2)] = q\gamma [a(a^2\eta + u\beta) - z\beta\gamma]. \quad (7)$$

$$z'^2 [\beta^2 - a^2(1 + \eta^2)] = q\gamma [-(u + \eta v)a + z\gamma(1 + \eta^2)]. \quad (8)$$

$$\beta = v - \eta u, \quad \gamma = fu - \varphi u, \quad a = f\eta - \varphi.$$

$$a^2 = \frac{x-1}{2} (1 - u^2 - v^2).$$

Here $f = f(\eta)$ and $\varphi = \varphi(h)$ are functions defined by Eqs. (4) and (5), while the prime denotes differentiation with respect to η .

3. In view of the complexity of the system of equations (6-8), a qualitative investigation of these equations entails much labor. We report below the preliminary results of such an investigation. We prove first that the integral curves in four-dimensional u, v, ρ , η space do

not cross the singular surface $v - \eta u = C$ in the finite portion of the space anywhere except the point $v = C$, $u = 0$, $\eta = 0$ (ρ is arbitrary).

Were this surface to be crossed by an integral curve at some $\eta = \eta_*$ this would mean, obviously, that the line $\eta = \eta_*$ can be regarded as a solid wall, i.e., the flow would be not over a plate, but over a wedge with a half-aperture angle $\epsilon = \text{arc tan } \eta_*$.

We shall prove this by contradiction. Assume that when $\eta = \eta_*$ the quantity $\beta = v - \eta u$ vanishes, and in the vicinity of $\eta = \eta_*$ the quantities u , v , and ρ do not become infinite. The system of equations (6-8) can be written in the vicinity $\eta = \eta_*$ in simplified form

$$u' = \frac{k_1}{\beta^3}, \quad v = \eta u', \quad \beta' = \frac{k_2}{\beta}, \quad (9)$$

where k_1 and k_2 are constants.

Assume that for some $\eta = \eta_0 \neq \eta_*$ we have $u = u_0$, $v = v_0$, $\rho = \rho_0$. From the equations (9) we have

$$u - u_0 = \lambda \ln \frac{\beta}{\beta_0}, \quad \lambda [\lambda(u - u_0) e^{\lambda(\eta - \eta_0)} - (v - v_0)] + \frac{k_1}{\beta_0} \ln \frac{\beta_0}{\beta} = 0, \quad (10)$$

$$\lambda = \frac{k_1}{k_2}$$

from which it follows that in the case when $k_1 > 0$ we have $\lim_{\beta \rightarrow 0} u = +\infty$ when $\lambda > 0$ and $\lim_{\beta \rightarrow 0} u = -\infty$ when $\lambda < 0$, which contradicts the assumption that the line $\beta = 0$ is reached in a finite part of space. On the other hand, when $k_1 < 0$ the surface $\beta = 0$ is not reached at all, for the value of β decreases in absolute magnitude from a value β_0 to a certain value β_* , after which it starts increasing again. Thus, the foregoing statement is proved. We consider now the equations near the surface of the plate. When $\eta = 0$ the condition $v = 0$, which represents blocking of the flow, is satisfied. The surface of the plate is a singular point for the system (6-8). Let us show that there exists a three-parameter family of solutions satisfying the condition for block-

ing the flow on the surface of the plate.

For this purpose we write down the system (6-8) near $\eta = 0$ in simplified form, expanding $f(\eta)$ and $\varphi(\eta)$ in series and using the smallness of y :

$$u' = -\frac{q}{\rho} \frac{v - \frac{\eta u}{2}}{v - \eta u}, \quad v' = \eta u', \quad \rho' = 0. \quad (11)$$

Introducing $\beta = v - \eta u$, we obtain the equations

$$\beta\beta'' + \frac{a}{2}\beta'\eta^2 - a\beta\eta = 0, \quad u = -\beta', \quad \frac{v}{\rho} = \beta + \eta u, \quad \rho = \rho_0 = \text{const} \quad (12)$$

where $a = q/\rho_0$.

Equation (12) admits of group transformation and can be reduced to a first-order equation in the quantities $x = \beta/\eta^3$, $y = \beta'/\eta^2$:

$$\frac{dy}{dx} = \frac{a(y - x) + 2xy}{x(3x - y)}, \quad \ln \left| \frac{y}{\eta_0} \right| = \int \frac{dx}{y - 3x}. \quad (13)$$

Equation (13) has two singular points — the origin (a combined saddle and node) and the point $x = -a/12$, $y = -a/4$ (a focus). It is easy to check that the point $x = -a/12$, $y = -a/4$ yields an analytic solution of Eq. (12) satisfying the condition $v = 0$ when $\eta = 0$. For u , v , and ρ we obtain in the vicinity of $\eta = 0$ the following expressions:

$$u = \frac{a}{4}\eta^2, \quad v = \frac{a}{6}\eta^3, \quad \rho = \rho_0. \quad (14)$$

It is important to emphasize that, as follows from (14), u also vanishes on the surface of the plate. This is the physical consequence of the fact that the magnetic field intensity on the forward edge of the plate becomes infinite. By making (14) more exact, it is possible to obtain an analytic solution of the equations under consideration near $\eta = 0$ from the exact equations (6-8). This solution has the form

$$u = \frac{q}{4\rho_0}\eta^2 - \frac{15q}{64\rho_0}\eta^4 + \left(\frac{518}{3072} + \frac{3-x}{x-1} \frac{29q^2}{5184\rho_0^2} \right) \frac{q}{\rho_0}\eta^6 + \dots$$

$$v = \frac{q}{6\rho_0}\eta^3 - \frac{3q}{16\rho_0}\eta^5 + \left(\frac{37}{256} + \frac{3-x}{x-1} \frac{43q^2}{42336\rho_0^2} \right) \frac{q}{\rho_0}\eta^7 + \dots$$

$$p = p_0 \left(1 - \frac{3}{x-1} \frac{\eta^2}{48 p_0^2} \right) + \dots \quad (15)$$

In addition to the solution (14) and (15), there exists an infinite set of nonanalytic integral curves, which approach this solution as $\eta \rightarrow 0$. To find these solutions we put in the first equation of (13)

$$x = -\frac{3}{12} + \xi, \quad y = -\frac{a}{4} + \eta.$$

Assuming ξ and η to be small quantities, we obtain

$$\frac{d\eta}{d\xi} = \frac{\frac{3}{2} - \frac{\eta}{3\xi}}{\frac{1}{4} - \frac{1}{12}\xi}. \quad (16)$$

The solution of this equation is

$$|\xi| = \frac{c_1}{\sqrt{\left(\frac{\eta}{\xi} - 3.5\right)^2 + \frac{23}{4}}} e^{-\frac{1}{\sqrt{23}} \operatorname{arc tg} \frac{2\left(\frac{\eta}{\xi} - 3.5\right)}{\sqrt{23}}}. \quad (17)$$

Using the second equation of (13), we obtain finally

$$\left| \frac{3}{\eta^2} + \frac{u}{12} \right| = \frac{c_1 \sqrt{\eta}}{\sqrt{1 + \operatorname{tg}^2 \left(\sqrt{23} \ln \frac{c_2}{\sqrt{\eta}} \right)}}. \quad (18)$$

where $\beta = v - \eta u$, while c_1 and c_2 are constants.

Equation (18) yields the sought solution; u , v , and ρ are determined in accordance with (12). Thus, the general solution near the singular point depends on the three arbitrary constants p_0 , c_1 , and c_2 .

We propose to consider in the future the question of the uniqueness of the construction of the solution for η close to zero, the solution having the form (18) and satisfying on the shock wave the ordinary gasdynamic relations for a shock wave.

APPROXIMATE METHOD OF INVESTIGATING PLANE
VORTICAL FLOWS IN MAGNETOHYDRODYNAMICS

I. I. Nochevkina
Moscow

We are investigating plane steady-state vortical motion of an ideal compressible liquid with infinite conductivity in an external magnetic field perpendicular to the plane of flow. The determination of the parameters of such a flow reduces mathematically to a simultaneous solution of the following system of electrodynamic and hydrodynamic equations

$$\text{rot}(\vec{v}\vec{H})=0, \quad \text{div}\vec{H}=0,$$
$$(\vec{v}\nabla)\vec{v} = -\frac{1}{\rho}\nabla p - \frac{1}{4\pi\rho}[\vec{H}\text{rot}\vec{H}], \quad \text{div}(\vec{\varphi}\vec{v})=0$$

for an equation of state specified in the form

$$p = A(\psi)\rho^* - B(\psi), \quad (1)$$

($A(\psi)$, $B(\psi)$ are functions characterizing the entropy distribution); this equation of state, as is well known, is valid for a tremendous majority of vortical flows. From the induction equation and from the continuity equation we can find the first integral of the system (1)

$$\frac{H}{\rho} = a(\psi). \quad (2)$$

The effect of the magnetic field on the motion of the conducting liquid reduces in this case to an additional pressure

$$p' = \frac{a^2(\psi)}{8\pi}\rho^*. \quad (3)$$

and therefore the general equation of state can be written in the form

$$P = \frac{a^2(\rho)}{8\pi} r^2 + A(\rho)z^2 - B(\rho). \quad (4)$$

We represent the velocity vector in the form

$$\vec{v}(x, y) = \lambda(x, y) \operatorname{grad} \varphi. \quad (5)$$

where $\lambda(x, y)$ is a proportionality coefficient and $\varphi(x, y) = \text{const}$ is a family of surfaces orthogonal to the stream lines. In this case the normal cross sections can be drawn also for current tubes of finite dimensions, since the Gromeka condition [1] is always satisfied for plane flow. The solution of the system (1) can be reduced to the solution of the differential equations

$$\lambda(x, y) \frac{\partial \varphi}{\partial x} = \frac{1}{\rho(x, y)} \frac{\partial \varphi}{\partial y}, \quad \lambda(x, y) \frac{\partial \varphi}{\partial y} = - \frac{1}{\rho(x, y)} \frac{\partial \varphi}{\partial x}, \quad (6)$$

which are obtained with the aid of (5) and the continuity equation, in the presence of the equation of state (4) and the projections of the equation of motion on the tangent and on the normal to the stream line. Let us consider the vortical flows for which the degree of regularity of the dependence of the velocity on the entropy is stronger than that on the density, and for which the coefficient of proportionality λ in (5) can be regarded approximately as a function of the density only. We break down the entire flow region into elementary regions within each of which the entropy has its own specific constant value $A_1, A_2, \dots, A_n \dots$. For such elementary regions, the equations (6) expressed in new specially selected independent variables ρ and Θ (Θ is the angle between the velocity vector and the x axis) assume the form

$$\frac{\partial \varphi}{\partial \rho} = - \left[\frac{1}{\rho^2} + \frac{1}{\rho} \frac{\partial \varphi}{\partial \rho} \right] \frac{\partial \varphi}{\partial \Theta}, \quad \frac{\partial \varphi}{\partial \Theta} = - \frac{1}{\rho \left[\frac{d\lambda}{d\rho} - \lambda(\rho) \frac{1}{\rho} \frac{\partial \varphi}{\partial \rho} \right]} \frac{\partial \varphi}{\partial \rho}. \quad (7)$$

The equations in (7) contain, for a constant density ρ^* in an adiabatically decelerated gas, the following invariant with respect to the stream lines:

$$\frac{1}{v} \left(\frac{\partial v}{\partial z} \right)_s = - \frac{1}{2(z^* - z)}. \quad (8)$$

In fact, using the Bernoulli equation, we obtain

$$v^2(p, \psi) = 4R(\psi)(p^* - p), \quad v \left(\frac{\partial v}{\partial p} \right) = -2R(\psi).$$

where

$$R(\psi) = \frac{a^2(\psi)}{8\pi} + A(\psi), \quad (n=2),$$

from which we verify that (8) is correct. It is easy to show also that the projection of the equation of motion on the normal to the stream line vanishes within the elementary regions. On the basis of (8), the equations in (7) are real for the entire gas flow region when $\lambda = \lambda(p)$. In the presence of a perpendicular magnetic field we have $p^* = v_{\max}^2(\psi)/4R(\psi)$, i.e., it depends on the character of the eddies (the distribution of the total energy along the stream lines) and on the specification of the function $a(\psi)$. For arbitrary vortical flows and for a definite specification of $a(\psi)$, p^* can be regarded as constant. Thus, it becomes possible to investigate the vortical flows in this case by means of the same methods that were developed for potential flows. Substituting the value $1/v (\partial v / \partial p)_s$ from (8) in (7) we obtain

$$\frac{\partial z}{\partial p} = - \left[\frac{1}{z^2} - \frac{1}{2p(z^* - z)} \right] \frac{\partial \psi}{\partial \lambda}, \quad \frac{\partial z}{\partial \lambda} = - \left[\frac{1}{p \left[\frac{dz}{dp} + \frac{1}{2(z^* - z)} \right]} \right] \frac{\partial \psi}{\partial p}. \quad (9)$$

A method of solving the equations in (9) by introducing the function of S.A. Chaplygin was detailed in [2]. It is possible to use that method to investigate the parameters of plane subsonic and supersonic nonisentropic flows with the equation of state specified in the general polytropic form

$$P = A(\psi)p^n - B(\psi) \quad (n=1, 2, 3 \dots).$$

We note that V.S. Tkalich obtained several results in magnetic gasdynamics with the aid of the transformation of S.A. Chaplygin.

With the aid of this method we can investigate also the parameters of plane steady-state flow in the presence of perpendicular magnetic fields and also in the case of finite conductivity of the medium. The mechanical problem reduces in this case to a solution of the system (1) with a modified induction equation

$$\text{rot}[\vec{v}\vec{H}] = -\eta \nabla^2 \vec{H}, \quad (10)$$

where $\eta = c^2/4\pi\sigma$ is the coefficient of magnetic viscosity. In the case of constant finite conductivity, $\eta = \text{const}$, we obtain from (10)

$$v_y H_z = \frac{\partial}{\partial y} (\eta H_x), \quad v_x H_z = \frac{\partial}{\partial x} (\eta H_x). \quad (11)$$

i.e., the velocity vector can be represented in the form

$$\vec{v} = \text{grad} \varphi, \quad (12)$$

where $\varphi = \eta \ln H_z$.

This method can be used to solve analogously the mechanical problems also in the case of variable conductivity of the medium, when $\text{grad } \sigma$ (and consequently also $\text{grad } \eta$) coincides in direction with the conduction current, as is the case, for example, with the cooling jet in a plasmotron. Then $[\text{grad } \eta \times \text{rot } \vec{H}] = 0$, and the induction equation can be represented, apart from a gradient of an arbitrary function, in the form

$$[\vec{v}\vec{H}] = \eta \text{rot} \vec{H}, \quad (13)$$

hence

$$\vec{v}(x, y) = \eta(x, y) \text{grad} \varphi, \quad (14)$$

where $\varphi = \ln H_z$, which is equivalent to a certain vortical flow with proportionality coefficient $\eta(x, y)$.

REFERENCES

1. I.S. Gromeka, Sobr. soch. [collected works], Izd-vo AN SSSR [Academy of Sciences USSR Press], 1952, 116.
2. I.I. Nochevkina, DAN SSSR [Proceedings of the Academy of Sciences

USSR], 126, 6, 1959.

Manu-
script
Page
No.

[Footnote]

212 To simplify the derivations we henceforth write for the polytropic exponent $n = 2$.

INVESTIGATION OF STEADY-STATE ULTRARELATIVISTIC ISENTROPIC
FLOWS IN THE PRESENCE OF MAGNETIC FIELDS

I. I. Nochevkina
Moscow

The motion of a relativistic gas in the presence of arbitrary magnetic fields can be represented in the form of the vanishing of the four-divergence of the summary mechanical and electromagnetic energy-momentum tensor. In the case of a gas of infinite conductivity, the energy-momentum tensor can be written in the form [1]

$$T_{\mu\nu} = \frac{W^*}{V} U_\mu U_\nu + p^* \delta_{\mu\nu} \quad (1)$$

where $W^* = pV + \rho Vc^2 + W'$ is the summary heat content of the gas and of the magnetic field, $p^* = p + p'$ is the summary pressure, V is the specific volume, U_1 is the 4-velocity, $x_{1,2,3} = x, y, z$; $x_4 = ict$.

It can be shown that in the presence of arbitrary electromagnetic fields it is sufficient to consider only the modified energy momentum tensor for macroscopic bodies, which includes the additional heat content W' and the additional pressure p' . In the general case W' and p' can be readily calculated from the formulas

$$W' = \frac{V}{4\pi} \left(F'_{ik} F'_{ii} + \frac{u^2}{c^2} \frac{F'_{lm}}{4\Theta^2} \delta_{ik} \right) U_i U_k$$
$$p' = - \frac{F'_{lm}}{16\pi\Theta^2} \cdot \left(\theta = \sqrt{1 - \frac{u^2}{c^2}} \right), \quad (2)$$

where F'_{ik} are the components of the tensor of the electromagnetic field in the K' frame, relative to which the element of the medium moves with velocity u . The advantage of reducing the summary energy

momentum tensor of the system comprising the gas and the electromagnetic field to a modified tensor of macroscopic bodies manifests itself in going over from one reference frame to another, since the Lorentz transformations for the components of the electromagnetic field tensor F'_{1k} are much simpler than those for the components of the electromagnetic energy momentum tensor $T_{1k}^{(1)}$.

If an isentropic mode is maintained, the investigation of the parameters of a plane steady-state flow of an ultrarelativistic gas in an arbitrary magnetic field can be carried out with the aid of the method described in [2].

We shall carry out the investigation for an infinitesimally small gas element in the laboratory frame K. In the case of isentropic flows, as is well known, there exists a relativistic analog of the potential

$$\frac{\partial \varphi}{\partial x_i} = U_i W^*, \quad (3)$$

from which we have for plane flows with $i = 1, 2$

$$W^* U_1 = \frac{\partial \varphi}{\partial x_1}, \quad W^* U_2 = \frac{\partial \varphi}{\partial x_2}. \quad (4)$$

Using also the relativistic continuity equation to introduce a relativistic analog of the stream function

$$\frac{U_1}{V} = \frac{\partial \psi}{\partial x_2}, \quad \frac{U_2}{V} = -\frac{\partial \psi}{\partial x_1}, \quad (5)$$

we obtain equations analogous to the equations describing a plane vortical flow of an ordinary gas [2], where the role of the proportionality coefficient λ is assumed by a quantity that is reciprocal to the summary heat content

$$\frac{1}{W^*} \frac{\partial \varphi}{\partial x} = V \frac{\partial \psi}{\partial y}, \quad \frac{1}{W^*} \frac{\partial \varphi}{\partial y} = -V \frac{\partial \psi}{\partial x}. \quad (6)$$

Thus, the problem reduces to a solution of Eqs. (6) using the relativistic Bernoulli equation (7)

$$\frac{W^*}{\Theta} = W_0^* = \text{const} \quad (7)$$

and the equation of state (8)

$$p^* = (\gamma - 1)\epsilon^*; \quad (1 < \gamma < 2). \quad (8)$$

which in the case of ultrarelativistic systems is completely defined by specifying a single thermodynamic function (for example, W^*).

By introducing new independent variables $\xi(W^*)$ and α , where α is the angle between the velocity 3-vector and the x axis, and noting that $u = u(W^*)$, $V = V(W^*)$, we represent the equations in (6) in the form

$$\begin{aligned} \frac{1}{W^*} \frac{\partial \varphi}{\partial \xi} &= \left(\frac{\partial V}{\partial W^*} - \frac{V}{u} \frac{\partial u}{\partial W^*} \right) \frac{dW^*}{d\xi} \cdot \frac{\partial \psi}{\partial z}, \\ \frac{1}{W^*} \left(\frac{1}{W^*} + \frac{1}{u} \frac{\partial u}{\partial W^*} \right) \frac{dW^*}{d\xi} \frac{\partial \varphi}{\partial z} &= V \frac{\partial \psi}{\partial \xi}. \end{aligned} \quad (9)$$

We have assumed here that the functions $\varphi(\xi, \alpha)$ and $\psi(\xi, \alpha)$ are continuous, finite, and single valued, while the Jacobian $\frac{\partial(x, y)}{\partial(\xi, \alpha)} \neq 0$ does not vanish in the entire flow region. Substituting into Eqs. (9) the values of $u(W^*)$ and $\partial u / \partial W^*$ determined from (7), and V and $\partial V / \partial W^*$ from (8) in the particular case when $\gamma = 4/3$, and imposing on ξ , as an arbitrary function of W^* , the simplifying condition

$$\frac{A_1(-3W^{*2} + 4)}{W^*(1 - W^*)} \frac{dW^*}{d\xi} = 1,$$

we reduce the equations of (9) to the form

$$\frac{\partial \varphi}{\partial \xi} = \frac{\partial \psi}{\partial z}, \quad \frac{\partial \varphi}{\partial z} = -K(W^*) \frac{\partial \psi}{\partial \xi}, \quad (10)$$

where

$$K(W^*) = \frac{A_1(-3W^{*2} + 4)}{W^{*2}(1 - 2W^{*2})}$$

is the Chaplygin function which we have introduced. The solution of the equations in (10) with the aid of the approximate Chaplygin method was described in [2].

The proposed method is used to investigate steady-state isentropic flow of an ultrarelativistic gas in a perpendicular magnetic field. It

is observed here that a perpendicular magnetic field does not affect the isentropic flow of an ultrarelativistic gas. In the case of a magnetic field with arbitrary orientation in the plane of flow, the isentropic mode is as a rule disturbed.

REFERENCES

1. K.P. Stanyukovich. ZhETF [J. Expt. Theor. Phys.], 36, 6, 1959.
2. I.I. Nochevkina. DAN SSSR [Proc. Acad. Sci. USSR], 126, 6, 1959.

DISCUSSION FOLLOWING THE PAPER

V.S. Tkach
Sukhumi

The method of S.A. Chaplygin was first used in magnetic gasdynamics by I.I. Nochevkina [1]; that paper generalizes the previously obtained results.

The successive application of the methods of I.S. Gromeka and S.A. Chaplygin turns out to be fruitful.

If all the principal quantities and the electrostatic potential are independent of one of the Cartesian coordinates (x_1, x_2, x_3) and of the time (t) ($\partial/\partial x_3 = \partial/\partial t = 0$), and if there is no dissipation or external ponderomotive forces, then, by using the method of I.S. Gromeka, we obtain the vector fields

$$\left. \begin{aligned} \vec{H} &= \nabla \psi \vec{x}_3 + h \vec{e}_3, \quad \vec{V} = (1, \nu) \nabla \psi_0 \vec{x}_3 + v \vec{e}_3, \quad \vec{E} = -\nabla \Phi, \\ h &= 4\pi p \left(\frac{\psi' Q - \psi'_0 \Phi'}{4\pi (\psi'_0)^2 - p (\psi')^2} \right), \quad v = \frac{4\pi \psi'_0 Q - p \psi' \Phi}{4\pi (\psi'_0)^2 - p (\psi')^2} \end{aligned} \right\}. \quad (1)$$

The quantities ψ , ψ'_0 , Φ , Q , and also the entropy s are arbitrary functions of the parameter $\xi = \xi(x_1, x_2)$. The prime denotes everywhere the derivative with respect to its argument.

In order for the transformation of S.A. Chaplygin to be possible,

it is sufficient for the effective pressure $P(\rho, \xi) \equiv p(\rho, s) + h^2/8\pi$ (where the ordinary pressure $p(\rho, s)$ is an arbitrary function of the density and of the entropy) to have the form

$$P = \rho^2 \frac{\partial}{\partial \rho} \left(\frac{H}{\rho} \right), \quad H \equiv H(E), \quad E \equiv (\dot{x}_0)^2 + (\dot{y})^2/4\pi. \quad (2)$$

where H is an arbitrary function of E . The first two components of the equation of motion (the system (1) – solution of all other equations) is transformed to the form

$$\frac{\partial \xi}{\partial \theta} + \frac{u}{E} \frac{\partial \eta}{\partial u} = 0, \quad \frac{\partial \eta}{\partial u} + u \left(\frac{d}{du} - \frac{1}{uE} \right) \frac{\partial \eta}{\partial \theta} = 0, \quad u^2 \equiv H'(E), \quad (3)$$

where φ is the analog of the two-dimensional velocity potential and θ is the angle between the x_1 axis and $\nabla \varphi$.

Putting in (1-3) $\psi = \text{const}$, $v = 0$, we obtain the plane flows in the presence of a magnetic field perpendicular to the plane of the flow.

REFERENCE

1. I.I. Nochevkina. DAN SSSR [Proc. Acad. Sci. USSR], 126, 6, 1959.

CONTRIBUTION TO THE THEORY OF
THE MAGNETOHYDRODYNAMIC PISTON

I.A. Akhiezar, G.Ya. Lyubarskiy, R.V. Polovin
Khar'kov

The types of waves arising in a magnetohydrodynamic medium with infinite conductivity under the influence of an ideally conducting piston moving uniformly in it are determined. Because of the adhesion of the magnetic force lines to the medium and to the piston, the relative velocity of the medium on the surface of the piston is zero. When the piston moves in a normal direction, two magnetic sound shock waves are produced on the side of the liquid; when the piston moves in the opposite direction, two self-similar magnetic sound waves are produced; there is no Alfven wave in either case.

The problem of the motion of a piston at an arbitrary angle to the normal is solved for the case when the magnetic pressure is appreciably smaller than the hydrostatic pressure. If the transverse velocity component of the piston exceeds the velocity of sound in the unperturbed medium, then a magnetic field is generated, i.e., the magnetic field increases from infinitesimally small to finite quantities; in this case the magnetic pressure is comparable in order of magnitude with the hydrostatic one. In the case of supersonic velocities, a vacuum region (cavitation) is produced between the piston and the medium. Compared with ordinary hydrodynamics, a conducting medium is subject to additional cases of cavitation when the piston moves in a direction perpendicular to the normal with supersonic velocity, and

also when the piston is inserted, provided the angle between the piston velocity vector and the normal to its surface exceeds 70° (for an ideal gas). An increase in the component of piston velocity perpendicular to the normal decreases the frontal resistance. In the presence of cavitation, the frontal resistance is one quarter as small as in the case when the piston moves in the direction normal to its surface.

The work was published in DAN SSSR, 128, 684 (1959); ZhETF, 38, 529 (1960); ZhETF, 38, 1544 (1960).

ON THE "LAW OF ACTION INVERSION"

IN MAGNETIC GASDYNAMICS

L.A. Vulis, P.L. Gusika

Alma-Ata

The equations of action inversion [1] are derived for the general case of a conducting gas for an arbitrary form of the equation of state and in the particular case of an ideal gas. The changes in flow velocity, Mach number, temperature, and other parameters are considered for stationary quasi-one-dimensional flows.

It is shown that the conditions for the inversion of action pertain to the transition through the magnetohydrodynamic speed of sound $\tilde{a} = \sqrt{a^2 + a_m^2}$, where a is the speed of sound in the absence of the fields and a_m is the speed of the magnetic sound oscillations. It is of interest, however, to investigate also the conditions of the transition through the hydrodynamic speed of sound.

Two limiting cases of flow, for large and small values of the magnetic Reynolds number Re_m , are analyzed in detail. In the first case ($Re_m \gg 1$) the results obtained are a direct generalization of the equations of ordinary gasdynamics, with $\tilde{a}^2 = a^2 + v_A^2$, where v_A is the

velocity of the Alfvén wave. In the second case ($Re_m \ll 1$ and $\tilde{a} \approx a$) the conditions for the transition through the speed of sound reduce essentially to those considered in [2]. For the intermediate case (finite but large conductivity), the results given in [3] are developed and made more exact.

The main results of the work is a generalization of the law of action inversion to include the case of magnetic gasdynamic flows. A detailed exposition of the problems considered is given in the paper by the authors "On the Inversion of Actions in Magnetohydrodynamics" (ZhTF, XXXI, 7, 806, 1961).

REFERENCES

1. L.A. Vulis. Termodinamika gazovykh potokov [Thermodynamics of Gas Flows], GEI [State Publishing House for Literature in Our Engineering], Moscow, 1950.
2. Ye.L. Resler and U.R. Sirs. Collection "Mekhanika" [Mechanics], 6, (52), 3, 1958; 6 (58), 39, 1959.
3. G.S. Golitsyn and K.P. Stanyukovich. ZhETF [J. Expt. Theor. Phys.], 33, 6 (12), 1417, 1957.

SOME PROBLEMS IN THE THEORY OF SIMPLE WAVES

R.V. Polovin
Khar'kov

The Riemann invariants in magnetohydrodynamics are calculated for the case when the magnetic pressure is appreciably smaller than the hydrostatic pressure. The formulas obtained are used to solve the problem involving the flow of a plasma in vacuum in the presence of a magnetic field. In the case of outgoing flow, three magnetohydrodynamic waves propagate in the plasma while an electromagnetic wave is radiated

in the vacuum. The Riemann invariants obtained make it possible to solve the problem of supersonic motion of a magnetohydrodynamic piston.

The paper was published in ZhETF, 39, 2(8), 463 (1960); ZhETF, 39, 3(9), 657 (1960).

RELATIVISTIC SHOCK WAVES IN MAGNETOHYDRODYNAMICS

L.M. Kovrzhnykh
Moscow

The properties of the shock adiabat in relativistic magnetohydrodynamics are investigated for the case of perpendicular shock waves. In several limiting cases (strong shock wave) simple expressions are obtained relating the values of the thermodynamic quantities on both sides of the discontinuity. The possibility is discussed of accelerating charged particles with the aid of shock waves. It is shown that in the ultrarelativistic case of perpendicular shock waves such an acceleration is possible.

The paper was published in ZhETF, 39, 4, 1042 (1960).

STRUCTURE OF LOW-INTENSITY SHOCK WAVES IN MAGNETOHYDRODYNAMICS

Ye.P. Sirotina, S.I. Syrovatskiy
Moscow

1. The problem is considered of the structure of weak shock waves of arbitrary type [1] in a viscous heat-conducting medium with finite conductivity.

2. Accurate to second-order terms, the system of magnetohydrodynamic equations for stationary one-dimensional flow, with allowance of

the dissipative terms, reduces to an equation analogous to that obtained in [2] for an ordinary gasdynamic shock wave. An exception is the vicinity of the singular point, at which the velocity of propagation of the discontinuity relative to the medium is equal to the Alfvén velocity. This point corresponds to a rotational discontinuity. It is obvious that a rotational discontinuity cannot be stationary in the presence of dissipation, since the boundary conditions for such a discontinuity call for the constancy of the entropy, in contradiction with the fact that the entropy must grow as a result of dissipation.

3. Linearizing the equation obtained, we can determine the damping coefficient of small amplitude waves. The damping coefficient is $\gamma = ak^2$, where k is the wave vector and

$$\begin{aligned} \epsilon = \frac{1}{2(\nu^4 - c^2 u_n^2)} & \left\{ c^2 (\nu^2 - u_n^2) \left[\frac{\chi}{\rho} \left(\frac{1}{c_v} - \frac{1}{c_p} \right) + \frac{\nu^2}{\rho c^2} \left(\frac{4}{3} \eta + \xi \right) \right] + \right. \\ & \left. + (\nu^2 + c^2) \left(\nu^2 \beta + \frac{u_n^2}{\rho} \eta \right) \right\}. \end{aligned}$$

Here ν is the phase velocity of the wave under consideration (see, for example, [1]), u_n is the Alfvén velocity, c is the velocity of sound, ρ is the density of the medium, c_v and c_p are the specific heats; η and ξ are the first and second viscosity coefficients, χ is the heat conduction coefficient, and β is the magnetic viscosity.

4. Inclusion of terms of second order of smallness leads to the following expression for the width of the discontinuity in magnetohydrodynamics

$$l = \frac{A}{p_2 - p_1},$$

where $p_2 - p_1$ is the pressure difference away from the discontinuity,

$$A = \frac{2c_p}{\nu} \frac{(\nu^4 - c^2 u_n^2) \alpha}{\nu^2 c^2 (\nu^2 - u_n^2) \left(\frac{\partial \alpha}{\partial \rho} \right)_s + 3(\nu^2 - c^2) \nu^2}$$

$\alpha = 1/\rho$ and the derivative is taken at constant entropy S .

5. The same expression for the width of the discontinuity can be obtained from qualitative considerations, by considering the equilibrium between two processes: the diffusion smearing of the discontinuity under the influence of the effective viscosity, and the opposing process of "entanglement" of the discontinuity, owing to the difference in the velocities of the disturbances on the two sides of the discontinuity.

The paper was published in ZhETF, 39, 3(9), 746, 1960.

REFERENCES

1. S.I. Syrovatskiy. UFN [Progress in the Physical Sciences], 62, 247, 1957.
2. L. Landau and Ye. Lifshits. Mekhanika sploshnykh sred [Mechanics of Continuous Media], 2nd edition, Moscow, 1954.

SPECIAL CASE OF INTERACTION BETWEEN A MAGNETIC FIELD AND A STRONG SHOCK WAVE

Yu. L. Zhilin

Moscow

A shock wave giving rise to ionization of a gas is considered, with the conductivity of the gas equal to zero outside the shock wave, and with a certain region inside the wave, in which electric currents flow and the electromagnetic field interacts with the motion. As a result of this interaction, the temperature of the gas drops and the conductivity disappears.

The structure of such a wave is analyzed for the case when the gas has ordinary and magnetic viscosities.

ABSORPTION OF MAGNETOHYDRODYNAMIC WAVES IN WAVEGUIDES

Yu.F. Filippov

Khar'kov

A paper by Gajewski [1] is devoted to an investigation of magneto-hydrodynamic waves of infinitesimally small amplitude in waveguides filled with an ideal conducting liquid. However, the formalism employed is unjustifiably complicated and difficult to check. Consequently [1] contains several incorrect results. In particular, it is shown in the present paper, in contrast with the statement made in [1], that no Alfvén wave can propagate in a rectangular waveguide and no Alfvén or sound wave can propagate in a coaxial waveguide.

The paper presents the derived dispersion relations for magneto-hydrodynamic waves with dispersion, the critical frequencies, and also expressions for the velocity field and for the magnetic field intensity in a rectangular and in a coaxial waveguide. The dependence of the absorption coefficient on the signal frequency and on the medium and waveguide parameters is considered for the propagation of waves in a conducting medium having viscosity and heat conductivity.

REFERENCE

1. Gajewski. The Physics of Fluids, 2, 633, 1952.

MERIDIONAL FLOWS OF A CONDUCTING LIQUID

G.L. Grodzovskiy, A.N. Dyukalov, V.V. Tokarev, A.N. Tolstykh
Moscow

It is shown that a broad class of self-similar solutions exist for the magnetohydrodynamic equations in the case of meridional flow of a conducting liquid. Examples of several exact solutions are considered.

TURBULENT FLOW OF A CONDUCTING LIQUID IN A HOMOPOLAR ENGINE

E.F. Fradkina, A.V. Kozyukov

Moscow

A study is made of the motion of solutions of cuprous oxide under the influence of crossed electric and magnetic fields between coaxial cylindrical electrodes (in a homopolar engine) at Reynolds numbers R from 6000 to 60,000 and at different ratios of the electrode radii $\epsilon = r_1/r_2$. The dependence of the resistance coefficient ξ on R and ϵ is found to be in agreement with the theory of turbulent flow of liquids in a homopolar engine as given by M.F. Shirokov and Ye.P. Vaulin.

CONCERNING THE STEADY FLOW OF A
CONDUCTING LIQUID IN A RECTANGULAR TUBE

Ya.S. Uflyand

Leningrad

1. For motion of a viscous incompressible electrically conducting liquid in a prismatic channel in the presence of a magnetic field perpendicular to the channel axis, the equations of magnetohydrodynamics can be reduced to a linear system of two differential second-order equations. In this case both the flow velocity and the induced magnetic field have only a single component directed along the channel axis.

2. In the case of a tube of rectangular cross section, a simple solution can be obtained for two limiting cases, when the channel walls have either very small or very large conductivity.

3. An exact solution of the problem was found with the aid of Fourier series for the case of ideally conducting tube walls. The form of the solution obtained is convenient for numerical calculations aimed at determining the influence of the lateral walls of the tube, since

the part of the solution corresponding to the one-dimensional mode has been separated out.

PLANE PROBLEM OF FLOW OF INCOMPRESSIBLE LIQUID
OF FINITE CONDUCTIVITY AROUND A SOLID BODY
IN A PERPENDICULAR MAGNETIC FIELD

K.A. Lur'ye

Leningrad

In the case considered, the magnetic field does not influence the velocity distribution, which is obtained by solving the corresponding hydrodynamic problem. Nondetached flow is assumed.

The magnetic field is determined from the induction equation. The latter can be reduced by mapping in the complex potential plane to a form that is independent of the velocity distribution in the flow. The boundary condition for the magnetic field in the complex potential plane are specified on straight-line segments if the flow is around obstacles of finite dimensions, and on rays in the opposite case. The shape of the obstacle does not play any role in this case.

As an example, symmetrical frontal flow around a parabolic dielectric profile is considered. The magnetic field is produced by current flowing out of a wire placed in a channel specially made in the dielectric.

The paper was published in ZhTF, XXX, 6, 736, 1960; 9, 1960.

ESTIMATE OF THE INFLUENCE OF THE EARTH'S MAGNETIC FIELD
ON THE TURBULENCE IN THE LOWER IONOSPHERE

G.S. Golitsyn

Moscow

The author has shown previously (DAN SSSR, 132, 2, 1960) that the density of the random currents induced in the turbulent flow of a poorly conducting liquid (magnetic viscosity much larger than the kinematic viscosity) is in a weak magnetic field a locally homogeneous random quantity, i.e., like the velocity or a passive impurity, it is determined locally, independently of what goes on on large scale. This theory makes it possible to determine the conditions under which one can neglect the reaction of the magnetic field on the turbulence. Violation of these conditions should be regarded as an indication that the influence of the magnetic field may prove to be appreciable for the dynamics of the medium. These premises were applied to an analysis of specific conditions of the upper atmosphere and it was shown that the influence of the magnetic field on the turbulence in the ionosphere is insignificant up to heights on the order of 150 km.

EFFECTIVENESS OF LOCAL MAGNETIC FIELD IN SOLAR CORONA

E.I. Mogilevskiy

Moscow Oblast

1. Calculation of the propagation of local magnetic fields of the solar photosphere in the region of the upper chromosphere and of the corona, taken in the form of magnetohydrodynamic and magnetic-sound waves in accordance with the Ferraro scheme, has shown that a magnetic field cannot propagate in this manner above the middle chromosphere.

2. The local magnetic field of the active region may be "carried

"out" by solar plasma clouds moving out of the chromosphere into the corona. In this case the magnetic field in the cloud may become appreciably intensified. A qualitative examination can be made of the interaction of such a cloud with the varying magnetic field of the active region. This enables us to judge whether the sun can eject geoeffective streams.

3. At large distances from the sun ($>3-4 R_{\odot}$) and near the earth ($>4 R_{\oplus}$) the quasi-stationary magnetic field does not change appreciably the parameters of the corpuscular solar streams.

EFFECT OF THE MAGNETIC FIELD
ON MOTION IN CHROMOSPHERIC FLARES

S.I. Gopasyuk
Crimea

The development of chromospheric flares is characterized by two stages: initial - expansion independent of the field direction, and subsequent - motion directed essentially along the magnetic field.

GENERATION OF COSMIC RAYS
IN A SOLAR FLARE

A.B. Severnyy, V.P. Shabanskiy
Moscow

It is assumed that the solar flare is none other than a reflected shock wave outgoing from the region of the neutral point of the magnetic solar fields; the shock wave energy comes from the opposing plasma motion brought about by a change in the magnetic field in the sun spots. An estimate of the temperature of the medium behind the front of the reflected shock wave, based on experimental data concerning the rate of expansion of the flare region with allowance for the fact that the front propagates in a plasma moving toward the neutral point, shows that in strong flares the temperature can be sufficiently high to effect thermonuclear fusion of the deuterium nuclei present in insignificant amounts in the solar chromosphere. The products of these and of the secondary thermonuclear reactions have sufficient energy to satisfy the necessary conditions for the acceleration of the particles upon reflection from the approaching magnetic mirrors under the conditions of the solar flare. The role of magnetic mirrors is played here by regions with large magnetic fields which extend inside the sun spots. It is shown convincingly that the minimum injection energy of the particles entering the region between these magnetic mirrors, necessary to satisfy the acceleration conditions, coincides precisely with the energy of the thermonuclear reaction products. There are also other indications that a thermonuclear reaction occurs in strong flares.

Estimates based on the picture so developed give satisfactory agreement with the experimental data.

Other acceleration mechanisms, which are compatible with this flare model, are considered: the Fermi statistical mechanism, acceleration between two approaching magnetic mirrors with field directed perpendicular to the plane of the mirrors, acceleration of a particle passing through the front of the shock wave in a magnetic field, and acceleration between the fronts of collapsing magnetohydrodynamic shock waves. It is shown that these mechanisms, which can play a certain role in other objects, are little effective compared with the first-order Fermi acceleration mechanism under the conditions of the solar flare.

FORMATION OF ACTIVE REGIONS IN
THE PRESENCE OF A MAGNETIC FIELD

S.B. Pikel'ner

Moscow

The active regions on the sun are closely related with magnetic fields. Even an intensity of 1-2 oersted gives rise to torches, floculas, coronal rays, and streams of geoactive particles. A mechanism is proposed whereby the convection becomes more intense in the presence of the fields, so that the indicated formations can appear. The mechanism is connected with the suppression of turbulence in convective streams, so that the turbulent viscosity is decreased. High latitude torches, the prominent wind from the sun, and other phenomena are given a natural explanation.

THEORETICAL PROBLEMS IN PLASMA PHYSICS

SOME PROBLEMS IN RELATIVISTIC GASDYNAMICS OF CHARGED PARTICLES

V.N. Tsytovich

Moscow

§1. INTRODUCTION

The relativistic motion of conducting gas masses has several specific features. Thus, for example, V.I. Veksler [1] showed that in collisions between an ionized mass and a condensation of magnetic force lines the ions transfer a considerable part of their energy to the electrons, which become relativistic. This means that even at negligibly low frequency v_{eff} of collisions between the electrons and the ions (i.e., high conductivity), in a reference frame that moves together with the given gas element, $\vec{E} + [\vec{vH}/c] \neq 0$ and is determined by the inertia force, the value of which can become large in the ultra-relativistic limit, owing to the relativistic increase in mass. Consequently the flux of the magnetic field through a liquid contour is not conserved and the adhesion of the magnetic force lines is violated.

Thus, one of the unique features of relativistic motion of conducting gas masses is the possible violation of the freezing in of the magnetic field force lines. As a consequence of this, it becomes impossible to describe such a motion with the aid of equations containing the two vectors \vec{v} and \vec{H} , the hydrodynamic velocity and the magnetic field (the vectors of relativistic magnetic gasdynamics). This remark pertains in particular to nonstationary processes, for which the force of inertia in the accompanying reference frame may be large.

Another qualitative difference, also connected with the creation of relativistic electrons, is, as is well known, the possible violation of electric neutrality, even in the stationary state. Thus, a collective effect is produced resulting from the action of the summary electric field produced by the gas.

To investigate these effects of relativistic motion of conducting masses, it is advantageous to turn to relativistic two-component gas-dynamics in electromagnetic fields. In the present paper we consider several general problems in relativistic gasdynamics of charged particles. We find an analog of potential motion in the presence of "relativistic current" and in its absence, and consider several one-dimensional nonstationary motions. Problems of relativistic gasdynamics of a neutral gas were considered by I.M. Khalatnikov [2]. In §2 of the present article we follow [2] closely, and generalize the corresponding results to the case when self-consistent and external electromagnetic fields are present.

§2. SOME GENERAL PROBLEMS

The relativistic motion equation for one of the components of a gas of charged particles situated in an electromagnetic field has obviously the form

$$\frac{\partial T_{\mu\nu}}{\partial x_\nu} = F_{\mu\nu} j_\nu \quad (1)$$

where [3] $T_{\mu\nu} = w u_\mu u_\nu + p \delta_{\mu\nu}$ is the gas energy in the momentum tensor, u_μ is the 4 velocity, p is the pressure, $w = \epsilon + p$ is the heat function per unit volume, ϵ is the internal energy per unit of the medium's own volume, $j_\mu = e n u_\mu$ is the current produced by the particles, n is the proper density, v is the three-dimensional velocity (the velocity of light c is assumed equal to unity), $F_{\mu\nu}$ is the electromagnetic field tensor, and

$$d\left(\frac{w}{n}\right) = T d\left(\frac{s}{n}\right) + \frac{1}{n} dp.$$

Taking into account the fact that $u_\mu F_{\mu\nu} j_\nu = 0$, we obtain as a consequence of (1) the conservation of the entropy per unit of own volume, s , along the particle trajectory:

$$\frac{d}{ds} \left(\frac{s}{n}\right) = 0, \quad (2)$$

where $d/ds = u_\mu (\partial/\partial x_\mu)$ is the substantial derivative with respect to the proper time. Confining ourselves to isentropic motion, introducing the heat function per particle $W = w/n$, and taking into account the thermodynamic identity $dW = (1/n)dp$, we can represent Eq. (1) in the simple form

$$\frac{d}{ds} W u_\mu = - \frac{\partial W}{\partial x_\mu} + e F_{\mu\nu} u_\nu \quad (3)$$

Let us find the analog of the potential motion for a gas of charged particles in an electromagnetic field. As was shown by I.M. Khalatnikov [2] and Frankel' [4], the relativistic analog of potential motion of a neutral gas is $W u_\mu = \partial \phi / \partial x_\mu$. It is easy to generalize this result to include the presence of electromagnetic fields. Introducing the 4 potential of the electromagnetic field $F_{\mu\nu} = \partial A_\nu / \partial x_\mu - (\partial A_\mu / \partial x_\nu)$, we can note that Eq. (3) has solutions of the following form

$$W u_\mu = -e A_\mu + \frac{\partial \phi}{\partial x_\mu}. \quad (4)$$

The fourth of the relations (4) is the analog of the Bernoulli equation. For a one-dimensional stationary case, the condition (4) is always satisfied; in other words, one-dimensional motion is always "quasipotential." Arguments analogous to those in [2] enable us to obtain from the equations of motion the relations

$$\frac{\partial}{\partial x_1} (W u_1 + e A_1) = \frac{\partial}{\partial x_0} (W u_0 + e A_0), \quad (5)$$

thus proving the "quasipotential nature" of the motion. Let us consider

now the case of one-dimensional motion in the presence of a current perpendicular to the direction of motion, as referred to in the introduction. We can assume that the charged liquid considered here is an electron gas, the charge of which is partially or completely neutralized by the ion gas, the contribution of which to the current density can be neglected. We assume that all the quantities dependent only on x_1 and x_4 , and in addition, since $u_3 \neq 0$, we also have $A_3 \neq 0$. Then the equations of motion (3) projected on the 3 axis yields

$$u_1 \frac{\partial}{\partial x_1} W u_3 + u_4 \frac{\partial}{\partial x_4} W u_3 = -e u_1 \frac{\partial A_3}{\partial x_1} - e u_4 \frac{\partial A_3}{\partial x_4} \quad (6)$$

or

$$\left(x_0 = -i x_4; u_1 = v \gamma; u_4 = i \gamma; \gamma = \frac{1}{\sqrt{1 - v^2 - v_3^2}} \right)$$

$$\frac{\partial}{\partial x_1} W v_3 \gamma + v \frac{\partial}{\partial x_4} W v_3 \gamma = e(E_3 + v H_2). \quad (7)$$

Equation (7) is the analog of Ohm's law,* but the left half of the equation is determined not by the friction force but by the inertia force. Owing to the inertia force, noticeable electric fields, which do not satisfy the relation $E_3 = -v H_2$, may arise in the ultrarelativistic limit. Instead of finding the connection between H_2 and E_3 , which follows from (7), it is convenient to find the condition imposed on the potential A_μ . Equation (6) can also be written in the form

$$\left(u_1 \frac{\partial}{\partial x_1} + u_4 \frac{\partial}{\partial x_4} \right) (W u_3 + e A_3) = \frac{d}{ds} (W u_3 + e A_3) = 0. \quad (8)$$

In other words, the quantity $W u_3 + e A_3 = p_3$ is conserved along the trajectory of particle motion. This result is valid not only for one-dimensional motion. To satisfy (8) it is sufficient that all the quantities be independent of x_3 ("cyclic coordinate"). If the inertial term $W u_3$ can be neglected, then the conservation law (8) reduces to the conservation of the flux through the liquid contour ($A_3 \sim \phi$). If at the initial instant of time p_3 is constant for all points, it re-

mains constant in all succeeding instants of time. Such one-dimensional nonstationary motion is also always quasipotential. Indeed, the first equation of (3) can in this case be represented in the form

$$(1+u_1^2)\frac{\partial W}{\partial x_1} + u_1 \frac{\partial}{\partial x_1} W u_1 + W u_1 \frac{\partial u_1}{\partial x_1} = \\ = e u_1 \left(\frac{\partial A_1}{\partial x_1} - \frac{\partial A_1}{\partial x_4} \right) + e u_3 \frac{\partial A_1}{\partial x_1}. \quad (9)$$

We use for the transformation of (9) the relations

$$u_1^2 + u_3^2 + u_4^2 = 1, \quad u_1 \frac{\partial u_3}{\partial x_1} + u_3 \frac{\partial u_1}{\partial x_1} + u_4 \frac{\partial u_4}{\partial x_1} = 0$$

and the relations $e(\partial A_3 / \partial x_1) = -u_3 (\partial W / \partial x_1) - W (\partial u_3 / \partial x_1)$, which follow from $W u_3 + e A_3 = \text{const}$. Then (9) is reduced to the form

$$\frac{\partial}{\partial x_1} (W u_1 + e A_1) = \frac{\partial}{\partial x_1} (W u_1 + e A_1), \quad (10)$$

which proves the quasipotential nature of the motion. For three-dimensional motion there exists a generalized Thomson theorem on the conservation of the circulation of the velocity

$$\frac{d}{ds} p_{\mu\nu} = p_{\mu\nu} \frac{\partial u_\alpha}{\partial x_\nu} - p_{\nu\nu} \frac{\partial u_\alpha}{\partial x_\mu}, \quad (11)$$

where

$$p_\mu = W u_\mu + e A_\mu; \quad p_{\mu\nu} = \frac{\partial}{\partial x_\nu} p_\mu - \frac{\partial}{\partial x_\mu} p_\nu$$

In the derivation of the last equation we made use of Eq. (6), of $u_\alpha = \partial u_\alpha / \partial x_\nu = 0$, and of the Maxwell equation $(\partial F_{\mu\nu} / \partial x_\alpha) + (\partial F_{\alpha\nu} / \partial x_\mu) + (\partial F_{\mu\alpha} / \partial x_\nu) = 0$. In the nonrelativistic limit we have $W \sim m$; $u_1 \approx v$; $u_4 \approx 1$; in the absence of electromagnetic fields, (11) reduces to the well-known conservation of the circulation along a liquid contour

$$\frac{d}{dt} \text{rot} \vec{V} = (\text{rot} \vec{V}, \vec{V}) \vec{V} - \text{rot} \vec{V} \text{div} \vec{V}. \quad (12)$$

§3. SOME ONE-DIMENSIONAL PROBLEM

a) Problem of Relativistic Scattering of a Layer of Charged Particles in Vacuum

The problem of the relativistic scattering of a layer of neutral gas in vacuum was first solved with logarithmic accuracy by L.D. Landau

[5] in connection with the hydrodynamic theory he proposed for multiple particle production in the collision of high-energy nucleons. Subsequently I.M. Khalatnikov [2] showed that the one-dimensional problem of relativistic hydrodynamics (using a certain transformation that he introduced) can be reduced to the problem of integrating a linear differential equation with constant coefficients, and also found an exact solution of the problem of the relativistic scatter of a neutral layer of gas in vacuum.

In the problem of the disintegration of a cluster of charged particles, the collective interaction of the summary electric field produced by the particles may exert a decisive influence on this disintegration.

In one-dimensional motion, it is advantageous to write down the four-velocity components in the form (see [3])

$$u_1 = \sinh \eta; u_4 = iu_0; u_0 = \cosh \eta; x_4 = ix_0. \quad (13)$$

Then the equations of motion (3), the continuity equation, and Maxwell's equations can be written in the form

$$\begin{aligned} \frac{\partial}{\partial x_0} W \sinh \eta + i \hbar \eta \frac{\partial}{\partial x_1} W \sinh \eta + \frac{1}{\cosh \eta} \frac{\partial W}{\partial x_1} - eE &= 0, \\ \frac{\partial}{\partial x_0} n \cosh \eta + \frac{\partial}{\partial x_1} n \sinh \eta &= 0; \quad \frac{\partial eE}{\partial x_1} = 4\pi n e^2 \cosh \eta, \\ \frac{\partial eE}{\partial x_0} &= -4\pi n e^2 \sinh \eta. \end{aligned} \quad (14)$$

Let us consider the limiting case of the scattering of a charged layer of cold gas into a vacuum.

For nonrelativistic temperatures and a monatomic gas we have

$$W = m + \frac{5}{2} T_0 \left(\frac{n}{n_0} \right)^{2/3}, \quad (15)$$

where T_0 and n_0 are certain initial values of the temperature and density of the gas, m is the rest energy (mass) of the particle, and $c = k = 1$.

By virtue of the proof given above, the one-dimensional motions are always "quasipotential": $Wu_1 = eA_1 + (\partial\varphi/\partial x_1)$; $Wu_4 = -eA_4 + (\partial\varphi/\partial x_4)$. Using the gauge invariance, we can put $\varphi = 0$; both the field and the motion of the gas are then described only by the potentials A_1 and $A_0 = -iA_4$. The electric fields are expressed in simple manner through .

$$W \text{ and } u \equiv u_1 (u_4 = i\sqrt{1+u^2}),$$

$$eE = \frac{\partial}{\partial x_0} Wu + \frac{\partial}{\partial x_1} W\sqrt{1+u^2}. \quad (16)$$

From the last two equations of (14) we can obtain as a consequence

$$\frac{\partial E}{\partial x_0} + \frac{u}{\sqrt{1+u^2}} \frac{\partial E}{\partial x_1} = 0. \quad (17)$$

To solve the posed problem of relativistic scatter of a charged layer, it is convenient to determine not u as a function of x_1 and x_0 , but x_1 as a function of x_0 and u ; $x_1 = \psi(x_0, u)$. Putting $\partial\psi/\partial u \neq 0$ and $\chi \equiv eE(x_0, u)/m$, we transform (17) to the variables x_0 and u :

$$\frac{\partial \chi}{\partial x_0} + \frac{\partial \chi}{\partial u} \frac{1}{\frac{\partial \psi}{\partial u}} \left(-\frac{\partial \psi}{\partial x_0} + \frac{u}{\sqrt{1+u^2}} \frac{1}{\frac{\partial \psi}{\partial u}} \right) = 0. \quad (18)$$

We make a similar transformation for (16):

$$\begin{aligned} \chi &= \left(1 + \frac{5}{2} \frac{T_0}{m} \left(\frac{n}{n_0} \right)^{2/3} \right) \left(-\frac{\frac{\partial \psi}{\partial x_0}}{\frac{\partial \psi}{\partial u}} + \frac{u}{\sqrt{1+u^2}} \frac{1}{\frac{\partial \psi}{\partial u}} \right) + \\ &+ \frac{5}{3} \frac{T_0}{m} \left(\frac{n}{n_0} \right)^{2/3} \left(\frac{u}{n} \frac{\partial n}{\partial x_0} - \frac{u}{n} \frac{\partial n}{\partial u} \frac{\frac{\partial \psi}{\partial x_0}}{\frac{\partial \psi}{\partial u}} + \frac{1}{n} \frac{1+u^2}{\sqrt{1+u^2}} \frac{\partial n}{\partial u} \frac{1}{\frac{\partial \psi}{\partial u}} \right). \end{aligned} \quad (19)$$

The coefficient of $\partial\chi/\partial u$ in (18) can be expressed in terms of χ (19) accurate to terms of first order in T_0/m . We obtain in place of (18) and (19)

$$\frac{\partial \chi}{\partial x_0} + \chi \frac{\partial \chi}{\partial u} = \frac{T_0}{m} G \frac{\partial \chi}{\partial u}; \quad \frac{\partial \chi}{\partial x} + \gamma \frac{\partial \chi}{\partial u} = \frac{u}{\sqrt{1+u^2}} + \frac{T_0}{m} G \frac{\partial \chi}{\partial u}, \quad (20)$$

where

$$G = 5 \left(\frac{n}{n_0} \right)^{2/3} \left[\frac{1}{2} + \frac{1}{3} \frac{u}{n} \left(\frac{\partial \chi}{\partial x_0} - \frac{\partial u}{\partial t} \frac{\partial \psi}{\partial x_0} \right) + \frac{1}{3} \frac{1}{n} \frac{1}{n^2} \frac{1}{\partial \psi / \partial u} \frac{\partial n}{\partial u} \right]. \quad (21)$$

The density n should be expressed in (20) in terms of χ and ψ :

$$n = \frac{1}{r_0 \sqrt{1+u^2}} \frac{\partial \chi}{\partial u}; \quad r_0 = 4\pi \frac{e^2}{m}. \quad (22)$$

Inasmuch as $T_0 \ll m$, the solutions of the system (20-22) can be sought in the form of expansions in the parameter

$$\chi = \chi_0 + \chi_1 \frac{T_0}{m} + \dots; \quad \psi = \psi_0 + \psi_1 \frac{T_0}{m} + \dots \quad (23)$$

We confine ourselves only to two terms of the expansion (23):

$$\begin{aligned} \frac{\partial \chi_0}{\partial x_0} + \gamma_0 \frac{\partial \chi_0}{\partial u} &= 0; \quad \frac{\partial \psi_0}{\partial x_0} + \gamma_0 \frac{\partial \psi_0}{\partial u} = \frac{u}{\sqrt{1+u^2}}; \\ \frac{\partial \chi_1}{\partial x_0} + \gamma_1 \frac{\partial \chi_1}{\partial u} + \gamma_0 \frac{\partial \chi_0}{\partial u} &= G_0 \frac{\partial \psi_0}{\partial u}; \\ \frac{\partial \psi_1}{\partial x_0} + \gamma_1 \frac{\partial \psi_1}{\partial u} + \gamma_0 \frac{\partial \psi_0}{\partial u} &= G_0 \frac{\partial \psi_0}{\partial u}; \end{aligned} \quad (24)$$

$$\begin{aligned} G_0 &= 5 \left(\frac{n^{(0)}}{n_0} \right)^{2/3} \left\{ \frac{1}{2} + \frac{u}{3n^{(0)}} \left(\frac{\partial n^{(0)}}{\partial x_0} - \frac{\partial n^{(0)}}{\partial u} \frac{\partial \psi_0}{\partial x_0} \right) + \frac{1}{3} \frac{1}{n^{(0)}} \frac{1}{n^{(0)}} \frac{\partial n^{(0)}}{\partial u} \frac{\partial \psi_0}{\partial u} \right\}, \\ n^{(0)} &= \frac{1}{r_0 \sqrt{1+u^2}} \frac{\partial \chi_0}{\partial u}. \end{aligned} \quad (25)$$

We see that the system (24) for the zeroth approximation of the functions χ_0 and ψ_0 turn out to be linear (the linearity of the equations for the higher approximations is trivial). Besides, the system of equations (24) can be solved successively, since the boundary or initial conditions for χ_0 can be specified independently from physical considerations, since χ coincides with the magnitude of the electric field accurate to the constant e/m . From the determined value of χ we can find the solution of the second equation of (24).

Let us give the results of an analysis of the scattering of a

charged layer of thickness $2l$. We assume that at the initial instant of time $x_0 = 0$ the gas density is zero, with the exception of a layer $-l < x_1 < l$, where it is constant and equal to n_0 . The electric field inside the layer is assumed to be static at the initial instant of time (linearly dependent on x_1)

$$\dot{\phi} = \frac{u}{n_0 r_0 x_0} + \frac{x_0}{u} (\sqrt{u^2 + 1} - 1). \quad (26)$$

$u = v\gamma = v/n_0 r_0 x_0$, where v is the hydrodynamic velocity. Putting $v = x_1$, we obtain an implicit expression for the velocity v as a function of x_1 and x_0 . The solution (26) holds true when

$$|\dot{\phi}| \leq l + \frac{1}{ln_0 r_0} (\sqrt{1 + F n_0^2 r_0^2 x_0^2} - 1).$$

The equality sign corresponds to the motion of the layer boundary. When $x_0 \ll 1/\ln_0 r_0$ the boundary of the layer moves with uniform acceleration and when $x_0 \gg 1/\ln_0 r_0$ it moves inertially. In the nonrelativistic limit $\gamma = 1 + \epsilon$, $\epsilon \ll 1$ it follows from (26) that

$$z = \frac{n_0^2 r_0^2 x_0^2}{2 \left(1 + \frac{1}{2} n_0 r_0^2\right)^2}. \quad (27)$$

The particle energy increases quadratically away from the center of the layer. At a fixed point it first increases in time, and then decreases. The latter is due to the fact that when x_0 is large slow particles start arriving at a given point from the center and these could not acquire large energies in the weak self-consistent field at the center, whereas the fast particles move away from this point. The characteristic time interval for the buildup of energy at a given point is $\sqrt{2/n_0 r_0}$. If $x_0 \ll 1/\ln_0 r_0$ and $2n_0 r_0^{-1} \ll 1$, then the maximum values of the particle energy on the layer boundary, $\epsilon_{\max} = n_0^2 r_0^2 x_0^{-2}/2 \ll 1$, are nonrelativistic. When $n_0 r_0^{-1} \gg 1$ and $1 \gg x_0 \gg 1/\ln_0 r_0$ the quantity $z_{\max} = \frac{n_0^2 r_0^2 x_0^2}{2 \left(1 + \frac{1}{2} n_0 r_0^2\right)^2}$ becomes relativistic. It is also easy to obtain

the distribution over the energies in the ultrarelativistic limit. The result is as follows: the energy increases linearly with increasing x . The distribution of the particle density can be obtained with the aid of (25)

$$\frac{n^{(2)}}{n_0} = \frac{1}{1 + n_0 r_0 c_0^2 \left[1 - \frac{(u^2 + 1)(\sqrt{1 + u^2} - 1)}{u^2 \sqrt{1 + u^2}} \right]}. \quad (28)$$

To determine the region of applicability of the results we used (23-25) to obtain the next approximation in T_0/m : the criterion obtained was $T_0/m \ll n_0 r_0 c_0^2$. The procedure described here was used also to solve problems involved in the scattering into vacuum of density distributions of other forms, particularly of a stratified structure.

b) Collisions Between Charged Layer and a Constant Electric Field

We assume that at the initial instant $x_0 = 0$ there exists a disintegrating layer of thickness $2l$, moving with initial relativistic velocity $u^H \gg 1$ toward a constant electric field $eE_H/m = \chi_H(x_1)$. Neglecting the temperature effect and using the gauge invariance, we obtain

$$\chi + \chi_H = \frac{\partial u}{\partial x_0} + \frac{\partial}{\partial x_1} \sqrt{1 + u^2}, \quad (29)$$

$$\frac{\partial \chi}{\partial x_0} + \frac{n}{\sqrt{1 + u^2}} \frac{\partial \chi}{\partial x_1} = 0. \quad (30)$$

Introducing, as above, $x_1 = \psi(x_0, u)$, we transform (29) and (30) into

$$\frac{\partial \chi}{\partial x_0} + (\chi + \chi_H) \frac{\partial \chi}{\partial u} = 0; \quad \frac{\partial \psi}{\partial x_0} + (\chi + \chi_H) \frac{\partial \psi}{\partial u} = \frac{u}{\sqrt{1 + u^2}}. \quad (31)$$

A solution of this system for the problem under consideration can be obtained in parametric form (the parameter t varies between the limits $\frac{1}{2}\sqrt{1 + u_H^2} < t < \frac{1}{2}\sqrt{1 + u_H^2}$):

$$x_0 = \int_t^{\frac{1}{2}\sqrt{1 + u_H^2}} \frac{\sqrt{u_H^2 + 1} + \chi_H(t)(\psi'' - t) + \int_t^{\psi''} \chi_H(\gamma) d\gamma}{\sqrt{\left[\sqrt{u_H^2 + 1} + \chi_H(t)(\psi'' - t) + \int_t^{\psi''} \chi_H(\gamma) d\gamma \right]^2 - 1}}. \quad (32)$$

$$\sqrt{1+u^2} - \sqrt{1+u_H^2} = \chi_H(t)(\gamma - t) + \int_t^\gamma \chi_H(\gamma') d\gamma'. \quad (33)$$

where $\chi_H(t)$ is the initial distribution of the layer's own electric field inside the layer.

For an initial density n_0 that is constant along the layer, we have $\chi_H = n_0 r_0 t$. The calculation of (32) even for an external field that increases linearly with distance already leads to elliptical integrals.

c) Collision Between Charged Layer and a Constant Magnetic Field

A magnetic field gives rise to a current, i.e., to a component u_3 in the velocity of the electron gas. We assume that at the initial instant of time $u_3 = 0$ and that there is no magnetic field inside the layer ($A_3 = 0$). Hence, if we neglect temperature effects, we obtain by virtue of the proof above that $u_3 = -eA_3/m$. We consider a case when the screening of the external field by the produced current is small and we assume that $u_3 \approx u_3^0 = -eA_3^0(x_1)/m$, where $A_3^0(x_1)$ is the potential of the external field. Proceeding to find $x_1 = \gamma(x_0, u)$, we obtain for small temperatures

$$\frac{\partial \gamma}{\partial x_0} + \left(\chi - \frac{u_3^0}{\sqrt{1+u^2+u_3^2}} \frac{eH_2^0}{m} \right) \frac{\partial \gamma}{\partial u} = \frac{u}{\sqrt{1+u^2+u_3^2}}, \quad (34)$$

$$\frac{\partial \chi}{\partial x_0} + \left(\chi - \frac{u_3^0}{\sqrt{1+u^2+u_3^2}} \frac{eH_2^0}{m} \right) \frac{\partial \chi}{\partial u} = 0, \quad (35)$$

where $H_2^0 = -\partial A_3^0 / \partial x_1$ is the external magnetic field and $\chi = eE/m$ is the own electric field. The solution of the systems (34, 35) for the case when the layer moves at the initial instant of time with relativistic velocity $u_H \gg 1$ toward a magnetic field, has the form

$$\sqrt{1+u^2+u_3^2}(\gamma) - \sqrt{1+u_H^2} = (\gamma - t) \chi_H(t), \quad (36)$$

$$x_0 = \int_t^\gamma d\gamma' \frac{\sqrt{1+u_H^2} + \chi_H(t)(\gamma' - t)}{(\sqrt{1+u_H^2} + \chi_H(t)(\gamma' - t))^2 - u_3^2(\gamma' - t)},$$

$$-l\sqrt{1+u_{H_1}^2} < t < l\sqrt{1+u_{H_2}^2} \quad (37)$$

For a magnetic field that increases linearly with the distance, the calculation of (37) leads to elliptic integrals. In the case of a jump in the magnetic field, the calculations can be carried through to conclusion.

In conclusion I consider it my pleasant duty to thank V.I. Veksler, M.S. Rabinovich, and A.A. Rukhadze for fruitful discussions of the results of the work.

REFERENCES

1. V.I. Veksler. DAN SSSR [Proceedings of the Academy of Sciences USSR], 118, 63, 1958.
2. I.M. Khalatnikov. ZhETF [Journal of Experimental and Theoretical Physics], 27, 529, 1954.
3. L.D. Landau, Ye.M. Lifshits. Mekhanika sploshnykh sred [Mechanics of Continuous Media], GITIL [State Publishing House for Technical and Theoretical Literature], Moscow, 1954.
4. F.N. Frankel'. DAN SSSR, 84, 1, 1952.
5. L.D. Landau. Izv. AN SSSR, ser. fiz. [Bulletin of the Academy of Sciences USSR, Physics Series], XVII, 5, 51, 1953.

Manu-
script
Page
No.

[Footnote]

238 At relativistic relative velocities the friction term causing the momentum transfer from the electrons to the ions is negligibly small.

PLANE AND CYLINDRICAL WAVES IN A MEDIUM
WITH FINITE CONDUCTIVITY

L.B. Levitin, M.I. Kiselev, K.P. Stanyukovich
Moscow

The investigation of the convergence of shock waves was first started by L.D. Landau and K.P. Stanyukovich in 1944 (see K.P. Stanyukovich "Nonsteady Flow of Continuous Media," Gostekhizdat, 1955, §64).

These ideas were subsequently used by A.D. Sakharov and I.Ye. Tamm to obtain high temperatures on the axes of a converging cylindrical wave in a plasma. However, preliminary calculations, and also later work (for example, by S.M. Osovets and M.A. Leontovich) were based on the notion of a plasma as an ideally conducting medium. In fact, in a weakly conducting plasma there are dissipative losses (Joule heat is released), and this leads during the course of the experiments to considerably lower temperatures than expected. The radiation produced upon convergence of a shock wave also leads to a decrease in the temperature.

In the present paper we attempt to consider the problem of compression of a plasma with allowance for finite conductivity of the medium.

1. FUNDAMENTAL EQUATIONS

The fundamental equations describing the motions of the medium with finite conductivity can be written in the following form [1]:

$$\begin{aligned} \rho \frac{du}{dt} + \text{grad } p + \frac{1}{4\pi} [\vec{B} \text{rot} \vec{H}] &= 0, \\ \frac{du}{dt} + \rho \text{div} \vec{u} &= 0, \quad \frac{\partial \vec{u}}{\partial t} - [\vec{u} \text{rot} \vec{u}] = \kappa \Delta \vec{u}. \end{aligned} \quad (1)$$

$$\rho \frac{d\left(i + \frac{u^2}{2}\right)}{dt} = \frac{\partial p}{\partial t} - \frac{cE}{4\pi} \text{rot} \vec{H}.$$

Here $\vec{B} = \sqrt{4\pi\rho} \text{rot} \vec{\varphi}$; $cE = -\sqrt{4\pi\rho} \frac{\partial \vec{\varphi}}{\partial t}$; $\chi = \frac{c^2}{3\pi\rho^2}$.

Eliminating \vec{B} ; $\vec{H} = \vec{B}/\mu$; \vec{E} , we arrive at a system of four equations

$$\begin{aligned} \rho \frac{du}{dt} + \text{grad } p + [\text{rot } \vec{\varphi} \Delta \vec{\varphi}] &= 0, \\ \rho \frac{d\left(i + \frac{u^2}{2}\right)}{dt} &= \frac{\partial p}{\partial t} + \frac{\partial \vec{\varphi}}{\partial t} \Delta \vec{\varphi}, \\ \frac{dp}{dt} + \rho \text{div } \vec{u} &= 0, \\ \frac{\partial \vec{\varphi}}{\partial t} &= [\vec{u} \text{rot} \vec{\varphi}] + \chi \Delta \vec{\varphi}. \end{aligned} \quad (2)$$

Besides, for any medium

$$di = c_v dT + T \left(\frac{\partial p}{\partial T} \right)_v dV + V dp = T dS + V dp. \quad (3)$$

In the case of an ideal gas $i = kp/(k - 1)\rho$, where $k = c_p/c_v$.

For motions with central symmetry [plane waves ($N = 0$) and cylindrical waves ($N = 1$)], the fundamental system of equations (1) has the form

$$\begin{aligned} \rho \left(\frac{\partial u}{\partial t} + u \frac{\partial u}{\partial r} \right) + \frac{\partial p}{\partial r} + \frac{B}{4\pi} r^{-mN} \frac{\partial}{\partial r} (r^{mN} H) &= 0, \\ \frac{\partial \vec{\varphi}}{\partial t} + u \frac{\partial \vec{\varphi}}{\partial r} + \rho \left(\frac{\partial u}{\partial r} + \frac{Nu}{r} \right) &= 0, \\ \rho \left\{ \frac{\partial}{\partial t} \left(i + \frac{u^2}{2} \right) + u \frac{\partial}{\partial r} \left(i + \frac{u^2}{2} \right) \right\} - \frac{\partial p}{\partial t} &= \frac{cE}{4\pi} r^{-mN} \frac{\partial}{\partial r} (r^{mN} H), \\ \frac{\partial (\tau r^{N(1-m)})}{\partial t} + u \frac{\partial (\tau r^{N(1-m)})}{\partial r} &= \\ &= \chi \left[\frac{\partial^2}{\partial r^2} (\tau r^{N(1-m)}) + \frac{(2m-1)N}{r} \frac{\partial}{\partial r} (\tau r^{N(1-m)}) \right]. \end{aligned} \quad (4)$$

Here $m = 1$ if $H = H_\theta$, $E = E_z$, $\varphi = \varphi_z$ and $m = 0$ if $H = H_z$, $E = E_\theta$, $\varphi = \varphi_\theta$. With this

$$E = -\frac{\sqrt{4\pi\rho}}{c} \frac{\partial \vec{\varphi}}{\partial t}; \quad B = \sqrt{4\pi\rho} r^{-N(1-m)} \frac{\partial}{\partial r} (r^{N(1-m)} \vec{\varphi}).$$

By eliminating E and B (and H) we can rewrite this system of equations in the form (with $\mu = \text{const}$)

$$\begin{aligned}
 & \rho \left(\frac{\partial u}{\partial t} + u \frac{\partial u}{\partial r} \right) + \frac{\partial p}{\partial r} + \\
 & + r^{-N} \frac{\partial}{\partial r} (r^{N(1-m)} \varphi) \frac{\partial}{\partial r} \left[r^{-N(1-m)} \frac{\partial}{\partial r} (r^{N(1-m)} \varphi) \right] = 0, \\
 & \frac{\partial p}{\partial t} + u \frac{\partial p}{\partial r} + \rho \left(\frac{\partial u}{\partial r} + \frac{Nu}{r} \right) = 0; \quad (5) \\
 & \rho \left\{ \frac{\partial}{\partial t} \left(I + \frac{u^2}{2} \right) + u \frac{\partial}{\partial r} \left(I + \frac{u^2}{2} \right) \right\} - \frac{\partial p}{\partial t} = \\
 & = - \frac{\partial \varphi}{\partial t} r^{-N} \frac{\partial}{\partial r} \left[r^{-N(1-m)} \frac{\partial}{\partial r} (r^{N(1-m)} \varphi) \right], \\
 & \frac{\partial}{\partial t} (\varphi r^{N(1-m)}) + u \frac{\partial}{\partial r} (\varphi r^{N(1-m)}) = \\
 & = x \left\{ \frac{\partial^2}{\partial r^2} (\varphi r^{N(1-m)}) + \frac{(2m-1)N}{r} \frac{\partial}{\partial r} (\varphi r^{N(1-m)}) \right\}.
 \end{aligned}$$

To find approximate solutions of the system (5), we use the same procedure as for the one-dimensional case [2, 3].

We first investigate the last equation of the system (5), which we now write in the form

$$\frac{\partial \xi}{\partial t} + u \frac{\partial \xi}{\partial r} = x \left(\frac{\partial^2 \xi}{\partial r^2} \pm \frac{N \partial \xi}{r \partial r} \right), \quad (6)$$

where for $N = 1$ and $m = 1$ we have $\xi = \varphi$ and we choose the plus sign, while for $m = 0$ we have $\xi = \varphi r$ and we choose the minus sign. When $N = 0$ we have $\xi = \varphi$. This expression is conveniently written in the form

$$\frac{\partial \xi}{\partial t} + u * \frac{\partial \xi}{\partial r} = x \frac{\partial^2 \xi}{\partial r^2}, \quad (7)$$

where

$$u^* = u \mp \frac{N}{r} x. \quad (8)$$

The equation written out in this form is perfectly analogous to the equation describing one-dimensional motions of the medium.

To solve Eq. (7) we can employ various methods. We shall use the method developed in the papers by G.A. Skuridin and K.P. Stanyukovich

[2, 3].

We assume that

$$\xi = A(r, t) e^{i\omega r, \theta}, \quad (9)$$

then Eq. (7) can be rewritten in the form of two equations

$$\frac{\partial A}{\partial t} + u^* \frac{\partial A}{\partial r} = x \left(\frac{\partial^2 A}{\partial r^2} - A \omega^2 \left(\frac{\partial f}{\partial r} \right)^2 \right), \quad (10)$$

$$\frac{\partial f}{\partial t} + u^* \frac{\partial f}{\partial r} = x \left(\frac{\partial^2 f}{\partial r^2} + 2 \frac{\partial f}{\partial r} \frac{\partial \ln A}{\partial r} \right). \quad (11)$$

We assume now that ω can be sufficiently large, such that we can neglect the first term of the right half of Eq. (10) compared with the second. We assume further that $\kappa \omega^2 (\partial f / \partial r)^2 = R^2(r) \tau^2(t)$, and then we can rewrite this equation in the form

$$\frac{\partial \ln A}{\partial t} + u^* \frac{\partial \ln A}{\partial r} + R^2 \tau^2 = 0. \quad (12)$$

Equation (11) then assumes the form

$$x \dot{T} + R \ddot{r} + u^* R \dot{r} = x \left(R \ddot{r} + 2 R \dot{r} \frac{\partial \ln A}{\partial r} \right);$$

where $a = \omega \sqrt{x}$; $R = \int r dr$; $T = T(t)$.

Hence

$$u^* = - \left(\frac{R \ddot{r}}{R \ddot{r} + R \dot{r}} + \frac{x \dot{T}}{R \ddot{r} + R \dot{r}} \right) + x \left(\frac{R'}{R} + 2 \frac{\partial \ln A}{\partial r} \right)$$

and after elimination of u^* Eq. (12) becomes

$$\frac{\partial \ln A}{\partial t} + \frac{\partial \ln A}{\partial r} \left\{ x \left(\frac{R'}{R} - \left(\frac{R \ddot{r}}{R \ddot{r} + R \dot{r}} + \frac{x \dot{T}}{R \ddot{r} + R \dot{r}} \right) \right) + 2x \left(\frac{\partial \ln A}{\partial r} \right)^2 + R^2 \tau^2 = 0. \quad (13) \right.$$

We put $\partial \ln A / \partial r = \Theta$, and then, differentiating (13) with respect to r , we arrive at the equation

$$\begin{aligned} & \frac{\partial \Theta}{\partial t} + \frac{\partial \Theta}{\partial r} \left\{ x \left(\frac{R'}{R} + 4\Theta \right) - \left(\frac{R \ddot{r}}{R \ddot{r} + R \dot{r}} + \frac{x \dot{T}}{R \ddot{r} + R \dot{r}} \right) \right\} + \\ & + \Theta \left\{ \frac{x \dot{T} R'}{R^2 \ddot{r}} + x \left(\frac{R'}{R} \right)' - \frac{\dot{r}}{r} \left(\frac{R'}{R} \right)' \right\} + 2RR' \tau^2 = 0. \end{aligned} \quad (14)$$

The set of functions R and τ , of the arbitrary function of time $T = T(t)$, and of the arbitrary function that arises upon integration of Eq. (14), will be more than enough to solve completely any problem

with the most general initial and boundary conditions.

2. PLANE WAVES

The problem of investigating plane waves by the method indicated above reduces first of all to a study of Eq. (14).

We put in this equation $R\tau = B = \text{const}$.

Then

$$u = 2x\theta - \frac{a}{B}t; \quad \frac{\partial \theta}{\partial t} + \frac{\partial \theta}{\partial x} \left(4x\theta - \frac{a}{B}t \right) = 0, \quad (15)$$

hence $x = 4x\theta t - (aT/B) + F(\theta)$; putting $F(\theta) = \beta\theta$, where $\beta = \text{const} < 0$, we obtain

$$x = (4x\theta + \beta)\theta - \frac{a}{B}t \quad (16)$$

and

$$u = 2x \frac{x + \frac{a}{B}t}{4x\theta + \beta} - \frac{a}{B}t. \quad (17)$$

Further

$$t = \frac{B}{a}x + T, \quad (18)$$

$$\theta = A_0(t) e^{\frac{a}{2}x + \frac{a}{B}t}, \quad (19)$$

$$\varphi = A_0(t) e^{\frac{a}{2}x + \frac{a}{B}t} \cos \omega \left(\frac{B}{a}x + T \right). \quad (20)$$

It is then easy to find $h = \partial\varphi/\partial x$. The arbitrary function $T(t)$ can be determined by knowing the conditions say on the piston or on the wall, assuming that the latter moves in accordance with the law

$$X_s = \dot{\gamma}(t); \quad u_s = \dot{X}_s = \ddot{\gamma}(t).$$

A complete solution of the problem with account of all the equations entails no difficulties (see [2]), and only the energy equation, which in itself is not accurate, is not accurately satisfied here.

We proceed to a description of a second effective method for obtaining the solutions of the equation

$$\frac{\partial \varphi}{\partial t} + u \frac{\partial \varphi}{\partial x} = \kappa \frac{\partial^2 \varphi}{\partial x^2}. \quad (21)$$

At the same time we consider the problem of the magnetic piston. We shall approximate the plasma velocity in the region between the front of the shock wave and the magnetic piston by means of a linear function of x , where the coefficients are arbitrary functions of the time

$$u(x, t) = a(t)x + b(t). \quad (22)$$

Then the equation for the magnetic field can be reduced to an ordinary heat conduction equation for a homogeneous rod by changing over to Lagrange coordinates and introducing the effective time scale [4]

$$x_0 = x e^{-\int^t_0 a dt} - \int^t_0 b(t) e^{-\int^t_0 a dt} dt, \quad (23)$$

$$\tau = \int^t_0 e^{-2 \int^t_0 a dt} dt. \quad (24)$$

Equation (21) assumes the form

$$\frac{\partial \varphi}{\partial \tau} = \kappa \frac{\partial^2 \varphi}{\partial x_0^2}. \quad (25)$$

In coordinates $\{x_0, \tau\}$ we obtain the ordinary skin effect. We can now carry through to conclusion the solution of the equations for plane one-dimensional motions.

The remaining equations have the form

$$\begin{aligned} \frac{\partial u}{\partial t} + \frac{\partial}{\partial x}(u \varphi) &= 0, \\ \frac{\partial u}{\partial t} + u \frac{\partial u}{\partial x} + \frac{1}{\rho} \frac{\partial p}{\partial x} + \frac{h}{\rho} \frac{\partial h}{\partial x} &= 0, \\ \frac{\partial p}{\partial t} + u \frac{\partial p}{\partial x} + k p \frac{\partial u}{\partial x} &= (k-1) \kappa \left(\frac{\partial h}{\partial x} \right)^2 \\ \left(\text{where } h = \sqrt{\frac{\mu}{4\pi}} H \right). \end{aligned} \quad (26)$$

The boundary and initial conditions for the magnetic field will be taken in the magnetic piston problem in the form

$$h(X_0(t), t) = \mu(t); \quad h(x, 0) = 0. \quad (27)$$

where

$$X_p(t) = e^{\int_a^t} \int b(t) e^{\int_a^t} dt \quad (28)$$

is the Euler coordinate of the piston (plasma boundary).

Conditions on the front of a perpendicular gas magnetic shock wave for finite conductivity have the following form for the case under consideration [4]:

$$\rho_1(u_1 - D) = \rho_2(u_2 - D), \quad (29)$$

$$\rho_1(u_1 - D)^2 + p_1 + \frac{h_1^2}{2} = \rho_2(u_2 - D)^2 + p_2 + \frac{h_2^2}{2}, \quad (30)$$

$$\begin{aligned} \frac{k}{k-1} \frac{p_1}{\rho_1} + \frac{(u_1 - D)^2}{2} + \left[\frac{h_1}{\rho_1} - \frac{x}{\rho_1(u_1 - D)} \left(\frac{\partial h}{\partial x} \right)_1 \right] h_1 = \\ = \frac{k}{k-1} \frac{p_2}{\rho_2} + \frac{(u_2 - D)^2}{2} + \left[\frac{h_2}{\rho_2} - \frac{x}{\rho_2(u_2 - D)} \left(\frac{\partial h}{\partial x} \right)_2 \right] h_2 \end{aligned} \quad (31)$$

$$(u_1 - D) h_1 - x \left(\frac{\partial h}{\partial x} \right)_1 = (u_2 - D) h_2 - x \left(\frac{\partial h}{\partial x} \right)_2. \quad (32)$$

The index 1 denotes here the quantities ahead of the wave front and the index 2 the quantities behind the front, $D = D(t) = dx_p(t)/dt$ is the velocity of the shock wave front. Condition (32) for the magnetic field on the discontinuity is rather complicated, but from physical considerations we can greatly simplify the solutions of Eq. (25). If the conductivity is high, we can assume that the magnetic field propagates in a semi-infinite space ($x_0 > 0$).

With increasing t , the front of the shock wave moves rapidly away (compared with the slow diffusion of the magnetic field) from the piston, the field on the front decreases rapidly, and the distribution of the magnetic field in the region between the piston and the front of the shock wave depends on the propagation of the magnetic field in the region ahead of the front of the discontinuity very weakly, and only in the narrow region which lies directly behind the front.

In this analysis we neglect the perturbing action of the weak mag-

netic field, which "seeps through" the front, and assume the gas ahead of the front to be at rest: $x_0 = x$, $u_1 = 0$. If we assume that the magnetic field accelerates the gas somewhat ahead of the front, the equation for the region behind the front and ahead of the front will be closer in form, and the error of our assumptions will become even smaller.

Thus, the magnetic field can be expressed with sufficient accuracy in the form of the derivative of the Duhamel integral ($x = \text{const}$):

$$h(x_0, t) = \frac{x_0}{2\sqrt{\pi} A_0} \int_0^t \frac{p(q)}{A(q) \left\{ \int_q^\infty A^{-2} dq \right\}^{1/2}} e^{-\frac{x_0^2}{4 \int_q^\infty A^{-2} dq}} dq, \quad (33)$$

where $A(t) = e^{\int_a^t dt'}$.

Here and in what follows it is convenient to assume $A(t)$ and $X_n(t)$ to be new approximating functions. The functions $a(t)$ and $b(t)$ are readily expressed in terms of the former:

$$a(t) = \frac{1}{A} \frac{dA}{dt}; \quad b(t) = A \frac{d}{dt} \left(\frac{X_n}{A} \right). \quad (34)$$

After determining $h(x_0, t)$, we can readily find the pressure and density, using the continuity equation and any equation of motion, or else the energy equation. The remaining equation is not satisfied exactly in the general case. It is possible, however, to choose the approximating functions $a(t)$ and $b(t)$ in such a way, as to have this equation satisfied approximately in the region of interest to us between the magnetic piston and the front of the shock wave. For this purpose it is necessary to satisfy the boundary conditions on the piston and on the fronts.

Let the initial conditions be constant:

$$p(x, 0) = p_0; \quad \rho(x, 0) = \rho_0 \quad (35)$$

Integrating the continuity equation, we obtain

$$\rho(x_0, t) = \frac{\rho_0}{A} \quad (36)$$

It is interesting to note that the density depends on the linear coordinate only through the initial distribution. This is understandable, since if the velocity depends linearly on x , the plasma becomes uniformly compressed (or rarefied).

This raises the question as to which of the equations is preferably used to determine the pressure. The point is that the energy equation itself has a more crude and approximate character. It is more strongly influenced than the equation of motion by the neglect of the viscosity, heat conduction, or radiation. It is therefore necessary to satisfy exactly the equation of motion, and satisfy the energy equation approximately, imposing on the functions $A(t)$ and $X_n(t)$ the condition of energy balance on the front of the shock wave.

Integrating the equation of motion, we obtain

$$p(x_0, t) = -\frac{h^2}{2} - \rho_0 A'' \frac{x_0^2}{2} - \rho_0 X_n'' x_0 + T(t). \quad (37)$$

The primes denote here differentiation with respect to t , and $T(t)$ is an arbitrary function of the time.

We now have four arbitrary functions: $A(t)$, $X_n(t)$, $X_p(t)$, and $T(t)$, with the aid of which we can satisfy the momentum balance equation on the piston and the conditions on the continuity (29-31).

On the piston, in fact, we have a contact discontinuity, and consequently the total pressure $p + h^2/2$ should be continuous. Hence

$$T(t) = \frac{p^2(t)}{2}. \quad (38)$$

The pressure has a final form

$$p(x_0, t) = \frac{p^2(t)}{2} - \frac{h^2}{2} - \rho_0 A'' \frac{x_0^2}{2} - \rho_0 X_n'' x_0 \quad (39)$$

The condition for the mass balance on the front of the shock wave yields an equation for $X_p(t)$, from which we readily obtain

$$X_0(t) = \frac{X_n}{1-A}. \quad (40)$$

The Euler and Lagrange coordinates of the front of the shock wave are equal, which incidentally is obvious beforehand as the result of the continuity.

Let us consider now the equation for the momentum balance (30)

$$\rho_1(u_1 - D)^2 + p_1 + \frac{h_1^2}{2} = \rho_2(u_2 - D)^2 + p_2 + \frac{h_2^2}{2}.$$

We note that in our case the right half of the equation is independent of the magnetic field behind the front (since it does not contain h_2).

Consequently, the left half should also be independent of the extent to which the magnetic field seeps through into the space ahead of the front. We can therefore, without introducing any new error whatever, assume that $h_1 = 0$ and then $u_1 = 0$; $\rho_1 = \rho_0$; $p_1 = p_0$ (this would hold true in the case of infinite conductivity ahead of the front).

We alternately obtain

$$\begin{aligned} \rho_0 + \rho_0 \frac{[(1-A)X'_n + A'X_n]^2}{(1-A)^2} + \frac{\rho_0}{2} \frac{A''X_n^2}{(1-A)^2} + \\ + \rho_0 \frac{X''X_n}{1-A} = \frac{p^2(t)}{2}. \end{aligned} \quad (41)$$

The influence of the magnetic field behind the front on the motion of the front is significant only for very small t . Neglecting these and assuming the medium ahead of the front to be at rest, we can write the energy balance equation in the form

$$\begin{aligned} \frac{k-1}{2k} \frac{\rho_0 (1+A)[(1-A)X'_n + A'X_n]^2}{A(1-A)^3} + \frac{\rho_0}{2} \frac{A''X_n^2}{(1-A)^2} + \\ + \rho_0 \frac{X''X_n}{1-A} + \frac{\rho_0}{A} = \frac{p^2(t)}{2}. \end{aligned} \quad (42)$$

The system of equations (41, 42) determines the approximating functions $a(t)$ and $b(t)$. From this we readily obtain an expression for the coordinates of the front

$$X_0(t) = \frac{X_0}{1-A} = \sqrt{2} c_0 \int \frac{dt}{[A(k+1)-(k-1)]}, \quad (43)$$

where $c_0 = \sqrt{\frac{k p_0}{\rho_0}}$ is the velocity of sound in the unperturbed medium. We see therefore that the function $A(t)$ can vary only within the limits

$$1 > A > \frac{k-1}{k+1}. \quad (44)$$

We note that the velocity of the front of the shock wave is inversely proportional to the square root of the medium density. This agrees with the results obtained in a different manner by Harris [5] and confirmed experimentally by Kolb [6].

Let $X_f = \sqrt{2c_0} B(t)$. The system (41, 42) readily reduces to a single third-order equation for the function $B(t)$:

$$B''' - \frac{3B''}{B''} + \frac{3B''}{B} + \frac{2B''}{BB''} + \frac{2B''}{B^2} - \frac{B''}{B^2} L(t) = 0, \quad (45)$$

where

$$L(t) = \frac{(k+1)\mu^2(t) + 2(k-1)p_0}{4kp_0}. \quad (46)$$

Let us determine the initial conditions for Eq. (45). From physical considerations $B(0) = 0$ and $B'(0) \neq \infty$ (the velocity of the front is finite). Then, from the equation (45) itself, after analyzing the order of the growth of the terms as $t \rightarrow 0$, we obtain

$$B'(0) = \sqrt{L_0/2}, \text{ where } L_0 = L(0) \geq 1 \text{ (we assume that } \mu^2(0)/2 \geq p_0).$$

If the magnetic field on the boundary is known as a function of the velocity (or coordinate) of the front or the piston, then the order of the equation can be lowered. When $B'(t) \neq \text{const}$ the substitution

$$y = -B'; z(y) = -BB'' \quad (47)$$

reduces Eq. (45) to an Abel equation

$$\frac{dz}{dy} + \frac{3}{y^2} z + \frac{L(y)y^2 - 2y^4}{z} + (2y^2 + y + 3) = 0. \quad (48)$$

Let us consider in detail the simplest case, when the magnetic field on the boundary is constant:

$$\mu(t) = \mu_0, \text{ i.e., } L = L_0.$$

Then the solution of (45) is a linear function of t

$$B(t) = \sqrt{\frac{L_0}{2}} t. \quad (49)$$

Hence

$$A = A_0 = \frac{(k-1)n_0^2 + 2(k+1)p_0}{(k+1)n_0^2 + 2(k-1)p_0}. \quad (50)$$

This corresponds to the following choice of approximating functions:

$$a(t) = 0; b(t) = \text{const} = (1 - A_0)c_0\sqrt{L_0}. \quad (51)$$

Now all the physical quantities are expressed in explicit form

$$\begin{aligned} h(x, t) &= \mu_0 \operatorname{erfc} \left(\frac{x - c_0(1 - A_0)\sqrt{L_0}t}{2\sqrt{xt}} \right), \\ p(x, t) &= \frac{p_0}{A_0} = \text{const}, \\ p(x, t) &= \frac{p_0^2}{2} \left[1 - \operatorname{erfc}^2 \left(\frac{x - c_0(1 - A_0)\sqrt{L_0}t}{2\sqrt{xt}} \right) \right], \\ x_0(t) &= c_0\sqrt{L_0}t. \end{aligned} \quad (52)$$

Thus, under the influence of a constant boundary layer, the plasma acquires a constant velocity $u = (1 - A_0)c_0\sqrt{L_0}$, which is approximately proportional to the square root of the ratio of the magnetic pressure to the initial density of the medium.

Let us consider a numerical example.

Let $\mu_0 = 1000$ oersted; the initial concentration is $n_0 = 10^{16}$ particles/cm³, and the initial temperature is $T_0 = 300^\circ\text{K}$. We then obtain

$$u_f \approx 7.7 \cdot 10^6 \text{ cm/sec (for atomic hydrogen).}$$

The magnetic field on the front of the shock wave is

$$h_0 \approx \mu_0 \operatorname{erfc}(1.5 \cdot 10^3 \sqrt{t}).$$

Thus, even at the instant of time $t = 10^{-6}$ sec the magnetic field on the front is already negligible in magnitude. Consequently, when the shock tube length has an order of not less than 50-100 cm, the magnetic

field on the front can be neglected and our approximation is justified.

3. CYLINDRICAL WAVES

To investigate cylindrical waves we may use only the first method proposed, where we put $\xi = Ae^{i\omega t}$.

Even a more simplified version of solution of the problem, when we put for simplicity (as was done in the case $N = 0$) that $Rt = B = \text{const}$, we already get a good approximation for the investigation of an axially symmetrical wave.

In this case

$$u^* = 2x\theta - \frac{\alpha}{B} T, \quad (53)$$

$$\frac{\partial \theta}{\partial t} + \frac{\partial \theta}{\partial r} \left(2x\theta - \frac{\alpha}{B} T \right) = 0, \quad (54)$$

hence

$$r = 4x\theta t - \frac{\alpha}{B} T + F(\theta). \quad (55)$$

Let

$$F(\theta) = \beta \theta^{1/\mu}. \quad (56)$$

(In the case $N = 0$ we assumed that $F(\theta) = \beta \theta$.) Then (55) assumes the form

$$\theta = \beta^{-\mu} \left(r + \frac{\alpha}{B} T - 4x\theta t \right)^{\mu}. \quad (57)$$

When $r + (\alpha T / B) \gg 4x\theta t$ we have, apart from terms of first order of smallness,

$$\theta = \beta^{-\mu} \left[\left(r + \frac{\alpha}{B} T \right)^{\mu} - 4x\theta t \left(r + \frac{\alpha}{B} T \right)^{\mu-1} \right]. \quad (58)$$

hence

$$\theta = \beta^{-\mu} \left(r + \frac{\alpha}{B} T \right)^{\mu} \left[1 - \frac{4x\theta t}{\beta^{\mu}} \left(r + \frac{\alpha}{B} T \right)^{\mu-1} \right]. \quad (59)$$

$$\begin{aligned} u &= u^* \pm \frac{Nx}{r} = -\frac{\alpha T}{B} + \\ &+ x \left\{ 2\beta^{-\mu} \left(r + \frac{\alpha}{B} T \right)^{\mu} \left[1 - \frac{4x\theta t}{\beta^{\mu}} \left(r + \frac{\alpha}{B} T \right)^{\mu-1} \right] \pm \frac{N}{r} \right\}. \end{aligned} \quad (60)$$

It is necessary to have at the center (at $r = 0$) $u \rightarrow \infty$ when $\kappa = 0$.

For $\kappa = 0$ we have $u = -\alpha T/B$. Let

$$T = T_0 \left[\left(1 - \frac{t}{\tau} \right)^n + \frac{n_1 t}{\tau} \right]; \quad (61)$$

where $0 < n_1 < 1$;

then

$$u = \frac{\alpha n_1 T_0}{B \tau} \left[\left(1 - \frac{t}{\tau} \right)^{n-1} - 1 \right]. \quad (62)$$

When $t = 0$ we have $u = 0$; when $t = \tau$ we have $u \rightarrow \infty$. This approximation, however, although it does give the correct result when $r = 0$ can be improved.

Let us stipulate, for example, that the following condition be satisfied

$$\frac{1}{\psi} = \pm \left(\frac{\dot{\psi} + \frac{\alpha}{B} T}{\beta} \right)^n [b(t - t_0) - 2]; \quad (63)$$

here ψ governs the motion of the plasma boundary, and then Eq. (60), neglecting the term $4\pi\kappa t/\beta(\psi + (\alpha T/B)/\beta)^n \ll 1$ can be readily integrated and we obtain

$$\psi = \pm \frac{1}{b(t - t_0) - 2} \left[(1 - n) \frac{x}{\beta} \frac{b}{2} (t - t_0)^2 \right]^{\frac{n}{n-1}}. \quad (64)$$

$$T = \frac{B}{\alpha} \left\{ \frac{1}{2} \left[(1 - n) \frac{x}{\beta} \frac{b}{2} (t - t_0)^2 \right]^{\frac{1}{n-1}} \pm \right. \\ \left. \pm \left[(1 - n) \frac{x}{\beta} \frac{b}{2} (t - t_0)^2 \right]^{\frac{n}{n-1}} \frac{1}{b(t - t_0) - 2} \right\}. \quad (65)$$

The constant b is determined from the condition $\psi|_{t=0} = r_0$. The vector potential of the field inside of a current-carrying plasma cylinder is now written in the form

$$\begin{aligned} \varphi = A(t) \cos \omega \left(\frac{B}{x} r + T \right) \exp \left\{ \frac{\beta}{n+1} \left(\frac{r + \frac{x}{B} T}{\beta} \right)^{n+1} \times \right. \\ \left. \times \left[1 - \frac{2x}{\beta} (n-1) \left(\frac{r + \frac{x}{B} T}{\beta} \right)^{n-1} \right] \right\} = A(t) \Phi(r). \end{aligned} \quad (66)$$

The function $A(t)$ is found from the boundary condition

$$H|_{r \rightarrow 0} = \frac{\partial \varphi}{\partial r}|_{r \rightarrow 0} = A(t) \frac{\partial \Phi}{\partial r}|_{r \rightarrow 0} = \frac{2I(t)}{c\psi}. \quad (67)$$

The ohmic power loss by unit volume is

$$\rho \frac{dQ}{dt} = \frac{\pi}{4\pi} (\Delta\varphi)^2 = \frac{\pi}{4\pi} \left[\varphi_r + N \left(\frac{\varphi_r}{r} - m \frac{\varphi}{r^2} \right) \right]^2. \quad (68)$$

i.e., the losses increase for small ψ in proportion to

$$\frac{\rho}{c^2} \frac{1}{\psi^2 r^2 \left(\frac{\partial \Phi}{\partial r} \right)^2|_{r \rightarrow 0}}.$$

When making a complete energy balance, it is necessary to take into account the inductive losses both in the electrical circuit and in the plasma pinch itself, as well as the radiation and losses through excitation of the internal degrees of freedom.

Let us make numerical estimates by means of a simple model example. Let $n = 1$, $\psi = r_0/(Dt + 1)$, with $D \gg \kappa/\beta \gg 1$, and then $T = r_0 \frac{B}{\alpha} \frac{Dt}{Dt + 1}$. Let at the same time $r_0 \sim \beta$; $B\omega/\alpha = 2\pi/M$, where $M \gg 1$, i.e., the current decreases monotonically away from the pinch boundary toward the axis. The expression for the vector potential assumes the following form

$$\begin{aligned} \varphi = A(t) \exp \left\{ \frac{1}{2} \left(r + \frac{r_0 Dt}{Dt + 1} \right)^2 \frac{1}{\beta^2} - \right. \\ \left. - \frac{1}{2} \left(\frac{r_0}{\beta} \right)^2 \right\} \cos \frac{2\pi}{M} \left(\frac{r}{r_0} + \frac{Dt}{Dt + 1} \right). \end{aligned} \quad (69)$$

We then have in order of magnitude

$$A(t) \approx \frac{2I}{c\psi}; \quad \rho \frac{dQ}{dt} \approx \frac{I^2 r_0^2}{c^2 \psi^2} \kappa. \quad (70)$$

and for $I \approx 10^5$ kA; $r_0 \approx 10$ cm; $\kappa \approx 10^{16}$, i.e., $\sigma \approx 10^{14}$ sec $^{-1}$, $\psi \approx 1$ cm. The ohmic loss power will have an order of 10^{16} erg/sec, i.e., 1 million kilowatts. When the pinch contracts to 0.3 cm, the loss power increases, obviously, by another almost three orders of magnitude.

Thus, in pinch accelerating systems it is necessary to avoid ex-

cessive compression of the plasma, since the "tail" of the accelerating pulse is expended for the most part in heating and not in acceleration.

It should be noted that the "magnetic piston" as a means of plasma acceleration has in general the following essential shortcomings: the forces exert a surface action, so that shock waves are produced in the accelerated plasmoid along with supplementary dissipation, and the character of the losses, as demonstrated by many examples, is close to that of volume losses.

In addition, the accelerated plasmoid can capture the field penetrating through its boundary, form an unstable magnetic gasdynamic configuration, and collapse on emerging from the accelerating unit. It is probably this type of plasmoid collapse that was observed in the conical chamber presented in the paper of D.V. Orlinskiy [7]. The field that seeped into the plasmoid then dissipates and heats the plasmoid somewhat.

We note that a certain increase in the rate of plasma ejection from conical chambers having a length and a diameter of merely a few centimeters, occurring upon increasing the aperture angle of the cone, is due to the increase in the average radius of the chamber, which improves somewhat the condition for the optimum utilization of the "magnetic piston."

Finite conductivity deteriorates also the quality of the "magnetic" wall as a means of plasma confinement and heat insulation, leading to a seeping of the plasma through the wall and to its departure from the plasmoid.

It is necessary in the future to look for schemes in which the accelerating force has not a surface but a volume character, and the electromagnetic energy is consumed essentially in an increase of the

electric conductivity of the plasma and its acceleration with minimum dissipation.

REFERENCES

1. K.P. Stanyukovich. Osnovnye uravneniya relyativistskoy magnitogazodinamiki [Basic Equations of Relativistic Magnetic Gas Dynamics], in present collection.
2. G.S. Skuridin and K.P. Stanyukovich, DAN SSSR [Proceedings of the Academy of Sciences USSR], 130, 6, 1960.
3. G.S. Skuridin and K.P. Stanyukovich, DAN SSSR, 131, 1, 1960.
4. L.B. Levitin and K.P. Stanyukovich, DAN SSSR, 134, 2, 1960.
5. E.G. Harris. Exact and approximate treatments of the One-Dimensional Blast Wave, NRL REport, 4858, 1956.
6. A. Kol'b, Magnitnaya gidrodinamika (materialy simpoziuma) [Magnetic Gas Dynamics (symposium material)], 1958, page 82.
7. D.V. Orlinskiy, Issledovaniye udarnoy volny v konicheskoy razryadnoy trubke [Investigation of Shock Wave in Tapered Discharge Tube], in present collection.

CONCERNING ONE ANALOGY BETWEEN WAVES ON THE SURFACE
OF A HEAVY LIQUID AND NONLINEAR PLASMA OSCILLATIONS

R.Z. Sagdeyev

Moscow

There is a well-known analogy between the theory of the so-called "shallow water" and the gasdynamics of plane isentropic motions. A generally arbitrary initial flow profile gets deformed in time, in both theories, in such a way that the steepness of the leading front increases continuously. In gasdynamics, there is ultimately established a stationary steepness, when the dissipative effects come into play. In the theory of waves on water, the finite nature of the depth of the channel becomes significant when the steepness of the leading front becomes sufficiently large. An account of this factor leads to dispersion effects. Thus, the analogy between gasdynamics and the theory of "shallow water" ends when dissipative effects appear in the former case and dispersion effects in the latter. This finds its manifestation also in the different character of the nonlinear steady-state motions. In the former case (in gasdynamics) we deal with shock waves, while in the latter case we deal with periodic or so-called solitary waves.

In the theory of nonlinear motions of a low-density plasma (in which the pair collisions play a small role), it is well known that a situation analogous to gasdynamics arises in many cases. Thus, for example, in the presence of a strong magnetic field in the plasma, the motion of the plasma in scales larger than the Larmor particle radii

is described formally by the Chew, Goldberger, and Low equations of anisotropic magnetic gasdynamics. To what effect does the increase in the steepness of the leading front of the perturbation lead in this case? One can show that at least in the case of a "cold" plasma (when the magnetic field pressure greatly exceeds the plasma pressure) there appear here, unlike in gasdynamics, effects of the dispersion type. The steady-state nonlinear motion has in this case, as in the theory of waves on water in a channel of finite depth, the form of periodic and solitary waves. These solutions exist only at Mach numbers that are smaller than a certain critical value. On going through this critical value, the "tumbling" of the front takes place. In the theory of waves on water, this should lead in final analysis to the formation of a "water spout" (or "twister"). In a plasma this can lead to an analogous phenomenon, namely a "collisionless" shock wave.*

We consider here a second case, a plasma without a magnetic field, but under the condition that the electron pressure greatly exceeds the ion pressure. As will be shown below, the situation arising in this case is very similar to that noted above.

As is known from linear theory, the propagation of sound waves in a plasma in the absence of pair collisions and of a magnetic field is possible only if $p_i \ll p_e$ ($p_{i,e}$ is the pressure of the ions or electrons). This condition can be realized both because the plasma is not isothermal, and because the ions are multiply charged (either $Z \gg 1$ or $T_e \gg T_i$).

Let us consider one-dimensional waves of arbitrary amplitude in such a plasma. Since the velocity of sound, $\sim \sqrt{(T_e + T_i)/M}$, greatly exceeds the thermal velocity of the ions, it is reasonable to neglect the thermal scatter in the velocities of the latter. On the other hand, if we confine ourselves to an examination of waves with propagation

velocities that are much smaller than the thermal velocity of the electrons, then the electric field in such a wave will be quasistatic relative to the electrons. Then, if the electron velocity distribution is Maxwellian, $f \sim e^{-mv^2/2T}$, in the region where the electric potential φ has a maximum, then the electron density at any point is determined by a Boltzmann distribution $n = n_0 e^{e\varphi/T}$. This corresponds to inclusion of the so-called "captured" electrons, inasmuch as the maximum of φ corresponds to a potential well $-e\varphi$ for the electrons (a minimum of potential energy), where $-e$ is the electron charge.

Taking the assumptions made into consideration, let us write down the initial system of equations for the one-dimensional motion:

$$M \left(\frac{\partial v}{\partial t} + v \frac{\partial v}{\partial x} \right) = -e \frac{\partial \varphi}{\partial x}, \quad (1)$$

$$\frac{\partial N}{\partial t} + \frac{\partial}{\partial x} (Nv) = 0, \quad (2)$$

$$-\frac{\partial^2 \varphi}{\partial x^2} = 4\pi e(N - n_0 e^{\frac{e\varphi}{T}}). \quad (3)$$

Here v is the ion velocity and N the ion density.

For motions with characteristic space scales that considerably exceed the Debye radius $(T/4\pi n e^2)^{1/2}$, the quasineutrality assumption $n \approx N$ is valid (one can leave out $\partial^2 \varphi / \partial x^2$ from Eq. (3)). Then, eliminating the electric field from the equations, we obtain a system of two equations for an adiabatically compressible gas with adiabatic exponent $\gamma = 1$ (isothermal case). In this case the solution in the form of a simple Riemann wave is valid, from which it follows that the front of the wave becomes steeper and steeper in time until it topples over completely. However, before this solution becomes multiple valued, the quasineutrality assumption becomes inapplicable, when the characteristic scale decreases to the Debye radius with increasing steepness of the leading front of the wave.

An account of the charge separation effect can be carried out for the case of a steady-state wave, in which all the quantities are functions of $(x - ut)$ only, where u is the velocity of wave propagation. The initial system (1-3) can be reduced to a single ordinary second-order differential equation for the potential φ

$$-\frac{d^2\varphi}{dx^2} = \epsilon n_0 e \left(\frac{u}{\sqrt{u^2 - \frac{2e\varphi}{M}}} - e^{\frac{\varphi}{T}} \right). \quad (4)$$

Depending on the choice of the integration constants, we can construct various steady-state waves. If it is assumed that at the initial instant of time we had a perturbation localized in a limited region of space with $\varphi \rightarrow 0$ as the distance from this region increases, and that such an initial perturbation approaches asymptotically with time to a steady-state motion described by Eq. (4), it is sensible to choose a solution in which $d\varphi/dx \rightarrow 0$ when $\varphi \rightarrow 0$. Such a choice gives a steady-state motion in the form of a symmetrical isolated wave. The propagation speed u of such a wave depends on the amplitude φ_{\max} . By assuming $d\varphi/dx = 0$ for $\varphi = \varphi_{\max}$ we obtain this dependence

$$u^2 = \frac{1}{2} \cdot \frac{T}{M} \cdot \frac{\left(e^{\frac{\varphi_{\max}}{T}} - 1\right)^2}{e^{\frac{\varphi_{\max}}{T}} - 1 - \frac{e^{\frac{\varphi_{\max}}{T}}}{T}}. \quad (5)$$

In the limiting case of small amplitudes, $u \rightarrow \sqrt{T/M}$ — the velocity of sound. At large amplitudes ($e\varphi_{\max} \gg T$) we have $u \rightarrow (1/2) \sqrt{(T/M)} \cdot e^{\varphi_{\max}/T}$. The explicit form of the profile of the solitary wave can be obtained for the case of small amplitudes by expanding the left half (4) in powers of $e\varphi/T$ and then integrating

$$\varphi = \frac{3}{2} \cdot \frac{T}{\epsilon} \cdot \left(1 - \frac{T}{Mu^2}\right) \operatorname{Sech}^2 \left\{ \frac{\sqrt{\pi n_0} e}{\sqrt{T}} \cdot \sqrt{1 - \frac{T}{Mu^2}} \cdot (x - ut) \right\}. \quad (6)$$

It is curious that a solution in the form of solitary waves for Eq. (4) exists for arbitrarily large Mach numbers, unlike waves on water or in a plasma with a magnetic field.

Manu-
script
Page
No.

[Footnote]

265 This part of the communication will be published in "ZhETF,"
and is therefore merely mentioned in the present text.

PROPERTIES OF A MAGNETIC TRAP IN A PLASMA EJECTED FROM THE SUN

L. I. Dorman

Moscow

§1. ELECTROMAGNETIC PROPERTIES OF A PLASMA EJECTED FROM THE SUN

In several investigations [1-4] carried out on the basis of the experimental data obtained by the international network of cosmic-ray stations, a study was made of different cosmic-ray effects: 1) the slow reduction in the intensity of cosmic rays preceding suddenly starting magnetic storms that give a Forbush drop, 2) the increase in the cosmic-ray intensity following this drop, which lasts only several hours and also occurs before the start of the magnetic storm, 3) the various profiles of the variation of the cosmic-ray intensity during the time of magnetic storms. A rather laborious analysis of all these effects, a study of their distribution for various secondary components in latitude and in longitude using the coupling coefficient method [5, Chapter IV] and data on the trajectories of charged particles of different energies in geomagnetic fields, have made it possible to determine the energy spectrum and the direction of arrival from different sources of cosmic-ray variations. A comparison of these results with the theoretical calculations [6, 7] of the cosmic-ray variations, expected from different suggested sources, makes it possible to interpret these effects as follows.

1. The increase effect, first observed in [1], is connected with the reflected particles from the forward nonmagnetic part of the solar plasma stream before the plasma envelops the earth (i.e., before the

magnetic storm starts on earth). In this case the particles acquire energy, just as in the case of reflection from a mirror moving head on [7].

2. The decrease effect, first observed in [8], is connected with the propagation in interplanetary space of a shock wave formed by the forward nonmagnetic part of the plasma stream moving with hypersonic velocity. Compression of the interplanetary medium behind the front of the shock wave and a corresponding intensification of the interplanetary magnetic field will lead to an increase in the scattering of the cosmic-ray particles and to an attenuation of their intensity on earth [9].

3. Different profiles of the variation of the intensity of cosmic rays are connected with the different velocity of motion and angular width of the plasma streams, different distribution of the frozen-in magnetic field, and, principally, with the different character of the capture of the earth by the solar plasma [6]. The point is that the earth can be captured by the forward front of the stream (and this brings about a magnetic storm with sudden start; such streams are connected essentially with solar flares). In this case a sharp decrease occurs in the cosmic-ray intensity. With this, the rate at which the intensity decreases is proportional to the velocity of the stream and to the degree of intensification of the magnetic field frozen in the forward part of the plasma stream.

Comparing the experimental data obtained from the world network of stations with the profiles expected under various assumptions, and using the method of coupling coefficients [5, Chapter IV], it is possible to determine the angular dimensions, the intensity of the frozen-in magnetic field, and its distribution in the plasma of the stream, as well as the degree of compression of the plasma and the field. An

analysis of this type [10] was carried out for more than 40 plasma streams, some of which gave rise to suddenly starting magnetic storms, and some to storms with gradual starts. The latter were connected with the enveloping of the earth by the lateral side of the stream (whereupon the intensity of the cosmic rays decreased rather slowly and was restored practically just as slowly). In particular, it was shown that the solar plasma streams carry frozen-in magnetic fields with intensity from 10^{-5} Oe to 10^{-4} Oe, and in the forward part the fields are greatly intensified (by a factor 3-6) as a result of the compression of the plasma, owing to interaction with the interplanetary medium and the formation of shock waves in it. The angular dimensions of the streams turn out to be quite different, ranging from several tens of degrees to π . The velocities observed also had a wide range, from $3 \cdot 10^7$ to 2×10^8 cm/sec.

The presence of frozen-in magnetic fields in the streams of solar plasma (there being in addition several serious arguments in favor of assuming that these fields are more or less regular and not turbulent) makes it possible for magnetic traps to be formed in such a plasma, capable of retaining particles whose radius of gyration is much smaller than the dimensions of the stream.

§2. INVESTIGATION OF COSMIC-RAY FLARES AND TWO POSSIBLE WAYS OF PROPAGATION OF SOLAR PARTICLES TO THE EARTH

Numerous investigations of cosmic-ray flares (for a review see [5], Chapters X, XI) have shown that even several hours after the start of the flare the flux of high-energy solar particles becomes isotropic and its intensity decreases with time in accordance with a power law, as $t^{-3/2}$. The power law was furthermore maintained for all the flares observed to date. The only differences were in the delay of the occurrence of isotropy relative to the start of the flare. This character

of variation of the intensity of the solar particles agrees with the diffuse model of propagation of particles in the interplanetary medium. Detailed calculations [11] show that on the basis of such a model it is possible also to understand the law governing the variation of intensity directly after the start of the flare.

At the same time, one cannot exclude also another possibility, namely the propagation of the particles generated in the solar atmosphere with the lowest energy (but still retained in the trap) via a relatively slow transport with a velocity $\sim 10^8$ cm/sec in a magnetized plasma ejected from the sun. However, it was only relatively recently that data demonstrating that such a possibility is apparently realized could be obtained.

§3. FLARE OF LOW-ENERGY SOLAR PARTICLES IN THE STRATOSPHERE ON 11-13 MAY 1959 AND PROPERTIES OF MAGNETIC TRAP

Low-energy particles, with energy lower than several hundred MeV, which can be captured in the trap, cannot penetrate through the earth's atmosphere and in order to observe them measurements must be carried out at high altitudes (where the absorption is low) and at high latitudes (where the geomagnetic cutoff is quite small). From this point of view, measurements of exceptional interest were made by the group of A.N. Charakhch'yan above Murmansk (geomagnetic cutoff 120 MeV) and by Winkler's group above Minneapolis (geomagnetic cutoff 300 MeV). These measurements showed the presence of a large number of flares of low-energy solar particles, which were not observed by instruments at sea level or by measurements at high altitudes, but in the region of low latitudes above points with large geomagnetic cutoff [12, 13]. Of particular interest are the data on the flare of 11-13 May 1959. A comparison of the data of A.N. Charakhch'yan et al. [12] and of Winkler et al. [13], and an analysis of the conditions of particle propagation

by diffusion in interplanetary medium and by transport in a magnetic trap, has shown [14] that what occurred here without any doubt was the formation of a trap in the forward end of the magnetized plasma ejected from the sun (the properties of this plasma stream were investigated in [15] on the basis of the data obtained by the world's station network). The following interesting phenomenon was observed here: after the start of the magnetic storm the intensity of the low-energy particles increased by almost 40 times, after which it decreased exponentially by a factor e in two hours (whereas the intensity of the particles propagating by diffusion decreases in accordance with a power law). Direct measurements of the energy spectrum [12, 13] have shown that it had the same form as during the time of large flares, i.e., $D(\varepsilon_k) \sim \varepsilon_k^{-(5+6)}$, where ε_k is the particle kinetic energy (such a spectrum could be traced with the aid of satellite measurements up to $\varepsilon_k \approx 30-40$ MeV). In addition, measurements of the spectrum [13] have shown also that a very interesting phenomenon takes place: during the time of the magnetic storm the geomagnetic cutoff greatly decreases, this being due to the effect of the stream plasma on the earth's magnetic field (compression of the cavity and intensification of the equatorial current ring). Calculations [16, 17], as well as investigations [18, 19] of the corresponding cosmic-ray variations, show that such changes in the geomagnetic cutoff are world-wide in character and can be understood on the basis of modern notions concerning the interaction between the stream plasma and the earth's magnetic field.

A comparison of the calculations with the experimental data, made in [14], shows that the particle density in each part of the trap corresponds to the density of the particles generated in the solar atmosphere for each instant of time, when the corresponding part of the plasma is ejected.

It follows therefore that a rather large particle density gradient is maintained in the trap and that the particles are not appreciably intermixed. The magnetic field in the trap should be directed perpendicular to the line of stream propagation. The compression of the plasma in the forward end of the stream leads to a corresponding increase of the density of the trapped particles. An estimate of the total energy of the particles transported in the trap shows that it is less than the energy of the frozen-in magnetic field. This relation between the particle energy density and the density of the magnetic field energy is retained also in the most forward part of the stream, where the particle density is the largest. It is necessary to assume here that the indicated particle spectrum extends not lower than 3-5 MeV. Such a limit on the spectrum agrees with the hypothesis that the particles are injected prior to the flare with an energy of several MeV, as the result of thermonuclear reactions, with subsequent acceleration by the first-order Fermi mechanism [20, 21]. We note that the total momentum of the generated particles turns out to be of sufficient order of magnitude for the ejection of a magnetized plasma from the solar atmosphere. Calculations based on a model with two possible paths of particle propagation show that the formation of the trap should occur at distances $1.5-2 R_{\odot}$ from the center of the sun, where R_{\odot} is the radius of the sun [14].

REFERENCES

1. Ya. L. Blokh, Ye.S. Glikova, L.I. Dorman, in collection entitled Variatsii kosmicheskikh luchey pod Zemley, na urovne morya i v stratosfere [Variations of Cosmic Rays Underground, at Sea Level and in the Stratosphere], Izd-vo AN SSSR [Publishing House of the Academy of Sciences USSR], Moscow, 1959, 7.
2. Ya.L. Blokh, L.I. Dorman, N.S. Kaminer, Trudy Mezhdunarodnoy

•

konferentsii po kosmicheskim lucham [Transactions of the International Conference on Cosmic Rays], IV, 154, Izd-vo AN SSSR, Moscow, 1960.

3. Ya.L. Blokh, L.I. Dorman, N.S. Kaminer. Trudy Mezhdunarodnoy konferentsii po kosmicheskim lucham [Transactions of the International Conference on Cosmic Rays], IV, 178, Izd-vo AN SSSR, Moscow, 1960.
4. Ya.L. Blokh, Ye.S. Glikova, L.I. Dorman, O.I. Inozemtseva. Trudy Mezhdunarodnoy konferentsii po kosmicheskim lucham [Transactions of the International Conference on Cosmic Rays], IV, 172, Izd-vo AN SSSR, Moscow, 1960.
5. L.I. Dorman, Variatsii kosmicheskikh luchey [Variations of Cosmic Rays], Gostekhizdat [State Publishing House for Technical and Theoretical Literature], Moscow, 1957.
6. L.I. Dorman, Trudy Mezhdunarodnoy konferentsii po kosmicheskim lucham [Transactions of the International Conference on Cosmic Rays], IV, 113, Izd-vo AN SSSR, Moscow, 1960.
7. L.I. Dorman, Trudy Mezhdunarodnoy konferentsii po komicheskim lucham [Transactions of the International Conference on Cosmic Rays], IV, 132, Izd-vo AN SSSR, Moscow, 1960.
8. A.G. Fenton, K.G. McCracken, D.C. Rose, B.G. Wilson. Canad. J. phys., 37, 970, 1959.
9. Ya.L. Blokh, L.I. Dorman, N.S. Kaminer, Rezul'taty MGG, ser. kosmich. luchey [Results of the IGY, Cosmic Radiation Series], 4, 49, 1961.
10. Ya.L. Blokh, L.I. Dorman, N.S. Kamner, in collection entitled Variatsii kosmicheskikh luchey i solnechnye korpuskulyarnye potoki [Variations of Cosmic Rays and Solar Corpuscular Streams], Izd-vo AN SSSR, Moscow, 1960, 7.

11. L.I. Dorman, Nuovo Cimento Suppl., VIII, No. 2, 391, 1958.
12. A.N. Charakhch'yan, V.F. Tulinov, T.N. Charakhch'yan, ZHETP [Journal of Experimental and Theoretical Physics], 38, 1031, 1960.
13. P.S. Frayer, Ye.P. Ney, Dzh.R. Vinkler, Trudy Mezhdunarodnoy konferentsii po kosmicheskim lucham [Transactions of the International Conference on Cosmic Rays], IV, 96, Izd-vo AN SSSR, Moscow, 1960.
14. L.I. Dorman Proc. of the Moscow cosmic ray conf., v. III, page 74, VINITI, Moscow, 1960.
15. Ya.L. Blokh, L.I. Dorman, N.S. Kaminer. Rezul'taty MGG ser. kosmich. luchey [Results of the IGY, Cosmic Radiation Series], 4, 59, 1961.
16. P. Rothwell. J. geophys. res., 11, 2026, 1959.
17. T. Obayshi. Rep. Ionosph. and space res. in Japan, 13 (3), 177, 1959.
18. I. Kondo K. Nagashima, S. Ioshida, M. Vada, Trudy Mezhdunarodnoy konferentsii po kosmicheskim lucham [Transactions of the International Conference on Cosmic Rays], IV, 210, Izd-vo AN SSSR, Moscow, 1960.
19. Ya.L. Blokh, L.I. Dorman, N.S. Kaminer, Rezul'taty MGG, ser. kosmich. luchey [Results of the IGY, Cosmic Radiation Series], 4, 5, 1961.
20. A.B. Severnyy. Astronomicheskiy zhurnal [Astronomical Journal], 36, 972, 1959.
21. L.I. Dorman Proc. Moscow cosmic ray. conf., v. III page 239. Moscow, 1960.

CONCERNING THE STABILITY OF A PLASMA PINCH

M. D. Ladyzhenskiy
Moscow

We investigate the stability of a plasma pinch situated in a medium with nonconducting liquid in vortical rotation.

A comparison is made of the regions of stability of a plasma pinch and of a vortex in "ordinary" hydrodynamics.

It was shown in [1, 2] that a plasma pinch is unstable against perturbations of the "sausage" and helix type. In connection with the instability observed, several methods were proposed for the stabilization of the pinch [3, 4].

We consider below the question of pinch stabilization with the aid of vortical motion of a nonconducting medium surrounding the pinch.

The problem is formulated in the following manner: a current of intensity I flows over the surface of a round cylinder of radius R of an ideally conducting incompressible liquid; the current flow is in the axial direction. The cylinder is placed in a medium in which a nonconducting incompressible liquid moves vortically. The system is in equilibrium: the hydrodynamic pressure from the inside of the cylinder is balanced by the sum of the hydrodynamic and magnetic pressures from the outside. It is required to investigate the stability of this system. The problem is solved in analogy with [1].

We introduce a cylindrical system of coordinates r, θ, z with z axis directed along the cylinder axis. We consider the system for a small deviation from the equilibrium position. The peripheral compo-

nents of the velocity vector v_θ and of the magnetic field h_θ in the unperturbed state are given by

$$v_\theta = V \frac{R}{r}, \quad h_\theta = H \frac{R}{r}, \quad (1)$$

where V and H are, respectively, the peripheral components of the velocity and the magnetic field on the surface of the cylinder. We denote by f , φ , and ψ the potentials of the perturbed motion for the external flow, internal magnetic field, and internal flow, respectively. These functions satisfy the Laplace equation with the following conditions on the axis and at infinity:

$$\begin{aligned} \psi &< \infty \text{ for } r=0, \\ \lim_{r \rightarrow \infty} f &= 0, \quad \lim_{r \rightarrow \infty} \varphi = 0. \end{aligned} \quad (2)$$

On the surface of the cylinder, the equation of which in cylindrical coordinates has the form

$$r = R + \xi(\theta, z, t),$$

the following conditions are satisfied: the internal and external flows do not penetrate the surface, the component of the magnetic field perpendicular to the surface of the pinch vanishes, and the pressures from the outside and from the inside of the cylinder are equal (the pressure is defined as the sum of the hydrodynamic pressure, determined by the Lagrange formula, and the magnetic pressure)

$$\frac{\partial f}{\partial r} - \frac{V \xi}{R \partial \theta} - \frac{\partial \xi}{\partial t} = 0, \quad (3)$$

$$\frac{\partial \varphi}{\partial r} - \frac{H \xi}{R \partial \theta} = 0, \quad (4)$$

$$\frac{\partial \psi}{\partial r} - \frac{\partial \xi}{\partial t} = 0, \quad (5)$$

$$-\rho_1 \frac{V \partial f}{R \partial \theta} - \rho_1 \frac{\partial f}{\partial t} - \frac{\rho_1 \xi}{2} \frac{\partial v_\theta^2}{\partial r} + \frac{H}{4\pi R} \frac{\partial \varphi}{\partial \theta} + \frac{\xi \partial h_\theta^2}{8\pi \partial r} + \rho_2 \frac{\partial \psi}{\partial t} = 0, \quad (6)$$

where ρ_1 and ρ_2 are the density outside and inside the cylinder.

We seek the solution in the form of a Fourier series. By satisfying the Laplace equation, the conditions at infinity, and the condition

that the velocity be finite on the cylinder axis, we obtain

$$\begin{aligned} f &= aK_m(kr)e^{i(m\theta + kz + \omega_{m,k}t)}, \\ \varphi &= bK_m(kr)e^{i(m\theta + kz + \omega_{m,k}t)}, \\ \psi &= cI_m(kr)e^{i(m\theta + kz + \omega_{m,k}t)}, \\ \zeta &= de^{i(m\theta + kz + \omega_{m,k}t)}, \end{aligned} \quad (7)$$

where k and m are integers, $I_m(kr)$ and $K_m(kr)$ are Bessel functions of imaginary argument, and a , b , c , and d are certain constants. From the condition that there exist a nonzero solution for a , b , c , and d , we obtain, by substituting (7) in Eqs. (3-6) an equation for $\omega_{m,k}$. Introducing the notation $\Omega = \omega_{m,k}R$, $\bar{k} = kr$ (the superior bar over k will be left out henceforth for the sake of brevity), we obtain the following equation:

$$\begin{aligned} \Omega^2[\rho_2 I_m K'_m - \rho_1 K_m I'_m] - 2\rho_1 V_m K_m I'_m \Omega + \\ + \left(\frac{H^2}{4\pi} - \rho_1 V^2 \right) (k K'_m I'_m + m^2 K_m I'_m) = 0. \end{aligned} \quad (8)$$

The condition that Ω have no complex roots in this quadratic equation yields the limit of the stability region of the flow under consideration.

Putting $\mu = 4\pi\rho_1 V^2/H^2$, $\bar{\rho} = \rho_1/\rho_2$ and using the following equation (retaining the notation of [1])

$$\begin{aligned} \frac{K'_m}{K_m} &= -\frac{K_{m-1}}{K_m} - \frac{m}{\bar{k}} \equiv -\frac{\varphi_2(k)}{k}, \\ \frac{I'_m}{I_m} &= \frac{I_{m-1}}{I_m} - \frac{m}{\bar{k}} \equiv \frac{\varphi_1(k)}{k}. \end{aligned}$$

we can write the stability condition in the form

$$\bar{\rho} \left[1 - \frac{m^2}{\varphi_2(k) + \bar{\rho}\varphi_1(k)} \right] + \frac{m^2}{\varphi_2(k)} - 1 > 0. \quad (9)$$

When $\mu = 0$, which corresponds to the absence of the external flow, Eq. (9) coincides with that obtained by V.D. Shafranov [1]. The stability regions given by this equation are as follows: when $m = 0$ and l the pinch is absolutely unstable. Starting with $m = 2$, a stability region

appears at small values of k , while at large values of m the stability region is given by the expression $k \leq m^2$.

When $\mu = \infty$ we arrive at the question of stability of a vortex with a core at rest. When $m = 0$ and $m = 1$ the vortex is absolutely stable. In other words, the vortex is absolutely stable against perturbations of the sausage and helix type, which are the most dangerous for a plasma pinch. For $m > 2$ there appears in the vortex an instability region which is given by the following relation (for large m)

$$k < \frac{m^2}{1 + \rho} \quad (10)$$

Perturbations with $m \geq 2$, with respect to which the vortex is unstable, have a "twist" character. Numerous observations have shown that the vortices are stable; it follows therefore that perturbations of the "twist" type are not dangerous and do not lead to a destruction of the vortex. We consider now the general case of arbitrary μ . The stability region is characterized in the following fashion. The configuration

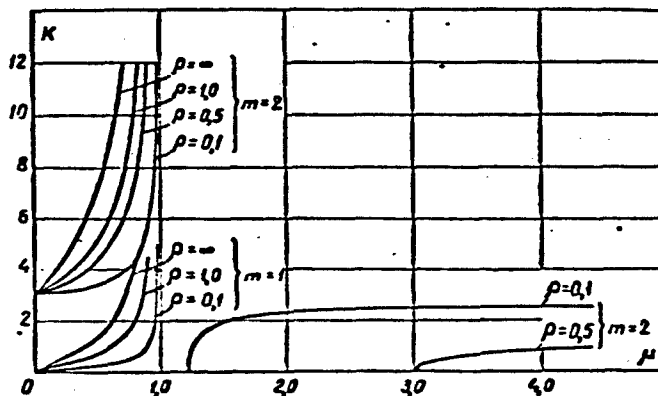


Fig. 1

considered at $1 < \mu < 1 + \bar{\rho}$ is absolutely stable with respect to any perturbation. Thus, complete stabilization of the pinch is possible for the indicated values of the parameters. Let us proceed to a more detailed description of the instability regions.

When $m = 0$ the system is stable if $\mu > 1$. When $m = 1$ the stability regions lie in the plane to the right of the lines shown in Fig. 1, each of which depends on a certain value of \bar{p} , i.e., in this case the system is also stable with respect to all perturbations if $\mu > 1$, but there are stability regions also for $\mu < 1$. When $m \geq 2$ in the half space $\mu > 1$, instability regions appear when $m > 1 + \bar{p}$, bounded by curves that depend on \bar{p} (see Fig. 1). The abscissas of the points of intersection of these curves with the line $k = 0$ are expressed in the following form (for large m)

$$\mu = \frac{\frac{m-1}{m}}{\frac{1}{1+\bar{p}} - 1}.$$

To the left, for $\mu < 1$, the boundary of the stability regions shifts toward the side of larger k with increasing m .

Furthermore, the following asymptotic relations hold true for large numbers m : when $\mu < 1$ the stability region is given by the relation

$$k < m^2 \frac{1 - \frac{\bar{p}}{1+\bar{p}}}{1 - \mu} \quad (11)$$

(qualitatively the configuration is similar to a plasma pinch). When $\mu > 1 + \bar{p}$ the stability region is given by

$$k > m^2 \frac{\frac{\bar{p}}{1+\bar{p}} - 1}{\mu - 1} \quad (12)$$

(the configuration is qualitatively analogous to a vortex).

CONCLUSIONS

1. In principle it is possible to stabilize a plasma pinch with respect to any perturbation with the aid of vertical motion of a non-conducting liquid surrounding the pinch.
2. Perturbations of the "twist" type are not dangerous, as can be seen with a vortex as an example.

We note in conclusion that the method of vortical stabilization can be combined with several other known methods [3, 4]. Then the speeds of vortical motion needed for stabilization will not be too large.

REFERENCES

1. V. D. Shafranov, Ob ustoychivosti tsilindricheskogo gazovogo provodnika v magnitnom pole [Stability of a Cylindrical Gaseous Conductor in a Magnetic Field], Atomnaya energiya [Atomic Energy], 5, 1956.
2. M. Kruskal, M. Schwarzschild. Some instabilities of a completely ionized plasma. Proc. Roy. soc. ser. A, math. a. phys. sci., 1154, 223, 1954.
3. M. A. Leontovich, V. D. Shafranov, Ob ustoychivosti gibkogo provoda v prodol'nom magnitnom pole [Stability of a Flexible Wire in a Longitudinal Magnetic Field], collection entitled Fizika plazmy i problema upravlyayemykh termoyadernykh reaktsiy [Plasma Physics and the Problem of Controlable Thermonuclear Reactions], Izd-vo AN SSSR, [Acadamy of Sciences USSR Press], Moscow, 1958, I, 207.
4. V. D. Shafranov, Ob ustoychivosti plazmennogo shnura pri nalichii prodol'nogo magnitnogo polya i provodyashchego kozhukha [On the Stability of a Plasma Pinch in the Presence of a Longitudinal Magnetic Field and a Conducting Sheath], ibid., II, 130.

NATURAL OSCILLATIONS OF A BOUNDED PLASMA

D. A. Frank-Kamenetskiy

Moscow

A plasma cylinder in a longitudinal static magnetic field can have the properties of an electromagnetic resonator or a waveguide over a wide frequency range. In the absence of a magnetic field, resonance is possible only at frequencies above the plasma frequency, where the ion motion can be neglected. Such plasma resonators operating in the microwave band were investigated by a group headed by Braun and their detuning is the basis of a widely used method of plasma diagnostics. In the presence of a magnetic field resonance phenomena occur also at much lower frequencies (in the UHF band), where the motion of the ions is significant. A study of such hydromagnetic and magnetic-sound resonators and waveguides is barely in the initial stage.

The dispersion equation of a plasma is of the fifth degree in the square of the frequency. Therefore a plasma volume has under given definite conditions, generally speaking, five different natural frequencies (real and imaginary) [1]. These frequencies are resonant in the direct meaning of this word, i.e., they are frequencies of standing waves that can exist in stationary manner in the given volume and satisfy the boundary conditions. They depend both on the properties of the plasma and on the geometrical form and dimensions of the volume under consideration. Such resonances we shall call buildup resonances; in radio language they correspond to the vanishing of the imaginary part of the plasma impedance. They must be distinguished from absorp-

tion resonances, which correspond to maxima of the real part of the impedance.

In unbounded plasma there is also a series of characteristic frequencies, which depend, naturally, only on the properties of the plasma itself. These frequencies are also customarily called resonant, although it would be more correct to call them the frequencies of anomalous dispersion. These include first of all the electron and ion cyclotron frequencies, at which the refractive index of the plasma along the magnetic field becomes infinite. For the refractive index transversely to the magnetic field, an analogous role is played by two frequencies which, using the very appropriate suggestion by Hurwitz [2], are called hybrid. In a dense plasma the lower one of these frequencies is close to the geometric mean of the electron and ion cyclotron resonances, and the upper one is close to the plasma frequency. At these frequencies the phase velocity of wave propagation in the plasma vanishes in the corresponding directions. The anomalous dispersion is accompanied by energy absorption. Therefore the characteristic frequencies of an unbounded plasma always correspond to absorption resonances.

One can point out, however, conditions under which there coincide with the anomalous dispersion frequencies also buildup resonances. The resonance condition for a standing wave requires that the time of propagation of the wave between the specified boundaries coincide with the period of the oscillation. Away from the anomalous dispersion frequencies, the rate of wave propagation both along the magnetic field and transversely to it tends to the Alfvén velocity. If the dimensions are small or the Alfvén velocity large (low densities, strong magnetic fields), then the resonance condition can be satisfied only by letting the phase velocity tend to zero, i.e., anomalous dispersion. Therefore, if we decrease the plasma density, decrease the dimensions of the vol-

ume occupied by it, or increase the intensity of the static magnetic field, then the resonance frequencies shift toward the anomalous dispersion frequencies, i.e., the buildup resonances coincide with the absorption resonances. To the contrary, in a dense plasma pinch of large radius, the most important of the buildup resonances, namely magnetic-sound resonance, can be realized in pure form.

The dispersion equation contains two wave numbers, the radial k_1 and the longitudinal k_3 . The longitudinal wave number is determined by the boundary conditions on the ends of the cylinder, while the radial one is determined by the conditions on its lateral surfaces. If the cylinder is surrounded on its lateral surface by ideally conducting walls, in which current flows, then the approximate boundary condition reduces to the vanishing of the azimuthal electric field on the wall. The total magnetic flux through the transverse cross section vanishes in this case, since the sign of the longitudinal alternating magnetic field reverses along the radius. If a gap exists between the wall and the plasma, then one can assume, in view of the large refractive index of the plasma, that the boundary condition is specified on the surface of the plasma and not on the surface of the wall. For a plasma cylinder of radius R_0 the boundary condition requires that $k_1 R_0$ be equal to the root of a definite combination of Bessel functions. In the simplest case of axially symmetrical oscillations for a cylinder surrounded by conducting walls, $k_1 R_0$ should be equal to one of the roots of a first-order Bessel function.

For free oscillations with radiation electromagnetic waves at infinity, an approximate boundary condition is imposed on the longitudinal alternating magnetic field, and for the case of axial symmetry this condition is that $k_1 R_0$ be equal to one of the roots of the zero-order Bessel function. In this case, owing to radiation of energy at

infinity, the frequency is complex, i.e., the oscillations are damped.

The attached plots show in dimensionless form the resonant frequency of a plasma cylinder for three cases with different values of the longitudinal wave number. The horizontal axis represents the square of the resonant frequency divided by the product of the electron and ion cyclotron frequencies:

$$\Omega = \frac{\omega^2}{\omega_e \omega_i}.$$

The vertical axis represents the quantity

$$z = \frac{k_1 c^2}{\omega_0^2},$$

where k_1 is the radial wave number, c is the velocity of light, and ω_0 is the plasma frequency. This quantity is inversely proportional to the running number of electrons in a length equal to the classical radius of the electron. We shall call the reciprocal quantity, $1/z$, the effective running number of electrons. The parameters of the curves are:

$A = \omega_0^2 / \omega_1 \omega_e = c^2 / u_A^2$ – the square of the refractive index corresponding to the Alfvén velocity;

$B = \omega_e / \omega_1 = M / zm$ – the ratio of the electron and ion cyclotron frequencies and $y = k_3^2 c^2 / \omega_0^2$, where k_3 is the longitudinal wave number. The values of A and B are taken for hydrogen at the density for which the plasma frequency is equal to the electron cyclotron frequency. The plots correspond to different values of y , increasing from Fig. 1 toward Fig. 3. Figure 1 represents pure radial oscillations of an infinite cylinder. There is one low-frequency branch corresponding to magnetic sound. When the running number of electrons is small ($z \rightarrow \infty$) the resonant frequency tends to the lower hybrid frequency (vertical line). In the case of a large running number of electrons ($z \rightarrow 0$, magnetoacoustic region), magnetic sound resonance is possible at frequen-

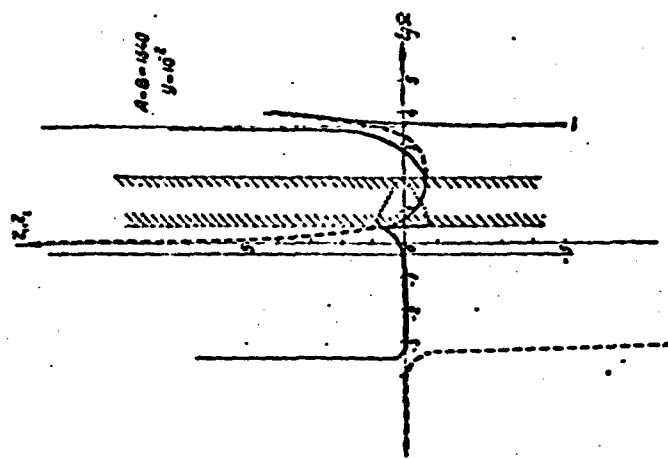


FIG. 3

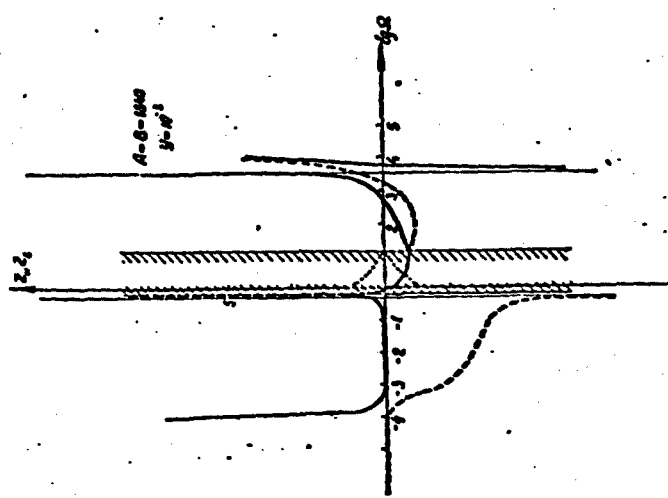


FIG. 2

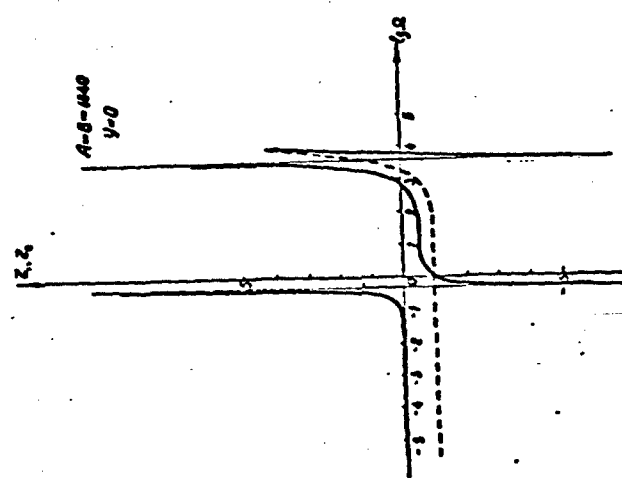


FIG. 1

cies as low as desired. Above the lower hybrid frequency there is a broad region where a wave propagating transversely to the field does not penetrate into the plasma (imaginary frequencies). Near the plasma frequency ($\Omega = A$) are located three branches of high-frequency electron oscillations. In the case of a cylinder of finite length (Figs. 2 and 3) the high-frequency branches vary little, while in the low-frequency regions a second branch arises (magnetohydrodynamic oscillations of the TEM type) with anomalous dispersion at the ion cyclotron frequency. These are oscillations propagating along the fields and reflected from the ends of the cylinder.

A very important difference between a finite cylinder and an infinite one is the behavior of the magnetic-sound branch near the lower hybrid frequency. The purely radial oscillations at the lower hybrid frequency are cut off. Oblique waves, on the other hand, propagate in the plasma even at frequencies above the lower hybrid one. In place of a region of total reflection, in a finite cylinder there is produced a region of complex values of the refractive index, shifting toward the higher frequencies. This region is represented in the plots by the shaded strip. The thin continuous line in the strip represents the real part, and the two thin dashed lines represent the imaginary parts of the two complex conjugate values of z . In the region of low frequencies there is also an imaginary branch, shown dashed in the figures.

In an incompletely ionized plasma [3] one can note two limiting cases: if the frequency of the charge-exchange collisions is small compared with the oscillation frequency, then the neutral particles are not entrained at all, and the opposite case, they are completely entrained by the magnetic-sound oscillations. In the intermediate region, where the oscillation and collision frequencies are of the same order of magnitude, a partial entrainment of the neutral particles should

occur and lead to strong damping.

Experiment [4] shows that in a finite but long cylinder, magnetic-sound oscillations that are of the standing-wave type along the radius are really excited, and resonance phenomena that depend on the plasma concentration are observed. The character of the resonance phenomena does not change on going through the hybrid frequency, thus indicating the role played by the oblique waves.

The combination of the buildup and absorption resonances can be used for ionization purposes [5] and for high-frequency heating of a plasma [6].

REFERENCES

1. D. A. Frank-Kamenetskiy, O sobstvennykh kolebaniyakh ogranicennoy plazmy [Natural Oscillations of a Bounded Plasma], ZhETF [Journal of Experimental and Theoretical Physics], 39, 9, 1960.
2. P. Auer, H. Hurwitz, R. Miller. Phys. fluids, 1, 501, 1958.
3. D. A. Frank-Kamenetskiy, Magnitnyy zvuk v trekhkomponentnoy plazme [Magnetic Sound in a Three-Component Plasma], ZhTF [Journal of Technical Physics], 30, 8, 893, 1960.
4. Akhmativ, Blinov, Zavoyskiy et al., Magnitno-zvukovoy rezonans v plazme [Magnetonic Resonance in Plasma], ZhETF, 39, 9, 1960.
5. Ye. K. Zavoyskiy, I. A. Kovar, B. I. Patrushev, V. D. Rusanov, D. A. Frank-Kamenetskiy, Magnitno-zvukovoy metod ionizatsii plazmy [Magnetonic Method of Plasma Ionization], ZhTF, 30, 1960.
6. D. A. Frank-Kamenetskiy, Magnitno-zvukovoy rezonans v plazme [Magnetonic Resonance in Plasma], ZhTF, 30, 8, 899, 1960.

MAGNETOHYDRODYNAMIC INSTABILITY OF A PLASMA STREAM
MOVING THROUGH AN IONIZED GAS

V.P. Dokuchayev

Gor'kiy

It is shown that when a plasma stream moves through an ionized gas with a velocity larger than the Alfvén wave velocity, the system comprising the stream and stationary plasma becomes unstable. In this case one of the normal magnetohydrodynamic waves builds up with time. A criterion for instability is discussed in detail and the buildup coefficient of this wave is analyzed.

* * *

A study of magnetohydrodynamic waves propagating in plasma streams is of certain interest for a whole series of astrophysical and geophysical problems. This pertains in particular to the dynamics of solar corpuscular streams, to arc protuberances on the sun, and possibly also to motions in the spiral arms of galaxies. However, in its general formulation, the investigation of the magnetohydrodynamic instability of a plasma stream moving through a completely ionized gas is a very complicated problem. By virtue of this it becomes necessary to employ several simplifying assumptions, making it possible to obtain the solution of the problem and consequently to clarify the conditions under which the plasma stream is unstable. Let us consider the problem of interest to us in the following formulation.

Assume a stream of strongly ionized quasineutral plasma with concentration N_s , moving through a strongly ionized quasineutral gas with

concentration N_p . Such a system is sometimes called a system of inter-penetrating unbounded moving media. The entire system is placed in an external homogeneous magnetic field \vec{H}_0 , which is parallel everywhere to the stream velocity \vec{V}_0 . These assumptions greatly facilitate the subsequent quantitative analysis of the problem of magnetohydrodynamic instability of the system comprising the stream plus stationary plasma, and at the same time enable us to establish a sufficiently general criterion the satisfaction of which indicates the occurrence of the instability. We note that the buildup of high-frequency electromagnetic waves occurring during the motion of electron and ion streams in a plasma has been considered in a whole series of papers [1-4]. We are interested in a different limiting case of instability, namely the stability of the aforementioned system against low-frequency electromagnetic waves (with frequency lower than the gyrofrequency of the ions), when the latter degenerate into magnetohydrodynamic waves [9]. Let us determine under what conditions magnetohydrodynamic waves that grow in time occur in the stream plus stationary plasma system, and consequently when the system becomes unstable.

The conservation laws for the momentum of electrons and ions in a strongly ionized gas, when the degree of ionization is so large that the interaction between the charged particles prevails over their interaction with the neutral atoms, can be written in the form [6]

$$\rho_e \frac{d\vec{v}_e}{dt} + \rho_e v_{ei} (\vec{v}_e - \vec{v}_i) = -eN_e \vec{E} - \frac{eN_e}{c} [\vec{v}_e \vec{H}] + \vec{F}_e \quad (1)$$

$$\rho_i \frac{d\vec{v}_i}{dt} - \rho_i v_{ei} (\vec{v}_e - \vec{v}_i) = eN_i \vec{E} + \frac{eN_i}{c} [\vec{v}_i \vec{H}] + \vec{F}_i \quad (2)$$

where $\rho_e = m_e N_e$ and $\rho_i = m_i N_i$ are the densities of the electron and ion masses in the plasma, \vec{v}_e and \vec{v}_i are the velocities of the electrons and the ions, \vec{F}_e and \vec{F}_i are the forces acting on the electron and ion gas, \vec{E} and \vec{H} are the intensities of the electric and magnetic

fields, v_{ei} is the number of collisions between an electron and the ions per unit time, e is the electron charge, m_e and m_i are the mass of the electron and the ion, and N_e and N_i are the concentrations of the electrons and the ions per cubic centimeter. We introduce the velocity \vec{v} of the motion of the entire plasma as a whole, and the density of the electric current \vec{j} , in the usual manner:

$$\vec{j} = eN(\vec{v}_e - \vec{v}_i), \quad (3)$$

$$\vec{v} = \frac{\rho_e \vec{v}_e + \rho_i \vec{v}_i}{\rho}, \quad (4)$$

where $\rho = \rho_e + \rho_i$. For a quasineutral plasma we have $N_e \approx N_i = N$, and consequently $\rho \approx \rho_i$. Using Relations (3) and (4) we can readily transform (1) and (2) into

$$\rho \frac{d\vec{v}}{dt} = \frac{1}{c} [\vec{J} \vec{H}] + \vec{F}_e + \vec{F}_i \quad (5)$$

$$\frac{d\vec{j}}{dt} + v_a \vec{j} + \omega_e [\vec{j} \vec{\tau}] = \frac{e^2 N}{m_e} \left(\vec{E} + \frac{1}{c} [\vec{v} \vec{H}] \right) + \frac{e}{m_i} \vec{F}_i - \frac{e}{m_e} \vec{F}_e \quad (6)$$

where $\omega_e = eH/m_e c$ is the gyrofrequency of the electron in the magnetic field \vec{H} , and $\vec{\tau}$ is the unit vector of this field. In the derivation of (5, 6) it was assumed that $m_i \gg m_e$. Equation (5) is the hydrodynamic equation for the plasma, while Eq. (6) for the electric current \vec{j} expresses the generalized Ohm's law. Unlike the relations given in [5, 6], in the derivation of Eq. (6) we have retained here the total derivatives with respect to time $d/dt = (\partial/\partial t) + (\vec{v} \nabla)$, which is of importance in the present case. From Maxwell's electrodynamic equations it follows that

$$\nabla^2 \vec{E} - \frac{1}{c^2} \frac{\partial^2 \vec{E}}{\partial t^2} = \frac{4\pi}{c^3} \cdot \frac{\partial \vec{j}}{\partial t}. \quad (7)$$

$$\text{rot } \vec{E} = - \frac{1}{c} \cdot \frac{\partial \vec{H}}{\partial t}. \quad (8)$$

Starting with Eqs. (5-8), we can readily set up linearized equations describing the electrodynamic processes in the stream plus stationary

plasma system:

$$\frac{\partial \vec{j}_s}{\partial t} + (\vec{V}_0 \nabla) \vec{j}_s + v_s \vec{j}_s + \omega_H [\vec{j}_s \vec{v}] = \frac{e^2 N_s}{m_e} \left(\vec{E} + \frac{1}{c} [\vec{V}_0 \vec{H}] + \frac{1}{c} [\vec{v}_s \vec{H}_0] \right), \quad (9)$$

$$\frac{\partial \vec{v}_s}{\partial t} + (\vec{V}_0 \nabla) \vec{v}_s = \frac{1}{\rho_s c} [\vec{j}_s \vec{H}_0], \quad (10)$$

$$\frac{\partial \vec{j}_p}{\partial t} + v_p \vec{j}_p + \omega_H [\vec{j}_p \vec{v}] = \frac{e^2 N_p}{m_e} \left(\vec{E} + \frac{1}{c} [\vec{v}_p \vec{H}_0] \right), \quad (11)$$

$$\frac{\partial \vec{v}_p}{\partial t} = \frac{1}{\rho_p c} [\vec{j}_p \vec{H}_0]. \quad (12)$$

$$\text{rot } \vec{E} = -\frac{1}{c} \frac{\partial \vec{h}}{\partial t}. \quad (13)$$

$$\nabla \cdot \vec{E} - \frac{1}{c^2} \frac{\partial^2 \vec{E}}{\partial t^2} = \frac{4\pi}{c^2} \frac{\partial (\vec{j}_s + \vec{j}_p)}{\partial t}. \quad (14)$$

The subscripts s and p pertain to quantities in the stream and in the resting plasma, respectively, \vec{V}_0 is the stream velocity, and \vec{H}_0 is the external magnetic field.

The system (9-14) allows us to obtain the dispersion equation for plane transverse electromagnetic waves propagating along the stream, and consequently along the force lines of the magnetic field \vec{H}_0 . Let us choose a rectangular coordinate system and direct the z axis along the magnetic field. For the sake of convenience we choose the complex quantities

$$E_{\pm} = E_x \pm iE_y, \quad h_{\pm} = h_x \pm ih_y, \quad v_{p\pm} = v_{px} \pm iv_{py}, \quad j_{p\pm} = j_{px} \pm j_{py}$$

and analogously represent the stream quantities $j_{s\pm}$ and $v_{s\pm}$. With this notation and under the assumption that all the indicated quantities vary as $\exp i(\omega t - kz)$, where ω and k are the frequency and the wave number, we obtain the following dispersion equation:

$$\begin{aligned} \omega^2 - c^2 k^2 &= \frac{\omega_{se}^2 (\omega - kV_0)}{\omega - kV_0 \pm \omega_H - iv_{st}^2 - [\omega_H \Omega_H / (\omega - kV_0)]} + \\ &+ \frac{\omega_{pe}^2 \omega}{\omega \pm \omega_H - iv_{st}^2 - (\omega_H \Omega_H / \omega)}, \end{aligned} \quad (15)$$

where $\omega_{se} = (4\pi N_s e^2 / m_e)^{1/2}$ and $\omega_{pe} = (4\pi N_p e^2 / m_e)^{1/2}$ are the plasma fre-

quencies of the electrons in the stream and in the stationary plasma, $\Omega_H = eH_0/m_1 c$ is the gyrofrequency of the ions. The plus sign corresponds to the ordinary wave and the minus sign to the extraordinary one. Dispersion Equation (15) describes the propagation of transverse electromagnetic waves only. The propagation of longitudinal high-frequency waves was considered in [7, 8]. In the absence of a stream, when $\omega_{se} = 0$, Eq. (15) goes over into the well-known equation for electromagnetic waves propagating in a plasma along the magnetic field [9]. When the entire plasma moves and $\omega_{pe} = 0$, and also when the ions are neglected, we obtain from (15) the equation derived in [4].

Let us consider the usual approximation of magnetohydrodynamics – the case of extremely low frequencies $\omega \ll \Omega_H$ – and let us assume that $kV_0 \ll \Omega_H$, and then we obtain from (15)

$$\kappa^2 = \frac{\omega^2}{c^2} + \frac{\omega^2}{V_{A\mu}^2} + \frac{(\omega - kV_0)^2}{V_{A\mu}^2}. \quad (16)$$

where we introduce the Alfvén wave velocities

$$V_{A\mu}^2 = \frac{\omega_H \Omega_H c^2}{\omega_{se}^2} = \frac{H_0^2}{4\pi\rho_s} \text{ and } V_{A\mu}^2 = \frac{H_0^2}{4\pi\rho_p}.$$

The solution of the dispersion equation (16) can be readily obtained and can be written in the form

$$\frac{\omega}{k} = \frac{V_0 \pm \sqrt{\frac{N_e}{N_i} \left[\left(1 - \frac{V_0^2}{c^2} \right) V_{A\mu}^2 + V_{A\mu}^2 + (V_{A\mu}^2 \cdot V_{A\mu}^2/c^2) - V_0^2 \right]}}{1 + (N_e/N_i) + (V_{A\mu}^2/c^2)}. \quad (17)*$$

For the analysis that follows it is convenient to rewrite the formula in a somewhat different form with account of the fact that we are considering a stream of particles with nonrelativistic velocities ($V_0 \ll c$):

$$\frac{\omega}{k} = \frac{N_e \pm \sqrt{N_e(N_e + N_p + N_{ip}) - N_e N_p}}{N_e + N_p + N_{ip}} V_0. \quad (18)$$

We have introduced here the notation $N_{kp} = H_0^2/4\pi m_1 c^2$ and $N_0 = H_0^2/4\pi m_1 V_0^2$. From (18) we can readily establish that if the condition

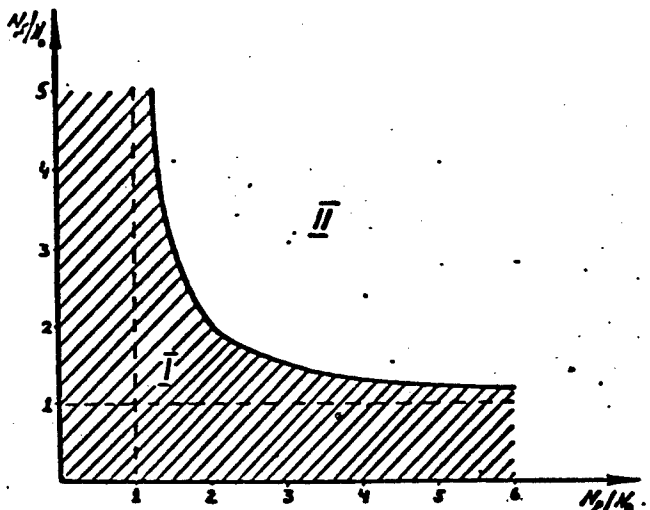


Fig. 1. Plane of the parameters N_p and N_s : I) system stability region; II) system instability region; the dashed lines are the asymptotes of the boundary curve.

$$NN_p > N_0(N_s + N_p + N_{kp}) \quad (19)$$

is satisfied there appear in the stream plus stationary plasma system waves that build up with time, i.e., the system becomes unstable. This type of magnetohydrodynamic instability differs from the instability of plasma streams against high-frequency electromagnetic perturbations, when $\omega \geq \Omega_H$ [1-4]. In magnetohydrodynamics, in addition to the condition $\omega \ll \Omega_H$, it is usually assumed that $N > N_{kp}$. In this case (19) can be rewritten in the form $V_0^2 > V_A^2 = V_{As}^2 + V_{Ap}^2$. Thus, a magnetohydrodynamic instability arises in the case when the stream velocity exceeds the Alfvén wave velocity in the stream plus stationary plasma system. In this case it is necessary to use for the system density the reduced density $1/\rho = 1/\rho_s + 1/\rho_p$. It must be noted that an analogous instability criterion is encountered in magnetohydrodynamics in the analysis of the instability of tangential discontinuities [11].

Figure 1 shows a plot of the stability boundary in the plane of the parameters N_p , N_s . The boundary curve is determined by the equation

$$\frac{1}{N_0} = \frac{1}{N_s} + \frac{1}{N_p} + \frac{N_{kp}}{N_s \cdot N_p}.$$

The shaded part of the plane together with the boundary is the region where the system is stable. The remaining part of the plane is the region of magnetohydrodynamic instability of the system. The boundary is an equilateral hyperbola with asymptotes parallel to the coordinate axes. It is easy to obtain the value of the plasma concentration corresponding to the asymptotic values of the curve. This value is N_0 for N_p and N_s .

If Condition (19) is satisfied in the stream plus plasma at rest, one of the normal waves builds up with time. The buildup coefficient γ is determined from (18) and has the form

$$\gamma = kV_0 \frac{\sqrt{N_p N_s - N_0(N_s + N_p + N_{kp})}}{N_s + N_p + N_{kp}}. \quad (20)$$

By regarding γ as a function of two variables $\gamma = \gamma(N_p, N_s)$, we can determine the condition for the maximum value of the buildup coefficient. It turns out that γ has a maximum if the equality $N_p = (N_s + N_{kp})(N_s + N_0)/(N_s - N_0)$ is fulfilled. In this case the maximum value of the buildup coefficient is $\gamma_{\max} = (kV_0/2)(N_s - N_0)/\sqrt{N_s(N_s + N_{kp})}$. We shall assume that N_p and $N_s \gg N_{kp}, N_0$, and then $\gamma = kV_0 \sqrt{N_p N_s}/(N_p + N_s)$, $\gamma_{\max} = kV_0/2$. Thus, γ assumes a maximum value in the case when the plasma concentration in the beam is approximately equal to the plasma concentration in the medium at rest.

In conclusion it must be noted that dispersion equations analogous to (17) or (18) are encountered also in ordinary hydrodynamics in the analysis of instability of jet flows [12].

REFERENCES

1. B. B. Kadomtsev, *Fizika plazmy i problema upravlyayemykh termoyadernykh reaktsiy* [Plasma Physics and the Problem of Controlled Thermonuclear Reactions], Iad-vo AN SSSR, [Academy of Sciences

- USSR Press], Moscow, 4, 364, 1958.
2. G.G. Getmantsev, ZhETF [Journal of Experimental and Theoretical Physics], 37, 843, 1959.
 3. V.V. Zheleznyakov, Izv. VUZ, Radiofizika [Bulletin of the Higher Educational Institutions, Radiophysics], 2, 14, 1959.
 4. R.Q. Twiss. Phys. rev., 84, 448, 1951.
 5. L. Spittser, Fizika polnostyyu ionizirovannogo gaza [Physics of the Fully Ionized Gas], Izd-vo inostr. lit., M. [Foreign Literature Press], Moscow, 1957.
 6. B.N. Gershman, V.L. Ginzburg, Uch. zapiski GGU, ser. fizich. [Scientific Reports of the Gorkiy State University, Physics Series], 30, 6, 1956.
 7. A.I. Akhierzer, Ya.B. Feynberg, ZheTF, 21, 1262, 1951.
 8. V.L. Ginzburg, V.V. Zheleznyakov, Astronom. zh. [Astronomical Journal], 35, 694, 1958.
 9. Ya.L. Al'pert, V.L. Ginzburg, Ye.L. Feynberg, Rasprostraneniye radiovoln [Propagation of Radio Waves], GITTL [State Publishing for Technical and Theoretical Literature], Moscow, 1953.
 10. V.P. Dokuchaev, ZheTF, 39, 413, 1960.
 11. S.I. Syrovatskiy, Tr. fiz. instituta AN SSSR im. P.N. Lebedeva [Transactions of the Lebedev Physics Institute of the Academy of Sciences USSR], 8, 13, 1956.
 12. P. Debye, J. Daen. Phys. fluids, 2, 416, 1959.

Manu-
script
Page
No.

[Footnote]

294 This formula is a generalization of the formula which we have derived previously [10].

INTERACTION OF ION BEAM WITH MAGNETOACTIVE PLASMA*

N. L. Tsintsadze, D. G. Lominadze
Tbilisi

It was shown in several investigations that in the absence of a magnetic field the state of an unmodulated electron beam with homogeneous density and with constant velocity is unstable as the beam moves through a plasma.

When the plasma is in an external magnetic field, passage of a particle beam through it may be accompanied by new types of instabilities, one of which is connected with the anomalous Doppler effect and the other with the low-frequency oscillation of the plasma.

We consider in the article the excitation of electromagnetic waves in an unbounded plasma situated in a magnetic field \vec{H}_0 brought about by a nonrelativistic cylindrical particle beam of radius r_0 passing through the plasma parallel to the external magnetic field.

The system of equations describing the interaction between the charged beam and the plasma will be specified by means of the self-consistent Maxwell equations together with the linearized kinetic equations for the electrons and ions of the beam and of the plasma.

By integrating the kinetic equation over the trajectory of the charges under the assumption that the magnetic field is strong, we determine the dielectric tensor

$$\epsilon_{ij} = \begin{pmatrix} \epsilon & Ig & 0 \\ -Ig & \epsilon & 0 \\ 0 & 0 & \eta \end{pmatrix}.$$

Assuming that the components of the electromagnetic field are pro-

portional to $\exp[i(kz - \omega t)]$, and solving Maxwell's equations, we obtain all the field components. The continuity of the tangential components of the electric and magnetic fields on the surface separating the cylindrical beam from the plasma determine the boundary conditions, from which we obtain the dispersion relation. This complicated dispersion equation describes both the longitudinal and the transverse oscillations. In view of its complexity, we consider only transverse oscillations, carrying out expansion in powers of $1/\eta$ in the frequency region $\omega \leq \omega_{H1} = eH/mc$. The resultant dispersion equation will be investigated for broad and narrow ion beams.

We first consider the cyclotron mechanism of wave excitation in a plasma with the aid of ion beams. If u is the velocity of the beam along the magnetic field, then, as a result of the anomalous Doppler effect, the frequency is given by $\omega = ku - \omega_H = \omega_H(u/V - 1)^{-1}$, where $V = \omega/k$ is the phase velocity of the waves. Neglecting the thermal motion in either beam or plasma for broad ion beams, we obtain the wave buildup increment

$$\nu = i \frac{u-V}{V} \Omega \left[1 + \frac{c^2}{2uV} \frac{(u-V)^2}{V_{A1}^2} + \frac{c^2}{4V^2} \frac{u-V}{\omega_H r_0} \right], \quad (1)$$

where $V_{A1} = H/\sqrt{4\pi m_1 n_1}$ is the Alfvén velocity of the plasma ions, and $\Omega = 4\pi n e^2/m$ is the Langmuir frequency of the beam ions.

The corresponding cases for narrow ion beams have the form

$$\frac{\nu}{\Omega} = i \frac{V}{2c} \left[\frac{\frac{\omega_H^2}{V_{A1}^2(u-V)} + \frac{a_n^2}{2V_{A1}^2}}{\frac{a_n^2}{V_{A1}^2} - \frac{\omega_H^2 V^3}{2V_{A1}^4 u^2}} \right]^{\frac{1}{2}} \quad (2)$$

$$r_0 < \sqrt{2} a_n \frac{u}{\omega_H} \left(\frac{V_{A1}}{V} \right)^3,$$

where a_n is the root of the Bessel function $J_0(xr_0) = 0$.

As follows from (1) and (2), waves are excited if $u > V$, the beam velocity exceeds the wave phase velocity.

For broad beams, taking into account the thermal scatter of the particle velocities in the beam and the low density of the particles, the oscillation buildup increment is

$$\nu = i \frac{\sqrt{\pi}}{4} \frac{u - V}{S} \frac{\Omega^2}{\Omega_i^2} \omega_H \left[1 - \frac{2(u - V)}{V^2} - \frac{V_A^2}{(u - V)V} \right]^{-1}. \quad (3)$$

where S is the thermal velocity of the beam ions, Ω_i is the Langmuir frequency of the plasma ions.

Analogously we have for narrow beams:

$$\nu = i \frac{\sqrt{\pi}}{4} \frac{\Omega^2}{\Omega_i^2} \frac{u - V}{S} \omega_H \left[1 + \frac{c^2(u - V)^2}{V^4} - \frac{c^2(u - V)(u - c)^2}{V^2(\Omega_f c)^2} \right]. \quad (4)$$

We conclude that oscillations are excited in the plasma in Case (3) when $u > V$ and $V \gg V_{A_1}$, and in Case (4) when $u > V$ and $r_0 > > (a_n c / \Omega_i) \sqrt{V/(u - V)}$.

This was followed by an investigation of the excitation of magnetohydrodynamic waves ($\omega \ll \omega_{H_1}$) with the aid of ion beams.

We determine the frequency for an interaction between a broad ion beam and a plasma (both cold) by assuming that the beam density is much smaller than the plasma density, $n \ll n_1$, $\Omega_i/k^2 r^2 \gg \omega_{n_1}^2/\omega^2 \gg 1$, and $\Omega^2/k^2 r^2 \gg 1$,

$$\omega \approx i\Omega \frac{V_A}{c} \left\{ 1 - \frac{i}{2kr_0} \sqrt{\frac{n}{n_1}} u^2 \right\}^{\frac{1}{2}}. \quad (5)$$

and for a narrow beam the imaginary part of the buildup increment is

$$Im\nu = \frac{\Omega^2}{c^2} \frac{V_A(u - V)}{\omega_H} \left(\frac{kr_0}{a_n} \right). \quad (6)$$

Wave excitation occurs for (5) when $u > V_A$ and in the case (6) when $u > V = V_A a_n / kr_0$.

We have also considered other cases of interaction between ion beams and a plasma; we conclude from all this that the excitation of certain waves is directly connected with the beam radius.

Manu-
script
Page
No.

[Footnote]

298

The article was published in "ZHTF," XXXI, 1039, 1961, where the question is examined in greater detail.

MAGNETOHYDRODYNAMIC EQUATIONS FOR A NONISOTHERMAL
COLLISION-FREE PLASMA

Yu. L. Klimontovich, V. P. Silin
Moscow

In spite of the large number of investigations devoted to the derivation of the magnetohydrodynamic equations for a plasma without collisions, the analysis of this question can nevertheless not be regarded as complete.

One of the main researches on this question is that by Chew, Goldberger, and Low [1]. Its results were the basis for many subsequent investigations devoted to magnetohydrodynamic theory of plasma.

It must be noted, however, that the main premise of this work, namely that the electric field is perpendicular to the magnetic induction in a collision-free plasma, is not satisfied, as will be shown below. This leads, in particular, to the violation of the adiabatic equation of Reference [1]. Only a correct allowance for the longitudinal field arising in the plasma (which was not made in [1]) leads to the correct spectrum of the magnetohydrodynamic waves in the plasma.

It must finally be noted that the magnetohydrodynamic equations obtained in [1] do not take account of dissipative processes. However, as will be shown below, even under the conditions when the collisions in the plasma are not significant, the magnetohydrodynamic equations contain dissipative terms due to the absorption of the arising magnetic sound waves by the electrons.

In the present article we consider the magnetohydrodynamic equa-

tions only for the case of a strongly nonisothermal plasma.

Correct estimates of the conditions under which the magnetohydrodynamic description is applicable for such a case are contained, for example, in the paper by S.I. Braginskii [2]. However, for example to investigate the spectrum and damping decrement of magnetic sound waves in a plasma, or to consider the question of the possibility of the existence of shock waves in a plasma, it is necessary to use the complete system of magnetohydrodynamic equations for a plasma with inclusion of the dissipative terms.

In a strongly nonisothermal plasma it is possible in many cases to neglect the thermal motion of the ions. Then, in the absence of collisions, the ion motion can be described by the continuity equation

$$\frac{\partial \rho}{\partial t} + \operatorname{div} \rho \vec{V} = 0 \quad (1)$$

and by Newton's equation

$$\rho \frac{d\vec{V}}{dt} = \frac{\partial \vec{V}}{\partial t} + \rho \left(\vec{V} \frac{\partial \vec{V}}{\partial r} \right) = q_i \left\{ \vec{E} + \frac{1}{c} [\vec{V} \vec{B}] \right\}. \quad (2)$$

Here ρ is the mass density, q_i the ion charge density, $\vec{V}(\vec{r}, t)$ the ion velocity, \vec{E} and \vec{B} the electric and magnetic field intensities.

To describe the motion of the electrons in a nonisothermal plasma, it is necessary to use the kinetic equation with self-consistent field

$$\frac{df}{dt} + \vec{v} \frac{\partial f}{\partial \vec{r}} + e \left\{ \vec{E} + \frac{1}{c} [\vec{v} \vec{B}] \right\} \frac{\partial f}{\partial p} = 0. \quad (3)$$

For frequencies ω that are small compared with the Larmor ion frequency (in a coordinate system bound to the ions), we obtain from Eq. (2), neglecting terms of second order of smallness,

$$\vec{E} = -\frac{1}{c} [\vec{V} \vec{B}] \quad (4)$$

Substituting this expression for \vec{E} into the field equation $\operatorname{rot} \vec{E} = -(1/c) \partial \vec{B} / \partial t$, we get

$$\frac{\partial \vec{B}}{\partial t} = \text{rot}[\vec{V}\vec{B}] \quad (5)$$

Equation (5) is indeed included in the system of magnetohydrodynamic equations for a plasma. Neglect of the collisions causes the conductivity to be infinite. The second equation has the form

$$\text{div } \vec{B} = 0. \quad (6)$$

If the Langmuir frequency of the ions is much larger than the considered frequency ω , then we can neglect the displacement current in the field equations, which assume the following form:

$$\vec{j} = (c/4\pi) \text{rot} \vec{B}, \quad q = 0. \quad (7)$$

Here $\vec{J} = q_1 \vec{V} + e \int \vec{v} f dp$ is the current density and $q = q_1 + e \int f dp$ is the plasma charge density.

To obtain a closed system of magnetohydrodynamic equations it is necessary, using Eqs. (3, 7), to determine the electric field in terms of the electron characteristics and to eliminate the field from Eq. (2).

We shall do this first without account of the dissipative processes. If the characteristic magnetohydrodynamic velocities are much smaller than the electron thermal velocities $\sqrt{kT/m}$, then we can neglect the term $\partial f / \partial t$ in the kinetic equation for the electrons (3) when we derive the hydrodynamic equations without the dissipative terms. This means that a stationary distribution can always be established for the electrons.

We denote by $\varphi(\vec{r}, t)$ the electric potential, and by $\vec{V}_e = \vec{J}_e/q_e$ the electron drift velocity, and attempt to satisfy Eq. (3) by means of a solution in the form

$$f = F \left(e\varphi(\vec{r}, t) + \frac{m(\vec{v} - \vec{V}_e)^2}{2} \right). \quad (8)$$

Here F is an arbitrary function. As a particular case, for example, the function f is a Maxwell-Boltzmann distribution.

Let us find an expression for \vec{E} as a function of ρ , T , \vec{V}_e , \vec{B} , for

which Expression (8) satisfies Eq. (3). For this purpose we multiply Eq. (3) with $\partial f / \partial t = 0$ by \vec{v} and integrate over the momenta. As a result we obtain a transport equation for the electron momentum density

$$\frac{\partial}{\partial r_i} \int v_i v_j d\mu = q_e \left(E_s + \frac{1}{c} [V_e B]_s \right). \quad (9)$$

Using Expression (8) we obtain

$$\int v_i v_j d\mu = \frac{q_e}{e} \left(V_{es} V_{ej} + \frac{xT}{m} \delta_{ij} \right). \quad (10)$$

Here

$$q_e = e \int d\mu = e \rho_e, \quad \frac{q_e xT}{m} = \frac{1}{3} \int (v - V_e)^2 d\mu.$$

Substituting Expression (10) in Eq. (9) and using the continuity equation, we obtain

$$\rho_e m V_{es} \frac{\partial V_{es}}{\partial r_i} + \frac{\partial x T \rho_e}{\partial r_i} = q_e \left(E_s + \frac{1}{c} [V_e B]_s \right). \quad (11)$$

Comparing (11) with (2) we see that in calculating the electric field intensity E we can neglect the first term in (11), owing to the smallness of the mass ratio m/M . As a result we obtain the sought expression for E

$$q_e E = \frac{\partial}{\partial r} (x T \rho_e) - \frac{q_e}{c} [V_e B]. \quad (12)$$

Substituting this expression in (2) and recognizing that in accordance with (7) $\rho_e = |e_1/e| \rho$ and $j = q_1 V + q_e V_e$, we obtain the magnetohydrodynamic equations of motion without account of the dissipative processes:

$$\frac{\partial V}{\partial t} + \left(V \frac{\partial}{\partial r} \right) V = - \frac{\sigma^2}{\rho} \frac{\partial \rho}{\partial r} + \frac{1}{4\pi\rho} [\text{rot } B, B]. \quad (13)$$

Here $v_s = \sqrt{|e_1/e| \kappa T / M}$ is the velocity of sound in the plasma ($T = \text{const}$). Equations (1, 13, 5, 6) do indeed form a closed system of magnetohydrodynamic equations. This system coincides with the corresponding system of equations for an ideal liquid, if the pressure is written in the form $p = v_s^2 \rho$.

If dissipative processes are included, a supplementary term $(1/\rho)F^{(\text{diss})}$ appears in Eq. (13), where $F^{(\text{diss})}$ is the force due to the radiation of magnetic sound waves. The expression for $F^{(\text{diss})}$ is obtained by solving the kinetic equation for the electrons (of course, with allowance also for the term $\partial f/\partial t$), and has the following form:

$$F_e^{(\text{diss})} = \frac{\rho_0 v_s^2}{B_0^2} \left\{ \left[B_{0z} \left(B_0 \frac{\partial}{\partial r} \right) + \left[B_0 \left[B_0 \frac{\partial}{\partial r} \right] \right]_e \right] \frac{1}{B_0^2} \left(B_0 \frac{\partial}{\partial r} \right) B_{0y} - \left[B_0 \left[B_0 \frac{\partial}{\partial r} \right] \right]_e \frac{\partial}{\partial r_y} \right\} \int Q(r-r') V_y(r',t) dr'. \quad (14)$$

Here B_0 is the external constant field, ρ_0 is the average density,

$$Q(r) = \frac{1}{(2\pi)^3} \int e^{i k r} \tau(k) dk.$$

$$\tau(k) = \int_0^\infty \exp \left\{ - \frac{\pi T}{2m} \left(\frac{k B_0}{B_0} \right)^2 i^2 - i \omega t \right\} dt \approx \sqrt{\frac{\pi m}{2\pi T}} \frac{B_0}{|k B_0|}. \quad (15)$$

It follows from (14) that the dissipative force is proportional to the square root of the electron temperature and to $\sqrt{m/M}$. It is important to note also that the dissipative force has in this case an essentially nonhydrodynamic form. Indeed, in the given case we arrive at an integral equation, because of the nonlocal character of the forces brought about by the absorption of magnetic sound waves.

The equations obtained were used for the analysis of the question of the spreading of a wave packet in a plasma. In the case under consideration, the spreading follows a linear law (the width of the packet is proportional to the time). The rate of spreading is $\gamma v/kv_s$, where v_\pm is the phase velocity of the magnetic sound waves:

$$v_\pm^2 = \frac{1}{2} \{ v_s^2 + v_A^2 \pm \sqrt{(v_s^2 + v_A^2)^2 - 4v_A^2 v_s^2 \cos^2 \alpha} \}, \quad v_A^2 = B_0^2 / 4\pi \rho_0,$$

and

$$\gamma_\pm = \frac{1}{4} \sqrt{\frac{\pi}{2}} \sqrt{\frac{e}{m}} v_A k \left\{ 1 \pm \frac{(\cos 2\alpha - \gamma) \cos 2\alpha}{\sqrt{1 + \gamma^2 - 2\gamma \cos \alpha}} \right\} \frac{1}{|\cos \alpha|}; \quad \gamma = \left(\frac{v_A}{v_s} \right)^2$$

is the damping decrement of the magnetic sound waves. The expressions

for v_{\pm}^2 and γ_{\pm} coincide with those obtained in [3].

On the basis of the system of hydrodynamic equations obtained, we investigated also the possibility of existence of stationary shock waves in a plasma. We first give here the corresponding formulas for the case when the magnetic field is equal to zero.

In this case the equation of motion assumes the form

$$\frac{\partial V}{\partial t} + \left(V \frac{\partial}{\partial r} \right) V = - \frac{v_i^2}{\rho} \frac{\partial \rho}{\partial r} + v_i^2 \frac{\partial}{\partial r} \int Q_0(r-r') \operatorname{div} V(r',t) dr'. \quad (16)$$

The kernel Q_0 differs from Q in that $|kB_0|/B_0$ is replaced by $|k|$. This equation together with the continuity equation comprises a closed system of hydrodynamic equations for the plasma with account of the dissipative processes when $B_0 = 0$. The kernel Q (or Q_0 in the absence of a magnetic field) decreases slowly with increasing r . This is connected with the fact that $\tau(k)$ has a singularity at $k = 0$. The appearance of this singularity is connected with the fact that in the case which we are considering the characteristic dimensions of the spatial inhomogeneities are assumed to be small compared with the mean free path.

For distances r that are comparable with or greater than the mean free path l , we must use in place of the given expression for Q_0 the expression

$$Q_0(r) = \frac{1}{(2\pi)^{3/2}} \sqrt{\frac{m}{\pi T}} \frac{d}{dr} K_0(r/l).$$

Here $l = \sqrt{2/\pi T}$; K_0 is the Macdonald function.

For the one-dimensional case, when V depends not on the coordinates y and z but only on x and t , the kernel $Q(r)$ must be integrated with respect to y and z . In this case we obtain in place of the expression for $Q(r)$

$$\bar{Q}(x) = \sqrt{\frac{m}{2\pi T |B_{0x}|}} \frac{B_0}{|B_{0x}|} K_0\left(\frac{x}{l} \frac{|B_0|}{|B_{0x}|}\right).$$

In the absence of a magnetic field we must replace $B_0/|B_{0x}|$ in this

expression by unity.

To investigate the possibility of the existence of shock waves, it is sufficient to consider Eqs. (1, 16) for the one-dimensional case. We introduce a coordinate frame fixed on the discontinuity surface and direct the x axis perpendicular to this surface. Using Eqs. (1, 2, 16) we obtain the conditions for the continuity of the matter flux and momentum flux of the discontinuity surface. Putting $\rho V = j_0$ and eliminating ρ from these continuity conditions, we write down the continuity condition for the momentum density flux in the form of an integral equation

$$\left(V + \frac{v_s^2}{V}\right)j_0 - \frac{a}{\sqrt{\pi}} v_s \rho_0 \int_{-\infty}^{+\infty} K_0\left(\frac{|x-x'|}{l}\right) \frac{dV(x')}{dx'} dx' = C. \quad (17)$$

where $a = \sqrt{mv_s^2/2kT}$.

We introduce a new constant V^- and write C in the form $V^- + v_s^2/V^-$. In this case the integral equation (17) assumes the form

$$(V - V^-) + v_s^2 \left(\frac{1}{V} - \frac{1}{V^-} \right) = \frac{a}{\sqrt{\pi}} v_s \rho_0 \int_{-\infty}^{+\infty} K_0\left(\frac{|x-x'|}{l}\right) \frac{dV(x')}{dx'} dx'. \quad (18)$$

Equation (18) is satisfied by definite constant values of the velocity V . To determine these constant values we obtain from (18) the equation

$$V - V^- + v_s^2 \left(\frac{1}{V} - \frac{1}{V^-} \right) = 0; \quad (19)$$

from which follow two constant values for V , namely $V = V^+$, $V = v_s^2/V^- \equiv V^-$. Both values coincide only if $V^- = v_s$.

To answer the question of whether shock waves exist in a plasma we must consider the possibility of a solution of Eq. (18) such that it assumes values V^+ and V^- , where $V^+ \neq V^-$, as $x \rightarrow \pm\infty$.

It follows from (18) that such a solution of the equation exists when the transition from V^- to V^+ is such that $V(x)$ changes little over distances on the order of the mean free path. Indeed, we can take

dV/dx in this case outside the integral sign, and the integral equation reduces in first approximation to the following differential equation

$$(V - V^-) + v_s^2 \left(\frac{1}{V} - \frac{1}{V^-} \right) = al \sqrt{\frac{\sigma \rho_0}{f_0}} \frac{dv}{dx}. \quad (20)$$

It is well known that Eq. (20) has a solution which assumes the values V^+ and V^- when $x \rightarrow \pm\infty$. In this case we must have $V^- > v_s$, $v_s > V^+$ in order for the solution to be stable. The width of the transition region is determined by the mean free path. In the approximation employed by us, this case is analogous to that considered in ordinary gasdynamics.

It follows from (18) that the plasma cannot support a stationary shock wave in which the transition from V^- to V^+ occurs over distances much shorter than the mean free path, i.e., under conditions when collisions can be neglected.

Indeed, in this case, if we assume that the transition from V^- to V^+ occurs near x_0 , Eq. (18) can be approximately written in the form

$$(V - V^-) + v_s^2 \left(\frac{1}{V} - \frac{1}{V^-} \right) = (V^- - V^+) \frac{\alpha \sigma \rho_0}{\sqrt{\pi f_0}} K_0 \left(\left| \frac{x - x_0}{l} \right| \right). \quad (21)$$

Since the right half differs from zero also when $x - x_0 \sim l$, it follows therefore that the assumption made in the derivation of Eq. (21) is not corroborated.

Thus, no stationary shock waves with width smaller than the mean free path exist in the plasma.

In the presence of a magnetic field, the corresponding integral equations will contain integral terms of the same type. Therefore in this case there are likewise no solutions describing stationary shock waves in the plasma, with width much smaller than the mean free path.

Let us note again the conditions under which the derived magneto-hydrodynamic equations are valid:

- 1) the mean free path is assumed to be infinitely large;

- 2) the plasma is strongly nonisothermal. The ion thermal velocity is equal to zero;
- 3) noticeable changes in the functions ρ , V , and B occur over distances that greatly exceed the Debye radius, the Larmor radius, and the length c/ω_L .

REFERENCES

1. G. Chew, M. Goldberger, F. Low. Proc. Roy. Soc., A236, 112, 1956.
2. S.I. Braginskiy, Voprosy magnitnoy gidrodinamiki i dinamiki plazmy [Problems of Magnetohydrodynamics and Plasma Dynamics], Riga, 1959.
3. K.N. Stepanov, Ukrainskiy fizicheskiy zhurnal [Ukrainian Physics Journal], 4, 5, 678, 1959.

INSTABILITY OF A SYSTEM OF TWO ELECTRON BEAMS
IN A MAGNETIC FIELD

V.N. Rutkevich
Khar'kov

1. INTRODUCTION

Two electron beams which move with different velocities represent under certain conditions an unstable system. The energy of translational motion of such beams changes over into the energy of oscillations that propagate along the system. The instability against longitudinal oscillations (space charge waves) has been well investigated and is used to amplify microwave frequencies in traveling wave tubes. It manifests itself in "pure form" either in the case of large transverse electron beam dimensions, when the edge effects are not significant and the motion is sufficiently completely described within the framework of the one-dimensional problem, or else in the case of a strong magnetic field, when the electrons move only along the magnetic force lines.

In other cases the transverse motion of the electrons can play an essential and even the principal role [1, 2] and must be taken into consideration in the analysis of the question of stability of a system of electron beams.

Allowance for the transverse motions is the main task of the present paper. It will be shown that a system of two beams can lose its stability not only because of space charge waves, but also because of interaction between transverse oscillations that are due to cyclotron

rotation of the electrons in the magnetic field (cyclotron waves [2]).

For simplicity we consider hollow coaxial beams (Fig. 1), thin enough to make the distribution of the fields over the thickness of the beam to assume a negligible role. In this case the electron layer is merely a surface on which the normal component of the electric field experiences a discontinuity equal to $4\pi\sigma$, where σ is the surface charge density. In addition, it is assumed that the phase velocity (v_p) of the waves propagating in the beam is small compared with the velocity of light, so that quantities of the order of v_p/c can be disregarded.

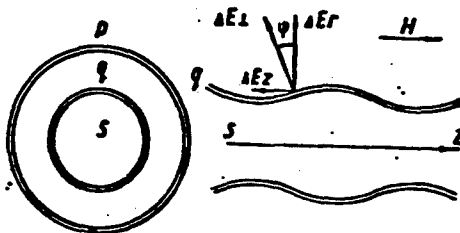


Fig. 1

2. FUNDAMENTAL EQUATIONS

Let us set up the equations that characterize the motion of the internal beam; the formulas for the external beam are similar.

We assume that the effect of the Coulomb forces is balanced by the magnetic forces, so that the distance from the electrons to the axis remains in the main unchanged. We superimpose on the equilibrium motion a small perturbation of velocity and of the charge surface density, symmetrical with respect to the z axis and propagating along the z axis in the form of a wave $e^{i(\omega t - \gamma z)}$.

The radial motion of the electrons causes the beam to become slightly corrugated. Denoting the inclination of the electron layer to the z axis by the letter ψ_1 (see Fig. 1), we have

$$\operatorname{tg} \psi_1 = \frac{\partial r_1}{\partial z} = - k_1 r_{1\sim}, \quad (1)$$

where $r_{1\sim}$ denotes a small deviation of the radius from the equilibrium value.

By virtue of the relations

$$v_{1r\sim} = \frac{dr_{1\sim}}{dt} = \frac{\partial r_{1\sim}}{\partial t} + v_1 \frac{\partial r_{1\sim}}{\partial z} = i\Omega_1 r_{1\sim}, \quad (2)$$

where

$$\Omega_1 = \omega - \gamma v_1, \quad (3)$$

v_1 is the mean velocity of motion of the electrons of the internal beam along the z axis and $v_{1r\sim}$ is the velocity of the radial motion of the electron, Eq. (1) can be rewritten in the form

$$\operatorname{tg} \psi_1 = - \frac{1}{\Omega_1} v_{1r\sim}. \quad (4)$$

The radial and axial components of the electric field experience on the electron layer discontinuities equal to $4\pi\sigma_1 \cos \psi_1$ and $4\pi\sigma_1 \sin \psi_1$, respectively. Therefore, denoting by E_s and E_q the variable components of the electric field in the regions s and q (see Fig. 1), and putting $\sigma = \sigma_1 + \sigma_{1\sim}$, we can write in the linear approximation

$$E_s(r_1) - E_s(r_1) = 4\pi\sigma_{1\sim}. \quad (5)$$

$$E_q(r_1) - E_q(r_1) = - \frac{4\pi\sigma_1}{\Omega_1} v_{1r\sim}. \quad (6)$$

The field acting on the electrons of the layer (1) will be assumed equal to the arithmetic mean of the fields on both surfaces of the layer:

$$\vec{E}_1 = \frac{1}{2} [\vec{E}_s(r_1) + \vec{E}_q(r_1)]. \quad (7)$$

As is well known [3], the motion of a particle in an axially symmetrical system can be treated as motion in the plane (r, z) with potential

$$\Phi = \frac{(p_\theta - \frac{e}{c} r A_\theta)^2}{2mr^2} + e\varphi. \quad (8)$$

where $p_\theta = mr^2\dot{\theta} + erA_\theta/c$ is the generalized momentum, which is a constant of the particle motion in the axially symmetrical system, A_θ is the azimuthal component of the vector potential, which in this case is equal to $rH/2$, and φ is the potential of the electric field. The motion of the particle in the (r, z) plane is represented by the equations

$$\frac{d^2z}{dt^2} = \frac{e}{m} E_r \quad (9)$$

$$\frac{dr}{dt} = \frac{1}{mr^2} \left[\frac{p_\theta^2}{r^2} - m \frac{\omega_H^2}{4} r^2 \right] + \frac{e}{m} E_r \quad (10)$$

where $\omega_H = eH/mc$ is the cyclotron frequency in the field H . Putting $r = r_1 + r_{1\sim}$ and using Relations (2), we obtain for the oscillatory velocity components the following equations

$$\frac{\partial v_{1z\sim}}{\partial t} + v_1 \frac{\partial v_{1z\sim}}{\partial z} = \frac{e}{m} E_{1z} \quad (11)$$

$$\frac{\partial v_{1r\sim}}{\partial t} + v_1 \frac{\partial v_{1r\sim}}{\partial z} + \frac{\omega_H^2}{i\Omega_1} v_{1r\sim} = \frac{e}{m} E_{1r} \quad (12)$$

We furthermore obtain from the equation for the conservation of the number of particles in the beam

$$\frac{\partial}{\partial t} (2\pi\sigma) + \frac{\partial}{\partial z} (2\pi\sigma v_z) = 0, \quad (13)$$

and in the linear approximation we get

$$\frac{\partial \sigma_{1\sim}}{\partial t} + v_1 \frac{\partial \sigma_{1\sim}}{\partial z} + \sigma_1 \frac{\partial v_{1z\sim}}{\partial z} + \sigma_1 \frac{v_{1z\sim}}{r_1} = 0. \quad (14)$$

Analogous equations can be set up for the external beam:

$$E_{px}(r_2) - E_{px}(r_1) = 4\pi\sigma_{2\sim}, \quad (15)$$

$$E_{pz}(r_2) - E_{pz}(r_1) = -\frac{4\pi\sigma_2}{\Omega_2} v_{2z\sim}, \quad (16)$$

$$\vec{E}_2 = \frac{1}{2} [\vec{E}_p(r_2) + \vec{E}_q(r_2)], \quad (17)$$

$$\frac{\partial v_{2z\sim}}{\partial t} + v_2 \frac{\partial v_{2z\sim}}{\partial z} = \frac{e}{m} E_{2z} \quad (18)$$

$$\frac{\partial v_{2r\sim}}{\partial t} + v_2 \frac{\partial v_{2r\sim}}{\partial z} + \frac{\omega_H^2}{i\Omega_2} v_{2r\sim} = \frac{e}{m} E_{2r} \quad (19)$$

$$\frac{\partial \sigma_{2\sim}}{\partial t} + v_2 \frac{\partial \sigma_{2\sim}}{\partial z} + \sigma_2 \frac{\partial v_{2z\sim}}{\partial z} + \frac{\sigma_2 v_{2z\sim}}{r_2} = 0. \quad (20)$$

3. DISPERSION RELATION

Eliminating the variable components of the velocities and of the charged surface densities, we obtain equations for the fields on the electron layers

$$E_{\nu}(r_1) - E_{\mu}(r_1) = Q_{11}[E_{\nu}(r_1) + E_{\mu}(r_1)] - iQ_{11}[E_{\nu}(r_1) + E_{\mu}(r_1)], \quad (21)$$

$$E_{\nu}(r_1) - E_{\mu}(r_1) = iQ_{11}\gamma r_1[E_{\nu}(r_1) + E_{\mu}(r_1)], \quad (22)$$

$$E_{\nu}(r_2) - E_{\mu}(r_2) = Q_{12}[E_{\nu}(r_2) + E_{\mu}(r_2)] - iQ_{12}[E_{\nu}(r_2) + E_{\mu}(r_2)], \quad (23)$$

$$E_{\mu}(r_2) - E_{\nu}(r_2) = i\gamma r_2 Q_{12}[E_{\nu}(r_2) - E_{\mu}(r_2)]. \quad (24)$$

We use here the notation

$$Q_{11} = \frac{\omega_1^2}{2(\Omega_1^2 - \omega_H^2)}, \quad (25)$$

$$Q_{12} = \frac{\omega_1^2 \gamma r_1}{2\Omega_1^2}, \quad (26)$$

$$Q_{22} = \frac{\omega_2^2}{2(\Omega_2^2 - \omega_H^2)}, \quad (27)$$

$$Q_{21} = \frac{\omega_2^2 \gamma r_2}{2\Omega_2^2}, \quad (28)$$

$$\omega_1^2 = \frac{4\pi e\sigma_1}{mr_1}, \quad (29)$$

$$\omega_2^2 = \frac{4\pi e\sigma_2}{mr_2}. \quad (30)$$

The electric fields in regions s, g, and p must satisfy the Laplace equation. It is obvious that in the case of slow waves ($\gamma > \omega/c$) the dependence of the potential ϕ_{∞} on the radius will be represented by linear combinations of modified Bessel functions:

$$\varphi_{\infty} = A I_0(\gamma r) + B K_0(\gamma r), \quad (31)$$

$$\varphi_{\infty} = C I_0(\gamma r) + D K_0(\gamma r), \quad (32)$$

$$\varphi_{\infty} = E I_0(\gamma r) + F K_0(\gamma r). \quad (33)$$

From the requirement that the fields be bounded on the system axis and at a considerable distance from the axis, we find that the coefficients

B and E must vanish. The remaining four coefficients are determined from the four equations (21-24), which represent the boundary conditions on the electron layers. The problem reduces to a system of homogeneous equations for A, C, D, and F.

Equating the system determinant to zero, we obtain the dispersion relation for the oscillations under consideration:

$$\begin{aligned}
 & 4 \frac{-I_1(\gamma r_1) I_0(\gamma r_1) Q_{11} +}{-\frac{1}{\gamma r_1} + Q_{11} I_0(\gamma r_1) K_1(\gamma r_1) - I_1(\gamma r_1) K_0(\gamma r_1)} + \\
 & \rightarrow \frac{+ I_0^2(\gamma r_1) Q_{11} - \gamma r_1 Q_{11} I_1^2(\gamma r_1)}{+ 2\gamma r_1 Q_{11} K_1(\gamma r_1) I_1(\gamma r_1) + 2Q_{11} K_0(\gamma r_1) I_0(\gamma r_1) - Q_{11} Q_{11}} = \\
 & = \frac{-\frac{1}{\gamma r_2} + Q_{12} I_0(\gamma r_2) K_1(\gamma r_2) - I_1(\gamma r_2) K_0(\gamma r_2)}{K_1(\gamma r_2) K_0(\gamma r_2) Q_{12}} + \\
 & \rightarrow \frac{2Q_{12} K_0(\gamma r_2) I_0(\gamma r_2) + 2\gamma r_2 Q_{12} I_1(\gamma r_2) K_1(\gamma r_2) - Q_{12} Q_{11}}{+ Q_{12} K_0^2(\gamma r_2) - \gamma r_2 Q_{12} K_1^2(\gamma r_2)}. \quad (34)
 \end{aligned}$$

4. CASE OF SMALL WAVELENGTH

In the general case the motion is quite complicated. However, under certain conditions it can be resolved into longitudinal and transverse oscillations in the first and second beams, after which the motion pattern becomes immediately clear.

We can consider the "partial" oscillations separately, and then take into account the connection between them and investigate the oscillations of the coupled systems. We shall be interested here in the appearance of growing solutions.

A weak coupling between oscillations of different types can be ensured by the following conditions:

$$\gamma r_1 \gg 1, \quad (35)$$

$$\gamma r_2 \gg 1, \quad (36)$$

$$\gamma(r_2 - r_1) \gg 1. \quad (37)$$

They are equivalent to requiring that the wavelengths in the beams be small compared with the differences in the radii of the first and sec-

ond beam. Using the asymptotic expressions for Bessel functions of large arguments, we now write down the dispersion equation (34) in the form

$$\left[(1 - \gamma r_1 Q_{11}) (1 - Q_{21}) - \frac{Q_{11}}{2\gamma r_1} \right] \left[(1 - \gamma r_2 Q_{12}) (1 - Q_{22}) - \frac{Q_{12}}{2\gamma r_2} \right] = a (Q_{21} - \gamma r_1 Q_{11}) (Q_{22} - \gamma r_2 Q_{12}), \quad (38)$$

where

$$a = e^{-2\gamma(r_2 - r_1)}. \quad (39)$$

In the limiting case of weak coupling, a vanishes and Eq. (38) breaks up into two independent dispersion relations for the waves in the first and second beams. Let us consider one of these equations

$$(1 - Q_{21}) (1 - \gamma r_1 Q_{11}) = \frac{Q_{11}}{2\gamma r_1}. \quad (40)$$

If its right half is small ($\gamma r_1 \gg 1$), it also breaks up into two independent equations

$$1 - Q_{21} = 0 \quad (41)$$

and

$$1 - \gamma r_1 Q_{11} = 0 \quad (42)$$

or

$$(\omega - \gamma v_1)^2 - \frac{\omega_1^2 r_1}{2} = 0 \quad (43)$$

and

$$(\omega - \gamma v_1)^2 - \omega_H^2 - \frac{\gamma r_1 \omega_1^2}{2} = 0. \quad (44)$$

Equation (43) pertains to space charge oscillations, while (44) pertains to cyclotron waves connected with the cyclotron rotation of the electrons. From these equations it follows that

$$\gamma_{1,2} = \frac{\omega}{v_1} + \frac{\omega_1^2 r_1}{2v_1^2} \pm \sqrt{\frac{\omega \omega_1^2 r_1}{v_1^3} + \frac{\omega_1^4 r_1^2}{4v_1^4}} \quad (45)$$

and

$$\gamma_{1,4} = \frac{\omega}{v_1} + \frac{\omega_1^2 r_1}{2v_1^2} \pm \sqrt{\frac{\omega \omega_1^2 r_1}{v_1^3} + \frac{\omega_1^4 r_1^2}{4v_1^4} + \frac{\omega_H^2}{v_1^2}}. \quad (46)$$

We see that the propagation constants are always real, therefore, as expected, the beams are stable against these oscillations.

An account of the coupling between the space charge waves and the cyclotron waves in one and the same beam likewise fails to lead to growing solutions.

Going over to the coupling between oscillations in different beams, let us retain in Eq. (38) the term with α , and let us leave out in the square brackets the small terms that characterize the coupling between oscillations in one and the same beam. As a result, the dispersion relation assumes the simple form

$$\frac{\alpha(Q_{21} - \gamma r_1 Q_{11})(Q_{22} - \gamma r_2 Q_{12})}{(1 - \gamma r_1 Q_{11})(1 - Q_{21})(1 - \gamma r_2 Q_{12})(1 - Q_{22})} = 1. \quad (47)$$

In the case of small coupling, $\alpha \ll 1$ and the last equation is satisfied only when the denominator of the left half approaches zero.

The vanishing of any of the brackets, as we have seen, does not lead to growing solutions. Let us assume that two brackets pertaining to different beams approach zero simultaneously. This can correspond either to the well-known coupling between space charge waves in two beams, or the coupling of the cyclotron oscillations with each other, or finally to the coupling of space charge waves in one beam with cyclotron oscillations in the other beam. An analysis of all the foregoing cases can be carried out following a single plan.

We consider the last case.

We assume that the following equations are approximately satisfied

$$1 - Q_{21} = 0. \quad (48)$$

$$1 - \gamma r_2 Q_{12} = 0. \quad (49)$$

and that their roots are

$$\gamma_{12} = \frac{\omega}{v_i} + \frac{\omega^2 r_1}{2v_i^2} \pm \sqrt{\frac{\omega^2 r_1}{v_i^2} + \frac{\omega^2 r_1}{4v_i^2}} \quad (50)$$

and

$$\gamma_{2,j} = \frac{\omega}{v_2} + \frac{\omega^2 r_2}{2v_2^2} \pm \sqrt{\frac{\omega^2 r_2}{v_2^2} + \frac{\omega^4 r_2^2}{4v_2^4} + \frac{\omega^2}{v_2^2}}. \quad (51)$$

The first index assigns γ to the internal or to the external beam, while the indices i and j assume values 1 and 3 or 2 and 4, depending on whether the radical is taken with the plus or with the minus sign.

Dispersion Equation (47) becomes particularly simple if (48) and (49) are satisfied:

$$-\frac{a}{(1-Q_{21})(1-\gamma_{21}Q_{12})} = 1. \quad (52)$$

Its roots should differ little from the roots of Eqs. (48) and (49), and we can put

$$\gamma = \gamma_{11}(1+x_1a) = \gamma_{21}(1+x_2a), \quad (53)$$

where x_1 and x_2 are the coefficients in the expansion of γ in powers of the small parameter a .

Substituting (53) in (52) and eliminating x_2 , we obtain the following expression for x_1 :

$$ax_1^2 + x_1 \left[\left(1 - \frac{\gamma_{21}}{\gamma_{11}} \right) + 2aM \right] + M = 0, \quad (54)$$

where

$$M = \frac{\omega_1^2 \omega_2^2 r_1 r_2}{4 \left(2\Omega_1 v_1 + \frac{\omega_1^2 r_1}{2} \right) \left(2\Omega_2 v_2 + \frac{\omega_2^2 r_2}{2} \right)}. \quad (55)$$

An imaginary component appears in the expression for x_1 , and consequently in the expression for γ , if

$$\left(1 - \frac{\gamma_{21}}{\gamma_{11}} \right)^2 < 4aM \frac{\gamma_{21}}{\gamma_{11}}. \quad (56)$$

This inequality can be fulfilled only when M is positive, something that can be assured by choosing identical signs, either plus or minus, in Expressions (50) and (51), i.e., by choosing the indices ($i = 1$, $j = 3$) or ($i = 2$, $j = 4$) for the coupled oscillations.

Thus, if the equalities $\gamma_{11} = \gamma_{23}$ or $\gamma_{12} = \gamma_{24}$ are approximately

satisfied, instability sets in; the boundaries of the instability regions are determined by the equations

$$1 - \frac{\gamma_2}{\gamma_1} = \pm 2 \sqrt{aM \frac{\gamma_2}{\gamma_1}} \quad (57)$$

or

$$\frac{\gamma_2}{\gamma_1} = (\sqrt{1 + aM} \pm \sqrt{aM})^2. \quad (58)$$

Let us consider in greater detail the particular case, when the electrons of one of the beams are on the average at rest ($v_2 = 0$). These may be electrons of an annular plasma layer, so that we are dealing essentially with excitation of plasma oscillations by a beam. Along with the well-investigated mechanism of excitation of space charge density waves [4], another mechanism may also be in operation, connected with the transverse motion of the plasma layer electrons. Small oscillations of beam density give rise to in-phase cyclotron rotation of the plasma electrons, which in turn intensifies the space charge oscillations of the beam.

The equation of the cyclotron oscillations will in this case be

$$\omega^2 - \omega_H^2 - \frac{\gamma_2 \omega_2^2}{2} = 0 \quad (59)$$

and consequently

$$\gamma = \gamma_{2,4} = \frac{2(\omega^2 - \omega_H^2)}{r_2 \omega_2^2}. \quad (60)$$

The instability, as in the general case, occurs upon appearance of imaginary roots of Eq. (54), in which the quantity M is now equal to

$$M = \frac{\omega_1^2 r_1}{2 \left(2\Omega_1 v_1 + \frac{r_1 \omega_1^2}{2} \right)}. \quad (61)$$

The condition $M > 0$ determines the choice of $i = 2$, i.e., the choice of a minus sign in front of the radical in (50).

The boundaries of the instability region are given by Relation (58). The equation

$$\frac{2(\omega^2 - \omega_H^2)}{r_0 v_i^2} = \frac{\omega_1^2}{v_1^2} + \frac{\omega_1^2 r_1}{2v_1^2} - \sqrt{\frac{\omega_1^2 r_1}{v_1^2} + \frac{\omega_1^4 r_1^2}{4v_1^4}} \quad (62)$$

determines the frequency near which the oscillations will be taken into account; in the case of low charge densities, it is close to the cyclotron frequency ω_H .

5. CASE OF LARGE WAVELENGTH AND LOW DENSITY

We analyze in similar fashion the case when the wavelengths in the plasma are large compared with the radii of the beams:

$$r \ll 1. \quad (63)$$

The dispersion equation has in this case the form

$$\begin{aligned} & \left(-\frac{1}{r_1} + \frac{\omega_1^2}{2r_1(\Omega_1^2 - \omega_H^2)} + \frac{\omega_1^2 r_1 l_1}{\Omega_1^2} - \frac{\omega_1^2 r_1}{4\Omega_1^2 (\Omega_1^2 - \omega_H^2)} \right) \times \\ & \times \left(-\frac{1}{r_2} + \frac{\omega_2^2}{2r_2(\Omega_2^2 - \omega_H^2)} + \frac{\gamma r_2 \omega_2^2 l_2}{\Omega_2^2} - \frac{\omega_2^2 r_2}{4\Omega_2^2 (\Omega_2^2 - \omega_H^2)} \right) = \\ & = \left(\frac{\gamma r_1 \omega_1^2}{\Omega_1^2} - \frac{\gamma r_1 \omega_1^2}{2(\Omega_1^2 - \omega_H^2)} \right) \left(\frac{\omega_2^2 (l_2 - 1)}{\gamma r_2 (\Omega_2^2 - \omega_H^2)} + \frac{\omega_2^2 r_2^2 l_2^2}{\Omega_2^2} \right). \end{aligned} \quad (64)$$

where

$$l = \ln \frac{1.12}{\gamma}.$$

In order to consider the oscillations that are possible in one beam, we put $\omega_2 = 0$, and then (64) reduces to

$$-\frac{1}{r_1} + \frac{\omega_1^2}{2r_1^2(\Omega_1^2 - \omega_H^2)} + \frac{\omega_1^2 r_1 l_1}{\Omega_1^2} - \frac{\omega_1^2 r_1}{4\Omega_1^2 (\Omega_1^2 - \omega_H^2)} = 0. \quad (65)$$

Assuming the frequency ω_1 to be small, we can discard the last term in (65):

$$-\frac{1}{r_1} + \frac{\omega_1^2}{2r_1^2(\Omega_1^2 - \omega_H^2)} + \frac{\omega_1^2 r_1 l_1}{\Omega_1^2} = 0. \quad (66)$$

Because of the smallness of ω_1 , the roots of Eq. (66) will be close to the roots of the equations

$$\Omega_1^2 = 0 \quad (67)$$

and

$$\Omega_1^2 - \omega_H^2 = 0. \quad (68)$$

If (67) is approximately satisfied, we obtain from (66)

$$-\frac{1}{\gamma r_1} + \frac{\omega_1^2 r_1 l_1}{\Omega_1^2} = 0 \quad (69)$$

and

$$\gamma_{1,2} = \frac{\omega}{v_1 \pm \omega_1 r_1 \sqrt{l_1}}; \quad (70)$$

on the other hand, if (68) is approximately satisfied, we get

$$-\frac{1}{\gamma r_1} + \frac{\omega_1^2}{2\gamma r_1 (\Omega_1^2 - \omega_H^2)} = 0 \quad (71)$$

and

$$\gamma_{1,2} = \frac{\omega}{v_1} \pm \frac{1}{v_1} \sqrt{\omega_H^2 + \frac{\omega_1^2}{2}}. \quad (72)$$

We have obtained dispersion relations for the space charge waves and for the cyclotron waves in a single beam. Let us now take into account the coupling between them. In the dispersion relation (64) the coupling between the waves of the first beam is represented by a term with ω_1^4 , that in the second beam by a term with ω_2^4 , and the coupling between oscillations in the first and the second beam is represented by the right half of (64), which is proportional to $\omega_1^2 \omega_2^2$. At low charge densities, the coupling terms are significant only if two quantities of the form Ω^2 or $(\Omega^2 - \omega_H^2)$ vanish simultaneously. In other words, the coupling comes into play only when the propagation constants of the two waves approximately coincide (this follows also from the general theory of interacting waves, developed by J.R. Pierce [5] in 1954). The coupling between oscillations in one and the same beam cannot be appreciable, since Eqs. (68) and (69) cannot be satisfied simultaneously. The coupling between the space charge waves in two beams has been well investigated (traveling wave tubes with interacting electron beams). We shall consider the interaction between the space charge wave in the first (internal beam) and the cyclotron wave in the second beam. It is realized if one of the equations

$$\frac{\omega}{v_1 \pm \omega_1 r_1 l_1} = \frac{\omega}{v_2} \pm \frac{1}{v_2} \sqrt{\omega_H^2 + \frac{\omega_1^2}{2}},$$

is satisfied, i.e., when

$$\omega = \frac{\pm \sqrt{\omega_H^2 + \frac{\omega_1^2}{2}}}{\frac{v_2}{v_1} \pm \frac{\omega_1 r_1 v_2 \sqrt{l_1}}{v_1} - 1}. \quad (73)$$

If the external beam is stationary ($v_2 = 0$), Eq. (73) goes over into

$$\omega = \sqrt{\omega_H^2 + \frac{\omega_1^2}{2}}. \quad (74)$$

In order to find the boundaries of the instability region, let us return to Eq. (64) and put in it $v_2 = 0$. It has a solution that is simultaneously close to the roots of the equations $\Omega_1 = 0$ and $\Omega_2^2 - \omega_H^2 = 0$ in the form

$$\gamma = \frac{\omega v_1 + P r_1 \pm \sqrt{(\omega v_1 + P r_1)^2 - \omega^2(v_1^2 - \omega_1^2 r_1^2 l_1)}}{v_1^2 - \omega_1^2 r_1^2 l_1}, \quad (75)$$

where

$$P = \frac{r_1}{2r_2} \frac{\omega_1^2 \omega_2^2 (l_2 - 1)}{\omega^2 - \omega_H^2 - \frac{\omega_1^2}{2}}.$$

The instability region is determined by the equation

$$(\omega v_1 + P r_1)^2 < \omega^2(v_1^2 - \omega_1^2 r_1^2 l_1)$$

or

$$\frac{r_1^2}{4r_2} \frac{\omega_1^2 \omega_2^2}{\omega v_1} < \omega_H^2 - \omega^2 + \frac{\omega_1^2}{2} < \frac{l_2 - 1}{l_1} \frac{\omega_1^2 v_1}{\omega r_1}. \quad (76)$$

With decreasing charge density, the instability region contracts toward the frequency (74). Thus, the system comprising a beam and a plasma layer can support oscillations at a frequency close to cyclotron frequency.

In conclusion, the author expresses his sincere gratitude to Professor K.D. Sinel'nikov for continuous interest in the work.

REFERENCES

1. J.R. Pierce. IRE Transaction ED-3, 183, 1956.

2. A.E. Siegman. J. Appl. Phys., 31, 17, 1960.
3. C.C. Wand. Proc. IRE, 38, 135, 1950.
4. A.I. Akhiyezer and Ya.B. Feynberg. ZhETF [J. Expt. Theor. Phys.], 21, 1262, 1951.
5. I.R. Pierce. J. Appl. Phys., 25, 179, 1954.

CHERENKOV GENERATION OF HYDROMAGNETIC AND MAGNETIC SOUND WAVES
IN LOW-DENSITY ANISOTROPIC PLASMA

N.L. Tsintsadze, A.D. Pataraya
Tbilisi

We consider the excitation of hydromagnetic and magnetic sound waves in a low-density anisotropic plasma, resulting from the motion of current loops at high velocities.

If the low-density plasma is in a strong magnetic field and the mean free path of the particles is considerably larger than the characteristic dimensions, then the pressure in it will generally speaking be anisotropic [1-3].

The propagation of hydromagnetic and magnetic sound waves in a plasma with anisotropic pressure was investigated in the linear approximation in References [2, 3].

The present work is devoted to an analysis of Cherenkov generation of hydromagnetic and magnetic sound waves in an anisotropic plasma.

Expressions are obtained for the power of Cherenkov radiation from moving sources. The wave sources are assumed to be current loops and a charged filament, moving at high velocities.

In the present work we use the equations of Chew, Goldberger, and Low [1]. These equations, however, which are analogous to the magneto-hydrodynamic system of equations, are valid only for a plasma moving transverse to the magnetic field.

We have used these equations in the analysis of the excitation of waves in an anisotropic plasma with the aid of a charge filament and

current carrying loops, moving both transversely to and along the magnetic field. The authors do not claim that the results are rigorous in the case when the motion of the loops in the plasma coincides with the direction of the magnetic field, although they would be exact were the plasma to be replaced by a conducting liquid.

Of particular interest is the case when the motion of a charged filament transversely to the magnetic field through an anisotropic plasma is considered. The main difference from the case of an isotropic plasma is the existence in the anisotropic plasma of strong excitations of hydromagnetic waves. This effect is brought about by the occurrence of anisotropic Alfven waves in the region under consideration.

An analogous problem for an isotropic plasma, in the case when the current loop moves along an external magnetic field, was considered by A. I. Morozov [4]. Those results which we have obtained for the motion of loops along the magnetic field agree qualitatively with the results of A. I. Morozov.

We consider a plasma situated in a strong homogeneous magnetic field H_0 directed along the y axis. In the presence of external currents j_0 , the motion of the plasma is determined by the following magnetohydrodynamic equations [1, 2]:

$$\left. \begin{aligned} \hat{v} \left(\frac{\partial \hat{v}}{\partial t} + (\hat{v} \nabla) \hat{v} \right) &= -\hat{F} + \frac{1}{c} (\vec{j} \cdot \vec{H}), \\ \frac{\partial \vec{H}}{\partial t} &= \text{rot} [\vec{v} \cdot \vec{H}], \quad \text{rot } \vec{H} = \frac{4\pi}{c} (\vec{j} + \vec{j}_0), \\ \frac{\partial p}{\partial t} + \text{div} (p \vec{v}) &= 0, \quad \text{div } \vec{H} = 0, \quad \frac{d}{dt} \left(\frac{p_{\perp} H^2}{\rho} \right) = 0, \quad \frac{d}{dt} \left(\frac{p_{\parallel}}{\rho H} \right) = 0, \\ \vec{F}_i &= \frac{\partial p_{\perp}}{\partial x_i}, \quad p_{\perp} = p_{\perp} \delta_{ij} + h h_s (p_{\parallel} - p_{\perp}), \quad \vec{h} = \frac{\vec{H}}{H}. \end{aligned} \right\} \quad (1)$$

where p_{\perp} , p_{\parallel} are the transverse and longitudinal pressures, respectively, \vec{H} is the magnetic field, \vec{v} and ρ are the velocity and density of the plasma, and \vec{j} is the density of the current flowing in the medium.

It is assumed here that $v_0/c \ll 1$, where $v_0 = H_0/\sqrt{4\pi\rho}$, and c is the velocity of light.

The system of equations (1) can be linearized if J_0 is small. Solving the linearized system of equations without an external current, and assuming that the dependence of the alternating components on the coordinates and on the time has the form const $\int e^{i(\vec{k}\vec{r} - \omega t)} d\vec{k} d\omega$, we obtain the dispersion equation for the waves in a low-density anisotropic plasma in the presence of a strong field:

$$\omega^2 - k_y^2 V_A^2 = 0$$

$$\omega^2 - \omega^2 \{V_A^2 + S_1^2(1 + 2\cos^2\vartheta) + \sin^2\vartheta S_{\perp}^2\} +$$

$$+ \cos^2\vartheta \{3S_1^2 [V_A^2 + \sin^2\vartheta S_{\perp}^2 + S_1^2 \cos^2\vartheta] - S_1^2 \sin^2\vartheta\}, \quad (2)$$

$k = \sqrt{k_x^2 + k_y^2 + k_z^2}$, $V_A^2 = \sqrt{S_1^2 + v_0^2 - S_{\parallel}^2}$ is the Alfvén velocity, and $S_{\perp} = \sqrt{P_{0\perp}/\rho_0}$, $S_{\parallel} = \sqrt{P_{0\parallel}/\rho_0}$ are the transverse and longitudinal velocities of sound, respectively, $P_{0\perp}$, $P_{0\parallel}$ are the equilibrium transverse and longitudinal pressures, ρ_0 is the equilibrium plasma density, and ϑ is the angle between the direction of propagation of the wave and the magnetic field.

This equation has three different solutions, corresponding to three different types of waves capable of propagating in a low-density anisotropic plasma. The first factor corresponds to "hydromagnetic" waves, and the second to magnetic sound waves. The phase velocities of the "hydromagnetic" and magnetic sound waves are, respectively,

$$V_{1,2} = \pm V_A \cos\vartheta, \quad (3)$$

$$V_{1,2} = \pm \frac{1}{2} \sqrt{V_A^2 + S_1^2 \sin^2\vartheta + S_1^2 [1 + 2\cos^2\vartheta] \pm}$$

$$\pm \sqrt{(V_A^2 + S_1^2 \sin^2\vartheta + S_1^2 [1 + 2\cos^2\vartheta])^2 -}$$

$$- 4\cos^2\vartheta \{3S_1^2 [V_A^2 + (S_1^2 + S_{\perp}^2) \sin^2\vartheta] - S_1^2 \sin^2\vartheta\} \quad (4)$$

From (2) and (3) follow the conditions for the stability of the anisotropic plasma:

$$V_A^2 > 0, \quad (5)$$

$$S_1^2 > \frac{S_1^4}{3(S_1^2 + S_1^2 + V_A^2)}, \quad (6)$$

which should be satisfied simultaneously [2, 3].

We now proceed to consider the generation of hydromagnetic waves.

We consider the generation of hydromagnetic waves with an infinitesimally thin charged filament moving in an unbounded anisotropic plasma perpendicular to the magnetic field. Assume that the charged infinite filament moves with a velocity u along the y axis, and then the current density is equal to

$$j_{ox} = qu\delta(y)\delta(z - ut).$$

The power of the Cherenkov radiation from the filament can be determined by the formula

$$P = -quE_x \Big|_{y=0} = \frac{I_0}{c} [\vec{v} \vec{H}_0]_x \Big|_{z=0}, \quad (7)$$

where we made use of the relation

$$\vec{E} = -\frac{1}{c} [\vec{v} \vec{H}]$$

Linearizing the system of equations (1) we obtain v_x . Substituting v_x in (7), we get

$$P = \begin{cases} \frac{2q^2 u H_0^2}{c^2} Re \left(\frac{1}{V_A} \int_0^{\omega_{max}} dw \right), & V_A^2 > 0, \\ 0 & V_A^2 < 0. \end{cases} \quad (8)$$

The system of equations (1) is obtained under the assumption $\omega_{max} \ll eH/mc$, so that ω_{max} is bounded from above.

It is important to note that V_A^2 has a different meaning for an isotropic plasma, $V_A^2 = H^2/4\pi\rho_0$, and an anisotropic plasma, $V_A^2 = S_1^2 + V_0^2 - S_1^2$. Consequently, only in the anisotropic case as $V_A^2 \rightarrow 0$ does a strong excitation of hydromagnetic waves occur.

In addition, excitations of magnetic sound waves were considered in [5]. Three cases were investigated:

- 1) excitation of a magnetic sound wave with the aid of a charged current-carrying filament moving along a constant magnetic field with velocity u ;
- 2) in view of the fact that the plasma occupies the half space, the magnetic sound wave is excited by a straight loop moving along the surface of the plasma;
- 3) the generation of magnetic sound waves in a cylindrical plasma pinch is considered for the case of a moving annular current coaxial with the plasma cylinder.

REFERENCES

1. G. Chu, M. Gol'dberger and F. Lou, in collection entitled Problemy sovremennoy [Problems of Contemporary Physics], 7, 165, 1957.
2. L.N. Radakov, R.Z. Sagdeev, in collection entitled Fizika plazmy i problema upravlyayemykh termoyadernykh reaktsiy [Plasma Physics and the Problem of Controlled Thermonuclear Reactions], Izd-vo AN SSSR [Academy of Sciences USSR Press], Moscow, 3, 268-277, 1958.
3. R.V. Polovin and N.L. Tsintsadze, UFZh, [Ukrainian Physics Journal], IV, 1, 1959.
4. A.I. Morozov, in collection entitled Fizika plazmy i problema upravlyayemykh [Plasma Physics and the Problem of Controlled Thermonuclear Reactions], Izd-vo AN SSSR, Moscow, 4, 331-351, 1958.
5. N.L. Tsintsadze and A.D. Patraya, ZhTF [Journal of Technical Physics], 30, 1178, 1960.

EFFECT OF FLUCTUATING MICROFIELDS ON MULTIPLE COLLISIONS
IN A GAS OF CHARGED (OR GRAVITATING) PARTICLES

V. I. Kogan

Moscow

The questions considered of the influence of fluctuating microfields on multiple collisions in a gas of charged (or gravitating) particles, aimed at clarifying the following: a) the relation between the multiple and pair collisions; b) the structure of the "Coulomb logarithm." Using some typical problems in the theory of multiple collisions as examples, it is shown that the joint action of many field particles on the trial particle does not change the fundamental "binary" character of the collisions; however, the role of the maximum cutoff length in the Coulomb logarithm can be played (depending on the character of the problem) not only by the dimension of the system and the Debye screening radius, but also by the longitudinal range of the trial particle. In other words, multiple Coulomb (or Newton) scattering does not always have a strictly diffuse character. This nondiffusion, brought about by far order correlations, is essential for systems of the space charge or stellar cluster type. For a quasineutral plasma, it leads only to a certain correction (~10%) to the transport coefficients.

KINETIC ANALYSIS OF THE STRUCTURE OF THE
BOUNDRY OF A PLASMA IN A MAGNETIC FIELD

A. I. Morozov, L. S. Solov'yev
Moscow

Neglecting collisions, different versions of the transition layer between a plasma and a magnetic field are calculated.

Three basic cases are considered in the paper:

- a) plasma interface with and without field;
- b) interface in the presence of a field in all of space;
- c) structure of plasma layers whose width is of the order of the Larmor radius.

The results obtained in the first part are generalizations of the well-known Chapman-Ferraro theory.

STRUCTURE OF TRANSITION LAYER BETWEEN
A PLASMA AND A MAGNETIC FIELD

V. P. Shabanskiy
Moscow

The magnetohydrodynamic equations do not make it possible to determine the structure of the transition layer between regions occupied by a plasma on the one hand and by a magnetic field on the other. Yet a knowledge of the structure of this layer is important for problems in which one considers questions of the confinement of a plasma by a magnetic field and questions of stability.

The character of motion of the electrons and ions and the depth of penetration of the magnetic field in the plasma are similar in such a problem to the behavior of the electrons and ions in the surface layer of a plasmoid reflected from a magnetic wall.

Consequently, from the mathematical point of view, the problems are equivalent to a certain degree of approximation.

The paper considers first the character of motion of electrons and ions in the case of reflection by a magnetic wall of a neutral plasmoid of sufficiently low density to be able to neglect the influence of the magnetic field of the surface currents themselves, and incident with sufficiently low velocity to be able to neglect the polarization effect.

A similar problem is then solved more rigorously. The motion of the electrons and the ions is described by means of the equations of mechanics for individual particles in self-consistent fields. In this approach we neglect the dispersion in the absolute magnitudes of the velocities and in the directions of the plasma particles. This formulation yields a better approximation for the problem involving an incoming plasmoid, than for the problem involving the confinement of a hot plasma, but even in the second problem the qualitative results should not differ greatly from the results expected in the rigorous approach with the aid of the kinetic equation. It is shown that when the incoming beam has sufficiently low velocity, so that the energy of the incident protons is less than mc^2 (where m is the electron mass), the entire longitudinal energy of the protons goes over into transverse electron energy at the instant of reflection. At greater velocities, the polarization effect becomes appreciable and changes the conditions of the redistribution of the energy between the electrons and the ions in a way as to decrease the energy transfer from the ions to the electrons. The thickness of the layer and the character of the variation of the magnetic field and of the electron and ion velocities in the layer are determined, and an expression is obtained for the surface current. The layer in a collision-free plasma turns out to be so thin

that the orbital theory does not apply to it.

EFFECT OF EXTERNAL MAGNETIC FIELD
ON THE BOUNDARY LAYER IN A PLASMA

E.I. Andriankin, Yu.S. Sayasov
Moscow

The influence of an external magnetic field on an incompressible laminar boundary layer in a plasma with finite temperature-dependent conductivity was investigated.

It is shown that under certain simplifying assumptions, depending on the temperature difference ΔT between the incoming gas and the surface walls, two streaming modes are possible:

- 1) at sufficiently small ΔT , the friction η on the surface increases monotonically with increasing H , following approximately the linear law $\eta \sim H$ as $H \rightarrow \infty$ (H is the component of the magnetic field perpendicular to the velocity of the incoming stream);
- 2) if ΔT is sufficiently large, then the friction decreases with increasing H and detachment of the boundary layer occurs at a certain critical value of H .

Results of numerical calculations of the dependence $\eta = \eta(H)$ are presented for a wide range of variation of H for two examples, pertaining to cases 1 and 2, respectively.

MOTION OF VISCOUS PLASMA IN A MAGNETIC FIELD
FOR ARBITRARY ωr .

A. I. Gubanov, Yu. P. Lun'kin
Leningrad

1. An exact comparison is made of the equations of the one-liquid and two-liquid approximation in the theory of viscous plasma. It is shown that the usually employed equations $p = \Sigma p_s$; $\pi_{ik} = \Sigma \pi_{sik}$, etc., where p_s and π_{sik} are the partial pressure and the viscous stress tensor of the individual mixture components, hold true only with accuracy to the first degree of the current.

2. Expressions are obtained for the viscous stress tensor and for the heat flux of a completely ionized plasma in the one-liquid approximation for arbitrary ωr , both in a special system of coordinates (magnetic field along the z axis) and in an arbitrary Cartesian coordinate system.

3. The equations of motion and heat flux are derived for the plasma and are expressed in terms of the components of the current velocity and the temperature gradient. The equations are written out in both the special and in the arbitrary coordinate systems. Unlike ordinary hydrodynamics, which holds true when $\omega r \ll 1$, the Hall effect is taken into account here, as is the dependence of the viscosity and heat conduction on the magnetic field.

4. The equations obtained are solved in the simplest case of Couette flow of an incompressible liquid, which is also of practical interest, inasmuch as it approximately describes the laminar boundary layer.

Different directions of the external magnetic field are considered. In the first approximation the induced magnetic field is neglected.

5. In the case of an external magnetic field perpendicular to the

plates, the velocity profile, the current components, and the induced magnetic field components are calculated. A specific effect of arbitrary ωr is the motion of the plasma in a direction perpendicular to the velocity u_x of the moving plate, i.e., $v_y \neq 0$, and also the occurrence of a space charge, the current j_x , and the induced magnetic field H_y .

6. The case of a magnetic field oriented in the plane of the plates, the velocity profile is linear, as in the absence of a magnetic field, but a decrease in viscous friction occurs with increasing magnetic field.

7. The case of arbitrary direction of the external magnetic field is also considered.

MAGNETIC "WRINGING" OF FREE-MOLECULE PLASMA CURRENT

V. N. Zhigulev
Moscow

The problem is considered of the interaction between a magnetic field and a free-molecule plasma current incident on it; this problem leads to a study of the behavior of the plasma and of the magnetic field in the "return" layer. The problem of interaction is formulated for the case when the thickness of the "return" layer is small compared with the characteristic dimension of the interaction. By way of an example, the problem of the flow of the corpuscular streams of the sun around the earth's magnetic dipole is considered with the corpuscular stream regarded as free-molecular.

STABILITY OF PLANE POISEUILLE FLOW OF A PLASMA WITH
FINITE CONDUCTIVITY IN A MAGNETIC FIELD

Yu.A. Tarasov

Moscow

We consider the stability of plasma flow in longitudinal and transverse magnetic fields against infinitesimally small perturbations, for magnetic Reynolds numbers $R_m \sim 1$. This case includes the region of large velocities and of temperatures on the order of $5000-10,000^{\circ}\text{K}$.

A differential equation of sixth order for the z-component of the perturbations of the magnetic field is solved for the longitudinal magnetic field. Four nonviscous and two viscous solutions are obtained. The three symmetrical solutions obtained in this manner are substituted in the boundary conditions. A series of neutral curves is obtained for several values of R_m . In order to fix the values of the Alfvén number A , the curves are closed on the side of the large Reynolds numbers R , and for a certain value A_{kr} they contract to a point, i.e., there are no instabilities upon further increase in the Alfvén number. The dependence of A_{kr} on R_m is plotted and the curve shows that as R_m changes from about 3-4 to infinity, the value of A_{kr} changes little (from 0.17 to 0.1).

For flow in a transverse magnetic field, it is shown that the results obtained by Lock for values $R_m \ll 1$ can be extrapolated to the region of values $R_m \sim 1$.

The paper was published in ZhETF, 37, 6(12), 1708, 1959.

INVESTIGATION OF THE STABILITY OF A PLASMA WITH
THE AID OF THE GENERALIZED ENERGY PRINCIPLE

V. F. Aleksin, V. I. Yashin

Khar'kov

Using the generalized energy principle, account is taken of the fact that the plasma has a neutral charge under the assumption that the magnetic field is constant along the force line.

Stability criteria are obtained for a plasma with an anisotropic distribution of particle velocities, the plasma being situated in a magnetic field with cylindrical symmetry. Cases of longitudinal and azimuthal magnetic fields are considered.

The work was published in ZhETF, 39, 822, 1960.

SOME PROBLEMS IN THE MAGNETOHYDRODYNAMIC STABILITY
OF A THIN ANNULAR PINCH

Yu. V. Vandakurov

Leningrad

The stability is considered of a thin annular pinch without active resistance, against long-wave perturbations (long wave comparable with the length of the torus). It is assumed that there are no volume currents in the stationary state and that there is no ideally conducting jacket.

It is shown that the most difficult to stabilize are perturbations with wavelength that is several times smaller than the length of the torus. The conditions for the stabilization of certain types of perturbations are mutually contradictory.

Part of the paper was published in ZhTF, XXX, 6, 711, 1960; 7, 781, 1960.

INSTABILITY OF ELECTROMAGNETIC WAVES
IN A SYSTEM OF INTERPENETRATING PLASMAS

A.A. Rukhadze

Moscow

The investigation covered electromagnetic oscillations in a system of interpenetrating plasmas. Both high-frequency and low-frequency (hydrodynamic) oscillations are considered. Instability criteria are obtained for oscillations in the system, and the corresponding expressions are obtained for the wave buildup increments.

PROPAGATION OF ELECTROMAGNETIC WAVES IN
A HALF SPACE FILLED WITH PLASMA

Yu.N. Dnestrovskiy, D.P. Kostomarov

Moscow

Electromagnetic waves are considered in a half space filled with a magnetoactive plasma, propagating transversely to the magnetic field. It is assumed that the plasma is contained by a stationary magnetic field \vec{H} , and the structure of this field is investigated for the case when the ratio of the pressure to the magnetic field pressure is low. It is shown that the electromagnetic wave with electric vector parallel to the stationary magnetic field \vec{H} , has at large distances from the plasma boundary the form of a plane wave with a propagation constant determined by the dispersion relation for an unbounded plasma. The coefficients of reflection and transmission are calculated for a plane wave incident from vacuum on the plasma.

The paper was published in ZhETF, 39, 3(9), 845, 1960.

SOME SINGULARITIES OF TRANSVERSE PROPAGATION OF ELECTROMAGNETIC WAVES
IN A PLASMA SITUATED IN A CONSTANT MAGNETIC FIELD

B.N. Gershman

Gor'kiy

In 1951 Gross established interesting singularities in the behavior of plasma waves in a plasma situated in a constant magnetic field \vec{H}_0 and for waves propagating in a direction transverse to the field \vec{H}_0 , on the basis of the kinetic theory he developed for the propagation of electromagnetic waves in a plasma. These singularities consisted of the appearance of narrow frequency regions (Gross' "gaps"), in which the propagation was impossible. These regions arise in the vicinity of the gyroresonant frequencies, and their width decreases with increasing number of the resonance.

It is shown that if a nonrelativistic analysis is used, then the "gaps" arise not only for plasma waves, but also for the ordinary and extraordinary waves. It is particularly simple to study the structure of forbidden regions for ordinary waves, where the "gaps" arising starting with the first gyroresonance ($\omega \approx \omega_H$, where ω is the frequency of the wave and ω_H is the gyrofrequency of the electrons), and subsequently occur at the resonances $\omega \approx 2\omega_H, 3\omega_H$, etc.

It is further shown that if collisions are taken into account, and also in the case of deviations, sometimes rather small, from the direction of propagation perpendicular to \vec{H} , the "gaps" may disappear. The latter is most probably due to the high gyroresonances.

However, the most essential factor for a final solution of the problem of the reality of the Gross "gaps" is an inclusion of the relativistic effects. An analysis carried out with account of the variation of the relativistic Doppler effect shows that for a strictly transverse propagation one can speak of noticeable changes in the behavior of the

waves, which at the same time have no direct correspondence with Gross' conclusions, for a plasma wave at $\omega \approx 3\omega_H$, for the extraordinary wave at $\omega \approx 2\omega_H$, and for the ordinary wave at $\omega \approx \omega_H$. Accordingly, for each of the types of the waves no noticeable singularities whatever occur for resonances whose order is higher than the one indicated. For plasma waves at $\omega \approx \omega_H$ the propagation is impossible, and the forbidden region arising at $\omega \approx 2\omega_H$ will not have the character of a narrow "gap." For the extraordinary wave at $\omega \approx \omega_H$, no essential singularities arise in the transverse case.

TENDENCY OF COMPRESSION WAVES TO "TUMBLE" AND LOSE THEIR
ISENTROPIC NATURE IN THE ABSENCE OF COLLISIONS BETWEEN
THE PARTICLES OF THE PLASMA MEDIUM

V.A. Belokon'

Moscow

It can be shown that under conditions encountered both in experimental setups and in nature (stellar atmospheres, etc.), the collisions cease to influence noticeably the change in the entropy of the medium, so that the hydrodynamic equations can be written for a collision-free plasma in the isentropic form [1]. This vanishing of the "traditional" dissipative factors of the viscosity type leads to a formal (within the framework of the hydrodynamic equations, which are maintained in this case) paradox, for nothing prevents the compression wave from "tumbling" or even "billowing over." Although the absurdity of the latter follows from obvious considerations, i.e., any dissipation should hinder the "tumbling" from pure retrospective considerations, it is important to derive more rigorous arguments in favor of the hindrance of the "tumbling" of the waves. So far only particular arguments were advanced, for example, that the width of the wave cannot be smaller than the Debye length, etc. A similar theory was developed by Kantrowitz and Petschek, where it is shown that under definite conditions the width of the transition is determined by the mean free path of the magnetohydrodynamic perturbations, which is much smaller than the mean free path of the particles of the medium, by virtue of which the entropy starts increasing when the wave becomes very steep and the tumbling stops. Yet the solution of the problem should in principle be more

general and turns out to be simpler, independent of the special conditions, and arguments can be advanced which are valid also outside magnetohydrodynamics.

I. Inasmuch as a situation can be encountered in general, wherein the equations of motion can be recast in hydrodynamic form, and the nature of the dissipative factors is not clear, it is useful to turn to the most fundamental laws, which are more general than any dissipation law in terms of viscosity, etc. Such a law is the Heisenberg uncertainty principle, which has a direct bearing to entropy.

The uncertainty principle yields the absolutely possible minimum of transition time of a medium particle through the front of the wave (with the entropy of the medium zero everywhere):

$$\tau_{\min \text{ min}} \gg \delta t \geq \frac{\hbar}{\delta E} \gg \frac{\hbar}{\Delta E},$$

since the information that the medium element, being adiabatically compressed, has acquired a different internal energy is compatible only with the condition that the change in energy ΔE is much larger than the uncertainty in the energy δE , and the uncertainty in time δt associated with that uncertainty is much smaller than the time τ of the transition process, or else the transition time loses its physical meaning. It can be shown that in case of a finite initial entropy of the medium, the absolute lower limit of the transition time of the medium particle in a state with a different (specified) energy increases exceedingly rapidly with increase in the specified initial entropy of the medium.

Thus, when the front of a compression wave that tends to topple over becomes sufficiently narrow, then in spite of the fact that the isentropic solution tends to form a "billowing over," i.e., to become multiple valued, the fundamental uncertainty principle goes into opera-

tion, so that further decrease in the width of the front, i.e., a reduction in the time of transition from one specified state to another, would lead to an uncertainty in the energy that the particle of the medium would acquire ultimately, i.e., to a physically sensible multiple valuedness, in contradiction to the "absurd" multiple valuedness obtained by formal solution of the isentropic (or other) hydrodynamic equations. In other words, information concerning a sufficiently rapid transition of the medium particle from one energy state to another is incompatible with information that this transition occurs isentropically, in splendid agreement with the theory of fast adiabatic processes at which the entropy increases [2].

II. If we make the very general assumption that excitations that in the limit are photons can exist in the plasma (this is quite likely if the plasma is regarded as an aggregate of Faraday force filaments which are loaded with masses), then the first law of thermodynamics, in the particular case of a plasma which is sufficiently cold that the medium makes no contribution whatever to the thermodynamic functions, is written in the form

$$T\delta S = \delta \langle E \rangle - \langle \delta E \rangle; \quad E \equiv H^2 V / 8\pi,$$

and from the statistical procedure for deriving this law it is even seen for states close to thermodynamic equilibrium that T is the temperature of the plasma "excitation gas" which can in the particular case be identified with the "avcon" gas, the hypothesis of which was advanced by the theoretical group of the Avco firm (Kantrowitz, Petschek). In the case of "frozen-in" force lines in the medium, we have

$$\dot{T}\delta S = (\delta \langle H^2 V \rangle + \langle H^2 \rangle \delta V) / 8\pi \neq \langle H \rangle \delta \langle HV \rangle / 4\pi \equiv 0,$$

i.e., the entropy of the plasma can change also when the medium does not play any role.

If the medium does make an appreciable contribution to the thermodynamics of the plasma, then the aforementioned factor of energy change nevertheless remains and this factor is the only observable one when the dissipation via collisions becomes too slow under the given conditions.

This result can be regarded as a somewhat generalized interpretation of the work of the theoretical group of the Avco company, carried out from the point of view of fundamental simple laws of statistical thermodynamics.

REFERENCES

1. Pechek. Kosmicheskaya gazodinamika [Cosmic Gas Dynamics], Izd-vo inostr. lit. [Foreign Literature Press], 1960 (report); report at Upsala, 1959.
2. R.C. Tolman. Principles of Statistical Mechanics. Oxford, 1938.

OSCILLATIONS OF AN INHOMOGENEOUS PLASMA

L. I. Rudakov
Moscow

The kinetic equation is used to consider the problem of the damping and buildup of magnetohydrodynamic waves in an inhomogeneous plasma in a magnetic field.

The main contents of the work was published in ZhETF, 37, 5(11), 1337, 1959.

PLASMA OSCILLATIONS BETWEEN TWO ELECTRODES

S.V. Iordanskiy
Moscow

The problem is considered of the excitation of electronic one-dimensional oscillations in a plasma when a beam of electrons is passed between two electrodes that have a specified negative potential relative to the plasma. The plasma and beam electrodes are assumed cold and the hydrodynamic approximation is used. The solution of the linearized equations with allowance of suitable boundary conditions on the electrodes and on the boundaries of the ion layers shows that an infinite number of oscillations that increase exponentially in time arises, with frequencies located near the plasma frequency. The formulas obtained for the case of low beam intensity and for large distance between electrodes show that the dependence of the frequency of the oscillation with the largest increment on the plasma frequency has a

steplike character, and that the maximum increment is obtained when the oscillation frequency is exactly equal to the plasma frequency. These results agree qualitatively with the experiments of Looney and Brown [1], which were carried out at high beam intensities.

REFERENCE

1. D. Luni and S. Braun, Collection of translations entitled *Dinamika plazmy* [Plasma Dynamics], 2, 176, 1956.

NONLINEAR LANGMUIR OSCILLATIONS OF IONS IN A PLASMA

M. V. Konyukov
Moscow

Nonlinear oscillations of a one-dimensional plasma are considered in the quasihydrodynamic approximation.

In addition to the already considered nonlinear electron oscillations, nonlinear ion oscillations in the plasma are investigated.

The solution is presented for two cases:

- a) localized oscillations of the ions with the frequency, arising in the plasma at infinite electron temperature;
- b) electroacoustic waves, existing at finite electron temperatures.

In the first case, an exact solution can be found.

In the second case, the solution is obtained in quadratures; the dependence of the period on the plasma parameters and on the initial conditions is obtained, and the region of existence of nonlinear electroacoustic waves is also established.

The paper was published in *ZhETF*, 37, 3(9), 799, 1959.

TRANSITION RADIATION OF A CHARGE
ON THE FRONT OF A SHOCK WAVE

L.S. Bogdankevich, B.M. Bolotovskiy, A.A. Rukhadze
Moscow

The problem is solved of transition radiation of a fast charged particle passing through the front of a strong shock wave which ionizes the medium. Formulas are obtained for the energy loss of the particle under different assumptions concerning the properties of the media ahead of and behind the wave front.

CYCLOTRON RADIATION OF A PLASMA

V.I. Pakhomov, K.N. Stepanov
Moscow

The radiation of an electron moving along a helix in a plasma situated in a magnetic field is considered. It is assumed that the velocity of the electron is of the order of the mean thermal velocity of the plasma electrons.

The angular distribution of the radiation intensity is obtained for different harmonics. Losses to cyclotron radiation from a bounded plasma are estimated.

The paper was published in ZhETF, 38, 5, 1564, 1960.

EXPERIMENTAL PROBLEMS OF PLASMA PHYSICS

BEHAVIOR OF A PLASMA IN STRONG ELECTRIC FIELDS

L. V. Dubovoy, A.G. Ponomarenko, O.M. Shvets
Khar'kov

The behavior of a plasma in electric fields with intensities 0.1-100 v/cm was investigated by high-frequency diagnostic methods. It was observed that in discharges with charged particle concentrations 10^8 - 10^{10} per cubic centimeter for electric field intensities larger than 1-10 v/cm, the effects of the interaction of the ions and electrons in the plasma cannot be explained by means of the pair collision theory that takes into account collisions of the type occurring between a charged particle and a neutral particle (under the experimental conditions the contribution of the Coulomb collisions was negligibly small).

Rapid thermalization of the beams of charged particles in low pressure discharges (the "Langmuir paradox" [1]), experiments on ohmic heating of plasma in stellarators, attempts to create a plasma betatron, and an investigation of the feasibility of heating ions by the cyclotron resonance method [2, 3] disclose interaction effects between particles, greatly in excess of those expected from the pair collision theory.

At the same time, an investigation of an electron plasma in thermal equilibrium [1] shows that the interaction between particles corresponds in this case to the theory. Consequently, the "X" mechanism, which is possible in the Langmuir paradox, etc., should be the result of the fact that the discharge plasma is not in thermal equilibrium, which in particular is disturbed by the extensive use of electric

fields in most modern structures used to investigate discharges.

In connection with the indirect character of the data available on this problem (the increased frequency of the collisions that bring about a reinforced exchange of energy between particles can be judged from the increase in the diffusion coefficient of the charged particles transversely to the magnetic field, from the Maxwellization rate, etc.), we undertook to determine directly the effective collision frequency [4] of the electrons and ions in the plasma as a function of the electric field intensity. The method used for the measurement was the one previously developed by the author [5] for the determination of the particle collision frequency in a plasma by measuring the transverse component of the discharge conductivity in a magnetic field in the region of cyclotron resonance for the given species of particles.

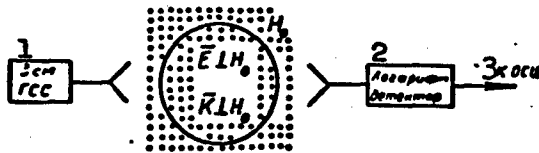


Fig. 1. Setup for measuring the effective electron collision frequency in a plasma. 1) 3-cm standard signal generator; 2) logarithmic detector; 3) to oscilloscope.

The main measurements were carried out in discharges, in which for the case of weak electric fields, which guarantee the smallness of the perturbation Δv in the particle velocity compared with the thermal velocity v_T , the principal role is played by collisions between charged particles and neutral ones (a unique model of a high-temperature plasma).

A block diagram of the experiments on the determination of the effective collision frequency of the electrons in the plasma is shown in Fig. 1.

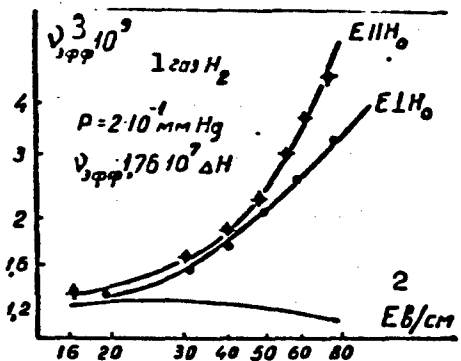


Fig. 2. Dependence of effective collision frequency of the electrons in a plasma on the electric field intensity. 1) Gas. 2) ev/cm; 3) v_{eff} .

A quartz or pyrex discharge bulb was placed between two dielectric antennas, one of which was connected to a low-power klystron generator with frequency $\omega_1 = 9000$ megacycles, and the other was connected to the detector. The electric component of the measuring signal \tilde{E} was oriented perpendicular to the static field H_0 , produced by an iron core magnet. The electronic circuitry made it possible to measure the logarithm of the ratio of the amplitude of the incident wave of the sounding signal to the transmitted wave (a quantity proportional to the plasma conductivity for the case $\omega_0^4/\omega_1^2 v_{\text{eff}}^2 \ll 1$, where ω_0 is the Langmuir frequency of the plasma and v_{eff} is the effective frequency of the electron collisions in the discharge), in the region of cyclotron resonance of the electrons, from which the value of v_{eff} was directly determined.

A spatially homogeneous electric field E was produced in the plasma by means of a parallel plate capacitor connected to a 60-megacycle generator. The minimum concentration of the neutral particles in the experiments (10^{14} - 10^{15} per cubic centimeter) was chosen such that the amplitude of the electron oscillations did not exceed several percent of the smallest dimension of the bulb in the maximum field $E_M =$

= 100 v/cm, used in the measurements; this amplitude had a value $\mu(p)E_M/\omega$, where $\mu(p)$ was the mobility of the electrons at a pressure p , and ω is the frequency of the field E . This ensured also the conditions for the penetration of the field E into the plasma ($v_{eff}/\omega \gg 1$ [6]) in a wide range of variation of the charged particle density in the discharge.

The obtained dependence of the electron collision frequency in the plasma on the intensity of the electric field E , oriented parallel to the magnetic field H_0 , is shown in Fig. 2. The same figure shows the dependence, calculated from [6, 7], of the effective frequency of the collisions between the electrons and the neutral particles. The sharp discrepancy between the measured values of v_{eff} and those expected in fields larger than 20 v/cm offer evidence of appearance of an additional mechanism whereby the electron energy is dissipated. Since $E > 20$ v/cm, the role of the neutral particles in the collision processes becomes insignificant, and one can expect the obtained dependence to be valid for all values of residual gas pressure. Preliminary measurements confirm the correctness of this assumption.

In connection with the fact that when $E \parallel H$ the plasma density changes somewhat with variation of E , the dependence of v_{eff} on E shown in Fig. 2 is apparently exaggerated. Indeed, when $E \parallel H$, when discharge conditions could be obtained under which the density, estimated from the intensity of the light emitted by the discharge and from the absorption of the sounding signal at the instant of resonance, remain practically constant over a wide range of variation of E , the dependence $v_x = v_{eff}(E)$ for $E > 20$ v/cm turns out to be close to linear for $E > 20$ v/cm (see Fig. 2).

As for the case of electrons, in the investigation of the effective ion collision frequencies in the plasma, at low electric field inten-

sity values that perturb little the initial value of the ion temperature T_1 , the interaction cross sections obtained were in satisfactory agreement with the theoretical predictions for the resonant charge exchange process [5, 8]. However, on going over to field intensities E sufficient to make the ion energy exceed the mean plasma temperature, the typical dependence obtained was of the type $E^{0.8} - E^{1.2}$, i.e., always much stronger, in place of the well-investigated increase in frequency of collision between the ions and the neutral particles, proportional to the square root of the field intensity. It is characteristic that in the presence of intrinsic noise in the plasma, which is a unique indicator of the possibility of the occurrence of instabilities in the discharge, the exponent of E in the function $v_x(E)$ is as a rule larger than 0.7.

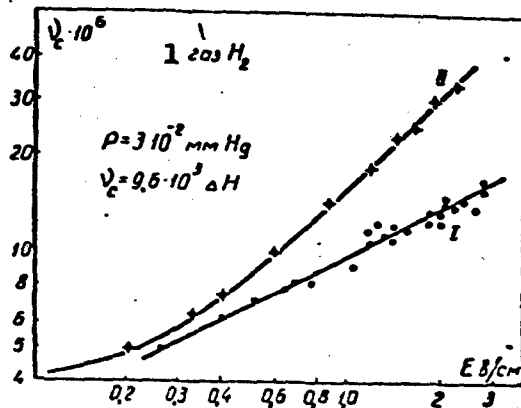


Fig. 3. Dependence of the effective ion collision frequency in a plasma on the electric field intensity. 1) Gas.

Figure 3 shows the measured dependence of the ion collision frequency in an electrodeless discharge on the intensity of the electric field E , perpendicular to the magnetic field and varying with a frequency equal to the ion cyclotron frequency (the usual measurement techniques were used [2, 3]).

Curve I was obtained for the specific case of a low-density (10^7 per cubic centimeter) plasma with low level of intrinsic noise, and is in good agreement with the expected theoretical dependence $\nu_{\text{eff}} \sim E^{0.5}$. However, on going over to larger densities, characterized by a ratio $\omega_{01}^2/\omega^2 \gtrsim 1$, where ω_{01} is the Langmuir frequency of the ions, the dependence of the effective collision frequency (curve II), which is most typical for ordinary discharges (relatively high noise level, and densities 10^9 - 10^{10} per cubic centimeter), is close to linear for fields $E > 1$ v/cm. It is seen that when $E > 0.5$ v/cm, a new interaction mechanism appears for ions, connected with the presence of the electric field.

For transverse fields E with frequencies that differ from cyclotron frequency ($\omega \ll \omega_{c_1}$) the instant of occurrence of the anomaly is shifted toward the larger values of the electric field, coinciding practically with the case of electrons ($E_{kr} \sim 10$ - 15 v/cm), which apparently is connected with the fact that when the resonance conditions are satisfied a sufficiently strong anisotropy of the ion velocities arises at much smaller values of E .

The influence of the longitudinal electric field on the ion collision frequency in the plasma was not investigated, since the presence of analogous effects are evidenced by experiments on the heating of plasma by the method of ion cyclotron resonance in stellarators [2]. A comparison of the efficiency with which the high-frequency ion heating energy is absorbed in this case indicates an anomalously high collision frequency for the ions during the time of existence of the electric field of the ohmic heating, compared with the conditions in a decaying plasma with the same parameters. One can also attribute to analogous effects, apparently, the shorter time of plasma confinement in stellarators in the presence of an ohmic heating field, since an in-

crease in the collision frequency leads to a direct increase in the diffusion coefficient.

In conclusion we must note the strong influence of the noise level in the discharge on the processes of particle interaction in the plasma. At the same time, it was observed in many cases that an increase in the electric field intensity in the plasma leads to a clearly pronounced increase in the noise level.

Unfortunately, the data presently available are not sufficient for a specific comparison with one of the numerous models considered in many theoretical papers [9, 10]. One can assume with respect to the nature of the observed phenomenon that the presence of strong electric fields in the plasma, contributing to the appearance of directed particle streams with different velocities for components of different species, leads to the occurrence of microfluctuations, which increase the interaction between the particles with subsequent rapid thermalization.

One can also assume that for fields larger than 10-20 v/cm, the instability in discharges of the "runaway electron" type will be greatly attenuated, and anomalies must appear in the behavior of the plasma conductivity along with a strong dependence of the diffusion processes in the charged particles on the intensity of the electric field.

It would be extremely interesting to investigate the behavior of the quantities v_{xi} and v_{xe} as functions of the plasma density and the magnetic field intensity.

The authors are grateful to Professor K.D. Sinel'nikov for practical remarks.

REFERENCES

1. E. Ash, G. Gabor. Proc. Roy. Soc., a 228, 447, 1955.

2. T. Stix, R. Palladino. Phys. Fluids, I, 446, 1958.
3. L. Dubovoy, O. Shvets, S. Ovchinnikov. Atomnaya energiya [Atomic Energy], 8, 316, 1960.
4. V.L. Ginzburg, A.V. Gurevich. UFN [Progress in Physical Science], XX, 201, 1960..
5. L. Dubovoy, O. Shvets. Izd. [sic] AN SSSR, ser. fiz.. [Bull. Acad. Sci. USSR, Physics Series] (in press); see also J. Schneider, F. Hofman. Phys. Rev., 116, 244, 1959.
6. L. Varnerin, S. Brown. Phys. Rev., 79, 946, 1950.
7. Landolt-Börnstein. Tabellen [Tables], Berlin, 1950.
8. A. Dalgarno, H. Jadav. Proc. Phys. Soc., a 72, 1087, 1958.
9. P.A. Sturrock. Proc. Roy. Soc. (L), a242, 277, 1957.
10. O. Buneman, Phys. Rev., 115, 503, 1955.

ON THE ROLE OF SPACE CHARGE IN A DISCHARGE WITH
OSCILLATING ELECTRONS IN A MAGNETIC FIELD

M. N. Vasil'yeva, E.M. Reykhrudel'
Moscow

The ignition and development of a discharge at low pressures in a magnetic field depend essentially on the kinetics of the electrons. A discharge with oscillating electrons in an inhomogeneous electric and in a constant magnetic field has found use in many devices: manometers, pumps, ion sources, etc. The arrangement of the electrodes and the direction of the magnetic field are shown in Fig. 1-a. The kinetics of the electrons in such a discharge, without account of space charge, was considered in many recently published papers [1-3]. At the given configuration of the electric and magnetic fields, the electrons leaving different spots on the cathode, and also the electrons formed in the discharge gap, oscillate in the discharge, forming a negative space charge. A typical distribution of the potential along the z axis and along the radius r of the tube in the plane of the anode ring, without a discharge and in a hot discharge, is shown in Fig. 1-b [4]. It is clear from Fig. 1 that the presence of space charge greatly changes the potential distribution curves, and consequently also the character of motion of the electrons in the discharge.

The real potential distribution along the discharge axis z and in the anode plane $r\theta$, taking place in a hot discharge, can be represented in the form

$$\varphi(z) = \frac{5\varphi_0}{d(6p-d)}(-z^2 + 2pz), \quad (1)$$

$$\varphi(r) = \frac{\varphi_0 - k\varphi_0}{r_a(r_a - 2q)}(r^2 - 2qr) + k\varphi_0. \quad (2)$$

where d is the distance from the cathode to the plane of the anode ring, p is the value of z at which the distribution curve of the potential $\varphi(z)$ has a maximum, φ_0 is the potential of the center of the tube (at $z = d$) in the case when there is no space charge, i.e., $p = d$, and the potential distribution along z is given by curve 1 (see Fig. 1), r_a is the radius of the anode ring, q is the value of r corresponding to the minimum of the function $\varphi(r)$, and k is a coefficient with value $k = (r_a - 2q)/(r_a - q)$. When $p = d$ and $q = 0$, the functions $\varphi(z)$ and $\varphi(r)$ describe the distribution of the potential in the absence of a discharge (curve 1 on Fig. 1-b). This case is considered in detail in [1].

The problem is solved of the motion of an electron in a longitudinal magnetic field H and in an electric field whose potential distribution is described by the functions $\varphi(z)$ and $\varphi(r)$. The equations of motion for this case have the form

$$m\ddot{z} = e\frac{\partial\varphi}{\partial z}, \quad (3)$$

$$m(\ddot{r} - r\dot{\theta}^2) = e\frac{\partial\varphi}{\partial r} - \frac{e r \dot{\theta} H}{c}, \quad (4)$$

$$m\frac{1}{r}\frac{d}{dt}(r^2\dot{\theta}) = \frac{e r \dot{H}}{c}. \quad (5)$$

From (1) and (3), under the initial conditions $t = 0$, $z = z_0$, $\dot{z} = \dot{z}_0$, we obtain

$$z = A \sin(\omega t + \alpha) + p, \quad (6)$$

where

$$\omega = \sqrt{\frac{10e\varphi_0}{md(6p-d)}}; \quad A = \sqrt{(z_0 - p)^2 + \frac{\dot{z}_0^2}{\omega^2}}; \quad \tan \alpha = \frac{z_0 - p}{\dot{z}_0}.$$

The given solution (6) describes the behavior of the electron in the

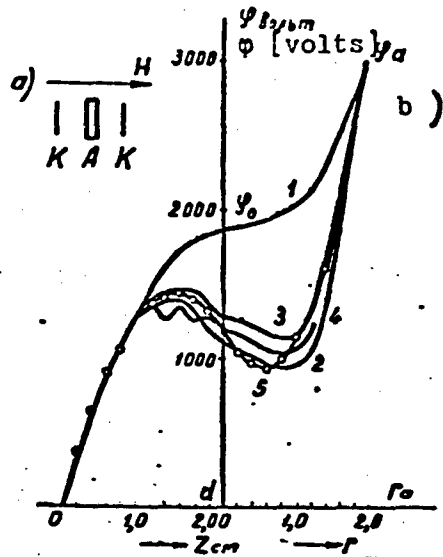


Fig. 1. a) Schematic diagram of the discharge gap: K - disk cathodes, A - ring anode; b) distribution of the potential along the z axis and along the radius r of the tube in the plane of the anode ring for different values of the magnetic field; $p = 3 \cdot 10^{-4}$ mm Hg; 1) potential distribution in the absence of a discharge; 2-4) in the presence of space charge; 2) $H = 280$ oersted; 3) $H = 315$ oersted; 4) $H = 350$ oersted; 5) theoretical.

interval from $z = 0$ to $z = d$, since $\phi(z)$ coincides with the experimental potential distribution only in that interval of variation of z . The potential distribution in the discharge is symmetrical with respect to the anode plane ($z = d$), and the motion of the electron in the interval from $z = d$ to $z = 2d$ will be described by the same function $\phi(z)$, but with origin at $z = 2d$.

An analysis of the solution (6) shows that, depending on the initial conditions z_0 and \dot{z}_0 , the motion of the electron along the z axis will be either anharmonic or harmonic. If the initial conditions are such that $A > d - p$, then the electron will execute anharmonic os-

cillations about the plane of the anode with frequency ω_1 , which depends on the initial conditions

$$\omega_1 = \frac{\pi\omega}{2(\pi - \arccos \frac{d-p}{A})}$$

The frequency ω_1 is always smaller than the frequency of the harmonic oscillations, which would arise under the same discharge conditions, were there to be no space charge. When $A \leq d - p$ the motion of the electron will be harmonic with frequency ω , which is independent of the initial conditions z_0 and z'_0 . In this case the electron will not pass through the anode ring into the space adjacent to the second cathode, and will execute harmonic oscillations with respect to the plane corresponding to the maximum of the potential distribution curve $\phi(z)$. The frequency of these harmonic oscillations ω will always exceed the frequency of the harmonic oscillations which would arise in the absence of space charge. If the space charge is disregarded, then the motion of the electron will always be harmonic relative to the plane of the anode, with frequency $\omega_0 = \sqrt{2e\phi_0/md^2}$, which is independent of the initial conditions. Figure 2 shows the curves of the electron motion along the discharge axis z for different initial conditions in the presence and in the absence of space charge.

Thus, the space charge leads to the occurrence of two types of dielectric oscillations in the discharge, with frequency on the order of 10^9 sec⁻¹, and to the presence of high-frequency noise in the discharge [2, 4]. Several ionization regions are produced along the discharge axis z , as confirmed by the presence of ion groups of different velocities in the discharge [5].

The solution of Eqs. (4, 5) subject to Condition (2), describing the motion of the electron in the anode plane $r\theta$, reduces to the solution of an equation of the type $\ddot{r} + Ar - (B/r^3) + C = 0$, where $A =$

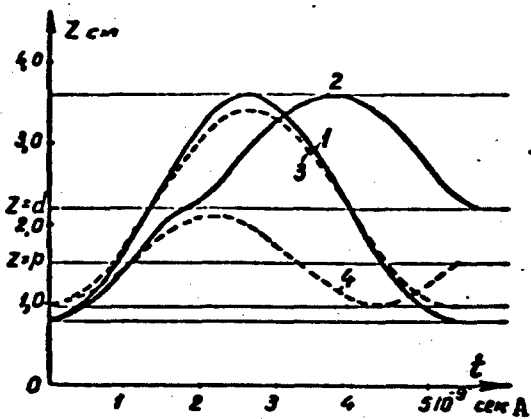


Fig. 2. Character of motion of electron along the discharge axis z in the presence of space charge (2, 4) and in its absence (1, 3) for different initial conditions: 1, 2) $z_0 = 0.8 \text{ cm}$; 3, 4) $z_0 = 1.0 \text{ cm}$. A) sec.

$$= (eH/2mc)^2 - e2P/m; B = (eH/2mc)^2 r_0^4,$$

$$C = \frac{e}{m} \cdot 2Pq; P = \frac{v_a - k\tau_0}{r_a(r_a - 2q)}.$$

After integration we have

$$\dot{r}^2 + Ar^2 + \frac{B}{r^2} + 2rC = C_1 \quad (7); \quad C_1 = r_0^2 + Ar_0^2 + \frac{B}{r_0^2} + 2r_0C.$$

From the given equation we can obtain the value of the critical magnetic field H_{kr} , at which the electron trajectory is tangent to the surface of the anode

$$H_{kr} = \frac{2mc}{e} \cdot \frac{r_a}{r_a^2 - r_0^2} \sqrt{\frac{2e}{m} P(r_a - r_0)(r_a + r_0 - 2q) + r_0^2}.$$

The calculations performed show that H_{kr} is the greater, the farther away from the axis the electron was produced and the larger its initial radial velocity r_0 is. The values of H_{kr} , calculated with allowance for space charge, always exceed the values of H_{kr} obtained without allowance for space charge.

Equation (7) reduces to an integral of the form

$$t = \int_{r_0}^r \frac{dr}{\sqrt{-Ar^2 - 2Cr + C_1 r^2 - B}},$$

which cannot be accurately calculated. Expanding the integrand in a series, we obtain

$$t = \int_{r_0}^r \frac{dr}{R^{1/2}} + \frac{B}{2} \int_{r_0}^r \frac{dr}{r^2 R^{1/2}} + \frac{3B^2}{8} \int_{r_0}^r \frac{dr}{r^4 R^{1/2}} + \dots,$$

where $R = -Ar^2 - 2Cr + C_1$. A comparison of the results of the numerical integration and of the results obtained upon integration of the terms of the given series, one can restrict oneself to the first two terms of the expansion with accuracy up to 25%.

When $H > H_{kr}$, $A > 0$ we obtain

$$\begin{aligned} t = & \frac{1}{\sqrt{A}} \arcsin \frac{C + Ar}{\sqrt{AC_1 + C^2}} + \frac{B}{2} \left[\left(\frac{3C}{C_1} - \frac{1}{C_1 r} \right) \frac{1}{R^{1/2}} + \right. \\ & + \left(\frac{3C^2}{C_1} + \frac{2A}{C_1} \right) \frac{Ar + C}{(AC_1 + C^2) R^{1/2}} - \frac{3C}{C_1^2 \sqrt{C_1}} \ln \frac{2}{r} (C_1 - Cr + \right. \\ & \left. \left. + \sqrt{C_1 R}) \right] + C_2, \end{aligned} \quad (8)$$

where C_2 is a constant equal to the expression in the right half taken with $r = r_0$ and with the sign reversed. If $H \leq H_{kr}$, then the electron will move away to the anode, so that

$$\begin{aligned} t = & \frac{1}{\sqrt{-A}} \ln 2 (\sqrt{-Ar} - Ar - C) + \frac{B}{2} \left[\left(\frac{3C}{C_1} - \frac{1}{C_1 r} \right) \frac{1}{R^{1/2}} + \right. \\ & + \left(\frac{3C^2}{C_1} + \frac{2A}{C_1} \right) \frac{Ar + C}{(AC_1 + C^2) R^{1/2}} - \frac{3C}{C_1^2 \sqrt{C_1}} \ln \frac{2}{r} (C_1 - Cr + \right. \\ & \left. \left. + \sqrt{C_1 R}) \right] + C_3, \end{aligned} \quad (9)$$

where C_3 is determined in analogy with C_2 .

To plot the electron trajectory in the $r\theta$ plane it is necessary to know also the dependence $\theta(t)$. From Eq. (5) under the condition $t = 0$, $r = r_0$, $v_\theta = 0$ we have

$$\dot{\theta} = \frac{eH}{2mc} \left(1 - \frac{r_0^2}{r^2} \right).$$

Since r cannot be explicitly expressed from (8) and (9), we seek the trajectory equation in the form $\Theta = \Theta(r)$

$$\Theta = \frac{eH}{2mc} t - \frac{eH}{2mc} r_0^2 \left\{ -\frac{1}{C_1 r} + \frac{B}{2C_1 R} \left[\frac{5C}{2C_1} \left(\frac{7C^2}{C_1} + 3A \right) - \frac{1}{3C_1 r^3} - \frac{7C}{6C_1 r^2} - \frac{1}{r} \left(\frac{35C^2}{6C_1} + \frac{4A}{3C_1} \right) + \left(\frac{35C^2}{2C_1} + \frac{115AC^2}{6C_1} + \frac{8A^2}{3C_1} \right) \frac{Ar + C}{AC_1 + C^2} \right] - \frac{1}{\sqrt{C_1}} \left[C_1 + \frac{B}{2} \left(\frac{35C^2}{2C_1} + \frac{15AC^2}{2C_1} \right) \right] \ln \frac{2}{r} (C_1 - Cr + \sqrt{C_1 R}) + C_4 \right\},$$

where C_4 is equal to the expression in the braces, taken with $r = r_0$ and the sign reversed. Depending on the value of H , we determine t either from (8) or (9).

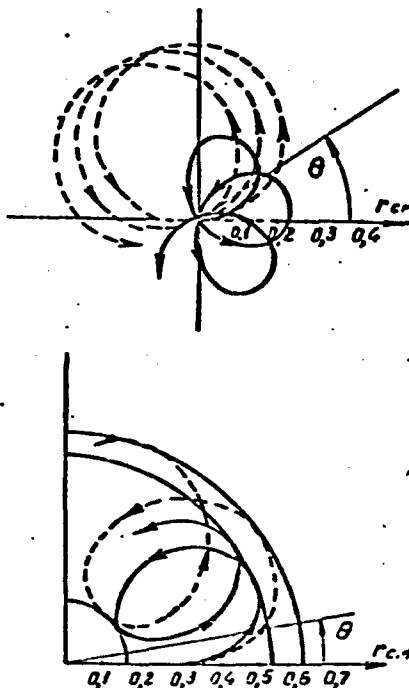


Fig. 3. Motion of electron in the plane $r\theta$ of the anode ring. The solid curves are plotted with allowance for space charge, while the dashed ones are without allowance of the space charge. Above — $r_0 = 0$; below — $r_0 = 0.3$ cm.

If the electron was produced at the center of the tube ($r_0 = 0$),

then $B = 0$ and the equations of motion can be integrated exactly. Figure 3 shows the trajectories of the electron motion in the plane $r\theta$, calculated with and without account of space charge. It is seen from the figure that the space charge contributes to additional contraction of the discharge and to an increase in the frequency of the gyromagnetic oscillations. The frequency of these oscillations depends on the initial conditions and is of the same order (10^9 sec^{-1}) as the frequency of electron oscillations along the discharge axis z . Consequently, resonant oscillations can set in [2]. If the space charge is disregarded, then the frequency of the oscillations is independent of the initial conditions r_0 and \dot{r}_0 and there are no resonance conditions.

The obtained dependence of H_{kr} on the magnitude of the space charge and on the initial conditions, as well as the increase of the contraction of the discharge with increasing space charge, make it possible to explain some complicated discharge characteristics $I = f(H)$, $I = f(\varphi_a)$. It is known that under pressures on the order of 10^{-4} - 10^{-5} mm Hg, the curves showing the dependence of the discharge current on the magnitude of the magnetic field and on the anode voltage display a series of maxima and minima [4, 5]. A typical curve showing the dependence of the discharge current on H with the first maximum is shown in Fig. 4.

With increasing H , the discharge current increases because of the ever-increasing number of electrons that are retained in the discharge, thereby increasing the ionization in the volume. Simultaneously, the increase in H leads to a larger contraction of the discharge. The negative space charge at the center of the tube increases, since the ions move out of the volume. The formation of the space charge contributes to an even greater contraction of the discharge. Under certain values of H , the space charge reaches as it were a critical value, when the

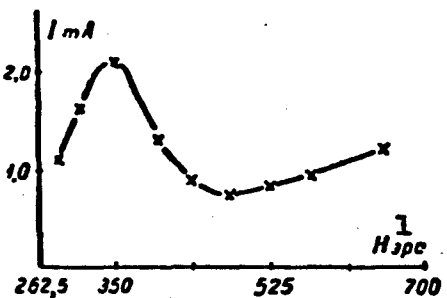


Fig. 4. Dependence of the discharge current on H ; $V_a = 2.4$ kv; $p = 3 \cdot 10^{-4}$ mm Hg. 1) Oe.

existing magnetic field is no longer sufficient to retain the electrons in the discharge (H_{kr} increases with increasing q). Consequently, further increase in the magnetic field causes a realignment of the space charge, the electrons move out from the discharge, and the current I decreases. At still larger values of H , the discharge current again increases; the magnetic field becomes sufficiently strong to retain the electrons in the discharge. At the same time, the electrons become more and more twisted with larger r_0 and r'_0 . The space charge at the center of the tube again increases with increasing magnetic field. Thus, the occurrence of the second maximum can be attributed to the same causes, but at a larger space charge density. The region of the second maximum is as a rule broader, because of the spreading of the space charge resulting from the repelling action of the electrons.

With increasing anode voltage V_a , the maxima shift toward the larger magnetic fields. In this case the electrons acquire larger values of r_0 and to retain them in the discharge larger values of H_{kr} are necessary. The critical space charge preventing further increase in the discharge current is produced at large magnetic fields. With increase in pressure, the maxima shift to the left, since the concentration of the electrons in the discharge increases and the realignment

of the discharge occurs at smaller values of H .

CONCLUSIONS

1. A solution is presented of the problem of the motion of the electron along the discharge axis z and in the anode plane $r\theta$ in a longitudinal magnetic field H and in an inhomogeneous electric field, in which the potential distribution is described by functions $\varphi(z)$ and $\varphi(r)$, which take into account the presence of space charge.
2. An analysis of the solution shows that depending on the initial conditions the motion of the electrons will be anharmonic or harmonic. The frequency of the anharmonic oscillations ω_1 depends on the initial conditions z_0 and z'_0 , whereas the frequency of the harmonic oscillations ω is independent of the initial conditions.
3. The electrons having a radial velocity component $r_0 \neq 0$ will also execute gyromagnetic oscillations, rotating in the $r\theta$ plane. The frequency of the gyromagnetic oscillations in the presence of space charge depends on the initial conditions, and resonance is possible between the gyromagnetic oscillations in the $r\theta$ plane and the oscillations along the discharge axis z .
4. The space charge contributes to the contraction of the discharge by changing the radial potential distribution.
5. An account of the space charge leads to a larger value of the critical magnetic field and helps explain complicated characteristics of the discharge.

REFERENCES

1. G.V. Smirnitskaya, E.M. Reykhrudel', Radiotekhnika i elektronika [Radio Engineering and Electronics], 2, 1303, 1957; Vestn. Mosk. univ. [Herald of Moscow University], 121, 2, 1958; ZhTF [Journal of Technical Physics], 29, 153, 1959.
2. G. Dumas. Rev. gener. d'electr. [General Revue of Electrical

- Engineering], 64, 331, 1955.
3. Miyagawa Nabukhadzu, Rep. sci. Rec. inst. Tokyo, 31, 4, 1955.
 4. E.M. Reykhrudel', G.V. Smirnitskaya, Izv. vyssh. uch. zaved., Radiofizika [Bulletin of the Higher Educational Institutions, Radiophysics], 1, 36, 1958.
 5. E.M. Reykhrudel', G.V. Smirnitskaya, M.N. Vasil'eva, Radiotekhnika i elektronika [Radio Engineering and Electronics], 5, 662, 1960.

EXPERIMENTAL DETERMINATION OF THE NATURE AND CONCENTRATION
OF EASILY IONIZED IMPURITIES BY MEANS OF ABSORPTION
OF RADIO WAVES BEHIND A SHOCK WAVE

T.V. Bazhenova, Yu.S. Lobastov

Moscow

In order to obtain a high degree of gas ionization at still relatively low temperatures ($\sim 2000\text{-}4000^{\circ}\text{K}$), it is customary to add to the heated gas easily ionized impurities. In addition, in experiments on the heating of a gas in adiabatic and shock tubes, the presence of an indeterminate amount of different impurities is unavoidable, some of which exert an influence on the thermal ionization of the gas.

In this paper we present results of experiments on the measurement of the absorption of radio waves by argon heated in a shock tube to a temperature $2000\text{-}4000^{\circ}\text{K}$. Simultaneously, we measure the velocity of the shock wave and the pressure behind it with the aid of piezoelectric pressure transmitters and Schlieren apparatus with drum type slit scanning. The measured damping decrement of the radio waves can be related by means of the well-known formulas with the concentration of the free electrons behind the shock wave. The ionization potential of the impurity, which gives the basic number of electrons n_e at the given temperatures, can be determined with the aid of the Saha formula from the slope of the straight line representing the dependence of the logarithm of n_e^2 on $1/T$. The value of the temperature and of the gas pressure behind the shock wave is determined from the measured value of its rate of propagation and from the initial conditions with the aid of the conservation laws for the direct jump. After the nature of the

easily ionized impurity is determined, the initial concentration of this impurity is found with the aid of the Saha formula.

§1. DESCRIPTION OF EXPERIMENTAL SETUP

The experimental setup is shown in Fig. 1.

A. The high-pressure chamber K_1 is connected through a system of metallic valves with a RVN-20 vacuum pump and with a standard vacuum meter on one side, and with a manometer for 25 atmospheres and 2 bulbs (through reduction valves) on the other.

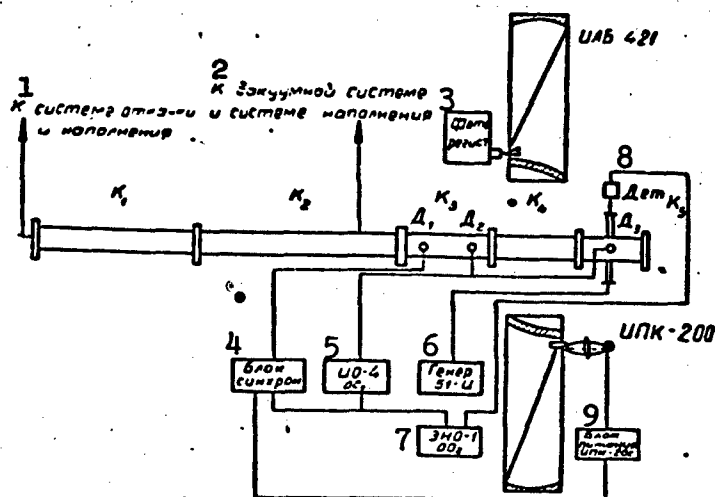


Fig. 1. 1) To evacuation and filling system; 2) to vacuum system and filling system; 3) photoregister; 4) synchronization block; 5) LO-4 oscilloscope; 6) ST-4 generator; 7) ENO-1 oscilloscope; 8) detector; 9) power supply IPK-200s.

B. The low-pressure chamber consists of four sections K_2 , K_3 , K_4 , and K_5 . Section K_2 is a copper waveguide 70 x 70 mm in cross section, 5 m long, with wall thickness 3-2.5 mm, with flanges made of ST-3 silver soldered on both ends. In order to protect K_2 against deformation during high-pressure experiments, this section is contained in steel clamps 15 mm thick. Section K_3 is made of duraluminum ingot 500 mm long and has an internal channel 70 x 70 mm. In this section are in-

serted two pairs of electric pressure transmitters D_1 and D_2 [1], and also a two-way vacuum valve, through which K_3 is connected to the measuring vacuum tube LT-2 and to the filling system. The same section is used to pump out the entire low-pressure chamber by means of a VN-1 pump. The section K_3 has an internal channel 70×70 mm and two ground glasses for the registration of the processes with the aid of a IAB-451 Toepler installation. The IAB-451 works with an IPK-200 flash lamp and a photographic register, which has a linear film speed $v = 117$ m/sec.

Section K_5 (MVK-2 chamber), with the aid of which the radio measurements are carried out, consists of a 70×70 mm waveguide section 140 mm long, with flanges on the ends. Two rectangular openings are cut on the side of the waveguide, and through these two antennas A_1 and A_2 are introduced into the chamber. In order to keep the system sealed, the following measures were adopted: the antennas were carefully soldered to the chamber, flush with the internal channel and rubber gaskets 2.5 mm thick were placed at the inlet A_1 and at the outlet A_2 (P_1 and P_2), between the cable ending kab_1 and A_1 , A_2 , and the detector. The waveguide slots in the antennas were covered with foamed plastic inserts that were transparent to the radio waves. In the upper part of the MVK there is a brass boss P , in which a hole is cut for the piezoelectric transmitter D_3 . The chamber is tuned for a standing wave minimum by means of a moving end piston.

§2. MEASURING APPARATUS AND CALCULATION OF n_e FROM THE READINGS

During the performance of the present investigation, the apparatus was used to measure the velocity of the shock waves and to measure the absorption of radio waves in shock waves.

The measurement of the velocity was carried out with the aid of three piezoelectric pressure transmitters, a synchronization block, and a cathode-ray oscilloscope of the IO-4 type.

The shock wave passes in succession past the transmitters D_1 , D_2 , and D_3 . A signal from D triggers the synchronization block which applies a triggering signal to the IO-4 oscillograph, which operates in the driven sweep mode. D_2 and D_3 are connected to the input of the IO-4 oscillograph amplifier. From the pressure oscillogram recorded with the aid of these two transmitters one can calculate the speed of the shock wave if the sweep duration is known.

For exact measurement of the length of the shock probe, the IAB-451 installation was used.

Absorption of radio waves was measured with the aid of a 3-cm 51-I generator, a MVK-2 chamber, a detector, and a ENO-1 oscillograph, which had a broad band amplifier and operated in the driven sweep mode.

The 51-I generator was tuned to the maximum radiated power. The output power control dial on the attenuator was set at an attenuation 5-10 db in order to exclude the reaction of the gasdynamic process on the reflex klystron.

Before carrying out the experiment, both the level of the total passage of the signal, and the level of the total absorption (reflection) were absorbed on the ENO-1 screen, by introducing a large value of attenuation (100 db) in the attenuator.

Thus, the presence of a DC amplifier, which passed the DC component of the signal, made it possible to carry out experiments with the aid of unmodulated oscillations and greatly simplified the reduction of the experimental data obtained.

The sweep of the ENO-1, like that of the IO-4, was triggered by a signal obtained from the synchronization block. Therefore the starts of both oscillograms coincide in time. The transmitter D_3 is located exactly halfway between the antennas A_1 and A_2 . This makes it possible to determine which section of the shock wave corresponds to the given

absorption of radio waves.

To calculate the degree of ionization from the readings of the apparatus, it is first necessary to calibrate the receiving apparatus with the aid of the attenuator. A null signal from the generator is applied through the antennas and the detector to the input of the oscillograph amplifier. By varying the amplitude v_1 of the signal coming from the generator, we obtain the dependence of the deflection of the beam \underline{l}_1 on the ENO-1 oscillograph screen on v_1 . We then plot $\underline{l}_1/l_{\max} = f(v_1/v_{\max})$, where v_{\max} is taken with an attenuation on the order of 5-10 db in the attenuator.

We then determine from the experimentally obtained oscillogram the ratio v_1/v_{\max} , where \underline{l}_{\max} is obtained for the same attenuation at which the calibration was carried out. The corresponding ratio v_1/v_{\max} will indeed be the sought radio wave transmission coefficient A_1 . Knowing A_1 , the temperature T , and the pressure p we can determine the number of electrons per cubic centimeter n_e .

Indeed [2],

$$n_e = \frac{m\sigma(\omega^2 + v^2)}{e^2 v}, \quad (1)$$

where σ is the conductivity (sec^{-1}); v is the number of collisions (sec^{-1}); m is the electron mass; e is the electron charge;

$$\sigma = \frac{\delta^2 e^2}{2\pi m}, \quad (2)$$

where δ is the radio wave damping decrement (cm^{-1}),

$$v = v_0 \sqrt{\frac{T_0}{T}} \frac{p}{p_0}, \quad (3)$$

consequently,

$$v_0 = V_{\text{sat}} \cdot K \cdot \text{const} = 4 \cdot 10^3 \text{ sec}^{-1},$$

$$v = 5.02 \cdot 10^{12} \frac{p}{\sqrt{T}}. \quad (3a)$$

$$A = e^{-v}, \quad (4)$$

where r is the thickness of the layer of gas (cm) absorbing the radio waves.

In our case $r = 7$ cm.

Thus,

$$n_e = 0.185 \frac{(39.5f^2 - v^2)}{v} \ln \frac{1}{A}. \quad (5)$$

where f is the frequency of the radio waves from the generator, in cps.
(In our case $f = 10^{10}$ cps.)

§3. MEASUREMENT OF THE DEGREE OF IONIZATION OF THE IMPURITIES IN THE ARGON

The experiments were carried out at pressures (in the low-pressure chamber) on the order of 10 mm, and at incident shock wave velocities from 3 to 5 m/sec. The absorption of the radio waves was measured only in the reflected waves with parameters $p \sim 10$ atm; $T = 2000 + 4000^\circ\text{K}$. As is well known, the ionization becomes noticeable in argon only starting with $T \sim 10,000^\circ\text{K}$, and therefore ionization at $T < 10,000^\circ\text{K}$ must apparently be attributed to the impurities contained in the argon and on the tube walls. The task of the control experiments was precisely to clarify the nature and amount of these impurities.

It was also necessary to take into account the bending of the radio waves around the ionized probe traveling past the antennas. For this purpose, several Toeplergrams were plotted (Fig. 2), with the aid of which the length of both the incident and the reflected shock probes were determined. For those modes at which the experiments were carried out, the probe dimensions turned out to be much larger than the slits in the antennas. Therefore, in our case the effect of bending around can be neglected.

From the velocity of the incident waves we calculated the temperature, the pressure, and the velocity of the reflected wave (T_2 , P_2 , and M_2 , respectively).



Fig. 2

$$T_1 = \frac{[2\gamma M_1^2 - (\gamma - 1)][(\gamma - 1)M_1^2 + 2]T_0}{(\gamma + 1)^2 M_1^2}; \quad (6)$$

$$M_2 = \left[\frac{2\gamma M_1^2 - (\gamma - 1)}{2 + (\gamma - 1)M_1^2} \right]^{\frac{1}{2}}; \quad (7)$$

$$T_2 = \frac{[2\gamma M_2^2 - (\gamma - 1)][(\gamma - 1)M_2^2 + 2]T_1}{(\gamma + 1)^2 M_2^2}; \quad (8)$$

$$p_1 = \frac{2\gamma M_1^2 - (\gamma - 1)}{\gamma + 1} p_0; \quad (9)$$

$$p_2 = \frac{2\gamma M_2^2 - (\gamma - 1)}{\gamma + 1} p_1. \quad (10)$$

In our case for argon $\gamma = 1.67$, $T_0 = 293^\circ\text{K}$.

Thus, by measuring experimentally the absorption of the radio waves A, and knowing p_0 and M of the incident wave, we can determine P_1 , T_1 , P_2 , T_2 , v , and n_e . Writing the Saha formula in the form

$$\ln n_e^2 = \ln K + \ln p + \frac{1}{2} \ln T - \frac{\varphi}{kT},$$

where K is a certain constant independent of p and T, we obtain the dependence

$$\ln n_e^2 - \ln p - \frac{1}{2} \ln T$$

on $1/T$ in the form of a line. The slope of this line gives the value of φ/k .

In the experiments performed, the ionization potential of the impurities turn out to be 5.1 (Fig. 3), which corresponds to the ionization potential of sodium.

From the experimentally known values of n_e and φ we can establish the concentration of the sodium impurity in the gas. For this purpose we rewrite Saha's formula in the form

$$\frac{N_e^2}{N_{Na}} = \frac{K_p}{kT} = \left(\frac{2\pi m K}{h^2} \right)^{3/2} T^{3/2} e^{-\frac{V}{kT}}. \quad (11)$$

Here N_e is the number of electrons in a gram-mole of the vapor and N_{Na} is the number of sodium atoms in a gram-mole of gas.

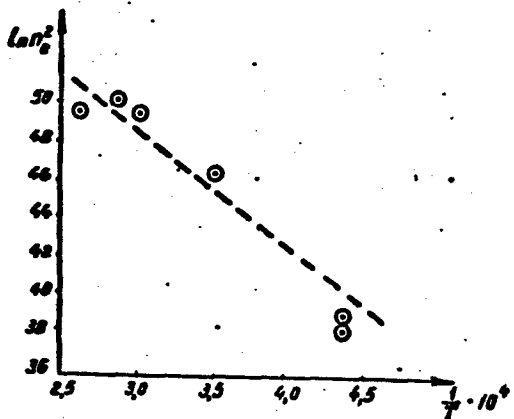


Fig. 3

In order to convert to the number of particles per cubic centimeter, we introduce the factor $V_{p,T}$, corresponding to the volume of a gram-mole of gas at a temperature and pressure corresponding to the experimental conditions. Then the number of atoms of sodium per cubic centimeter is expressed in terms of the number of electrons in the following form:

$$n_{Na} = V_{p,T} \frac{n_e^2 e^{\frac{V}{kT}}}{\left(\frac{2\pi m K}{h^2} \right)^{3/2} T^{3/2}}$$

Reduction of the data of Fig. 3 has shown that the content of sodium vapor in argon is on the order of $10^{-5}\%$.

The authors are grateful to Corresponding Member of the USSR Academy of Sciences, A.S. Predvoditelev, for valuable hints made concerning the present work.

REFERENCES

1. S.G. Zaytsev, PTE [Instruments and the Technique of Experiment],

6, 1958.

2. Y.L. Al'pert and V.L. Ginzburg, Rasprostraneniye radiovoln [Propagation of Radio Waves], Gostekhizdat [State Publishing House for Technical and Theoretical Literature], 1958.

EXPERIMENTAL DETERMINATION OF THE CONCENTRATION OF
CHARGED PARTICLES IN ARGON AND KRYPTON
BEHIND A SHOCK WAVE

V.N. Alyamovskiy, A.P. Dronov, V.F. Kitayeva,
A.G. Sviridov, N.N. Sobolev
Moscow

The present paper pertains to a cycle of investigations carried out at the Physics Institute of the Academy of Sciences on a spectroscopic study of the state of a gas behind a shock wave [1], and is devoted to the investigation of the state of argon and krypton behind a shock wave.

Experimental study of the state of inert gases is interesting from two points of view [2]. First, after the passage through them of a shock wave of an intensity that can be readily obtained under laboratory conditions, they are heated to relatively high temperatures, $10,000-15,000^{\circ}\text{K}$. Second, gasdynamic calculations of the state of inert gases are relatively simple and do not call for additional supplementary data, which must be used in the calculation of the state of more complicated molecular gases. This makes it possible to obtain rather simply the calculated data, to compare them with experiment, and thereby establish the validity of the premises on which the calculations are based.

One of the methods for the investigation of high-temperature plasma is based on a study of the contours of the spectral lines. An investigation of line contours makes it possible to obtain information on the concentration of the charged particles in the plasma behind the

shock wave, and in the case of thermal equilibrium it also furnishes data on the plasma temperature. It must be noted that the conditions for the excitation of lines in a plasma behind a shock wave are most suitable for a comparison of experimental data with the existing line broadening theories, since the plasma behind a shock wave is sufficiently homogeneous and is not perturbed by any external fields, unlike the ordinary employed electric light sources (arc, spark, etc.).

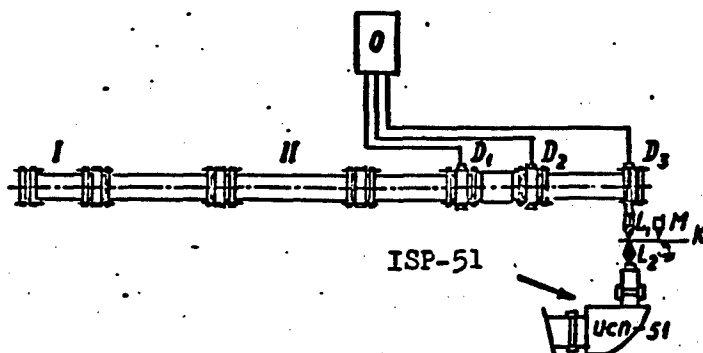


Fig. 1. Diagram of experimental setup.

In the present investigation we studied the hydrogen lines in krypton [3] behind an incident shock wave and in argon [4] behind a reflected shock wave.

To obtain shock waves, cylindrical shock tubes were used, made of metal for the argon investigation and of glass for the krypton investigation. The pushing gas was hydrogen. The low-pressure chamber was filled with argon or krypton with small addition of hydrogen, from 1-5% in krypton and about 2% in argon. The velocity of the incident shock wave was measured in the metallic tube with the aid of ionization transmitters and in the glass tube by registration of the light signals arriving from the probe to the photomultipliers.

In argon, the contour of the hydrogen line H_{β} was investigated behind the reflected shock wave. The experimental setup is shown in Fig. 1. The H_{β} line was registered photographically with the aid of an

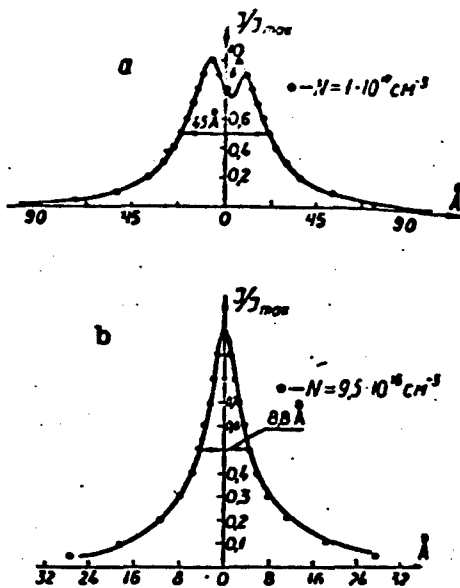


Fig. 2. Contours of hydrogen lines: a) H_{β} ; b) H_{α} . Solid lines — experimental contour; dotted lines — contour calculated by the theory of Griem, Kolb, and Shen.

ISP-51 spectrograph with a central camera ($f = 270$ mm). The radiation entering the spectrograph came from an end portion of the tube about 1 cm long. The radiation spectrum was swept in time by means of a rotated disk with holes placed in front of the spectrograph slit. The speed of rotation of the disk was chosen such as to prevent overlap of pictures from neighboring holes, and the resolution amounted to approximately 25 μ sec.

The time-swept spectrum consisted of two clearly delineated regions. The first region with duration ~ 100 μ sec pertained to the radiation after the first reflection, while the second pertained to the radiation after the succeeding reflections. The photometry of the H_{β} contour was carried out in the first region. Figure 2-a shows one of the obtained contours of the H_{β} line. Under the conditions investigated by us, the H_{β} line is characterized by a considerable half width (40-60 Å),

the presence of an intensity dip in the center of the line, and asymmetry. The distance between the violet and red maxima of the H_{β} line increased in proportion to the increase in the half width.

In [3, 4], in order to determine the concentration of the charged particles in the plasma behind the shock wave, the experimental contours were compared with the theoretical ones, calculated from Holtsmark's theory. However, as is well known, this theory is incomplete, and takes account of only the statistical action of the ions, neglecting the effect of electron impact broadening. In comparing the experimental and theoretical contours, this has led to the result that the contour of the H_{β} hydrogen line fitted the Holtsmark theory satisfactorily only in the skirt, while the central part of the line was not described by the Holtsmark theory. As a consequence of this, a discrepancy arose in the concentration of the charged particles determined from the half width and from the contour of the line. Recently a new theory was published by Griem, Kolb, and Shen [5] (G.K.S.). These authors calculated the distribution of the intensity in the hydrogen lines with allowance for the broadening both by the ions and by the electrons. Broadening by electrons was considered from the point of view of the impact theory with allowance for the transitions induced by the electrons between the Stark components (which split in the field E produced by the ions) of each individual level. For the ion field, the Ecker distribution function is used, which includes the effect of electron screening and ion-ion correlations. We have compared experimentally the H_{β} line contours obtained with the GKS theoretical contours. The results of the comparison of one of the contours of the H_{β} line are shown in Fig. 2-a. From 2-a we see that the experimental contour is described quite satisfactorily by the GKS theory. Figure 2-b shows by way of an example also an experimental contour of the H_{α} hy-

drogen line, obtained behind the shock wave in krypton, and a comparison is made with the GKS theory. The agreement between theory and experiment is fully satisfactory.

Figure 2 shows clearly that the GKS hydrogen line broadening theory, in spite of several simplifying assumptions and approximations, describes the phenomenon correctly. It must be emphasized here, however, that for narrower hydrogen lines the agreement between theory and experiment at the centers of the lines is less satisfactory than in Fig. 2, owing to the distorting influence of the Doppler effect and of the apparatus function.

TABLE I

1 Воздушное давле- ние (в атм)	2 Износ давле- ния смеси аргон + 2% води- ческого газа (в ми- нистерах)	3 скорость (в километрах в секунду)	4 Падающая ударная волнка	5 число Маха	6 Поглощени- е $\delta\lambda_{H\beta}$ (в Å)	7 напряженность поля E_0 (в киловольтах)	8 концентрация $N_i \cdot 10^{-17}$ см $^{-3}$	9 Параметры ударной волной аргона за отраженной (расчетные)	10 $N_i \cdot 10^{-17}$ см $^{-3}$	11 плотность n_5	12 степень иони- зации a_5	13 температура T_5 (в $^{\circ}$ К)	14 давление p_5 (в мм рт. ст.)
75	0.26	4.52	14.1	45	80	1.0	1.4	3.8	0.36	12700	490		
84	0.26	4.60	14.4	63	115	1.7	1.5	4.0	0.37	12900	530		
110	0.26	4.78	14.9	65	115	1.7	1.7	4.2	0.41	13300	570		
75	0.45	—	—	41	75	0.9	—	—	—	—	—		
90	0.45	4.06	12.7	42	75	0.9	1.3	4.9	0.26	12600	640		
115	0.78	3.92	11.9	54	96	1.3	1.4	6.6	0.21	12500	870		
110	1.16	3.60	11.2	52	96	1.3	1.4	8.5	0.17	12200	1070		

- 1) High pressure (atm); 2) low pressure of the mixture of argon + 2% hydrogen (in mm Hg); 3) velocity (km/sec); 4) incident shock wave; 5) Mach number; 6) half width $\delta\lambda_{H\beta}$ (in Å); 7) field intensity E_0 (in kv/cm); 8) concentration $N_i \cdot 10^{-17}$ cm $^{-3}$; 9) parameters of argon behind the reflected shock wave (calculated); 10) density; 11) degree of ionization a_5 ; 12) temperature T_5 in ($^{\circ}$ K); 13) pressure p_5 (in mm Hg).

From a comparison of the experimental and theoretical H_β contours we determine the value of the normal intensity of the intermolecular field E_0 , while from the relation $E_0 = 2.61eN^{2/3}$ we determine the con-

centration of the charged particles in the plasma behind the reflected shock wave. The results obtained are listed in Table 1. The same table shows the values of N_1 ₅* for argon behind the reflected shock wave, which we obtained by linear extrapolation of the Kantrowitz data [6]. Within the limits of experimental accuracy, the agreement between the values of N_1 , calculated from the H_β line contour, and those obtained from gasdynamic calculations following Saha is satisfactory.

In investigations made in krypton behind the incident shock wave, we registered the lines H_α , H_β , and H_γ . The H_γ line was observed up to $M = 11.5$ and after which, because of the strong broadening, it merged with the background. The H_δ was not observed at all. The H_α and H_β lines were used to determine the concentrations of the charged particles in the krypton plasma behind the incident shock wave in a relatively broad range of variation of the shock wave velocity (10-15 M). The concentrations N_1 were obtained from H_α and H_β by comparing the experimental distribution of the intensity in the line with the distribution calculated by the GKS theory.

The results of the determination of the charged particle concentration in krypton from the H_α and H_β lines at an initial pressure $p_1 = 5.2$ mm Hg are shown in Fig. 3 as a function of M . The solid curve 1 in the same figure shows the theoretical dependence of N_1 on M for pure krypton and for krypton with 2.5 and 4.0% hydrogen impurity.

The state of the krypton behind the shock wave was calculated on the basis of the laws of conservation of matter, momentum, and energy, and also the equation of state of the gas and the Saha equation, assuming single ionization. No account was taken in the calculation of the reduction in the ionization potential of the krypton. It was assumed that thermodynamic equilibrium is established behind the shock wave. The calculations for pure krypton are plotted in Figs. 4 and 5.

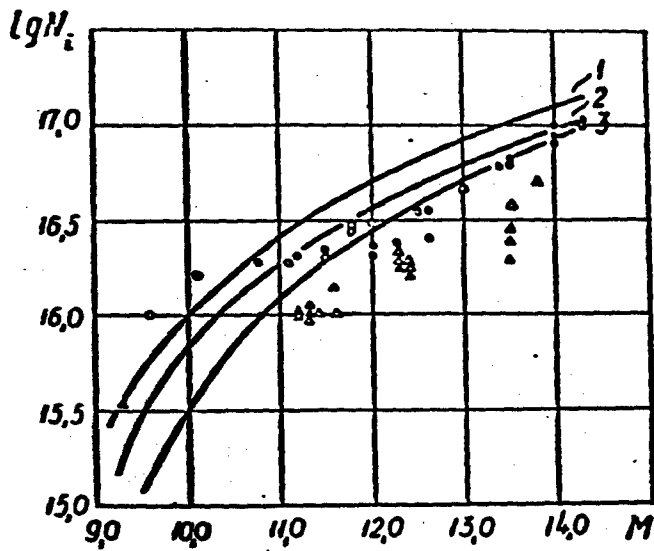


Fig. 3. Results of experimental determination of the concentration of charged particles from the hydrogen lines H_{α} and H_{β} :

Symbols: $\bullet H_{\alpha}$ } with hydrogen concentration
 $\circ H_{\beta}$ } less than 1%
 ΔH_{α} } with more than 1% H_2 added.
 $\blacktriangle H_{\beta}$

Solid curves — calculated values: 1) pure krypton; 2) with 2.5% H_2 added; 3) with 4.0% H_2 added.

It is seen from Fig. 4 that the temperature of the krypton plasma at $p_1 = 5.2$ mm Hg increased from 2000 to $17,000^{\circ}\text{K}$ as M increased from 5 to 30. Up to $M = 9$ ($T = 7000^{\circ}\text{K}$) the ionization is insignificant (see Fig. 5), so that the plasma temperature is independent of the initial pressure p_1 . For $M > 9$ the ionization begins to play an appreciable role. For small p_1 (and consequently small p_2), the value of the degree of ionization α is higher than for large pressures, and therefore all the $T(M)$ curves for small p_1 lie below the curves for high pressures. As M varies from 9 to 30, the degree of ionization increases from 10^{-4} to 0.9, and a particularly sharp increase is observed in the M interval

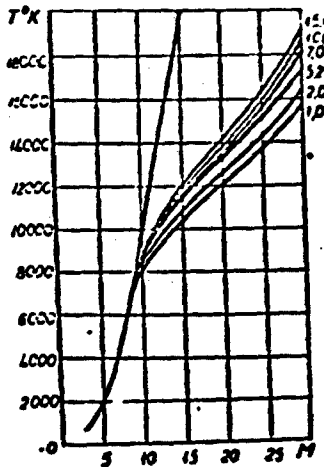


Fig. 4. Dependence of the plasma temperature behind the shock wave front in pure krypton on the velocity for initial pressures $p = 1.0, 2.0, 5.2, 7.0, 10.0$, and 15 mm Hg in the low-pressure chamber.

from 9 to 15.

It must be noted that in view of the neglect of losses for radiation and for secondary ionization, the results of the calculation given for $M > 20$ must be approached with caution (the temperature, the degree of ionization, and the concentration of the charged particles behind the shock wave may be lower than calculated for M values larger than 20).

Let us turn to a discussion of Fig. 3.

As can be seen from the figure, the experimental points corresponding to krypton with hydrogen impurity less than 1% lie near the theoretical curves with hydrogen content of 2.5 and 4%. This may be due to several factors: first, to the insufficient reliability with which the concentration of the hydrogen in the krypton was determined, second with failure to take into account the various losses, including those for radiation. Finally, a fact acting in the same direction may

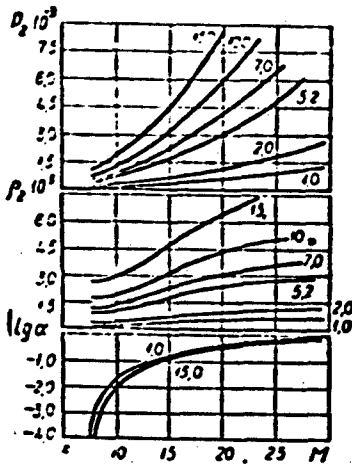


Fig. 5. Dependence of the degree of ionization α_1 , the pressure P_2 (mm Hg), and the density ρ_2 (g/cm^3) behind the shock wave front in pure krypton on the velocity. Symbols: 1) for $p_1 = 1.0 \text{ mm Hg}$; 2) for $p_1 = 2.0 \text{ mm Hg}$; 3) 5.2 mm Hg ; 4) 7.0 mm Hg ; 5) 10.0 mm Hg ; 6) 15.0 mm Hg .

be that, unlike the experiments with argons, the photographic plates register in this case the radiation from an inhomogeneous probe integrated over the time. Which of these factors plays the decisive role is difficult to say. However, in one way or another the discrepancy between the theoretical gasdynamic data and the experimental ones emphasizes the need for checking the gasdynamic calculations by experiments.

In conclusion, on the basis of our experiment, we deem it necessary to note that to determine the concentrations of charged particles in a plasma, in a range from several times 10^{15} cm^{-3} to several times 10^{17} cm^{-3} , we can recommend the use of the H_β line, and the determination can be carried out simply by using the half width of the H_β line, without a detailed investigation of the contour. To determine concen-

trations larger than 10^{17} cm^{-3} , the H_{α} line is perfectly suitable. On the other hand, to determine concentrations lower than 10^{17} by means of the H_{α} line, it is necessary to bear in mind, on the one hand, the distorting action of the Doppler effect, which is not taken into account in the GKS theory, and on the other hand it is essential to study the contour of the H_{α} line using a spectral instrument with large dispersion.

REFERENCES

1. Ye. M. Kudryavtsev, N. N. Sobolev, L. N. Tunitskiy, F. S. Fayzullov, Pirometricheskoe issledovaniye sostonyaniya gaza az udarnoy volnoy [Pyrometric Investigation of State of Gas Behind Shock Wave], in present collection.
2. S. R. Kholev, in collection entitled Voprosy magnitnoy gidrodinamiki i dinamiki plazmy [Problems of Magnetohydrodynamics and Plasma Dynamics], Izd-vo AN Latv. SSR [Publishing House of the Academy of Sciences of the Latvian SSR], Riga, 1959.
3. A. P. Dronov, A. G. Sviridov, N. N. Sobolev. Optika i spektroskopiya [Optics and Spectroscopy], 10, 312, 1961.
4. V. N. Alyamovskiy, V. F. Kitaeva, Optika i spektroskopiya, 8, 152, 1960.
5. H. R. Griem, A. C. Kolb, K. J. Shen. Phys. rev., 116, 4, 1960; Stark broadening of hydrogen lines in plasma. U. S. naval res. lab. Report 5455, March 4, 1960.
6. E. L. Resler, Shao-Chi-Lin, A. Kantrowitz. J. appl. phys., 23, 1390, 1952.

Manu-
script
Page
No.

[Footnote]

- 381 In agreement with [6], the parameters of the argon behind
the reflected shock wave are designated in Table 1 by the
subscript 5.

PYROMETRIC INVESTIGATION OF A GAS
BEHIND A SHOCK WAVE

Ye.M. Kudryavtsev, N.N. Sobolev, L.N. Tunitskiy, F.S. Fayzullov
Moscow

In recent years the need for solving the problem of the motion of bodies with hypersonic velocities, it has become acutely necessary to investigate both the gasdynamic phenomena occurring at these velocities, and the properties of gases at high temperatures and the kinetics of the processes occurring behind a shock wave. In all these investigations it is necessary to know the parameters of the gas characterizing its state behind the shock wave. These parameters can be calculated by the methods of gasdynamics. However, the existing one-dimensional theory is rather approximate. It is based, in addition to the conservation laws, on a whole series of idealizations: instantaneous formation of the shock wave front, one dimensionality of the flow, the absence of energy losses to viscosity and heat conductivity (and, in the case of high temperatures, also to radiation), and instantaneous establishment of thermodynamic equilibrium behind the front of the shock wave. Only direct experiment will show the extent to which these idealizations are valid. If it is recognized that the temperature of the gas behind the shock wave is the most sensitive parameter, it becomes clear that experiments must be set up on the measurement of the temperatures and the experimental results compared with theory. It was therefore decided to develop a method for measuring temperatures, to use this method for a pyrometric investigation of several gases, and to compare

the experimental data with the theory.

The objects of the investigation were nitrogen, air, argon, and carbon dioxide, which are gases of greatest interest from the practical point of view.

The observations were carried out both behind an incident and behind a reflected shock wave in a shock tube about 5 m long with inside diameter 92 mm. The working gas used was hydrogen at a pressure from 20 to 120 atm. The initial pressure p_1 of the investigated gas was chosen in the range from 2 to 150 mm Hg. Figure 1 shows schematically the shock tube and the apparatus used in the investigations (a detailed description of the apparatus is given in [1, 2]).

According to the one-dimensional gasdynamic theory, the instantaneous opening of the diaphragm gives rise to a plane shock wave which propagates over the investigated gas with constant velocity U_s and compresses and heats the gas rapidly (within a time equal to several collisions between molecules). At the same time, a region of homogeneously heated gas is produced between the front of the shock wave and the contact surface, called a plug, the length of which increases linearly with propagation of the shock wave. After reflection of the shock wave from the end of the tube, the shock wave passes through the plug, further compressing and heating the investigated gas (if the specific heat is constant we have $T_5 \approx 2T_2$, $P_5 = (10-20)P_2$).*

To compare the results of the pyrometric investigation with the one-dimensional theory it is necessary to know reliably the velocity of shock wave propagation U_s in each experiment, to investigate the distribution of shock wave velocity along the tube, and also to determine the length of the homogeneous flux (plug). All this information concerning the shock wave and the flux was obtained experimentally [2, 6].

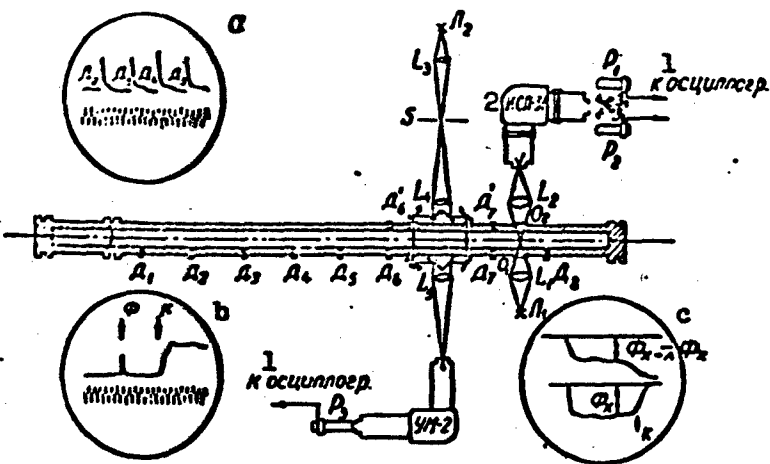


Fig. 1. Diagram of the apparatus: D_1, D_2, \dots, D_8 - ionization transmitters. Setup for investigations with the aid of the Schlieren method: L_2 - type SVDSH-1000 mercury lamp; L_3 - condenser ($f = 50$ mm); s - slit; L_4 - objective of collimator ($f = 800$ mm); L_5 - objective ($f = 800$ mm); P_3 - FEU-19 photomultiplier. Setup for temperature measurement: L_1 - DKSSH-1000 xenon lamp; L_1 and L_2 - objectives ($f = 90$ mm); O_1 and O_2 - windows; Z_1 and Z_2 - mirrors; P_1 and P_2 - FEU-17 photomultipliers. Appearance of typical oscillosograms for the measurement of the following: a) velocity of shock waves; b) length of plug (F - front of shock wave, K - start of contact region); c) temperature (F_{kh} - gas radiation flux in the spectral line, $F_{kh+1} - F_{kh}$ - radiation flux when light from the comparison source passes through the gas). 1) To oscillosograph; 2) ISP-31.

The velocity of the shock wave U_s was measured with the aid of a series of ionization transmitters located along the tube. Figure 1-a shows the form of the oscillosograms obtained in measurements of the velocity.

As the result of the investigation of the distribution of the shock wave velocity along the tube, it was established that the fact that the diaphragm is not instantaneously opened causes the velocity of the shock wave to be variable and to reach its maximum value not

immediately but only over a distance of about 2.5 meters from the diaphragm. The velocity of the shock wave then gradually decreases. This maximum velocity remains less than the theoretical value calculated for the given pressure drop on the diaphragm, owing to the energy lost to viscosity and heat conduction during the process of shock wave formation.

To determine the length of the plug we used a photoelectric version of the Schlieren method, a diagram of which is shown in Fig. 1. The same figure shows the appearance of a typical oscillogram (Fig. 1-b). This simple setup enables us not only to measure the length of the plug, but also to investigate the delay in the glow from the individual spectral lines relative to the front of the shock wave, and to carry out control experiments of the shock wave velocity [2].

A study of the flux with the aid of the photoelectric Schlieren method has shown that no contact surface separating the working and the investigated gases exists as such, but a rather extensive contact region is observed, which does not always have a clear-cut beginning. As a result of this, the length of the plug reaches only approximately half the theoretical value. It was also shown with the aid of the Schlieren method that the glow of the sodium D line begins directly in the front of the shock wave and reaches a maximum after 10-20 μ sec.

Pyrometric investigations of the gas behind the shock wave were carried out with the aid of a photoelectric generalized method for the inversion of spectral lines which we have developed [2, 5]. The gist of the method is to register simultaneously the absorption and emission intensities in the spectral line. The use of a two-channel optical system with two photomultipliers and a double beam pulsed oscillograph makes it possible to register simultaneously the gas radiation flux F_{kh} and the flux $F_{kh+1} - F_{kh}$ of the radiation produced when the light

from the comparison source passes through the gas. A typical oscillogram is shown in Fig. 1-c. Here

$$\Phi_s = a C_1 \lambda^{-3} \exp(-C_2 / \lambda T_s) \delta \lambda (d/f)^2 sh$$

and

$$\Phi_{s+s} - \Phi_s = \Phi_s - a C_1 \lambda^{-3} \exp(-C_2 / \lambda T_s) \delta \lambda (d/f)^2 sh,$$

where $\delta \lambda$ is the width of the spectral line, a the absorption ability in the line (the line shape is assumed rectangular), d/f is the relative aperture of the camera objective, s and h are the width and height of the exit slit of the monochromator, C_1 and C_2 are the radiation constants, T_{kh} is the true gas temperature, and T_1 the brightness temperature of the comparison source.

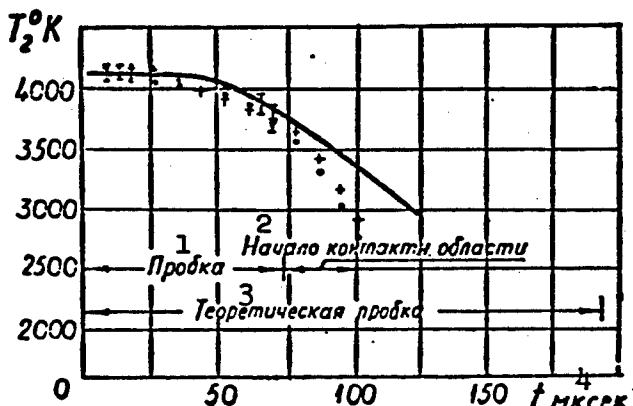


Fig. 2. Temperature distribution along the plug for the case of nitrogen ($p_1 = 10$ mm Hg). Continuous curve — temperature calculated with allowance for the variation of the shock wave velocity along the tube. Dots — experimental data: \circ — obtained from sodium D lines, $+$ — from barium line. Each point is an average of six experiments ($\bar{U}_s = 3.14$ km/sec). Data on the length of the plug were obtained with the aid of the Schlieren method. 1) Plug; 2) start of contact region; 3) theoretical plug; 4) μ sec.

From the relations given it is clear that by using Wien's formula and Kirchhoff's law and knowing the brightness temperature of the com-

parison source it is possible to determine the true gas temperature from the ratio of these two measured fluxes:

$$T_2 = T_1 \left[1 + \frac{\lambda T_1}{C_2} \ln \left(1 - \frac{\Phi_{x+L} - \Phi_x}{\Phi_x} \right) \right]^{-1}.$$

A pyrometric investigation of the gas behind the front of the shock wave [3/4, 6] has shown that there exists a definite correlation between the temperature distribution over the plug and the distribution of the shock wave velocity along the tube. The presence of such a correlation is illustrated by Fig. 2. The experimental data are represented by points. Each point is the average of six experiments ($p_1 = 10$ mm Hg, nitrogen; $U_s = 3.14$ km/sec). Curve represents the temperature distribution calculated with allowance for the variation of the shock wave velocity along the tube. It is seen from the same figure that the temperatures measured from the NaI and BaII lines agreed with each other, within the limits of experimental error, thus confirming further the existence of thermodynamic equilibrium in the nitrogen and air behind the shock wave.

The results of the measurement of the air and nitrogen temperature behind the shock wave over a wide range of initial pressures ($p_1 = 2-50$ mm Hg) and Mach numbers ($M = 6-12$) is in good agreement with the data of the theoretical calculations, thus indicating the correctness of the theory (Figs. 3 and 4).

In experiments with air under certain conditions ($p_1 = 50$ mm Hg and $U_s = 1.9-2.3$ km/sec) one observes in the contact region temperatures that greatly exceed the temperature of the plug. This temperature rise is due to the combustion of the hydrogen in the mixing zone.

At small initial nitrogen pressures and low temperatures ($p_1 = 10$ mm Hg, $T_2 = 2000-2500^{\circ}\text{K}$), immediately behind the front of the shock wave, during $10-30$ μsec , one observes a low temperature which may be

connected with the delay in the establishment of the equilibrium over the vibrational degrees of freedom of the N_2 molecule, since the measured excitation temperature is more readily determined by the effective vibrational temperature than by the translational one.

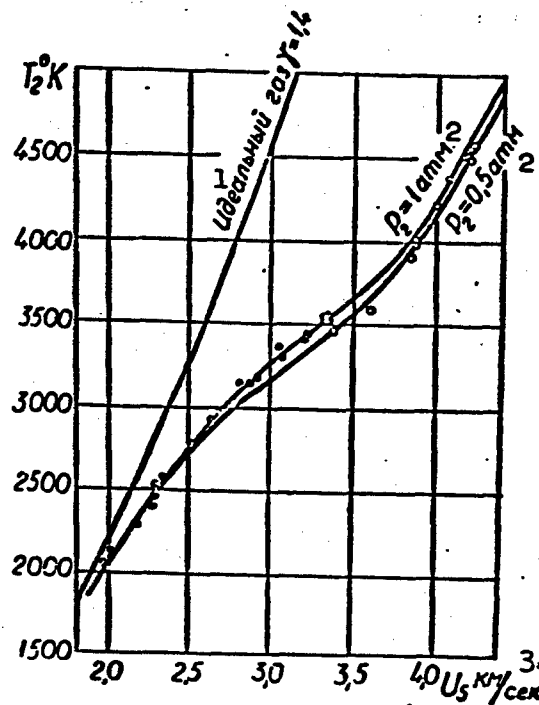


Fig. 3. Dependence of the temperature of the air behind the shock wave on the velocity of the shock wave.
Curves - calculation for $T_1 = 293^\circ\text{K}$.
Points - experiment: o) $p_1 = 10 \text{ mm Hg}$;
o) $p_1 = 2 \text{ mm Hg}$. 1) Ideal gas; 2)
atmospheres; 3) km/sec.

In pyrometric investigations of argon [3/4] it was established that the measured barium ion excitation temperatures at plug pressures ~ 0.4 and 4 atm are, respectively, 1000° and 400° lower than the equilibrium value (Fig. 5); with increasing pressure, the measured temperatures approach the equilibrium temperature and coincide with it at pressures $p_2 \sim 12$ atm. The observed disparity is obviously connected with the fact that the efficiency of the collisions between the barium

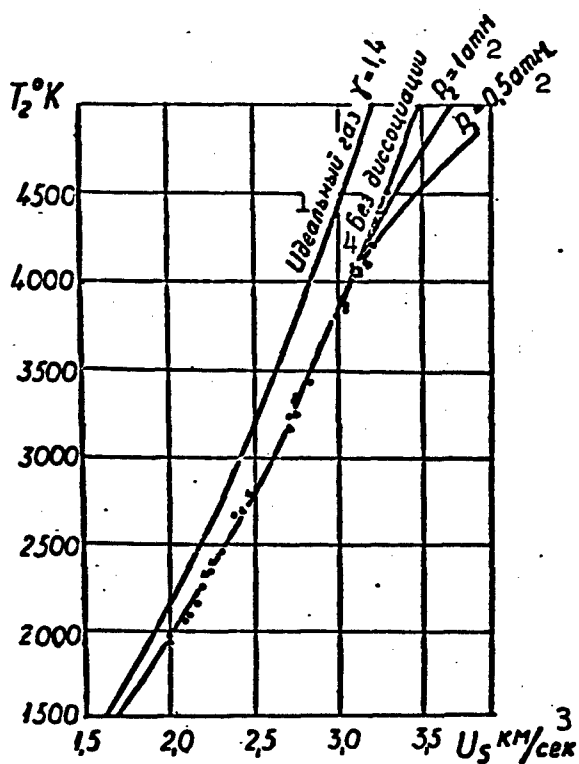


Fig. 4. Dependence of the temperature of nitrogen behind the shock wave on the shock wave velocity. Curves — calculation for $T_1 = 293^\circ\text{K}$. Points — experiment: • — $p_1 = 10 \text{ mm Hg}$; Δ — $p_1 = 50 \text{ mm Hg}$. 1) Ideal gas; 2) atmospheres; 3) km/sec; 4) without dissociation.

and argon ions is in this case insufficient to maintain an equilibrium population of the excited state of the barium ion, i.e., with the absence of radiation equilibrium. The effective cross section of impacts of the second kind between the excited ions of barium and the argon atoms was estimated on the basis of experimental data to be $\sim 4 \times 10^{-17} \text{ cm}^2$.

The results of a pyrometric investigation of the state of air, nitrogen, and CO_2 behind a reflected shock wave are given for Fig. 6. The measurements were carried out at 10 mm from the end. Temperatures

above 5000°K were measured with a DKSSh-1000 lamp, through which a shaping line (five capacitors each $100 \mu\text{f}$ at $U = 400 \text{ v}$) was discharged at the required instant of time so as to guarantee the production of a rectangular light pulse with duration of about $250 \mu\text{sec}$ and a brightness temperature $\sim 11,000^{\circ}\text{K}$.

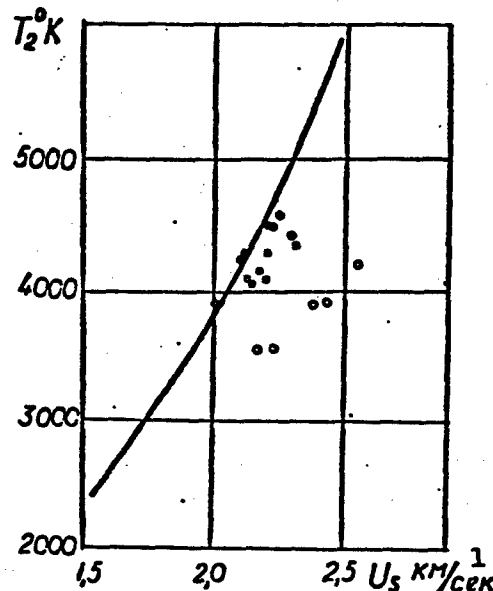


Fig. 5. Dependence of the temperature of argon behind a shock wave on the shock wave velocity. Curve - calculation, point - experiment. Values of pressure p_1 (in mm Hg): o) 5, □) 50; ●) 150. 1) km/sec.

The measured temperatures T_5 are in agreement with the theoretical values if they are referred to the maximum velocity U_s . The bars drawn through each point correspond to the changes in the gas temperature after a time of 45-50 μsec . These changes are in the main random.

In the case of nitrogen at temperatures up to 6500°K one observes in all experiments an increase in temperature directly behind the shock wave front, gradually decreasing to the equilibrium value. The fall-off time amounts to about $40 \mu\text{sec}$ at $T_5 = 5000^{\circ}\text{K}$ and about $20 \mu\text{sec}$

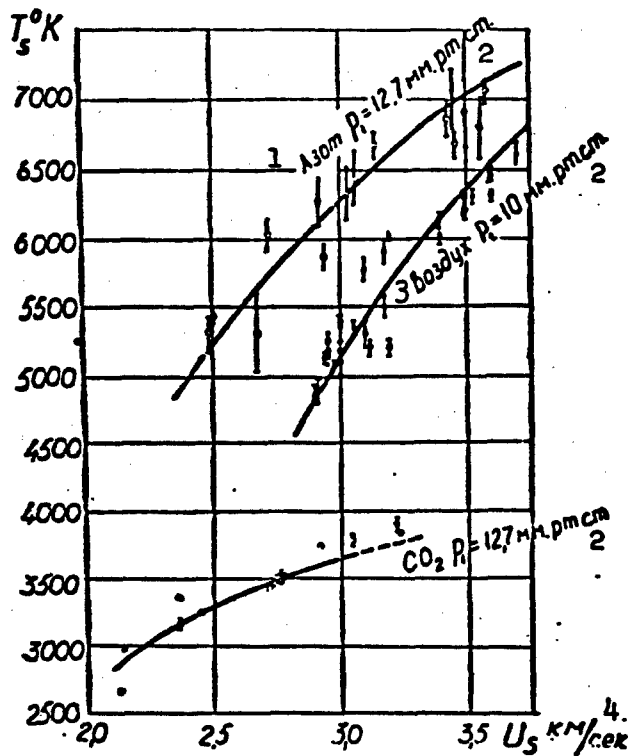


Fig. 6. Dependence of the temperature of nitrogen, air, and CO_2 behind a reflected shock wave on the shock wave velocity. Curves — calculation.* (Dashed — extrapolation.) Points — experiment.** 1) Nitrogen; 2) mm Hg; 3) air; 4) km/sec.

at $T_5 = 6000^\circ\text{K}$. This effect is apparently connected with the dissociation relaxation in the nitrogen.

We have investigated the temperature variation behind the reflected shock wave in nitrogen with increasing distance from the end. It was established that the temperature decreases gradually with increasing distance from the end. If $T_5 = 6900^\circ\text{K}$ at a distance of 10 mm from the end, then at a distance of 60 mm $T_5 = 6100^\circ\text{K}$ (i.e., a drop of 800°). The temperature drop may be due to the fact that the temperature is not constant along the plug behind the incident shock wave.

In pyrometric investigations of argon behind a reflected shock wave it was established that the measured barium ion excitation tem-

perature (at $p_1 = 50$ mm Hg) is approximately 1000° lower than the calculated value. At present we are unable to present a sufficiently reliable explanation for this discrepancy between the theoretical and experimental data.

In conclusion it must be noted that the method developed for temperature measurement can be used successfully for the following:

- a) investigations of flow under modes when the gasdynamic calculation cannot be carried out with sufficient reliability;
- b) a study of relaxation phenomena of vibration and dissociation of molecules;
- c) an estimate or determination of the effective cross sections of impact of the second kind, and
- d) an investigation of the state of the reaction products in the study of explosion and combustion in gases.

REFERENCES

1. N.N. Sobolev, A.V. Potapov, V.F. Kitayeva, F.S. Fayzullov, V.N. Alyamovskiy, Ye.T. Antropov, and I.L. Isayev. Optika i spektroskopiya [Optics and Spectroscopy], 6, 284, 1959.
2. F.S. Fayzullov, N.N. Sobolev, and Ye.M. Kudryavtsev. Optika i spektroskopiya, 8, 585, 1960.
- 3/4. F.S. Fayzullov, N.N. Sobolev, and Ye.M. Kudryavtsev. Optika i spektroskopiya, 8, 761, 1960.
5. N.N. Sobolev, A.V. Potapov, V.F. Kitayeva, F.S. Fayzullov, V.N. Alyamovskiy, Ye.T. Antropov, and I.L. Isayev. Izvestiya AN SSSR, seriya fizicheskaya [Bull. Acad. Sci. USSR, Phys. Ser.], 22, 730, 1958.
6. F.S. Fayzullov, N.N. Sobolev, and Ye.M. Kudryavtsev. DAN SSSR [Proc. Acad. Sci. USSR], 127, 541, 1959.

Manu-
script
Page
No.

[Footnotes]

- 388 T_2 , p_2 , T_5 , p_5 are the gas temperatures and pressures behind the incident and reflected shock waves, respectively.
- 396 The calculated values of the nitrogen and CO_2 parameters behind the reflected shock waves were graciously furnished by T.V. Bazhenova and S.G. Zaytsev.
- 396 The question of which value of U_s , the maximum or extrapolated to the end, should be used to calculate T_5 is discussed in detail, with use of new data, in our paper "Pyrometric Investigation of Gases Behind a Reflected Shock Wave," Trudy FIAN, XVIII.

Manu-
script
Page
No.

[List of Transliterated Symbols]

- 389 $\Pi = D$ = datchik = transmitter, sensor
- 390 x = kh
- 390 $\pi = \underline{l}$

MAGNETIC COMPRESSION OF PLASMA

I.M. Zolototrubov, Yu.M. Novikov, N.M. Ryzhov,
I.P. Skoblik, V.T. Tolok
Khar'kov

The use of time-varying magnetic fields for purposes of heating the plasma is based on the adiabatic invariance of the magnetic moment of the charged particle. When the magnetic field variation is sufficiently small compared with the Larmor period, the quantity $\mu = mv_1^2/2H$ remains constant, and this leads to a change in the particle energy connected with the velocity component perpendicular to the magnetic field. The final energy of the particle is determined in this case only by the initial energy and the ratio of the field at the end and at the start of the compression cycle

$$W_t = W_0 \frac{H_t}{H_0}$$

In experiments on the heating of a plasma by magnetic compression, an axial magnetic field that increases with time was used, along with mirrors on the ends. From the point of view of the attainable limiting energy of the charged particles, the rate of variation of the magnetic field does not exert any influence whatever. However, in a system with magnetic mirrors, an essential parameter is the time of plasma confinement, which for deuterons is defined in such systems [1] as

$$t = 2.6 \cdot 10^{10} \cdot W^{3/2} / n \text{ sec},$$

where W is the energy in kiloelectron volts, n is the particle density.

At small values of the initial energy, the confinement time is

small, and therefore the compression process should be carried out sufficiently rapidly so as to force a more vigorous departure of the ions from the trap at the start of the compression. This can be attained either 1) by using for compression purposes rapidly varying magnetic fields of large amplitude, which simultaneously ionize the neutral gas by inducing an eddy emf and compressing the plasma obtained in this manner, or 2) by separating these functions of the magnetic field; a rapidly varying magnetic field is used for ionization and preliminary heating, while the compression is effected by a slower field. The second method is more usable, for in this case the requirements imposed on the capacitor bank which stores the energy for the magnetic compression and imposed on the discharge units used for the switching are less stringent than in the former case. Experiments of the former type are described in [2] and those of the latter type in [3, 4].

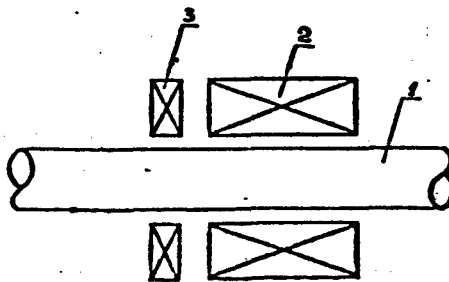


Fig. 1. 1) Discharge tube; 2) compressing field coil; 3) coil for excitation of shock waves.

In both experiments departure of neutrons was observed near the point of maximum compression and soft x-rays were produced, thus evidencing the high degree of heating of the plasma. It was pointed out by Kolb [3], in particular, that the heated plasma in such systems is stable. It was shown, however, in [5] with the aid of streak photographs that during the stage of maximum compression the state of the plasma is unstable. Powerful hydromagnetic oscillations observed in

the region of maximum compression are described in [6], and these also indicate instability in discharges of this type.

In the present paper we describe an experiment on the compression of a previously heated plasma by means of a relatively slow magnetic field.

The principal diagram of the experimental setup is shown in Fig. 1. The ionization and preliminary heating of the plasma were produced by shock waves excited by a single turn coil placed in tandem with the main field coil. A capacitor of $6.3 \mu\text{f}$, charged to 30 kv, was discharged into this coil. The discharge period was 6 μsec . The maximum value of the magnetic field intensity under the coil was 60 kiloersted.

The main field with intensity up to 85 kiloersted was produced by a coil consisting of 15 turns of copper bus of rectangular cross section potted in epoxy resin. In the center of the coil, between the turns, a transverse slot was left to photograph the discharge. The inside diameter of the coil was 4 cm and the total length 11 cm. The mirror ratio on the axis, obtained by changing the pitch of the winding, was 1.2.

The inductance of such a coil, L_k , is much larger than the parasitic inductance of the discharge circuit L_p , and consequently the coefficient of utilization of the energy stored in the capacitor, $k = L_k / (L_k + L_p)$, was 0.95.

The interconnection between the capacitors and the supply of energy to the coil were effected by means of wide copper buses with organic glass liners between them. In order not to disturb the plane-parallel geometry of the system, the discharge gap was made in the form of a break in the transmission line with an igniting unit. The same method was used for the connection and discharging of the capacitors producing the shock waves.

The discharge tube was made of quartz with inside diameter 3 cm and 1 meter length. A deuterium stream was established in the tube at a specified pressure through a palladium leak valve. During the course of operation, the pressure varied between 10^{-1} and $5 \cdot 10^{-2}$ mm Hg.



Fig. 2

Figure 2 shows a streak photograph of the propagation of shock waves along the axis of the discharge tube. The main coil was removed in this case. In the first half cycle the velocity of the wave is low, but with increasing development of the discharge, the velocity of propagation also increases, and on the portion of the path where the gas was ionized by the wave of the preceding half cycle, the velocity of the wave was approximately 5-6 times larger than on the portion where the gas was not yet ionized. With decreasing amplitude of the magnetic field, the velocity of the wave tends to a certain constant limit. For a shock wave this limit is a sound wave, the velocity of which is connected with the temperature by the following relation:

$$c = \sqrt{\frac{\gamma k T}{M}}$$

where $\gamma = C_p/C_v$, k is Boltzmann's constant, T is the temperature in $^{\circ}\text{K}$, and M is the mass of the molecule.

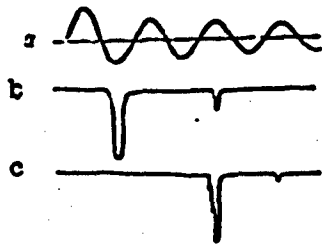
The plasma temperature as estimated from this formula is about 1 ev.

The main compressing field was turned on later than the field producing the preliminary ionization, and the instant of its application was varied by changing the delay.

Figure 3 shows oscillograms of the magnetic field and of the x-ray pulses. The instant of appearance of the radiation pulse depends to a

great degree on the delay time. In the oscillogram of Fig. 3-b, the first pulse appears during the second half cycle of the main magnetic field.

The delay chosen in this manner is optimal, since when it is varied in one direction or another the radiation pulses appear later. The optimum delay corresponds to turning on the main field during the sixth half cycle of the preliminary ionization field.



From the streak photograph of Fig. 2 it is seen that by that instant of time the state established in the tube is characterized by a constant velocity of the propagation of the waves excited by the single turn coil.

Fig. 3. 1) μ sec. Turning on the main coil during the time interval between the sixth and tenth half cycles is unavoidably accompanied by the appearance of a pulse in the second half cycle of the compressing field, but its amplitude decreases from the start toward the end of this interval.

Figure 3-c shows an oscillogram of the radiation pulse in the case of a very large delay; this oscillogram is analogous to the oscillosograms obtained in the absence of preliminary ionization. In this case the pulse appears in the fifth or sixth half cycle.

In addition to the main pulse, we see on the oscillosograms pulses of small magnitude, appearing one or two half cycles later. The absence of pulses in the third and succeeding half cycles (Fig. 3-b) is not connected with the damping of the magnetic field, for otherwise it would be impossible for them to appear in later instants of time. In all probability the compression of the plasma by the main field leads to the appearance of instabilities and of x-ray pulses associated with them. The character of the instabilities that develop in such a system

is shown on the streak photograph of Fig. 4. This photograph has been plotted for argon at a pressure of 0.1 mm Hg.



Fig. 4

To determine the dimensions of the region of emission of radiation, photographic film was located under the coil along the axis of the discharge tube. The blackening of the film was local in character, i.e., it had the form of individual dark spots, which were randomly scattered in the region from the center of the coil to the edge on the side opposite the turn exciting the shock waves. This character of film blackening agrees with the instabilities observed with the aid of the streak photography, which lead to the ejection of plasma on the wall of the discharge tube. The γ radiation energy, estimated from its absorption in aluminum, is 50 kev.

Thus, it follows from the results of the experiment that in a system comprising a trap with time-varying magnetic field, instabilities may arise.

REFERENCES

1. Tr. Vtoroy mezhdunarodnoy konferentsii po mirnomu ispol'zovaniyu atomnoy energii (Zheneva, 1958). Izbr. dokl. inostrannyykh uchenyykh [Transactions of the Second International Conference on the Peaceful Uses of Atomic Energy (Geneva, 1958). Selected reports of foreign scientists], Vol. I - Fizika goryachej plazmy i upravlyaemye termoyadernyye reaksii [Physics of the High-Temperature Plasma and Controlled Thermonuclear Reactions], Atomizdat M. str. [State Publishing House for Literature on Atomic Energy], Moscow, 1959, page 548.

2. Elmor, Litl, Kuinn [Elmore, Little and Quinn], *ibid.*, page 639.
3. Kolb, *ibid.*, page 270.
4. A.C. Colb. Dobbie, H.R. Griem. *Phys. rev. Letters*, 3, 5, 1959.
5. I.F. Kvartskhava, K.N. Kervalidze and Yu.S. Gvaladze, *ZHTF* [Journal of Experimental and Theoretical Physics], 38, 1641, 1960.
6. I.M. Zolotobrubov, N.M. Ryzhov, I.P. Skobli, and V.T. Tolok, *ZHTF* [Journal of Technical Physics], XXX, 7, 769, 1960.

NEW DATA ON THE INFLUENCE OF A MAGNETIC FIELD
ON THE DEPARTURE OF IONS FROM THE PLASMA OF INERT GASES

I.A. Vasil'yeva, V.L. Granovskiy
Moscow

1. INTRODUCTION AND FORMULATION OF THE PROBLEM

The theory of the diffusion of charged particles in a magnetic field, in which only paired collisions in a weakly ionized gas are taken into account [1], leads to the following dependence of the particle diffusion coefficient D on the magnetic field:

$$D(B) = \frac{D(0)}{1 + \omega^2 \tau^2} = \frac{D(0)}{1 + \left(\frac{e\tau}{mc_0}\right)^2 B^2}, \quad (1)$$

where $\omega = eB/mc_0$, $c_0 = 3 \cdot 10^{10}$ cm/sec, and τ is the transit time of the particle.

The dependence of the coefficient of ambipolar diffusion (D_a) on the magnetic field has the form

$$D_a(B) = \frac{D_a(0)}{1 + \omega_e \tau_e \omega_p \tau_p} = \frac{D_a(0)}{1 + \left(\frac{e}{c_0}\right)^2 \frac{\tau_e \tau_p}{m_e m_p} B^2}. \quad (2)$$

An experimental check has shown that these dependences are not always confirmed [2-6]. However, the experiments were carried out either in the presence of complications, such as conducting walls, or else by indirect methods. It is desirable to ascertain the following by means of a direct method readily amenable to interpretation: 1) to what extent does a magnetic field weaken the departure of charge carriers in a direction perpendicular to the magnetic field; 2) what is the character of the carrier diffusion in the presence of a magnetic

field (bound or independent diffusion); 3) what factors give rise to anomalies in the dependence of the rate of carrier departure from the magnetic field.

2. METHOD OF INVESTIGATION AND CONDITIONS OF THE EXPERIMENTS

The departure of ions from a plasma is characterized by the density of the ion current on the tube wall (j_{pw}). The coefficient diffusion or the coefficient of carrier departure (D) is determined from the relation

$$j_{pw} = -D \frac{dp_p}{dr}, \quad (3)$$

where ρ_p is the charge density of the positive ions near the walls [7].

The experimental glass tubes contained an indirectly heated oxide cathode and a cone-shaped anode. The current of the ions on the wall was determined by means of a flat wall probe in the form of a disk with guard ring. To determine $d\rho_p/dr$, a cylindrical probe was used, which was moved along the section of the tube with the aid of a ground-glass stopper. The charge density of the positive ions in each probe position was determined from the ionic parts of the probe characteristics.

In the two tube versions, the cathode was located either inside or outside the magnetic field.

The investigations were carried out in helium and argon at pressures from $5 \cdot 10^{-3}$ to 1.1 mm Hg, in a magnetic field range from 0 to 2600 gauss, and at tube currents from 0.03 to 1 amp.

3. RESULTS OF THE INVESTIGATION

I. Figure 1 shows the dependence of the relative value of the departure coefficient D on the magnetic field. The parameter of the curves is the gas pressure p . It is clear from the figure that the smaller the pressure, the steeper the decrease in D under the influence

of the magnetic field. At the lowest pressures one can note deviations from a monotonic decrease.

The steepness of the decrease can be characterized by a magnetic field in which D is decreased to one half its value ($B_{1/2}$). As can be seen from Fig. 2, the dependence of the experimental values of $B_{1/2}$ on the pressure is close to linear (the scale of the drawing is bilogarithmic and the line is inclined at 45°). This is in agreement with Formulas (1) and (2).

In Fig. 3 one of the experimental $D(B)$ curves is compared with the calculated curves. The calculation is based on Formula (1) in the

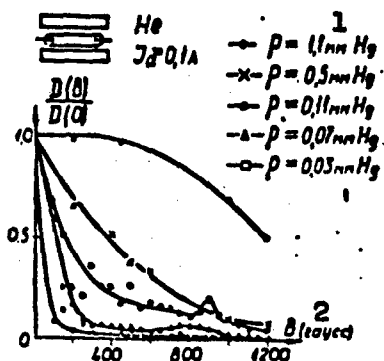


Fig. 1. 1) mm Hg; 2)
gauss.

case of independent diffusion of the ions and electrons (dashed curves), and by Formula (2) in the case of ambipolar diffusion (thin solid curve). It is seen from the figure that the curve closest to the experimental one is that corresponding to ambipolar diffusion.

Thus, in the region of monotonic decrease, the dependence $D(B)$ turns out to be quadratic and the diffusion is ambipolar in character.

II. To investigate the deviations from the monotonic decrease of $D(B)$, it was necessary to expand the range of magnetic fields and to improve the experimental tubes.

Let us consider the results of the measurements in tubes with the cathode located outside the magnetic field.

Figure 4 shows the dependence of the density of the ion current in the wall on the magnetic field. The parameter of the curves will from now on be the current strength. It is seen from Fig. 4 that at helium pressure of 0.055 mm Hg the current on the wall decreases mono-

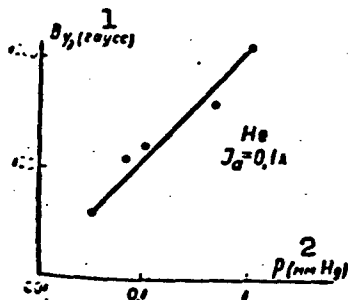


Fig. 2. 1) Gauss; 2)
mm Hg.

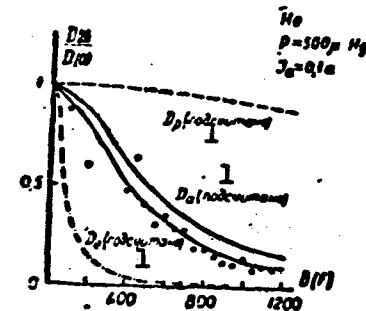


Fig. 3. 1) Calculated.

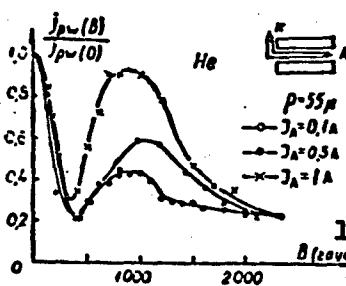


Fig. 4. 1) Gauss.

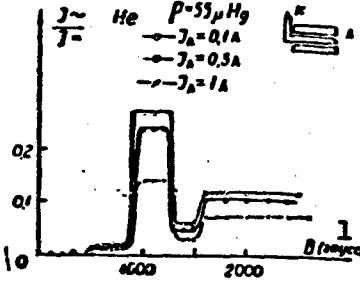


Fig. 5. 1) Gauss.

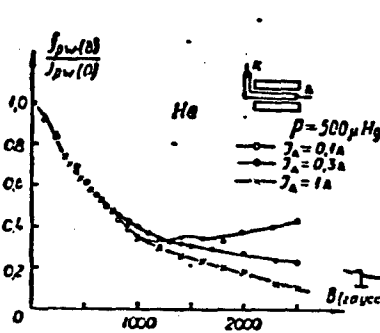


Fig. 6. 1) Gauss.

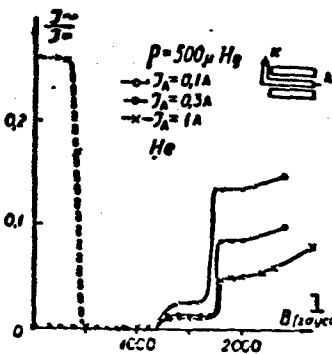


Fig. 7. 1) Gauss.

tonically to a magnetic field value $B_{krit} \approx 400$ gauss, after which it increases and passes through a maximum for all the currents investigated in the tube. Figure 5 is a plot of the anode current noise amplitude ($I\sim$) as a function of the magnetic field. It is seen from the figure that in a magnetic field $B_{krit} \approx 400$ gauss, the current noise increases, and then passes through a maximum.

Figure 6 pertains to a pressure of 0.5 mm Hg. It is seen from Fig. 6 that the $J_{pw}(B)$ curves for different currents in the tube coincide up to fields of 1200 gauss, after which they diverge and a deviation from monotonic decrease appears. Figure 7 shows that at this value of the magnetic field $B = B_{krit}$ noise oscillations (continuous curves) arise, which then grow. The dashed curve of the same figure represents the dependence on the magnetic field of the amplitude of the striations with frequency 40 kcs, which exist at a current of 1 amp and $B < 500$

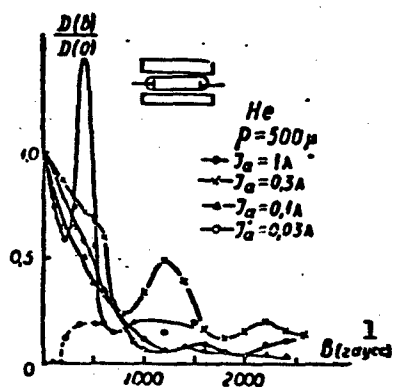


Fig. 8. 1) Gauss.

gauss. In such magnetic fields, the departure of the ions changes with increasing B in similar fashion for all anode currents, and this change is furthermore monotonic (see Fig. 6). This means that the striations exert no appreciable influence on the departure of the carriers.

Thus, in tubes where the cathode is located outside the H field, the appearance of anomalies (the value of B_{krit}) depends on the pressure, is connected with the increase in the noise oscillation amplitude, and is independent of the current strength and of the presence of striations.

These experimental facts are in qualitative agreement with the theory that predicts the appearance of anomalies in the rate of departure of the currents starting with a certain $B = B_{krit}$.

The curves of Fig. 8 have been obtained in a tube with cathode located inside the magnetic field (helium pressure 0.5 mm Hg). It is seen from the figure that deviation from a monotonic decrease occurs the earlier and are the more brightly pronounced, the larger the current in the tube. The dashed curve in the same figure shows in arbitrary units the amplitude of the noise oscillations, referred to a cur-

rent of 1 amp. The noise increase in the same magnetic field, in which $D(B)$ starts increasing at a current of 1 amp.

Consequently, in tubes where the cathode is located in the magnetic field, B_{krit} depends on the current and is related to the increase in the noise amplitude of the anode current in the same way as in the case when the cathode is outside the H field.

III. To explain the large rate of departure of the ions perpendicular to the H field, Simon [6] advanced the hypothesis of "short circuiting" of the plasma by the conducting end walls of the tube, in connection with the anisotropy of the plasma conductivity in a strong H field. To verify this hypothesis, we investigated the effect produced on the departure of carriers from a plasma by inserting a metal wall in the end part of the tube.

The measurements were carried out by the method described above, but were repeated twice for the positions of the wall perpendicular to the magnetic field. The wall could be displaced with the aid of a ground-glass stopper; in one position it was placed on the same force lines of the magnetic field, where the measuring probes were located, and in the other position it was moved away to the side. The experiments were repeated many times in helium at $p = 0.08$ mm Hg and $B = 2500$ gauss ($\omega_e \tau_e = 450$) and in argon at $p = 5 \cdot 10^{-3}$ mm Hg and at the same value of B ($\omega_e \tau_e = 3 \cdot 10^3$). The ion and electron currents on the wall were constant in this case, within the experimental accuracy (1-2%). The coefficient of departure was also practically constant as the metallic wall was displaced. This means that Simon's hypothesis does not explain under the conditions of our experiments the existence of anomalies in the dependence of the departure of the ions from the plasma in a magnetic field.

CONCLUSIONS

1. The diffusion of ions and electrons from a plasma corresponds to the theory of pair collisions and is ambipolar up to $B = B_{krit}$.
2. When $B > B_{krit}$, anomalies are observed in the $D(B)$ and $j_{pw}(B)$ dependences.
3. The value of B_{krit} increases with increasing pressure and depends on the position of the cathode relative to the region where the magnetic field is effective.
4. The appearance of anomalies in the $D(B)$ and $j_{pw}(B)$ dependences is connected with the appearance of random electric oscillations in the plasma. Striations do not influence $D(B)$ and $j_{pw}(B)$.
5. The influence of different factors on the appearance of anomalies at $B = B_{krit}$ agrees with the theory of B.B. Kadomtsev and A.V. Nedospasov.
6. The hypothetical effect of "short circuiting" of the plasma, advanced by Simon, could not be observed in experiments specially set up for the purpose.

REFERENCES

1. T.S. Townsend. Phil. Mag., 25, 7, 459, 1938. S. Chapman, T.G. Cowling. The Mathematical Theory of Nonuniform Gases, Cambridge, 1950. T.G. Cowling. Proc. Roy. Soc., A, 183, 995, 453, 1945.
2. A. Guthrie, D.K. Wakerling. The Characteristics of Electrical Discharges in Magnetic Fields. New York, 1949 (Chapt. 2, 9).
3. B. Lehnert. Dokl. na 2-y mezhdunar. konf. po mirnomu isp. atomn. energii [Report to the Second International Conference on the Peaceful Uses of Atomic Energy], 1958; T.C. Hoh, and B. Lehnert, Dokl. na 4-y mezhdunar. konf. po ioniz. yavleniyam v gazakh [Report to the Fourth International Conference on Ionization Phenomena in Gases], 1959.

4. A. V. Zharinov, Atomnaya energiya [Atomic Energy], 7, 3, 1959.
5. V. Bostik and M. Levin, Probl. sovr. fiz [Problems of Contemporary Physics], 2, 161, 1956.
6. A. Simon. Phys. rev., 98, 437, 1955. A. Simon, R. V. Neidigh, Dokl. na 2-y mezhdunar. konf. po mirn. isp. atomn. energii [Report to the Second International Conference on the Peaceful Uses of Atomic Energy], 1958.
7. I.A. Vasil'eva and V.L. Granovskiy, Rad. i el. [Radio Engineering and Electronics], 12, 2051, 1959; I.A. Vasil'eva, V.L. Granovskiy and A.F. Chernovolenko. Rad. i el., 9, 1508, 1960.

Manu-
script
Page
No.

[Footnote]

406 The subscript e pertains to electrons and the p to positive ions.

Manu-
script
Page
No.

[List of Transliterated Symbols]

409

κ_{crit} = krit = kriticheskiy = critical

INVESTIGATION OF THE MOTION OF A CONDUCTING GAS
ACCELERATED BY CROSSED ELECTRIC AND MAGNETIC FIELDS

A. K. Musin, V. L. Granovskiy
Moscow

(PART I - THEORETICAL)

Let us consider the motion of a viscous conductive medium in a magnetic field in the presence of a plane current layer produced by an external alternating electric field. We start here from the magneto-hydrodynamic equations for the momenta and for the magnetic induction, written in the simple symmetrical form

$$\begin{aligned}\vec{u}_t + \vec{\omega}_x \vec{u}_{x_2} + \vec{e}_x \vec{\Phi}_{x_2} &= (\vec{a} \vec{u} + \vec{b} \vec{w})_{x_2 x_2}, \\ \vec{\omega}_t + \vec{u}_x \vec{\omega}_{x_2} + \vec{e}_x \vec{\Phi}_{x_2} &= (\vec{a} \vec{w} + \vec{b} \vec{u})_{x_2 x_2}.\end{aligned}\quad (1)$$

We use here the notation [1]

$$\begin{aligned}\vec{u} &= \vec{v} + \vec{H}/\sqrt{4\pi\rho}; \vec{\omega} = \vec{v} - \vec{H}/\sqrt{4\pi\rho}, \\ \vec{\Phi} &= p/\rho + (\vec{u} - \vec{\omega})^2/8; 2a = v + v_m; 2b = v - v_m,\end{aligned}\quad (2)$$

v is the kinematic viscosity, v_m is the magnetic viscosity of the medium. The remaining symbols used in (1) and (2) are standard,* and $a = 1, 2, 3$.

The physical meaning of the functions $\vec{u}(t, x_\alpha)$ and $\vec{w}(t, x_\alpha)$ given in (2) lies in the fact that in the coordinate frame fixed in the moving medium we introduce into consideration two hydrodynamic waves propagating in opposite directions with equal speeds $\vec{v}_A = \pm \vec{H}/\sqrt{4\pi\rho}$. Inasmuch as propagations occurring in a conducting medium with constant physical properties propagate with velocities that do not exceed $2\vec{v}_A$ [2], these waves do not interact with each other.

In the stationary case this reduces the problem of integrating the simultaneous system of equations to the integration of several independent equations. In the nonstationary case, under certain particular assumptions, the problem is likewise simplified. Let us consider, in particular, plane nonstationary motions of a viscous conducting medium with a variable current layer along an external electric field $\vec{E} = \vec{E}(t)$ in a transverse magnetic field $\vec{H} = \text{const}$. Let the electric field $\vec{E}(t)$ be parallel to the x_2 axis, so that in the region under consideration there flows an alternating current parallel to the x_2 axis with the following current strength per unit length in the x_1 direction

$$\vec{j}(t) = j_0 \exp i(\omega t + \psi). \quad (3)$$

The external magnetic field is directed along the x_3 axis; the motion is along the x_1 axis and is bounded by parallel nonconducting planes $x_3 = \pm R$.

The relative placement of the fields and of the direction of motion are shown in Fig. 1.

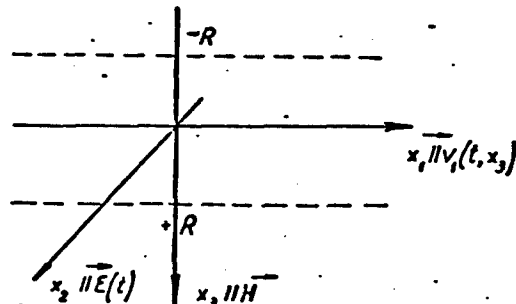


Fig. 1

Projecting Eqs. (1) on the x_1 axis, we obtain in our case a parabolic system of equations

$$\begin{aligned} u_{11} + \omega_1 u_{1x_1} + \Phi_{x_1} &= (au_1 + bw_1)_{x_1}, \\ \omega_{11} + u_1 \omega_{1x_1} + \Phi_{x_1} &= (aw_1 + bu_1)_{x_1}. \end{aligned} \quad (4)$$

Assume that when $t < 0$ the electric field is zero and the motion occurs

only under the influence of the constant pressure gradient $\partial p / \partial x_1 = \text{const}$, i.e.,

$$u_1(t, x_3) \Big|_{x_3=0} = \tilde{u}_1(x_3); \quad w_1(t, x_3) \Big|_{x_3=0} = \tilde{w}_1(x_3), \quad (5)$$

where $\tilde{u}_1(x_3)$ and $\tilde{w}_1(x_3)$ are the stationary solution of the system (1) in the case when there is no current layer. Owing to the adhesion of the viscous medium to the boundary surfaces and owing to the continuity of the tangential component of the magnetic field in the absence of surface currents we have

$$-w_1 \Big|_{x_3=R} = \omega_1 \Big|_{x_3=-R} = u_1 \Big|_{x_3=R} = -u_1 \Big|_{x_3=-R} = \frac{h_0(t)}{\sqrt{4\pi\rho}}; \quad (6)$$

$$h_0(t) = (2\pi j_0/c_0) \exp i(\omega t + \psi).$$

The system (4) can be reduced to a system of algebraic equations if we use the operator equation [5]

$$s^m \tilde{\gamma} - \{\tilde{\gamma}^{(n)}(\lambda)\} = s^{m-1} \{\tilde{\gamma}^{(n-m)}(0)\},$$

where $m = 1, \dots, n$; s is the operator of differentiation with respect to λ . In this case Conditions (5) and (6) are included directly in these algebraic equations, where $h_0(t)$ goes over into $h(k)$:

$$h(k) = (2\pi j_0/c_0) [\exp i(\psi + \arctg \omega/k)] / (\omega^2 + k^2)^{1/2}, \quad (7)$$

where k is the operator of differentiation with respect to the variable t . In order to avoid cumbersome calculations connected with the simultaneity of the system of equations, we can use equations that follow by virtue of the known analysis theorems from the symmetry of the problem and from Conditions (6):

$$(u_s + w_s)_{s=0} = (u - w)_{s=0} = 0. \quad (8)$$

We shall not write out here the solution obtained in general form; we note only that it is most convenient for analysis purposes to use directly the solution of the algebraic system, which is a solution of the problem in operator form.

Depending on the character of the active moving forces and on the

conditions of motion, we can separate from this general solution several special cases. In this case the general solution becomes appreciably simpler, and the particular solution can be readily written down in the notation of classical analysis.* We consider here only one special case, when the gradient of the total pressure is $(\partial P/\partial x_1) \equiv 0^{**}$ and the motion occurs only under the influence of the electromagnetic forces. In addition, we assume $\psi = \pi/2$ in Formula (7). We then use the well-known theorems on contour integration [4] to write down the expressions for the velocity of motion and for the induced magnetic field in series form:

$$\begin{aligned} v_1(t, x_3) &= \{G_1 p_1 p_3 e^{kt} (\text{ch} p_1 R \text{ch} p_3 x_3 - \text{ch} p_1 R \text{sh} p_3 x_3) / (\partial D / \partial k)\}_{k=k_1}, \\ H_1(t, x_3) &= \{G_2 e^{kt} [p_1(k - \nu p_3^2) \text{ch} p_1 R \text{sh} p_3 x_3 - \\ &\quad - p_3(k - \nu p_1^2) \text{ch} p_3 R \text{sh} p_1 x_3] / (\partial D / \partial k)\}_{k=k_1}, \\ D(k) &= (k^2 + \nu^2) [p_1(k - \nu p_3^2) \text{sh} p_1 R \text{ch} p_3 R - \\ &\quad - p_3(k - \nu p_1^2) \text{sh} p_3 R \text{ch} p_1 R], \end{aligned} \quad (9)$$

$$p_{1,3}(k) = (1/2ka + v_A^2 + 2kl \pm \sqrt{1/2ka + v_A^2 - 2kl})/l,$$

$$G_1 = j_{00} l I_3 / 2c_0 \rho; \quad G_2 = 2v_{00} \omega / c_0; \quad l^2 = v v_m;$$

k_1 are the roots of the equation $D(k) = 0$; summation is carried out over 1.

Assume now that the inequality $v \ll v_m$ or $v\sigma \ll c_0^2/4\pi\mu$ is satisfied, i.e., the conductivity and viscosity of the medium are not too large. Then Expressions (9) greatly simplify, and the formulas for the velocity and for the magnetic field can be written in analytic form. These formulas are rather complicated, but if we stipulate in addition that $(\omega v_m/v_A^2)^2 \ll 1$ and neglect the quantity $(\omega v_m/v_A^2)^2$ compared with unity, something that can be done if the external magnetic field is sufficiently large and the densities low, then we obtain for the maximum velocity on the flow axis, attainable at the instant of time $t \approx \omega\psi = \pi\omega/2$, a formula which is convenient for analysis and calculation:

$$v_0 = \frac{J_{\alpha} \sqrt{\omega_m} (\sin 2\tilde{z}_1 \cos \tilde{z}_2 + \sin 2\tilde{z}_2 \sin \tilde{z}_3)}{2 J_p c_s (\sin^2 \tilde{z}_1 \sin^2 \tilde{z}_3 + \sin^2 \tilde{z}_2 \cos^2 \tilde{z}_3)}; \quad (10)$$

$$\tilde{z}_1 = R v_A 2 J_p \sqrt{\omega_m}; \quad \tilde{z}_2 = m_A / 2 v_A^2; \quad \tilde{z}_3 = R \omega_m / 4 v_A \sqrt{\omega_m}.$$

At still larger magnetic fields, when $\omega v_m / v_A^2 \ll 1$, we neglect $\omega v_m / v_A^2$ compared with unity and obtain from (10) for the maximum velocity

$$v_0 = \frac{J_{\alpha} \sqrt{\omega_m} [\exp(RH_3/2\sqrt{\omega_m}) - 1]}{c_s J_p [\exp(RH_3/2\sqrt{\omega_m}) + 1]}. \quad (11)$$

We see therefore that the velocity of motion tends asymptotically with increasing magnetic field toward a certain limiting value, and at large magnetic fields it no longer depends on the magnetic field — a "saturation" of sorts sets in. The smaller the density of the medium, the smaller the magnetic field at which the saturation occurs. The physical meaning of this phenomenon is that with increasing magnetic field, its accelerating action is gradually balanced by the induction deceleration resulting from the interaction between the external magnetic field and the increasing induction current.

At low densities and slow changes in the external magnetic field,

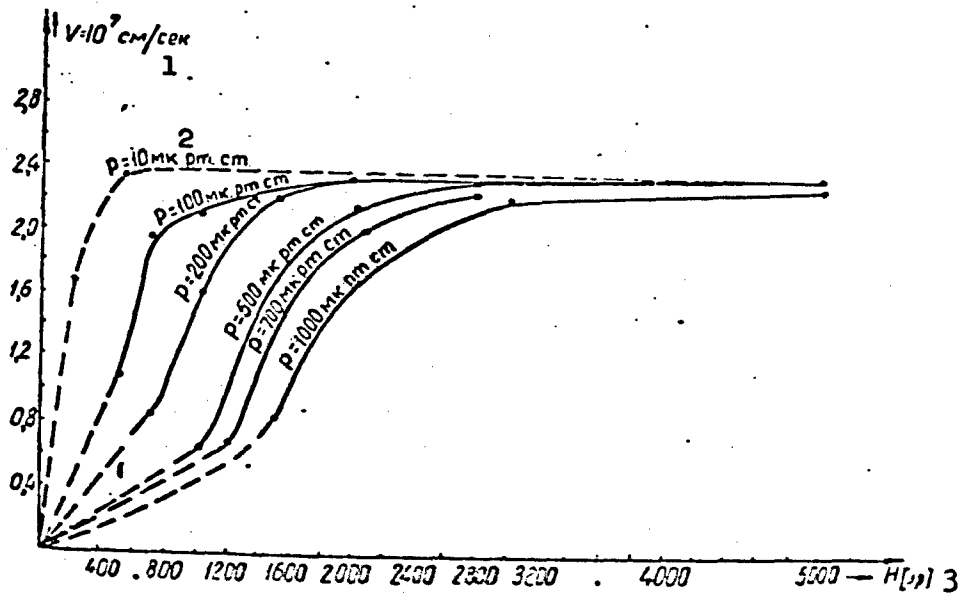


Fig. 2. 1) cm/sec; 2) μ G; 3) oersted.

the rate of motion ceases to depend likewise on the density of the medium. The reason for it is that under such conditions the inertial terms are small and the resistance to the motion is determined entirely by the viscous dissipation.

The limiting value of the velocity is determined by the amplitude of the electric current falling through the medium and by the conductivity of the medium; it is obtained the later, the larger the density ρ of the medium. It is clear therefore that an increase in the magnetic field above the values at which saturation sets in, although it does not bring about an increase in the velocity of motion for a constant J_0 , nevertheless makes it possible to set a larger mass in motion.

Figure 2 shows the curves calculated by means of Formula (10).

At a current density $J_0 = 430 \text{ a/cm}$ and $\sigma = 10^{13} \text{ sec}^{-1}$, the limiting value of the velocity v_{pred} equals $2.4 \cdot 10^7 \text{ cm/sec}$.

REFERENCES

1. W.M. Elsasser. Phys. Rev., 79, 183, 1950.
2. Kh Al'fven, Kosmicheskaya elektrodinamika [Cosmic Electrodynamics], Izd-vo inostr. lit. [Foreign Literature Press], 1952.
3. S.A. Regirer, IFZh [Engineering-Physics Journal], 8, 43, 1959.
4. A.I. Markushevich, Teoriya analiticheskikh funktsiy [Theory of Analytic Functions], Moscow, 1950.
5. Ya. Mikusinskiy, Operatornoe ischisleniye [Operator Calculus], Izd-vo inostr. lit., 1956.

[Footnotes]

414

Here and throughout, in order to abbreviate the notation, the derivatives with respect to the time t and with respect to the coordinates x_a are denoted by suitable indices and summation is carried out over repeated indices (for example,

$$u_a \dot{v}_a = \sum_{a=1}^3 u_a \cdot \dot{v}_a$$

417

For example, by putting $\bar{J}(t) \equiv 0$, $(\partial p / \partial x_1)|_{t<0} = 0$, $(\partial p / \partial x_1)|_{t>0} = \text{const} \neq 0$, we can obtain from the general solution, after making suitable simplifications, the solution of the problem considered in [3].

417

The total pressure is $P = p + (H^2/8\pi)$.

INVESTIGATION OF THE MOTION OF A CONDUCTING GAS
ACCELERATED BY CROSSED ELECTRIC AND MAGNETIC FIELDS

L.S. Lomonosova, V.I. Serbin, G.G. Timofeyeva, V.L. Granovskiy
Moscow

(PART II - EXPERIMENTAL)

1. The motion of a conducting medium accelerated in crossed electric and magnetic fields was considered in [1]. In the particular case when there is no pressure gradient and the motion occurs only under the influence of the electromagnetic forces, formulas that are convenient for calculation were presented and the dependence of the velocity on the external magnetic field was plotted. It was also shown in [1] that when the magnetic field is sufficiently large the velocity of the plasma ceases to depend on the magnetic field, i.e., "saturation" sets in (see [1], Fig. 2). With increasing initial gas pressure p_0 , the "saturation" sets in at ever-stronger magnetic fields. It was also shown that, other conditions being equal (p_0 , H, the type of gas), the velocity of the plasma increases with increasing amplitude I_A of the discharge current.

2. For an experimental investigation of these phenomena, a setup was assembled in accord with the diagram shown in Fig. 1. The plasma was obtained and accelerated in a cruciform glass tube 32 mm in diameter. The plasma source was an arc produced in tube A following the discharge of a capacitor bank with capacity $C = 2 \mu\text{f}$. The cruciform portion of the tube was placed between the poles of an electromagnet, so that the magnetic field produced by the latter ($6 \cdot 10^3$ oersted) was

perpendicular to the electric field of the arc. Under the influence of the magnetic field, the plasma was ejected into tube B, about 1 meter in length. In our experiments we varied the amplitude of the arc current from 1.2 to 5 kiloamperes, the magnetic field intensity from 250 to 6000 oersted, and the pressure from 10^{-2} to $7 \cdot 10^{-1}$ mm Hg. We measured the plasma velocity on a portion of tube B of length 18-28 cm in hydrogen, air, and krypton.

The motion of the plasma was investigated by two methods:

a) with an electron optical converter operating as a photoregistrator;

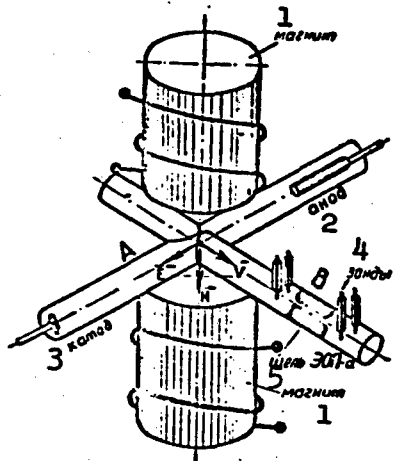


Fig. 1. Diagram of apparatus. 1) Magnet; 2) anode; 3) cathode; 4) probes; 5) slit of electron optical converter.

b) with probes sealed in tube B as shown in Fig. 1. In this case the velocity of the plasma was determined from the known distance between probes and the time interval between the appearance of the probe signals on the oscilloscope screen.

The main results, which are presented below, were obtained by the probe method. It turns out that the velocity of the plasma increases:

a) with increasing amplitude of the discharge current (Fig. 2);

b) with decreasing initial gas pressure at low magnetic fields (Fig. 3);

c) with decreasing atomic weight of the gas (Table 1).

It was observed that for the same values of I_A and p_0 , the velocity of the plasma increases with increasing H . However, with further increase of the magnetic field H , the increase in the velocity slows

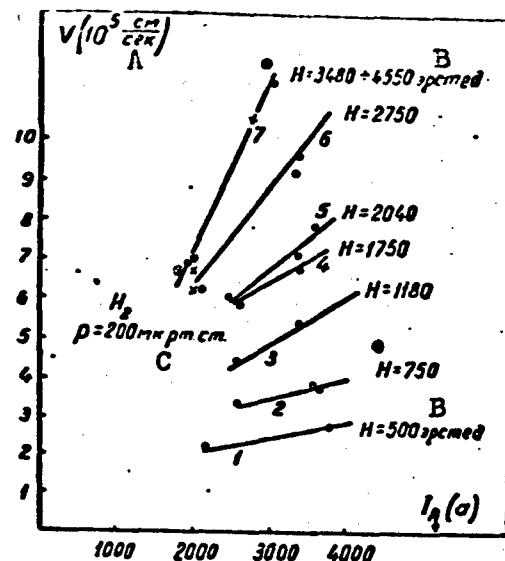


Fig. 2. Dependence of v on the discharge current I_A in hydrogen, at $p_0 = 0.2$ mm Hg and at different magnetic field intensities H :
 1) $H = 500$ oersted; 2) $H = 750$ oersted; 3) $H = 1180$ oersted; 4) $H = 1750$ oersted; 5) $H = 2040$ oersted; 6) $H = 2750$ oersted; 7) $H = 3480-4550$ oersted. Measured on the portion $l = 15-28$ cm from the start of tube B. A) cm/sec; B) oersted; C) microns mercury.

TABLE 1

1) Gas type	2) p_0 (mm Hg)	3) I_A (kA)	4) H (oersted)	5) v (cm/sec)
6) Воздух	28,8	0,15	3,4	$4,1 \times 10^3$
7) Криpton	83,7	0,15	3,6	$1,5 \times 10^3$
6) Воздух	28,3	0,15	2,6	$0,6 \times 10^3$
8) Водород	2,0	0,15	2,75	$(5-6) \times 10^3$

1) Type of gas; 2) mm Hg; 3) kiloamperes; 4) oersteds; 5) cm/sec; 6) air; 7) krypton; 8) hydrogen.

down, after which the plasma velocity remains constant (the limiting velocity is reached) (Fig. 4). In hydrogen at $p_0 = 0.15$ mm Hg and $I_A = 2.1$ kiloamperes, the "saturation" sets in at $H = 4500-5000$ oersted,

and the limiting velocity attained thereby at a distance of 26 cm from the axis of tube A is $v = 7.5 \times 10^5$ cm/sec. This "saturation" in the course of the dependence of the plasma velocity on H agrees with the theoretical deductions [1].

3. In comparing the theoretical and experimental dependences of the velocity on the magnetic field intensity, the following must be kept in mind. In the theoretical calculations [1] we deal with the velocity of the plasma directly in the acceleration region, i.e., under the poles of the electromagnet. What we determined experimentally, however, was the velocity of the plasma at a certain distance from this region. Thus, for example, the first probe was located at a distance of 13 cm from the discharge tube axis, and the longitudinal slots, when working with an electron optical converter, started at a distance of 10 cm from the axis. When moving in tube B, the plasma was slowed down by the following two phenomena:

a) the transfer of momentum to the wall tubes and to the stationary gas;

b) deceleration by the force exerted on the induced currents in the moving plasma by the transverse stray field of the electromagnet.

Figure 5 shows a plot of the motion of a plasma in hydrogen in tube B at $I_A = 2.6$ kiloamperes, $p_0 = 0.185$ mm Hg, and $H = 1200$ oersted.

Figure 6 shows on a semilogarithmic scale the dependence of the plasma velocity in tube B on the distance covered, as calculated from the plot of the motion (Fig. 5). It is seen that as the plasma moves along the tube B, its velocity decreases approximately exponentially. The velocity with which the plasma begins its motion from the accelerating region can be obtained by extrapolating the plot of Fig. 6 to the start of the tube. In the example shown in Figs. 5 and 6 (Curve 1), this velocity turns out to be $v = 2 \cdot 10^6$ cm/sec, whereas its theoretical

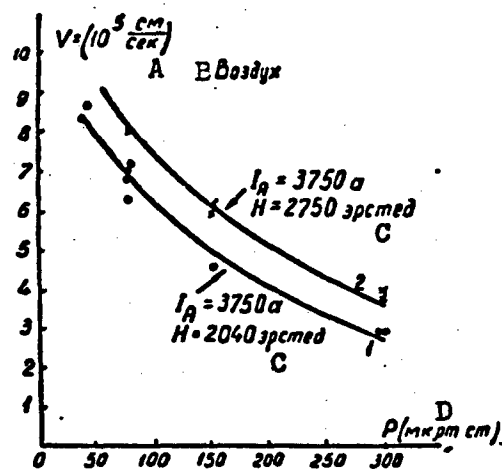


Fig. 3. Dependence of the plasma velocity v on the initial pressure of the gas (air) p_0 in two modes: 1) $I_A = 3.75$ kiloamperes, $H = 2040$ oersted; 2) $I_A = 3.75$ kiloamperes, $H = 2750$ oersted. Measured in a portion $l = 0-15$ cm from the start of tube B. A) cm/sec; B) air; C) oersted; D) microns mercury.

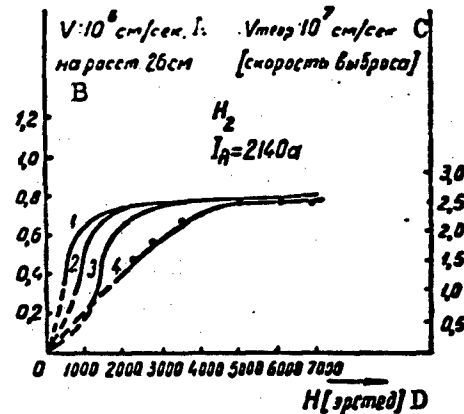


Fig. 4. Dependence of v on the magnetic field H in hydrogen at $p_0 = 0.15$ mm Hg and $I_A = 2.1$ kiloamperes. Curves 1-3 are theoretical and their vertical scale is on the right; curve 4 is experimental with vertical scale on the left. A) cm/sec; B) at distance 26 cm; C) $V_{\text{теор}}$ 10^7 cm/sec [velocity of ejection]; D) oersted.

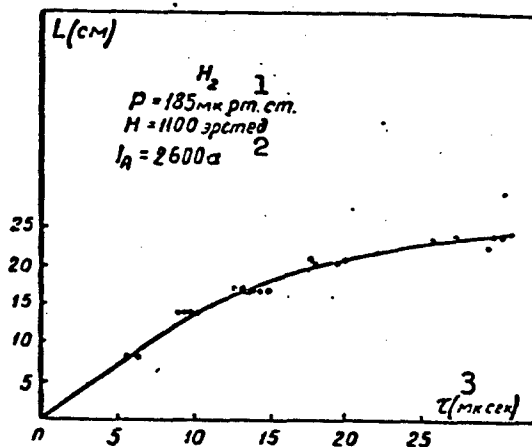


Fig. 5. Plot of motion of plasma in hydrogen in tube B at $I_A = 2.6$ kiloamperes, $p_0 = 0.185$ mm Hg, and $H = 1200$ oersted. 1) Microns mercury; 2) oersted; 3) μsec .

value is 2.4×10^7 cm/sec. The plasma ejection velocities obtained by extrapolating the experimental data turn out to be nevertheless lower than those obtained by calculation. Thus, one can state that there is good qualitative agreement between the character of the experimental and theoretical dependences of the plasma velocity on the type of gas, on its initial pressure, on the current amplitude, and on the intensity of the external magnetic field. However, the absolute values of the measured velocities, and also of the limiting magnetic fields, differ

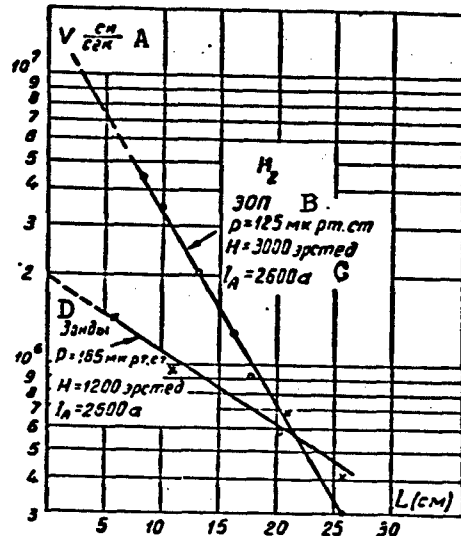


Fig. 6. Dependence of v in hydrogen on the distance covered along the tube B: 1) $p_0 = 0.185$ mm Hg, $I_A = 2.6$ kiloamperes, $H = 1200$ oersted; 2) $p_0 = 0.125$ mm Hg, $I_A = 2.6$ kiloamperes, $H = 3000$ oersted. A) cm/sec; B) microns mercury; C) oersted; D) probes.

from the theoretical ones in that the experimental values of the ejection velocities are lower than the theoretical ones, while the limiting fields are larger. The reason for these disparities is still not completely explained. One of the possible reasons is the difference in

the conditions of the calculation and of the experiments, inasmuch as the theory developed in [1] pertains to a planar configuration while the experiment pertains to a cylindrical one.

REFERENCE

1. A.K. Musin, V.L. Granovskiy. Issledovaniye dvizheniya provodящego gaza, uskorennogo skreshchennymi elektricheskimi i magnitnymi polyami (chast' I - teoreticheskaya) [Investigation of the Motion of a Conducting Gas Accelerated by Crossed Electric and Magnetic Fields (Part I - Theoretical)]. In the present collection, page 414.

OBSERVATION OF HYDROMAGNETIC OSCILLATIONS IN THE PLASMA
OF A PULSED ELECTRODELESS DISCHARGE

M.D. Gabovich, I.M. Mitropan
Kiev

The discharge of a capacitor bank into two single-turn coils 70 mm in diameter (current oscillation period 6 μ sec) excited an electrodeless pulse discharge in hydrogen. By means of a magnetic probe and belts it was possible to observe the radial oscillations of the plasma connected with the annular current. A comparison of the observed period of these oscillations with the calculated value makes it possible to determine the concentration of the ions, which is in satisfactory agreement both with the concentration of the neutral atoms and with the concentration of the ions as determined from the width of the spectral lines. A distinguishing feature of the case considered here is that the oscillations of the plasma ring occur upon compression of a magnetic field that opposes the external field, i.e., a field whose lines are connected with the internal currents in the plasma, and not with the currents in the external turn. In a heavy gas (krypton), as expected under our conditions, there is neither compression of the frozen-in field nor oscillations of the plasma ring.

SCHEMES OF ELECTROGASDYNAMIC MACHINES

Ye. I. Yantovskiy
Khar'kov

Electrogasdynamic generators are intended for direct conversion of the energy of a gas stream into electricity. This obviates the need for introducing blades in the stream of the high-temperature gas and it becomes possible to increase appreciably the maximum temperature of the thermodynamic cycle, and consequently also the thermal efficiency.

In most cases the energy conversion does not call for rotating parts to be present in the machine.

As regards the operating principle, all the known types of electro-gasdynamic machines (EGM) do not differ from ordinary electric machines. The main distinction of the EGM is that it has a gaseous rotor as a moving part which directly serves as the operating body of the heat engine which carries out the thermodynamic cycle. The EGM is therefore a unification of the heat engine and the electric machine.

Electric current can flow in a gas either if the gas contains a sufficient number of free electrons and ions moving under the influence of an electric field, or when the gas contains overwhelmingly charged particles of one sign, carried by the gas stream.

As is customary in magnetic gasdynamics, the current density is written in accord with the generalized Ohm's law in the form

$$\vec{j} = \sigma(\vec{E} + \vec{v} \times \vec{\mu} \vec{H}) + \rho \vec{v}; \quad (1)$$

here \vec{j} is the current density; σ is the electric conductivity of the gas; \vec{E} is the intensity of the electric field; \vec{v} is the velocity of

gas in the reference frame in which \vec{E} is measured; \vec{H} is the magnetic field intensity; μ is the magnetic permeability; ρ_e is the density of free charges.

We shall a machine magnetogasdynamics if the energy exchange in it is effected by the work of the conduction current (first term of the right half of (1)).

It is customary to call a machine convective if the gas flow in it does the work necessary to transport the charges together with the gas against the forces of the electric field. Use is made here of the convection current (second term of the right half of Eq. (1)).

Magnetogasdodynamic machines can be divided into two classes, depending on the method by which the external electric field \vec{E} is produced.

In conduction machines the field \vec{E} is applied directly to the boundaries of the gas stream with the aid of electrodes.

In induction machines there are no electrodes and the external electric field is produced by time variation of a magnetic field.

Each of the foregoing types of machines is also used in ordinary electric machine building. The conduction scheme is the equivalent of the unipolar electric machines, the prototype of which was the Faraday disk. One can classify as induction machines the ordinary synchronous and induction AC machinery. The convection scheme corresponds to an electrostatic generator with moving belt.

In view of the exclusive advantages of the EGM as compared with ordinary machines, many proposals were made by which to bring into being each of the three mentioned possible types of machinery.

Although none of these proposals have been realized to date on an industrial scale, they are of great interest. The use of modern theoretical and experimental data on magnetic gasdynamics and plasma phys-

ics as applied to specific schemes will apparently make it possible to choose in the nearest future the most suitable scheme for each technical problem. Particular interest is attached in EGM for station power, since in principle the upper limit on the power is eliminated by the absence of rotating parts.

We present below a brief review of different schemes which we were able to find in the literature. Within each class, the description is in chronological order.

I. CONVECTION GENERATORS

In Braun's scheme [1] (Fig. 1) steam or some other vapor from source A is fed into two nozzles, each of which is surrounded by oppositely charged belts B_1 and B_2 .

When the expanding steam flows past each sharp point S_1 and S_2 , ions of different signs are obtained by electric induction. These serve

as condensation centers and are dragged by the steam toward grid electrodes K_1 and K_2 , to which they give up their charge. The steam is then fully condensed in a cooler and the liquid is pumped to the heater. The electrodes K_1 and K_2 , on which a potential difference is produced and maintained by the steam flow, are connected to the useful load.

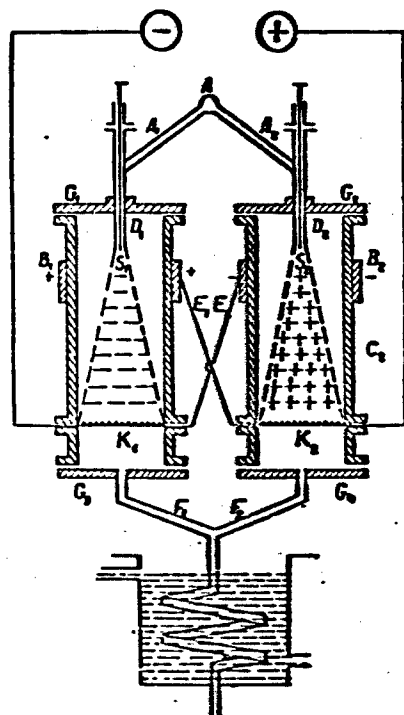


Fig. 1

In the scheme of Ye.M. Sinel'nikov [2] (Fig. 2), provision is made for externally heating the cathode 3, which is provided with sharp points and which is covered by a substance having a large thermionic emission. The electrons emit-

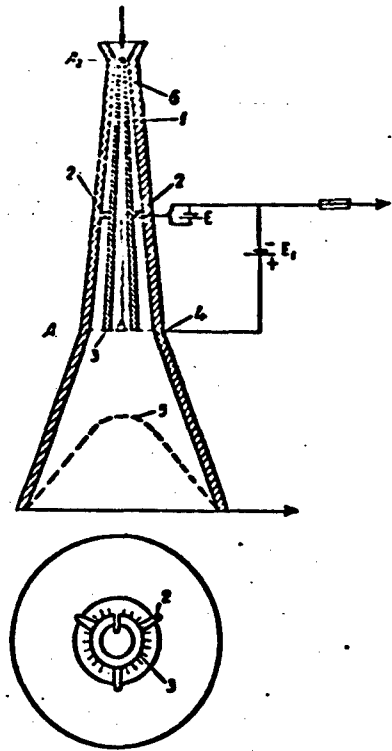


Fig. 2

ted by the cathode are dragged by the jet of mercury vapor to a grounded charge collector 5, so that the potential of the cathode is reduced relative to ground. The working current flows through the useful load which is connected to the cathode and the collector.

In the AEG scheme [3] (Fig. 3), provision is made for the use of spherical electrodes to obtain high voltage with the aid of a convection generator. To avoid vorticity and hydraulic losses it is proposed to pass the steam jet inside an insulated tube provided with metallic honeycombs or Raschig rings and placed

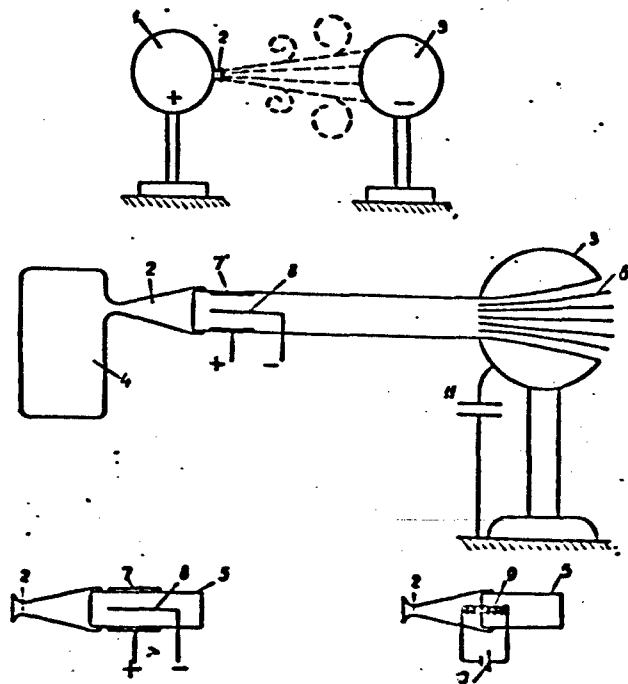
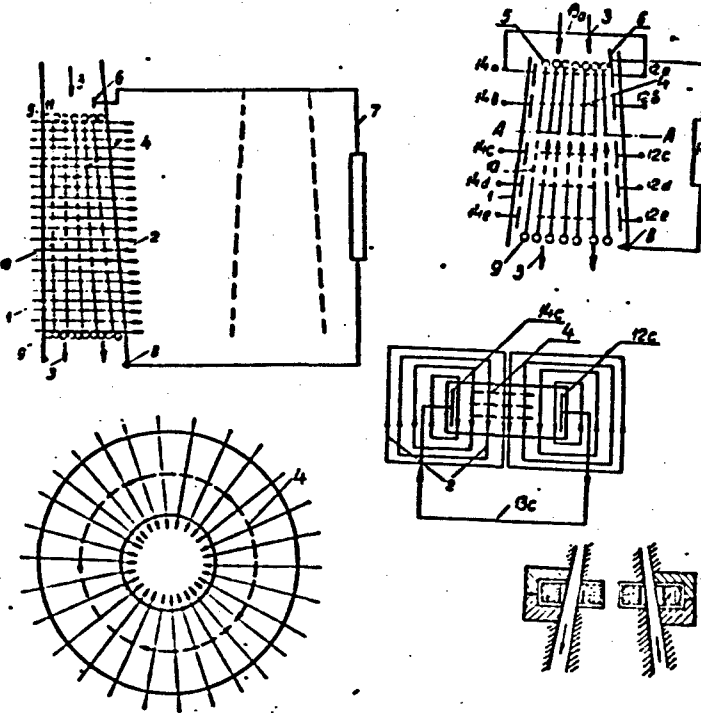


Fig. 3

inside a spherical electrode.

In the scheme of Karlovitz and Halasz [4] (Fig. 4), a stream of previously ionized combustion products (in the mean, neutral) is fed to a jet of annular section with radial stationary magnetic field of such intensity as to retain the electrons, which have a large mobility, but pass the ions. At the entrance to the magnetic field there is formed an annular electron current and a negative pole, while at the exit from the nozzle there is an accumulation of positive ions.*



The possibility is afforded of changing the magnetic field strength with changing load, and also with changing velocity along the channel. Mention is made of the possibility of feeding into the combustion chamber air heated by cooling its walls, and also the possibility of iso-thermal combustion in a channel of variable cross section.

According to the scheme of G.I. Babat and R.P. Zhezherin [5] (Fig. 5), mercury vapor supercooled in nozzle C is partially condensed on the positive ions which diffuse toward the grid electrode C from an arc burning between electrodes F and A, or from another ionizer. Schemes are presented wherein three generators are connected together by means of a mechanically rotating switch in order to feed the steam into the

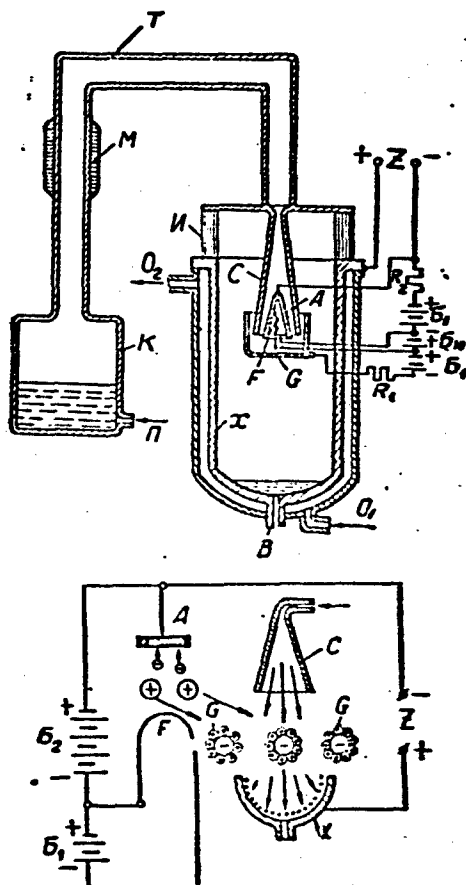


Fig. 5

nozzles by pulses and obtain three phase AC of varying frequency.

A model of such a generator [6] delivered a current of 50 ma at 100 v. According to calculations by the authors, at a voltage of 1000 v the density of the convection current may reach $0.25 \cdot 10^{-3}$ amp/cm².

B.I. Ostreyko [7] proposed to charge by electrostatic induction mercury particles and then, to obtain small particles with increased charge at high potential, propel the mercury mechanically through a grid with capillary apertures, and entrain the resultant small jets by means of a jet of steam; he also pointed out the possibility of feeding the steam generator with a liquid containing an admixture of metallic particles in suspended state.

A.S. Semenov [8] (Fig. 6) proposed still another generator construction with two oppositely charged vapor streams and mutual electric induction.

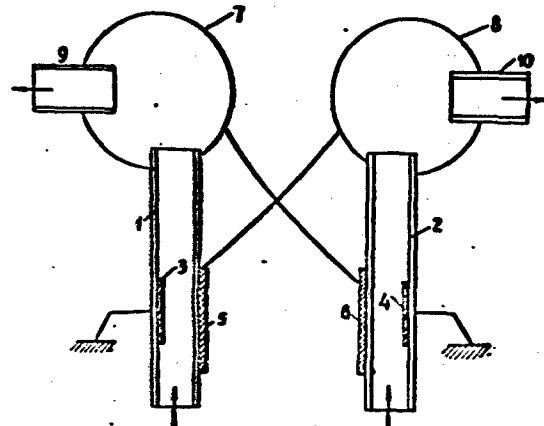


Fig. 6

Marks [9] carried out extensive calculations and proposed a convection generator using aerosols; this generator consists of a large number of short small-diameter nozzles. When gas of high dielectric strength is used (freon or carbon tetrachloride) the possible convection current density as calculated by the author is 50 amp/m². In his

calculations the author uses the data of Pauthenier [10] on the limiting charge of spherical particles in high-voltage convection generators.

In the scheme by Krapf [11] (Fig. 7), positive ions are obtained by surface ionization when gas flows past an electrode having a work function larger than the ionization potential of the gas, with subsequent neutralization on an electrode having a work function smaller than the ionization potential. The convection current flows between the electrodes, which are used as a cathode and an anode, with the circuit closed by the useful load. The voltage is increased by connecting generators in series.

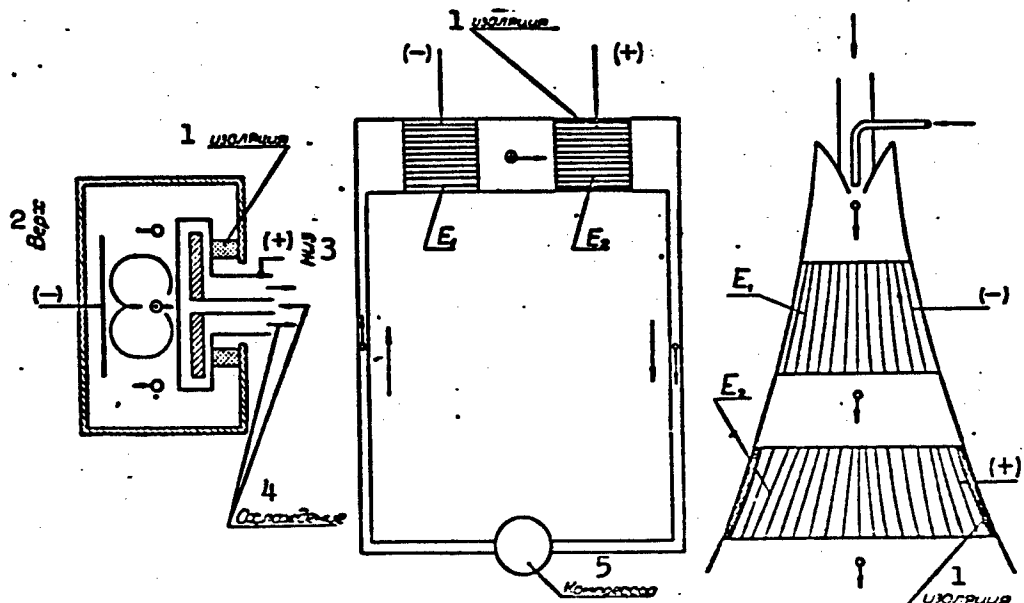


Fig. 7. 1) Insulation; 2) top; 3) bottom; 4) cooling; 5) compressor.

In the scheme of B.M. Molchanyuk [12] (Fig. 8), the specific power of the convection generator is increased by constructing the intermediate insulated electrode in the form of a lattice of aerodynamic streamlined profiles. At the instant when the circuit is closed, the potential difference between electrodes 1 and 3 gives rise to a corona discharge. The positive ions produced are distributed by the gas stream.

over the surface of an insulating cover 2, forming as it were the second electrode of a capacitor, made up of the ionized gas. The working current is drawn through electrodes 3 and 4.

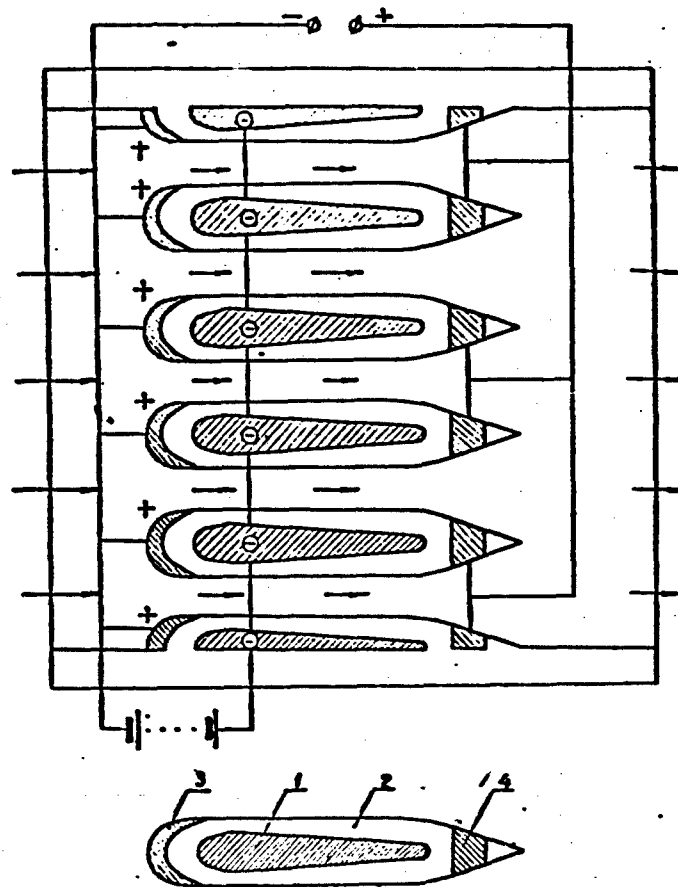


Fig. 8

The convection generator schemes considered above, by virtue of the difficulties involved in producing a high density of free charges, are characterized by low current density even when the gas velocity is high. They are therefore of no interest for stationary power, but can be useful in those cases when low power DC at high voltage is necessary.

II. CONDUCTION GENERATORS

The first magnetic gasdynamic scheme known to us is that of Scherer [13] (Fig. 9).

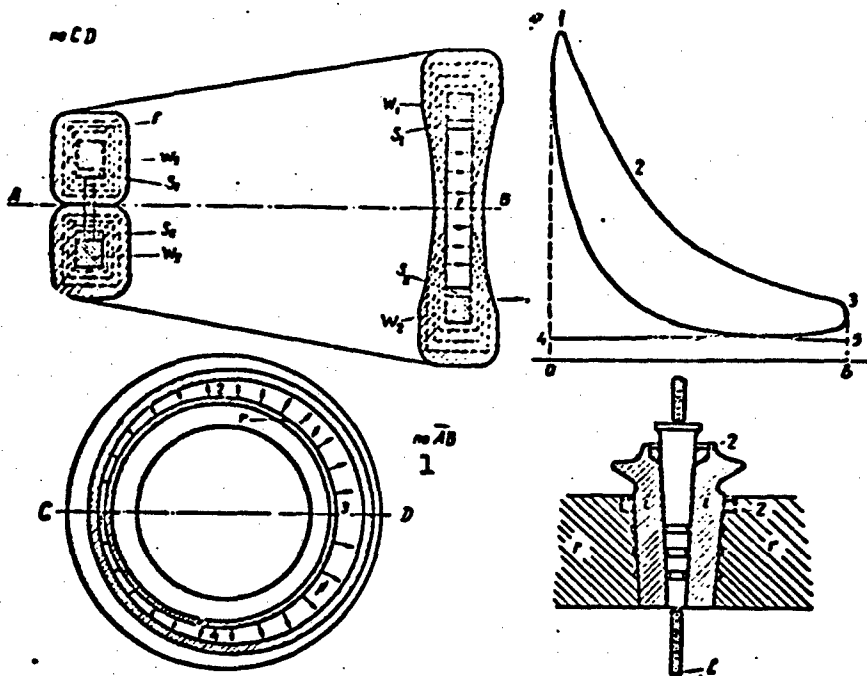


Fig. 9. 1) Section AB.

A stationary transverse magnetic field is produced in a channel of rectangular cross section of variable area, closed in the form of a ring and filled with electrically conducting gas, using two excitation windings W_1 and W_2 .

The opposite walls of the channels are made up of metal buses - electrodes S_1 and S_2 . If a potential difference is applied to the buses, current will flow through the gas in a direction perpendicular to the magnetic field. The interaction between the current and the magnetic field produces a force that compresses the gas as the latter flows into the narrower portion of the channel 4-1, after which heat is fed to the gas from a source not indicated in the diagram. The gas then flows into the expanding portion of the channel, where the voltage induced by the moving gas as a result of the increase in the distance between the buses exceeds the voltage applied for the compression. After expansion, the gas is cooled in sector 3-4 and is again compressed.

In sector 1-2-3 (expansion) the current and the induced emf coincide in direction and the energy of the gas flow is converted into electricity, while in sector 3-4-1 (compression) the current and the induced emf are opposite in sign and the electricity is consumed by the gas. Inasmuch as heated gas is expanded and cold gas is compressed, the expansion work exceeds the compression work and the resultant electricity can be usefully employed.

An analogous process occurs in any heat engine, for example in a diesel engine, and is represented by an equivalent indicator diagram in pressure-specific gas volume coordinates.

The proposed engine converts the heat energy obtained from the heater into electricity delivered by the buses.

The author refers to earlier predictions of similar processes (Zeitschr. f. Electr., No. 17, 1898).

The construction of a mercury-field contact for removing the current from the buses is given.

No methods are indicated for obtaining a gas of sufficient electric conductivity.

Meszlang [14] proposed to make the medium electrically conducting by ionization with ultraviolet, x-ray, or other radioactive radiation, and also to use high temperatures and glow discharge. To obtain a high voltage, which calls for a large gas velocity, it is proposed to use a Laval nozzle.

Kramolin [15] (Fig. 10) proposed a generator scheme in which gas flows in a transverse magnetic field, and in order to reduce the voltage near the electrodes it is proposed to use materials with low work functions and incandescent electrodes.

In a series of patents by the Siemens-Schuckert firm [16-19] schemes are described of AC conduction generators and methods of con-

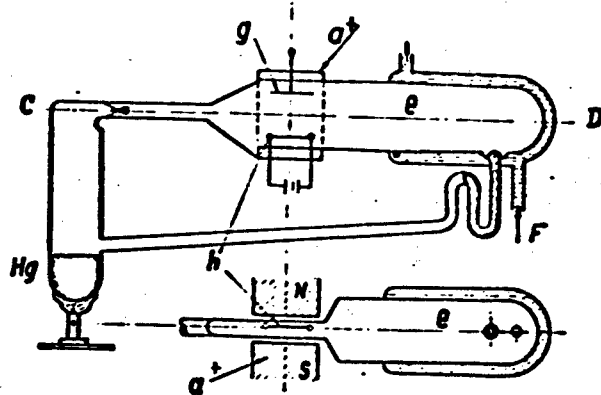


Fig. 10

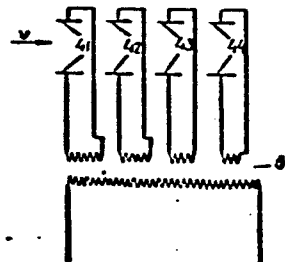
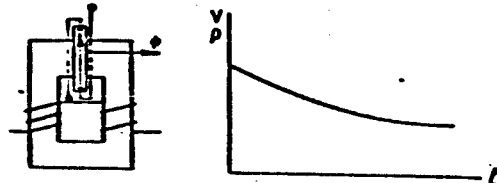
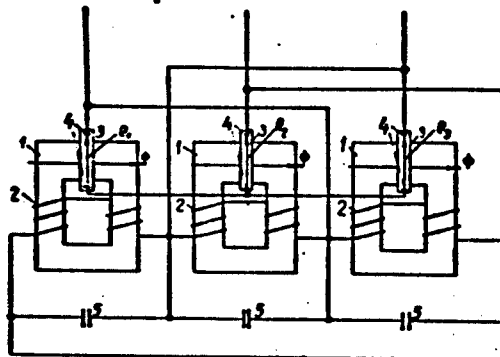


Fig. 11

necting them [19] (Fig. 11) in order to obtain three phase currents, with capacitors that produce reactive power for the excitation bind-

ings, and with such an arrangement of the working current conductors as to neutralize the armature reaction.

It is proposed to place the generators in succession along the gas stream and to couple them by means of transformers to the line, so as to reduce the induced AC voltage along the gas channel.

Kolbasko [20] (Fig. 12) makes mention in a description of a conduction pump for current conducting liquids that such a pump is reversible, i.e., that it can operate as a generator, and proposes a series excitation system by which the magnetic field is produced by the variable working current.

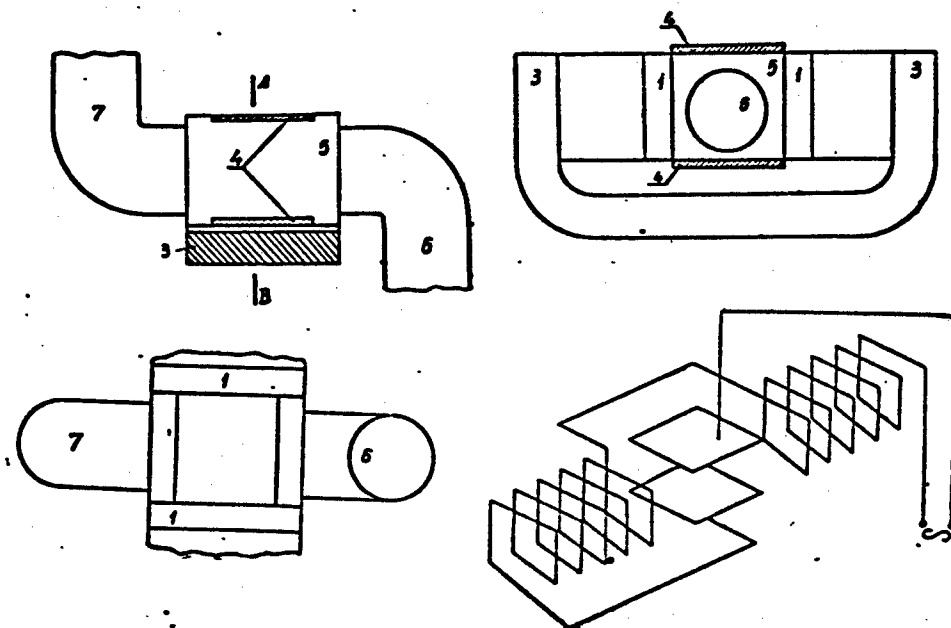


Fig. 12

Sporn and Kantrovitz [21] have proposed a scheme for a large scale power installation with a conduction magnetogasdynamic generator, in which the working mediums employed are the combustion products of coal (Fig. 13). The total power of the installation is 462 megawatts, of which 97 megawatts is obtained by an ordinary steam turbine unit using

the gases in which the electroconductivity has been decreased upon reduction in temperature. The total efficiency of the installation is estimated to be 55%. The combustion chamber is fed with air heated by the combustion products in a regenerator to 2000°C at a pressure of 10 atmospheres. The maximum temperature in the combustion chamber is 2940°C , which ensures sufficient ionization if a small amount of additive with low ionization potential is added. The resultant DC is converted into AC with the aid of a special unit.

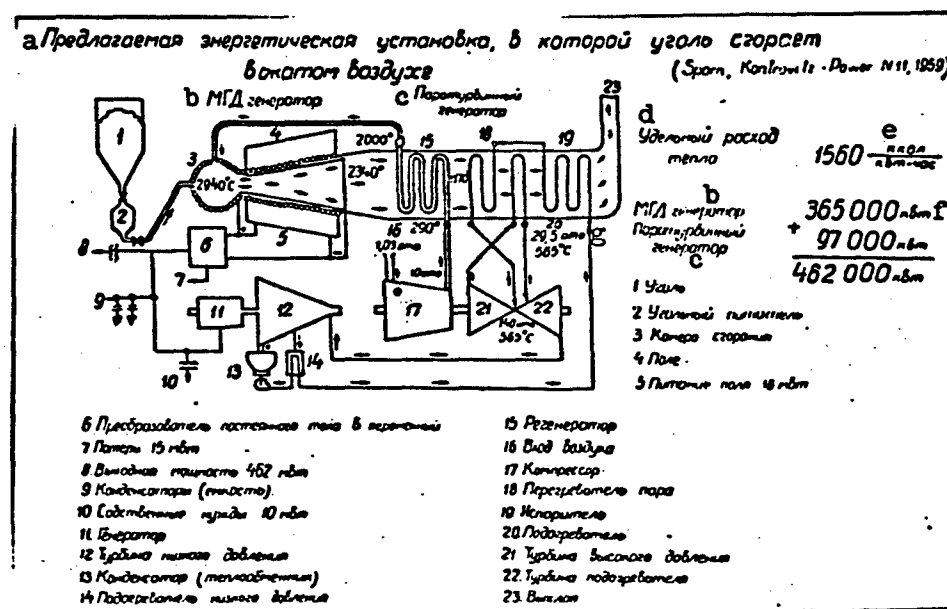


Fig. 13. a) Proposed power installation in which coal is burned in compressed air; b) magnetohydrodynamic generator; c) steam turbine generator; d) specific heat flow; e) kcal/kw-hr; f) kw; g) atmospheres. 1) Coal; 2) coal feed; 3) combustion chamber; 4) field; 5) field supply 18 megawatts; 6) DC to AC inverter; 7) losses 15 megawatts; 8) output power 462 megawatts; 9) capacitors; 10) station needs, 10 megawatts; 11) generator; 12) low-pressure turbine; 13) condenser (heat exchanger); 14) low-pressure feed water heater; 15) regenerator; 16) air inlet; 17) compressor; 18) steam superheater; 19) evaporator; 20) feed water heater; 21) high-pressure turbine; 22) feed water heater; 23) exhaust.

A recently published communication reports the construction of a model of a conduction generator with a capacity 10 kw, as well as other

models [22, 23].

Conduction generators can produce both direct and alternating current, but at the practically attainable gas velocities and dimensions, the voltage obtained can be on the order of a thousand volts, which is insufficient for stationary power generation, although in individual cases it is usable.

The main difficulty in developing induction generators is the elimination of the voltage drop in the boundary layer near the electrode, and the attainment of a sufficient service life for the electrodes. In the case of intense cooling of the electrodes, one can expect the near electrode layer to have a high electric resistance resulting from the drop in thermal ionization owing to the temperature decrease:

III. INDUCTION GENERATORS

The first of the induction generator schemes known to us is that described in [24] (Fig. 14), where the working medium is mercury vapor.

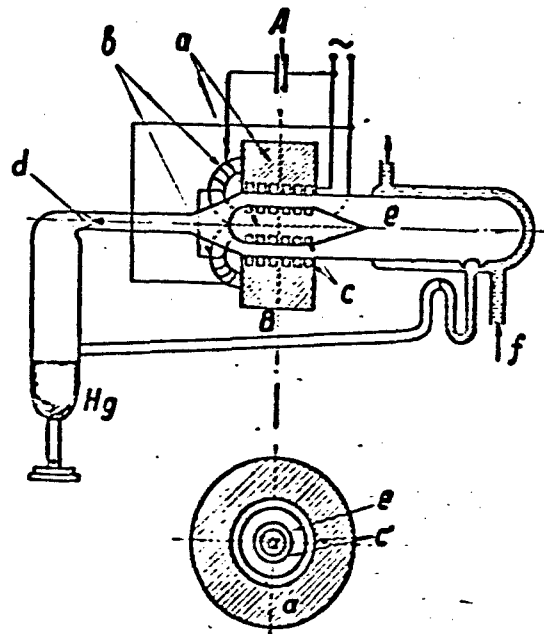


Fig. 14

On the whole the scheme is analogous to that of [15], except that the energy from the vapor flow and its conversion into electricity occurs with gas flowing in a channel of annular cross section, formed by the external and internal magnetic circuits a. The magnetic circuits have windings C, in which voltage is induced when the electrically conducting gas flows in a radial alternating magnetic field produced by separate excitation winding b.

In this scheme, the current in the gas flows in a ring produced in a plane perpendicular to the gas velocity, and there are no electrodes. The excitation winding is connected through a capacitor in parallel to the working winding C.

Among the induction type generators one can include a gas nuclear fission reactor proposed by Colgate and Aamodt [25], in which the thermal energy is released in a shock wave in gaseous uranium. The layer of conducting gas moving behind the front of the shock wave is periodically reflected from the end walls of the cylindrical volume of the reactor thus performing work in an alternating magnetic field of a short solenoid which surrounds the reactor.

Several schemes for induction generators for stationary power were considered at the NIIELEKTRO.

The radial scheme of an induction magnetogasdynamic generator [26] (Fig. 15) is a modification of a plane linear magnetic circuit used in magnetofugal electric machines and induction pumps for liquid metal. However, in plane linear schemes a "transverse edge effect" arises, as a result of which the effective electric conductivity of the gas decreases. In the radial system the transverse edge effect is apparently weakened. In addition, it is easier to obtain here a constant gas velocity at subsonic speed by specially shaping the channel. In this scheme an alternating magnetic field which moves in an almost radial

direction is produced with the aid of a winding on a stator consisting of two disks.

The conducting gas moves radially from the inside to the outside at a velocity larger than that of the field. A three-phase operating

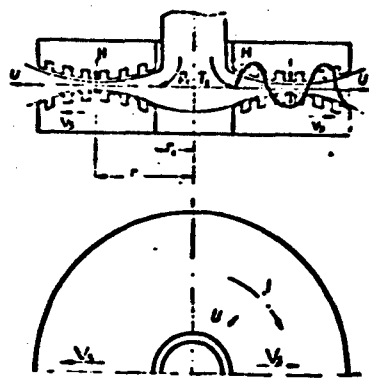


Fig. 15

current shifted in phase relatively to the excitation current is induced, as in an ordinary induction generator, by the current in the gas.

At the electric conductivity that is practically attainable for combustion products, the power factor of such generators is relatively small and consequently additional synchronous machines or

capacitors are necessary to provide the reactive power.

In one machine, the complete cycle of conversion of the chemical energy of the fuel into electricity can be effected by using a rotating rotor. The energy of the combustion products is in this case also extracted by magnetogasdynamic interaction; as in all other systems, there is no need for turbine blades, so that the limitations on the maximum cycle temperature become weaker.

An example of such a scheme is the disk generator [27] (Fig. 16). The magnetic excitation field (the external field) is produced by a rotating inductor 7, which is fed with DC, as in an ordinary synchronous generator.

When fuel is burned in chamber 5, which is placed in a gap between the inductor and stator 1, a flow of electrically conducting combustion products is produced. Because the peripheral component of the gas velocity, which is guided by partitions 6, exceeds the speed of the inductor, closed currents interacting with the inductor field and the force

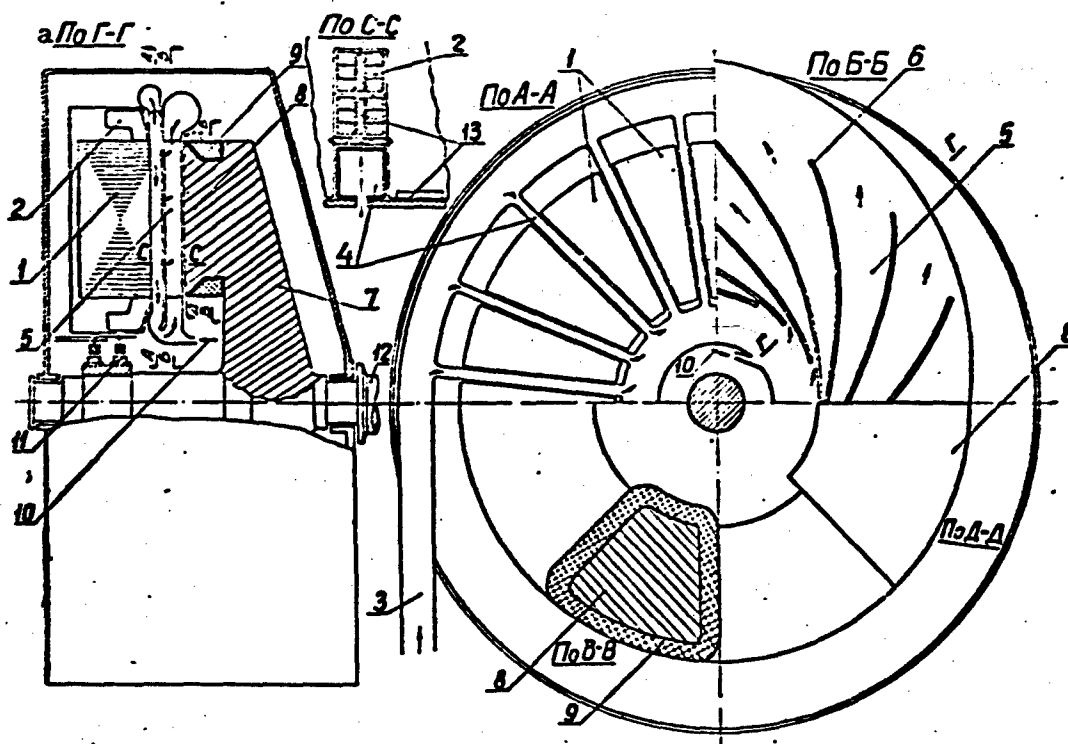


Fig. 16. a) Section.

maintaining the latter in rotation are produced in the gas.

In this case the magnetic field of the inductor poles plays the role of the turbine blades and if there is no winding in the stator, such a device could be called a magnetic turbine, since it transforms the energy of the gas stream into mechanical rotation energy.

If a three-phase winding 2 is placed on a stator, the alternating magnetic flux of the rotating inductor induces a voltage and a current in the latter, as in an ordinary synchronous generator.

The air necessary for the combustion is compressed in a compressor mounted on the shaft and is fed into the channels 4 above the stator slots and from there, through openings in the wall, into the combustion chamber. The disk form of the stator makes it possible to obtain the necessary increase in the transmission cross section of the chamber as

the gas expands.

In the case of low expansion, such a machine can be built using an ordinary synchronous generator and a cylindrical rotor which has a sufficiently large gap to hold the chamber with the stream of conducting gas [28] (Fig. 17).

The air compressed in compressor 2 is fed to a spiral chamber 5, made of refractory material and located in the gap of an ordinary large synchronous generator. The areas fed through the openings in the walls into the spiral combustion chamber 7, to which fuel and ionizing additives are supplied. The combustion occurs over the entire length of chamber 7. The combustion products, which become electrically conductive because of the thermal ionization of the additives and because of chemical ionization, flow in the magnetic field produced in rotor 9, and cause the rotor to turn as a result of the eddy currents in the gas.

This scheme is effective if the expansion is incomplete and the heat of the exhaust gas is utilized in an ordinary gas turbine or some other cycle.

The use of guiding partitions in the chamber is not essential. By making the poles of the inductor of special shape, it is possible to obtain such a magnetic field configuration, as to change the direction of the gas entering into the chamber and thereby producing a rotating torque. A preliminary examination of such a generator scheme with skewed poles is contained in the paper by L.Yu. Ustimenko and Ye.I. Yantovskiy (Izv. AN SSSR, OTN, Mekhanika i mashinostroyeniye, 5, 1960).

Inasmuch as the generation of electricity in schemes with rotating inductor is similar to that in an ordinary synchronous generator, such machines are best called synchronous magnetogasdynamic generators, bearing in mind their drive, which does not contain a blade-type turbine.

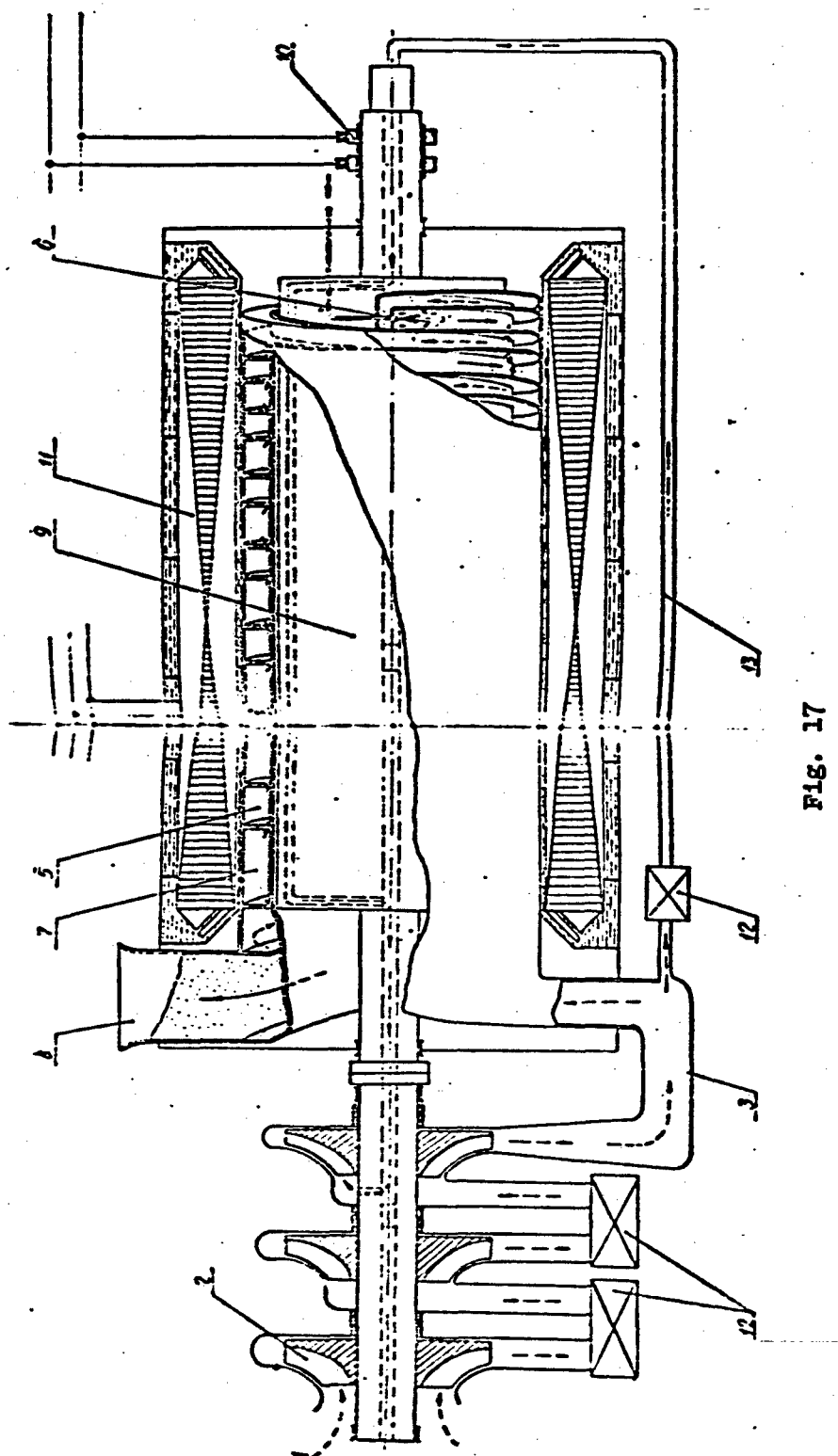


FIG. 17

The walls of the chamber of any induction type generator can be intensely cooled, say with liquid, so that the maximum temperature of the thermodynamic cycle is not limited by their construction.

Unlike the conduction scheme, the electrode problem is eliminated, but a need arises for reactive power sources or for a rotating inductor.

Induction generators produce only alternating current of any power and any voltage, which, like ordinary generators, are limited by the insulation of the stator winding.

If the attainable electric conductivity of the gas (with the aid of 1% of potassium salt as an additive) is on the order of $1-10 \text{ ohm}^{-1}\text{cm}^{-1}$, it is possible to generate in one cubic centimeter of working space some 10-100 watts, so that one can count on a power on the order of 100 megawatts and higher in machinery of tolerable dimensions, already attained in turbine generator construction.

Inasmuch as the electric conductivity of the gas decreases with decreasing temperature, but its heat content still remains rather large, it is possible to obtain a high thermal efficiency by combining a magnetogasdynamic generator with an ordinary steam turbine or gas turbine unit.

For stationary power generation it is probable that the most appropriate will be the installation of an induction magnetogasdynamic generator in an existing station, where the synchronous generators can provide the necessary reactive power for excitation and the active power to drive the air compressor. On the whole, one can expect an appreciable increase in thermal efficiency of the cycle by increasing its maximum temperature.

REFERENCES

1. G. Braun, German Patent 329422, Class 21 g, Group 35, dated 22 March 1917.
2. Ye.M. Sinel'nikov, Author's Certificate 30773, Class 21 g, 31, dated 26 August 1931.
3. AEG. German Patent 666127, Class 21 g, 35, dated 16 May 1934.
4. B. Karlovitz and D. Malasz, German Patent 725433, Class 21 g, 35 dated 31 August 1935.
5. G.I. Babat and R.P. Zhezherin, Author's Certificate 48753, Class 21 d², 5 dated 29 August 1935.
6. G.I. Babat, ZhTF [Journal of Technical Physics], 8, 1936.
7. B.I. Ostreyko, Author's Certificate 58195, Class 21 g, 35 dated 20 October 1936.
8. A.S. Semenov, Author's Certificate 54939, Class 21 d¹, 7 dated 29 November 1937.
9. A.M. Marks, US Patent 2,638,555, Class 310 - 4 dated 14 December 1949.
10. M. Pauthenier. Rev. Gen. de l'Electric., 6, May 1939, 583 - 595.
11. S. Krapf, Federal Republic of Germany Patent 842233, Class 21 g, 35 dated 28 June 1950.
12. B.M. Molchanyuk, Author's Certificate 117379, Class 21 g, 35 dated 22 January 1958.
13. E. Scherer, German Patent 241970, Class 21 g, 35 dated 4 May 1907.
14. M. Meszlang, German Patent 245672, Class 21 g, 35 dated 6 April 1910.
15. L. Kramolin, German Patent 621990, Class 21 g, 35 dated 4 May 1932.
16. A.G. Siemens-Schuckertwerke, German Patent 685559, Class 21 g, 35 dated 14 April 1933.
17. A.G. Siemens-Schuckertwerke, German Patent 704505, dated 14 April

1933.

18. A. G. Siemens-Schuckertwerke, German Patent 622131 dated 24 May 1933.
19. A. G. Siemens-Schuckertwerke, German Patent 692706 dated 24 May 1933.
20. Ye.I. Kolbasko, Author's Certificate 42798, Class 21 d², 5 dated 9 August 1934.
21. P. Sporn, A. Kantrovitz. Power, 11, 1959.
22. Electr. Engineering, 1, 1960, 114, 28.
23. Atomnaya tekhnika za rubezhom [Atomic Engineering Abroad], 1, 1960, 45.
24. L. Kramolin, German Patent 632443, Class 21 g, 35 dated 4 May 1932.
25. S. A. Kolgeyt and R. Kh. Aamodt, At. tekhn. za rubezhom [Atomic Engineering Abroad], 4, 1957.
26. Ye.I. Yantovskiy, Doklad na Vsesoyuznom s"ezde po mekhanike [Report to the All-Union Congress on Mechanics], January 1960. Izv. AN SSSR, OTN, Mekhanika i mashinostroeniye, [Bulletin of the Academy of Sciences USSR, Division of Technical Sciences, Mechanics and Machinebuilding], 2, 1961.
27. Ye.I. Yantovskiy, Author's Certificate 127770, Class 21 g, 35 dated 5 June 1959.
28. Ye.I. Yantovskiy, Author's Certificate 128542, Class 21 g, 35 dated 31 March 1959.

Manu-
script
Page
No.

433

[Footnote]

This scheme can also be regarded as using Hall current and we consider it to be the start in the development of a special class of Hall type conduction generators.

Manu-
script
Page
No.

[List of Transliterated Symbols]

429 ЭГМ = EGM = elektrogazodinamicheskaya mashina = electrogas-
dynamic machine

444 НИИЭЛЕКТРО = NIIELEKTRO = Scientific-Research Institute
"Elektro"

CIRCLE DIAGRAM OF AN INDUCTION MAGNETOGASDYNAMIC GENERATOR

L.M. Dronnik

Khar'kov

The induction magnetogasdynamics generator (AMG) does not differ in principle from the ordinary induction generator. The only exception is the gaseous compressible rotor, which is capable of changing its volume with change in pressure.

The process of slowing down a gas stream in a rotating magnetic field is accompanied by a decrease in the total enthalpy of the gas due in general both to the decrease in temperature and to the decrease in velocity. The change in gas parameters over the length of the machine is obtained by solving the gasdynamic equations (usually in the one-dimensional approximation). The theory of ordinary induction machinery has been developed in detail, and it can be used in the design of AMG, provided the magnetogasdynamics generator with a speed that is variable along the machine is reduced to an equivalent generator with solid bulky rotor, having the same electric conductivity as the gas.

One can approach this problem in the following manner: the split is defined as the ratio of the Joule losses in the rotor to the value of the electromagnetic power

$$S = P_g / P_e; \quad (1)$$

the power given up by the gas is in the usual case (electromagnetic power)

$$P_g = \rho u \Delta i_0 F, \quad (2)$$

where ρ is the gas density, u is the gas velocity, F is the transverse

area of the gas channel.

Here Δi_0 is the decrease in the slowing down enthalpy with allowance for the Joule losses (without heat exchange).

Let us define $\Delta i'_0$ as the reduction in the slowing down enthalpy for an isentropic release of energy (no energy dissipation in the form of Joule heat).

The difference $\Delta i'_0 - \Delta i_0$ is due to the presence of heat losses in the gas.

The Joule losses are

$$P_e = \rho u (\Delta i'_0 - \Delta i_0) F, \quad (2)$$

$$S = \frac{\Delta i'_0 - \Delta i_0}{\Delta i_0}; \quad (3)$$

on the other hand $S = (v_s - v_{ekv})/v_s$, where v_{ekv} is the speed of the equivalent generator and v_s is the speed of the field,

$$v_{ekv} = v_s \left(1 - \frac{\Delta i'_0 - \Delta i_0}{\Delta i_0}\right); \quad (4)$$

Δi_0 and $\Delta i'_0$ are determined from the solution of the equations, particularly the energy equation,

$$1) \rho u \frac{di_0}{dx} = \sigma (\mu H^*)^2 (v_s - u) u + \sigma (\mu H^*)^2 (v_s - u)^2;$$

$$2) \rho u \frac{di'_0}{dx} = \sigma (\mu H^*)^2 (v_s - u) u.$$

Let us proceed to the construction of the circle diagram.

We consider a case in which the induction magnetogasdynamic generator is part of a power system, i.e., a generator with independent excitation (the voltage U and the frequency f are constant).

To construct the circle diagram it is sufficient to know the following:

I. The machine parameters:

a) active resistance of stator winding r_1 ;

b) reactance of the stator winding due to the leakage flux x_1 ;

- c) reactance of the stator winding due to the main flux x_m ;
- d) reduced active resistance of the gaseous rotor r'_2 ; (the electric conductivity of the gas is constant and sufficiently small, so that there is no skin effect and the resistance is the same as for a bulky rotor);
- e) the reactance of the rotor x'_2 ;
- f) the active resistance of the magnetizing circuit r_m .

II. The magnetizing current.

All this is determined from the check calculations and is independent of the operating mode of the machine (whether it is operated as a motor, a generator, or in plugging).

III. The equivalent slip.

Calculations have shown the following:

- a) the reactance of the rotor winding can be neglected;
- b) the active component of the magnetizing current, due to the iron and copper losses at no load, is so small compared with the reactive component, that it can also be neglected and the active resistance of the magnetizing circuit can be assumed equal to zero.

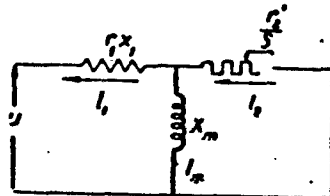


Fig. 1

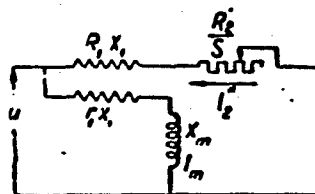


Fig. 2

The equivalent circuit referred to the locked rotor is shown in Fig. 1.

Further construction of the circular diagram does not differ in any respect from the construction for an ordinary induction machine [1].

As in an ordinary induction machine, the T-shaped circuit is re-

placed by an L-shaped circuit with suitable change in the parameters (Fig. 2).

The ideal no-load current is drawn, the diameter of the circle diagram is determined, as are also the currents in the rotor corresponding to $S = 1$ and $S = \infty$, and the slip scale is constructed.

Knowing the slip, we can determine the nominal current in the rotor and in the stator, the power factor, the electromagnetic power, and the efficiency (Fig. 3).

The circle diagram of the AMG has its own peculiarities:

a) inasmuch as the rotor has a very high resistance, the portion of the diagram between $s = 0$ and $s = 1$, corresponding to the motor mode, is very small; this indicates that at the existing electric conductivities it is difficult to use an induction magnetogasdynamic ma-

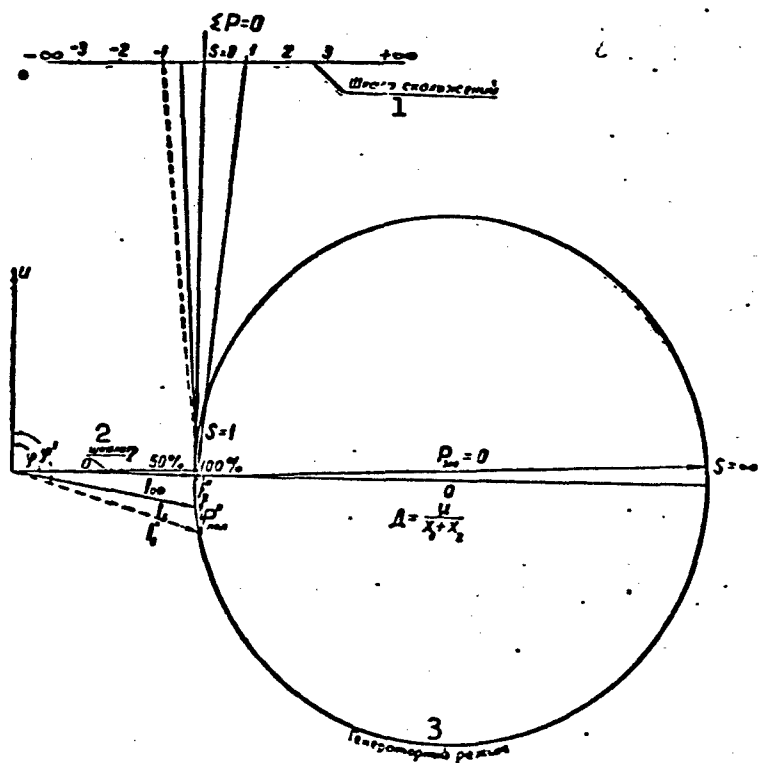


Fig. 3. 1) Slip scale; 2) scale; 3) generator mode.

chine as a motor;

b) the electric efficiency is defined as the ratio of the useful power to the electromagnetic power, the latter being equal to the decrease in the slowing down enthalpy multiplied by the gas flow.

After constructing the circle diagram, it is possible to determine all the operating characteristics of the generator (useful power, stator current, and efficiency), and only magnetogasdynamic calculations are necessary.

REFERENCE

1. M.P. Kostenko and L.M. Piotrovskiy, Elektrocheskiye mashiny [Electrical Machinery], Vol. II, 1958.

Manu-
script
Page
No.

[List of Transliterated Symbols]

452	AMГ = AMG = asinkhronnyy magnitogazodinamicheskiy generator = induction magnetogasdynamic generator
452	з = e = elektromagnitnyy = electromagnetic
453	зKB = ekv = ekvivalentnyy = equivalent

SOME EXPERIMENTS WITH A PLASMA JET

B.F. Bobylev, V.Ye. Stryzhak
Khar'kov

In order to accumulate experience on the development of plasma devices, we have designed and constructed a small plasma generator with a water-stabilized arc and graphite electrodes, with a power rating up to 40 kw.

It was planned to carry out a series of experiments, making it possible to determine the character of the destruction of the graphite electrodes and the character of the action of the plasma jet on various materials.

The anode employed was a graphite rod 15 mm in diameter, which could be displaced relative to the cathode. The cathode was a copper disk in the center of which was inserted an interchangeable graphite insert with a hole about 3 mm in diameter.

The power was delivered by an ordinary DC generator at 220 or 110 volts.

A stabilizing resistance (0.2 ohms) was connected in the arc circuit.

The duration of operation was on the order of one minute and was limited to the time required to burn out the graphite insert in the cathode.

In the operation of the plasma generator it was noted that the graphite insert is destroyed relatively more rapidly than the anode rod. Whereas the graphite insert permits in practice only one operating

cycle to be performed, the anode can be used for several cycles, although to be sure it is necessary to reset the anode so as to compensate for the wear of the graphite.

The rate of wear of the anode turned out to be not more than 0.5-1 mm/sec. Cases of the cathode melting outward (Fig. 1) and melting inward (Fig. 2) were noted.

The plug produced in the inward-melting hole was in the form of radially arranged spokes.

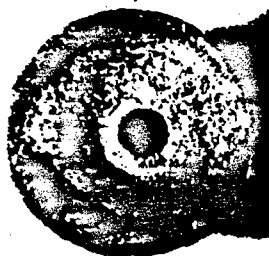


Fig. 1



Fig. 2



Fig. 3

In graphite cathodes the following changes were observed: first, formation of a thin outward-melting film on the end side of the cathode. Under a microscope one could see in such a film graphite particles as well as particles of a colorless glasslike substance (not more than 3-4%). Chemical analysis of the employed cathodes showed

their ash contents to be about 1.1%, but the high temperature obviously caused the glasslike substance to migrate to the surface of the cathode;

Second, the inward melting of the hole in the cathode. In examining a fracture of the cathode it was seen that near the exit aperture a graphite "plug" was produced, formed by radial spokes resulting from the melting of the graphite. Under the microscope, the portions of the molten graphite represent a black structureless mass.

Experiments were carried out in order to ascertain the character of the action of the plasma jet on solid and refractory materials (chamotte, granite).

One must take particular notice of the rapid destruction of granite. Figure 3 shows the outward appearance of granite after 5-10 seconds of plasma jet action. The energy concentration in this action was approximately 5 kw/mm^2 , with the hole in the cathode having a 3 mm diameter. Such an energy concentration cannot be produced apparently by any of the other means used in drilling.

We therefore consider it worthwhile to examine the question of the technical feasibility of using plasma installations for drilling in very hard rocks.

ACCELERATION OF A CONDUCTING GAS BY A TRAVELING MAGNETIC FIELD

V.B. Baranov

Moscow

Let us consider the problem of the acceleration, in a plane channel, of a weakly conducting gas by means of a traveling magnetic field, the direction of which is perpendicular to the direction of its motion.

The principle of producing a ponderomotive force acting on a liquid with the aid of a traveling magnetic field was used, for example, in pumps for liquid metals [1].

We analyze the problem in the one-dimensional formulation. All the parameters depend only on the coordinate x along the channel. The magnetic field is directed along the y axis in the plane of the flow.

We assume first that the magnetic field induced in the gas can be neglected. Then the average system of equations will have the form

$$\left\{ \begin{array}{ll} \rho u S = \rho_0 u_0 S_0 = G & (1) \text{ the continuity equation,} \\ \rho u \frac{du}{dx} + \rho \frac{dp}{dx} = \frac{\sigma H_0^2}{2c^2} (u_n - u) & (2) \text{ the equation of motion,} \\ c_1 \rho u \frac{dT}{dx} + p \rho u \frac{dp}{dx} = \frac{\sigma H_0^2}{2c^2} (u_n - u)^2 & (3) \text{ the equation of energy,} \\ p = pRT & (4) \text{ the equation of state.} \end{array} \right.$$

Here u_n is the velocity of the magnetic field along the x axis, u is the gas velocity, ρ is the density, p is the pressure, T is the temperature, S is the transverse area of the channel, G is the gas flow, σ is the conductivity, and c is the velocity of light. In order for the ponderomotive force to accelerate the gas we must have $u_n > u$.

When $S = \text{const}$ and $T = \text{const}$ the system (1-4) can be integrated to the end. The solution in the first case has the form

$$\bar{x} = A \ln\left(\frac{1-\bar{u}_0}{1-\bar{u}}\right) + B \ln\left(\frac{m-\bar{u}_0}{m-\bar{u}}\right) + C\left(\frac{1}{m-\bar{u}} - \frac{1}{m-\bar{u}_0}\right). \quad (5)$$

$$\bar{T} = -\frac{\bar{K} - (1-\bar{u})^2}{1 - \frac{m}{\bar{u}}}; \quad \bar{\rho} = m \cdot \frac{\bar{T}}{\bar{u}}; \quad \rho = \frac{1}{\bar{u}}. \quad (6)$$

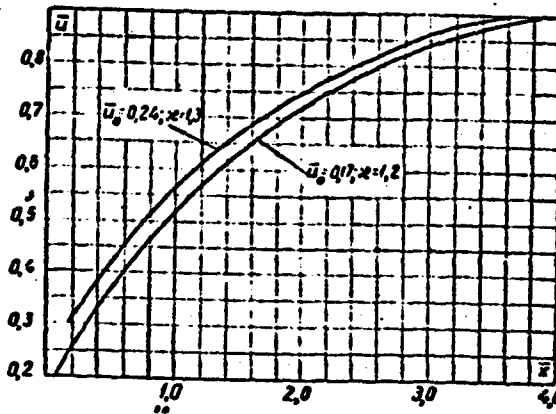


Fig. 1. $\bar{x} = \frac{a K_0^2}{c^2} \cdot \frac{S}{G} \cdot x; \quad S = \frac{m}{m_0}; \quad K_0 = \frac{u_0^2}{m_0}; \quad S = \text{const}$

$$\bar{K} = \frac{(1-\bar{u}_0)^2}{2} + \frac{\bar{u}_0^2}{\bar{u}-1} - \frac{\bar{u}_0}{\bar{u}}$$

(when \bar{u}_0 is equal to the velocity of sound).

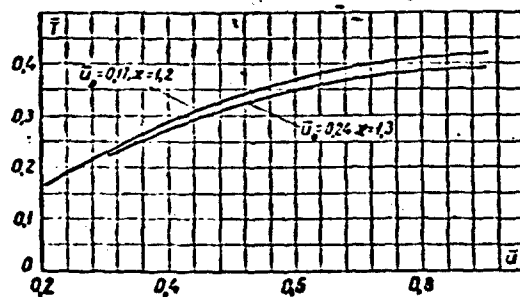


Fig. 2. $\bar{T} = \frac{T}{c_p^2}; \quad S = \frac{m}{m_0}; \quad S = \text{const}$

Here $\bar{x} = \frac{\sigma H_0^2 S}{c^2 G} x$; $\bar{u} = \frac{u}{u_0}$; $\bar{u}_0 = \frac{u_0}{u_a}$;

A, B, and C are constants that depend on $\kappa = c_p/c_v$ and K (K is the dimensionless constant of the energy integral).

$$K = \frac{K}{u_a^2}; \quad m = \frac{x-1}{x}; \quad \bar{T} = \frac{T}{u_a^2/c_v}; \quad \bar{p} = \frac{p}{\rho_0 u_0^2 u_a}; \quad \bar{\rho} = \frac{\rho}{\rho_0 u_0^2 / u_a}.$$

The index (0) pertains to values of the parameter in a certain initial section of the channel.

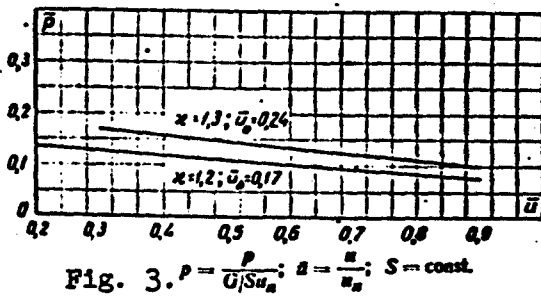


Fig. 3. $\bar{p} = \frac{p}{G/Su_a}$; $\bar{u} = \frac{u}{u_a}$; $S = \text{const}$.

Curves calculated from Formulas (5, 6) are plotted in Figs. 1-3.

In the second case the solution has the form

$$\bar{S} = \frac{1}{u} \exp z M_0^2 \left[\frac{1}{2} (\bar{u}^2 - 1) - \frac{1}{3 \bar{u}_a} (\bar{u}^3 - 1) \right]. \quad (7)$$

$$\bar{\rho} = z M_0^2 \bar{p} = \exp z M_0^2 \left[-\frac{1}{2} (\bar{u}^2 - 1) + \frac{1}{3 \bar{u}_a} (\bar{u}^3 - 1) \right], \quad (8)$$

$$\tilde{x} = \int \frac{\bar{u}^2 \bar{p} d\bar{u}}{\bar{u}_a - \bar{u}}. \quad (9)$$

Here $\bar{u} = u/u_0$; $\bar{\rho} = \rho/\rho_0$; $\bar{p} = p/p_0 u_0^2$; $\bar{S} = S/S_0$;

$$\bar{u}_a = \frac{u_a}{u_0}; \quad \tilde{x} = \frac{\sigma H_0^2 \bar{u}_a}{2 c^2 \rho_0 u_0} x,$$

M_0 is the Mach number in the initial section.

Plots calculated from Formulas (7-9) are shown in Figs. 4-6.

In the case when the channel varies in accordance to some specified law, the system of equations (1-4) reduces to a system of two non-linear first-order equations for u and T , which can be solved with respect to the derivatives du/dx and dT/dx .

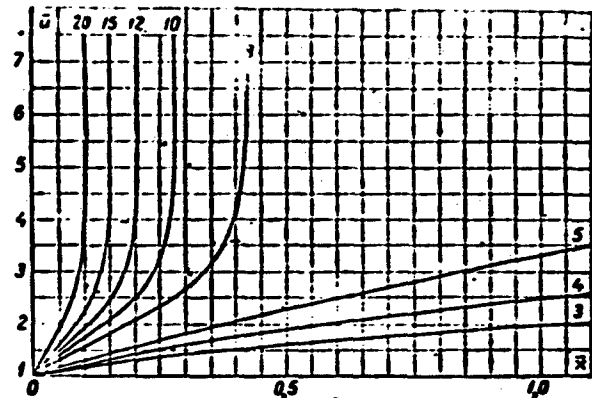


Fig. 4. $a = \frac{u}{u_0}$; $u_n = \frac{u_n}{u_0}$; $\bar{x} = \frac{ax^2 u_0}{2c^2 p_0 u_0}$; $x \cdot M_0^2 = 1$.

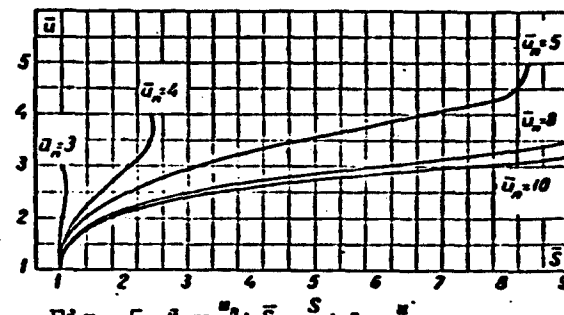


Fig. 5. $a_n = \frac{u_n}{u_0}$; $\bar{S} = \frac{S}{S_0}$; $a = \frac{u}{u_0}$; $x \cdot M_0^2 = 1$.

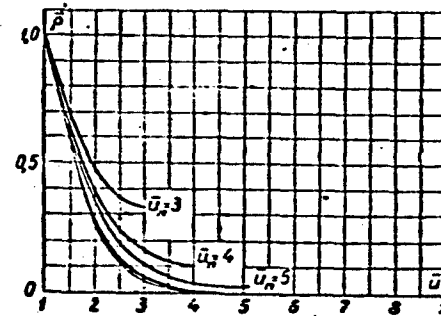


Fig. 6. $a_n = \frac{u_n}{u_0}$; $\bar{P} = \frac{\bar{P}}{p_0 u_0^2}$; $\bar{P} = \frac{P}{p_0}$; $a = \frac{u}{u_0}$; $T = \text{const}$; $x \cdot M_0^2 = 1$.

The results of the numerical calculations for a channel that expands gently in accordance with a linear law are shown in Figs. 7-10.

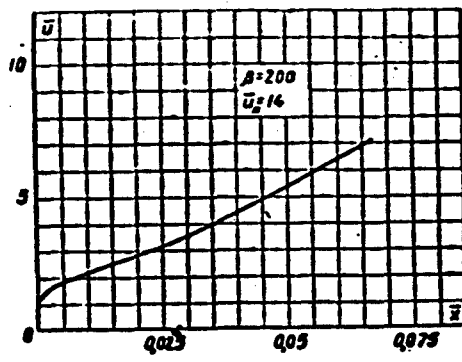


Fig. 7. $\bar{u} = \frac{\alpha H_0^2}{2c^2 \rho_0 \mu_0} \cdot x$; $B = \frac{H}{\mu_0}$; $S = 1 + \beta \bar{x}$; $\beta = \frac{\lg \alpha}{\alpha H_0^2}$
 $\rho_0 = \frac{1}{2c^2 \rho_0 \mu_0}$

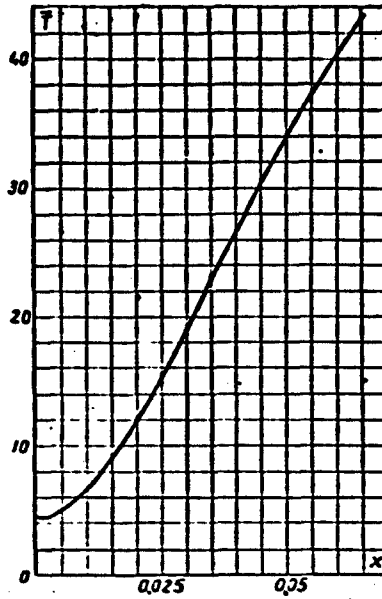


Fig. 8. $\bar{B} = \frac{\alpha H_0^2}{2c^2 \rho_0 \mu_0} \cdot x$; $T = \frac{B^2}{\mu_0^2 c_p} \dots$

As a result of the analysis made it is possible to conclude that it is most advantageous to accelerate the gas by suitably varying along the x direction both the shape of the channel and the velocity of motion of the magnetic field. In this case when $\sigma \sim 10^{11} \text{ sec}^{-1}$, $H_0 \sim 3000$ oersted, and $G \sim 1 \text{ g/sec}$ it is possible to accelerate the gas, under our assumptions, to a velocity $\sim 12 \text{ km/sec}$ over a distance of $\sim 1.5 \text{ m}$.

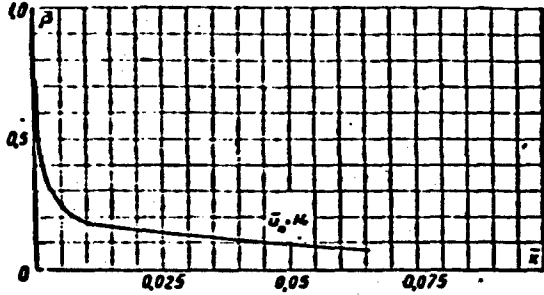


Fig. 9. $\bar{x} = \frac{cH_0^2}{2c^2 p_0 u_0} \cdot x; \bar{p} = \frac{p}{p_0}$.

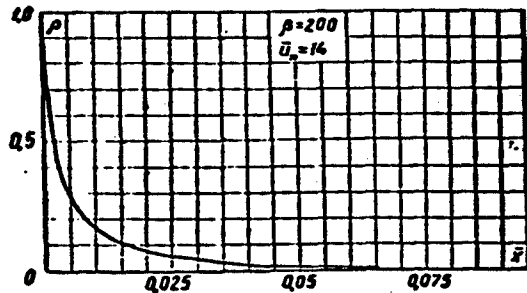


Fig. 10. $\bar{x} = \frac{cH_0^2}{2c^2 p_0 u_0} \cdot x; \bar{p} = \frac{p}{p_0}; S = \frac{S}{S_0} = 1 + \beta \bar{x}$

with $u_0 \sim 1$ km/sec (u_0 corresponds to the velocity of sound).

An estimate of the effect of the magnetic field induced in the gas on the acceleration has been made for the case $S = \text{const.}$

The following system of equations was integrated

$$\rho u = \rho_0 u_0, \quad (10)$$

$$\rho u \frac{du}{dx} + \frac{dp}{dx} = \frac{\sigma}{c^2} (u_s - u) H_s^2, \quad (11)$$

$$\frac{1}{x-1} u \frac{dp}{dx} - \frac{x}{x-1} \frac{p}{\rho} u \frac{du}{dx} = \frac{\sigma}{c^2} (u_s - u)^2 H_s^2, \quad (12)$$

$$\frac{dH_s}{dx} + \frac{4\pi\sigma}{c^2} (u_s - u) H_s = 0. \quad (13)$$

It is possible to obtain two integrals of this system:

$$\frac{u^2}{2} + \frac{x}{x-1} \frac{p u}{\rho_0 u_0} - \left(u + \frac{p}{\rho_0 u_0} \right) u_s = A_1, \quad (14)$$

$$\rho_0 u_0 u + p + \frac{H_y^2}{8\pi} = B_1. \quad (15)$$

Using (10, 13-15) and the initial condition $u = u_0$ when $x = 0$, we obtain

$$\begin{aligned} \tilde{x} &= L \ln \frac{u - \frac{x-1}{x} u_n}{u_n - \frac{x-1}{x} u_n} - M \ln \frac{u_n - u}{u_n - u_0} + \\ &+ \frac{N}{2a_1} \ln \frac{a_1 u^2 + b_1 u + c_1}{a_1 u_n^2 + b_1 u_0 + c_1} + \frac{P - N \frac{b_1}{2a_1}}{\sqrt{b_1^2 - 4a_1 c_1}} \times \\ &\times \ln \frac{(2a_1 u + b_1 - \sqrt{b_1^2 - 4a_1 c_1})(2a_1 u_0 + b_1 + \sqrt{b_1^2 - 4a_1 c_1})}{(2a_1 u + b_1 + \sqrt{b_1^2 - 4a_1 c_1})(2a_1 u_0 + b_1 - \sqrt{b_1^2 - 4a_1 c_1})}. \end{aligned} \quad (16)$$

$$H_y = \sqrt{\frac{8\pi}{3} \left[B_1 - \frac{\rho_0 u_0 \left(\frac{1}{2} \frac{x+1}{x-1} u^2 + A_1 \right)}{\frac{x}{x-1} \left(u - \frac{x-1}{x} u_n \right)} \right]}. \quad (17)$$

Here

$$\begin{aligned} \tilde{x} &= \frac{8\pi\sigma}{c^2 \rho_0 u_0} x; \quad a = -\frac{1}{2} \frac{x+1}{x-1}; \quad b = \frac{x+1}{x} u_n; \\ a_1 &= \frac{1}{2} \rho_0 u_0 \frac{x+1}{x-1}; \quad b_1 = -B_1 \frac{x}{x-1}; \quad c_1 = B_1 u_n + \rho_0 u_0 A_1; \\ L &= \frac{x \left[\left(\frac{x-1}{x} \right)^2 a u_n^2 + \frac{x-1}{x} b u_n + A_1 \right]}{u_n \left[\left(\frac{x-1}{x} \right)^2 a_1 u_n^2 + \frac{x-1}{x} b_1 u_n + c_1 \right]}, \quad M = \frac{x(a u_n^2 + b u_n + A_1)}{u_n(a_1 u_n^2 + b_1 u_n + c_1)}; \end{aligned}$$

$$N = a_1(M - L); \quad P = -\left(\frac{x-1}{x} a_1 u_n + b_1 \right) L + (b_1 + a_1 u_n)M - a.$$

The pressure, density, and temperature are obtained from (10, 14, 15) and from the equation of state. Calculations have shown that the magnetic field induced in the gas improves the characteristics of the acceleration (larger velocities are obtained over one and the same length, as compared with the case when the induced magnetic field was neglected). To determine the constant B_1 we used the condition that $H_y \rightarrow H_0$ when $u \rightarrow u_n$ (H_0 is the intensity of the external applied magnetic field).

If we put $u_n = E/H$ and $H_y = H$ (E and H are the mutually perpendicular electric and magnetic fields), then the solution of the system

(10-13) yields the solution of the problem of the acceleration of a gas in crossed electric and magnetic fields [2].

It must also be noted that simultaneously with our paper, another paper was presented to the Conference [3], in which a system of equations analogous to the system (10-13) was integrated, something the author found out later.

REFERENCES

1. Prikladnaya magnitogidrodinamika [Applied Magnetohydrodynamics], Trudy Instituta fiziki AN Latv. SSR [Transactions of the Physics Institute of the Academy of Sciences of the Latvian SSR], VIII, 1956.
2. Resler and Sirs, Perspektivy magnitnoy aerodinamiki [Outlook for Magnetic Aerodynamics], Mekhanika [Mechanics], 6, 1958.
3. I. B. Chekmarev, O kvazidomernom statsionarnom techenii szhimаемого provdyashchego gaza v kanale postoyannogo secheniya pri nalichii poperechnykh elektricheskogo i magnitnogo poley [Quasi-one-dimensional Steady-State Flow of a Compressible Conducting Gas in a Channel of Constant Section in the Presence of Transverse Electric and Magnetic Fields], Prikladnaya metematika i mekhanika [Applied Mathematics and Mechanics], XXIV, 3, 1960.

EQUATIONS OF MOTION OF PLASMOIDS
IN EXTERNAL MAGNETIC FIELD

K.D. Sinel'nikov, N.A. Khizhnyak, B.G. Safronov
Khar'kov

The Lagrangian is investigated of a system of nonrelativistic particles forming a quasineutral plasmoid, and the equations of motion of this plasmoid in external magnetic fields are determined. The forces acting on the plasmoid are obtained under the assumption that the kinetic energy of the plasmoid particles is small compared with the energy of their electrostatic interaction, and are represented in the form of an expansion in powers of the polarization. The zero-order terms of the expansion coincide with the forces acting on a flexible current loop in an external magnetic field.

The motion of a plasmoid in a linearly growing axially symmetrical magnetic field and in a homogeneous field during a time that is small compared with the time of thermal decay of the plasmoid is considered. The natural oscillations of the plasmoid are considered.

CONCERNING THE INTERACTION BETWEEN
PLASMOIDS AND A MAGNETIC FIELD

I.M. Podgornyy, V.I. Sumarokov
Moscow

Plasmoids accelerated by the electrodynamic method were injected in a magnetic field produced by two coils connected to buck each other. It is shown that the lifetime of the plasma in such a system amounts to several times ten microseconds. The capture of the plasmoid is accompanied by the appearance of an annular current in the gas. The reasons for the stability of this current remain unclear for the time

being.

The paper will be published in the foreign journal "Journal of Nuclear Engineering."

CONDUCTIVITY OF A PLASMA OF A STRAIGHT-LINE PINCH

M.D. Borisov, V.A. Suprunenko, Ye.A. Sukhomlin,
Ye.D. Volkov, N.I. Rudnev
Khar'kov

We investigated with the aid of magnetic probes the conductivity of a plasma of a straight-line strong-current discharge (pinch). A decrease in the conductivity of the plasma and in the lifetime of the pinch with increasing intensity of the electric field in the plasma was observed. In the case of ordinary strong-current discharges, it is pointed out that even a small amount of neutral atoms (on the order of 1%) has a great influence on the conductivity of the plasma.

INVESTIGATION OF THE PROPAGATION OF SHOCK WAVES IN A DISCHARGE TUBE

L.G. Chernikova, M.D. Ladyzhenskiy
Moscow

The paper reports on experimental investigations carried out on the conditions of electrical discharge necessary to obtain a uniform speed of propagation of a shock wave along a discharge tube.

Estimates are presented of the dependence of the energy release in the discharge gap of the tube on the parameters of the resonant circuit and the discharge conditions.

INVESTIGATION OF A SHOCK WAVE IN A CONICAL DISCHARGE TUBE

D. V. Orlinskiy

Moscow

By means of high-speed photography, an investigation is made of the dependence of the velocity of the front of a shock wave produced in a conical discharge chamber and propagating along the axis of a glass cylinder on the angle at the vertex of the cone, on the initial gas pressure, and on the voltage on the capacitor bank. The maximum velocity, $\sim 2 \cdot 10^7$ cm/sec, is obtained under the experimental conditions at $\alpha/2 = 12^\circ$.

The paper was published in ZhETF, 36, 3, 717, 1959.

INSTABILITY OF A PLASMA WITH ANISOTROPIC DISTRIBUTION OF ION AND ELECTRON VELOCITIES

A. B. Kitsenko, K. N. Stepanov

Khar'kov

The propagation of low-frequency magnetohydrodynamic waves in an unbounded plasma with anisotropic distribution of the velocities of the charged particles is investigated on the basis of the kinetic equation.

The conditions are obtained for the occurrence of instability, due to the anisotropy of the distribution function. It is shown that the kinetic analysis leads to an increase in the instability region compared with that obtained in the quasihydrodynamic approximation.

The paper was published in ZhETF, 38, 6, 1841, 1960.

INTERACTION OF AN ELECTRON BEAM WITH
A PLASMA IN A MAGNETIC FIELD

I.F. Kharchenko, Ya.B. Faynberg, R.M. Nikolayev,
Ye.A. Kornilov, Ye.I. Lutsenko, N.S. Pedenko
· Khar'kov

Results are presented of an experimental investigation of the interaction between a modulated and unmodulated beam of electrons with energy of 5 kev with a plasma in a magnetic field.

On passage of an unmodulated beam through a plasma, oscillations at the electron cyclotron frequency are produced in the beam.

In a magnetic field of definite value, large energy losses are observed in the beam (up to 2 kev), accompanied by an increase in the intensity of the glow of the beam and an increase in the intensity of the oscillations in the beam, over a wide range of frequencies.

Analogous effects were obtained for a beam modulated at the electron-cyclotron frequency and at frequencies that are multiples of it.

The paper was published in ZhETF, 38, 3, 685, 1960.

INVESTIGATION OF THE HIGH-FREQUENCY OSCILLATIONS OF
THE PLASMA PINCH OF A VACUUM ARC

B.G. Safronov, R.V. Mitin, A.A. Kalmykov, V.G. Konovalov
Khar'kov

The high-frequency oscillations accompanying the combustion of a loose vacuum arc were investigated. The arc was ignited in a vacuum $\sim 10^{-6}$ mm Hg at a current of 150-300 amp and in a magnetic field of 100-5000 gauss.

Strong high-frequency oscillations with frequencies of 1-2 megacycles were observed. The frequency of the oscillations depends linearly on the magnetic field. The distribution of the high-frequency

fields of these oscillations was investigated. It is concluded from the measurements that these oscillations are magnetohydrodynamic waves.

STUDY OF MAGNETIC PROPERTIES OF A PLASMA
BEHIND THE FRONT OF A STRONG SHOCK WAVE

K.D. Sinel'nikov, V.G. Safronov, G.G. Aseyev,
Yu.S. Azovskiy, V.S. Voytsenya
Khar'kov

The currents in a plasma behind the front of a strong shock wave (Mach number $M = 30-70$), arising as the shock wave moves in an axially symmetrical magnetic field (up to 400 oersted) were investigated. The nature of these currents is discussed in the case of a homogeneous and inhomogeneous magnetic field.

The dependence of the currents on the magnitude of the magnetic field and on the distance to the shock wave source in a homogeneous magnetic field are obtained. The applicability of this method for the determination of the conductivity and temperature behind the front of a strong shock wave ($M = 20$) is discussed.

Magnetic signals corresponding to successive shock waves were observed.

Preliminary experiments on the study of the polarization of a plasma behind the front of the shock wave in a transverse magnetic field (up to 2000 oersted) are described.

The paper is published in ZhTF, 31, 8, 893, 1961.

EXPERIMENTS WITH PLASMA JETS IN A MAGNETIC FIELD

A.M. Kostylev, A.A. Porotnikov
Moscow

METHODS OF OBTAINING HIGH-TEMPERATURE GAS

The solution of many physical and technical problems, and particularly problems in magnetic gasdynamics, calls for the use of a high-temperature gas heated to the so-called plasma state, when thermal ionization is significant. In shock tubes, in explosion of wires, in pulsed strong current discharges in gases, high temperatures are obtained, but for a very short time. This circumstance is a serious difficulty in the performance of many experiments. It is possible to produce and maintain high gas temperatures, of several times ten thousand degrees, for a long time, namely tens of minutes, in electric arcs with compressed discharge channels.

In an ordinary open electric arc it is impossible to supply a large amount of power per unit gas volume and consequently it is impossible to obtain high temperatures. The reason for it is that as the arc current increases the diameter of the discharge channel increases and the current density in the arc remains practically constant, while the intensity of the electric field changes little at large currents.

Generally speaking, the current density tends to a definite limit with increasing current strength in open arcs. This has been confirmed experimentally by many investigators [1]. Thus, the specific energy released per unit volume of gas in an open arc hardly changes with increasing current. The temperature of open electric arcs is $6000-8000^{\circ}$.

Contained arcs in a high-pressure chamber did not result in an appreciable rise in temperature. As the pressure in the chamber was increased to 1000 atm, the temperature in the arc rose to $12,000^{\circ}$ [2].

It is possible to increase the temperature of an electric arc to $30,000-50,000^{\circ}$ by restricting the diameter of the arc discharge channel. An effective method of increasing the temperature in an electric arc turned out to be the well-known method of Guerdien, proposed by him already in the thirties and consisting of limiting the diameter of the arc discharge by means of a special water-cooled diaphragm [3]. In the literature there are many reports in which the use of this method is described. Similarly, in our electric arc installations the diameter of the arc discharge was limited by diaphragms with internal or external cooling with liquid or gas. We have reported details of the installations and the first results of the methodological investigations on them in our paper presented to the Congress on Mechanics. We give here only the main parameters of the electric arcs and the plasma jets, which can be of interest for those engaged in magnetic gasdynamics.

MAIN PARAMETERS OF THE PLASMA OBTAINED IN THE INSTALLATIONS

In the 115 kw plasma installation, an over-all view of which is

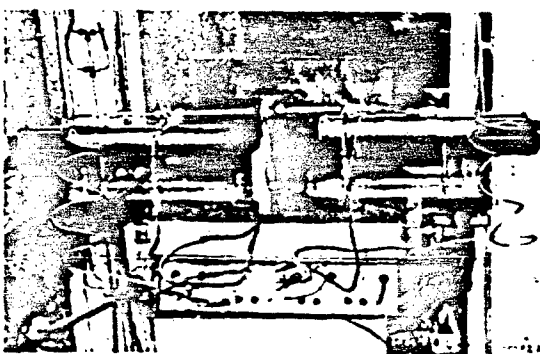


Fig. 1. Over-all view of plasma installation $N = 115$ kw.

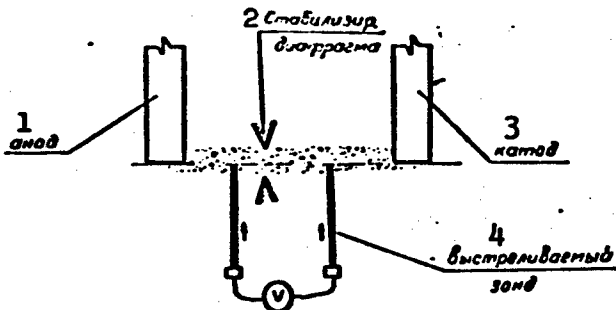


Fig. 2. Diagram of experiment on the measurement of the conductivity in the arc column. 1) anode; 2) stabilized diaphragm; 3) cathode; 4) expellable probe.

shown in Fig. 1, the current density was 7100 amp/cm^2 and the intensity of the electric field 115 v/cm . The arc lengths in this installation ranged from 30 to 105 mm. In the 4000-kw installation, the current density reached $74,000 \text{ amp/cm}^2$ and the power per unit volume $37,000 \text{ kw/cm}^3$, while the intensity of the electric field was 500 v/cm . The changeover to larger powers is necessary not only in order to obtain larger plasma flows, but also to increase the lifetime of the plasma outside the discharge, since the ratio of the volume to the surface of the plasma jet becomes more favorable. The high temperature is maintained in a jet of such a plasma over a greater length.

In the experiments with these installations, the electric conductivity of the plasma was measured with the aid of specially expelled probes. The experimental setup is illustrated in Fig. 2. In order to exclude the potential drops occurring near the electrodes from the calculations of the electric field intensity, the distance between the probes was varied in the various experiments, or else the length of the arc was varied. By measuring the intensity of the electric field E of the arc, the current strength I , the length of the arc \underline{l} , and the diameter of the arc discharge column d , we calculated the resistance and electric conductivity in the arc channel. The measurements per-

formed enabled us to calculate the electric conductivity of the plasma.

An estimate of the electric conductivity of the plasma in an arc with large current density gave a value of $\sim 10^{14}$ CGS esu, which is three orders of magnitude lower than in copper but one order of magnitude higher than in open arcs. This is a sufficiently large value for many magnetic gasdynamic experiments.

At the present time there are still no fully mastered reliable methods for determining a plasma temperature of several times ten thousand degrees. One of the methods of estimating the temperature is to calculate it from the flow of the plasma and the amount of energy delivered to it. For the installation parameters indicated above, such a calculation yields an average temperature of about $20,000^{\circ}$. It is possible to estimate the temperature more accurately by measuring the conductivity of the plasma in the discharge. Assuming that at the prevailing degrees of ionization the conductivity is determined by the interaction between the electrons and the ions only, and using Gvozdover's formula, we obtain

$$j = \sigma E = \frac{2(kT)^{3/2}}{\pi e^2 l' 3m \ln \left(\frac{3kT}{2e^2 n_e^{1/3}} \right)} \cdot E; \quad (1)$$

here σ is the measured conductivity, k is the Boltzman constant, e and m are the discharge and mass of electron, n_e is the concentration of electrons, T is the temperature to be determined.

The calculation of the temperature in the discharge from the measured electric conductivity, assuming that the temperature remains constant over the diameter, yields a value $\sim 28,000^{\circ}$. Assuming the temperature distribution over the cross section to follow a quadratic parabola, we can calculate the integral conductivity over the cross section of the discharge and, by comparing it with the measured value, determine the temperature on the discharge axis. Calculation yields a

value of 35,000°.

Using the assumption that the temperature is parabolically distributed over the cross section of the arc, and using Formula (1), we can plot nomograms relating the current in the arc, the electric field intensity, the temperature on the arc axis, and the discharge diameter.

This was done in Maecker's work [4] for a water plasma at atmospheric pressure. The curves calculated in this manner were marked with the experimental points and the temperature in the arc was measured in these experiments spectrographically. The nomogram in Fig. 3 shows also our own experimental points.

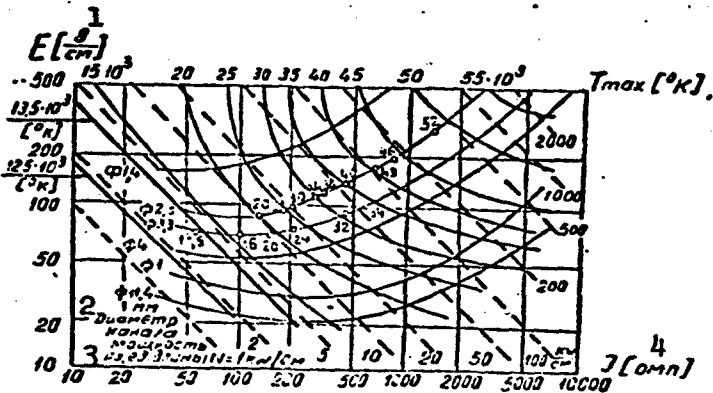


Fig. 3. Nomogram for estimating the temperature in the arc channel. 1) v/cm; 2) diameter of channel; 3) power per unit length $N = 1$ kw/cm; 4) amp.

The high-temperature plasma installations operated also at increased pressure. For this purpose the arc was enclosed in a housing with the plasma jet leaving from one side. The pressure was raised to several tens of atmospheres. The rate of escape of the plasma jet in the case of large currents and narrow channels reaches a very large value, several kilometers per second. The high velocities are the result of the action of the high temperature and the large pressure drop. In the 115-kw installation the velocity of the plasma escaping from a hole in the electrode was estimated to be 4 km/sec. In the 4000-kw in-

stallation (for a photograph of the operating plasmotron see Fig. 4) the rate of escape of the plasma reached 5-6 km/sec. Estimates of the velocity were made from the known plasma flow and its temperature, and also by means of high-speed motion picture photography (using frame or streak photography). The speed of the jet leaving the plasmotron did not exceed the local velocity of sound, owing to the high temperature. Table 1 summarizes the most interesting experimental results. At the present time methods are being developed for a more accurate determination of the physical plasma parameters such as the composition, temperature, velocity, and other parameters.

TABLE 1

№ посл.	I амп	E в/см	d мм	J а/см ²	Плот- ность тока	Мощ- ность на сз. дз.	7 Макс. т-ра на ах дуги	8 измерен. сопротив.	9 Макс. врем. экспер.	10 рабочее давлен.
N (кв)	I (амп)	E (в/см)	d (мм)	J (а/см ²)	Ne (квт/см)	T _{max} (°К)	a (CGSE)	t (мин)	P (кг/см ²)	
11	12	13	14	15	16	17	18	19		
115	500	115	3	7100	50	35000	$\sim 10^{14}$	>5	1	
4000	5200	500	3	71000	2600	35000	$\sim 10^{14}$	>1	1	

1) Power; 2) current; 3) voltage; 4) minimum arc diameter; 5) current density; 6) power per unit length; 7) maximum temperature on arc axis; 8) measured conductivity; 9) maximum time of one experiment; 10) working pressure; 11) kw; 12) amp; 13) v/cm; 14) mm; 15) amp/cm²; 16) kw/cm; 17) CGS esu; 18) min; 19) kg/cm².

Using the values obtained above for the plasma jet velocity, the conductivity, the temperature, etc., we can estimate a few magnetogasdynamic plasma parameters. For the plasma obtained in these installations the magnetic viscosity is

$$\nu_m = 10^6 \text{ cm}^2/\text{sec}$$

(two orders of magnitude lower than in mercury). At the exit from the

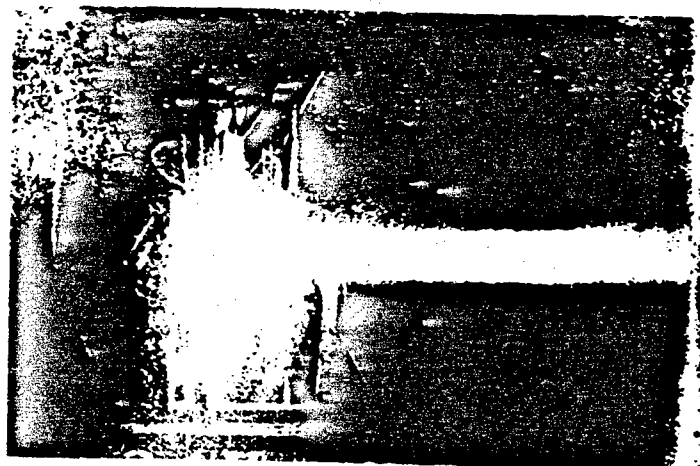


Fig. 4. Over-all view of the operating plasmotron with $N = 4000$ kw.

plasmotrons, the plasma velocity reached 10^5 - 10^6 cm/sec. If we take as the characteristic dimension the diameter of the jet $L \approx 1$ cm, then for the parameters indicated above the magnetic Reynolds number is $R_m \approx 1$. As a rule, in laboratory experiments with liquid metals and with a low temperature plasma we have $R_m < 1$.

The interaction between electromagnetic and hydrodynamic phenomena is characterized by the so-called Stewart criterion q :

$$q = A^2 R_m = \frac{H^2 I_\alpha}{v^2 \rho \sigma},$$

where A is the Alfven number, H is the intensity of magnetic field in gausses, L is the characteristic plasma dimension in cm, σ is the conductivity in CGS esu, v is the plasma velocity in cm/sec, ρ is the plasma density in g/cm³.

If $q > 1$ in the medium, then the electromagnetic forces will prevail over the hydrodynamic ones. Even at large magnetic fields H , i.e., at large Alfven numbers A , the influence of the electromagnetic forces on the hydrodynamics can be appreciable only in the case of good conductivity (i.e., large R_m numbers). When $H = 10,000$ gauss, $L = 1$ cm, and $v = 10^5$ cm/sec, assuming the plasma density to be $\rho \approx 10^{-5}$ g/cm³,

we get $q = 10$. This criterion can be improved by working with larger magnetic fields or at reduced pressures.

The given values of R_m and g for the plasma of electric arc installations make it possible to observe some magnetohydrodynamic effects.

STABILIZING ACTION OF LONGITUDINAL MAGNETIC FIELD ON PLASMA JETS

In carrying out several experiments with plasma jets, we had to fix accurately the axis of the jet. The high-speed motion picture photography indicated that the axis of the plasma jet oscillated relative to the axis of the aperture in the electrode. We undertook to stabilize (to fix) the jet by means of a constant external magnetic field. The experimental setup is shown in Fig. 5. The plasma of our arc installations was far from magnetized, since the free paths of the particles are negligibly small compared with the Larmor radii. The conductivity, although high, was finite.

We were unable to "fix" the plasma jet with the available magnetic field, but we were able to note the stabilizing action of even a weak magnetic field (several hundred gauss) on the discharge channel and on the plasma jet behind the electrode. When a constant external longitudinal magnetic field with intensity up to 300 gauss was applied to the plasma jet and simultaneously an electric current was made to flow through the jet, the jet became "fixed" on the axis. This can be explained in the following fashion. The external magnetic field is coaxial with the flow in current, and a deviation of the jet from this direction by a certain angle causes it to rotate as a result of the convective, electrodynamic, and other possible forces; the centrifugal forces displace the hot plasma, which has a lower density as compared with the surrounding gas, toward the axis of rotation. Thus, the current carrying channel occupies a stable position along the magnetic

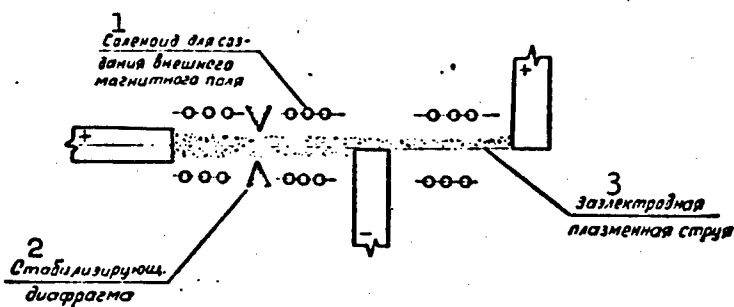


Fig. 5. Diagram of experiment on the stabilization of a plasma by a magnetic field. 1) Solenoid for producing the external magnetic field; 2) stabilizing diaphragm; 3) plasma jet behind the electrode.

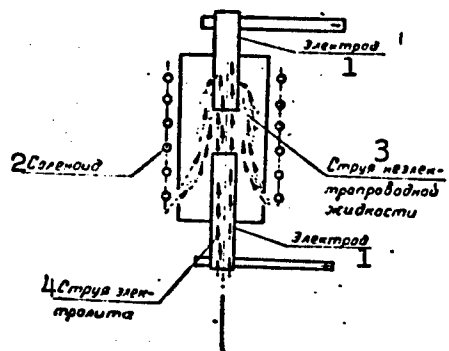


Fig. 6. Diagram of experiment with destabilization of an electrolyte jet by a magnetic field. 1) Electrode; 2) solenoid; 3) jet of electrically nonconducting liquid; 4) jet of electrolyte.

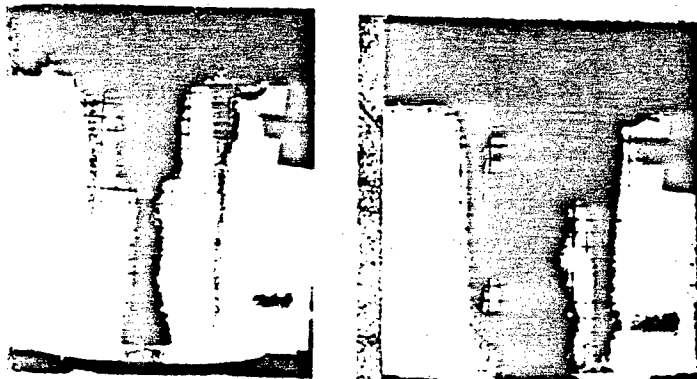


Fig. 7. Stable and unstable flow of a small electrolyte jet.

field. A similar stabilizing action is exerted by an external longitudinal magnetic field of small magnitude on an arc discharge proper between electrodes. The operating stability of the arc is noticeably increased and the current and voltage fluctuations are decreased. The conditions for igniting the arc by exploding a wire are greatly improved.

In order to verify the reality of such a rotation mechanism in the stabilization by means of a constant external magnetic field, we set up an experiment in which the internal electrically conducting jet had a greater density than the surrounding medium. By using an electrolyte jet around which a nonconducting liquid flowed, a current was made to flow and an external longitudinal magnetic field was applied; when the magnetic field was turned on, the jet of the electrolyte became twisted, flowed away from the center, and broke apart. A diagram of the experiment is shown in Figs. 6 and 7..

On the basis of these experiments it was concluded that although the influence of the magnetohydrodynamic effects is small, there does exist an influence of the centrifugal effect, which is the cause of the stability of the plasma which is lighter than the surrounding medium, and of the instability of the electrolyte which is heavier than the surrounding liquid. The results described have found practical application in work with these installations.

GENERATION OF MAGNETIC FIELD IN A PLASMA

When a plasma moves in an external magnetic field, currents are generated in it and these are associated with magnetic fields which are superimposed on the external magnetic field and distort the latter. The plasma "stretches out" the force lines. The kinetic energy of the plasma goes over into the energy of the magnetic field and into Joule heat of the plasma

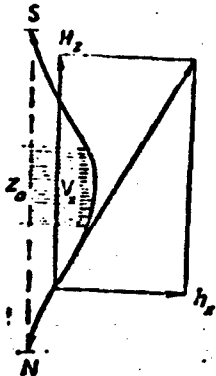


Fig. 8. Distortion of magnetic field of a moving plasma.

$$\Delta E_{\text{max}} = \int \left(\frac{\Delta H^2}{8\pi} + \frac{J^2}{2} \right) d\sigma.$$

If a plane jet with conductivity σ , thickness z_0 , and velocity v_x moves in an external field H_z (Fig. 8), then the value of the generated magnetic field h_x can be estimated from the equation

$$\text{rot } h_x = \frac{4\pi}{c} J_y = \frac{4\pi}{c} \sigma E_y = \frac{4\pi}{c} \sigma \frac{v_x H_z}{c},$$

hence

$$h_x \sim \frac{4\pi}{c} \sigma \frac{v_x H_z}{c} z_0 = \frac{\sigma z_0}{v_x} H_z = \text{Re}_m H_z.$$

In this case the circuits of the generated current are closed at infinity. For example, the plane jet is in fact a cylinder with complete axial symmetry, having an infinitely large radius.

If on the other hand the jet of finite dimensions is not closed, then on entering the magnetic field the charges will become separated in it, and polarization currents will flow in it until the electric field of the separated charges neutralizes the induced electric field vH/c , whereupon the separation of the charges will stop, the displacement currents will become equal to zero, and the plasma will pass through the magnetic field without distorting it. The charged particles will experience no acceleration whatever in the region where $E_{\text{polyar}} = vH/c$ and will have a constant velocity, just like neutral particles, and therefore the polarized jet will flow in the constant magnetic field with constant velocity without distorting the field or interacting with it. If the polarization charge is removed in some place, for example if the opposite (+, -) sides of the plasma jet are short circuited with a conductor, then the separation of the charges will resume and currents will flow, whose kinetic energy will be converted into magnetic energy and into heat. Thus, the magnetic field component

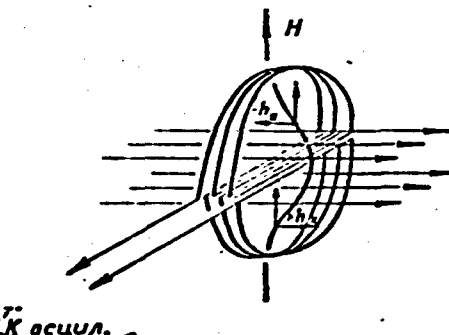


Fig. 9. Measurement of the component of the magnetic field generated by a plasma by means of a compensated magnetic probe. 1) To oscilloscope.

h_x generated by the plasma can be measured not only at the entrance to the magnetic field, but also inside a constant magnetic field. At the entrance to the field it is important to know the rate at which the intensity of the external magnetic field builds up, so as to be able to determine the value of the polarization current density and compare it with the measured h_x . It must be noted that in addition to the polarization, closed currents can flow in a plasma in the presence of a velocity gradient along the radius of the jet of conducting gas.

In our experiments this was apparently excluded. The jet leaving the plasmotron consists of a conducting core, where the charges are separated, and an almost nonconducting gas jacket, which moves with a velocity close to that of the core, followed by a boundary layer, where the velocity drops to zero. Were the jacket and the boundary layer to be conducting, then they would short circuit the polarization potential and would carry closed current loops, but in view of the fact that the conductivity decreases rapidly along the radius in the place where the velocity is hardly changed as yet, only the separation of the charges can take place and only displacement currents can flow.

Measurement of the component h_x generated by the plasma was car-

ried out by a compensated magnetic probe (Fig. 9). Near the exit from the plasmotron there were installed permanent magnets provided with thermal insulation, and the plasma jet flowed perpendicular to the field of these magnets. The intensity of the magnetic field as a function of the distance between the poles could vary from one to four or five thousand oersted and was monitored with the aid of an IMI-3. The plasma flowed through two coils connected to buck each other (see Fig. 9). One half of the probe measured the change of $-h_x$ and the other that of $+h_x$; to prevent errors it is necessary that the axis of the jet coincide with the symmetry plane of the probe. Since the coils are connected to buck, the signal was additive and the external induced stray currents, which were the same in both coils, canceled out, for which purpose the coils were made of minimum dimension, so as not to permit the inhomogeneity of the alternating external fields (due to turning the plasmotron on, etc.) from coming into play. The probe was secured on a frame made of organic glass and was inserted by means of a nonmagnetic pipe into the gap between the magnet poles, 2-5 cm away from the place of exit of the jet from the plasmotron. The plasmotron was turned on and the signal from the probe was registered on the oscilloscope. The optimum expected results should give a generated field of about 1000 oersteds, if it is assumed that the magnetic Reynolds number is on the order of unity. However, all the results obtained were lower than expected. For example, the results of one of the experiments were as follows: the number of probe turns $n = 100$, probe area $S = 2 \text{ cm}^2$ ($1 + 1$), signal magnitude $E = 7 \text{ mv}$, signal duration $\Delta t = 0.01$ sec. The average value of the generated magnetic field is therefore

$$B_h = 10^4 \frac{E\Delta t}{S \cdot n} = 35 \text{ oersted.}$$

The measured value of h_x deviates by almost two orders of magni-

tude from the expected value, probably owing to the fact that the magnetic Reynolds number at the measurement point is lower than that obtained from the optimal estimates, while at the other points the value of h_x can also be higher than that measured. For example, the average value Δh_x is measured experimentally, and from the sharp variation of the conductivity along the radius it follows that near the jet axis there should be generated fields h_x which are much larger than the average values (and these we may fail to measure when the jet deviates from the center of the probe). On approaching the plasmotron along the jet, and also when the plasmotron power is increased, the values of h_x will increase and conditions under which the generated fields will play no less a role than the external fields become quite possible.

REFERENCES

1. A. Maecker. Der elektrische Lichtbogen [The Electric Arc], Ergebni. exakt. Naturwess. [Progress in the Exact Natural Sciences], 25, 1951.
2. Peters. Zshcr. Phys. [Journal of Physics], 135, 5, 1953.
3. O. Prayning, Uspekhi fizicheskikh nauk [Progress in the Physical Sciences], 55, 4, 1955.
4. F. Burchorn, H. Maecker, T. Peters Zschr. Phys. 131, 28, 1951.

HIGH-FREQUENCY DISCHARGE IN MOVING GAS

A. M. Khazen

Moscow

A high-frequency discharge between two electrodes in a gas stream is considered. The frequency of the high-frequency field and the gas pressure are such that during the time of one half cycle of the voltage supplying the discharge gap the electron does not have time to pass through all the discharge gap. The change in the external electric characteristics of the discharge is determined as the magnitude and the direction of the gas stream velocity is changed.

CONTRIBUTION TO THE THEORY OF THE SYNCHRONOUS MAGNETOGASDYNAMIC MACHINE

L. Yu. Ustimenko, Ye. I. Yantovskiy

Khar'kov

A machine is considered, in which part of the energy of the flow of an electrically conducting gas is converted into electricity or into mechanical energy of a rotor, without the need for introducing blades in the stream.

It is shown that it is possible to obtain a rotating torque by axial flow around a smooth rotor with skewed poles.

Assuming that there is no transverse edge effect, the characteristics of "magnetic blades" are obtained for an incompressible liquid with constant electric conductivity.

The paper was published in "Izv. AN SSSR, Mekhanika i mashinostroyeniye," 5, 1960.

ELECTRIC DIPOLE FIELD IN A PLASMA
IN AN EXTERNAL MAGNETIC FIELD

B.P. Kononov, A.A. Rukhadze, G.V. Solodukhov
Moscow

The behavior of the field of an electric dipole in a plasma situated in an external magnetic field was investigated theoretically and experimentally. The predicted singularities in the behavior of the electric field were confirmed by experiment. The possibility is discussed in the paper of using these singularities to measure the concentration of electrons in a plasma and to measure the magnetic field intensity.

APPLIED MAGNETOHYDRODYNAMICS

STATUS AND PROBLEMS INVOLVED IN THE DEVELOPMENT OF
THE THEORY OF ELECTROMAGNETIC PROCESSES
IN INDUCTION PUMPS AND IN MACHINERY WITH OPEN MAGNETIC CIRCUITS

A.I. Vol'dek

Tallin

1. Investigation made by G.I. Shturman of the distribution of the magnetic field in the air gap of an inductor with open magnetic circuit. Development of G.I. Shturman's research, a criticism of this research, and its justification.
2. Methods of neutralizing pulsating fields with the aid of end pieces, the degree of their development, and further problems.
3. Windings with smooth variation of the linear load on the ends of an inductor and the degree of their development.
4. Investigation of the longitudinal edge effect in the secondary circuit, status and further problems.
5. Losses in the secondary circuit due to pulsating fields of the inductor.
6. Transverse and thickness edge effects in the secondary circuit, status of the theory.
7. Parameters of electric circuits, design features, and further problems.

TRANSVERSE EDGE EFFECT IN PLANAR INDUCTION PUMPS
USING A LIQUID METAL CHANNEL WITH CONDUCTING WALLS

A.I. Vol'dek, Kh.I. Yanes

Tallin

The main factor that reduces the efficiency of a linear planar induction pump is the transverse edge effect in the secondary circuit. The finite width of the layer of liquid metal, $2a$ (Fig. 1) gives rise to current density components directed along the x axis. These components do not participate in the production of useful forces, and the pressure developed by the pump decreases compared with the theoretical pressure which would be produced in the case of infinitely broad channel and inductor and in the absence of a phase shift. In practical cases the pressure is always appreciably smaller than the aforementioned theoretical value and in some of our calculations it does not even exceed 5 or 10%.

An effective measure for reducing the influence of this effect is to use conducting sidewalls for the channel. This is frequently realized by using special short circuiting buses or even a simple broadening of the channel with nonconducting walls, to extend beyond the limits of the inductor. The currents along the x axis can flow in this short circuiting strip (Fig. 2) and also in the inductor zone, where the distribution of the primary field is assumed to be rectangular and the current density lines are oriented to a great degree (compared with the dashed lines of Fig. 2, which show the approximate distribution of the current lines in the case when there are no side

strips) in the direction of the y axis.

In the general case the width $2a$ of the channel, the width $2c$ of the inductor (assumed width of the primary field), and the width $2t$ of the channel together with the short circuited strips are not equal to one another. Let us confine ourselves to an examination of two particular cases: $2a = 2c < 2t$, namely short circuiting strips outside the inductors, and $2a < 2c = 2t$, namely short circuiting strips between the inductors. The conductance of the remaining walls of the channel, except for the side walls, does not exert any special influence on the current distribution.

If the field in the gap is assumed to be plane parallel, then Maxwell's equations are expressed in symbolic form as follows [1]

$$\left. \begin{aligned} \frac{d\dot{H}_x}{dy} &= \gamma \dot{E}_z, \\ j_2 \dot{H}_z &= \gamma (\dot{E}_y + E_3), \\ j_2 \dot{E}_y + \frac{d\dot{E}_x}{dy} &= j_{10} \omega \dot{H}_x. \end{aligned} \right\} \quad (1)$$

All the components of the field intensity except E_Δ are the proper components of the current in the liquid metal layer. The quantity

$$E_3 = 2\tau/B_1$$

represents the induced electric field intensity due to the primary magnetic field, in which the maximum value of the normal component of the magnetic induction is B_Δ .

SHORT CIRCUITING STRIPS OUTSIDE THE INDUCTORS

Equations (1) apply in the form represented here to the zone between inductors, that is, to zone I (see Fig. 2). For zone II, that is, for the short circuiting strips situated outside the inductors, we have $E_\Delta = 0$. For this zone we can also neglect the magnetic induction due to the induced currents, since the magnetic lines pass

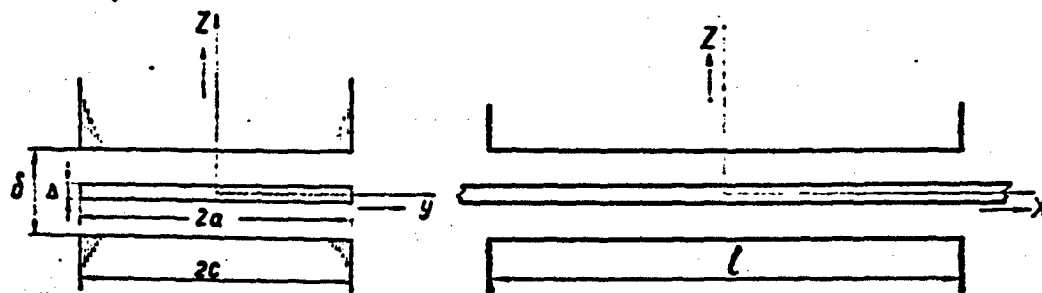


Fig. 1

completely through a nonmagnetic medium. Formally we can substitute $\mu_0 = 0$ in the third equation of (1).

In solving this system (1) we obtain for the magnetic field intensity in zone I

$$\dot{H}_z = C_1 \sinh \lambda y + C_2 \cosh \lambda y - \frac{j x \gamma E_3}{\lambda^2}. \quad (2)$$

Zone II we get accordingly

$$\dot{H}_z = C_1' \sinh \alpha y + C_2' \cosh \alpha y. \quad (2a)$$

Here $\alpha = \pi/\tau$ where τ is the pole pitch,

$$\begin{aligned} \lambda &= \alpha \sqrt{1 + j \epsilon}, \\ \epsilon &= \frac{\mu_0 \sigma}{\alpha^2} \gamma', \end{aligned} \quad (2b)$$

where γ' is the equivalent specific conductivity of the medium in the nonmagnetic gap. According to Fig. 1,

$$\tau = \frac{\Delta}{\delta}.$$

To determine simultaneously the four integration constants we make use of the following boundary conditions:

In zone I

$$\dot{H}_z|_{\epsilon} = \dot{H}_z|_{-\epsilon}. \quad (3)$$

In zone II

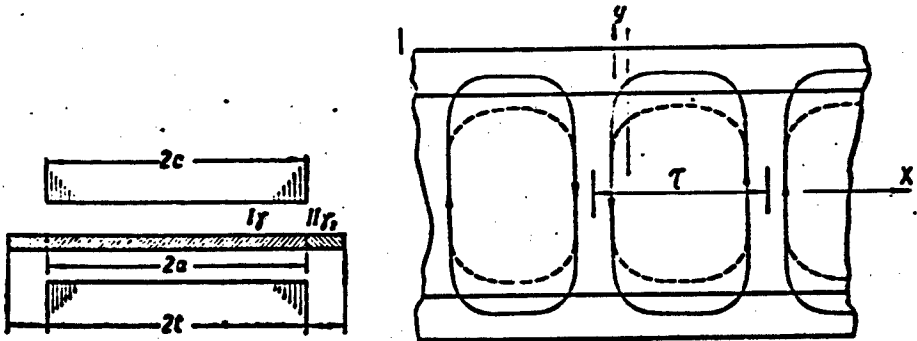


Fig. 2

$$\left. \begin{aligned} \dot{H}_x \Big|_{y=0} &= 0, \\ \gamma \dot{E}_y \Big|_I &= \gamma_2 \dot{E}_y \Big|_{II}, \\ \dot{E}_x \Big|_I &= \dot{E}_x \Big|_{II}. \end{aligned} \right\} \quad (4)$$

The last two relations are the continuity conditions for the normal components of the current density and for the tangential components of the electric field intensity on the boundaries between zones I and II.

Finally, the intensity of the magnetic field and the useful component of the current density in zone I will be

$$\dot{H}_x = -\frac{j_x \gamma E_1}{\lambda^2} \left[1 - \frac{x_1 \text{ch} \lambda y}{x_1 \text{ch} \lambda c + \gamma_2 \lambda \text{th} \lambda (t - c) \text{sh} \lambda c} \right]. \quad (5)$$

$$\dot{\delta}_y = \frac{x_1^2 \gamma E_1}{\lambda^2} \left[1 - \frac{x_1 \text{ch} \lambda y}{x_1 \text{ch} \lambda c + \gamma_2 \lambda \text{th} \lambda (t - c) \text{sh} \lambda c} \right]. \quad (6)$$

The mean pressure over the width of the channel will be

$$p = \frac{l}{2c} R e \int_{-a}^a \dot{\delta}_y B_\Delta dy = k_{os} p_0, \quad (7)$$

where k_{os} is the so-called attenuation coefficient and p_0 is the pressure for an infinitely broad channel and infinitely broad inductor, and in the absence of a phase shift between $\dot{\delta}_y$ and B_Δ .

$$k_{os} = R e \frac{a^2}{\lambda^2} \left[1 - \frac{x_1 \text{sh} \lambda c}{\lambda c [x_1 \text{ch} \lambda c + \gamma_2 \lambda \text{th} \lambda (t - c) \text{sh} \lambda c]} \right]. \quad (8)$$

$$p_0 = \frac{\gamma \alpha l}{2x} B_x^2. \quad (9)$$

When $t = c$ or when $\gamma_2 = 0$, Eq. (8) becomes

$$k_{os} = Re \frac{\epsilon^2}{\lambda^2} \left(1 - \frac{lh\lambda c}{\lambda c} \right). \quad (10)$$

which coincides with (12) in [1].

When $\gamma_2 = \infty$ we obtain from (8) and (2b)

$$k_{os} = Re \frac{\epsilon^2}{\lambda^2} = \frac{1}{1 + \epsilon^2}. \quad (11)$$

In this case k_{os} is due only to the presence of the phase shift between δ_y and B_Δ .

If the specific conductivity γ is so small that $\epsilon \ll 1$ and we can put $\lambda = a$ then we obtain from (11) $k_{os} = 1$ and from (8)

$$k_{os} = 1 - \frac{\operatorname{sh} \lambda c}{ac [\operatorname{ch} \lambda c + \frac{\gamma_2}{\gamma} \operatorname{th} \lambda c (t - c) \operatorname{sh} \lambda c]}. \quad (12)$$

If the side wall of the channel is actually nonconducting, but the width of the channel exceeds the width of the inductor $2a = 2t > 2c$, then k_{os} is determined from (8) with $\gamma_2 = \gamma$. If, in addition $\epsilon \ll 1$ and we can put $\lambda = a$, then

$$k_{os} = 1 - \frac{\operatorname{sh} \lambda c \operatorname{ch} \lambda c (t - c)}{ac \operatorname{ch} \lambda c t}. \quad (13)$$

The average pressure over the entire width of the channel decreases here further by c/t times. Consequently

$$p = p_0 \frac{c}{t} k_{os}.$$

SHORT CIRCUITING STRIPS BETWEEN CONDUCTORS

If the conducting side strips are situated in zone $2c$, that is, between the inductors (Fig. 3), the induced electric field intensity in the short circuited strips differs from zero. For zones I and II we have for the magnetic field intensity expressions analogous to (2). Only the specific conductances γ and γ_2 differ in the two zones. For

a simultaneous determination of the four integration constants it is necessary to replace in conditions (3) t by c and c by a.

Finally, the intensity of the magnetic field and the useful component of the current density in zone I will be given by

$$H_x = -\frac{j_{x'} E_1}{\lambda^2} \left\{ 1 - \frac{[(\gamma \lambda_2^2 - \gamma_2 \lambda^2) \operatorname{ch} \lambda_2 (c-a) + \gamma_2 \lambda^2] \operatorname{ch} \lambda y}{\lambda_2 [\gamma_2 \operatorname{sh} \lambda_2 (c-a) \operatorname{sh} \lambda a + \gamma_2 \lambda_2 \operatorname{ch} \lambda_2 (c-a) \operatorname{ch} \lambda a]} \right\}, \quad (14)$$

$$\dot{J}_y = -\frac{x^2 E_1}{\lambda^2} \left\{ 1 - \frac{[(\gamma \lambda_2^2 - \gamma_2 \lambda^2) \operatorname{ch} \lambda_2 (c-a) + \gamma_2 \lambda^2] \operatorname{ch} \lambda y}{\lambda_2 [\gamma_2 \operatorname{sh} \lambda_2 (c-a) \operatorname{sh} \lambda a + \gamma_2 \lambda_2 \operatorname{ch} \lambda_2 (c-a) \operatorname{ch} \lambda a]} \right\}. \quad (15)$$

The average pressure over the width of the channel is determined from the integral (7). The attenuation coefficient assumes in this case the form

$$k_{os} = Re \frac{a^2}{\lambda^2} \left\{ 1 - \frac{\operatorname{sh} \lambda a [(\gamma \lambda_2^2 - \gamma_2 \lambda^2) \operatorname{ch} \lambda_2 (c-a) + \gamma_2 \lambda^2]}{\lambda a \lambda_2 [\gamma_2 \operatorname{sh} \lambda_2 (c-a) \operatorname{sh} \lambda a + \gamma_2 \lambda_2 \operatorname{ch} \lambda_2 (c-a) \operatorname{ch} \lambda a]} \right\}. \quad (16)$$

When $a = c$ expression (16) turns into (10). When $\gamma_2 = 0$ and $\lambda_2 = \alpha$, that is, when the pump channel is narrower than the inductor but there are no short circuiting strips, the expression for k_{os} is similar to (10), except that c is replaced by a.

When $\gamma_2 = \infty$ and $\lambda_2 = \infty$, expression (16) turns into (11).

When $\gamma_2 = \gamma$ and $\lambda_2 = \lambda$, expression (16) simplifies to

$$k_{os} = Re \frac{a^2}{\lambda^2} \left(1 - \frac{\operatorname{sh} \lambda a}{\lambda a \operatorname{ch} \lambda a} \right). \quad (17)$$

If the width of the channel $2a$ is reduced to zero expression (16) for k_{os} assumes in the limit the form

$$k_{os} \Big|_{a=0} = \frac{\gamma_2}{\gamma} Re \frac{a^2}{\lambda_2^2} \left(1 - \frac{1}{\operatorname{ch} \lambda_2 c} \right). \quad (18)$$

If the specific conductivities γ and γ_2 are so small that $\epsilon \ll 1$

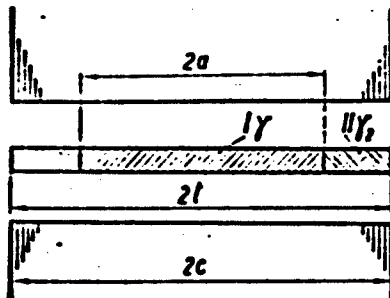


Fig. 3

and $\epsilon_2 \ll 1$, and therefore we can put $\lambda = \gamma_2 = a$, we obtain from (16) for the attenuation coefficient

$$k_{ac} = 1 - \frac{\sinh[\gamma_2 - (\gamma_2 - \gamma) \operatorname{ch} z(c-a)]}{\gamma_2 [\gamma_2 \sinh z(c-a) \sinh z a + \gamma \operatorname{ch} z(c-a) \operatorname{ch} z a]} \cdot (19)$$

This expression disregards the inductance of the secondary circuit, and the current distribution is determined

only by the specific conductances. When $\gamma_2 \gg \gamma$ the value of k_{os} approaches the limit

$$k_{ac} \Big|_{\gamma_2 \gg \gamma} = 1 - \frac{1 - \operatorname{ch} z(c-a)}{a \sinh z(c-a)}. \quad (20)$$

If the specific conductivities are small and the channel narrow, cases are possible when the coefficient of attenuation becomes even greater than unity in the presence of short circuiting strips between the inductors.

* * *

Table 1 compares the results of the calculation of the attenuation coefficient by means of formula (12), variant 1 and by formula (19), variants 2-4, for different ratios of the specific conductivities. In variants 1, 3, and 4 the width of the inductor is 85.2% of the pole pitch. In variant 1 there is a short circuiting strip outside the inductors. Furthermore, $t - c = 0.43 c$. In variants 3 and 4 the width of the channel is smaller than the width of the inductor, and $c - a$ is respectively equal to 0.43 c and 0.86 c. In variant 2 there is an inductor with conducting strips of the same width as in variant 1. The second column of the table shows the relative widths. Comparison of the first and second variants shows that at the ratios under consideration an increase in the width of the inductor to the outer edges of the conducting strips does not produce any special additional

effect. However, if we narrow down in this case the channel within the limits of the inductor and employ highly conductive strips up to the width of the inductor, the attenuation coefficient increases by several times. This procedure of course increases only the pressure, and decreases the delivery of the pump.

Expression (18) was checked experimentally for $\gamma_2 = \gamma$. The mechanical forces were determined using two brass plates in the air gap of the inductor. One plate had a width equal to that of the inductor, and the second was 43% broader, that is, $t = 1.43 c$. In this case $a = 0.214$ and $\epsilon = 1.694$, $c/\tau = 0.476$. The attenuation coefficient as given by (10) is 0.243 and as given by (18) is 0.338, that is, k_{os} is increased by a factor of 1.39. The ratio of the mechanical forces in the experiment was 1.38.

TABLE 1

No variant	Dimensions, mm	k_{oc}				
		$\gamma_2 = 0$	$\gamma_2 = \gamma$	$\gamma_2 = 2\gamma$	$\gamma_2 = 10\gamma$	$\gamma_2 = 100\gamma$
1	$\frac{c}{\tau} = \frac{a}{\tau} = 0.476$	0.395	0.610	0.700	0.901	0.999
	$\frac{a}{\tau} = 0.631$					1
2	$\frac{c}{\tau} = \frac{a}{\tau} = 0.631$	0.395	0.670	0.805	1.074	1.204
	$\frac{a}{\tau} = 0.476$					1.207
3	$\frac{c}{\tau} = \frac{a}{\tau} = 0.176$	0.187	0.519	0.705	1.166	1.375
	$\frac{a}{\tau} = 0.272$					1.362
4	$\frac{c}{\tau} = \frac{a}{\tau} = 0.476$	0.015	0.568	0.980	2.35	3.5
	$\frac{a}{\tau} = 0.631$					3.68

1) Number of variant; 2) relative widths.

REFERENCE

1. A. I. Vol'dek. Toki usiliya v sloye zhidkogo metalla ploskikh induktsionnykh nasosov [Currents and Forces in Liquid-Metal Layer of Flat Induction Pumps], Izvestiya vysshikh uchebnykh zavedeniy. Elektromekhanika [Bulletin of the Higher Educational Institutions. Electromechanics], 1, 1959.

Manu-
script
Page
No.

[List of Transliterated Symbols]

493

oc = os = oslableniye = attenuation

LONGITUDINAL EDGE EFFECT IN SECONDARY CIRCUIT OF
LIQUID METAL INDUCTION PUMPS WITH OPEN MAGNETIC CIRCUIT

A.I. Vol'dek, Kh.K. Ross

Tallin

1. The longitudinal edge effect in the secondary circuit manifests itself in the fact that the secondary currents "leak away" beyond the limits of the active zone, and consequently the power losses in the secondary circuit increase and certain other side effects appear. This problem must therefore be investigated in greater detail.
2. The theoretical problem is investigated by electromagnetic field theory methods. Formulas are derived for the determination of the necessary quantities.
3. The character of variation of the secondary fields of the edge effect and of the corresponding distribution of the currents in the secondary circuit is investigated.
4. The significance of the secondary fields and currents with respect to the aforementioned edge effect is analyzed.
5. The problem is investigated without account of the influence of the magnetic fields of the given edge effect.
6. The question of losses due to the corresponding circuits in the secondary circuit is considered.

EQUIVALENT CIRCUIT OF D.C. PUMP CHANNEL

Yu. A. Birzvalk

Riga

Conformal mapping is used in the paper to solve the problem of the distribution of the potential in the edge zone of a d.c. pump. Based on the solution, an equivalent circuit is derived for the pump channel, in which account is taken (within the limits of the assumptions made) of all the singularities that are introduced by the longitudinal edge effect.

The parameters of the equivalent circuit are calculated with the aid of dimensionless so-called current coefficients κ , numerical values of which are summarized in a table and are plotted as functions of two quantities — the relative pole excess and the ratio of the width of the channel to the size of the nonferromagnetic gap.

The energy properties of the edge zone of the pump are analyzed and ideas are advanced concerning the rational choice of the pole axis.

A detailed report of the content of the work can be found in the article "Equivalent Circuit for a D.C. Pump Channel and Design of Pump for Maximum Efficiency" published in the twelfth collected works of the Institute of Physics, Academy of Sciences of the Latvian SSR "Applied Magnetohydrodynamics" (Riga 1961).

DETERMINATION OF CERTAIN PARAMETERS
OF ELECTROMAGNETIC PUMPS WITH
THE AID OF AN ELECTROLYTIC TROUGH

L.V. Nitsetskiy, E.K. Yankop
Riga

At the first conference on problems of applied and theoretical magnetohydrodynamics, the feasibility was demonstrated of using electrolytic troughs and other potential models for the investigation of fields with continuously distributed emf's. In paper [1], the general principles of such modeling were established and examples were presented of the solution of problems connected with electromagnetic pumps. The boundary conditions were specified in the course of modeling on the basis of representing the normal component of the current density on the boundaries of the operating region of the pump, j_n , in the form of a sum of terms:

$$j_n = j_{n0} + j_{n1} + j_{n2}, \quad (1)$$

where j_{n0} is the component due to the motion of the liquid in the magnetic field (induced component);

j_{n1} is the component due to external voltage applied to the electrodes;

j_{n2} is the component that takes into account the influence of the pump channel walls.

Integrating (1) over the area, we obtain a relation between the current functions similar to formula (1)

$$I = I_0 + I_1 + I_2$$

where the meaning of all the quantities is analogous to the meaning of the corresponding quantities in (1).

The term I_0 was calculated while the terms I_1 and I_2 were obtained by modeling in an electrolytic trough.

References [1] and [2] presented data obtained with the aid of a direct modeling system, in which the current lines in nature corresponded to analogous current lines on the model. However, what is measured directly on the model are the potentials, so that it is difficult to change over to the currents and a special calculation procedure must be developed.

This shortcoming can be eliminated. Using the equivalents of the equipotential lines and of the current lines in plane-parallel fields, it is proposed to employ a reciprocal or dual modeling system. In the reciprocal circuits, the conductors on all boundaries are replaced by dielectrics and the dielectrics are replaced by conductors. Because of this, the equipotential lines and the current lines are interchanged. Thus, the current lines in nature correspond here to the equipotentials, thus greatly facilitating the calculations and simplifying the modeling.

The potential on a plane model is proportional to the value of the current I_k between the point where the given potential ϕ_k is determined, and the point where the potential is assumed equal to zero, that is,

$$I_k = C \phi_k,$$

where C is a constant. The determination of the constants and the calculation procedure are described in [3].

The influence of partitions on the effectiveness of the pump operation was determined with the aid of dual models. The effective-

ness was estimated from the ratio of the stray current I_s to the productive current I_p , equal to

$$I_s = \frac{1}{a} \int \int j_s ds dx,$$

where a is the distance between electrodes and s is the area of the cross section of the working zone, parallel to the surface of the electrodes, passed at a distance x from one of the electrodes.

In the dual model, the current I_p is proportional to the average potential on the boundary of the working zone. The determination of the average potential was carried out with the aid of a series of probes installed on the entire boundary at equal distances from one another, and the average potential was measured directly by a pointer type instrument with the aid of a simple summing unit.

The stray current I_s was determined as the difference between the total current I (corresponding to the voltage applied to the electrodes of the dual model) and the productive current I_p .

Measurements of the ratios I_s/I_p were carried out for a different number of partitions n and for different partition lengths, d , and it turned out that this ratio is almost directly proportional to the length of the electrode l and inversely proportional to the distance between electrodes a .

This made it possible to reduce appreciably the number of plots, for the quantity I_s/I_p could be replaced by the quantity $k = I_s/I_p \cdot l/a$.

For example, it turned out that for a stationary liquid the ratio is

$$k = \frac{I_s l}{I_p a} \approx 0.45.$$

It is obvious that for a specific pump with a known ratio l/a no great difficulty is entailed in determining I_s/I_p .

If a single partition is installed, the value of k depends not only on the length of this partition, but also on its position. The smallest value was assumed by k when the partition was placed along the channel axis. The discrepancy of the values of k as a function of the ratio l/a did not exceed 7%.

Figure 1 shows curves of k as a function of the ratio d/a for the optimal partition position, when k is minimal.

It is clear from the curves that by using one partition it is possible to improve k by approximately 30%. It is also seen from the curves that $(1-2)a$ is a sufficient length for the partition.

Further increases in the length did not yield a noticeable effect, and it is possible that the hydrodynamic losses caused by the longer length of the partition will offset the reduction in the leakage of the current, so that a partition of considerable length is obviously undesirable.

In place of using one long partition, it is better to install two, three, or more shorter ones.

Three partitions of length $d = a$ attenuate the leakage of the current by more than a factor of 2.

If the liquid is in motion, this relation changes appreciably. No general laws were observed here, but for each specific pump with a definite data it is possible to calculate here the current ratio I_s/I_p on the basis of the procedure proposed.

It is very simple to calculate these relations for a case when the magnetic field beyond the limits of the zone bounded by planes passing through the edges of the electrodes is assumed to be very small and can be neglected. Then the boundaries of the active zone, which coincide with the boundaries of the magnetic field, will pass through these planes and the motion of the liquid will cause only a

change in the productive current:

$$I_{\text{stray}} = I_p - I_s$$

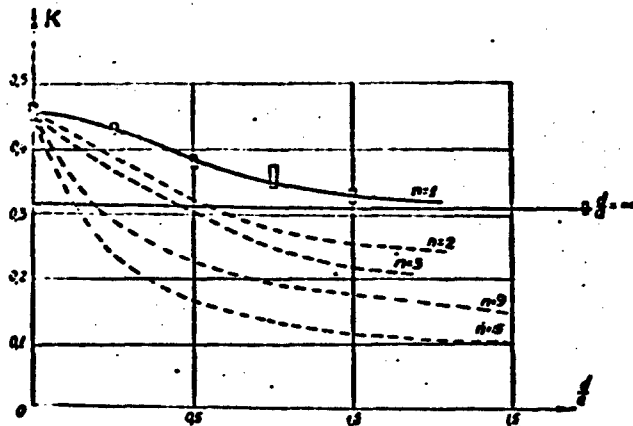


Fig. 1

The ratio I_s/I_p which becomes worse, so that the use of partitions becomes more justified and necessary. On the other hand, if the magnetic field is still appreciable beyond the limits of the electrodes, it is necessary to determine the boundary of the magnetic field (the line beyond which the influence of the field can be neglected) and to mount the probes on this boundary. The productive current is determined by starting from the average potential on this boundary, but the currents I_0 and I_2 must also be taken into account here.

Another example of the use of dual models is for the determination of the parameters of the equivalent circuit of the pump.

To determine the parameters of the equivalent circuit of the pump, the dual models are used to find the current components I_p and I_s for stationary liquid. Then the resistance to the productive current in the liquid is

$$R_p = \frac{U_H}{I_p}. \quad (2)$$

and the resistance to the stray current in the liquid is

$$R_s = \frac{U_H}{I_s} \quad (3)$$

where U_H is the voltage applied to the pump.

We see that calculation of parameters by means of the proposed method is elementary. On the other hand, to determine these parameters analytically is quite difficult.

Dividing (2) by (3) we get

$$\frac{R_p}{R_s} = \frac{I_s}{I_p}$$

Thus, the curves in Fig. 1 enable us also to estimate the ratio R_p/R_s .

A third example of the use of dual models is to determine the form of the pole piece, at which the ratio of the current density in the liquid to the magnetic field induction would obey a definite law. In particular, some authors indicate that it is desirable that this ratio be constant at all points of the working zone.

To determine the required ratio we can use successive modeling of the magnetic field and the current field.

The modeling of the magnetic field has been well developed and described in many papers (see, for example, [4]). By specifying a certain pole piece form, we determine with the aid of the model the law of the field distribution. Then, using the obtained distribution for the magnetic field, we determine the distribution of the current. A comparison of the two obtained relationships demonstrates the character of their ratio in all the points of interest to us and simultaneously allows us to draw conclusions concerning what ways to follow in changing the form of the pole piece in order to obtain the desired ratio, if the present ratio does not satisfy the designer.

REFERENCES

1. L. V. Nitsetskiy. Printsip modelirovaniya elektricheskogo polya elektromagnitnykh nasosov v elektroliticheskoy vanne i na elektroprovlyashchey bumage [The Principle of Simulating the Electric Field of Electromagnetic Pumps in the Electrolytic Bath and on Electrically Conductive Paper], Voprosy magnitnoy gidrodinamiki i dinamiki plazmy [Problems of Magnetohydrodynamics and Plasma Dynamics], Riga, 1959.
2. L. V. Nitsetskiy. Modelirovaniye elektricheskogo polya elektromagnitnykh nasosov v elektroliticheskoy vanne i na elektroprovlyashchey bumage [Simulation of the Electric Field of Electromagnetic Pumps in the Electrolytic Bath and on Electrically Conductive Paper], Elektromagnitnye protsessy v metallakh. Trudy Instituta fiziki AN LSSR [Electromagnetic Processes in Metals. Transactions of the Physics Institute Academy of Sciences Latvian SSR], XI, 1959.
3. L. V. Nitsetskiy and E. K. Yankop. Elektroliticheskaya vanna dlya opredeleniya nekotorykh parametrov elektromagnitnykh nasosov postoyannogo toka. Elektricheskoye [An Electrolytic Bath for Determining Certain Parameters of Direct-Current Electromagnetic Pumps. Electrical Simulation], Uchenye zapiski RPI [Scientific Reports of the Riga Polytechnic Institute], V, 1961.
4. I. M. Tetel'baum. Elektricheskoye modelirovaniye [Electrical Simulation], Moscow, 1959.

Manu-
script
Page
No.

[List of Transliterated Symbols]

505 $\ddot{\alpha}\ddot{\alpha}\ddot{\alpha}$ = dvizh = dvizheniye = motion

EXPERIMENTAL INVESTIGATION OF PLANAR INDUCTION PUMPS

A.I. Vol'dek, Kh.I. Yanes
Tallin

In solving theoretical and practical problems in the field of electromagnetic pumps, it is particularly important to carry out an experimental investigation of the corresponding problems. Only an experimental investigation of ready made pumps or models can cover the entire aggregate of the complicated electromagnetic processes.

An experimental model of a planar two-way induction pump with two-way three-phase double-layer diametral winding and open slots was investigated at the Tallin Polytechnic Institute. The measurements were carried out principally with a 35 mm nonmagnetic gap. The cross section or the equivalent conductor in the inductor winding was 6.18 mm^2 . With the current density in the winding at 2.5 a/mm^2 , the total power was 8.5 kva. The winding was of the four-pole type with two slots per pole and per phase. The arrangement of the coil sides of the individual phases in the inductor slots is shown in Fig. 1 under the x axis.

On the ends of the inductor there are the so-called correcting coils, one side of each filling the slots in the active zone ($2p_1$, 24 slots), and the other side of each located in the extreme three slots. The measurements and observations of the current and voltage curves by means of an oscillograph have shown that the circuit is linear, but the phases are asymmetrical. The phase which is centrally located on the inductor with respect to the placement of the windings

(C-Z) has 9% less inductance than the outside phases. The mutual inductance between two outside phases is 33% less than the mutual inductance between the central phases and any of the outside phases.

When the correcting coils are not connected, the inductances of the phases are equal, but the mutual inductance between the outer phases is 60% less than the mutual inductance between the central phase and the outside phase.

If the system of line voltages is symmetrical, the phase currents differ by 6%, and if no correcting coils are used, they differ by 20%.

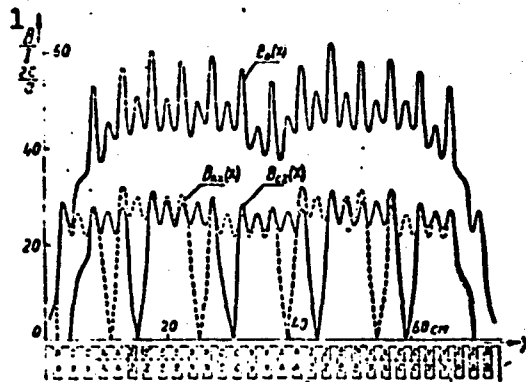


Fig. 1. 1) Gausses/ampere.

An investigation of the distribution of the magnetic induction was carried out by means of probing with an electrical coil with diameter 7.5/3.5 mm and height 3.0 mm. A magnetic induction of 1.32 Gauss produced a voltage of 1 mv at 50 cps. The measurements were with an MVL-2M vacuum-tube voltmeter with a 10-mv scale.

The distribution of the transverse component of the electric induction at no load over the length of the inductor is plotted in Fig. 1. The measurements were carried out along the axis of the inductor with a gap of 35 mm, at a height of 5 mm above the surface of the teeth. The induction curves are shown for a 1 ampere current in the winding. The curve $B_{Ax}(x)$ is plotted with the outside phase fed

with current. The curve $B_{CZ}(x)$ is plotted with the central phase fed with current. The curve $B_0(x)$ pertains to three-phase current supply, with the correcting coils included. If the inductor would contain all the normal traveling field, then the $B_0(x)$ curve would have no dropping portions in the center of the inductor and at the ends, but only the waviness due to the teeth. The influence of the tooth harmonics is strong near the surface of the teeth.

The curves of Fig. 2 show the values of the transverse component of the magnetic induction at the center of the air gap, with the curve $B_0(x)$ corresponding to three-phase excitation of the windings with correcting coils, and $B_{\delta k}(x)$ pertaining to windings without the correcting coils. The influence of the correction is clearly seen on these curves.

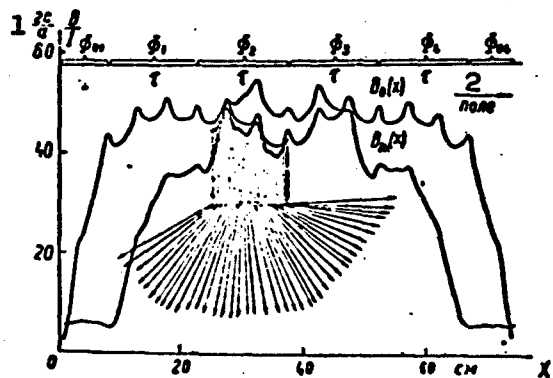


Fig. 2. 1) Gauss/amp; 2) field.

The effect of secondary currents on the resultant magnetic field is seen in Fig. 3. Both curves represent the distribution of the transverse component of the magnetic induction at a height of 5 mm above the surface of the teeth with three-phase excitation. The curve $B_0(x)$ is the no-load curve. The $B(x)$ curve was plotted in the presence of a brass plate 5 mm thick, with width and length the same as of the inductor (140 X 750 mm) in the center of the inductor. The resultant

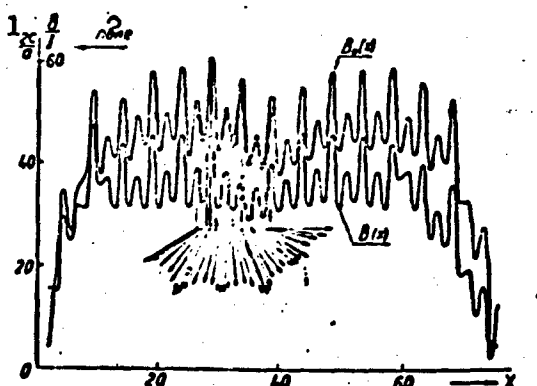


Fig. 3. 1) Gauss/amp; 2) field.

induction for the same value of the current and averaged over the entire length of the inductor was much less. However, in that end of the inductor where the traveling field goes out of the inductor, the secondary current field, as can be seen on the left side of the plot, intensifies the primary field.

The variation of the transverse component of the magnetic in-

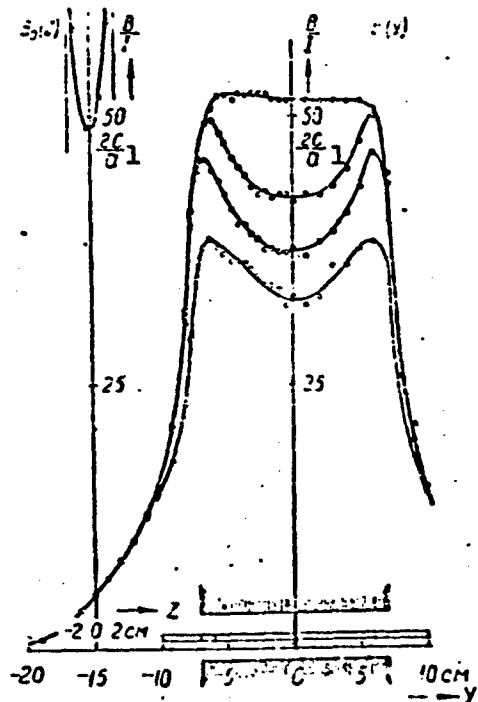


Fig. 4. 1) Gauss/ampere.

duction in a direction transverse to the inductor axis is shown in Fig. 4. The curves $B(y)$ were plotted on the axis of the tooth at a height of 9 mm above the surface of the tooth. The upper curve corresponds to no load. The three lower curves are plotted in the presence of a 5 mm brass plate in the center of the gap, with a width of 120, 140 (width of the inductor) and 200 mm, respectively. The secondary currents screen the field in the central portion of the inductor width. The

6

variation of the transverse component of magnetic induction over the thickness of the gap is shown for no-load in the form of the $B_0(z)$ plot in Fig. 4.

The time phase of the magnetic induction or of the magnetic flux is determined from the phase of the induced emf in the measuring coil. The phase of the emf is determined with the aid of a cathode ray oscilloscope. Two voltages are applied simultaneously to the input of the oscilloscope, one from the measuring coil and the secondary voltage from a three-phase induction regulator. By turning the rotor of the regulator, the phase of the secondary voltage is varied until the Lissajous ellipse on the screen of the oscilloscope becomes a straight line. The position of the induction regulator rotor determines the phase of the measuring coil emf.

The variation of the phase of the transverse component of the magnetic induction along the length of the inductor is shown in Figs. 2 and 3 at no load. In addition to the magnitude, the phase of the induction was determined in a segment several tooth pitches wide. The results of the induction measurements are represented by vectors starting at the corresponding points. The angles between the vectors correspond to the phase shifts. At the center of the gap (see Fig. 2) the phase varies smoothly. On the surface of the inductor (see Fig. 3), the phase changes abruptly in the slots and has a constant magnitude within the limits of each tooth.

To determine the pulsating components in the magnetic field of the inductor, the magnitude and phases of the fluxes of all four poles and the two end parts of the induction outside the active zone were measured. Parts of these fluxes are shown schematically in the upper part of Fig. 2. The results of the measurements are shown for three-phase supply in the form of a vector flux diagram on Fig. 5a for

a winding with correcting coils and on Fig. 5b without the correcting coils. Also shown are the resultant fluxes of the entire active zone, Φ_{47} , and the resultant fluxes of the two halves of the active zone, Φ_{12} and Φ_{34} . These resultant fluxes characterize the pulsating components in the magnetic field. The flux Φ_{47} characterizes the pulsating components, which according to the equations of Professor G.I. Shturman has a hyperbolic cosine distribution, and the difference between the fluxes Φ_{12} and Φ_{34} characterizes the pulsating component, which has a hyperbolic sine distribution. From the diagrams of Fig. 5 we can conclude that the correcting coils of the double-layer winding almost completely cancel the pulsating component which has a hyperbolic sine distribution, while the component with the hyperbolic cosine distribution is highly suppressed.

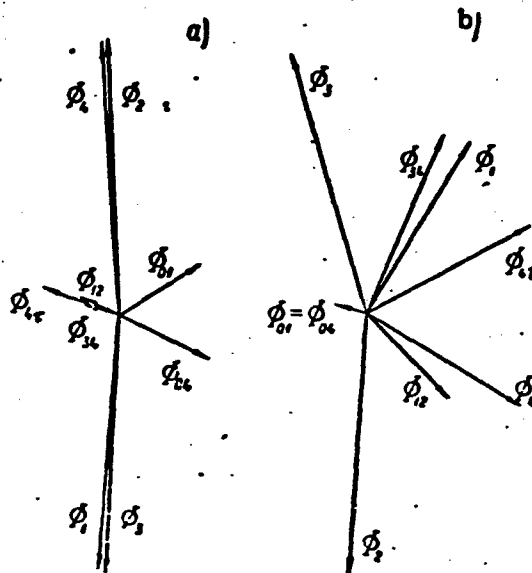


Fig. 5

Other magnetic measurements with the aid of special coils have established the stray fluxes from all the surfaces of the inductor and the stray fluxes of the end parts of the windings.

To investigate the magnetic field of the inductor, one can make successful use, as shown above, of the method of probing the magnetic induction and measuring the magnetic fluxes along with a determination of the phase relationships.

DESIGN OF D.C. PUMP FOR MAXIMUM EFFICIENCY

Yu.A. Birzvalk

Riga

The paper considers some of the most important problems in the design of a d.c. pump, with limitation to compensated pumps with series excitation.

The conditions on which the efficiency of the pump design depends are divided into two groups - external and internal.

The external conditions determine the choice of specific load, while the internal conditions determine the rational combination of specific loads, design dimensions, and number of turns of the pump such as to ensure pump operation (in the nominal mode) at maximum efficiency. Considerations are advanced regarding the choice of the specific loads, and their influence on the performance of the pump is considered.

The limitations imposed by the discrete number of turns are analyzed. The main relationship between the magnetic induction, the electromagnetic pressure, the number of turns, and three dimensionless coefficients, namely the saturation coefficient, the ratio of the total current to the productive current, and the ratio of the gap to the height of the pump channel, are established and analyzed.

The concepts of relative productivity \bar{Q} and relative pressure \bar{p} are introduced and used to investigate the maximum pump efficiency conditions in two modes: with the current constant and with the supply voltage constant. It is shown that the maximum electromagnetic

efficiency occurs in both modes for an equal value of the productivity, characterized by the criterion "relative optimal productivity Q_0 ." The influence of the hydraulic pump losses is considered.

Previously known criteria, such as the "optimal slip" of Watt and "optimal induction" of Barnes are analyzed. It is shown that they are particular cases of the proposed criterion Q_0 .

A detailed exposition of the content of the work can be found in the article "Equivalent Circuit for a D.C. Pump Channel and Design of Pump for Maximum Efficiency," published in the twelfth collection of the works of the Institute of Physics of the Academy of Sciences, Latvian SSR "Applied Magnetohydrodynamics" (Riga, 1961).

CENTRIFUGAL INDUCTION PUMP

A.K. Veze, I.M. Kirkko, O.A. Lielausis
Riga

If a closed cylindrical vessel with liquid metal is placed in a vertical stator of an induction motor, then the rotating magnetic field will cause the metal to rotate. A pressure difference due to the centrifugal forces is produced between the axis of the vessel and the periphery. Consequently, such a system is a simple modification of an induction pump. In the present work we investigated a laboratory model of such a centrifugal induction pump both in the pumping mode and in the batching mode.

A plastic vessel with diameter $d = 7.3$ cm and height $h \approx d$ was placed in the stator of an induction motor with one pair of poles and with pole pitch $\tau = 22$ cm. The stator was fed with alternating current of frequency 50, 100, and 200 cps. The maximum current used was $I = 15$ amperes, corresponding to a magnetic field induction on the surface of the vessel $B = 400$ Gauss. The liquid metal was mercury at room temperature. The mercury was fed to the pump through an inlet in the center of the bottom of the vessel and was removed through a tube at the edge of the cover.

The pressure p developed by the pump (in millimeters of mercury) was determined from the difference in the level of the mercury column in glass tubes placed at the center and on the periphery of the vessel, while the productivity of the pump Q in cm^3/sec . was determined from the liquid flow.

The pump characteristics $p = f(Q)$ were plotted for the peculiar static and total pressure at different current frequencies and at different currents in the stator winding. To plot the "static" pressure, due only to the centrifugal forces, the end of the outlet tube was placed in the plane of the wall, that is, parallel to the flow. To plot the total pressure, the end of the tube was directed against the stream.

To describe the operation of the described setup as a pump, Fig. 1 shows the dependence of the relative pressure p/p_0 on the relative productivity

$$\frac{Q}{d^2} \sqrt{\frac{\rho}{2p_0}}$$

where p_0 is the pressure developed by the pump at a productivity $Q = 0$; ρ is the density of the liquid metal.

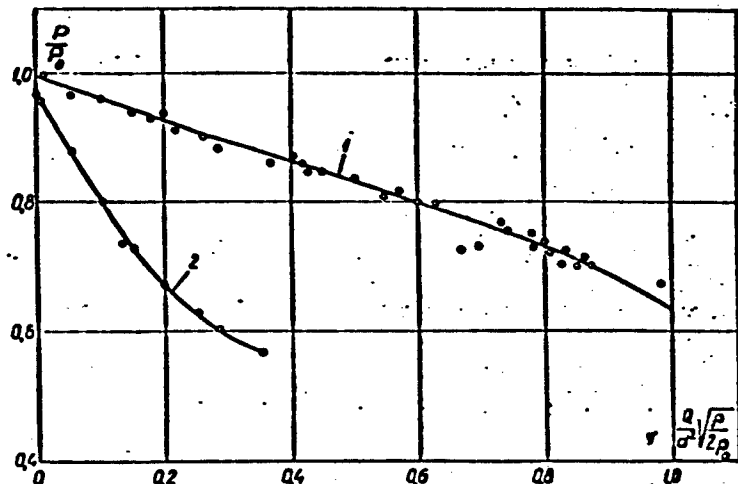


Fig. 1

Curve 1 pertains to the case of total pressure, while curve 2 pertains to the case of static pressure.

The centrifugal induction pump can be used also as a batching unit. Figure 2 shows the working characteristics of such a batching

unit - the delivered mercury batch V in cm^3 as a function of the time t during which the pressure is turned on at a current $I = 14.4$ amperes and a frequency 50 cps. The same figure shows the dependence of the batch on the current in the stator winding for a constant operating time $t = 10$ sec and a frequency 50 cps.

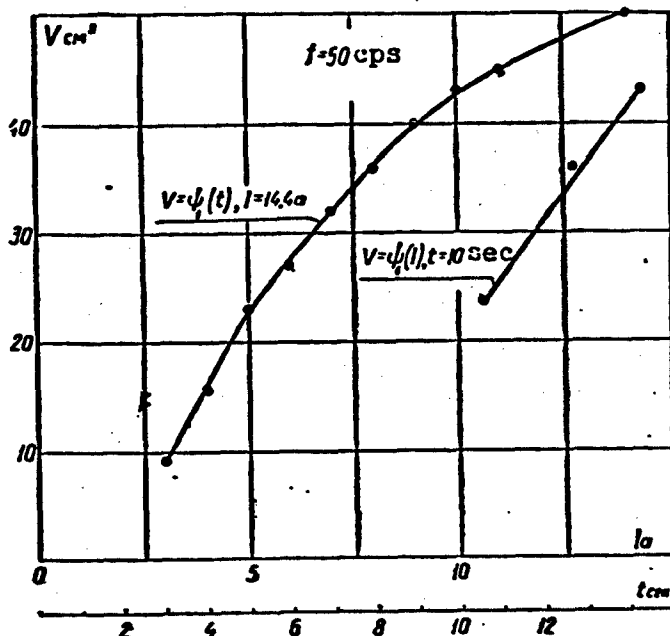


Fig. 2

Figure 3 shows the dependence of the batch on the frequency of the supplying current ($\omega = 2\pi f$) at $I = 10.5$ amperes and $t = 30$ sec. Figure 3 shows also the dependence of the batch V and the additional resistance ξ , introduced in the outlet of the liquid metal in the form of a diaphragm with different relative apertures. The corresponding resistance coefficients are taken from the book of N.N. Pavlovskiy [1]. In analogy with the increase in the delivered batch with increasing induction frequency, one can expect the batch also to increase with improved conductivity of the liquid metal. It is natural to expect that the batch in cm^3 will also increase with decreasing density.

The purpose of the present research was a tentative determination

of the feasibility of a centrifugal batcher. In the experiments we used metal with the worst parameters. If the inductor is specially

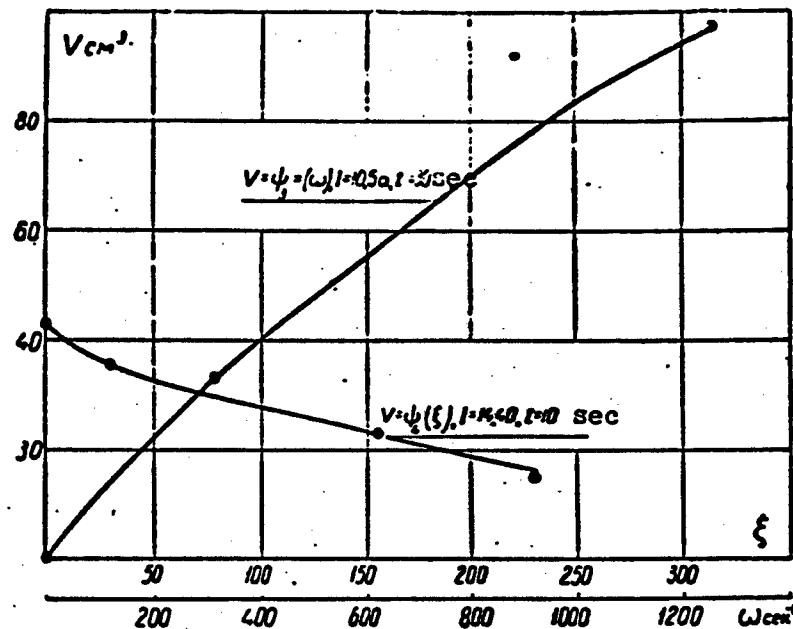


Fig. 3

constructed, the induction can also be greatly improved. From the described experiments it follows that it is possible to construct a centrifugal induction batcher to supply small amounts (several hundred cm^3) of liquid metal. It should be recognized that the metal is vigorously mixed in the vessel of the pump, and this may be suitable for the performance of several technological operations directly before pouring.

REFERENCE

1. N.N. Pavlovskiy. Gidravlicheskiy spravochnik [Hydraulic Handbook], Moscow, 1937.

MAGNETOHYDRODYNAMIC PHENOMENA IN A CHANNEL
OF A PLANAR INDUCTION PUMP WITH
ACCOUNT OF ATTENUATION OF THE ELECTROMAGNETIC FIELD

N.M. Okhremenko

Leningrad

Magnetohydrodynamic phenomena in the channel of a planar induction pump with a one-dimensional stationary laminar flow in the absence of the surface effect were investigated in sufficient detail [1, 2]. Less investigated were the features of magnetohydrodynamic processes in the case when considerable attenuation of the electromagnetic field occurs over the height of the channel. Such phenomena exist in pumps of large productivity, in which the height of the channel reaches several centimeters.

In some regions of technology, there is a noted tendency towards using electric equipment of increased frequency. For example, in shipbuilding, the question of the use of 400 cps alternating current is quite timely. The question therefore arises of the possibility of using increased-frequency current to supply induction pumps. In all these cases the choice of the height of the channel of the induction pump should be closely related with an account of the attenuation of the electromagnetic field. The study of these phenomena is therefore of definite practical interest.

In the present paper we report results of an investigation of magnetohydrodynamic phenomena with account of attenuation of the electromagnetic field over the height of the channel in laminar steady-

state flow.

Let a channel filled with liquid metal and having the form of a narrow slot with height $2a$ have a length L (Fig. 1). We shall assume that high-conduction buses (2) are located on the sides of the channel, so that we can expect only the z component of the vector potential of the magnetic field \bar{A} to exist in the region of the liquid metal ($\text{curl } \bar{A} = \bar{B}$, where \bar{B} is the magnetic induction vector), and the transverse edge effect can be neglected. We shall likewise disregard phenomena due to the fact that the magnetic circuit is open and that the length of the channel is limited.

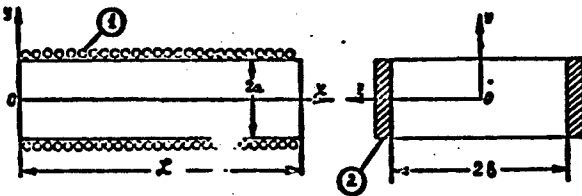


Fig. 1. Channel of planar induction pump.
1 - Winding; 2 - current conducting buses.

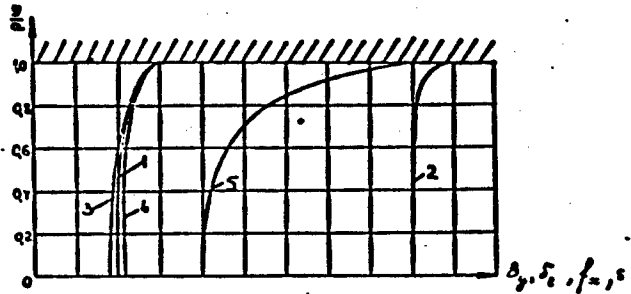


Fig. 2. Distribution of electromagnetic quantities and of the slip in the induction pump channel for laminar flow and for considerable field attenuation:
1 - B_y and δ_z for $V = 0$; 2 - s ; 3 - δ_0 for $V > 0$; 4 - B_y for $V > 0$; 5 - f_x for $V > 0$.

Let us consider first the influence of the attenuation of the electromagnetic field over the height of the channel on the magneto-

hydrodynamic phenomena from the physical point of view, bearing in mind the previously stipulated assumptions. If the attenuation of the field is appreciable, then the distribution of the normal component of induction B_y and of the current density δ_z in the region of the liquid metal, when the latter is stationary, can be represented by only curve 1 of Fig. 2. In the case of laminar one-dimensional flow of the liquid along the channel axis, the unevenness of the distribution δ_z increases. Indeed, the distribution of the current density over the height of the channel is determined in this case by the relation

$$\delta_z(y) = C \cdot B_y(y) \cdot s(y),$$

where C is a constant and s is the slip. Since the slip of the layers of the liquid relative to the traveling field decreases on approaching the channel axis (curve 2), the current density will also decrease with decreasing y (curve 3).

On the other hand, the unevenness in the distribution of the induction over the height of the channel decreases in the case of flow (Fig. 4), owing to the weakening of the demagnetizing action of the induced currents on approaching the channel axis.

The degree of disparity between the curves 3 and 4 will be determined by the value of the slip. In view of the fact that in laminar motion the absolute velocity of the flow is small, the change in the distribution of δ_z and B_y due to the flow will be insignificant. The dependence of the useful electromagnetic force $f_x = \delta_z B_y$, which gives rise to the pressure drop along the channel, on the coordinate y in the case of laminar flow will be represented by curve 5. It will differ little from the plot of the distribution of the same force in the absence of flow. The electromagnetic force will have a maximum at the channel walls and a minimum at the axis. The average values of the

electromagnetic force and of the pressure developed by the pump will decrease somewhat, and the velocity profile may change compared with the case when B_y and δ_z are constant over the height of the channel.

In addition to the singularities noted above, the attenuation of the field leads also to the appearance of an induction component B_x , an electromagnetic force, and a pressure gradient acting in the direction of the O_y axis.

Under the assumptions made above, we can obtain from the magneto-hydrodynamic equations describing planar laminar flow of a viscous incompressible conducting liquid in the channel of a planar induction pump [2] the following equations:

$$\begin{aligned} \frac{\partial \Omega}{\partial t} + V_x \frac{\partial \Omega}{\partial x} + V_y \frac{\partial \Omega}{\partial y} - v \Delta^2 \Omega = & \frac{\sigma a^2 A_m^2}{\rho} \left\{ (\varphi \varphi' + \psi \psi') \left(V_x - \frac{\omega}{a} \right) + \right. \\ & + \left[\frac{V_x}{a^2} (\varphi'' \psi + \varphi' \psi') - \frac{2}{a} \frac{dV_x}{dx} \varphi' \psi + \left(\varphi^2 \frac{\partial V_x}{\partial y} - \frac{\varphi'^2}{a^2} \frac{\partial V_x}{\partial x} \right) \right] \times \\ & \times \sin^2(\omega t - ax) + \left[- \frac{V_x}{a} (\varphi \varphi'' + \psi \psi'') + \frac{2}{a} \frac{\partial V_x}{\partial x} \varphi \psi' + \right. \\ & \left. + \left(\varphi^2 \frac{\partial V_x}{\partial y} - \frac{\varphi'^2}{a^2} \frac{\partial V_x}{\partial x} \right) \right] \cos^2(\omega t - ax) + \left[\frac{V_x}{2a} (\varphi \varphi'' - \psi \psi'' + \varphi^2 - \right. \\ & \left. - \psi'^2) + \frac{1}{a} \frac{\partial V_x}{\partial x} (\varphi \varphi' - \psi \psi') - \right. \\ & \left. - \left(\varphi \frac{\partial V_x}{\partial y} + \frac{\varphi' \psi'}{a^2} \frac{\partial V_x}{\partial x} \right) \right] \sin 2(\omega t - ax), \end{aligned} \quad (1)$$

$$\Omega = \frac{\partial V_x}{\partial x} - \frac{\partial V_y}{\partial y}, \quad (2)$$

$$\begin{aligned} \left[\mu \sigma z \left(\frac{\omega}{z} - V_x \right) \varphi + \mu \sigma \psi' V_y + a^2 \psi^2 - \psi'' \right] \cos(\omega t - ax) = \\ = \left[\mu \sigma z \left(\frac{\omega}{z} - V_x \right) \varphi + \mu \sigma \varphi' V_y - a^2 \varphi + \varphi'' \right] \cdot \sin(\omega t - ax). \end{aligned} \quad (3)$$

$$A = A_m [\varphi(y) \cdot \sin(\omega t - ax) + \psi(y) \cdot \cos(\omega t - ax)] \quad (4)$$

with boundary conditions

$$\begin{aligned} \varphi(\pm a) = 1, \quad \psi(\pm a) = 0, \\ V_x = V_y = 0 \text{ for } y = \pm a. \end{aligned} \quad (5)$$

We use here the same notation as in [2], while $\varphi(y)$ and $\psi(y)$ together with V_x and V_y are the unknown functions. Expression (1) is the generalized Helmholtz equation with allowance for the electromagnetic mass forces. The right half of this equation contains the derivatives of the electromagnetic forces with respect to the coordinates.

Following the method of S.M. Targ and N.A. Slezkin [8, 9], let us replace in Eqs. (1-3) the real velocities by their values averaged over the period $T = 2\pi/\omega$. In this case we can leave out from (1) the derivative of Ω with respect to the time and integrate the equations (1) and (3) with respect to time from 0 to T .

Solution of the nonlinear equations obtained in this case is fraught with great difficulties. In view of the symmetry of the problem, we can assume that V_x is independent of x , and that $V_y = 0$. We then obtain in place of (1-5)

$$\frac{d^2V}{dy^2} = \frac{M^2}{a^2} (\varphi^2 + \psi^2) \left(V - \frac{\omega}{a} \right) + B, \quad (6)$$

$$\mu\sigma a \left(\frac{\omega}{a} - V \right) \varphi + a^2 \psi - \psi'' = 0, \quad (7)$$

$$\mu\sigma a \left(\frac{\omega}{a} - V \right) \psi - a^2 \varphi + \varphi'' = 0, \quad (8)$$

where M is the Hartmann number, $V = V_x$ and B is a constant to be determined.

The system of equations (6-8) with boundary conditions (5) can be solved by successive approximations. For the zero approximation we obtain the following equation for the velocity:

$$\frac{d^2V_0}{dy^2} - \frac{M^2}{a^2 k^2} \frac{\cosh 2\beta y + \cos 2\beta y}{2} V_0 = B - \frac{M^2}{a^2 k^2} V_f \frac{\cosh 2\beta y + \cos 2\beta y}{2} \quad (9)$$

with boundary conditions

$$V_0 = V, \quad V'_0 = 0 \text{ for } y = 0, \quad (10)$$

$$V_0 = 0 \text{ for } y = a,$$

where $\frac{1}{\beta} = \sqrt{\frac{2}{\mu \sigma \omega}}$ is the depth of penetration of the electromagnetic wave (assuming $\mu \sigma \omega \gg (\pi/\tau)^2$,

$$k = \sqrt{\frac{\operatorname{ch} 2\beta a + \cos 2\beta a}{2}},$$

$V_f = \omega/a$ is the velocity of the magnetic field, V is the velocity at the center of the stream.

Particular solutions of this equation have been obtained in the form of rapidly converging power series, in which only the first terms are retained. The general approximation of the solution of Eq. (9) has the form*

$$V_0 = V_{\text{osc}} + V_{\text{add}}, \quad (11)$$

$$V_{\text{osc}} = V \frac{\operatorname{ch} \frac{M}{k} - \operatorname{ch} \left(\frac{M}{k} \frac{y}{a} \right)}{\operatorname{ch} \frac{M}{k} - 1}, \quad (12)$$

$$\begin{aligned} V_{\text{add}} = & \frac{c^4 V_f}{c^4 - 1} \left\{ \left[k^2 - 1 + \frac{\operatorname{ch} 2\beta a - \cos 2\beta a}{2c^2} \right] \frac{\operatorname{ch} \frac{M}{k} - \operatorname{ch} \left(\frac{M}{k} \frac{y}{a} \right)}{\operatorname{ch} \frac{M}{k} - 1} - \left[k^2 + \right. \right. \\ & \left. \left. + \frac{\operatorname{ch} 2\beta a - \cos 2\beta a}{2c^2} - \frac{\operatorname{ch} 2\beta y - \cos 2\beta y}{2} - \frac{\operatorname{ch} 2\beta y - \cos 2\beta y}{2c^2} \right] \right\}, \quad (13) \\ c = & \frac{M}{2\beta a k}. \end{aligned}$$

The attenuation of the electromagnetic field manifests itself in the main velocity component (12) in a reduction of the average value of the induction and of the "effective Hartmann number" by a factor k , so that the velocity profile becomes less flat.

If $\beta \approx 0$, then $k = 1$ and the second velocity component (13) vanishes, so that we obtain from formulas (11) and (12) the well known expression for the velocity profile in the absence of surface effect.

The velocity component (13) appears only as a result of the attenuation of the field, when $s > 0$. This component is equal to zero on the walls and at the center of the channel. It is proportional to the velocity of the traveling field. Its relative share is the greater, the larger the depth of penetration of the electromagnetic field and the larger the height of the channel.

With decreasing slip s_0 , the velocity of flow in the center of the stream increases, and the relative share of the additional component of velocity in formula (11) decreases. Figures 3 and 4 show the profiles of the velocity $V_0 = f(y/a)$ and its components, calculated by formulas (11) and (13) for a planar induction pump for sodium at 400°C and having the following data: the frequency is

$$f = 50 \text{ cps}, \quad 2a = 2 \text{ cm}, \quad 2\beta a = 0.626,$$
$$s_0 = 0.99, \quad M = 5 \text{ and} \quad M = 10.$$

Because of the unevenness in the distribution of the electromagnetic forces, the velocity profile at $M = 10$ assumes a saddle-like form. This profile has two points of inflection.

It is known that the presence of a point of inflection is in ordinary hydrodynamics a necessary and sufficient condition for violation of flow stability (in the sense of nonviscous instability) [5].

We can therefore assume that the uneven distribution of the electromagnetic forces, brought about by the attenuation of the electromagnetic field, may be the reason of the changeover from laminar to turbulent conditions.

The curves of Figs. 3 and 4 have been plotted for $s_0 = 0.99$. When the slip is reduced say to 0.9, the abscissas of the additional velocity components in these figures decrease by a factor of 10, and the points of inflection disappear. However, saddle-like unstable

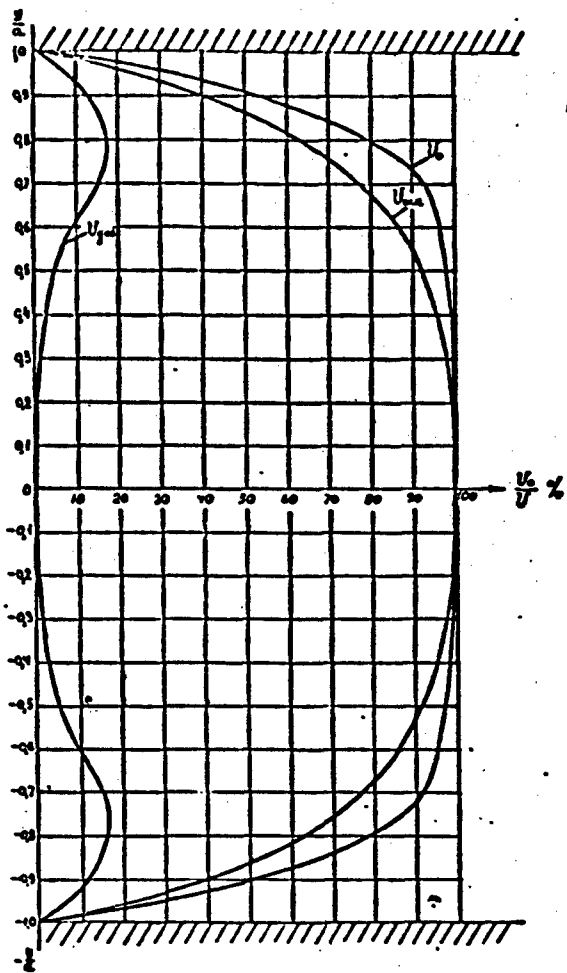


Fig. 3. Velocity profile at $M = 5$ and field attenuation.

profiles can be obtained also in the case of small slips s_0 , but considerable values of M and $2\beta a > 1$.

If we replace in formulas (11-13) the velocity at the center of the stream by its expression in terms of the average velocity over the channel cross section V_{sr} , we obtain the following dependence:

$$V_s = \left\{ V_{sr} - \frac{c^4 V_s}{c^4 - 1} \left[\left(k^2 - 1 + \frac{\operatorname{ch} 2\beta a - \cos 2\beta a}{2c^2} \right) \frac{\operatorname{ch} \frac{M}{k} - \operatorname{ch} \left(\frac{M}{k} \frac{y}{a} \right)}{\operatorname{ch} \frac{M}{k} - 1} - \right] \right\}$$

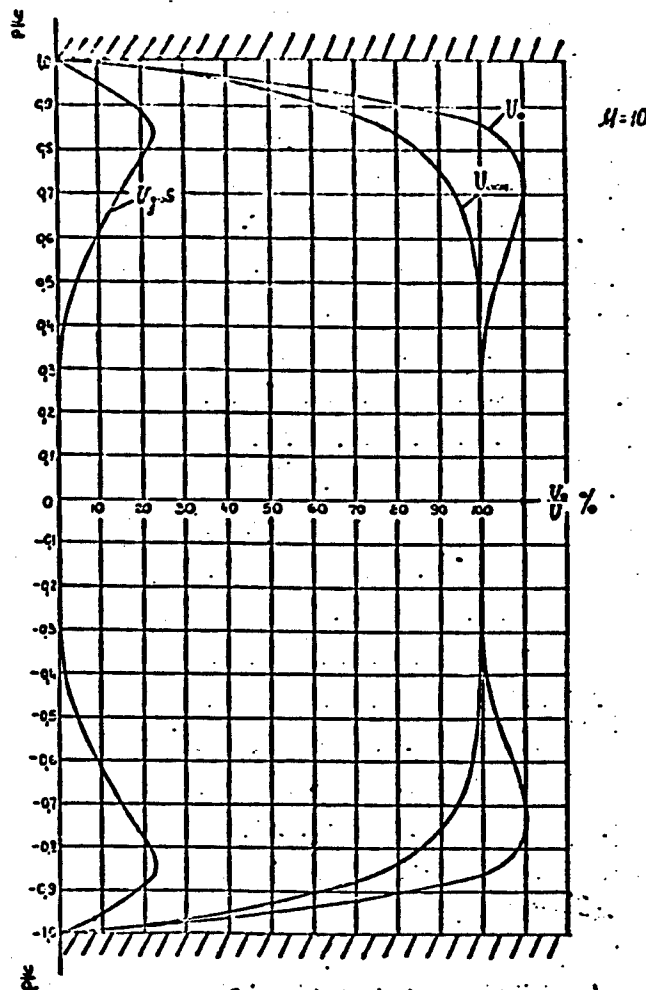


Fig. 4. Velocity profile at $M = 10$ and field attenuation.

$$\left. \begin{aligned}
 & - \left(k^2 + \frac{\operatorname{ch} 2\beta a - \cos 2\beta a}{2c^2} - \frac{\operatorname{sh} 2\beta a - \sin 2\beta a}{4\beta a} \right. \\
 & \left. - \frac{\operatorname{sh} 2\beta a - \sin 2\beta a}{4\beta a c^2} \right) \right\} \times \frac{\operatorname{ch} \frac{M}{k} - \operatorname{ch} \left(\frac{M}{k} \frac{y}{a} \right)}{\operatorname{ch} \frac{M}{k} - 1} + V_{104}. \quad (14)
 \end{aligned}
 \right.$$

Putting $V_{sr} = 0$ in this formula, we determine the velocity profile for an induction pump operating as a metal mixer or an electromagnetic valve, in the following form:

$$V_{sp} = \frac{c^4 V_f}{c^4 - 1} \left\{ \left(k^2 + \frac{\text{ch } 2\beta a - \cos 2\beta a}{2c^2} \right) \frac{k \cdot \text{sh } \frac{M}{k} - \text{ch } \left(\frac{M}{k} y \right)}{\text{ch } \frac{M}{k} - \frac{k}{M} \text{sh } \frac{M}{k}} + \right. \\ \left. + \left(\frac{\text{ch } 2\beta y + \cos 2\beta y}{2} + \frac{\text{ch } 2\beta y - \cos 2\beta y}{2c^2} \right) - \left(\frac{\text{sh } 2\beta a + \sin 2\beta a}{4\beta a} + \right. \right. \\ \left. \left. + \frac{\text{sh } 2\beta a - \sin 2\beta a}{4\beta a c^2} \right) \frac{\text{ch } \frac{M}{k} - \text{ch } \left(\frac{M}{k} y \right)}{\text{ch } \frac{M}{k} - \frac{k}{M} \text{sh } \frac{M}{k}} \right\}. \quad (15)$$

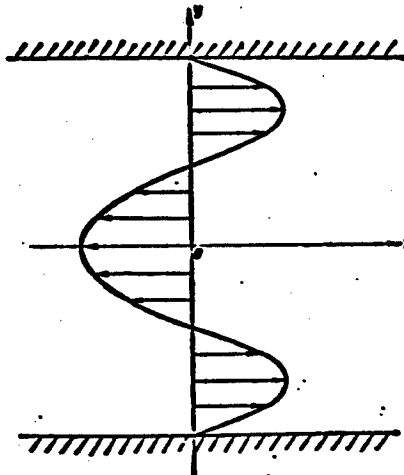


Fig. 5. Velocity profile of induction pump operating as an electromagnetic valve.

amount to:

$$\Delta p = \Delta p_1 + \Delta p_2, \quad (16)$$

where

$$\Delta p_1 = \frac{\eta I M V}{a^2 k} \cdot \frac{\text{th } \frac{M}{k}}{1 - \frac{1}{\text{ch } \frac{M}{k}}}, \quad (17)$$

$$\Delta p_2 = \frac{\gamma L M V_f c^4}{a^2 k (c^4 - 1)} \left[\left(k^2 - 1 + \frac{\operatorname{ch} 2\beta a - \cos 2\beta a}{2c^2} \right) \frac{\operatorname{th} \frac{M}{k}}{1 - \frac{M}{\operatorname{ch} \frac{M}{k}}} - \right. \\ \left. - \frac{1}{c} \left(\frac{\operatorname{sh} 2\beta a - \sin 2\beta a}{2} + \frac{\operatorname{sh} 2\beta a + \sin 2\beta a}{2c^2} \right) \right]. \quad (18)$$

The first component of the pressure loss is due to the main velocity component. When $\beta = 0$ we obtain from (17) a formula that disregards the field attenuation [2]. The second component (18) is due to the skin effect.

Calculations show that for the example given above the ratio

$$\frac{\Delta p_2}{\Delta p_1} \cdot 100$$

amounts to 13.8% when $M = 5$ and 44.5% when $M = 10$.

The attenuation of the field, in addition to increasing the pressure losses, leads to a decrease in the electromagnetic pressure, something already noted in the literature [6, 7].

The question of magnetohydrodynamic phenomena in the channel of an induction pump in the presence of field attenuation was also solved by I.A. Tyutin [2]. In this case he discarded in the Navier-Stokes equation the terms due to the viscosity. Such a simplification of the equations has led to an expression for the velocity which, of course, does not satisfy the adhesion conditions and in addition does not take full account of the specific nature of the phenomena. It lies in the fact that it is precisely at the walls where the electromagnetic forces and the velocity gradients are large, and the viscosity forces become appreciable so that they can no longer be neglected. I.A. Tyutin's solution therefore does not make it possible to determine the pressure losses.

Manu-
script
Page
No.

[Footnote]

525 An estimate of the accuracy of the solution (11-13) can be made by the methods indicated in [3, 4].

REFERENCES

1. I.M. Kirko.. O modelirvaniii magnitogidrodinamicheskikh yavleniy v zhidkikh metallakh [Simulation of Magnetohydrodynamic Phenomena in Liquid Metals], Tr. In-ta fiziki AN Latv. SSR [Transactions of the Physics Institute Academy of Sciences Latvian SSR], VIII, 3, 1956.
2. I.A. Tyutin. Elektromagnitnyye nasosy dlya zhidkikh metallov [Electromagnetic Pumps for Liquid Metals], Izd-vo AN Latv. SSR [Publishing House of the Academy of Sciences Latvian SSR], 1959.
3. V.P. Il'in. Otsenka pogreshnosti v metode Rittsa dlya obyknovenykh differentsial'nykh uravneniy [Estimation of Error in Ritz method for Ordinary Differential Equations], Tr. matematicheskogo instituta imeni V.A. Steklova [Transactions of the Mathematics Institute named for V.A. Steklov], 53, 43, 1959.
4. K. Tatarkewicz. Une methode d'estimation de l'erreur dans procede de Ritz [A Method of Estimating the Error in the Ritz Process], Ann. polon. math. [Annals of Polish Mathematics], 1955, Vol. 1, No. 2, 346 to 359.
5. G. Shlikhting. Teoriya pogranichnogo sloya [Theory of the Boundary Layer], Izd-vo inostr. lit. [Foreign Literature Press], 1956.
6. I.A. Tyutin, E.K. Yankop. Elektromagnitnyye protsessy v induktsionnykh nasosakh dlya zhidkikh metallov. [Electromagnetic Processes in Induction Pumps for Liquid Metals], Tr. in-ta

- fiziki AII Latv. SSR, VIII, 65, 1956.
7. N.M. Okhremenko. Elektromagnitnyye yavleniya v ploskikh induktsionnykh nasosakh dlya zhidkikh metallov. [Electromagnetic Phenomena in Planar Induction Pumps for Liquid Metals], Elektrichestvo [Electricity], 3, 1960.
8. S.M. Targ. Osnovnyye zadachi teorii laminarnykh techeniy [Basic Problems of Laminar-Flow Theory], GITTL [State Unified Publishing House for Technical and Theoretical Literature], 1951.
9. N.A. Slezkin. Dinamika vyazkoy neszhimaemoy zhidkosti [Dynamics of the Viscous Incompressible Fluid], GITTL, 1955.

Manu-
script
Page
No.

[List of Transliterated Symbols]

525	осн = osn = osnovnoy = main
525	доб = dob = dobavochnyy = additional, secondary
527	ср = sr = sredniy = average
529	кр = kr = kriticheskiy = critical

HYDRODYNAMIC PROCESSES IN THE CHANNEL
OF AN ELECTROMAGNETIC INDUCTION PUMP

Ya.Ya. Lielpeter
Riga

The electromagnetic induction pump operates on the principle of the induction motor, in which the role of the rotor is assumed by the pumped liquid metal. The presence of a liquid "rotor" in the induction pump gives rise to several hydrodynamic phenomena, a study of which is part of the theory of such a pump.

From the hydrodynamic point of view the induction pump represents a certain portion of a common pipe of a hydraulic system (pump channel), in which a traveling (or rotating) magnetic field of the form $B = B_0 \cos(\omega t - \alpha x)$ is produced, where B is the induction of the magnetic field, ω is the angular frequency, $\alpha = \pi/\tau$, τ is half the distance between two nearest points of the same phase of magnetic induction, and x is the coordinate, directed along the pipe. The ponderomotive forces arising upon interaction between the traveling magnetic field and the currents induced in the liquid metal give rise to a certain pressure difference on the ends of the segment — the pump pressure head. In the stationary mode, the latter is balanced by the pressure drop in the remaining part of the hydraulic system.

The determination of the pump pressure for a specified magnetic field is one of the main problems of the theory. For a solid body, such a problem is solved by integrating the electromagnetic forces acting on each elementary volume of the body:

$$p_0 = \frac{1}{S} \int \vec{e}_x \vec{J} \times \vec{B} dV, \quad (1)$$

where p_0 is the pressure produced by the electromagnetic forces, S is the transverse cross section of the pump channel, \vec{e}_x is a unit vector directed along the coordinate x , and \vec{J} is the current density in the conducting solid.

The pressure of the pump in the presence of a liquid current conductor can be determined analytically only by solving the corresponding equations of motion, which comprise the nonlinear system of magnetohydrodynamic equations for an incompressible medium. The solution of the latter can be obtained only for very simplified particular cases, which do not satisfy completely the practical needs. Therefore, the main method for investigating hydrodynamic processes in an induction pump remains experiment, all the more since we deal almost always with a turbulent flow mode. Analytic methods serve principally for a qualitative analysis of the processes and for generalization of the experimental data.

Practice has shown that in many cases the electromagnetic processes in a liquid body correspond to a sufficiently high degree of accuracy to the processes in a solid body, provided the latter moves with the average velocity of the liquid body. The pump pressure p_a is in this case smaller than the pressure p_0 by an amount equal to the hydraulic losses p_f , due to the viscosity of the liquid:

$$p_a = p_0 - p_f. \quad (2)$$

It is also noted that the pressure losses for the turbulent flow mode can be determined from the formulas of ordinary hydrodynamics, neglecting the influence of the magnetic field [1, 2]. In Fig. 1 the solid lines represent the theoretical curves, with the resistivity coef-

ficient determined by the Blasius formula, and the pressure p_0 determined from the average velocity of the liquid metal. The individual points represent the measurement results.

We can determine the order of magnitude of the influence of the magnetic field on the pressure losses in the case of turbulent flow by starting from an analysis of the equations of the averaged motion [2]. The turbulent viscosity v_T in the case of plane flow of a non-conducting liquid is expressed, as is well known [3], by the formula

$$-\bar{v'_x v'_z} = v_T \frac{\partial \bar{v}_x}{\partial z}, \quad (3)$$

where v_x and v_z are the velocity components, the primes ('') denote pulsating quantities and the bar (-) denotes averaging.

In the case of plane flow of a conducting liquid in a magnetic field, we can introduce analogously a certain effective turbulent viscosity v_T^* , which takes into account the influence of the magnetic field.

$$-\bar{v'_x v'_z} + \frac{1}{\mu \rho} \bar{B'_x B'_z} = v_T^* \frac{\partial \bar{v}_x}{\partial z}, \quad (4)$$

where B'_x and B'_z are the components of the turbulent pulsations of the magnetic induction, brought about by the velocity pulsations, while μ and ρ are respectively the magnetic permeability and the density of the liquid.

Estimating the order of magnitude of the first and second terms of (4), we arrive at the following condition under which the second term is insignificant:

$$N_B \cdot Re^{1/2} \ll 1, \quad (5)$$

where N_B is the ratio of the densities of the magnetic energy and the kinetic energy of the liquid

$$N_B = \frac{B_0^2}{\mu \rho v_0^2}, \quad (6)$$

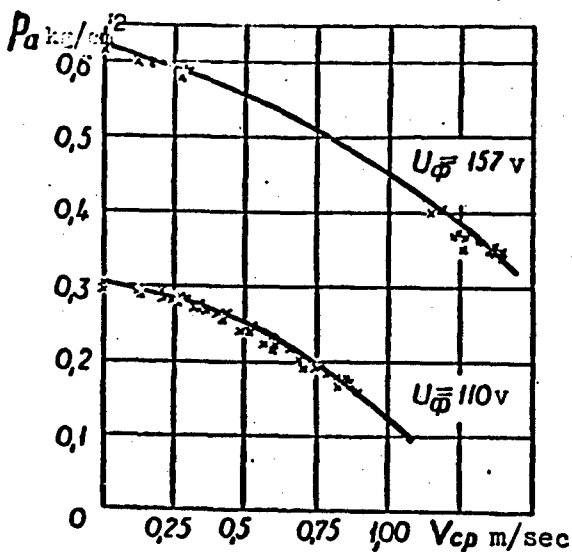


Fig. 1

Re_m' is the magnetic Reynolds number for turbulent pulsation

$$\text{Re}'_m = v' l_p \sigma \mu. \quad (7)$$

In these expressions B_0 and v_0 are certain values of induction and velocity, which are characteristic for the phenomenon under consideration, l_p is the scale of turbulent pulsation, and σ is the specific electric conductivity of the liquid metal.

Relation (5) can be used to estimate the influence of the magnetic field on the turbulent viscosity, that is, we can obtain qualitative considerations of pressure losses in the channel of the induction pump.

When estimating the quantity $N_B \cdot \text{Re}_m'^2$ for the constructed induction pumps we find that it is actually appreciably smaller than unity. Inasmuch as the turbulent viscosity is determined principally by the large-scale pulsations, we can approximately take as the characteristic values of v' and l_p the quantities v_0 and l_0 . It must be noted that the estimate made above pertains to the case when the skin effect can be neglected for the induction currents in the liquid metal.

Thus, we have arrived in different ways at one and the same conclusion: the pump pressure is determined by the flow velocity averaged over the cross section of the channel, and the energy dissipation due to liquid viscosity occurs in the same way as in ordinary flow without a magnetic field. Expression (5) determines the limits of applicability of such a theory, and it turns out that the theory is applicable for the overwhelming majority of induction pumps.

It must be noted that a direct experimental verification of these conclusions has been made only for large slip of the liquid metal relative to the magnetic field, when the density of the electromagnetic force is approximately constant over the cross section of the channel. There are grounds for assuming that in the case when the electromagnetic forces are highly unevenly distributed over the cross section of the channel, the profile of the average velocities may be appreciably distorted, and this will lead also to a change in the pressure losses.

There are three most important cases which lead to uneven distribution of the electromagnetic forces:

- a) a pronounced skin effect in the distribution of the induction currents in the direction of the magnetic field (over the thickness of the metal layer),
- b) a pronounced transverse edge effect in the distribution of the induction current in the liquid metal,
- c) small slip of the liquid metal relative to the magnetic field.

All these cases have not yet been sufficiently studied to date, and therefore no practical deductions can be drawn from them.

An attempt to study the velocity distribution of laminar flow with a pronounced skin effect in thickness was made by I.A. Tyutin [4], but he did not solve the problem to the end. Certain interesting

conclusions with regard to the same problem were obtained by N.M. Okhremenko [5]. The transverse edge effect in the distribution of the induction current was investigated in [6, 7], but only for the case of a solid.

We consider below by way of an example plane laminar flow of a liquid metal in the case when the unevenness in the amplitude of the traveling magnetic field over the thickness of the layer and the resultant unevenness in the distribution of the induction current are due to the commensurability of the pole pitch with the thickness of the metal layer. The skin effect due to the demagnetizing effect of the induction currents will be neglected.

Assume that the electrically conducting viscous liquid filling the space between two infinite parallel planes (Fig. 2) is set in stationary motion with the aid of a traveling magnetic field, the induction B_z of which is determined by the law

$$B_z = B_{m0} \frac{\operatorname{ch} \alpha z}{\operatorname{ch} \alpha b} \cos(\omega t - \alpha x), \quad (8)$$

where B_{m0} is the amplitude of the induction on the surface of $z = \pm b$, b is half the distance between the planes.

The equation of motion of the liquid can be written for the case under consideration in the following form:

$$\frac{\sigma B_m^2}{2} \frac{\operatorname{ch}^2 \alpha z}{\operatorname{ch}^2 \alpha b} \left(\frac{\omega}{\alpha} - v_x \right) - \frac{p_2 - p_1}{l} + \nu p \frac{d^2 v_x}{dz^2} = 0, \quad (9)$$

where p_1 and p_2 are the pressures in two sections of the channel spaced a distance l apart, ν is the kinematic viscosity of the liquid metal.

It will be convenient in what follows to use the concept of local slip $s(z)$, which depends in this case on the coordinate z :

$$s(z) = 1 - v_x(z) \cdot \frac{\nu}{\omega}. \quad (10)$$

Substituting the latter into Eq. (9) and carrying out simple transformations, we obtain

$$\frac{ds}{dz^2} - \frac{M^2}{m^2}(1 + \text{ch } 2az) \cdot s + D = 0, \quad (11)$$

where

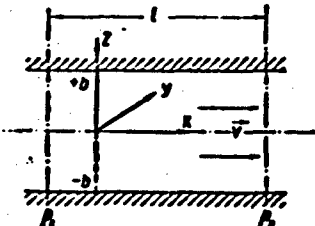


Fig. 2.

Equation (11) is an inhomogeneous modified Matthew type equation. It is easy to verify that its solution should be an even function. We shall seek it in the form of a power series containing even powers of the argument z:

$$s(z) = \sum_{n=0}^{\infty} A_{2n} \cdot z^{2n}, \quad (15)$$

where A_{2n} are the coefficients of the series and n is a positive integer or zero.

After substituting (15) in Eq. (11) we obtain the following expression for the determination of the coefficients A_{2n} of the series:

$$(2n+2)(2n+1)A_{2n+2} - \frac{M^2}{m^2}A_{2n} - \sum_{k=0}^{\infty} \frac{M^2}{m^2} \frac{(2a)^{2n-2k}}{(2n-2k)!} A_{2k} + D_s = 0, \quad (16)$$

which is an infinite system of equations from which we can determine the coefficients A_2 , A_4 , etc., relative to A_0 .

Solving this system, we obtain the coefficients

$$A_2 = \frac{2 \frac{M^2}{m^2} A_0}{2 \cdot 1} - \frac{D}{2 \cdot 1},$$

$$A_4 = \frac{2 \frac{M^2}{m^2} \left(2 \frac{M^2}{m^2} A_0 - \frac{D}{2 \cdot 1} \right)}{4 \cdot 3} + \frac{\frac{M^2}{m^2} (2a)^2}{4 \cdot 3 \cdot 2!} A_0, \quad (17)$$

$$A_6 = \frac{2M^2}{6 \cdot 5} \left[\frac{2M^2}{m^2} \left(\frac{2 \cdot M^2}{m^2} A_0 - \frac{D}{2 \cdot 1} \right) + \frac{M^2}{4 \cdot 3} \cdot \frac{(2a)^2}{21} A_0 \right] + \\ + \frac{M^2}{6 \cdot 5} \cdot \frac{(2a)^2}{21} \left(\frac{2 \cdot M^2}{m^2} A_0 - \frac{D}{2 \cdot 1} \right) + \frac{M^2}{6 \cdot 5} \cdot \frac{(2a)^2}{41} A_0.$$

The following recurrence formula can be set up for the determination of the coefficients A_2, A_4, A_6, \dots :

$$A_{2n} = \frac{\frac{M^2}{m^2} \cdot A_{2n-2}}{2n(2n-1)} + \frac{\frac{M^2}{m^2}}{2n(2n-1)} \cdot \sum_{k=0}^{n-1} A_{2n-2k-2} \cdot \frac{(2a)^{2k}}{(2k)!}. \quad (18)$$

The series (15) converges moderately rapidly. The coefficient A_0 plays the role of an arbitrary constant and is determined from the boundary conditions

$$s = 1 \text{ for } z = \pm b. \quad (19)$$

Taking (10) into account, we obtain the velocity distribution

$$v_x(z) = \frac{u}{a} [1 - s(z)] = \frac{u}{a} \left[1 - \sum_{n=0}^{\infty} A_{2n} \cdot z^{2n} \right]. \quad (20)$$

It is also easy to find the velocity averaged over the section of the channel

$$\bar{v}_x = \frac{1}{b} \int v_x(z) dz = \frac{u}{a} \left[1 - \sum_{n=0}^{\infty} A_{2n} \cdot \frac{b^{2n}}{2n+1} \right]. \quad (21)$$

Finally, let us find the magnetohydrodynamic pressure loss in the pump channel, taking into account the velocity distribution (20). For this purpose we use the equation

$$v_p \frac{\partial^2 p_x}{\partial z^2} = - \frac{p_{fz}}{l}, \quad (22)$$

which equates the viscosity force, acting on an elementary layer of liquid dz , to the pressure force. Substituting into (22) the second derivative of v_x we obtain

$$p_{fz} = \frac{u}{a} v_p l \sum_{n=0}^{\infty} (2n+2)(2n+1) A_{2n+2} \cdot z^{2n}. \quad (20)$$

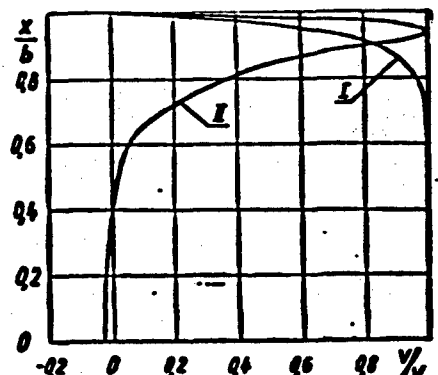


Fig. 3

ing parameters: $b = 2 \cdot 10^{-2}$ meters, $a = 50 \text{ m}^{-1}$, $\omega/a = 6.28 \text{ m/sec}$ and $M = 20$. Curve I corresponds to $D = 0$ and curve II to $D = 5 \cdot 10^5 \text{ m}^{-2}$.

The next hydrodynamic problem in the theory of the induction pump is a study of the turbulent flow of liquid metal for an uneven distribution of the electromagnetic forces.

REFERENCES

1. I. M. Kirko, Ya. Ya. Klyayin'sh, I. A. Tyutin, L. Ya. Ul'manis, Model' beskonechno dlinnogo kanala s zhidkim metallom, nakhodyashchimya v begushchem magnitnom pole [A Model of an Infinitely Long Channel with Liquid Metal Situated in a Traveling Magnetic Field], Nauchnye doklady vysshey shkoly. Energetika [Scientific Reports of the Higher Schools. Power Engineering], 3, 1958.
2. Ya. Ya. Liyelpeter. O turbulentnom rezhime raboty elektromagnitnogo indiktionsnogo nasosa [On the Turbulent Operating Mode of the Electromagnetic Induction Pump], Izv. AN Latv. SSR [Publishing House of the Academy of Sciences Latvian SSR], 1, 1960.
3. S. P. Loytsyanskiy. Mekhanika zhidkosti i gaza [Mechanics of Liquids and Gases], Gostekhizdat [State Unified Publishing House for Technical and Theoretical Literature], Moscow, 1957.

We obtain the total pressure loss by integrating the last expression with respect to z and dividing by the distance between the parallel planes. We then have

$$p_f = l \cdot p \sum_{n=0}^{\infty} (2n+2) A_{2n-2} b^{2n}. \quad (21)$$

By way of illustration Fig. 3 shows the velocity distribution curves in the pump channel under the follow-

4. I.A. Tyutin. Elektromagnitnye nasosy dlya zhidkikh metallov [Electromagnetic Pumps for Liquid Metals], Izd-vo AN Latv. SSR, 1959.
5. N.M. Okhremenko. Magnitogidrodinamicheskiye yavleniya v lineynykh induktsionnykh nasosakh s uchetom poverkhnostnogo effekta [Magnetohydrodynamic Phenomena in Linear Induction Pumps Taking the Surface Effect into Account], in present collection.
6. L.Ya. Ul'manis. K voprosu o kraevykh effektakh v lineynykh induktsionnykh nasosakh. Prikladnaya magnitogidrodinamika [On the Problem of Edge Effects in Linear Induction Pumps. Applied Magnetohydrodynamics], Tr. In-ta fiziki AN Latv. SSR Transacions of the Institute of Physics of the Academy of Sciences of the Latvian SSR], VIII, 1956.
7. A.I. Vol'dek. Toki i usiliya v sloe zhidkogo metalla ploskikh induktsionnykh nasosov [Currents and Forces in the Liquid Metal Layer of Planar Induction Pumps], Izv. vysshikh uchebnykh zavedeniy, Elektromekhanika [Bulletin of the Higher Educational Institutions, Electromechanics], 1, 1959.

NONSTATIONARY FLOW OF A LIQUID METAL
IN THE CHANNEL OF A PLANAR INDUCTION PUMP

N.M. Okhremenko

Leningrad

Nonstationary one-dimensional flow of a viscous liquid in pipes and between parallel planes has been investigated in detail within the framework of classical hydrodynamics. On the other hand, problems of unsteady flow in magnetohydrodynamics have not been sufficiently studied. There is a known paper by O.A. Ladyzhenskaya and V.A. Solonnikov [1], in which certain nonstationary magnetohydrodynamic problems are considered from the point of view of proving the theorem for the existence and uniqueness of the solution. S.A. Regirer [2] has considered one-dimensional nonstationary flow of a conducting liquid in a half space in the presence of a constant transverse magnetic field on the boundary.

In the present paper we report the results of a solution of the problem of unsteady linear-parallel flow of a liquid metal between two parallel walls $y = \pm a$ under the influence of a suddenly applied transverse traveling magnetic field

$$B_x = B_0 \sin(\omega t - \alpha x), \quad \alpha = \frac{\pi}{\tau}, \quad (1)$$

where ω is the angular velocity and τ is the pole pitch.

In induction pumps, as in induction motors, the electromagnetic transient occurs in the overwhelming majority of cases much more rapidly than the mechanical acceleration of the liquid metal. Therefore the

influence of the electromagnetic transients on the motion of the metal can be disregarded. If we neglect phenomena which are brought about by the fact that the magnetic circuit is open [4, 5] and disregard the transverse edge effect and the surface effect, then we obtain from the equations of magnetohydrodynamics for the channel of a planar induction pump [3] the following equations, which describe unsteady plane-parallel flow:

$$\begin{aligned} \frac{\partial u}{\partial t} &= -\frac{1}{\rho} \frac{\partial p}{\partial x} + v \frac{\partial^2 u}{\partial y^2} + \frac{\sigma B_0^2}{\rho} \left(\frac{u}{a} - u \right) \sin^2(\omega t - ax), \\ \frac{\partial p}{\partial y} &= \frac{\partial p}{\partial z} = 0, \\ \frac{\partial u}{\partial x} &= 0, \end{aligned} \quad (2)$$

with
conditions $u=0$ for $y=\pm a$,
 $u=0$ for $t=0$.

where ρ is the density, σ the electric conductivity, and v is the kinematic viscosity of the liquid, while p is the pressure and u the velocity in the direction of O_x .

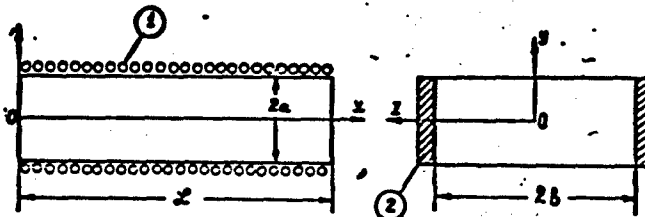


Fig. 1. Channel of planar induction pump:
1 - Winding; 2 - current conducting buses.

Equations (2) can be readily solved by operational methods under the assumption that the external pressure drop P is constant.

As a result of solving the problem for the velocity, the following expression was obtained:

$$u = \left(\frac{u}{a} - \frac{P_0^2}{\rho L M^3} \right) \left\{ \frac{\operatorname{ch} M - \operatorname{ch} \frac{M}{a} y}{\operatorname{ch} M} \left(1 - e^{-v \frac{M}{2} t} \right) + \right.$$

$$+ 2M^2 e^{-\eta \frac{M^2}{a^2} t} \sum_{k=1}^{\infty} \frac{(-1)^{k+1} \cos\left(\lambda_k \frac{y}{a}\right)}{\lambda_k (M^2 + \lambda_k^2)} (1 - e^{-\eta \frac{\lambda_k^2}{a^2} t}) \Bigg). \quad (3)$$

where

$$\lambda_k = \frac{2k-1}{2} \pi \quad (k=1, 2, \dots).$$

L is the channel length, η is the dynamic viscosity of the liquid, and M is the Hartmann number.

The series in the right half of formula (3) converges uniformly in the region $a \geq y \geq -a$, $0 \leq t \leq \infty$. Solution (3) satisfies Eq. (2) and vanishes when $t = 0$ and $y = \pm a$. It determines the law governing the variation of the velocity with time for any value of t .

Putting $t = \infty$ in (3) we obtain the steady-state value of the velocity:

$$u_{y_0} = \left(\frac{u}{a} - \frac{P_0 a^2}{\eta L M^2} \right) \frac{\operatorname{ch} M - \operatorname{ch} \frac{M}{a} y}{\operatorname{ch} M} = u_0 \frac{\operatorname{ch} M - \operatorname{ch} \frac{M}{a} y}{\operatorname{ch} M - 1}, \quad (4)$$

where u_0 is the steady-state value of the velocity at the center of the stream. Expression (4) coincides with the known solution [3].

The settling time of the stationary mode is determined by time constants of two types. The buildup of the first velocity component is due to the constant

$$T_1 = \frac{a^2}{M^2 \nu} = \frac{a^2}{B^2 \sigma} [\text{sec}], \quad (5)$$

which is proportional to the mass density and is inversely proportional to the square of the effective value of the induction B and the electric conductivity. It is characteristic that formula (5) contains neither the kinematic viscosity nor the height of the channel.

The buildup of the second term in the curly brackets of expression (3) is due both to T_1 and to a time constant of the form

$$T_2 = \frac{a^2}{\lambda_k^2 \nu} = \frac{4a^2}{\pi^2 (2k-1)^2} [\text{sec}], \quad (6)$$

which depends only on the kinematic viscosity and on the square of the half height of the channel. The values of T_k decrease rapidly with increasing k .

Figures 2 and 3 show velocity profiles for different instants of time, as calculated from formula (3).

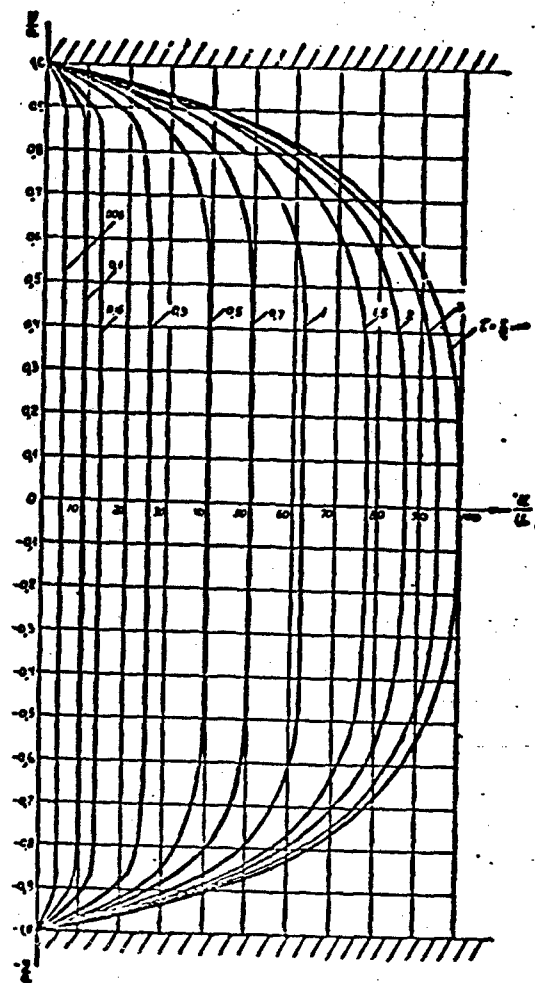


Fig. 2. Velocity profiles in the channel of an induction pump for different instants of time $\tau = t/T_1$ at $M = 5$.

The expression for the velocity in the absence of a magnetic field can be determined from (3) by putting in it $M \rightarrow 0$:

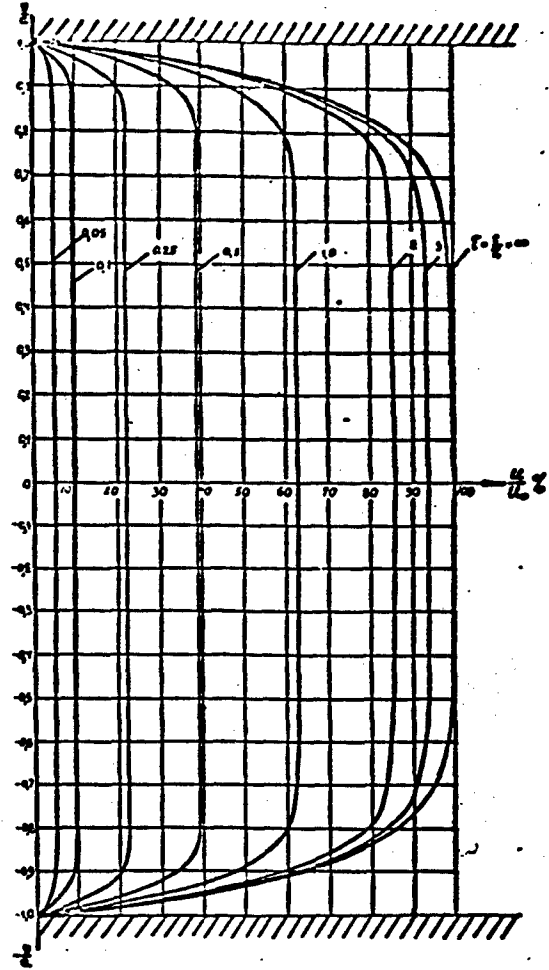


Fig. 3. Velocity profiles in the channel of an induction pump for different instants of time $\tau = t/T_1$, for $M = 10$.

$$u_{M \rightarrow 0} = -\frac{2Pa^2}{\eta L} \sum_{k=1}^{\infty} \frac{(-1)^{k+1}}{\lambda_k^3} \cos \left(\lambda_k \frac{y}{a} \right) \left(1 - e^{-\sqrt{\frac{\lambda_k^2}{a^2}} t} \right). \quad (7)$$

Recognizing that

$$2 \sum_{k=1}^{\infty} \frac{(-1)^{k+1}}{\lambda_k^3} \cos \left(\lambda_k \frac{y}{a} \right) = \frac{1 - \frac{y^2}{a^2}}{2}. \quad (8)$$

we obtain from (7) the formula of ordinary hydrodynamics

$$u_{M \rightarrow 0} = -\frac{Pa^2}{2\gamma L} \left[\left(1 - \frac{y^2}{a^2} \right) - \right. \\ \left. - \frac{32}{\pi^2} \sum_{k=1}^{\infty} \frac{(-1)^{k+1}}{(2k-1)^3} \cdot \cos \frac{(2k-1)\pi y}{2a} e^{-\frac{\pi^2(2k-1)^2 t}{4a^2}} \right]. \quad (9)$$

which determines when $t = \infty$ a parabolic velocity profile.

In conclusion let us determine the friction force stress

$$\tau = -\eta \left(\frac{\partial u}{\partial y} \right). \quad (10)$$

Using (3), we obtain after transformations

$$\tau = \left(\frac{\gamma_1 M^2}{a} \cdot \frac{\omega}{a} - \frac{Pa}{L} \right) \left[\frac{\ln M}{M} - 2e^{-\frac{t}{T_1}} \sum_{k=1}^{\infty} \frac{e^{-\frac{T_k}{T_1}}}{k^2 + M^2} \right], \quad (11)$$

where T_1 and T_k are determined by formulas (5) and (6).

It follows from (11) that $\tau = 0$ when $t = 0$. When $t = \infty$ we have the known expression [3]:

$$\tau_{\text{ext}} = \left(\frac{\gamma_1 M^2}{a} \cdot \frac{\omega}{a} - \frac{Pa}{L} \right) \frac{\ln M}{M}. \quad (12)$$

In the absence of a magnetic field we obtain from (11) the ordinary hydrodynamic result

$$\tau_{M \rightarrow 0} = -\frac{Pa}{L} \left[1 - \frac{8}{\pi^2} \sum_{k=1}^{\infty} \frac{e^{-\frac{\pi^2(2k-1)^2 t}{4a^2}}}{(2k-1)^2} \right]. \quad (13)$$

REFERENCES

1. O.A. Ladyzhenskaya and V.A. Solonnikov. O Razreshimosti nestatsionarnykh zadach magnitnoy gidrodinamiki [The Solvability of Nonstationary Problems in Magnetohydrodynamics], DAN SSSR [Proceedings of the Academy of Sciences USSR], 124, 1, 1959.
2. S.A. Regirer. Nestatsionarnaya zadacha magnitnoy hidrodinamiki dlya poluprostranstva [Nonstationary Problem of Magnetohydrodynamics for a Half-Space], DAN SSSR, 127, 5, 1959.
3. I.A. Tyutin. Vvedeniye v teoriyu induktsionnykh nasosov [Introduction to the Theory of Induction Pumps], Tr. In-ta Fiziki AN

Latv. SSR [Transactions of the Physics Institute Academy of Sciences Latvian SSR], VIII, 1956.

4. A.I. Vol'dek. Pul'siruyuchchiye sostavlyayushchiye magnitnogo polya induktsionnykh mashin i nasosov s razomknutym magnitoprovodom [Pulsating Components of Magnetic Field in Induction Machines and Pumps with Open Magnetic Circuit], Nauchnye doklady vysshey shkoly. Elektromekhanika i avtomatika [Scientific Reports of the Higher Schools. Electro Mechanics and Automation], 3, 1959.
5. N.M. Okhremenko. Elektromagnitnyye yavleniya v ploskikh induktsionnykh nasosakh dlya zhidkikh metallov [Electromagnetic Phenomena in Planar Induction Pumps for Liquid Metals], Elektrichestvo [Electricity], 3, 1960.

Manu-
script
Page
No.

[List of Transliterated Symbols]

539 cp = sr = sredniy = average
546 yct = ust = ustanovivshisyia = steady-state, stationary

DEVELOPMENT OF LAMINAR FLOW OF A VISCOSUS
ELECTRICALLY CONDUCTING LIQUID BETWEEN PARALLEL PLANES
UNDER THE INFLUENCE OF A TRANSVERSE MAGNETIC FIELD

N.M. Okhremenko

Leningrad

The problem of the stationary linear-parallel flow of a viscous incompressible liquid between infinite parallel stationary planes in the presence of an external constant homogeneous magnetic field perpendicular to the walls was first investigated by Hartmann [1].

A similar problem was solved by I.M. Kirko and I.A. Tyutin [2, 3] for the case when the conducting liquid moves under the influence of a traveling magnetic field. The solutions obtained can be regarded as valid for channels of limited length only if the section of the channel under consideration is located a distance exceeding the length of the initial portion away from the inlet section.

The investigation of the character of flow of a viscous incompressible liquid in the initial portion of round cylindrical pipes and channels of rectangular form, within the framework of classical hydrodynamics, has been the subject of an appreciable number of papers. The problem was first solved by Bussinek, and then by Schiller and L.S. Leybenzon [4-6]. S.M. Targ and N.A. Slezkin investigated the development of laminar flow in tubes and diffusers with the aid of approximate equations, in which the acceleration and viscosity terms were partially taken into account [7-9]. Such a method turned out to be quite effective and yielded results which for round pipes is in

satisfactory qualitative agreement with the experimental data [7].

As far as the author knows, the solution of the problem of development of laminar flow under the action of a transverse magnetic field was not developed in magnetohydrodynamics in either the domestic or the foreign literature.

Using the method of partially taking into account the inertial and viscosity forces, as used by S.M. Targ and N.A. Slezkin [7-9], we can investigate the development of laminar flow of a conducting liquid between parallel planes under the influence of a traveling magnetic field perpendicular to the walls. Such a flow occurs in the channel of a planar induction pump. The approximate magnetohydrodynamic equations describing plane-parallel flow of a viscous incompressible liquid between two parallel planes $y = \pm a$ under the influence of a transverse traveling magnetic field at

$$B_z = B_m \cdot \sin(\omega t - ax), \quad (1)$$

where ω is the angular frequency, $a = \pi/\tau$, and τ is the pole pitch, can be represented in the following form

$$\nu \frac{\partial u}{\partial x} = - \frac{1}{\rho} \frac{\partial p}{\partial x} + v \frac{\partial^2 u}{\partial y^2} + \frac{\sigma B_m^2}{\rho} \left(\frac{\omega}{a} - u \right) \cdot \sin^2(\omega t - ax), \quad (2a)$$

$$\frac{\partial p}{\partial y} = 0, \quad (2b)$$

$$\frac{\partial u}{\partial x} + \frac{\partial v}{\partial y} = 0. \quad (2c)$$

Here u is the velocity, p the pressure, v the velocity of the liquid in the inlet cross section, B_m is the amplitude of the magnetic induction, ρ is the density, σ the electric conductivity, and ν the kinematic viscosity of the liquid.

In these equations the inertial terms are partially taken into account in (2a), while the terms due to viscosity are taken into account in the same manner as in the boundary layer theory. Equations

(2) are obtained under the assumption that there is no transverse or longitudinal edge effect and no attenuation of the magnetic field over the height of the channel, and that the main component of the velocity is uniformly distributed over the initial section of the channel (Fig. 1). The boundary conditions for these equations are as follows:

$$\left. \begin{array}{l} \text{for } x=0, |y| < a, u = V; \\ \text{for } x > 0, y = \pm a, u = 0, v = 0 \end{array} \right\} \quad (3)$$

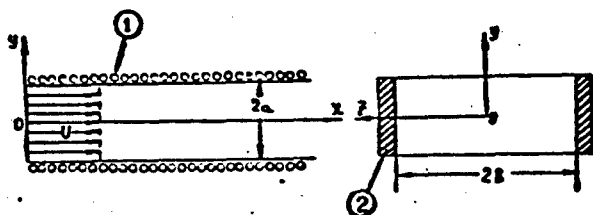


Fig. 1. Channel of planar induction pump:
1 - Winding; 2 - current conducting buses.

After time-averaging the mass forces and the pressure in Eq. (2a), the system (2-3) can be solved by operational methods. As a result of the solution we obtain the following expression for the velocity:

$$u(x, y) = V \left\{ \frac{\operatorname{ch} M - \operatorname{ch} \frac{M}{a} y}{\operatorname{ch} M - \frac{\operatorname{sh} M}{M}} - \right. \\ \left. - 2 \sum_{m=1}^{\infty} \frac{\cos \gamma_m - \cos \left(\gamma_m \frac{y}{a} \right)}{(M^2 + \gamma_m^2) \cos \gamma_m} e^{-\frac{x^2 + \gamma_m^2}{R}} \cdot \frac{x}{a} \right\}. \quad (4)$$

where $R = aV/v$ is the Reynolds number for a planar channel, M is the Hartmann number, γ_m are the roots of the transcendental equation

$$\operatorname{tg} z = z \quad (5)$$

The series in the right half of (4) is, in accordance with the Weierstrass tests, uniformly convergent, since the series $\sum_{m=1}^{\infty} \frac{1}{\gamma_m}$ converges.

This solution satisfies Eq. (2a) and the boundary conditions (3). It enables us to obtain the value of the velocity profile at any distance from the inlet in the presence of a transverse traveling magnetic field.

Formula (4) will hold true also in the case of a constant transverse field.

The value of the velocity at an infinite distance from the inlet

$$u(\infty, y) = V \frac{\operatorname{ch} M - \operatorname{ch} \frac{M}{a} y}{\operatorname{ch} M - \frac{\operatorname{sh} M}{M}} = u_0 \frac{\operatorname{ch} M - \operatorname{ch} \frac{M}{a} y}{\operatorname{ch} M - 1}. \quad (6)$$

where u_0 is the velocity of the center of the stream, coincides with the known solutions [1-3]. The velocity profiles at an infinite distance from the inlet to the channel and for different values of M are shown in Fig. 2.

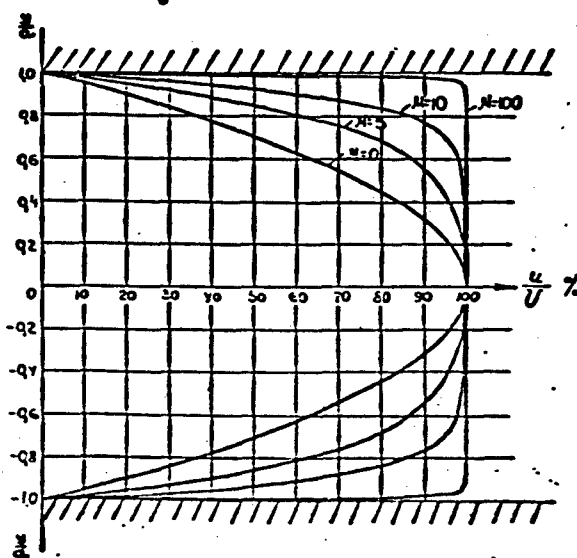


Fig. 2. Steady-state velocity profiles.

In the particular case when $M \rightarrow 0$, we obtain from formula (4) the expression derived by S.M. Targ [7, formula 6.59]):

$$u(x, y)|_{M \rightarrow 0} = \frac{3}{2} V \left(1 - \frac{y^2}{a^2} \right) - \\ - 2V \sum_{n=1}^{\infty} \frac{\cos \gamma_n - \cos \left(\gamma_n \frac{y}{a} \right)}{\gamma_n^2 \cos \gamma_n} e^{-\frac{\gamma_n^2}{ka} x}. \quad (7)$$

which at an infinite distance from the inlet determines a parabolic velocity profile.

It is of interest to determine the influence of an external transverse magnetic field on the length of the initial portion, over which the different disturbances, which unavoidably arise on entering the channel, become attenuated.

We shall define, following Bussinek's suggestion as used by S.M. Targ [7] the length of the initial portion L_M as that distance away from the inlet section, over which the actual velocity, calculated by formula (4), deviates from the actual velocity determined by formula (6) by not more than 1%. Then the approximate expression for the length of the initial portion can be obtained in the following form:

$$L_M = \frac{aR}{M^2 + \gamma_1^2} \ln \frac{200 \left(\operatorname{ch} M - \frac{\operatorname{sh} M}{M} \right) (\cos \gamma_1 - 1)}{(M^2 + \gamma_1^2) (\operatorname{ch} M - 1) \cos \gamma_1}. \quad (8)$$

where $\gamma_1 = 4.493$ is the smallest nonvanishing root of equation (5) [10].

When $M \rightarrow 0$ we obtain from formula (8) an expression for the length of the initial portion in the absence of a magnetic field [8, p. 356]:

$$L_{M=0} = \frac{aR}{\gamma_1^2} \ln \frac{400(\cos \gamma_1 - 1)}{3\gamma_1^2 \cos \gamma_1}. \quad (9)$$

Comparison of (8) with (9) shows that the influence of the transverse magnetic field on the reduction in the length of the initial portion is manifest in two ways, since the quantity M is contained in

formula (8) both under the logarithm sign and in the coefficient preceding it.

The expression under the logarithm sign determines the velocity profile. With increase in M , the steady-state velocity profile (see Fig. 2) approaches the velocity profile in the initial cross section, assumed in our problem, which formally leads to a reduction in the number contained under the logarithm sign.

On the other hand, the action of the electromagnetic mass forces shapes the stream more rapidly, suppressing the disturbances that arise upon entering into the channel.

This circumstance influences the magnitude of the coefficient preceding the logarithm. The effect of the latter on the value of the initial portion is more noticeable and is decisive.

To illustrate the quantitative influence of the magnetic field on the length of the initial portion, we present the following example.

By substituting the numerical value of the root γ_1 in (9), S.M. Targ [8] obtained an approximate value for the length of the initial portion of a planar tube:

$$L_{M=0} = 0.18 a R \quad (10)$$

Substituting the value of γ_1 in (8) we obtain

$$\begin{aligned} \text{for } M = 5 & \quad L_{M=5} = 0.0886 a R, \quad \frac{L_{M=0}}{L_{M=5}} = 2.03; \\ \text{for } M = 10 & \quad L_{M=10} = 0.0177 a R, \quad \frac{L_{M=0}}{L_{M=10}} = 10.16. \end{aligned}$$

Usually in electromagnetic pumps M is large and reaches $10^2 - 10^3$. At large values of M , and if the laminar mode is conserved, the length of the initial portion is of the order

$$L_{M \gg 1} \approx \frac{aR}{M^2}. \quad (11)$$

If $M = 100$ and $R = 10^4$, then $L_M \approx a$. For the case when $M = 0$ and $R =$

2000, the length of the initial portion is $L_M = 0 = 360$ a.

Under the influence of the magnetic field, the length of the initial portion is greatly reduced.

The dependence of the pressure distribution along the channel axis can be represented by the following expression:

$$p - p_0 = \rho V^2 \left\{ \frac{M^2}{R} \left(\frac{\epsilon}{zV} - \frac{1}{1 - \frac{1}{M}} \right) \cdot \frac{x}{a} - \right. \\ \left. - 2 \sum_{n=1}^{\infty} \frac{T_n^2}{(M^2 + T_n^2)^2} \left(1 - e^{-\frac{x^2 + T_n^2}{R} \cdot \frac{x}{a}} \right) \right\}, \quad (12)$$

where p_0 is the pressure on the initial section of the channel.

Formula (12) is valid only for a traveling field.

When $M \rightarrow 0$ we obtain from (12)

$$p - p_0 = - \rho V^2 \left[\frac{3}{R} \cdot \frac{x}{a} + 2 \sum_{n=1}^{\infty} \frac{1}{T_n^2} - 2 \sum_{n=1}^{\infty} \frac{1}{T_n^2} e^{-\frac{T_n^2}{R} \cdot \frac{x}{a}} \right], \quad (13)$$

which coincides with the dependence established in [7 (Formula 6.59)].

The relations (4), (8), and (12) which were established above are physically correct. The electromagnetic mass forces shape the velocity profile over a considerably shorter distance from the inlet into the channel. The author knows of no experimental data with which to estimate quantitatively the correctness of the relations obtained. The organization of proper experiments is highly desirable. However, the foregoing formulas can in themselves serve as a base for a suitable organization of experiments.

REFERENCES

1. Y. Hartmann. Hg-Dynamics-1, Det. Kgl. Danske Videnskab. Selskab. (Mat.-fys. Medd.), 1937, 15, 6.
2. I.M. Kirko. O modeliravani magnitogidrodinamicheskikh yavleniy v zhidkikh metallakh [Simulation of Magnetohydrodynamic Phenomena in Liquid Metals], Tr. In-ta fiziki AN Latv. SSR [Trans-

actions of the Physics Institute Academy of Sciences Latvian SSR], VIII, 1956.

3. I.A. Tyutin. Vvedeniye v teoriyu induktsionnykh nasosov [Introduction to the Theory of Induction Pumps], Tr. In-ta fiziki AN Latv. SSR, VIII, 1956.
4. J. Boussinesq. Compt. rend. Acad. sci., 113, 9, 49, 1891.
5. L. Shiller. Techeniye zhidkosti v trubakh [Flow of Liquid in Pipes], ONTI [State Unified Scientific and Technical Publishers], 1936.
6. L.S. Leybenzon. Rukovodstvo po neftepromyslovoy mekhanike. I. Gidravlika [Guide to Petroleum Mechanics. I. Hydraulics], GONTI [State Unified Scientific and Technical Publishers], 1931; DAN SSSR [Proceedings of the Academy of Sciences USSR], 54, 3, 1946.
7. S.M. Targ. Osnovnyye zadachi teorii laminarnykh techeniy [Basic Problems of the Theory of Laminar Flow], GITTL [State Publishing House for Technical and Theoretical Literature], 1951.
8. N.A. Slezkin. Dinamika vyazkoy neszhimaemoy zhidkosti [Dynamics of the Viscous in the Compressible Liquid], GITTL, 1955.
9. N.A. Slezkin. O razvitiyu techeniya vyazkoy zhidkosti mezhdu parallel'nymi poristymi stenkami [On the Development of Flow of a Viscous Liquid Between Parallel Porous Walls], Prikladnaya matematika i mekhanika [Applied Mathematics and Mechanics], 21, 4, 1955.
10. Ye. Yanke and F. Emde. Tablitsy funktsiy [Tables of Functions], GITTL, 1948.

BATCHING OF LIQUID METAL WITH THE AID OF
ELECTROMAGNETIC INDUCTION PUMPS*

I.M. Kirko, Ya.Ya. Lielpeter
Riga

The operating features of an electromagnetic induction pump used for batching of liquid metal are considered in the paper. Principal attention is paid to an analysis of the steady-state motion of the liquid metal for a specific batching scheme, in which the induction pump serves the lift the liquid metal to a given height and to measure a definite batch. The total cycle of supplying a single batch is divided into intermediate stages: filling the supply pipe, pouring out the liquid metal, and moving it by inertia after the pump is turned off. Approximate expressions are obtained for the dependence of the poured batch on the pump characteristics and on the pipe configuration; these expressions are of significance principally for qualitative derivations and estimates.

Some results of experiments performed on a batcher model are also reported.

The results of the experiments agree with the results of the derivations.

The paper was published in the collection "Works of the Physics Institute of the Academy of Sciences of the Latvian SSR" Vol. XII, 1961.

CONCERNING THE TRANSVERSE EDGE EFFECT IN INDUCTION PUMPS

L.Ya. Ulmanis

Riga

Experimental investigations of the transverse edge effect in induction pumps were carried out on metallic plates and in the channel of a mercury pump with flow $Q = 0$ [1]. The reduction of the experimental data yielded an empirical formula for the coefficient K_{Δ} which characterizes the transverse edge effect in induction pumps

$$K_{\Delta} = 1 + C \left(\frac{\tau}{a} \right)^2. \quad (1)$$

where τ is the pole pitch of the pump, a is the width of the metal layer in the orifice of the pump, C is the constant ($C \approx 1$).

A theoretical calculation of the transverse edge effect was carried out by A.I. Vol'dek [2] and N.M. Okhremenko [3]. A.I. Vol'dek derived the following formula*:

$$K_{\infty} = \frac{1}{1 + \gamma^2} \left[1 - \frac{(2\bar{\beta}_1^2 - \gamma^2)K + \gamma(2\bar{\beta}_1^2 + 1)L}{\bar{\beta}_1 a / 1 + \gamma^2} \right]. \quad (2)$$

where

$$K = \frac{\sinh \bar{\beta}_1 a}{\cosh \bar{\beta}_1 a + \cos \bar{\beta}_1 a}.$$

$$L = \frac{\sin \bar{\beta}_2 a}{\cosh \bar{\beta}_1 a + \cos \bar{\beta}_2 a}.$$

$$\bar{\beta}_1 = \frac{1}{\sqrt{2}} \sqrt{\gamma^2 + 1 + 1}.$$

$$\bar{\beta}_2 = \frac{1}{\sqrt{2}} \sqrt{\gamma^2 + 1 - 1}.$$

$$\gamma = \frac{4\pi\mu\sigma}{c^2}.$$

$$\bar{a} = a \cdot a.$$

$$a = \frac{\pi}{\gamma},$$

σ - electric conductivity, μ - magnetic permeability, c - velocity of light, ω_1 - circular frequency of traveling magnetic field relative to the moving medium,

$$\omega_1 = \omega - \alpha v,$$

ω - circular frequency of traveling magnetic field relative to the stationary system, v - velocity of the medium, K_{os} - attenuation coefficient, equal to $1/K_\Delta$.

When $\gamma = 0$ formula (2) becomes

$$K_{os} = 1 - \frac{2\ln \frac{v}{\gamma}}{a}. \quad (3)$$

N.M. Okhremenko derived an analogous formula for the attenuation coefficient $K_{os}^{(v)}$ for individual harmonics

$$K_{os}^{(v)} = \frac{8}{\pi^2 v \left[1 + \left(\frac{v}{a} \right)^2 \right]}. \quad (4)$$

Here v is the serial number of the harmonic. Summing $K_{os}^{(v)}$ over all the harmonics we obtain formula (3).

A formula similar to the one derived by the two aforementioned authors was obtained also by modeling [4] of the electromagnetic phenomena in induction pumps by means of an electrolytic trough and on electrically conducting paper.

In the present article we attempt to check the applicability of the methods for calculating K_Δ , confirmed by experiment for $Q = 0$, to the design of induction pumps in the operating mode ($Q \neq 0$).

The ratio

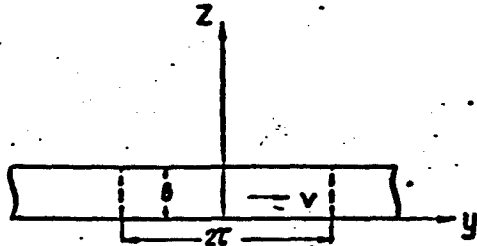


Fig. 1

$$\xi = \frac{p_1}{p_2} \quad (5)$$

$$\xi' = \frac{\bar{p}_1}{\bar{p}_2} \quad (6)$$

Here p_1 and p_2 are the pressures

developed by the traveling magnetic

field in the induction-pump model in the presence of solidified and liquid metal in the channel, respectively, while \bar{p}_1 and \bar{p}_2 are the theoretical relative pressures under the same conditions.

If the expression for K_Δ holds true also when $Q \neq 0$, then obviously

$$\frac{p_1}{p_2} = \frac{\bar{p}_1}{\bar{p}_2} \quad (7)$$

To calculate \bar{p}_1 and \bar{p}_2 we assumed that 1) a layer of electrically conducting medium of thickness b (Fig. 1) extends without limit in the x and y directions, 2) the medium moves as a unit, that is, the redistribution of the velocity in the pump channel is neglected.

The normal component of induction B_z of the traveling magnetic field in the conducting medium is

$$B_z = Re[\dot{B}_0 e^{i(\omega t - \varphi)}], \quad (8)$$

where \dot{B}_0 — induction amplitude, t — time, $i = \sqrt{-1}$.

The following boundary conditions were assumed

$$\begin{aligned} 1) \text{for } z=0 & \quad \dot{B}_0 = iB_1, \\ 2) \text{for } z=b & \quad \dot{B}_0 = iB_2 e^{\varphi}, \end{aligned} \quad (9)$$

where B_1 and B_2 are respectively the induction amplitudes in the layer of the conducting medium at $z = 0$ and $z = b$, while φ is the angle through which the magnetic induction vector is rotated on passing through the layer of the conducting medium.

Solving the system of Maxwell's equations by a method similar to

I. A. Iyulin's [5] and using boundary conditions (9), we obtain

$$\dot{B}_x = \frac{i}{\sinh \beta b} [B_1 \sinh \beta(b-z) + B_2 e^{i\theta} \sinh \beta z], \quad (10)$$

$$\dot{B}_y = \frac{\beta}{a \sinh \beta b} [B_1 \sinh \beta(b-z) + B_2 e^{i\theta} \sinh \beta z], \quad (11)$$

$$j = -\frac{i \omega_1 \sigma}{c \sinh \beta b} [B_1 \sinh \beta(b-z) + B_2 e^{i\theta} \sinh \beta z]. \quad (12)$$

where

$$\begin{aligned} \beta &= \sqrt{\alpha^2 + i\gamma} = \beta_1 + i\beta_2; \\ \beta_1 &= a\bar{\beta}_1, \quad \beta_2 = a\bar{\beta}_2. \end{aligned} \quad (13)$$

Let us cut out mentally a region of width a and length $2n\tau$ from the infinite layer of the medium. The average \bar{p} of the pressure over the section of the layer in the region under consideration V will be

$$\bar{p} = \frac{1}{2cab} \iiint_V j^* B_x dV. \quad (14)$$

Corresponding to a definite current in the stator is a definite value of the tangential component of the induction on the surface of the layer of electrically conducting medium (at $z = 0$). Consequently, in order to compare the calculations with experiment, it is convenient to refer \bar{p} to the square of the tangential component of induction at $z = 0$:

$$\bar{p} = \frac{\bar{p}}{B_{x1}^2}. \quad (15)$$

After several mathematical transformations we obtain from expressions (10-12, 14, 15)

$$B_{x1} = \frac{B_x N}{a R}. \quad (16)$$

$$\bar{p} = \frac{n \omega_1 \sigma B_x^2 M}{c^2 a b R}. \quad (17)$$

$$\bar{p} = \frac{n \omega_1 \sigma R M}{c^2 b N^2}. \quad (18)$$

where

$$\operatorname{ch} 2\beta_1 b - \cos 2\beta_2 b = R, \quad (19)$$

$$\frac{1}{B_1} \operatorname{sh} \beta_1 b [(1+x^2) \operatorname{ch} \beta_1 b - 2x \cos \beta_2 b \cos \varphi] -$$

$$-\frac{1}{B_2} \sin \beta_2 b [(1+x^2) \cos \beta_2 b - 2x \operatorname{ch} \beta_1 b \cos \varphi] = M, \quad (20)$$

$$2 \operatorname{sh} \beta_1 b \cos \beta_2 b (\beta_1 \cos \varphi - \beta_2 \sin \varphi) + 2 \operatorname{ch} \beta_1 b \sin \beta_2 b (\beta_1 \sin \varphi + \beta_2 \cos \varphi) - x(\beta_1 \operatorname{sh} 2\beta_1 b + \beta_2 \sin 2\beta_2 b) = N, \quad (21)$$

$$x = \frac{B_1}{B_2}. \quad (22)$$

From (17, 18, 7) we get that if the expression for K_Δ is correct, we should have at $Q \neq 0$

$$\xi = \frac{\sigma_1 \omega R_1 M_1 N_1^2}{\sigma_2 (\omega - \alpha v) M_2 N_2^2 R_2} \quad (23)$$

The subscript 1 refers here to the solid metal and 2 refers to the liquid metal.

The measurements were carried out in a model of an infinitely long channel [6]. The liquid metal moved through a closed annular gap between two cylinders placed in the stator of an induction motor. Measurements were made of the pressure developed by the rotating magnetic field in a layer of sodium in both the solid and in the liquid state, and of the average speed of motion of the metal in the gap between cylinders. The average gap radius was 9.25 cm, $\tau = 7.26$ cm, $b = 1.64$ cm and $a = 10$ cm. The moment of inertia of the moving system of the measuring installation was $6.39 \cdot 10^5$ g cm², while the elastic torsion of the wire was 2220 g·cm²/sec². The temperature of the solid sodium was 88°C and that of the liquid 116°C. The stator was fed with 50 cycle three-phase current. The coefficient K_Δ of the experimental channel calculated from formula (1) was 1.52.

The phase lag of the induction resulting from penetration through the layer was measured with the aid of coils located on both sides of the channel. The voltages U_1 and U_2 induced in the coils were fed to a phase sensitive voltmeter, which in this case was used as a null

indicator. The maximum values of U_1 and U_2 were measured with a vacuum tube voltmeter. The quantity κ was defined as

$$\kappa = k \frac{U_1}{U_2}$$

where k is a proportionality coefficient which depends on the parameters of the coil.

Knowing γ , κ , and the parameters of the apparatus, a value $\xi' = 1.24$ was obtained theoretically from formulas (19-21 and 23). The experimental value of ξ obtained with the apparatus was 1.27. The discrepancy between the results is 2.4%. This is fairly good agreement if it is recognized that the theoretical calculation does not take account of the bending of the channel and of the metal velocity distribution of the cross section of the channel.

We can thus conclude from the experiment that at slips $0.83 \leq s \leq 1$, at which the measurement was carried out, it is possible to use formula (1) in the design of induction pumps.

The work was carried out under the guidance of I.M. Kirko.

555 The Gaussian system of units is used in the present paper.

REFERENCES

- 1. L. Ya. Ulmanis. K voprosu o kraevykh effektakh v lineynykh induktsionnykh nasosakh [Edge Effects in Linear Induction Pumps], Tr. In-ta fiziki AN Latv. SSR [Transactions of the Physics Institute Academy of Sciences Latvian SSR], VIII, 1956.
2. A. I. Vol'dek. Toki i usiliya v sloye zhidkogo metalla ploskikh induktsionnykh nasosov [Currents and Forces in Liquid-Metal Layer of Planar Induction Pumps], Izvestiya vysshikh uchebnykh zavedeniy. Elektromekhanika [Bulletin of the Higher Educational Institutions. Electromechanics], 1, 1959.
3. N. M. Okhremenko. Elektromagnitnyye yavleniya v plokhikh induktsionnykh nasosakh dlya zhidkikh metallov [Electromagnetic Phenomena in Planar Induction Pumps for Liquid Metals], Elektrichestvo [Electricity], 3, 1960.
4. L. V. Nitsetskiy. Modelirovaniye elektricheskogo polya, elektromagnitnykh nasosov v elektroliticheskoy vanne i na elektroprovod-yashchey bumage [Simulation of Electric Field of Electromagnetic Pumps in Electrolitic Bath and on Electrically Conductive Paper], Tr. In-ta fiziki AN Latv. SSR [Transactions of the Physics Institute Academy of Sciences Latvian SSR], XI, 1959.
5. I. A. Tyutin. Elektromagnitnyye nasosy dlya zhidkikh metallov [Electromagnetic Pumps for Liquid Metals], Izd-vo AN Latv. SSR [Publishing House of the Academy of Sciences Latvian SSR], 1959.
6. I. M. Kirko, Ya.Ya. Klyavin', I. A. Tyutin, L.Ya. Ulmanis. Model' beskonechno dlinnogo kanala s zhidkim metallom, nakhodyashche-

gosya v tegushchem magnitnom pole [Model of an Infinitely Long Channel with Liquid Metal Situated in a Traveling Magnetic Field], Tr. In-ta. fiziki AN Latv. SSR [Transactions of the Institute of Physics Academy of Sciences Latvian SSR], XI, 1959.

Manu-
script
Page
No.

[List of Transliterated Symbols]

555 oc = os = oslableniye = attenuation

MEASUREMENT OF VELOCITIES OF A LIQUID
IN MAGNETOHYDRODYNAMICS BY THE ELECTROMAGNETIC METHOD

Yu.M. Mikhaylov

Moscow

The measurement of liquid velocities is of great interest for experimental magnetohydrodynamics. In the experimental investigations [1,2], the velocities were measured, as in ordinary hydrodynamics, with the aid of a Pitot tube. It must be noted that in the investigation of magnetohydrodynamic phenomena the Pitot tube distorts not only the flow profile but also the distribution of the electromagnetic forces. This is particularly important in experiments where the volume of the metal or electrolyte is small.

In the paper presented here we consider the possibility of employing an electromagnetic method for the measurement of liquid velocity. This method, by virtue of certain inherent features (small dimensions of the measuring probes, possibility of working over a wide range of temperatures and in active media, possibility of remote recording of the readings, etc.) can in many cases turn out to be more convenient than the ordinary hydrodynamic method.

In the case of magnetohydrodynamic motions, there exist in the liquid strong electric and magnetic fields, E_0 and H_0 , which greatly influence the motion of the liquid. These fields will from now on be called force fields. Their frequency is usually that of the commercial line (50 cps). Even if constant electric and magnetic fields are used, the 50 cps background component usually has sufficiently large magni-

tude.

The gist of the proposed method consists of the following.

An auxiliary indicator field H_{ind} , with a frequency that differs appreciably from the force field frequency, is applied to the investigated volume of liquid. The amplitude of the indicator field is chosen to be small so as to exclude the possibility of interaction between the liquid and the indicator field. The measurements are carried out in the indicator field in accordance with the ordinary procedure employed when working with a.c. electromagnetic flow meters.

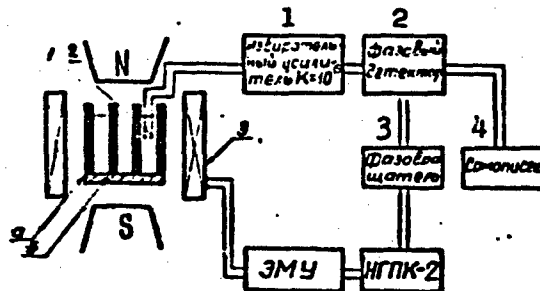


Fig. 1. Diagram of apparatus for the measurement of the velocity of liquid in a homopolar unit.

- 1) Selective amplifier, $k = 10^6$;
- 2) phase detector; 3) phase shifter; 4) automatic recorder.

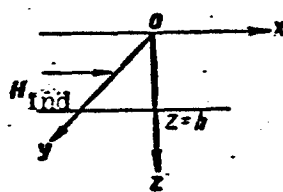


Fig. 2. Vertical section through planar flow. The velocity of the liquid is directed perpendicular to the plane of the figure in the direction of the y axis.

Figure 1 shows a block diagram of an infralow frequency electromagnetic flow meter, suitable for the aforementioned measurements. The flow meter operates at frequencies from 1 to 5 cps. A similar flow meter for 11 cps was described by James [3], so that we shall not present a detailed description here. We only point out that the apparatus is synchronized by a NGPK-2 low-frequency generator, the signal from which is fed through an amplidyne (EMU) to

the winding of the indicator coil 3.

The emf is proportional to the velocity of motion and is picked up from the measuring electrodes and then fed to a narrow band vacuum tube amplifier tuned to the flow meter frequency. Special measures are used in the apparatus to eliminate the influence of the force fields on the reading of the instruments.

The signal from the amplifier is fed to a phase detector, which generates a signal proportional to the velocity and in which the signal due to the variation of the magnetic flux is suppressed.

The electromagnetic method makes it possible to measure both average and local liquid velocities. In the latter case, however, its use is limited, and therein lies the shortcoming of the electromagnetic method. One can point out only individual flow geometries in which measurement of the potential gradients yields directly the distribution of the flow velocity. In the case of planar flow (Fig. 2) bounded by walls $z = 0$ and $z = h$, in the presence of small velocity gradients at a distance h in the x direction, the direction of the indicator field can be chosen to be along the x axis; in this case, the distribution of the potential gradient $\partial\phi/\partial z$ is proportional to velocity $\partial\phi/\partial z = v \cdot H_{ind}$ [4].

Analogously, for a rotating liquid with axial symmetry, it is advantageous to choose an axial magnetic indicator field. In this case the distribution of the potential gradient $\partial\phi/\partial r$ is proportional to the φ component of the velocity of the liquid $\partial\phi/\partial r = v \cdot H_{ind}$.

There exist also other flow geometries, in which the local velocity of the liquids can be measured directly [5].

In experiments carried out in the magnetic laboratory, the indicated method was used to measure the average velocity of electrolyte in a homopolar unit of small dimensions ($r_1 = 10$ mm, $r_2 = 25$ mm).

Figure 1, as already indicated, shows the general arrangement of the apparatus. N and S are the poles of the electromagnet used to produce the vertical field H_0 . a and b are the concentric cylindrical electrodes of the homopolar unit, 1 and 2 are the measuring probes, and 3 is the indicator coil. The velocities measured were on the order of 1 cm/sec, and the small dimensions of the homopolar unit didn't make it possible to compare quantitatively this method with the ordinary hydrodynamic methods. This comparison will be made once apparatus of larger size is constructed.

REFERENCES

1. A.E. Mikel'son, in present collection.
2. G.G. Branover and O.A. Liyelausis, in present collection.
3. W. Sames. Rev. Sci. Instr., 22, 12, 1951.
4. M.S. Longuett-Higgins. Monthly Not. Roy. Astron. Soc., 5, 13, 1949.
5. A. Kolin. J. Appl. Phys., 15, 2, 1944.

Manu-
script
Page
No.

[List of Transliterated Symbols]

563 3MY = EMU = elektromashinnyy usilitel' = amplidyne

USE OF ELECTROMAGNETIC FLOW METERS FOR THE MEASUREMENT
OF THE FLOW OF LIQUID MEDIA WITH IONIC CONDUCTIVITY

L.M. Korsunskiy

Kharbkov

The work dealt with a theoretical and experimental investigation of electromagnetic flow meters with rectangular channel. The result of the experiment confirmed the theoretical conclusions that the readings of electromagnetic flow meters with rectangular channels and with electrodes that average out the electric field are independent of the velocity diagram for any arbitrary distribution of the velocities in the channel of the instrument.

The paper was published in the journal "Measurement Technique," 10, 1960.

SOME RESULTS OF AN EXPERIMENTAL INVESTIGATION OF
TURBULENT FLOW OF LIQUID METAL IN A TRANSVERSE MAGNETIC FIELD

G.G. Branover, O.A. Lielausis

Riga

The question of the flow of liquid metal in channels in the presence of a magnetic field occupies a somewhat unique position in magnetohydrodynamics. Some of the specific magnetohydrodynamic phenomena are missing here. A flow takes place, in which in addition to the force fields that are customary in hydrodynamics, such as gravitation, viscosity, and inertia, it is also necessary to take into consideration the field of electromagnetic ponderomotive forces. As shown by Hartmann [1, 2] the foregoing forces give rise in the case of turbulent flow in a transverse magnetic field to an equalization of the velocities in the central part of the section (the Hartmann effect) and to the appearance of turbulent velocity pulsations. The influence of the magnetic field on the hydraulic resistance is determined by the relationship between these two oppositely directed but interrelated effects. For turbulent flow at low Reynolds numbers (Hartmann's experiments) [2] the resistance decreases with increasing magnetic field. In the case of large Reynolds numbers (the Murgatroyd experiments [3]), the resistance increases. For a definite Reynolds number interval, the resistance will not change with increasing field, that is, the two mentioned effects cancel each other.

In the case of flow in a longitudinal field [4], one cannot expect the Hartmann effect. The resistance in this case decreases mono-

tonically with the increasing field, this being due to the suppression of turbulent pulsations.

Harris [5] attempted to develop a semi-empirical theory based on the results of Hartmann's and Murgatroyd's experiments and on several assumptions. Another scheme for constructing a semi-empirical theory was proposed by G.G. Branover [6]. However, the available experimental data are undoubtedly insufficient for a satisfactory development of the foregoing theories. Experiments must be carried out to study the internal structure of turbulent streams in a magnetic field. It is necessary first of all to develop a procedure for such experiments.

We have undertaken an attempt at an experimental study of the influence of the transverse field on the velocity distribution. In an earlier paper [7] we traced the Hartmann effect in the case when there is a sharply pronounced nonuniformity in the velocity distribution, brought about by the curvature of the channel.

In the present work the experiments were continued as applied to the case when the velocities without the field have the distribution usually prevailing for turbulent flow in channels.

The experimental setup (Fig. 1) comprised a hydraulic system with closed circulation of mercury, set in motion by means of a d.c. electromagnetic pump K. The operating parts of the setup were two straight-line rectangular channels three centimeters wide, one of which, 150 cm long, was placed between the poles of an electromagnet, which produced a field up to 1750 Gauss, while the second, 100 cm long, was used for comparison. The channels were glued together of organic glass and interconnected with polyethylene tubes with inside diameter 4.5 cm. The average depth of the mercury in the channel was 4.5 cm. The flow was measured with a Venturi type flow meter made of organic glass.

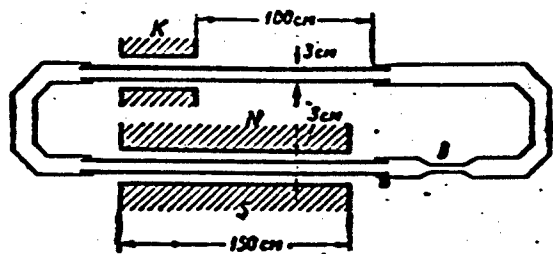


Fig. 1. Diagram of experimental setup (plan).

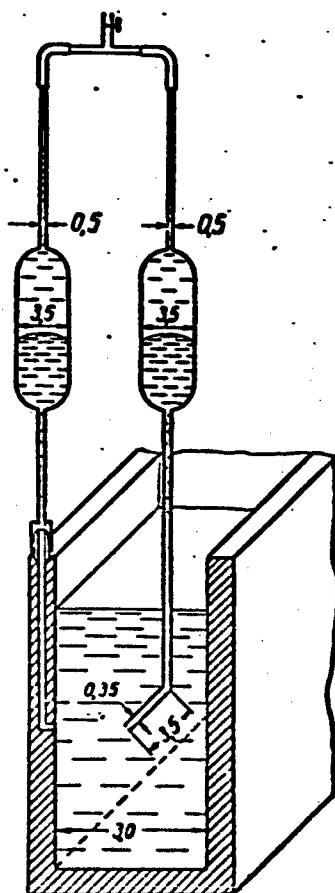


Fig. 2. Diagram of Pitot tube and differential manometer.

The motion in the channels was without pressure head, so that the velocities could be measured with the aid of a Pitot tube. The tube was so installed that the dynamic pressure transmitter, which comprised a glass fitting 0.35 cm in diameter and 3.5 cm long, with an inlet aperture of 0.15 cm diameter, could move over the entire area of the channel section and come in the limit as close as 0.175 cm to the walls. The static pressure transmitter was a piezometric aperture in the channel wall in the same section. The transmitters were connected to a differential manometer (Fig. 2). The minimum velocity that could still be measured was about 3 cm/sec at an error on the order of 10-15%. At higher velocities the measurement accuracy increased correspondingly.

All the experiments were carried out with turbulent flow conditions. The velocities were measured in a section 130 cm away from the entrance of the flow into the magnetic

field. Control measurements have shown that this length is sufficient for complete development of the effect of the magnetic field on the flow.

The Reynolds number

$$Re = \frac{\rho v R}{\eta}$$

where ρ - density of the liquid, v - average flow velocity, η - dynamic viscosity coefficient, R - hydraulic radius, equal to the ratio of the cross section area to the wetted perimeter* ranged in the experiments from $Re = 6680$ to $Re = 18,400$.

The Hartmann number

$$M = BR \sqrt{\frac{\sigma}{\eta}}$$

where B - induction of the field, σ - electric conductivity, ranged in the experiments from $M = 0$ to $M = 41.5$.

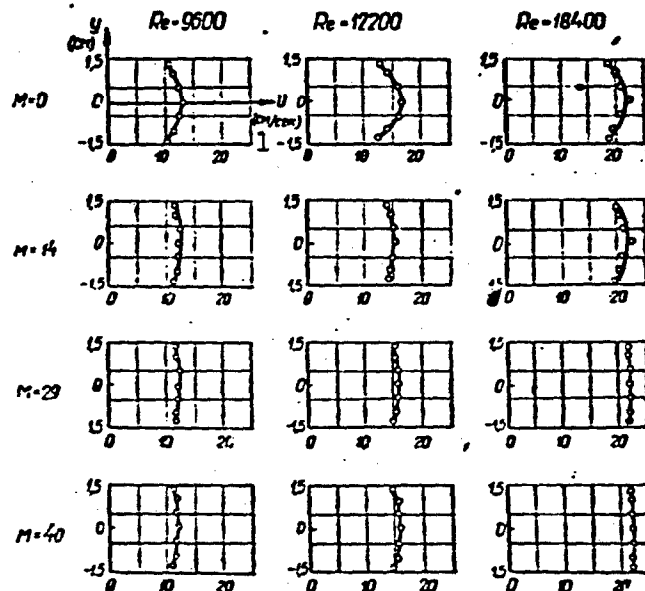


Fig. 3. Velocity distribution in a channel with smooth walls as a function of the field intensity. 1) cm/sec.

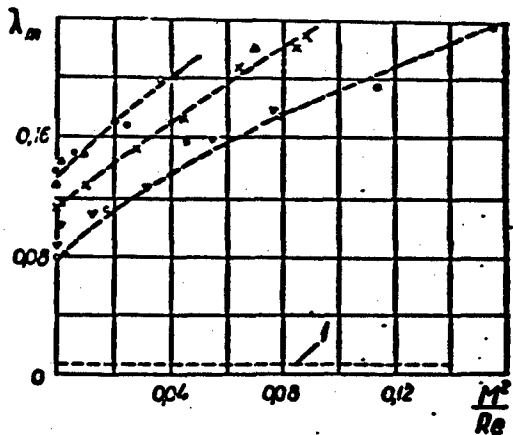


Fig. 4. Variation of the coefficient of resistance in a channel with artificial roughness, as a function of the field intensity. The Reynolds number values are: ○ - 6680, ▽ - 9650, X - 11,900, ● - 13,000, △ - 14,900. Curve 1 corresponds to the Blasius value of λ at $Re = 12,000$.

Some of the results of the measurement of the velocities in different points of the channel width, at half depth, are shown in Fig. 3, where one can trace the flattening of the velocity diagram with increasing M , that is, the Hartmann effect at different values of Re .

The equalization of the velocities can be characterized by the ratio of the velocity at the point closest to the wall to the velocity on the flow axis. As a result of all the measurements it turned out that this quantity ranged on the average from 0.7 or 0.8 at $M = 0$ to 0.97 at $M = 29$.

The measurements of the velocities at different depths have shown that the vertical velocity diagram does not experience any changes upon application of the field, up to the largest value of M at which the measurements were still carried out.

In addition to measuring the velocities, we measured in the

experiments the change in depth over a length of 95 cm and calculated the resistance coefficient. However, for all the experimental values of the Reynolds number, the changes in the resistance coefficient turned out to lie within the limits of the measurement accuracy, which, in view of the small absolute value of the depth difference, was approximately $\pm 10\%$.

Until recently all the investigations of the flow of a liquid metal in a transverse magnetic field, whether experimental or theoretical, pertained only to flows bounded by smooth walls. One of the main results of these investigations is the conclusion that the coefficient of hydraulic resistance varies with the field only insignificantly over a considerable portion of the region where the turbulent flow exists, and corresponds approximately to the Blasius formula for smooth pipes. We have attempted to study experimentally the flow of a liquid metal in a transverse magnetic field between walls that had artificial roughness.

We used the experimental setup described above (see Fig. 1). Artificial roughness was created on the side walls of the channel, in the form of rectangular strips 5 mm wide and 2 mm high, placed at intervals of 5 mm. The roughness was made so coarse in order to disclose primarily the principal features of the phenomenon.

The experiments were carried out in the same Reynolds number interval as for the smooth walls. It turned out that in the case of rough walls the neutralization of the Hartmann effect by the suppression of the turbulent pulsations, which apparently occurs in the case of smooth walls, no longer holds true, and a sharp increase in the resistance coefficient is observed with increasing magnetic field induction.

Figure 4 shows the dependence of the resistance coefficient

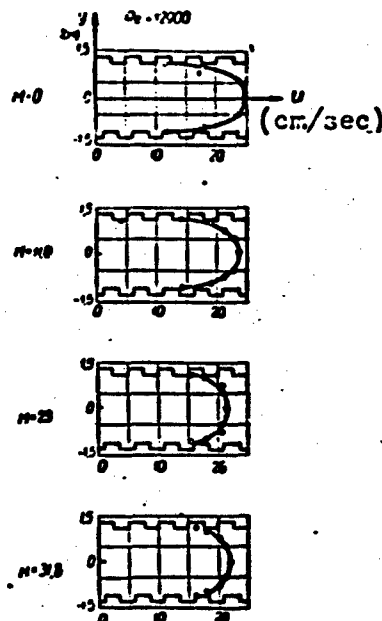


Fig. 5. Velocity distribution in a channel with rough walls as a function of the field intensity.

in a magnetic field, λ_m , on the ratio M^2/Re for different values of Re . Figure 5 shows the modification in the velocity diagram over the width of the channel resulting from the magnetic field. The procedure for measuring the velocities was the same as in the case of a channel with smooth walls.

REFERENCES

1. J. Hartmann. Kgl. Danske Vidensk. Selskab (Math.-Fys. Medd.), 15, 6, 1937.
2. J. Hartmann. F. Lazarus. Kgl. Danske Vidensk. Selskab (Math.-Fys. Medd.), 15, 7, 1937.
3. W. Murgatroyd. Phil. Mag., 44, 1348, 1937.
4. S. Globe. The Supression of Turbulence in Pipe Flow of Mercury by an Axial Magnetic Field. Heat Transfer and Fluid Mech. Inst. (Los Angeles, Calif., 1959) Stanford Calif. Univ. Press, 1959, 68-79.
5. L. P. Harris. Hydromagnetic Channel Flows. N.Y. - L. 1960.
6. G. G. Branover, Tr. In-ta fiziki AN Litv. SSR [Transactions of the Physics Institute, Academy of Sciences Latvian SSR], XII, 1961.
7. G. G. Branover, I. M. Kirko and O. A. Liyelausis, Tr. In-ta Fiziki AN Latv. SSR, XII, 1961.

EFFECT OF THE MAGNETIC FIELD ON THE
RESISTANCE IN THE FLOW OF MERCURY AROUND SOME BODIES

O.A. Lielausis, A.B. Tsinober
Riga

In the present communication we report the results of experiments on the measurement of the resistance in the case of the flow of a homogeneous mercury stream around bodies in a homogeneous transverse magnetic field. The bodies tested were a sphere and a plate.

1. EXPERIMENTAL SETUP

An annular magnetohydrodynamic channel of rectangular cross section was used in the experiments. The channel comprised a ring of rectangular section with average diameter 50 cm, width 3 cm, and depth 6 cm, placed in the gap K of a magnetic circuit M, in which the coil O is located under the bottom of the channel [1].

The entire channel was uniformly rotated, and after a relatively short time interval the mercury in the channel acquired a velocity equal to the velocity of the channel, that is, was stationary relative to the channel. Thus, a homogeneous stream of mercury was incident on a stationary body placed in the gap of the channel, if we neglect the curvature of the channel.

Three gold spheres 0.5 cm were immersed in the mercury, secured with molybdenum wires P 0.3 mm in diameter at the vertices of an equilateral triangle T, which formed a trifilar suspension over the channel (Fig. 1).

The depth of immersion was half the total depth of the mercury,

which in turn was 5 cm. To prevent corrosion, a protective layer of BF-2 glue was placed on the sphere.

The resistance force was measured by determining the angle of rotation of the trifilar suspension.

The resistance of a plate 0.8 cm wide and 0.1 cm thick, immersed at a depth of 3 cm, was also measured, and photographs were taken of the Karman vortex street in the magnetic field.*

Figure 1 shows a schematic section through the apparatus.

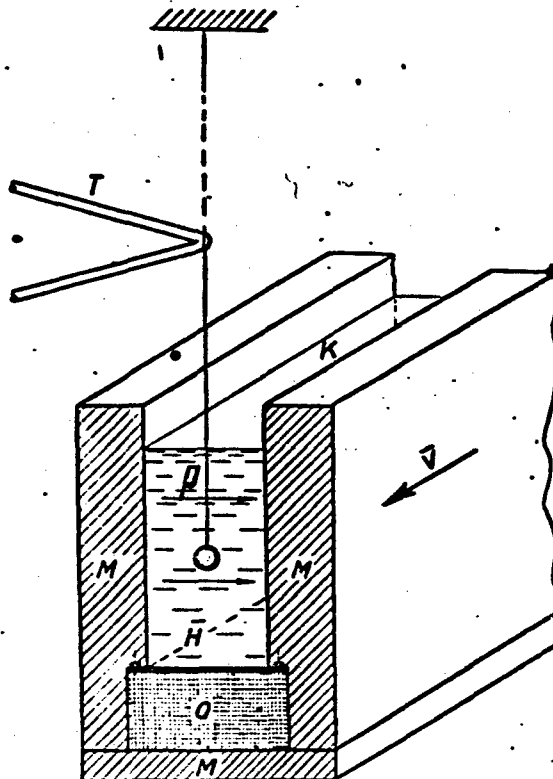


Fig. 1. Schematic section through the apparatus.

2. EXPERIMENTAL RESULTS

Figure 2 shows the experimental curves of the dependence of the resistance coefficient of a sphere at $C_r = \frac{1}{\frac{1}{2} \rho v^2 \frac{\pi d^2}{4}}$ on the Hartmann

number $M = Bd\sqrt{\frac{\sigma}{\eta}}$ for four values of the Reynolds number $Re = \rho v d / \eta$, where f is the resistance force, ρ , v , σ , and η are the density, velocity, specific electric conductivity, and the dynamic viscosity of the mercury, respectively, B is the magnetic induction and d is the diameter of the sphere.

In the upper left corner of Fig. 2 are shown the experimental curves of the dependence of the resistance coefficient of a plate, at

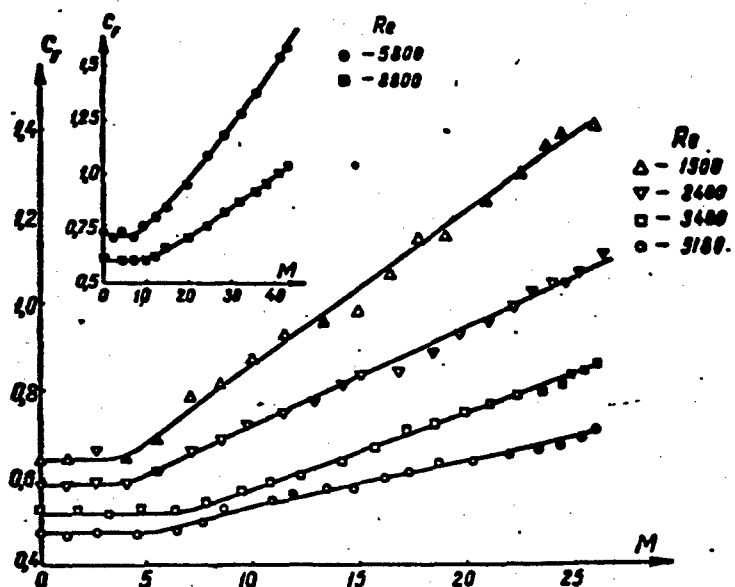


Fig. 2. Curves showing the dependence of the resistance coefficient C_f of a sphere and of a plate on the Hartmann number M .

$C_f = \frac{1}{2} \rho v^2 S$ on the Hartmann number $M = Bd\sqrt{\frac{\sigma}{\eta}}$ for two values of the Reynolds number $Re = \rho v a / \eta$, where S is the area of the immersed part of the plate and a is the width of the plate.

Figure 3 shows photographs of the Karman vortex street in mercury behind a plate in a magnetic field ($Re = 7000$).

As can be seen from Fig. 2, at small magnetic fields the resistance of the bodies in the stream changes little, and then monotonically in-

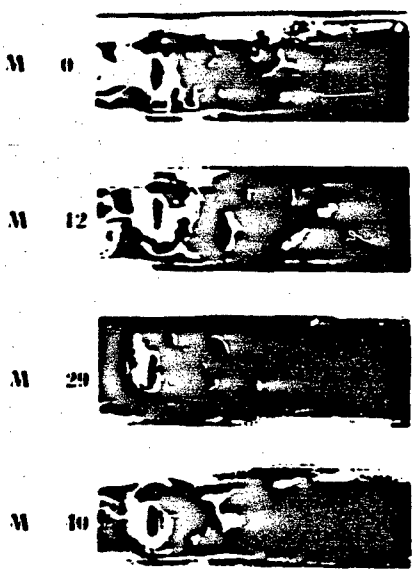


Fig. 3. Effect of transverse magnetic field on the Karman vortex street in mercury behind a plate.

creases with the increasing magnetic field.

Photographs of the Karman vortex street in mercury behind a plate in a magnetic field show that with increasing field the apparent length of the street decreases, which confirms the fact that the magnetic field suppresses the vortices.

In conclusion, several remarks should be made.

As is well known, under ordinary conditions the surface of mercury is not a liquid, but is covered by a practically solid film.

In order to eliminate this film, the surface of the mercury was covered with a 3-5% solution of nitric acid, making it possible to greatly attenuate (but not completely eliminate) the effect of the surface film on the measurements.

It must also be emphasized that the described experiments are preliminary and are aimed at disclosing the character of the phenomena, so as to set up more accurate experiments.

Manu-
script
Page
No.

[Footnotes]

575 G. Branover and R. Dukure participated in the photography
 of the Karman vortex street.

EFFECT OF TRANSVERSE MAGNETIC FIELD ON THE
LOCAL HYDRAULIC RESISTANCE IN A MERCURY STREAM

G.G. Branover, O.A. Liebaumis

Riga

The question of the sudden expansion of a turbulent stream, which has been investigated in detail in ordinary hydrodynamics [1, 2], has so far not been considered for the case when a magnetic field is present and the liquid is conducting. Yet such a question has applied significance and is also of interest from the point of view of the investigation of the influence of the field on the internal structure of the turbulent stream, and on the dissipation of energy in the eddies that are observed whenever the transverse cross section of the stream changes form abruptly.

In the present paper we report the results of an experimental investigation of this question as applied to plane-parallel flow of mercury in a transverse magnetic field. The experimental setup shown in Fig. 1 comprised a closed system consisting of a d.c. pump K, the operating part P, and a Venturi type flow meter B, interconnected by rubber tubing. The operating portion of the setup was in the form of a channel 4.0 cm high and 0.3 cm wide in its narrow portion and 0.8 cm wide in the broad portion. The channel was glued together of organic glass. It was placed between the poles of an electromagnet producing a field up to 4000 Gauss, corresponding to a Hartmann number $M = 41.4$.

The purpose of the experiments was to make sure the pressure drop

caused by the local hydraulic resistance, for which purpose two piezometers were used, brought out of points located 0.5 cm ahead of the expansion and 3.0 cm behind it. The third piezometer was brought out from a ledge in the wall in the cross section where the abrupt expansion took place. As can be seen from the figure, the measuring tubes of the piezometers had cylindrical thickened portions, in which the mercury bordered on water poured above it. With the thicker portion having a diameter 3.5 cm and the thin tube having a diameter 0.5 cm, the changes in the level in the thin tubes were magnified 13 times compared with ordinary piezometers [3].

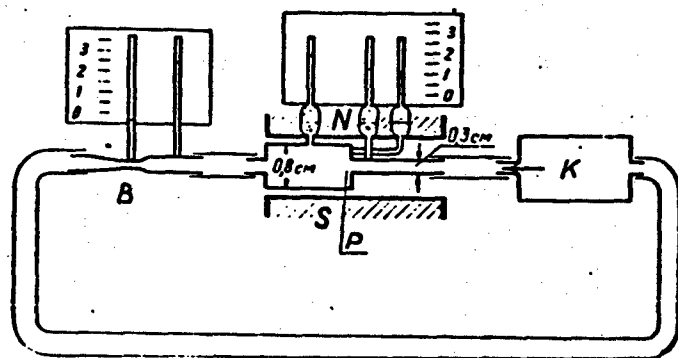


Fig. 1. Diagram of experimental setup.

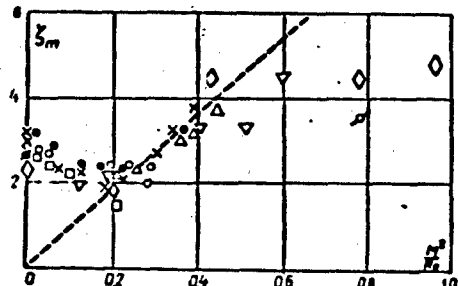


Fig. 2. Change in the coefficient of resistance as a function of the magnetic field intensity.

sively increasing values of the magnetic field induction. The results of the measurements of the pressure drop are shown in Fig. 2. The

- 580 -

In the experiments, the flow ranged from 6.0 to 52.3 cm^3/sec , corresponding to a variation in the Reynolds numbers over the investigated portion of the stream from $Re = 680$ to $Re = 5960$. In each of the experiments, a certain constant value of the flow was maintained, and the readings of the piezometers were fixed for success-

vertical axis represents here the local resistance coefficient

$$\zeta_m = \frac{\Delta p}{\frac{1}{2} \rho v_2^2}$$

where Δp — pressure drop, v_2 — average flow velocity in the broad part of the channel, ρ — density of the mercury.

The horizontal axis represents the ratio M^2/Re (M is the Hartmann number

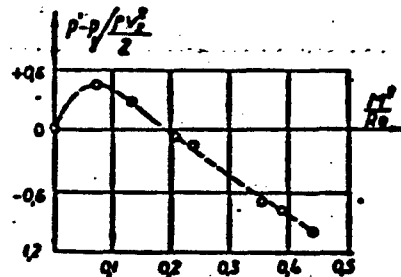


Fig. 3. Change in pressure on the ledge of the wall as a function of the magnetic field intensity.

referred to the half-width or the channel past the expansion and Re is the Reynolds number, referred to the same width), which, as is well known, has the meaning of the ratio of electromagnetic forces to the inertia forces.

It is easy to show that the specific per second energy loss necessary to overcome the magnetic braking of the eddies formed on both sides of the jet is proportional to M^2/Re . In the absence of a field, the values of ζ_m are in approximate agreement with the Borda theorem. When the field is applied, the values of ζ_m begin to decrease, the explanation of which must apparently be sought in the suppression of the turbulent pulsations by the field; a minimum of these values is reached when M^2/Re is close to 0.2. Further increase in M^2/Re causes the braking effect to predominate over the suppression of the turbulence, and the experimental points approach the straight line $\zeta_m \sim -M^2/Re$. There are still not enough experimental points to be able to suggest what takes place when $M^2/Re > 0.4$.

Accurate to the scatter of the experimental data shown in Fig. 2, we can assume that ζ_m is independent of Re .

Figure 3 shows an example of the variation of the pressure on the ledge of the wall with increasing field induction. The vertical

axis represents the difference between the pressure p' on the ledge and the pressure p_1 in the channel prior to the expansion, referred to the velocity head.

REFERENCES

1. G.N. Abramovich. Izv. OTN AN SSSR [Bulletin of the Academy of Sciences USSR, Division of Technical Sciences], 12, 1956.
2. G.N. Abramovich. Tr. TsIAM [Transactions of the Central Scientific Research Institute for Aircraft Engines], 322, 1958.
3. G.G. Branover, I.M. Kirko and O.A. Lelyausis, Tr. In-ta fiziki AN Latv. SSR [Transactions of the Physics Institute, Academy of Sciences Latvian SSR], XI, 1961.

EFFECT OF MAGNETIC FIELD ON TURBULENT TRANSPORT
PROCESSES IN A STREAM OF MERCURY.

G.G. Branover, O.A. Lielausis
Riga

Various magnetohydrodynamic installations with liquid metal have already proved their effectiveness. However, for a better utilization of their capabilities, and also to take into account the specific features in the construction of these devices, more accurate information is necessary concerning the influence of the magnetic field on turbulent transport processes in liquid metals. Even Hartmann [1] advanced the suggestion that radical changes take place in the structure of turbulence in a magnetic field. This is directly evidenced by the work of Globe [2], who established that a longitudinal field that does not act on the average velocity diagram decreases the resistance in turbulent flow. Such a deduction follows indirectly also from our own work [3, 4].

It is necessary to stop and discuss the specific features of the analysis of experimental results on the influence of the transverse magnetic field on the coefficient of turbulent resistance. We make use of the remarkable experimental fact that the coefficient of resistance λ_m , at which the flow loses its laminar character, is independent of the applied transverse magnetic field. We find that for the region of turbulent flow where λ at $H = 0$ exceeds the value $\lambda_{m_{kr}} = \text{const}$, the magnetic field will decrease the resistance down to total laminarization at $\lambda_m = \lambda_{m_{kr}}$. The results of Hartmann's work

pertain to this region. For Reynolds numbers such that λ at $H = 0$ is less than λ_{mkr} , an increase in the field gives rise to an increase in the resistance. This is seen from the work of Murgatroyd [5]. It follows from the foregoing that a study of the influence of the magnetic field on the turbulent flow of a liquid metal in which only the change in the coefficient of resistance is taken into account may be misleading. There exists a region of Reynolds numbers in which the magnetic field does not influence the coefficient of resistance, in spite of the fact that the structure of the flow is greatly modified.

It is possible to study the influence of the magnetic field also by using other features, say the change in the mass transfer process. A study of the influence of the field on mass transfer is of great significance in itself. In almost all magnetohydrodynamic installations we encounter the problem of corrosion of the structural materials in the liquid metals, and the phenomena of turbulent mass transfer play a primary role here.

We have set up experiments on the study of the influence of the magnetic field on the dissolution of lead in a turbulent stream of mercury. An amalgamized specimen of lead of rectangular form ($3 \times 1.5 \times 0.25$ cm) was inserted in a cut made at the center of a rectangular organic glass plate measuring $25 \times 3 \times 0.25$ cm. This was a crude imitation of the conditions under which a material is dissolved away from a wall. One plate with the specimen was placed in the mercury stream vertically along the axis of the experimental portion of a straight magnetohydrodynamic channel [3]. The second plate was immersed horizontally to half the depth of the mercury in the channel. Two other plates, intended for comparison, were placed in strictly analogous fashion in a second linear portion of the channel where $H = 0$. After a certain time the plates were removed and the reduction in the

weights of the lead specimens determined. All the specimens had the same dimensions, so that the absolute reduction in the weight of the specimens can be regarded as characteristic. Table 1 lists the average values of the experimental results. As can be seen from the table, the magnetic field slows down the dissolution of the lead. This must be attributed to a reduction in the turbulent mass transfer, that is, to a reduction in the pulsating components of the velocity in the magnetic field.

TABLE 1

1 Среднее со- щество теку- щего (см/сек)	2 Магнитное поле (Гаусс)	Re	M	Абсолютное зменение веса образца вне магнит- ного поля		Абсолютное зменение веса образца в магнитном поле		$\Delta p_1^v(r)$	$\Delta p_1^h(r)$	$\frac{\Delta p_1^v}{\Delta p_1^h}$
				5 погреш- ность 2%	6 погреш- ность 2%	5 погреш- ность 2%	6 погреш- ность 2%			
8	1500	1950	21.1	2.7	2.1	2.0	1.6	0.74	0.76	

1) Average flow velocity v (cm/sec); 2) magnetic field induction B (Gauss); 3) absolute decrease in the weight of the specimen outside the magnetic field; 4) absolute decrease in the weight of the specimen in the magnetic field; 5) vertical specimen $\Delta p_1^v(r)$; 6) horizontal specimen $\Delta p_1^h(r)$.

REFERENCES

1. J. Hartman, F. Lazarus. Kgl. Danske Vidensk. Selskab. (Math.-fys. Medd.), 15, 7, 1937.
2. S. Globe. The Supression of Turbulence in Pipe Flow of Mercury by an Axial Magnetic Field. Heat Transfer and Fluid Mech. Inst. (Los Angeles, Calif., 1959) Standford, Calif. Univ. Press, 1959, 68-79.
3. G.G. Branover and O.A. Liyelausis, in present collection.
4. G.G. Branover, I.M. Kirko and O.A. Liyelausis. Tr. In-ta fiziki AN Latv. SSR [Transactions of the Physics Institute, Academy

of Sciences Latvian SSR], XII, 1961.

5. W. Murgatroyd. Phil. Mag., 44, 1348, 1953.

Manu-
script
Page
No.

[List of Transliterated Symbols]

583 kp = kr = kriticheskiy = critical

CERTAIN PROBLEMS IN THE
CONTACT PROPERTIES OF METALLIC SURFACES

R.K. Dukure, G.P. Upit

Riga

In the present investigation we measured the electric resistance in the zone of contact between a solid metal and a liquid metal. Systems comprising stainless steel with mercury, gallium, sodium, potassium, lead, and its alloy with bismuth were investigated.

The contact resistance was determined as the difference between the system resistance in the presence of contact resistance on the investigated surfaces and in the absence of the contact resistance, using a direct method with a Thomson double bridge.

The absence of contact resistance was attained by wetting the solid metal with liquid metal.

It was established as a result of the measurements that in the presence of wetting the contact resistance completely disappears.

In the absence of wetting, the contact resistance is unstable and may assume different values depending on the thickness of the oxide films and the degree of contamination of the surfaces by the adsorption films.

When the system is heated to 400°C , the adsorption films disappear and the contact resistance drops to a stable minimum.

The paper was published in the collection "Works of the Institute of Physics, Academy of Sciences Latvian SSR," Vol. XII, 1961.

CONCERNING THE STABILITY OF FREE SUSPENSION OF A
DROP OF LIQUID METAL IN AN ALTERNATING MAGNETIC FIELD

I.M. Kirko, A.E. Mikel'son

Riga

In a paper delivered to the Magnetohydrodynamic Conference of 1958, R.G. Zhezherin indicated [1] that the realization of an "electromagnetic crucible," namely a freely suspended floating mass of metal, is frequently hindered by instability. The center of gravity of the drop of the suspended liquid sometimes goes into oscillation with increasing amplitude for some unknown reasons.

Our own investigations have shown that the buildup of oscillations in a drop suspended in an alternating field is not a specific property of the liquid state, but is brought about by the electromagnetic interaction between the suspended body and the electric circuit of the inductor.

Let us consider first the general conditions for the equilibrium of a solid body suspended in an annular inductor. Figure 1 shows the diagram of the installation and the dependence of the expulsion force acting on the sphere on the distance between the centers of the lower inductor and the sphere for a constant value of the current I flowing through the inductor. We see that the force has a maximum $F = F_{\max}$ at a certain finite value $x = x_m$. If the condition $I = \text{const}$ is not fulfilled, and only the condition that the electromotive force E in the circuit be constant is in effect, then the current in the inductor increases with decreasing x and reaches a maximum when $x = 0$.

(see Fig. 1, curve I), which in turn influences the value of the maintaining force F .

The equilibrium position of the suspended sphere at $x = x_0$ is determined by the equality of the expulsion force to the force of gravity acting on the sphere.

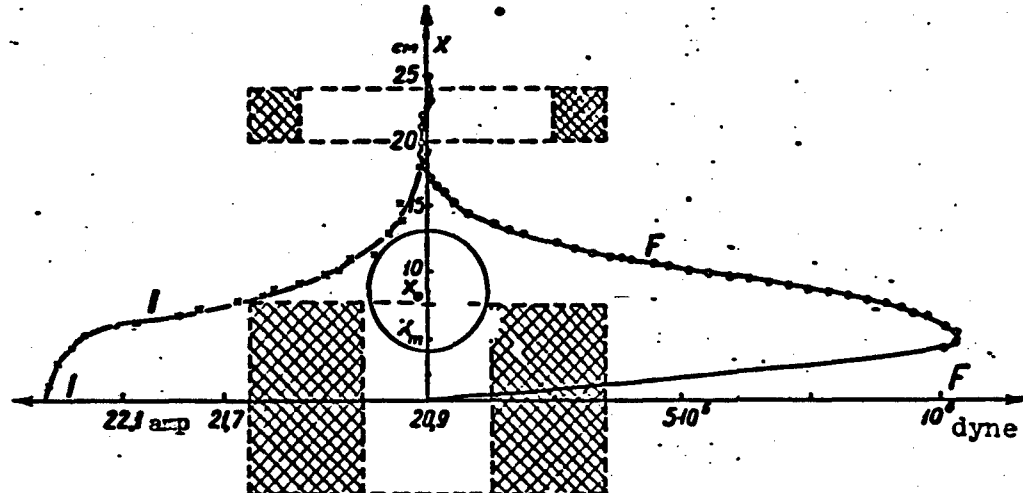


Fig. 1. Diagram of setup for the investigation of stability: curve I — dependence of the current flowing through the inductor on the distance between the centers of the sphere and of the lower solenoid at constant voltage; curve F — dependence of the force acting on the sphere on the distance between the centers of the sphere and the lower solenoid.

Figure 2 (curve 1) shows the dependence of the maximum force F_{\max} acting on an aluminum sphere 9.6 cm in diameter on the ratio $\bar{d} = d/d_0$, where d is the diameter of the sphere and d_0 the inside diameter of the solenoid.

To estimate the mass that can be suspended under given conditions by a given inductor, Fig. 2 (curve 2) shows the dependence of the weight of an aluminum sphere on the value of \bar{d} . The condition for the sphere to be suspended will obviously be $\bar{d} > d_0$. For spheres made of denser material (such as lead) it may turn out that curve 2 is always above curve 1. The given spheres will not stay suspended when the

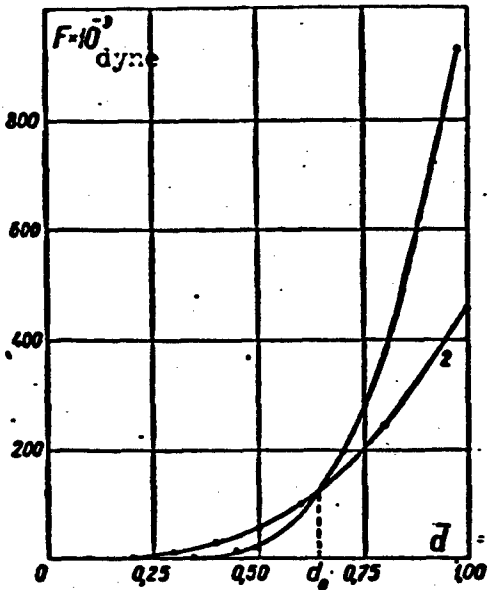


Fig. 2. Dependence of the maximum force acting on the sphere on the diameter of the supporting solenoid.

this interaction is the occurrence of self oscillations, which cause the sphere to be ejected from the potential well of the electromagnetic field.

In the case of small deviations from the equilibrium positions, the oscillation of the sphere in the magnetic field can be described by the following system of equations:

$$m \frac{d^2x}{dt^2} + r \frac{dx}{dt} = F - mg. \quad (1)$$

$$L_1 \frac{dI_1}{dt} + R_1 I_1 + \frac{d(MI_2)}{dt} = E_0 \cos \omega t, \quad (2)$$

$$L_2 \frac{dI_2}{dt} + R_2 I_2 + \frac{d(MI_1)}{dt} = 0, \quad (3)$$

$$M = M_0 - \beta(x - x_0); \quad (4)$$

here m — mass of sphere; g — acceleration due to gravity, I_1 — current in the inductor circuit, I_2 — equivalent current in the sphere, M —

current in the inductor corresponds to curve 1.

Let us proceed now to examine the connection between the sphere position and the circuit parameters. As was already noted, a change in the position of the suspended sphere relative to the inductor leads in the case of constant voltage to a change in the current flowing through the inductor (see Fig. 1). The latter, in turn, causes a change in the force acting on the sphere, and consequently on the position of the sphere. A result of

mutual inductance of the sphere and the turn, L_1 — self inductance of the inductor, L_2 — self inductance of the sphere, β — proportionality coefficient which depends on the form of the inductor and which is determined from experiment.

Inasmuch as the frequency of the sphere oscillations is as a rule much smaller than the frequency of the alternating current feeding the inductor, we can regard the sphere velocity dx/dt in Eqs. (2) and (3) as a constant quantity.

Then the current in both circuits can be expressed in sinusoidal form

$$I_1 = \frac{E_0 e^{j\omega t}}{R_1 + j\omega L_1 + \frac{(j\omega M - \beta \frac{dx}{dt})^2}{R_2 + j\omega L_2}}, \quad (5)$$

$$I_2 = \frac{E \left(j\omega M - \beta \frac{dx}{dt} \right)}{(R_1 + j\omega L_1)(R_2 + j\omega L_2) - (\beta \frac{dx}{dt} - j\omega M)^2}. \quad (6)$$

The effective electromagnetic force acting on the sphere is

$$F = \frac{1}{2} k \cdot \text{Re}[I_1 I_2^*], \quad (7)$$

where k is a certain proportionality coefficient which depends on the form of the inductor. Upon substitution of (7) in (1) we obtain the equation for the oscillations

$$m \frac{d^2x}{dt^2} + (r - AR_2\beta) \frac{dx}{dt} - A\omega^2 L_2 \beta (x - x_0) = 0, \quad (8)$$

where

$$A = \frac{k E_m^2}{[R_1 R_2 - \omega^2 L_1 L_2 - \beta^2 \left(\frac{dx}{dt} \right)^2 + \omega^2 M^2] + [R_1 \omega L_2 + R_2 \omega L_1 + 2\omega M \beta \frac{dx}{dt}]}$$

and

$$-\omega^2 L_2 M_s = mg.$$

It follows from (8) that the condition for the occurrence of self oscillations is

$$r - AR_2 \beta < 0. \quad (9)$$

With increasing coefficient of dissipated forces, r , resulting from placing the sphere in a more viscous medium than air, the self oscillations vanish and the suspension becomes stable. Self oscillations can also be suppressed by superimposing an additional constant magnetic field, which gives rise to a unique type of magnetic viscosity, proportional to the velocity of the sphere. Finally, a decrease in the frequency ω decreases the relative magnitude of the second term in (9), which also leads to a disappearance of the self oscillations. Figure 3 shows the experimentally obtained dependence of the logarithmic damping decrement δ on the relative frequency criterion $\bar{\omega} = 4\pi\mu\sigma d^2$ (σ , μ and d are respectively the specific conductivity, the magnetic permeability, and the diameter of the sphere). We see that when $\bar{\omega} < 60$ the damping decrement becomes positive meaning that the oscillations damp out.

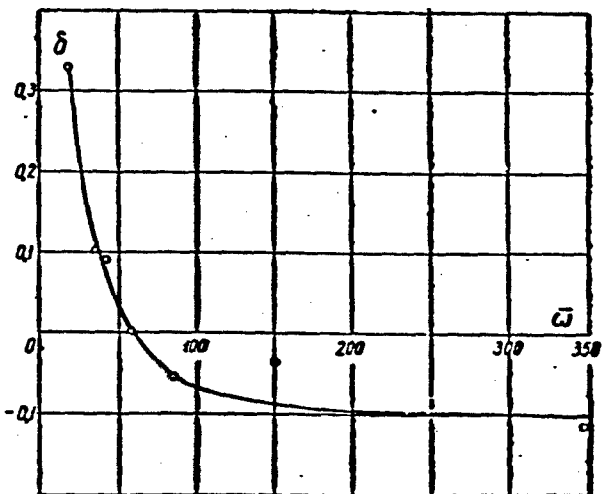


Fig. 3. Dependence of the logarithmic damping decrement on the relative frequency criterion.

Many papers dealing with the equilibrium of a conducting medium or infinite conductivity in a magnetic field have been published.

B.B. Kadomtsev and S.I. Braginskiy [2] and Berkowitz and Friedrichs et al. [3] have shown that in such media stability will be attained only if the centers of curvature of the interfaces between the conducting liquid and the magnetic field lie in the magnetic field.

Thus, a "cusped geometry" is produced — a system of bodies bounded by surfaces with negative curvature.

In accordance with these notions, the figure shown in Fig. 4a can stay in equilibrium in a system comprising two coaxial turns.

However, in the case which we are considering, where a liquid-metal medium is in equilibrium, such a cusped form obviously is not realizable, since the Laplace pressure of the curved surface of the liquid would reach infinity at the cusps. In the experiment set up by the authors where a large sodium sphere was suspended in paraffin oil, the liquid assumes a pear-shaped form with the stem on the bottom, as shown in Fig. 4b.

Let us consider the total pressure at a given level in such a liquid-metal sphere.

For a certain fixed value of x we obviously have

$$p = \frac{B^2}{8\pi\mu} + \alpha \left(\frac{1}{r_1} + \frac{1}{r_2} \right) - \rho_M g (h - x) - \rho_n g (x_0 - h), \quad (10)$$

where B — effective value of the field, α — surface tension, r_1 and r_2 — maximum and minimum radii of curvature at the given section, ρ_M , ρ_n — the density of the metal and surrounding medium, respectively. x_0 — coordinate of the liquid surface (see Fig. 4b).

In the upper and lower points of the body we have $B = 0$ and the corresponding pressures will be

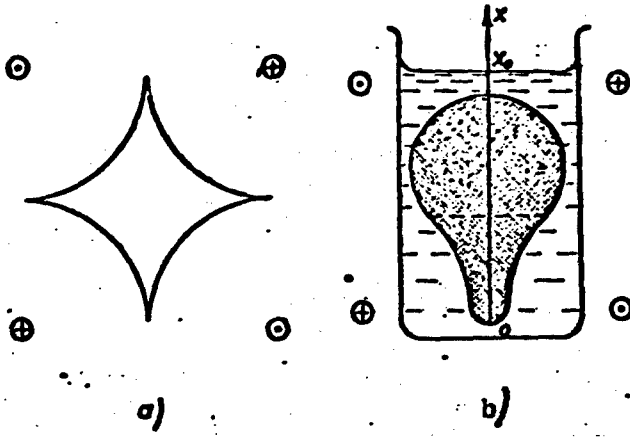


Fig. 4

$$p_b = \frac{2\alpha}{r_b} + p_a gh - p_a gx_0$$

$$p_a = \frac{2\alpha}{r_a} + p_a gh - p_a gx_0 - p_M gh.$$

Subtracting one equation from the other we obtain a relation between the height of the body and the radii of curvature of the upper and lower surfaces:

$$h = \frac{2\alpha}{(p_M - p_a)g} \left(\frac{1}{r_a} - \frac{1}{r_b} \right).$$

Sometimes [1] folds begin to form on the surface of the sphere, in its lower portion, parallel to the magnetic field force lines, as a result of which the stability of such a configuration sharply decreases. The projection between two neighboring folds begins to grow rapidly, for no apparent reason, and all of the metal pours out through the resulting "slot."

It is easy to visualize this phenomenon. The appearance of folds increases the resistance to the induced currents flowing over the surface of the suspended mass, and decreases the secondary current I_2 . The reason for the appearance of the folds is the secondary pinch effect: when the current I_2 reaches a certain density it starts inter-

acting with its own field and compresses the conductor, tending to decrease its cross section.

In order to combat this type of instability, the double frequency method is used [1], and also special inductors are produced with a strong field gradient preventing the appearance of progressing stubs. Both methods give under certain conditions good results, but call for considerable elaborations.

REFERENCES

1. R.P. Zhezherin. Problema elektromagnitnogo tiglya [The Problem of the Electromagnetic Crucible], Voprosy magnitnoy gidrodinamiki i dinamiki plazmy [Problems of Magnetohydrodynamics and Plasma Dynamics], Izd-vo AN Latv. SSR [Publishing House of the Academy of Sciences Latvian SSR], Riga, 1959.
2. B.B. Kadomtsev and S.I. Braginskiy. Stabilizatsiya plazmy s pomoshch'yu neodnorodnykh magnitnykh poley [Stabilization of Plasma with the Aid of Nonuniform Magnetic Fields], Trudy II Mezhdunarodnoy konferentsii po mirnomu ispol'zovaniyu atomnoy energii [Transactions of the International Conference on the Peaceful Uses of Atomic Energy], Geneva, 1958.
3. Berkovich, Fridriks et al. Ostrokonechnaya geometriya [Cusp Geometry], ibid.

MOTION OF NONINTERMING LAYERS OF LIQUID METAL AND
NONELECTRICALLY CONDUCTING LIQUID IN A TRAVELING MAGNETIC FIELD

V.A. Briskman

Perm'

The article reports the results of the measurement of the distribution of the velocity of mercury in a bath made of stainless steel, and also in vessels of different shapes. The motion of the metal is produced by a traveling magnetic field.

The article was partially published in "News of the Academy of Sciences of the Latvian SSR," 8, 145, 1959.

MIXING OF METAL INSIDE A FREELY SUSPENDED DROP

A.E. Mikel'son
Riga

When using melting without a crucible [1], it is desirable to know the character or motion of the metal inside the freely suspended molten mass of liquid metal, particularly in order to determine the place where alloying elements should be added to the melt, to establish the instant when the melt is ready, etc. The character of motion of the metal is of interest also when it comes to explaining the distribution of the electromagnetic forces acting on the liquid metals in the magnetic field, to studying the stability of the suspension of liquid metals in apparatus of similar types, to explaining the possibility of modeling by means of metals the processes occurring in a plasma, etc.

In order to simplify the experiment, the measurements were carried out with a suspended drop contained in a glass bulb. The diagram of the setup is shown in Fig. 1. A bulb with liquid sodium was placed in a potential well of an electromagnetic field produced by coils L_1 and L_2 . The bulb could be freely suspended in the space between the inductors. In order for the bulb not to turn over, its neck was held by a special mechanism in a vertical position. The numbers of the inductor turns were $L_1 = 50$ and $L_2 = 700$.

To measure the velocity of the metal in the bulb, the Pitot tube principle was used. The velocity of the sodium was determined from the difference in the levels in the tube and in the neck of the bulb with

and without a magnetic field. The diameter of the measuring tube was chosen to be 10 mm. If thinner tubes are used for the measurements, the hydrodynamic pressure forces become commensurable with the forces of interaction between the metal and the material of the tube, so that the tube gives false results. In order for the tube dimensions not to influence noticeably the velocity distribution pattern in the bulb, it was necessary to make the measurements with relatively large volumes of sodium. In our case, the diameter of the bulb with the sodium was chosen to be 135 mm.

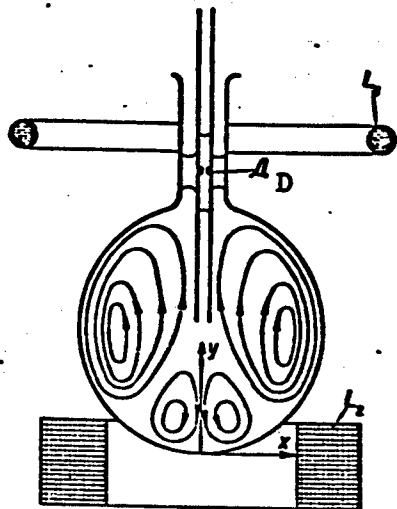


Fig. 1. Sketch of overall view of installation and approximate velocity distribution pattern in the bulb.

Measurements have shown that the motion of the metal inside the bulb has a strongly developed turbulent character. The velocity fluctuation exceeded in many cases by a factor of several times the average value of the velocity of the metal at the given point. In order for the fluctuations not to affect the readings of the measuring tube, a diaphragm D (see Fig. 1) was placed inside the tube, somewhat above the level of the sodium. The layer of paraffin oil, located above the sodium, had a high viscosity and on passing through the diaphragm strongly suppressed the fluctuation oscillations in the tube, resulting from the fluctuation of the sodium velocity in the bulb. Before the measurements, the tube was calibrated under identical conditions with the aid of water. The results of the measurements are shown in Figs. 2-4. Figure 2 shows the distribution of the vertical (in y direction) component of velocity along the x axis at y = 6 cm. The distribution of the vertical compo-

cosity and on passing through the diaphragm strongly suppressed the fluctuation oscillations in the tube, resulting from the fluctuation of the sodium velocity in the bulb. Before the measurements, the tube was calibrated under identical conditions with the aid of water. The results of the measurements are shown in Figs. 2-4. Figure 2 shows the distribution of the vertical (in y direction) component of velocity along the x axis at y = 6 cm. The distribution of the vertical compo-

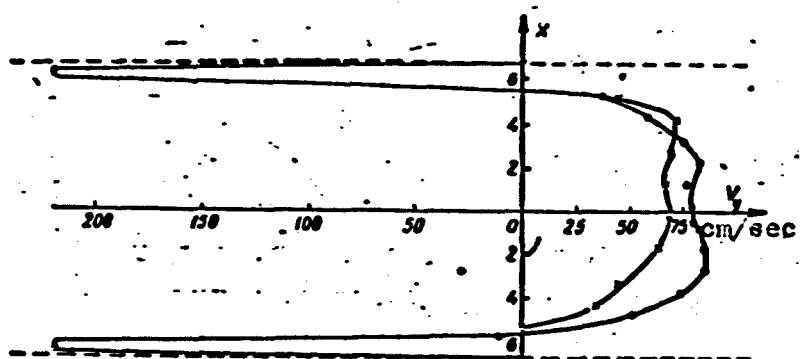


Fig. 2. Distribution of vertical component of velocity of sodium along the x axis for $I = 20$ A:
 O - 50 cps; X - 200 cps.

ment of the velocity along the y axis at $x = 0$ is shown in Fig. 3.

We see that the main volume of the liquid in the suspended bulb moves upward. Along the walls of the bulb, in a layer approximately 1.5 cm thick, the metal moves with much larger velocity in the opposite direction.

Inasmuch as in the present case the thickness of the layer in which the metal moves downward was comparable with the dimensions of the measuring tube, it turned out impossible to measure the distribution of the velocity in the stream moving along the walls. To measure the velocity in the surface layer we used a different method. The bulb with the sodium was cooled to a temperature close to the solidification temperature of the sodium. The colder bulb walls caused the sodium to crystallize primarily on the walls of the bulb. After such dendrite formations and individual crystallites were formed, the magnetic field was turned on and the surface of the bulb photographed in intermittent light. An intermittent trail of the sodium crystallites which were torn away from their location and moved together with the metal was traced on the surface of the bulb. From the length of the trail and from the time of elimination one determined the velocity of motion of the metal on the surface. The measurement results obtained

by photography at an inductor current frequency of 50 cps are shown in Fig. 2.

Since the motion in the bulb is closed, the volume of the liquid flowing per unit time in one direction should equal the volume flowing along the walls in the opposite direction. Graphic integration of the volumes moving in the bulb in opposite directions has shown good agreement between the methods of measuring velocity with the aid of tubes and with the aid of photography.

Control measurements of the vertical component of the velocity along the y axis were made with the aid of a bronze sphere 0.6 cm in diameter. The velocity of the sodium was determined from the force acting on the sphere suspended in the sodium. The results of the measurements are shown in Fig. 3.

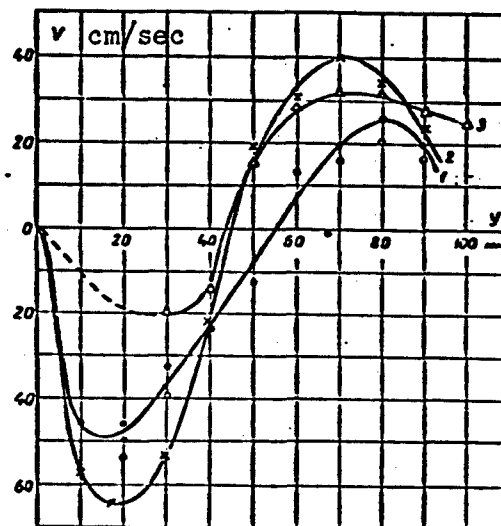


Fig. 3. Determination of the vertical components of the velocity along the y axis in a bulb and suspended drop: ● — measurement with Pitot tubes at $f = 50$ cps; X — the same at $f = 200$ cps; ○ — measurement with bronze sphere at $f = 50$ cps; Δ — measurements with Pitot tube in a suspended drop 11 cm high and transverse diameter 5.6 cm at $f = 200$ cps.

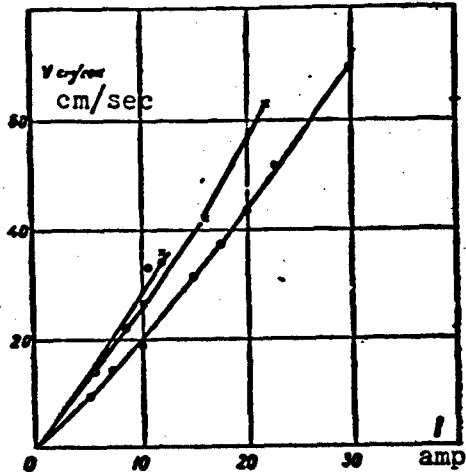


Fig. 4. Dependence of the velocity of the metal in the bulb on the current in the inductor winding.

In order to ascertain the influence of the walls of the bulb on the velocity profile in the suspended drop, that is, in order to ascertain the extent to which the processes occurring in the suspended bulb with sodium are similar to those in a freely suspended drop, we measured the vertical component of the velocity of the metal inside the mass of liquid sodium freely suspended in paraffin oil. The results of the measurements are shown in Fig. 3.

We see from the course of the curves that the absence of the bulb does not make any essential changes in the velocity distribution pattern inside the freely suspended drop. The results obtained by measurements in a bulb can be extrapolated with certain approximation to the case of metal suspended without a bulb. Obviously, the mixing of a metal freely suspended in vacuum or in an inert gas medium will be somewhat more intense, in view of the fact that the velocity of the metal on the surface will not be zero in this case, as was the situation in the experiments with sodium.

It is interesting to note that measurements of the velocity distribution for a freely suspended drop were carried out with a measur-

To determine the dependence of the velocity of motion of the sodium on the intensity of the magnetic field, the bulb was fixed in position and the vertical component of the velocity was measured at $x = 0$, $y = 7$ cm for different values of the current flowing through the inductor winding. The results of the measurements are shown in Fig. 4.

In order to ascertain the influence of the walls of the bulb on the

ing tube without a diaphragm, but no fluctuation oscillations were observed. Obviously, the velocity fluctuations are the result of the interaction between the sodium stream and the stationary walls of the bulb.

The results presented here enable us to present the following picture of velocity distribution in a suspended mass of liquid sodium. A recalculation of the results obtained by measurement in sodium for other metals can be carried out by methods of similarity theory. It is necessary to produce here experimental conditions such that equality of the following defining criteria holds true for both the model, that is, the sodium drop, and the drop of the given metal:

$$\bar{I} = (4\pi\mu)^{3/2} n^2 \sigma^3 \rho^{-1}, \quad (1)$$

$$\bar{\omega} = 4\pi\mu\sigma\alpha d^2, \quad (2)$$

$$\bar{m} = 4\pi\mu^2 n^2 \rho^{-1} g^{-1} d^4, \quad (3)$$

$$\bar{a} = \frac{\alpha}{(\rho - \rho_1) d^2}. \quad (4)$$

Here I — current in the solenoid winding, n — number of solenoid turns, σ , ρ , μ , α and d — the conductivity, density, magnetic permeability, coefficient of surface tension, and dimension of the suspended liquid metal drop, respectively, ρ_1 — density of the medium in which the drop of given metal is suspended, g — acceleration due to gravity.

The constancy of the foregoing system of criteria in the model and in nature guarantees the constancy of the nondefining criterion

$$R_M = 4\pi\mu\sigma\alpha d,$$

which characterizes the velocity v of motion of the metal at the corresponding point of the drop.

REFERENCE

1. R.P. Zhezherin. Problema elektromagnitnogo tiglya [The Problem of the Electromagnetic Crucible], Voprosy magnitnoy gidrodinamiki i dinamiki plazmy [Problems of Magnetohydrodynamics and Plasma Dynamics], Riga, 1959.

BASIC PARAMETERS AND CONSTRUCTIONS OF ELECTROMAGNETIC STIRRING DEVICES FOR ELECTRIC ARC FURNACES

Ya.P. Zvorono

Leningrad

In the melting of high grade steel in arc furnaces of large capacity, the liquid metal must be stirred. At the present time electromagnetic stirring of liquid steel is finding an ever increasing application.

Electromagnetic stirring is produced by means of a developed stator which is located above the furnace and produces a traveling magnetic field in the furnace bath. The traveling magnetic field of the stator interacts with the eddy currents induced by the field in the liquid steel, and the mechanical forces produced thereby give rise to directed motion which causes stirring of the entire mass.

BASIC ELECTRIC PARAMETERS

Number of Stator Poles

Since the lining of large furnaces is 60-100 cm thick, the weakening of the stator field is quite large.

The dependence of the induction component normal to the borel surface of the stator on the distance above the bored surface in air has the following form for a flat stator:

$$B_0 = B_0 \cdot e^{-\frac{\pi x}{R}}. \quad (1)$$

Accordingly, for a stator in arc form

$$B_0 = B_0 \cdot \left(\frac{R - \delta}{R} \right)^{\frac{\pi R}{\delta} - 1}. \quad (2)$$

where B_z - induction at a height δ above the bored surface, B_0 - induction on the bored surface, δ - height above the bored surface, τ - pole pitch, R - boring radius.

Both formulas disregard the influence of edge effects.

Formulas (1 and 2) show that the attenuation of the field is inversely proportional to τ and, inasmuch as the stator dimensions are bounded, it is best to use a two-pole stator.

Frequency

To obtain circulation of the molten steel it is necessary that the forces act only on its lower layers: from the bottom to half the depth of the bath. Since the depth of the bath in a large furnace amounts to 50-100 cm, to obtain the necessary depth of field penetration the frequency of the current supplying the stator should be quite low, on the order of a fraction of a cycle. Nonetheless, even at such a frequency the jacket of the furnace must be nonmagnetic so as to avoid appreciable screening of the stator field. Usually only the bottom of the jacket, directly above the stator, is made nonmagnetic.

Number of Phases

The stator is made two-phase with a split phase the winding of which is located on the ends of the magnetic circuit. Such a placement of the winding guarantees better wave form of the induction above the stator.

Inasmuch as the stator has an open magnetic system, and coils belonging to one phase are located on the ends of the core, the phase windings are subjected to different conditions. Therefore, in order for the phase impedances to be equal, the number of turns in the phase winding should be different. Usually the ratio of the phase turns ranges between 3/4 and 4/5.

The use of a two-phase stator simplifies the supply equipment.

Line Load of the Stator

Inasmuch as the stator field is highly attenuated at the location of the liquid steel (by a factor of several times), the line load on the bored surface should be on the order of 1000-1500 A/cm in order to obtain the necessary stirring intensity.

STATOR CONSTRUCTION

The fact that the magnetic circuit is open and the singularities of the electric parameters of the stator exert an appreciable influence on its construction, which differs appreciably from the constructions of ordinary electric machines.

Owing to the low frequency of the current, the losses in the active core steel are negligible, so that the stator can be assembled of relatively thick laminations of ordinary non-electrotechnical steel.

Such a core is quite rigid and does not require a special mounting housing.

The skin effect in the winding can likewise be neglected and the

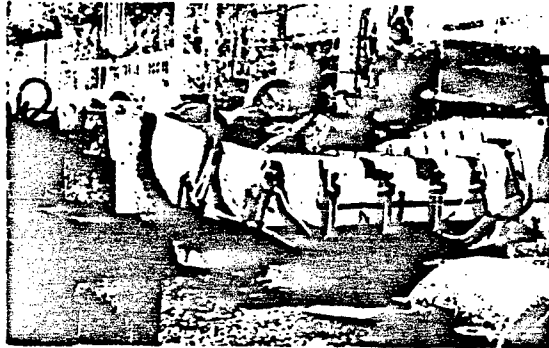


Fig. 1. Type SEP/40 1 - 400/100
stator for a furnace of 40-ton ca-
pacity (without covers).

winding made of solid conductors of large cross section.

The relatively high line load of the stator, and also the heat radiated from the furnace jacket, the temperature of which reaches 300°C , raise difficulties with cooling of the winding. The stator

winding can be cooled both with air and with water, but the latter is preferable.

Since the stator has no rotating part, its ventilation can be effected only by external means and no closed cycle can be used. This leads to contamination of the winding and reduces the operating reliability of the stator. In the case of air cooling, individual parts of the winding are considerably overheated, so that silicone insulation must be used.

In a directly water cooled winding made of hollow conductors the temperature drop between the copper and water is a fraction of a degree, resulting in both a low average winding temperature and in high uniformity of cooling.

A typical stator construction is shown in Fig. 1.

The main core assembly is made of type ST. 3 sheet steel 10 mm thick. The core is clamped together on insulated pins. A drum type winding consisting of four coils, two for each phase, is placed on the side of the core facing the bottom of the furnace. The coils are made of copper tubing of rectangular cross section measuring 22 X 22 mm with a round aperture of 111 square mm, which is continuously wound on a form. The coil turns are insulated by liners made of asbestos-textolite 3 mm thick.

The stator is covered on the top with a refractory cover made of asbestos-cement plates; this cover protects the stator against the entrance of liquid steel or slag.

The stator winding is cooled with water that runs directly through the hollow conductors.

The main parameters of some of the stators designed by the Leningrad branch of the Scientific Research Institute for Electric Machinery and the "Elektrosila" plant are listed below.

Characteristics of Stators for Electric Stirrers

Capacity of furnace (tons)	20	40	80	180
Rating (kva)	830	460	520	1100
Voltage (V)	160	115	130	230
Current (A)	2600	2000	2000	2400
Power factor	0.55	0.6	0.6	0.67
Line load (A/cm)	1500	1160	1080	1500
Frequency range (cps)	0.8-1	0.5-1.5	0.55-1	0.3-0.6
Double pole pitch (cm)	360	400	400	460
Length of active steel (cm)	110	100	160	180
Number of turns in phase I	44	52	48	64
Number of turns in phase II	60	64	60	80
Total weight of stator (tons)	18	16	20	40

SUPPLY UNIT

The stator is fed from a dynamo electric supply unit, a simplified diagram of which is shown in Fig. 2.

The supply assembly consists of five machines: two single-phase low-frequency slip ring generators, a synchronous drive motor with exciter, and a constant voltage generator intended to supply the frequency transmitter and the control circuits.

The low frequency generators are revamped series "P" d.c. machines and have cast bedplates.

The three-unit exciter consists of two type EMU 110 amplitidynes and an induction drive motor.

The pre-exciter consists of a d.c. drive motor, a two-phase rheostatic converter (low frequency transmitter) and a tachometer generator. The transmitter is a stationary drum commutator, similar to the commutator used in a d.c. machine, with two pairs of brushes, shifted relative to each other by one-quarter of a cycle, rotating around the commutator. A sinusoidally subdivided potentiometric resistor is connected to the commutator segments.

The frequency of the transmitter is regulated by varying the velocity of the pre-exciter motor.

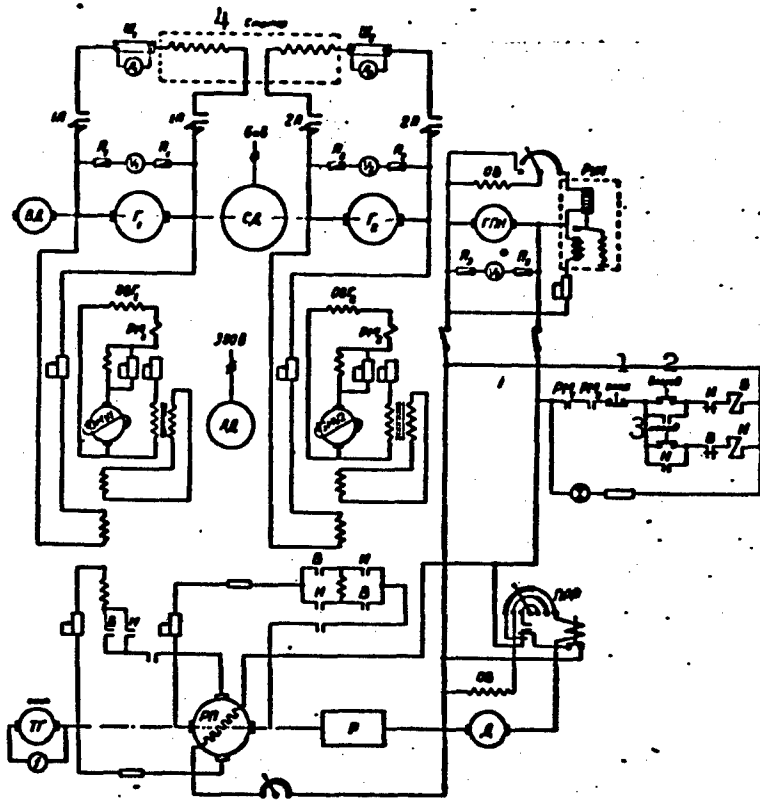


Fig. 2. Typical power supply circuit for stator.
Designations used in circuit:

SD - synchronous motor; G₁, G₂ - main generator;
GPN - constant voltage generator; VD - exciter
for synchronous motor; AD - induction motor; EMU 1,
EMU 2 - amplidyne; RP - rheostatic converter; D -
motor of rheostatic converter; R - reduction gear;
TG - tachometer generator; Sh₁, Sh₂ - shunts, 0.5
cps; 1 A, 2 A - automatic circuit breakers; PRR -
starting rheostat; RUN - voltage regulator; A₁,
A₂, A₃ - ammeter; V₁, V₂, V₃ - voltmeter; P₁, P₂,
P₃ - fuses; f - frequency meter.

1) Off; 2) forward; 3) reverse; 4) stator.

OPERATING RESULTS

At the present several electromagnetic stirring units of domestic construction are in operation in furnaces of 20, 40 and 80-ton capacity.

Detailed tests of the installation in the 80-ton furnace of the

Novolipetsk metallurgical plant made in May of 1959 yielded results that agreed with the calculations. The power fed to the liquid steel was about 3.5 kw, and the corresponding stator efficiency about 1.5%.

At nominal current and at a frequency of 0.55 cps, the speed of a brick floating in the bath reached 0.35-0.4 m/sec. The closed cycle water cooling system maintained the stator winding temperature below 50°C.

FURTHER DEVELOPMENT OF ELECTROMAGNETIC STIRRING UNITS

The operating experience with the installed stirring units has shown that they work to the metallurgist's satisfaction, so that further development of these units is aimed at simplification and cost reduction.

One of the ways of reducing the stator cost is to make its winding of aluminum.

The power supply can be simplified and its cost reduced by replacing the motor-generator system with an ionic frequency converter. The ionic frequency converter is best made of sealed rectifiers with an electronic frequency transmitter. In this case the entire stirring unit will have no rotating machinery, so that its operation becomes greatly simplified. Among the advantages of the ionic converter are its lower dimensions, lower weight, and lack of foundation, something of particular value when the electromagnetic stirrer is installed in furnaces already in operation, where limitations in shop area make it difficult to locate the dynamo electric installation.

At the present time all the large arc furnaces produced in the Soviet Union are being equipped with electromagnetic stirring units.

Manu-
script
Page
No.

[List of Transliterated Symbols]

609	СИ = SD = sinkhronnyy dvigatele' = synchronous motor
609	Ш = Sh = shunt = shunt
609	Г = G = generator = generator
609	ГПН = GPN = generator postoyannogo napryazheniya = constant voltage generator
609	ВД = VD = vozbuздitel' dvigatelya = motor exciter
609	РУН = RUN = reguliyator ...napryazheniya = voltage ...regulator
609	АД = AD = asinkhronnyy dvigatele' = induction motor
609	ЭМУ = EMU = elektromashinnyy usilitel' = amplidyne
609	РП = RP = reostatnyy preobrazovatel' = rheostat converter
609	Д = D = dvigatele' = motor
609	Р = R = reduktor = reducing gear
609	ТГ = TG = takhogenerator = tachometer generator
609	А = A = avtomat = circuit breaker; = ampermetr = ammeter
609	ПРР = PRR = puskoregulirovochnyy reostat = starting rheostat
609	П = P = predokhranitel' = fuse

ELECTROMAGNETIC STIRRING OF STEEL IN THE LADLE

M.G. Rezin
Sverdlovsk

Metallurgists have long been aware of the need for stirring metal in many melting processes. Effective stirring using the simplest means is made difficult by the high temperature of the molten steel. The use of electromagnetic stirring in arc steel melting furnaces yields certain advantages compared with other methods and points to the possibility of extending this method to other steel production processes such as vacuumizing, desulfurizing pig iron, etc.

In vacuuming without stirring, the degasification takes place only in the upper layers of the liquid steel. The operating depth of the vacuum is determined essentially by the boiling of the bath. In the lower layers, owing to the appreciable metallostatic pressure, practically no gas is liberated. These lower nondegasified layers must be raised upward in order to subject them to the direct action of the vacuum, and the degasified layers of the metal must be moved downward, that is, the metal must be stirred. Electromagnetic stirring in the ladle, in addition to providing degasification and ultimate deoxidation, can make it possible to dissolve the alloying additives directly in the ladle, which in addition to reducing the melting time affords appreciable economy of expensive alloying additives, considerable waste of which occurs in steel-smelting furnaces.

As a result, various installations intended for stirring in the ladle during the degasification of the steel have appeared recently

in the USSR and abroad. These installations can be subdivided into those using electromagnetic devices and those without such devices.

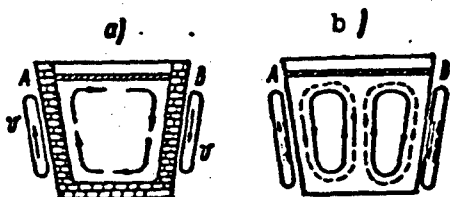


Fig. 1. Stirring with one or two stators ("A" and "B") installed outside the jacket of the ladle.

Without considering all the installations in which electromagnetic units are used, let us stop to discuss only two:

1) installation with flat stator, the winding of which is fed with low frequency current;

2) installation using the circulating degasification method.

The use of low frequency for the stator supply in place of the commercial 50 cycles makes it possible to place the stator outside the ladle jacket (Fig. 1) and in addition increases the stirring effect while appreciably reducing the reactive power.

In many cases the hydrodynamics of the liquid steel can be modified and its speed increased by using in addition to stator "A" a second stator "B" diametrically opposite the stator "A".

Simulation of the hydrodynamic processes has shown that in the presence of two stators the hydrodynamics of the liquid steel can be appreciably modified by changing the direction of the current in the phases of the stator, as a result of which the direction of a portion of the field of stators "A" and "B" is changed. If the field of stator "B" is directed opposite to the field of stator "A", then the motion will be produced essentially in accordance with the scheme of Fig. 1a. If the fields of stators "A" and "B" have the same direction, for example from the surface of the metal towards the bottom, then the motion of the metal will be produced in accordance with Fig. 1b (the arrows of the solid line). If the direction of the traveling field is simultaneously reversed in stators "A" and "B", the

metal will move as shown in Fig. 1b (arrows of the dashed line). In this case the metal near the walls of the ladle will move upward, flow over the surface, and drop downward outside the active zone of the stators.

The Department for Electric Machinery and the Department of General Electrical Engineering, together with the MOMZ Department of the S.M. Kirov Ural Polytechnic Institute, have prepared designs of electromagnetic stirrers for a ladle of 70-ton capacity.

For effective stirring of liquid steel using two diametrically located stators, the depth of penetration of the field should be equal to half the average diameter of the ladle.

If $D = 210$ cm is the average ladle diameter, $\rho = 1.36 \text{ ohm-mm}^2/\text{M}$ is the specific resistivity of the liquid steel, then the necessary frequency is given by the expression $\frac{D}{2} = \frac{100}{2\pi} \sqrt{\frac{10 \cdot \rho}{f}}$, hence $f = 0.315$ cps. The range of frequency variation adopted in the design is 0.3-1 cps.

In order to reduce the cost of the power supply and to simplify the construction of the stator winding, a two-phase winding is used.

To guarantee minimum damping of the normal component of the induction in the air gap, the stator has been made of the two-pole type in accordance with the expression

$$B = B_0 \cdot l^{-\frac{1}{2}}$$

where B — induction at a distance δ from the stator; B_0 — induction on the surface of the stator; τ — pole pitch of the stator.

The stator is made flat in order to fit it better into the chamber, and the ladle needs less revamping if the stator is flat.

The winding used is annular, since under the vacuum chamber conditions a stator with such a winding occupies less place than other types of windings.

An essential feature of the stators is the lack of any artificial cooling, something made possible if the stators operate for 15-20 minutes. The two stators are fed from rotating generators with a total rating 160 kva.

The stator is placed vertically in the vacuum chamber housing and is driven by a special mechanism to the wall of the ladle after the latter is installed in the chamber. When the stirring is completed, the stator is moved away from the ladle and placed in its previous nonoperating position.

Let us consider the installation with circulating degasification, which can be used in comparison with the previously considered installation with flat stator whenever large masses of metal are processed, for it is not necessary in this case to place the ladle into the vacuum chamber, to close the chamber and to seal it after the

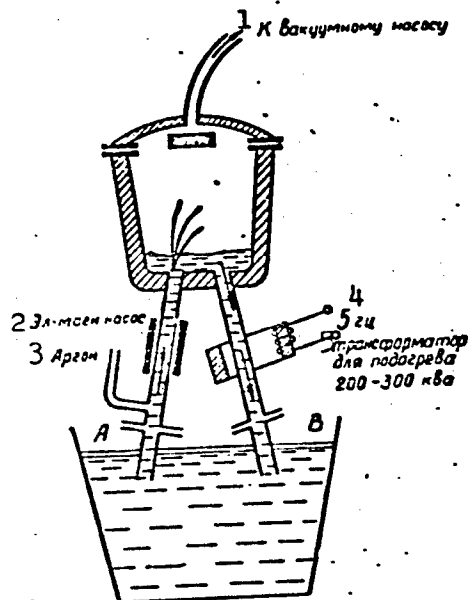


Fig. 2. Degasification of steel by the method of pumping through vacuum.
1) To vacuum pump; 2) electromagnetic pump; 3) argon;
4) 5 cps; 5) transformer for heating, 200-300 kva.

installation of the ladle.

This process is characterized by pumping the molten steel through a vacuum chamber of small size as compared with the ladle. The steel is continuously driven by an electromagnetic pump from the ladle through an intake tube "A" inside the degasification chamber, and after degasification it flows back into the ladle through a drain pipe "B" (Fig. 2).

The power for this circulation is produced additionally by the gas released from the steel under the influence of the vacuum chamber.

An advantage of this process is the favorable redistribution of the steel for vacuuming in the degasification chamber. The rising gas bubbles due to the dissolved gases in the steel will increase in volume with time as they float upward, and the steel enters into the degasification chamber, under the influence of these gases and the action of the pump, at a high velocity, causing it to be ejected upward, splash vigorously, and get rid of the dissolved gases.

Other important features of the process are the insignificant heat losses, inasmuch as the volume of the degasification chamber is small, and the possibility of offsetting these heat losses by simply using transformer heating. This is effected by placing on the drain pipe "B" a magnetic circuit with a winding fed at commercial frequency. The secondary winding is the closed circuit of the molten metal, which comprises a single turn of the secondary winding.

The degasification chamber gives rise to constant heat losses independently of the volume of the metal in the ladle. Therefore if the volume of the metal in the ladle is low, the temperature drop will be greater. To offset the heat losses, the temperature of the melt is raised or additional heating is used.

The use of an electromagnetic pump to replace the compression action of the neutral gas in such installations does not lead to a deterioration of the vacuum.

The use of a neutral gas (argon) to exert pressure on the metal in pipe "A" deteriorates the vacuum in the degasification chamber and calls for the use of powerful vacuum pumps.

Calculations show that the necessary pressure on the metal can be produced by an electromagnetic pump.

The choice of the type of pump to move the liquid steel depends on many factors, the most important of which are indicated below.

The material of the neck or pipe walls cannot be steel, as is usually the case for pumping metals at low temperature. The high temperature of liquid steel (1600°C) calls for the use of ceramic materials which have the necessary properties.

The thickness of the ceramic wall of the neck (pipe) must exceed by a factor of several times ten the thickness of a metallic wall which is used for pumps for low temperature metals, in order to provide mechanical strength and thermal insulation.

The thickness of the layer of liquid steel cannot be assumed to be the same as in pumps for metals with lower temperature, since the steel may cool down on the walls of the pipe, in spite of preliminary heating.

If the thickness of the ceramic wall of the neck is assumed to be 45 mm and the minimum thickness of the liquid steel to be 30 mm, then the minimum distance between the inductors (in the case of a flat induction pump) is 120 mm. Such an "air" gap calls for rather large magnetizing current and consequently for high line current loads on the surface of the stators.

With so large a gap, it is desirable to produce the current in the secondary circuit of the pump (in the layer of liquid metal) by conduction using direct or alternating current. However, to supply current to a layer of liquid steel is a rather difficult matter. The electrodes that supply the current to the liquid steel must withstand a high temperature, be good electric conductors and poor heat conductors, and must not dissolve in the steel and deteriorate its properties. The most suitable electrode for this purpose could be graphite, but it may carburize the steel. In addition, direct contact between the metal and the electrodes causes the latter to wear and makes it necessary to displace the electrodes through a high vacuum seal or to

replace the electrodes completely. All this makes the pump construction very complicated. The difficulties connected with providing reliable current supply to liquid steel make it necessary to forego for the time being the use of conduction pumps.

It becomes necessary to choose a flat induction pump, where the current in the liquid metal is produced by induction, and the problem of electrodes and the associated tight seals is eliminated.

The Departments of Electric Machinery, General Electrical Engineering, and MOMZ of the S.M. Kirov Ural Polytechnic Institute have completed a design for a degasification unit for liquid steel using the circulation method with an electromagnetic pump at two frequencies:

- a) at 50 cps with a liquid steel layer 30 mm thick, power $P =$
 $= 2050$ kva, and a rating of $85 \text{ m}^3/\text{hr}$;
- b) at 16 cps, 80 mm layer of liquid steel, $P = 1650$ kva, and rating $173 \text{ m}^3/\text{hr}$.

The practical utilization of the designs calls for the installation of pipes made of high grade refractories.

The refractory material used to manufacture the pipe should have high mechanical strength at a temperature $1600\text{-}1800^\circ\text{C}$. In addition, the wall of the pipe should be sufficiently resistant to wear resulting from friction produced by the moving metal at this temperature, and also dense so as to prevent air from being sucked in through the walls of the pipe.

Electromagnetic stirring can find extensive use in the desulphurization of cast iron. Usually cast iron is desulphurized in a drum into which the liquid cast iron is poured from a ladle and covered with a slag of necessary composition, after which the drum is rotated so as to mix the cast iron and the slag. After the end of the process the

metal is again poured out into a pouring ladle.

This process has appreciable shortcomings. It is not technologically sound, since it calls for repouring the molten cast iron through the neck of the ladle into the opening of the drum. Multiple repouring of the cast iron leads to large heat loss and to the cooling of the cast iron. When the drum rotates, its lining is damaged by the molten cast iron and calls for time-consuming repairs.

The use of electromagnetic stirring makes it possible to desulphurize cast iron directly in the ladle, thus yielding appreciable technical and economical advantages.

In many cases it may prove advantageous to use electromagnetic stirring in open hearth furnaces, in foundry production, etc.

REFERENCES

1. A. I. Vol'dek. Elektromagnitnye nasosy dlya zhidkikh metallov [Electromagnetic Pumps for Liquid Metals], Elektrichestvo [Electricity], 5, 1960.
2. Tal'man, Maas. Degazatsiya stali pri tsirkulyatsii ee v vakuumme [Degassing of Steel by Circulating it in a Vacuum], Problemy sovremennoy metallurgii [Problems of Contemporary Metallurgy], 4, 1959.

POWER SUPPLIES FOR INSTALLATIONS FOR
ELECTROMAGNETIC STIRRING OF LIQUID STEEL IN LADLES

Ya.I. Drobinin

Sverdlovsk

Unlike the installations used for stirring in arc furnaces, where the depth of the bath does not exceed 0.8 meters and the required depth of penetration is not larger than 0.4 meters, when steel is mixed in large ladles with capacity on the order of 100 tons, a large depth of penetration of the magnetic field into the liquid metal (up to 1 meter) is required, and consequently the frequency of the current fed to the stirrer must be lower (on the order of 0.2-0.4 cps).

On the other hand, the small thickness of the ladle lining, which usually does not exceed 10 or 20 centimeters, is several times less than the lining of electric arc furnaces, where it reaches 0.8-1 meter, so that the rating of the power supply can be reduced and consequently a different power supply system can be used and different equipment.

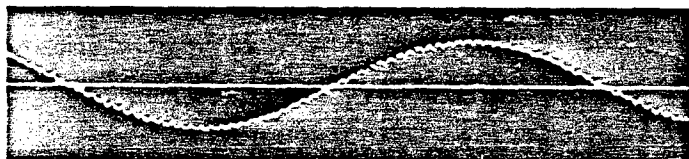


Fig. 1. Oscillogram of the voltage of a slip ring type two-phase low frequency 0.5 cps converter.

The system used for stirrers in the USSR is that of the "Elektro-

sila" plant [1], which contains 10 machines. This system can be reduced to four or even three machines by replacing the rheostatic frequency transmitter and the amplidyne by a slip ring frequency converter. The use of a slip ring converter as a transmitter for infralow frequency was investigated at the Ural Polytechnic Institute. An oscillogram taken from a two-phase 0.5 cps transmitter is shown in Fig. 1.

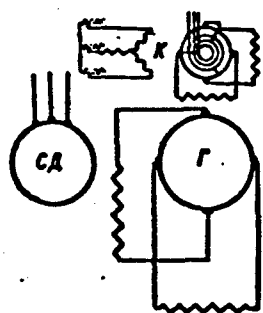


Fig. 2. Three-machine system:
G - two-phase generator;
SD - drive motor;
K - slip ring converter used as exciter.

The machine stage can be simplified by replacing two single-phase generators with one two-phase generator, which saves, by calculation, about 30% of material and reduces the area occupied and the weight of the foundation. The diagram of such an installation is shown in Fig. 2. Two-phase low frequency generators for stirring purposes have been in operation in Swedish installations for ten years and have given good results.

The system can be further simplified by feeding the stator directly from a slip ring converter of suitable rating (Fig. 3). The Ural Polytechnic Institute has developed the design of such an installation, and its technical and economic indices as compared with other rotating-machine systems are listed in Table 1. The converter power rating is 500 kw. The stator voltage is 130 volts, the frequency is 0.5 cps (adjustable), and the current is 2000 A. The slip ring converter can be made in two variants: with rotating armature and with stationary armature and rotating brushes.

If the armature is stationary, the machine can be made of the vertical type to reduce the occupied area, but the rotating brushes make the construction more complicated, although the overall losses are reduced.

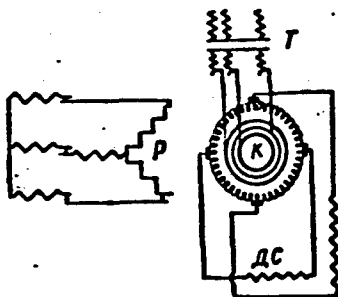


Fig. 3. Slip ring converter as the main generator of two-phase low frequency current:
K - converter; T - regulating transformer;
R - rotary winding (imbedded in the stator steel); DS - two-phase stator.

To obtain current at infralow frequency, one can also use ionic frequency converters. An ionic frequency converter with pumped-out rectifiers was considered previously [1-3]. Less power is needed to stir in ladles, and the converter can also be made with sealed rectifiers of the Zaporozh'ye electric apparatus plant in accordance with the circuit of Fig. 4. Contacts K-1 and K-2 have been introduced into the circuit to shut the rectifiers off during the time when the low frequency

TABLE I

Name of System	Cost of Equipment, Thousands of Rubles	Annual Operating Cost, Thousands of Rubles	Hourly Losses, Rubles
System of the "Elektrosila" plant	18.34	1.13	1.03
System with two-phase generator	12.91	0.81	1.08
System with slip ring converter	7.92	0.53	0.79

current reverses polarity. The contacts are made necessary by the fact that the rectifiers have a common cathode for all the anodes of a given rectifier. The grid control, as in installations with isolated cathodes, is operated by a selsyn rheostat. Contacts K-1 and K-2 are turned on and off by a frequency transmitter, with which they are mechanically coupled. Thus, they operate in synchronism with the frequency of the voltage applied to the control grids. The switches have each two pairs of normally closed and two pairs of normally open contacts. Simultaneously with the switching of the rectifiers, the null point of the two-phase stator is switched over, thereby reversing

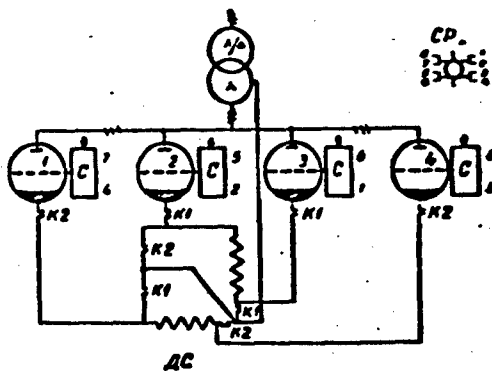


Fig. 4. Ionic frequency converter using sealed rectifiers with common cathode:
1, 2, 3, 4 - multiphase rectifiers with common cathode;
 K_1 and K_2 - contacts operated by the drive of the selsyn rheostat; SR - selsyn rheostat; T - transformer; S - grid control; DS - two-phase stator of electromagnetic stirrer.

is made up of four rectifiers (see Fig. 4).

A promising development for further use in circuits for generating infralow frequency is a mechanical frequency converter which has higher efficiency than all others as a result of the smaller voltage drop in the converter contacts (1-2 V) as against 15-20 V voltage drop in the rectifier arc, which is particularly important at the low voltage used to operate the stator of the electromagnetic stirrer. which usually does not exceed 100-200 V.

The mechanical frequency converter is based on a mechanical rectifier with adjustable voltage. The converter diagram is shown in Fig. 5. In analogy with the ionic converter, the role of the grid in the adjustable mechanical converter is assumed by rotation of the stator of a synchronous motor, which regulates the phase shift at which the converter contacts are closed. By periodically varying the stator angle as set by the drive mechanism in accordance with a

the current in both stator phases, and the disconnecting of the inoperative cathodes makes it possible to avoid a short circuit between the rectifiers. Sealed rectifiers are produced by the Zaporozh'ye plant with a rating of 250 A with 6 rectifiers in a single cabinet. The use of two cabinets makes feasible an installation rated at 750A in accordance with a circuit previously described [1]. Sealed rectifiers with common cathode are manufactured with a rating of 500 A. This circuit

specified law, we change the voltage at the output of the converter from zero to the maximum. At a frequency of 0.5 cps, the duration of one half cycle of the alternating current will be one second. During that time the contacts of the converter, which are operated by a synchronous motor at 3000 rpm, will close 50 times per phase, and in the case of three-phase current and full wave rectification the contacts will close $50 \times 6 = 300$ times, which provides a sufficiently smooth variation of the voltage wave form.

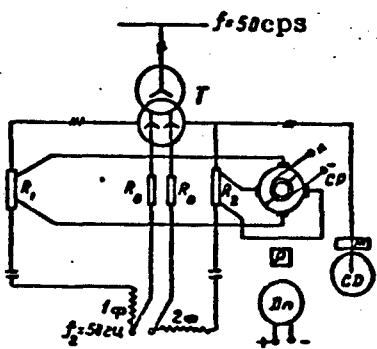


Fig. 5. Mechanical frequency converter:
T - transformer; R_1 and
 R_2 - adjustable reactors;
 D_p - drive motor;
R - reduction gear to
rotate the selsyn rheo-
stat and the mechanism
(M) which rocks the
stator of the synchron-
ous motor (SD); 1f and
2f - 2 phases of the
low frequency 0.5 cps
stator.

elements necessary for the converter, that is, to leave the number of contacts the same as in ordinary rectifying circuits. Inasmuch as in this case a periodically repeated process is necessary (the generation of a current at a frequency 0.2-1 cps), the stator must also be rotated periodically to permit the contacts to operate at reversible

The wave form of the current will be smoothed by the inductance of the circuit and of the reactor in the neutral lead. The angle of stator rotation governs also the direction of the current flowing through the converter contacts. Rotation in one direction causes the converter to operate on the positive half wave, and rotation in the opposite direction causes operation on the negative half wave.

Unlike the ionic converter, which does not pass current in the opposite direction, the mechanical converter is indifferent to the direction of the current flowing through its contacts. This makes it possible to reduce the number of circuit ele-

polarity, something effected by a mechanism which rocks the stator with a periodicity corresponding to the operating frequency. The voltage of the mechanical converter can be regulated by magnetizing an adjustable reactor connected in the supply circuit of the converter. In both cases the start of the commutation is shifted relative to the voltage of the supply line, so that the magnitude of the rectified current changes, and by shifting at the same time the stator angle (from $+a$ to $-a$) we change periodically also the polarity of the curve. The auxiliary winding of the commutation choke makes it possible to shift the hysteresis loop, and consequently to control the current through the contact during the time that they are at a given step and control the slowing down of the on time. This can also be attained independently of the commutation chokes by connecting in the primary or secondary side of the main transformer an adjustable reactor, in which the magnetization is produced with direct current. This method yields smooth and rapid regulation, which can be made periodic or to follow a specified law by suitable design of the steps of the selsyn rheostat (SR - Fig. 5), which feeds current to the magnetization winding of the adjustable reactor, that is, a sinusoidal wave form can be obtained for the current. A two-phase current with a phase shift of 90° is produced by magnetizing reactors R_1 and R_2 by currents from the selsyn rheostat, which are shifted 90° by mounting the brushes on the rheostat at an angle of 90° .

REFERENCES

1. Ya.I. Drobinnin. Skhemy pitaniya ustyanovok dlya elektromagnitnogo peremeshivaniya metalla v elektrudugovykh pechakh [Power Circuits for Installations for Electromagnetic Stirring of Metal in Electric-Arc Furnaces], Voprosy magnitnoy gidrodinamiki i dinamiki plazmy [Problems of Magnetohydrodynamics and

- Plasma Dynamics], Riga, 1959.
2. N. S. Siunov, M. G. Rezin, Ya. I. Drobinnin and Ye. M. Glukh. Ionnyy preobrazovatel' chastoty 0,5-2,5 gts [Ionic Converter for Frequencies from 0.5 to 2.5 cycles], Elektrichestvo [Electricity], 11, 1959.
3. Ya. I. Drobinnin, M. G. Rezin, Ye. M. Glukh and Ye. L. Ettinger. Preobrazovatel' trekhfaznogo toka sverkhnizkoy chastoty [A Three-Phase Superlow-Frequency Converter], Author's Certificate No. 115359 dated 10 January 1959.

Manu-
script
Page
No.

[List of Transliterated Symbols]

620	Γ = G = generator = generator
620	СД = SD = sinkhronnyy dvigatel' = synchronous motor
620	K = K = kollektorny = collector, slip-ring
621	P = R = rotor = rotor
621	K = K kollektorny preobrazovatel' = slip-ring converter
621	ДС = DS = dvukhfaznyy stator = two-phase stator
622	СР = SR = selsinnyy reostat = selsyn rheostat
622	K = K kontakt = contact
622	C = S = setochnyy = grid (adj.)
623	Дп = Dp = dvigatel', privodnoy = motor, drive

HYDROGAS ANALOGY IN MAGNETOHYDRODYNAMICS

L.A. Vulis, P.L. Gusika

Alma-Ata

The advisability of generalizing and employing in magnetohydrodynamics the well known hydrogas analogy proposed in the works of N.Ye. Zhukovskiy is pointed out. The gist of the analogy is to simulate isentropic flow of a conducting compressible gas with the aid of a hydraulic trough, by observation of the flow of an incompressible conducting liquid (with free surface) subjected to the action of electric and magnetic fields. The use of this analogy for one-dimensional and two-dimensional flows is briefly discussed. The decisive significance of the magnetic Reynolds number Re_m is indicated, and features of simulation in limiting cases of large and small values of this number are discussed.

A complete exposition is found in the authors' article "Hydrogas Analogy in Magnetohydrodynamics" (ZhTF, 7, 31, 819, 1961).

CERTAIN PROPERTIES OF SUSPENDED LAYER
OF FERROMAGNETIC PARTICLES IN A MAGNETIC FIELD

M.V. Filippov

Riga

In the present communication we describe certain properties of a suspended layer of ferromagnetic particles in a magnetic field.

The suspended layer is a two-phase mixture which has a far reaching similarity to a liquid which is in the state of turbulent motion, and is therefore frequently called semi-liquefied. If the particles of the solid phase of the suspended layer are ferromagnetic, then the latter can be regarded in many respects as a certain ferromagnetic pseudoliquid, a study of which is of interest all the more since there are no known liquid ferromagnets. The lack of a theory and of much information on the mechanism of the phenomenon makes the accumulation of experimental data and laws even more important.

Among the main parameters of a suspended layer is primarily the critical velocity, that is, the velocity of the stream at which the stationary layer goes into the suspended state.

This is followed by the expansion law, that is, the connection between the porosity, the fractions of the free volume of the layer, ϵ , and the velocity of the stream v , usually expressed in criterial form in terms of the Reynolds number $Re = v \cdot d / \nu$ and the Archimedes number $Ar = (g \cdot d^3) / \nu^2 (\rho_b - \rho_c) / \rho_c$, for example in the form

$$\epsilon = \left(\frac{18Re + 0.36Re^2}{Ar} \right)^{0.25}$$

where d - defining linear dimension of the particle, ν - kinematic viscosity of the suspended medium, ρ_c - its density, ρ_b - density of the solid-phase substance.

Among the important characteristics of the suspended layer are also its resistance, which is practically equal to the weight of the layer per unit area of the column cross section, and the viscosity. The purpose of the investigations performed was to establish the character of the influence exerted on all these parameters by a homogeneous longitudinal alternating magnetic field.

The ferromagnetic phase was made up of small iron cylinders and small cast iron spheres, with average diameter 1.67 ± 0.07 mm, and also particles of ground natural magnetite from the Kursk magnetic anomaly, measuring 0.07-0.4 mm. The suspending medium in the experiments with the iron and cast iron particles was water, while in the experiments with magnetite air was used.

Measurements of the dependence of the height of the layer on the stream velocity, carried out at magnetic field intensities up to 150 oersted, have established that the suspension of the layer, in either water or in air streams, occurs at the same value of the critical velocity v_k as without the field. At velocities greater than v_k , the layer broadens, but the characteristic random motion of the particles no longer sets in. The motion of the particles now reduces to slow displacements - migrations in the direction of the magnetic field flux lines. The particles gather gradually along the flux lines, and the pattern of the gathering depends on their hydrodynamic resistance. Thus, whereas spherical particles form chains stretching along the axis of the column and separated by channels that are free of the solid phase as they are gradually slowed down in the magnetic field, cylindrical particles, which have a larger hydrodynamic resis-

tance, behave somewhat differently in this respect.

The cylindrical particles gather into coarse clusters with a pronounced although incomplete longitudinal orientation, reminiscent of the ramified complexes of polymerized molecules. so that we can figuratively call the state of the suspended layer stopped by the magnetic field a pseudopolymer state.

The external appearance of a pseudopolymer layer of spherical and cylindrical particles is shown in Fig. 1.

The upper edge of such a layer is usually outlined by formations of ramified character, making it difficult to determine exactly its height, the measurement of which has in this case a tentative character.

With further increase in the stream velocity, the pseudopolymer structure of the layer breaks up and its particles are gradually set into motion; the layer becomes pseudoliquefied.

This occurs at relatively low magnetic field intensities. However, if the magnetic field intensity at which the above-described phenomenon takes place is sufficiently large, then when the stream velocity approaches the soaring velocity of a single particle, the entire pseudopolymer layer is carried out as a unit from the working volume of the column.

Sometimes such a layer along with being carried out of the column also breaks up into pieces of larger or smaller dimensions.

It should be pointed out that there is a difference in the structure of the pseudopolymer layer of particles suspended by water streams and those suspended in air. Whereas in the former case all the particles of the layer are in a stationary state, in the latter, even when the intensity of the retarding field was large, one or more sources of particle gushing was always observed. These sources

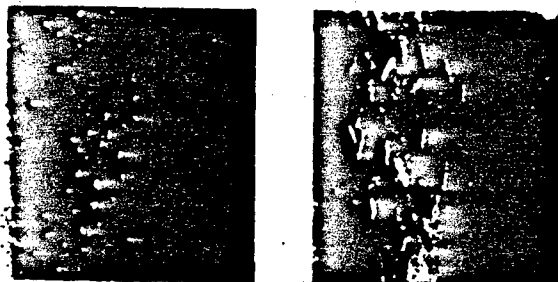


Fig. 1. External view of pseudopolymer layer of spherical and cylindrical particles.

were channels along which the suspending air stream flows with a velocity which greatly exceeds its average value, so that it breaks away individual particles, carries them with it, and ejects them upward out of the pseudopolymer layer.

The described gushing phenomenon must be taken into consideration in the development of practical applications of this phenomenon.

To ascertain the feasibility of controlling a layer of ferromagnetic particles by means of a magnetic field, it is interesting to establish the character of the influence that the latter exerts on its height.

Figure 2 shows the dependence of the porosity of the layer on the Reynolds number, plotted at different values of H from 0 to 75 oersted, for cylindrical particles suspended by a water stream. The course of this dependence discloses the existence of two regions. in each of which the magnetic field acts on the suspended layer in different fashion.

At expansions up to $\epsilon \approx 0.65$, the magnetic field hardly influences the height and it is perhaps more correct to speak here only of a tendency towards a certain compression of the layer subjected to the retardation by the magnetic field. Regardless of the magnetic

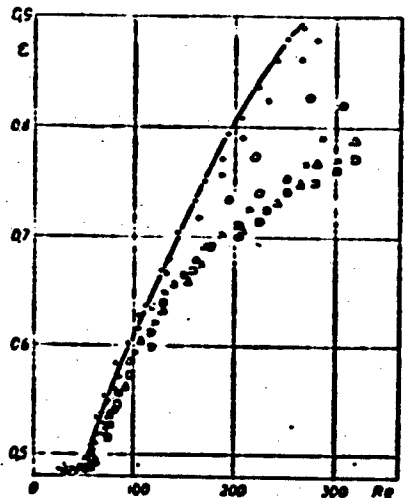


Fig. 2. Connection between the porosity of the layer and the Reynolds number for different magnetic fields: $\cdot - H = 0$; $+ - H = 10$ oe; $\circ - H = 20$ oe; $\times - H = 30$ oe; $\Delta - H = 40$ oe; $\blacksquare - H = 60$ oe; $\blacksquare - H = 75$ oe.

gushers, which give rise to nonuniform escape of groups of particles and to sharp fluctuations in the pressure, etc., so that the stream conditions become unstable. The start of the precipitation of the layer coincides with a sharp decrease in the velocity of the random

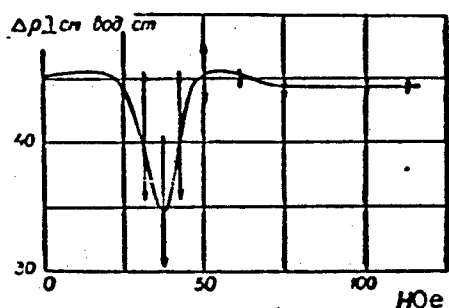


Fig. 3. Connection between the resistance of the suspended layer and the magnetic field intensity.
1) centimeters water column.

field intensity. the expansion of the layer follows here the law that holds true when $H = 0$.

When the expansion of the layer exceeds $\epsilon \approx 0.65$, the influence of the magnetic field on the porosity ϵ (and consequently also on the height h) of the layer increases and it becomes possible to control the height of the layer by means of the magnetic field within technically acceptable dimensions. It must be recognized, however, that when the layer is sharply precipitated under the influence of the magnetic field, it is subject to such phenomena as channels, plugs, bubbles, and

motions of the particles and precedes the transition of the bulk of the layer into the pseudopolymer states at an even larger increase in H . Thus, the process of controlling the height of a suspended layer of ferromagnetic particles by means of a magnetic field occurs at different rates of particle motion.

Figure 3 shows the variation of the resistance Δp for a suspended layer of iron particles of cylindrical form in a magnetic field. As can be seen from the plot, small fields do not exert a noticeable influence on the resistance of the layer. Then, at a certain value of H , sharp oscillations of the resistance begin, which usually tend to decrease it. This corresponds phenomenologically to the start of a sharp precipitation of the layer and to the formation of disturbances to the stream conditions in it, and also a considerable decrease in the velocity of motion of the particles. As the layer is gradually stopped and the pseudopolymer structure formed, the resistance of the layer becomes equalized and assumes the same value as when $H = 0$, although the height of the stopped layer is much smaller than that of a layer suspended without the field.

The reason for it must be sought in the presence of channels in the pseudopolymer layer, which separate the accumulations of the particles stretched out along the field, and through which the stream moves with decreased resistance. The formation of a pseudopolymer state of a suspended layer proceeds in such a way as to guarantee automatically the constancy of its resistance by suitable clustering of the particles in accordance with their hydrodynamic properties.

The viscosity of the pseudopolymer layer is much higher than that of the layer when $H = 0$, as was demonstrated by many researches of qualitative character.

The effect of a magnetic field on a suspended layer of ferromagnetic particles can be greatly intensified by placing one or several thin iron rods either inside the layer or above its upper edge.

The high induction of these ferromagnetic bodies contributes to the occurrence of new peculiarities in the suspension of the layer. Although the experiments carried out in this direction were tentative

in character, it was possible to establish nevertheless that this method can greatly increase the critical velocity and the rate of removal of the layer, and also to change the course of the expansion curve and reduce the resistance of the layer.

Further experiments in this direction are being continued.

In conclusion let us discuss the use of this phenomenon.

When speaking of practical applications, it must be pointed out that the magnetic field can be used as a supplementary regulating factor in all processes involving boiling-layer techniques, where the solid phase comprises ferromagnetic particles. We note, in particular, the possibility of using a magnetic field in coal-dressing installations with magnetite filler used to reduce the inhomogeneities of the suspension conditions. Favorable results are obtained also by using a magnetic field to separate a suspended mixture of particles, one component of which has ferromagnetic properties.

The retardation of the particles and the formation of a pseudo-polymer structure of the ferromagnetic phase in the magnetic field make it possible to assume that this method makes feasible the control of the heat exchange process in the suspended layer, the intensity of which is connected with the velocity of the pulsation motions of the particles. Further study of the properties of the suspended layer of ferromagnetic particles in a magnetic field will undoubtedly disclose many other ways of employing this phenomenon.

MAGNETIC SEPARATION OF PARTICLES IN SUSPENDED STATE

A.T. Filippov

832

The presence of random pulsational motions in a suspended layer brings about a continuous displacement of the particles, thus preventing the separation from the mixture of components that differ from one another in dimensions, density, etc.

If the particle mixture components have different ferromagnetic properties, they can be separated in a state of suspension in an air stream by placing the column C in the magnetic field of a coil X, as shown in Fig. 1.

The experiments were carried out with a mixture of quartz sand and a ground ferromagnet, namely magnetite, in a weight ratio 13/14, so that the height of the stationary layer in a column 8.4 cm in diameter was $d_0 = 9.7$ cm. The effective diameters of the particles, which were determined experimentally by measuring the "stream velocity vs. pressure head" characteristic for the stationary layer, amounted to $d = 0.012$ cm for both the sand and for the magnetite fraction.

The specific densities of the sand and of the magnetite material were 2.65 and 4.75 g/cm^3 , respectively.

The measured critical velocity of the mixture suspension was $v_k = 4.15 \text{ cm/sec}$ and was in between the value for sand, $v_k = 3.2 \text{ cm/sec}$, and for magnetite, $v_k = 5.7 \text{ cm/sec}$, for the investigated diameter.

The particles were suspended in an air stream flowing through the

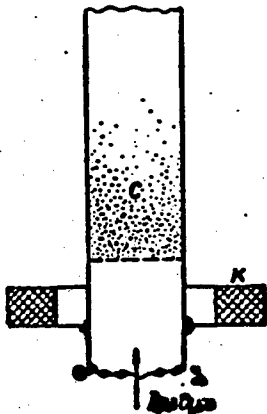


Fig. 1. Schematic diagram of the installation.

3) Air.

free section of the column with a velocity $v = 7.5$ cm/sec. The relative suspension height was in this case $h/h_0 = 1.15$. The boiling of the layer was quiet; small bubbles were continuously formed inside the layer, and above the edge there were always two or three constantly gushing moving concretes. The motion of the layer particles, which was very slow in the main mass of the layer, was appreciably accelerated near the gushing regions.

The duration of the suspension was five minutes both with and without magnetic field, after which the mixture was removed from the column layer by layer. In each fraction obtained in this manner, the magnetite was separated from the sand by means of an a.c. electromagnet, and then the relative fraction of each component in the given layer of the mixture was weighed.

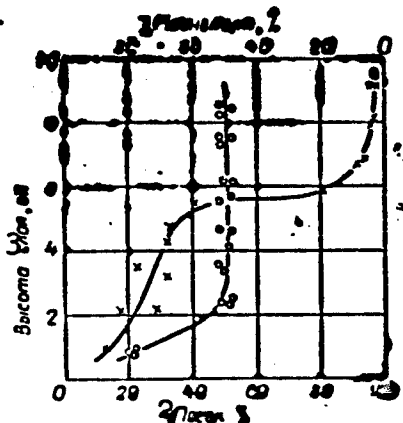


Fig. 2. Connection between the height of the layer and the relative content of the mixture components: O - in the absence of a field, X - in a magnetic field.
1) Magnetite; 2) sand;
3) height of layer, cm.

The results of the experiments are shown in Fig. 2, where the vertical axis shows the height of the layer, and the horizontal axis shows the per cent con-

The longitudinal alternating (50 cps) magnetic field produced by a coil X mounted coaxial with the column had such a degree of inhomogeneity, that it decreased in the upward direction along the height of the layer from 48 to 30 oersted, following a nearly linear law.

The results of the experiments are shown in Fig. 2, where the vertical axis shows the height of the layer, and the horizontal axis shows the per cent con-

circles denote the results of the experiments made in the absence of the field, and the crosses those in a magnetic field.

It is seen from the course of the curves that whereas without a field, complete mixing of the particles occurred in the entire layer during a given suspension mode, with the exception of the lowest part of the layer, in a magnetic field a clear cut separation effect was observed. The upper part of the layer was richer in sand and the lower was richer in the ferromagnetic magnetite.

Observations of the exterior picture of the suspension of the mixture in the magnetic field near the walls of the column disclose the following peculiarities of this phenomenon. The magnetite particles stop, descend downward, and gather into clusters of pseudopolymer structure. The sand particles, on the other hand, which are situated in the gaps between the magnetite clusters, fall into the faster air streams. This increases the porosity in these gaps and forces the sand into the upper part of the layer.

This is also accompanied by a continuous separation of a certain fraction of the magnetite particles from the boundaries of the clusters and a penetration of these particles upward, so that the separation is not perfect. The boiling and the motion of the particles in the upper portion of the mixture, which is enriched with sand, is more intense in the magnetic field than without a magnetic field.

After the suspension terminates and the particles are stopped, one can see clearly the separation boundary between the mixture components which is made choppy by the termination of the ramified groupings of the pseudopolymer structure of the magnetite layer.

The quality of the separation depends to a great degree on the correct choice of the working magnetic field intensity.

Manu-
script
Page
No.

[List of Transliterated Symbols]

634 K = K = katushka = coil

EXPERIMENTAL STUDY OF THE INFLUENCE OF
ELECTROMAGNETIC FORCES ON THE FLOW OF AN
ELECTROLYTE AROUND SOME BODIES*

R.K. Dukure, O.A. Lielausis

Riga

Recently several papers were published in which the influence of electromagnetic forces on the flow of an electrolyte around bodies is demonstrated [1-3]. In these experiments, an obstacle in the form of a round cylinder [3] or a semicylinder [1, 2] is placed in a laminar stream having a velocity on the order of 10 cm/sec. Electric current is made to flow through the electrolyte perpendicular to the generatrix of the cylinder. The cylinder is clamped between pole pieces of a magnet, that is, a magnetic field is directed along the generatrix of the cylinder. The liquid around the body is acted on here by a ponderomotive electromagnetic force, directed along the body parallel to the velocity field.

In all the cases under consideration, the gradient of the electromagnetic forces in a direction perpendicular to the surface of the body is determined principally by the decrease in the magnetic field intensity in the zone of the stray field beyond the limits of the volume contained between the pole pieces. As is well known, the field decreases here approximately exponentially and decreases by a factor 2.7 over a distance on the order of the distance between the pole pieces, which in the aforementioned experiments was approximately 1 cm. This means that the gradient of the electromagnetic forces near

the body is also characterized by a distance on the order of 1 cm. One cannot speak in this case of the action of electromagnetic forces in a boundary layer, the thickness of which under these conditions is on the order of 1 mm. The ponderomotive electromagnetic forces act on much larger liquid masses. Naturally, under such conditions the effect of improved flow around the body is most clearly pronounced if the electromagnetic forces are concentrated in the stagnation region behind the body [3].

It is possible to produce an electromagnetic force field with large gradient, for example, by placing on the surface of the body magnetic poles of alternate signs, between which electrodes of alternate polarities are placed. The force gradient in such a case is characterized by a distance which is of the same order of magnitude as the distance between the poles [4, 5]. However, in small-scale experiments where the characteristic dimension of the body is on the order of several centimeters, it is difficult to realize such a system in practice. To localize the electromagnetic forces near the surface we have set up experiments with a liquid of uneven conductivity. A stream of nonconducting liquid, distilled water, was made to flow on the obstacle. The electrolyte was used to color the boundary layer only.

A stationary fixed body made of organic glass in the form of a semicylinder or wedge was placed in an annular magnetohydrodynamic channel. The arrangement of the channel is described in [4]. The channel was rotated uniformly together with the distilled water placed in it. Under such conditions, liquid with uniform velocity distribution flowed around the stationarily fixed body. The location of the body in the channel is shown in Fig. 1. The figure is not to scale. A coloring liquid having the same density as water (ethyl alcohol, HCl, and the organic dye methyl orange) were introduced into the

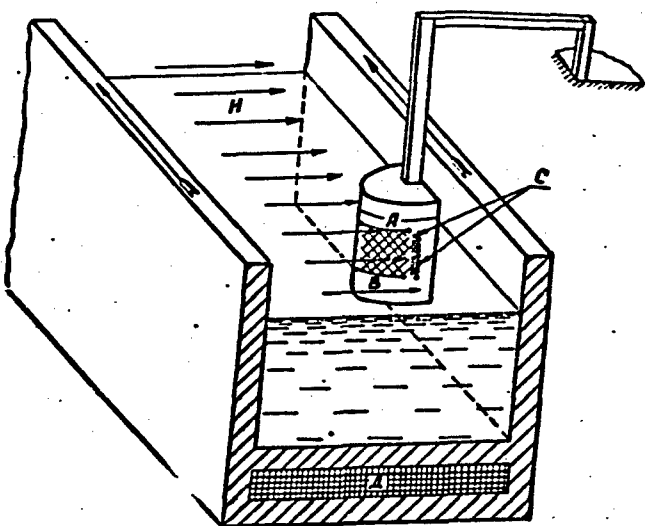


Fig. 1. Diagram of the experiment.

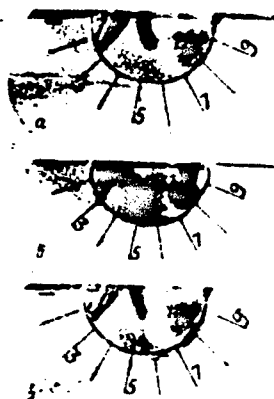


Fig. 2. Pattern of flow around a semi-cylinder: a - without application of magnetic field; b - electromagnetic forces act in the flow direction; c - electromagnetic forces act against the flow.

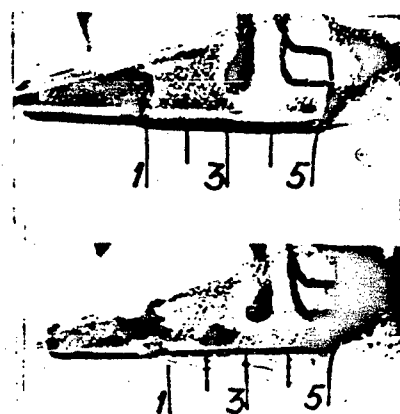


Fig. 3. Pattern of flow around a wedge: a - electromagnetic forces act against the direction of flow; b - without application of magnetic field.

boundary layer through apertures C in the front part of the body. The body was in a relatively homogeneous magnetic field, directed perpendicular to the direction of the stream and to the generatrix of the body. The magnetic field was produced in the channel with the aid of a coil D,

fed through slip rings. Electric current was made to flow along the generatrix of the body through the colored boundary layer. The electrodes were two copper wires A and B. It must be noted that in the case of a semicylinder the wires were drawn in such a way as to make the electromagnetic forces act in the boundary layer only up to the point of detachment (shaded region in Fig. 1). In the case of a wedge, the zone where the electromagnetic forces were in effect occupied the distance from the holes for the coloring to the rear edge. Depending on the orientation of the magnetic and electric fields, the electromagnetic forces acted either in the flow direction or against it.

Figure 2 shows photographs of the streamlined patterns around a semicylinder of radius 1 cm and of height 1.5 cm. The distance between electrodes was 1 cm. The upper photograph shows the case when there are no electromagnetic forces. The central photograph is for electromagnetic forces acting in the flow direction, while the lower one is for forces against the flow. The current between electrodes was 2 mA, and the magnetic field intensity was 2000 Gauss.

Figure 3 shows photographs of the streamlined pattern around a wedge 1.5 cm wide and 2.5 cm long. The distance between electrodes was 1 cm and the electrodes were 1 cm long. The liquid flowed over the investigated side of the wedge at an angle of attack equal approximately to 5° . The lower photograph shows the case when there are no electromagnetic forces. In the upper photograph the electromagnetic forces are against the flow, causing detachment of the stream. The current between electrodes was 2 mA, and the magnetic field intensity was 2000 Gauss.

In all cases the water flowed against the obstacle with a velocity on the order of 5 cm/sec.

REFERENCES

1. E. Crausse, P. Cashou. C r. Acad. Sci., 238, 26, 2488, 1954.
2. E. Crausse, Y. Poirier. 9th Congr. Internat. Med. Appl., III, 26, Bruxelles 1957.
3. M. L. Kuznetsov. Sb. nauchnykh rabot studentov fiz.-mekh. f-ta Leningr. politekhn. in-ta [Collected Scientific Works of Students in the Physical-Mathematical Department of Leningrad Polytechnic Institute], II, 42-47, 1959.
4. A. Gaylitis and O. Liyelausis. Trudy In-ta Fiziki AN Latv. SSR [Transactions of the Physics Institute Academy of Sciences Latvian SSR], XII, 1961.
5. E. Grinberg. Trudy In-ta fiziki AN Latv. SSR, XII, 1961.
6. I. L. Kuznetsov. ZhTF [Journal of Technical Physics], 30, 9, 1041-1045, 1960.

HEAT TRANSFER TO LIQUID METALS

V.M. Borishanskiy

Leningrad

Polhausen, Schlichting, Kruzhilin, Schwab, Levich, Kutateladze and others use the concept of thermal layer for the calculation of heat transfer in different flow conditions (internal and external problems). As applied to liquid metals flowing in pipes, the general theory of the problem, which was developed by Levich, gives a computational solution in the form of a two-layer thermal flow scheme (turbulent thermal core and a thermal molecular-transport layer near the wall), with simultaneous use of the two-layer dynamic stream scheme of Prandtl and Taylor in the calculations. Calculation based on this scheme gives qualitative agreement with experiment.

This theory can be further developed by using the concept of a three-layer thermal scheme for the stream (thermal turbulent core, intermediate thermal region, and molecular heat transport layer near the wall), with simultaneous assumption of the three-layer dynamic flow scheme of Korman and Schwab.

A comparison of the experimental material on the velocities and the temperature fields in the flow of liquid metal, available in the literature, confirms the theoretical notion that the dimensionless fields of the velocity defect and of the temperature coincide in the thermal turbulent core of the stream. On this basis, the connection between the thermal and dynamic boundaries of the turbulent core can be written in the form

$$y_m = y_s P_e^{-1}$$

where y is the distance from the wall to the boundary of the thermal and dynamic turbulent core;

$$P_e = \frac{U_\infty L}{v}$$

is the Prandtl number.

The determination of the boundary of the molecular transport thermal layer near the wall is calculated on the basis of the relation

$$y = y_s P_e^{1/2}$$

This approximate relation, derived by us here in the calculation of heat transfer under conditions where a laminar boundary layer flows over a plate, should be regarded only as a first approximation and calls for further refinement.

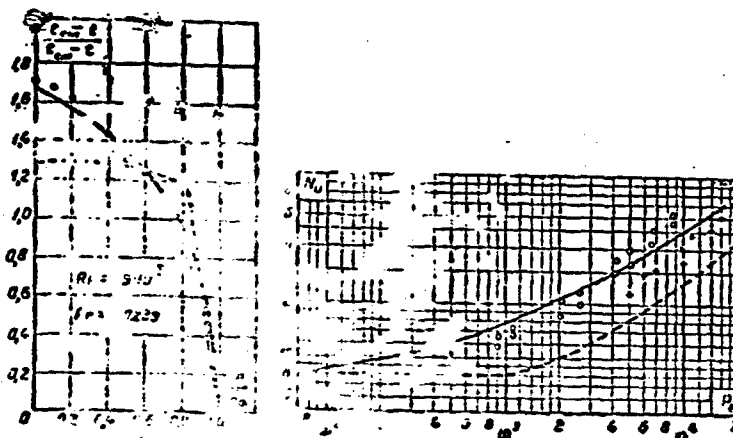


Fig. 1. Calculation based on three-layer thermal scheme (Borshanskiy); - - - - calculation based on two-layer thermal scheme (Levich); O - experiments of Isakov and Drew (heating of mercury); + - experiments of Brown, Amsted, and Short (cooling of mercury); a - temperature field; δ - coefficient of heat transfer ($Nu = f(Pe)$).

The calculations of the temperature fields and the heat transfer coefficients carried out in accordance with the proposed three-layer thermal flow scheme (using the Lyon integral) gave indication of

qualitative agreement with the experimental data for the temperature fields and the heat transfer coefficients obtained in the absence of oxides in the stream and on the wall (Figs. 1a and 1b).

The existing experimental data on heat transfer accompanying the flow of liquid metals show rather noticeable discrepancies (up to a factor 3-4) at not very large Peclet numbers. This is usually attributed to the presence of the so-called "contact thermal resistance" on the boundary between the stream and the wall of the contour. A study of the distribution of oxides and other impurities over the cross section of the stream, and also of the physical and chemical phenomena on the boundary with the wall will make it possible to develop engineering methods for increasing the intensity of heat transfer.

Manu-
script [List of Transliterated Symbols]
Page
No.

641 τ = t = teplovoy = thermal
641 π = d = dinamicheskiy = dynamic

SOME PHYSICAL AND CHEMICAL PHENOMENA
OBSERVED IN FLOWS OF LIQUID METAL COOLANTS

A.S. Andreyev
Leningrad

In an operating heat exchanger, a dynamic equilibrium is established between the liquid metal coolant and the parts of the system in contact with it (the metal of the circuit walls, the protective gases, etc.). Contact with gases causes the latter to be dissolved in the metal, and insufficient purification of the gases leads to formation of oxides, hydrides, and other compounds. Metals predominantly from the iron group are dissolved from the walls of the circuit, and the dissolution may be selective in character. The composition and the state of the coolant which is in constant contact with the metal of the circuit walls and with the protective gases changes continuously, and its change depends on the properties of the liquid metal and its temperature.

At high temperatures, sodium oxides and hydrides are dissolved in the metallic sodium, along with the metal from the circuit walls. In the cooled portions of the circuit one observes the opposite picture — the release of gases, oxides, hydrides, and solid metallic phases, resulting from the decrease in their solubility.

Particles of the solid phases (oxides, metals) can be released both directly on the cooling surfaces, as well as in various points of the metal stream. In the former cases crusts may form, causing a reduction in the cross section and the plugging of the main lines of the

heat exchange circuit. The solid metallic particles carried by the stream into the high temperature zone are again dissolved in the liquid metal, to be again separated in the cold portions. In the zone of the magnetic fields of flow meters and magnetic pumps, these may cluster together and reduce the passage area of pipes and the flow of liquid, and also shield the magnetic fields and disturb the operation of the magnetic pumps.

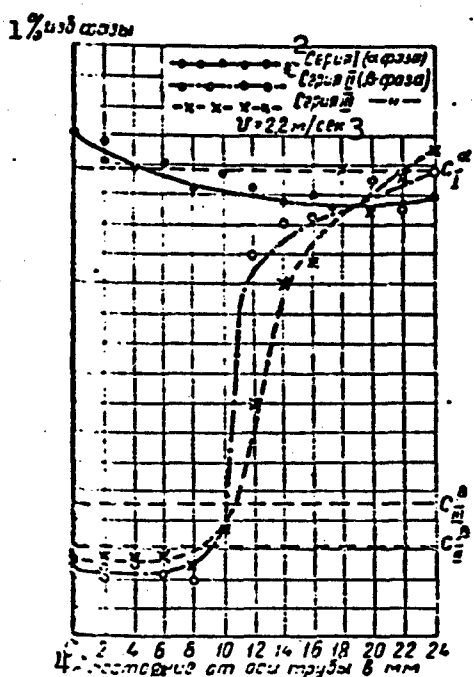


Fig. 1. Change in concentration of the excess phase (α or β) over the cross section of the stream (Pb-Sb alloy): Series I (excess of α phase), alloy 5% Sb, 95% Pb at $t = 280^\circ\text{C}$. Series II (excess of β phase), alloy 26% Sb, 74% Pb at $t = 300^\circ\text{C}$. Series III (excess of β phase), alloy 32% Sb, 68% Pb, at $t = 300^\circ\text{C}$; $v = 2.2 \text{ m/sec}$. 1) Excess phase; 2) series; 3) m/sec ; 4) distance from pipe axis in mm.

character, which include in addition to the formation on the separa-

- 644 -

tion boundary of a layer consisting of oxides and gases with low thermal conductivity, also the following phenomena which should be thoroughly studied: a) diffusion of liquid metal into the adjacent metal of the contour and formation of a diffusion layer with different structure in the layer at the contact; b) increased concentration of carbon and change in the composition of the layer near the contact, resulting from the selective dissolution of individual steel components, c) thermal phenomena (on the separation boundary), connected with the appearance of the Peltier effect, and many others.

To prevent oxidation of the heavy metals, it is advisable to protect them not with pure inert gases, but to produce a reducing medium (mixture of hydrogen or water gas with an inert gas).

Control over the chemical composition (principally the impurity content) should be exercised on local samples taken from different spots in the stream, which characterize not only the content but also the relative distribution of the suspensions in the given portion of the circuit.

DISTRIBUTION LIST

DEPARTMENT OF DEFENSE	Nr. Copies	MAJOR AF COMMANDS	Nr. Copies
HEADQUARTERS USAF			
AFCIN-3D2	1	AFSC	1
ARL (ARB)	1	SCFLD	25
OTHER AGENCIES			
CIA	6	ASPA	5
NSA	2	TECL	5
DIA	2	TEWDP	5
AID	2	AMTC (AEY)	1
OTS	2	SSD (PSF)	2
AEC	2	ESD (LSY)	1
PWS	1	RADC (RAY)	1
NASA	1	AFSWS (SWF)	1
ARMY	1	AFMTC (MTW)	1
NAVY	1	APGC (PGF)	1
RAND	1	AFMDG (MDF)	1
SPECTRUM	1	AFITC (FTY)	1